UNITED STATES
DEPARTMENT OF THE INTERIOR
GEOLOGICAL SURVEY

# NATIONAL EARTHQUAKE HAZARDS REDUCTION PROGRAM, SUMMARIES OF TECHNICAL REPORTS VOLUME XXVI

Prepared by Participants in

NATIONAL EARTHQUAKE HAZARDS REDUCTION PROGRAM

Compiled by

Muriel L. Jacobson

The research results described in the following summaries were submitted by the investigators on May 20, 1988 and cover the period from October 1, 1987 through May 1, 1988. These reports include both work performed under contracts administered by the Geological Survey and work by members of the Geological Survey. The report summaries are grouped into the five major elements of the National Earthquake Hazards Reduction Program.

Open File Report No. 88-434

The data and interpretations in these progress reports may be reevaluated by the investigators upon completion of the research. Readers who wish to cite findings described herein should confirm their accuracy with the author.

# CONTENTS

## Earthquake Hazards Reduction Program

Page

ELEMENT I - Recent Tectonics and Earthquake Potential

Determine the tectonic framework and earthquake potential of U.S. seismogenic zones with significant hazard potential

Objective (I-1): Regional seismic monitoring....................1

Objective (I-2): Source zone characteristics

Identify and map active crustal faults, using geophysical and geological data to interpret the structure and geometry of seismogenic zones.

1. Identify and map active faults in seismic regions
2. Combine geophysical and geologic data to interpret tectonic setting of seismogenic zones..................55

Objective (I-3): Earthquake potential

Estimate fault slip rates, earthquake magnitudes, and recurrence intervals for seismogenic zones and faults disclosed by research under Objectives T-1 and T-2, using geological and geophysical data.

1. Earthquake potential estimates for regions of the U.S. west of 100½W.
2. Earthquake potential estimates for regions of the U.S. east of 100½W.
3. Support studies in geochemistry, geology, and soils science that enable fault movements to be accurately dated.....................................................125

Page

## ELEMENT II. Earthquake Prediction Research

Collect observational data and develop the instrumentation, methodologies, and physical understanding needed to predict damaging earthquakes.

Objective (II-1): Prediction Methodology and Evaluation

Develop methods to provide a rational basis for estimates of increased earthquake potential. Evaluate the relevance of various geophysical, geochemical, and hydrological data for earthquake prediction.

1. Develop, operate and evaluate instrumentation for monitoring potential earthquake precursors.
2. Analyze and evaluate seismicity data collected prior to medium and large earthquakes.
3. Obtain and analyze data from seismically active regions of foreign countries through cooperative projects with the host countries.
4. Systematically evaluate data and develop statistics that relate observations of specific phenomena to earthquake occurrence.
5. Develop, study and test prediction methods that can be used to proceed from estimates of long-range earthquake potential to specific short-term predictions.........................................185

Objective (II-2): Earthquake Prediction Experiments

Conduct data collection and analysis experiments in areas of California capable of great earthquakes, where large populations are at risk. The experiments will emphasize improved coordination of data collection, data reporting, review and analysis according to set schedules and standards.

1. Collect and analyze data for an earthquake prediction experiment in southern California, concentrating on the southern San Andreas fault from Parkfield, California to the Salton Sea.
2. Collect and analyze data for an earthquake prediction experiment in central California, concentrating on the San Andreas fault north of Parkfield, California..........................................278

Page

### Objective (II-3): Theoretical, Laboratory and Fault Zone Studies

Improve our understanding of the physics of earthquake processes through theoretical and laboratory studies to guide and test earthquake prediction observations and data analysis. Measure physical properties of those zones selected for earthquake experiments, including stress, temperature, elastic and anelastic characteristics, pore pressure, and material properties.

1. Conduct theoretical investigations of failure and pre-failure processes and the nature of large-scale earthquake instability.
2. Conduct experimental studies of the dynamics of faulting and the constitutive properties of fault zone materials.
3. Through the use of drilled holes and appropriate down hole instruments, determine the physical state of the fault zone in regions of earthquake prediction experiments................................394

### Objective (II-4): Induced Seismicity Studies

Determine the physical mechanism responsible for reservoir-induced seismicity and develop techniques for predicting and mitigating this phenomena.

1. Develop, test, and evaluate theories on the physics of induced seismicity.
2. Develop techniques for predicting the character and severity of induced seismicity.
3. Devise hazard assessment and mitigation strategies at sites of induced seismicity.......................447

## ELEMENT III Evaluation of Regional and Urban Earthquake Hazards

Delineate, evaluate, and document earthquake hazards and risk in urban regions at seismic risk. Regions of interest, in order of priority, are:

1) The Wasatch Front

2) Southern California

3) Northern California

Page

4) Anchorage Region

5) Puget Sound

6) Mississippi Valley

7) Charleston Region

Objective (III-1): Establishment of information systems......449

Objective (III-2): Mapping and synthesis of geologic hazards

Prepare synthesis documents, maps and develop models on surface faulting, liquefaction potential, ground failure and tectonic deformation..........................539

Objective (III-3): Ground motion modeling

Develop and apply techniques for estimating strong ground shaking...........................................556

Objective (III-4): Loss estimation modeling

Develop and apply techniques for estimating earthquake losses

Objective (III-3): Implementation.............................587

ELEMENT IV Earthquake Data and Information Services

Objective (IV-1): Install, operate, maintain, and improve standardized networks of seismograph stations and process and provide digital seismic data on magnetic tape to network-day tape format.

1. Operate the WWSSN and GDSN and compile network data from worldwide high quality digital seismic stations.
2. Provide network engineering support.
3. Provide network data review and compilation..........572

Page

Objective (IV-2): Provide seismological data and information services to the public and to the seismological research community.

1. Maintain and improve a real-time data acquisition system for NEIS. (GSG)
2. Develop dedicated NEIS data-processing capability.
3. Provide earthquake information services.
4. Establish a national earthquake catalogue............595

ELEMENT V: Engineering Seismology

Objective (V-1): Strong Motion Data Acquisition and Management

1. Operate the national network of strong motion instruments.
2. Deploy specialized arrays of instruments to measure strong ground motion.
3. Deploy specialized arrays of instruments to measure structural response..................................603

Objective (V-2): Strong Ground Motion Analysis and Theory

1. Infer the physics of earthquake sources. Establish near-source arrays for inferring temporal and spatial variations in the physics of earthquake sources.
2. Study earthquake source and corresponding seismic radiation fields to develop improved ground motion estimates used in engineering and strong-motion seismology.
3. Development of strong ground motion analysis techniques that are applicable for earthquake-resistant design.......................................619

Index 1: Alphabetized by Principal Investigator........................629

Index 2: Alphabetized by Institution..................................634

# Southern California Seismic Arrays

Cooperative Agreement No. 14-08-0001-A0257

Clarence R. Allen and Robert W. Clayton
Seismological Laboratory, California Institute of Technology
Pasadena, California 91125 (818-356-6912)

## Investigations

This semi-annual Technical Report Summary covers the six-month period from 1 October 1987 to 31 March 1988. The Cooperative Agreement's purpose is the partial support of the joint USGS-Caltech Southern California Seismographic Network, which is also supported by other groups, as well as by direct USGS funding to its own employees at Caltech. According to the Agreement, the primary visible product will be a joint Caltech-USGS catalog of earthquakes in the southern California region; quarterly epicenter maps and preliminary catalogs have been submitted as due during the Agreement period. About 250 preliminary catalogs are routinely distributed to interested parties.

## Results

This six-month reporting period includes two significant southern California earthquake sequences: (1) the 1 October 1987 Whittier Narrows sequence, including two events which caused damage in the Los Angeles area ($M_L$ = 5.9 on 10-1-87, and $M_L$ = 5.3 on 10-4-87), and (2) the November 1987 Superstition Hills sequence, the largest of which measured $M_S$ = 6.2 and 6.6.

Figure 1 shows the southern California seismicity for the reporting period. Because of the large number of aftershocks in the Superstition Hills sequence, data from 27 November to 31 December have only been partially processed. The catalog for this period currently includes all events above about $M_L$ 2.3, whereas data for the remainder of the reporting period should be complete down to about the $M_L$ 1.5 level.

Figure 2 shows epicenters of the Whittier Narrows sequence. The primary shock ($M_L$ = 5.9) and its immediate aftershocks occurred on a previously unknown thrust fault beneath the Elysian Park anticline (Hauksson et al., 1988). The second large shock ($M_L$ = 5.3), three days later, occurred on an approximately north-trending strike-slip fault, which may be an extension of the mapped Whittier fault. The third sizable shock ($M_L$ = 4.7) occurred much later, on 11 February 1988; this event took place on the eastern edge of the aftershock area, apparently on the thrust fault. Damage from the two large October shocks was concentrated in Whittier, but also occurred in large sections of Pasadena, Alhambra, Rosemead, Los Angeles, and adjacent communities. Even though it contained a few rather large events, the Whittier Narrows aftershock series was actually a rather sparse sequence when compared to those of many mainshocks in the region (e.g., the 1986 North Palm Springs and Oceanside sequences, the latest members of which can still be seen in Figure 1.)

The first of the Superstition Hills earthquakes ($M_L$ = 5.8; $M_S$ = 6.2) occurred on a left-slip fault, now known as the Elmore Ranch fault, which trends northeast from the Superstition Hills across the southern end of the Salton Sea--toward the southernmost end of the San Andreas fault (Fig. 3). This event occurred at about 5:54 pm local time on 23 November. The proximity of its rupture to the southern end of the locked segment of the San Andreas fault near Bombay Beach caused a tense night at the Seismological Laboratory. The second large event at 5:15 am the following morning ($M_L$ = 6.0; $M_S$ = 6.6) occurred, however, at the other end of the Elmore Ranch fault and was associated with right-slip of several centimeters along some 30 km of the northwest-trending Superstition Hills fault. The second earthquake caused significant damage in El Centro and surrounding areas. It seems logical that the first event may have effectively "unlocked" the Superstition Hills fault, which then ruptured 12 hours later. Inasmuch as both the southernmost San Andreas and Superstition Hills faults have demonstrated episodic creep in recent years, the Superstition Hills earthquake sequence must increase our concern for the southernmost San Andreas fault, which might well rupture in a much larger event.

On 25 January 1988, yet another event above magnitude 5 ($M_L$ = 5.6) occurred in northern Baja California, Mexico, bringing the total of such events to five for the reporting period. The highlights of seismic activity during the 6-month reporting period are as follows:

Total number of events processed to date: 604
Number of events of magnitude 3.0 and greater: 315
Number of events of magnitude 4.0 and greater: 38
Magnitude 5.0 and greater events:
  (1) 1 October 1987, 1442 GMT, $M_L$ = 5.9 (Whittier Narrows)
  (2) 4 October 1987, 1059 GMT, $M_L$ = 5.3 (Whittier Narrows)
  (3) 24 November 1987, 0154 GMT, $M_S$ = 6.2 (Elmore Ranch fault)
  (4) 24 November 1987, 1315 GMT, $M_S$ = 6.6 (Superstition Hills fault)
  (5) 25 January 1988, 1317 GMT, $M_L$ = 5.6 (Northern Baja California)
Number of earthquakes reported felt: 84

Late in March 1988 we received a new Digital Equipment Corp. MicroVAX to replace one of our aging PDP 11/34 on-line systems. We plan to run the version of the CUSP on-line software written by Robert Dollar for use in the Parkfield array, and we await its installation soon.

## Reference

Hauksson, E., et al., 1988, The 1987 Whittier Narrows earthquake in the Los Angeles metropolitan area, California: Science, v. 239, p. 1409-1412.

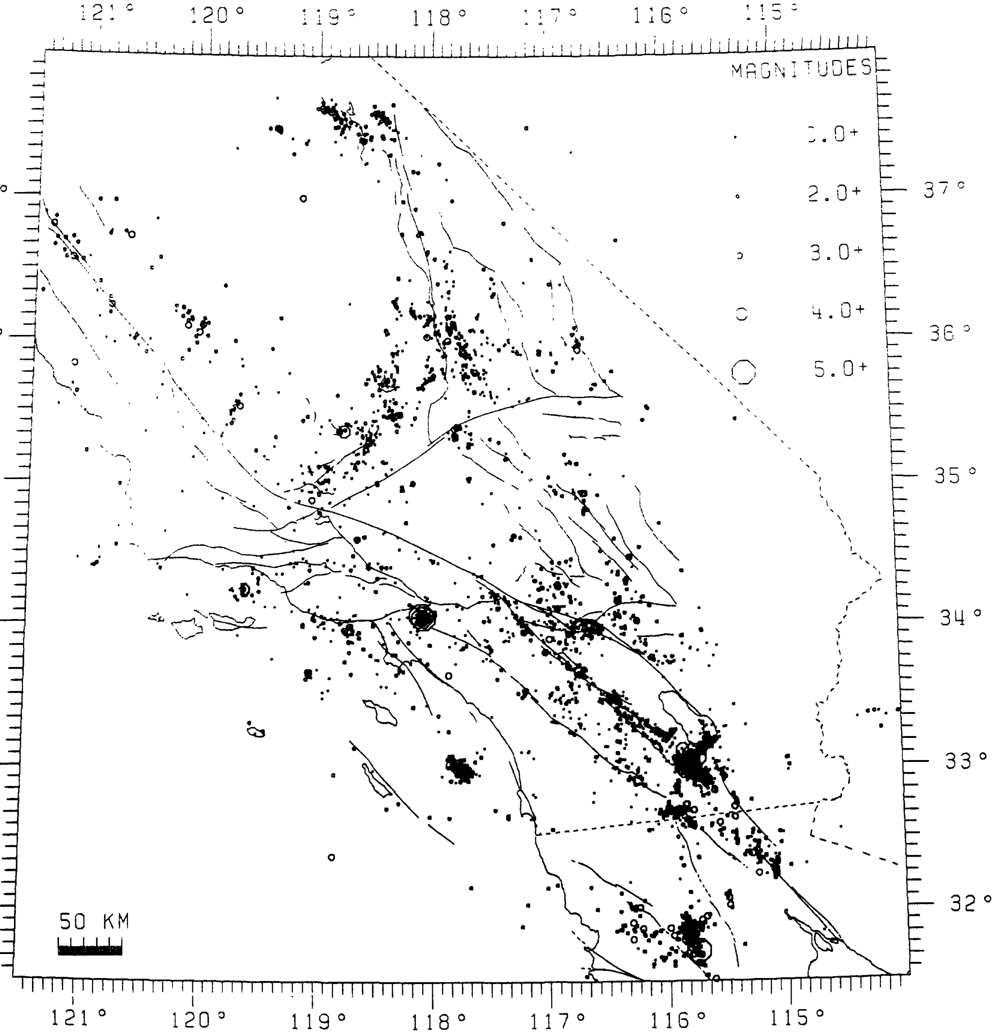

Fig. 1.--Epicenters of earthquakes in the southern California region, 1 October 1987 to 31 March 1988.

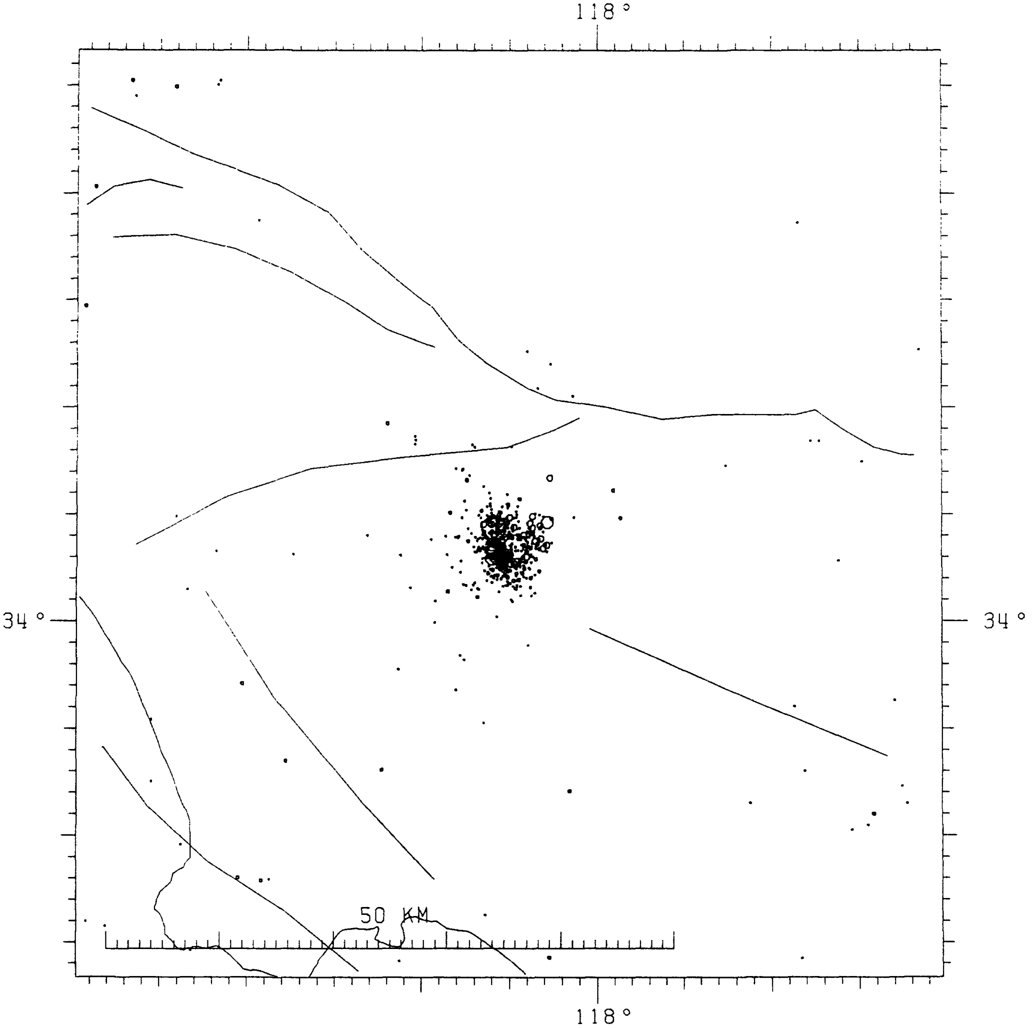

Fig. 2.--Epicenters of principal events of the Whittier Narrows earthquake sequence, 10-1-87 and following. Lines show coastline and major surface faults of the region. Symbols are as in Fig. 1.

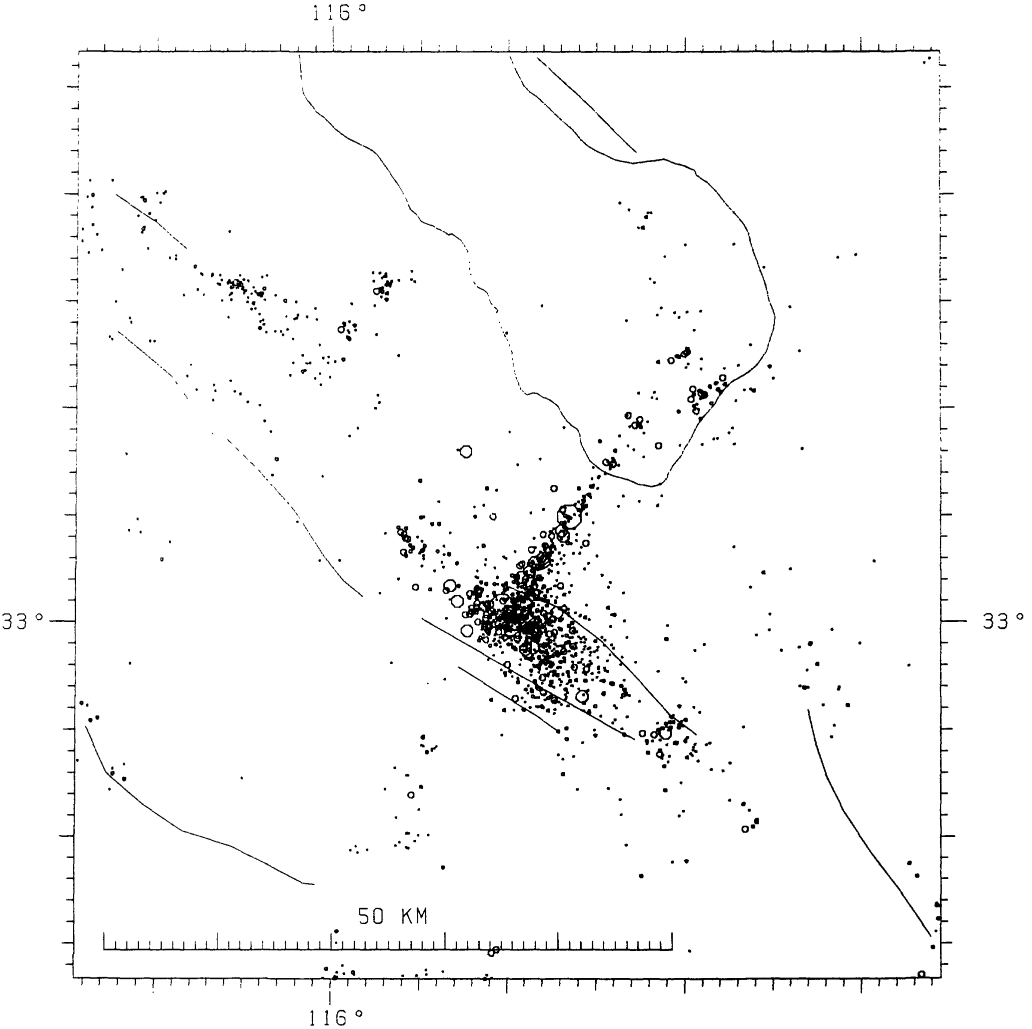

Fig. 3.--Epicenters of principal events of the Superstition Hills earthquake sequence, 11-23-87 and following. Lines shows outline of Salton Sea and major surface faults of the region. Symbols are as in Fig. 1.

# Regional Seismic Monitoring Along The Wasatch Front Urban Corridor And Adjacent Intermountain Seismic Belt

14-08-0001-A0265

W. J. Arabasz, R.B. Smith, J.C. Pechmann, and E.D. Brown
Department of Geology and Geophysics
University of Utah
Salt Lake City, Utah 84112
(801) 581-6274

## Investigations

This cooperative agreement supports "network operations" associated with the University of Utah's 85-station regional seismic telemetry network. USGS support focuses on the seismically hazardous Wasatch Front urban corridor of north-central Utah but also encompasses neighboring areas of the Intermountain seismic belt. Primary products for this USGS support are quarterly earthquake catalogs and a semi-annual data submission, in magnetic-tape form, to the USGS Data Archive.

During the report period, significant efforts were made in: (1) performing *in-situ* calibration on remote telemetry stations—and resolving discrepancies between observations and system responses predicted from circuit analysis; (2) refining software for system calibrations involving curve-fitting applications; (3) designing and fabricating new compact low-noise VCO/mixers; and (4) installing and operating temporary telemetry stations in and around an earthquake source zone in the Great Salt Lake Desert.

## Results

### *1. Network Seismicity*

Figure 1 shows the epicenters of 405 earthquakes ($M_L \leq 4.7$) located in part of the University of Utah study area designated the "Utah region" (lat. 36.75°-42.5°N, long. 108.75°-114.25°W) during the six-month period October 1, 1987, to March 31, 1988. The seismicity sample includes eleven shocks of magnitude 3.0 or greater and seven felt earthquakes.

The largest earthquake during the six-month report period was a shock of $M_L$4.7 ($m_b$4.3, USGS) on October 26 (04:16 GMT) near Lakeside west of the Great Salt Lake. This earthquake was felt from Wendover (on the Utah-Nevada border) to the Salt Lake Valley and northward into southern Idaho, and it was part of an earthquake sequence that included an $M_L$4.8 event on September 25 (Figure 2). An $M_L$4.2 event in the same area on October 23 was felt strongly by workers close to the epicenter. Other felt earthquakes during the report period include: An $M_L$3.4 event on October 2, located 50 km southwest of Logan and felt at the Golden Spike National Historic Site; an $M_L$3.6 shock on October 19, located 50 km west of Price and felt in the northern Sanpete Valley, and an $M_L$3.5 event on January 2, located 30 km west of Kanab on the southern border of Utah and felt in nearby small towns.

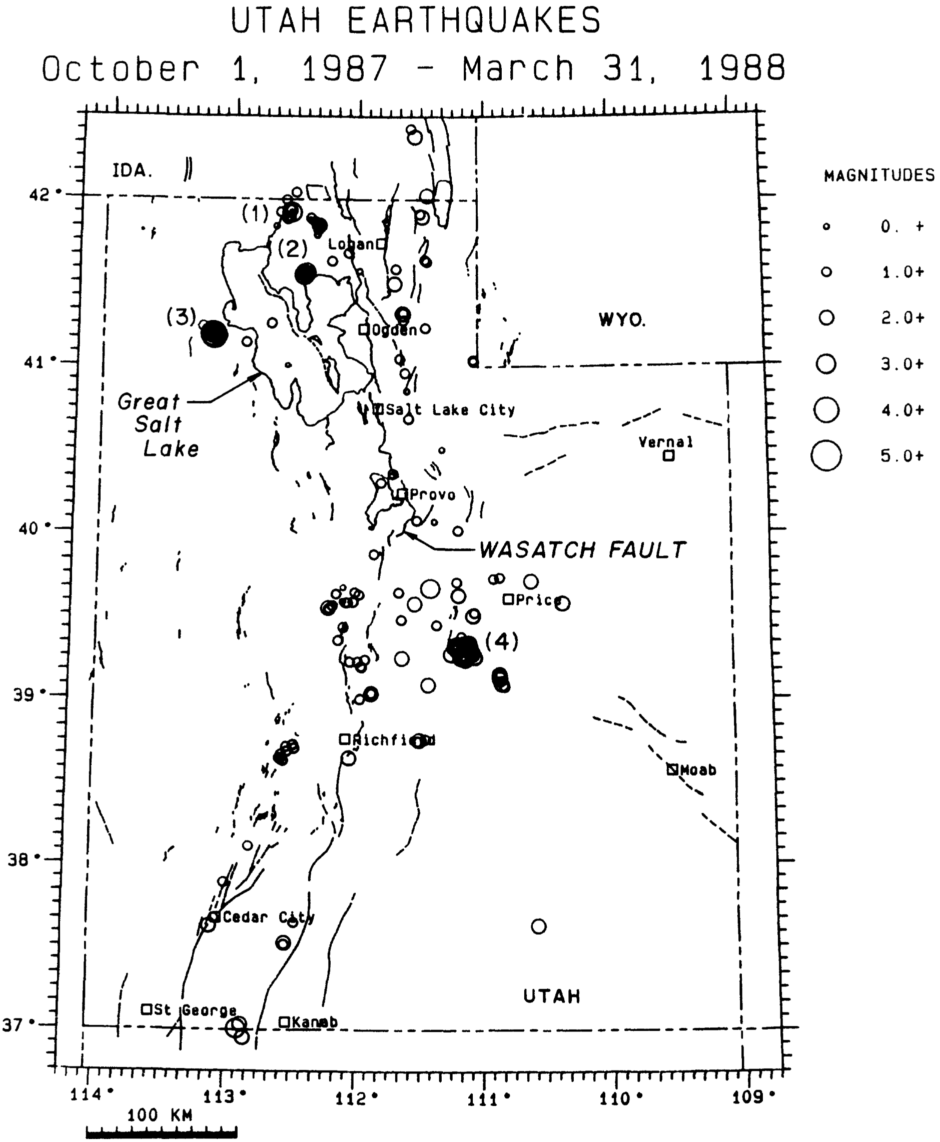
UTAH EARTHQUAKES
October 1, 1987 - March 31, 1988
IDA.
WYO.
UTAH
MAGNITUDES
0. +
1.0+
2.0+
3.0+
4.0+
5.0+
(1)
(2)
(3)
(4)
Logan
Ogden
Salt Lake City
Great Salt Lake
Vernal
Provo
WASATCH FAULT
Price
Richfield
Moab
Cedar City
St George
Kanab
42°
41°
40°
39°
38°
37°
114°
113°
112°
111°
110°
109°
100 KM

Figure 1

The scattered seismicity depicted in Figure 1 is typical of a pattern repeatedly observed during the last decade. Four prominent spatial clusters are labeled in Figure 1 (1) near the Utah-Idaho border, (2) north of the Great Salt Lake, (3) west of the Great Salt Lake, and (4) 40 km southwest of Price. Cluster (1), including a subgroup immediately to the east, contains 28 events of $M_L \leq 3.2$. These earthquakes are in the same area as a sequence active between October 1986 and April 1987 that included seven events greater than magnitude 3.5. Cluster (2) includes 21 events of $M_L \leq 3.4$, which occurred in October and November. Cluster (3), containing 198 events of $M_L \leq 4.7$, is part of a decaying sequence of earthquakes that began in September 1987 (Figure 2). Cluster (4) was active throughout the report period and includes 52 seismic events ($M_L \leq 3.3$) in an area of active underground coal mining.

## Reports and Publications

Brown, E.D., Utah earthquake activity, *Wasatch Front Forum,* v. 3, no. 3-4, p. 22, 1986.

Brown, E.D., Utah earthquake activity, July through September, 1987, *Survey Notes (Utah Geological and Mineral Survey),* v. 21, no. 2-3, p. 11, 1987.

[For other reports and publications and for additional details of the Lakeside, Utah, earthquake sequence, see technical summary for companion research award—R.B. Smith, W.J. Arabasz, J.C. Pechmann, and E.D. Brown, University of Utah, this volume.]

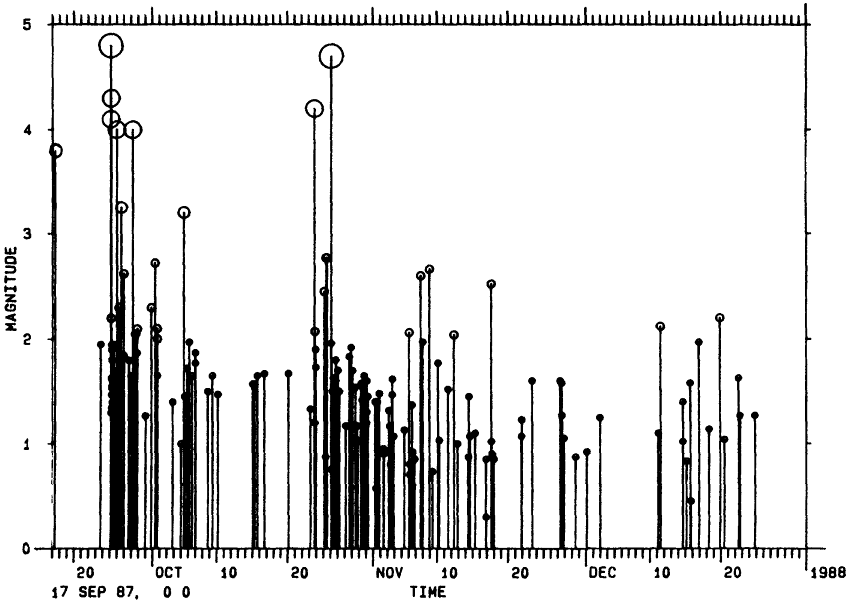

Figure 2. Magnitude as a function of time for Lakeside, Utah, earthquake sequence. A total of 165 earthquakes were recorded from September 17 to December 31, 1987. The mainshock ($M_L$=4.8) on September 25 was followed a month later (October 26) by a $M_L$ 4.7 event.

# Regional Seismic Monitoring in Western Washington

14-08-0001-A0266

R.S. Crosson and S.D. Malone
Geophysics Program
University of Washington
Seattle, WA 98195
(202) 543-8020

## Investigations

Operation of the western Washington regional seismograph network and routine preliminary analysis of earthquakes in western Washington are carried out under this contract. Quarterly catalogs of seismic activity in Washington and Northern Oregon are available for 1984 through 1987. Final catalogs are available though 1986. These catalogs were funded jointly by this contract and others. The University of Washington operates approximately 80 stations west of 120.5°W. Twenty eight are funded under this contract.

Data are provided for USGS contract 14-08-0001-G1390 and other research programs. Efforts under this contract are closely related to and overlap objectives under contract G1390, also summarized in this volume. Publications are listed in the G1390 summary. This summary covers a six month period from October 1, 1987 through March 31, 1988.

Excluding blasts, probable blasts, and earthquakes outside the U. W. network, 381 earthquakes west of 120.5°W were located during this period. Seventy-eight of these were located near Mount St. Helens, which has not erupted since October of 1986. Two earthquakes $M_c$ 4.1 and 4.3 were located near Yakima, Washington on December 2 at depths of about 20 km. The largest earthquake located in western Washington/northern Oregon between October 1 and March 31 had a $M_c$ of 3.9, and occurred near the southern end of Puget Sound on March 11, at a depth of 65 km.

# Earthquake Prediction Experiments in the Anza-Coyote Canyon Seismic Gap

14-08-0001-A0258

Jonathan Berger and James N. Brune
Institute of Geophysics and Planetary Physics
Scripps Institution of Oceanography
University of California, San Diego
La Jolla, CA 92093
(619) 534-2889

## 1. Investigations

This report covers the progress of the research investigating the Anza-Coyote Canyon seismic gap for the period of the second half of 1987. The objectives of this research are: 1) To study the mechanisms and seismic characteristics of small and moderate earthquakes, and 2) To determine if there are premonitory changes in seismic observables preceding small and moderate earthquakes. This work is carried out in cooperation with Tom Hanks, Joe Fletcher and Linda Haar, of the U.S. Geological Survey, Menlo Park.

## 2. Network Status

During the period of this report, nine stations of the Anza Seismic Network were telemetering three component data. The network was set at a low gain for most of the time of this report to try to record earthquakes up to magnitude 4 occurring inside the array.

There were no significant modifications to the data acquisition equipment.

## 3. Seismicity

In the six months of fall and winter, the Anza network recorded over 32 events which were large enough to locate and determine source parameters. These events had moments ranging from $2.5\times10^{18}$ to $4.3\times10^{21}$ dyne-cm, and stress drops ranging from about 1 to 56 bars (Brune model). The seismicity pattern seems unchanged from what has been observed before (Figure 1). The seismicity does not appear to be associated with the main trace of the San Jacinto fault on the north-west end of the array. These events in this area tend to be between the Hot Springs fault and the San Jacinto fault at depths of 12 to 19 km. The events on the south-east end of the array near the trifurcation of the San Jacinto fault also do not have any obvious associations with the identified fault traces. These earthquakes are occurring at depths between 8 and 12 km. The shallowest events are still occurring in the Cahuilla area.

The Anza network recorded many off-array events from the Superstition Hills earthquakes in November and December, and from the Whittier earthquakes in October.

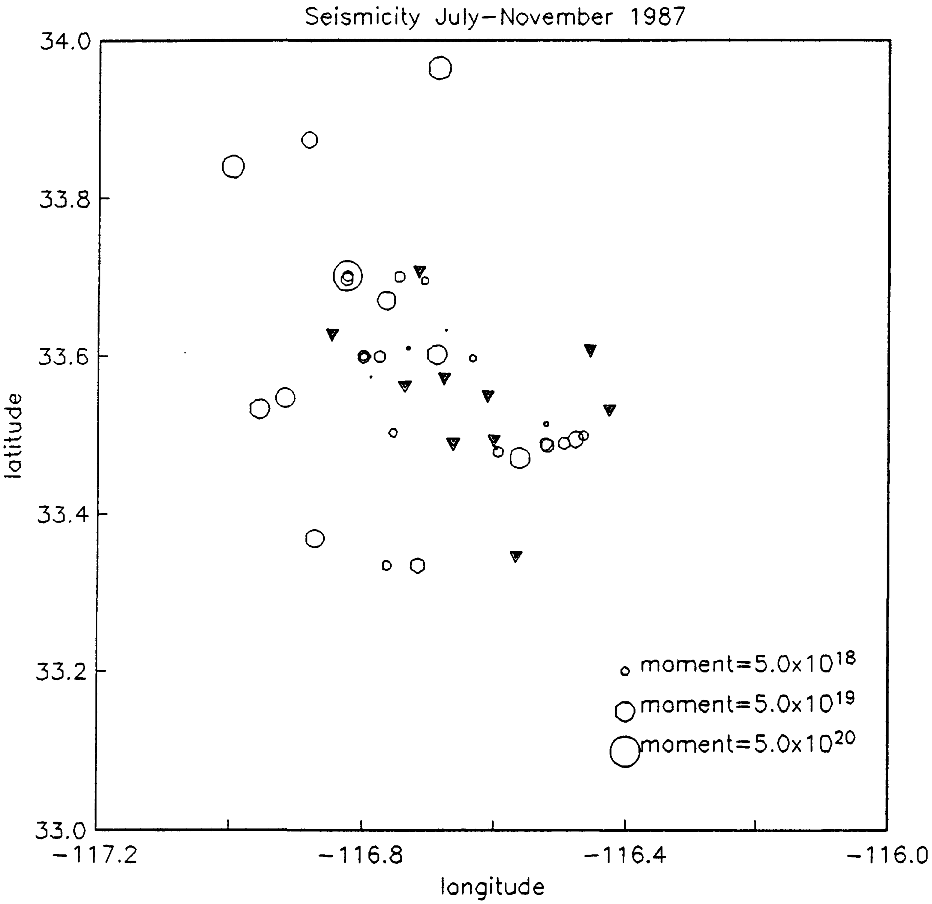

Figure 1. Seismicity scaled by moment. Anza stations (▼).

# Central California Network Operations

9930-01891

Wes Hall
Branch of Seismology
U.S. Geological Survey
345 Middlefield Road - Mail Stop 977
Menlo Park, California 94025
(415) 329-4730

## Investigations

Maintenance and and recording of 336 seismograph stations (415 components) located in Northern and Central California. Also recording 78 components from other agencies. The area covered is from the Oregon border south to Santa Maria.

## Results

1.Bench Maintenance Repairs

| | |
|---|---|
| seismic VCO units - | 115 ea |
| discriminators - | 48 ea |

2.Production/Fabrication

| | |
|---|---|
| seismic test units - | 2 ea |
| seismic VCO units - | 15 ea |
| VCO printed circuit boards | 38 ea |

3.Modifications

| | |
|---|---|
| seismic VCO units - | 6 ea |
| VCO printed circuit boards | 16 ea |
| summing amplifiers | 12 ea |
| discriminators - | 83 ea |

4. Completed wiring and documentation of new Signal Distribution Frame for Cusp and RTP computer systems.

5. Began uploading a file to isunix on seismic stations with known problems and which ones have been fixed. the file is called troubles DD report, where DD is a Julian day (1 to 365...) and is in /we/calnet/hall.

6. Installed a new microwave facility at Black mountain FAA Facility, Santa Margarita, CA. Data from Simmler, Vandenburg, Cambria and Shandon are now being routed through this facility.

7. Increased the capacity of the Hog Canyon microwave facility by installing a thirty (30) foot free standing tower. Installed additional link from Hog Canyon to Black Mountain.

8. Discontinued operation and removed Cuesta Peak microwave facility.

9. Replaced antenna tower and Mount Hamilton facility with a new 25 foot free standing tower.

10. Haliburton House (Parkfield) - Supported installation of a 20KW emergency generator and UPS system. Completed electrical installation. Added computer data transmission capability from Haliburton to Menlo Park via USGS microwave system.

11. Deleted and removed following seismic stations HCP, PCG

12. Installed new seismic stations at PTA (Tassajera Peak), PMB (Black Mountain), SIM (Simmler), PHFV, PHFE, PHFN (Heflinger Ranch)

13. Recording new telemetry circuits 1GD 6333 from Pasadena CA.
77FDDJ290686 from Pasadena Quarry, Cupertino, CA

# Central Aleutian Islands Seismic Network

Agreement No. 14-08-0001-A0259

Carl Kisslinger
Cooperative Institute for Research in Environmental Sciences
Campus Box 449, University of Colorado
Boulder, Colorado 80309

(303) 492-6089

## Brief Description of Instrumentation and Data Reduction Methods

The Adak seismic network consists of 13 high-gain, high-frequency, two-component seismic systems and one six-component system (ADK) located at the Adak Naval Base. Station ADK has been in operation since the mid-1960s; nine of the additional stations were installed in 1974, three in 1975, and one each in 1976 and 1977.

Data from the stations are FM-telemetered to recording sites near the Naval Base, and are then transferred by cable to the Observatory on the Base. Data were originally recorded by Develocorder on 16 mm film; since 1980 the film recordings are back-up and the primary form of data recording has been on analog magnetic tape. The tapes are mailed to CIRES once a week.

At CIRES the analog tapes are played back at four-times the speed at which they were recorded into a computer which digitizes the data, automatically detects events, and writes an initial digital event tape. This tape is edited to eliminate spurious triggers, and a demultiplexed tape containing only seismic events is created. All subsequent processing is done on this tape. Times of arrival and wave amplitudes are read from an interactive graphics display terminal. The earthquakes are located using a program developed for this project by E. R. Engdahl, which uses corrections to the arrival times which are a function of the station and the source region of the earthquake.

## Data Annotations

A major earthquake ($M_S$ 7.6) occurred immediately to the east of the network coverage area on May 7, 1986 (at 22:47). Thousands of aftershocks of that earthquake occurred within the network coverage area. At the time of this writing, the local catalog of hypocenters is still incomplete for the immediate time period following the mainshock. A discussion of research on that earthquake and its aftershocks is published under the report of Grant. No. G1368 (Kisslinger) elsewhere in this volume.

The network was serviced from mid-July through September, 1986. Due to major logistic problems, two of the westernmost stations could not be reached at that time, and we were also unable to make a needed return trip to one other far-west station. Of the 28 short-period vertical and horizontal components, 21 were operating for most of the time period of May through July, 1986. By the end of the 1986 summer field trip to Adak, 23 of the 28 components were operating (AK2z, AK5h, AD3 and AD5 having been brought back up).

During the time period of August 1986 through August of 1987, AK2z, AK3, and AK4 were not operating. In addition, there were some periods of time during this year when AD6 and ADK were intermittently down. Maintenance was performed on the network between mid-August and mid-October of 1987. By the end of the 1987 summer field trip to Adak, 23 of the 28 components were operating (AD6 and ADK having been brought back up). Again, due to logistic problems, AK2z, AK3, and AK4 could not be reached.

### Current Observations

So far, 611 earthquakes have been located with data from the network for the period between the time (20:43) of the $M_S$ 6.0 foreshock of the May 7 mainshock and 24:00 on May 14. During the past six months, project personnel have located 30 aftershocks occurring on May 14, 1986. We have also skipped ahead in time and located 44 events which occurred in July, 1986. Epicenters of *all* the events for May 14, as well as events occurring July 14 through July 26 are shown in Figures 1a and 1b and vertical cross-sections are given in Figures 2a and 2b. The aftershocks, May 7 through May 14, are shown in Figure 3.

Three of the events located with data from the Adak network for May 14 were large enough to be located teleseismically (USGS PDEs). A number of other teleseismically located aftershocks within the network region are difficult for us to locate due to their arrivals being masked by the codas of other aftershocks. Also, 7 of the events located with data from the Adak network for the specified dates in July, 1986, were large enough to be located teleseismically (USGS PDEs). No attempt is being made to locate aftershocks with duration magnitudes ($m_d$) of less than 2.3. More detailed information about the network status and a catalog of the hypocenters determined for the time period reported here are included in our semi-annual data report to the U.S.G.S. Recent research using these data is reported in the Technical Summary for U.S.G.S. Grant No. G1368.

### Move to the New Building

The entire solid earth geophysics research group at the CIRES Computing Facility will move from the present building to a newly constructed CIRES building in early April 1988. This move requires the shutdown of all computers and a temporary break in the earthquake location process. New computer equipment is also being installed. It is anticipated that our work should resume by mid-May.

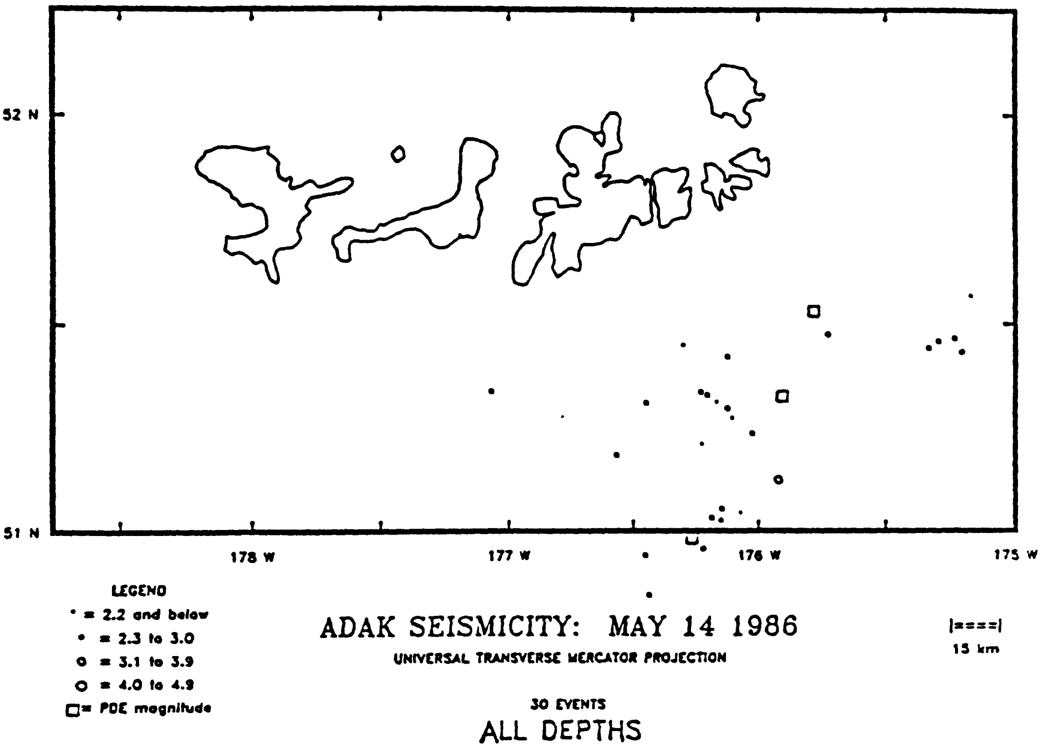

Figure 1a: Map of seismicity which occurred May 14, 1986. All epicenters were determined from Adak network data. Events marked with squares are those for which a teleseismic body-wave magnitude has been determined by the USGS; all other events are shown by symbols which indicate the duration magnitude determined from Adak network data. The islands mapped (from Tanaga on the west to Great Sitkin on the east) indicate the geographic extent of the Adak seismic network.

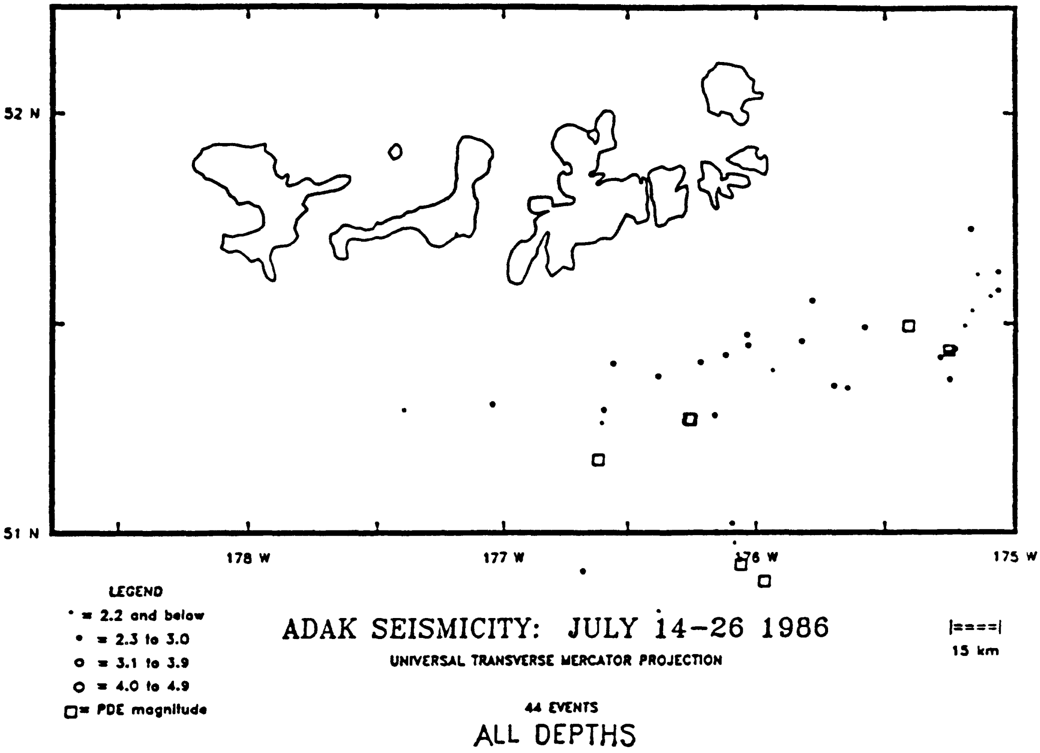

**Figure 1b:** Map of seismicity which occurred July 14 - 26, 1986. Symbols as in Figure 1a.

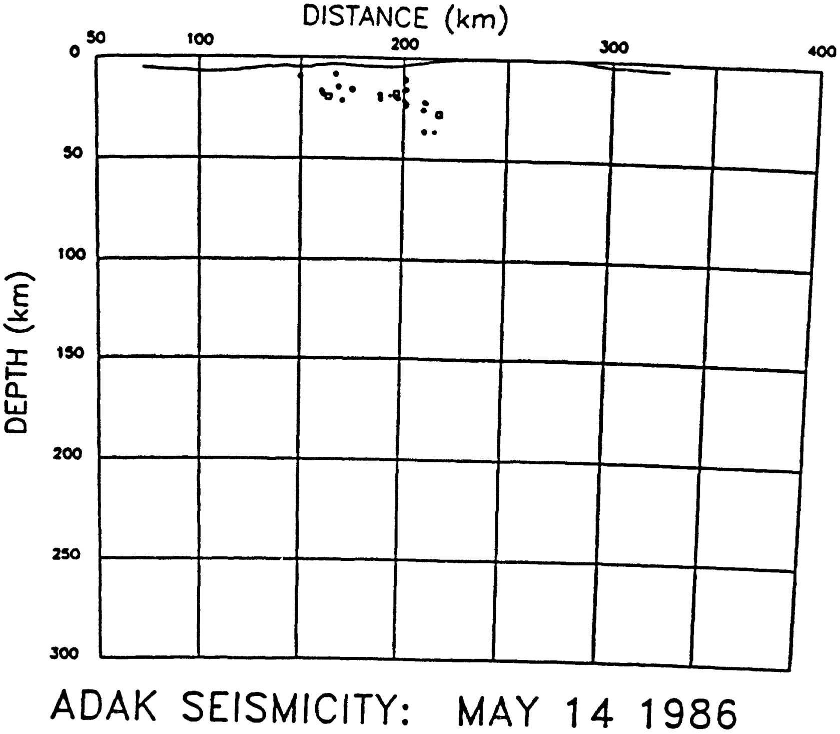

**Figure 2a:** Vertical cross section of seismicity which occurred May 14, 1986. Events are projected according to their depth (corresponding roughly to vertical on the plot) and distance from the pole of the Aleutian volcanic line. The zero-point for the distance scale marked on the roughly-horizontal axis of the plot is arbitrary. Events marked with squares are those for which a teleseismic body-wave magnitude has been determined by the USGS; all other events are shown by symbols which indicate the duration magnitude determined from Adak network data. The irregular curve near the top of the section is bathymetry.

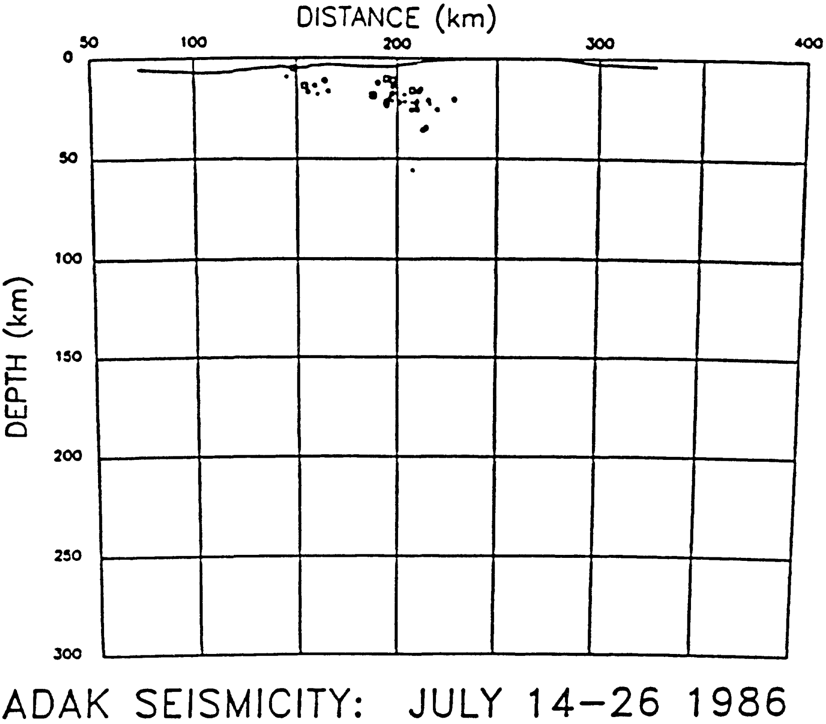

**Figure 2b:** Vertical cross section of seismicity which occurred July 14 - 26, 1986. Projection and symbols as in Figure 2a.

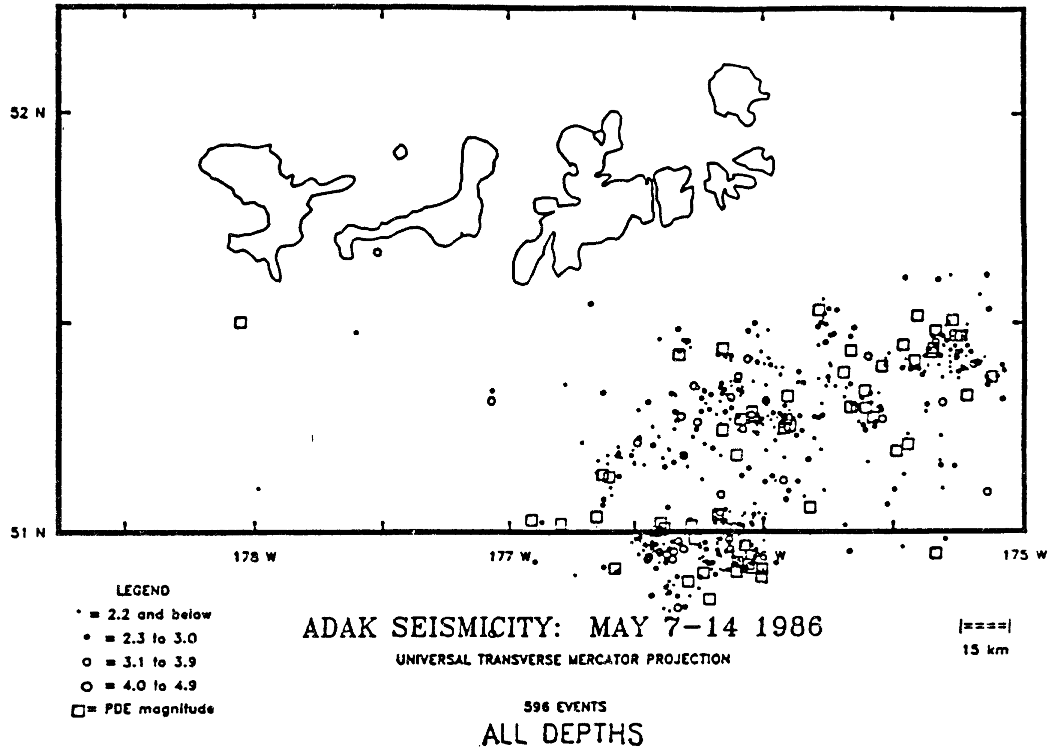

Figure 3: Map of seismicity which occurred May 7 - 14, 1986. Symbols as in Figure 1a.

# Alaska Seismic Studies

9930-01162

John C. Lahr, Christopher D. Stephens, Robert A. Page, Kent A. Fogleman
Branch of Seismology
U. S. Geological Survey
345 Middlefield Rd., MS 977
Menlo Park, California 94025
(415) 329-4744

## Investigations

1) Continued collection and analysis of data from the high-gain short-period seismograph network extending across southern Alaska from the volcanic arc west of Cook Inlet to Yakutat Bay, and inland across the Chugach Mountains. This region spans the Yakataga seismic gap, and a special effort is made to note changes of activity within and adjacent to the gap that might change our assessment of the imminence of a gap-filling event.

2) Cooperated with the Branch of Engineering Seismology and Geology in operating 17 strong-motion accelerographs in southern Alaska, including 12 between Icy Bay and Cordova in the area of the Yakataga seismic gap.

3) Began planning for increased monitoring of the Cook Inlet volcanoes as part of the Alaskan Volcano Observatory being established as a cooperative program between the U.S.G.S., the Geophysical Institute of the University of Alaska, and the Alaska Division of Geological and Geophysical Surveys.

## Results

1.) During the past six months preliminary hypocenters were determined for 1580 earthquakes that occurred between August 1987 and January 1988 (Figures 1 and 2). A total of 168 events had coda-duration magnitudes ($M_D$) of 3 or larger. Ninety-five of these larger shocks were located west of longitude 145° W, and all but 4 had computed depths greater than 30 km. Of the remaining 73 larger earthquakes located east of longitude 145° W, all but 3 were associated with the November 17 ($M_S$ 6.9) and November 30 ($M_S$ 7.6), 1987 earthquakes in the northern Gulf of Alaska, which are discussed under item 2.

A $M_D$ 4.1 (4.8 $m_b$) shock that occurred on October 31 beneath the eastern Kenai Peninsula was located at a well-constrained depth of 64 km, which is about 10 km below the lower depth range of Aleutian Wadati-Benioff seismicity typically observed in this area. A preliminary focal mechanism determined from P-wave polarities recorded on high-frequency regional seismographs has a subhorizontal, N-S-trending axis of greatest compressive stress and an E-W-trending axis of least compressive stress. The dip of the T-axis is not well contrained and can range from moderately westward- to moderately eastward-dipping. The stress orientation inferred from this mechanism and those of shallower earthquakes within the Aleutian

Wadati-Benioff zone in this area suggest that throughout the depth range of its elastic thickness, the subducting Pacific plate has a tension axis oriented approximately downdip.

On November 14, a $M_D$ 3.8 (5.2 $m_b$, NEIC) crustal shock occurred in southeastern Alaska approximately 75 km northwest of Juneau. Felt reports (NEIC) include MM intensity V at Haines, and intensity IV at Douglas, Juneau, and Skagway. The largest aftershock ($M_D$ 3.6, $m_b$ 4.9) occurred three days later on November 17 and was felt V at Haines, IV at Skagway and III at Juneau. The mainshock and three largest aftershocks are located a few km east of the mapped trace of the Chatham Strait fault.

On November 19, two days after the first large northern Gulf of Alaska earthquake, an intense sequence of low magnitude crustal earthquakes began near Waxell Ridge (60.5°N, 143.0°W), which is located near the center of the Yakataga seismic gap. The largest event on the first day was a $M_D$ 1.7 shock that occurred early in the sequence. At least 73 shocks with magnitudes ranging up to $M_D$ 1.5 were detected within 24 hr of this first large shock, and 75 more occurred within the next three days. The largest earthquake in the sequence, a $M_D$ 2.7 shock, occurred on November 23. Three foreshocks of magnitude $M_D > 1.0$ preceded this event, and at least 181 aftershocks, most smaller than $M_D$ 1.0, were detected within 24 hr. By the end of a week, 88 more aftershocks were detected. The Waxell Ridge area of the Yakataga seismic gap is characterized by a notably high rate of microseismicity relative to adjacent areas in a 75-km wide band that parallels and extends inland from the coast. The last time similar earthquake sequences were observed in this area was in June and July of 1979, following by a few months the February 1979 St. Elias earthquake ($M_S$ 7.1) that occurred north of Icy Bay along the eastern edge of the Yakataga gap.

On November 23, a $M_D$ 4.2 (5.7 $m_b$) crustal shock occurred near the intersection of the Totschunda and Duke River faults (near latitude 61.5° N, longitude 141.3° W), and was felt with intensity IV at Chitina and Copper Center. Through the end of January 1988, 47 aftershocks with magnitudes as large as 2.7 $M_D$ were located, with the largest aftershock occurring on December 13. P-wave polarities from the mainshock suggest dextral slip on a nearly vertical fault plane trending northwest-southeast, in general agreement with the trend and type of faulting exhibited by the Totschunda fault. Magnitude 5 shocks on the Totschunda fault are infrequent; the largest recent shock was a magnitude 4.3 event in 1978.

2.) On November 17 and November 30, 1987, two large ($M_S$ 6.9 and 7.6, NEIC) shallow shocks occurred within the Pacific plate beneath the northern Gulf of Alaska and south of the convergent boundary between the Pacific and North American plates (Figure 3). Aftershocks of the two earthquakes define two spatially distinct, nearly orthogonal zones. For the November 17 event, all but one of the aftershocks in the first 6 hr are confined to a zone about 40 km long, 20 km wide, and trending nearly E-W. Numerous shocks that occurred in the following two weeks are located as much as 25 km outside of this zone, with most of these shocks clustered along the E-W trend of the earlier activity. The trend in the distribution of early aftershocks and later expansion of aftershock activity primarily along the same trend are compatible with rupture on an E-W striking fault, such as the near vertical E-W plane of the focal mechanism determined from P-wave polarities (Figure 4).

The November 30 earthquake was a multiple event initiated by a 4.5 $m_b$ shock that was followed about 4 sec later by the much larger $M_s$ 7.6 event. The intial event is located about 30 km ENE of the November 17 mainshock. Aftershocks that occurred within 6 hrs are located in a N-S-trending zone that extends about 20 km north and 100 km south of the epicenter of the initial event, and is wider in its southern half. The aftershock distribution and focal mechanism of the November 30 shock are compatible with dextral slip on a nearly vertical plane. Continuing activity over the following three months extended the aftershock zone about 25 km to the north, and possibly as far as 75 km to the south, as indicated by a few shocks located between latitudes 57.1° and 57.8°N. Numerous aftershocks were located off the principal N-S trend of the aftershock zone, including an apparent E-W trend of epicenters that crosses the main zone near latitude 58.2°, and a cluster at the SW end of the November 17 aftershock zone. The aftershock zone of the November 17 shock appears not to have been reactivated for at least 5 1/2 days after the November 30 mainshock. It is not yet clear whether the apparent E-W trend in the seismicity forms a continuous band that may indicate the presence of a major cross-cutting fracture.

On March 6, 1988, the sequence of large shocks resumed with a $M_s$ 7.6 earthquake that broke the Pacific plate south of the November 30 aftershock zone (Figure 3). Most of the aftershocks that occurred within 6 hr of the March mainshock were located in two groups, a diffuse one near the mainshock at latitude 57° N, longitude 143° W, and a tight cluster about 70 km to the north near the epicenter of the largest aftershock (6.2$m_b$). These early aftershocks define a principal N-S-trending zone about 130 km in length, but near the latitude of the mainshock a few aftershocks were located up to 60 km west of the mainshock epicenter, and an isolated shock ($m_b$ 4.3) was located about 140 to the east. The focal mechanism for the mainshock determined from P-wave polarities (Figure 4) is compatible with dextral slip on a N-S-trending plane dipping 70° to the west, similar to the mechanism for the November 30 mainshock, but with a less steeply dipping slip plane. The distribution of early aftershocks also suggests that the March 6 earthquake primarily involved unilateral rupture to the north into the southern end of the November 30 aftershock zone; the northern limit of aftershocks from the March 6 earthquake is approximately coincides with the distinct E-W broadening in the principal aftershock zone of the November 30 earthquake. The broadening in the aftershock distribution and the termination of rupture from the November 30 and March 6 earthquakes in this area may reflect the presence of a change or complication in fault geometry, such as a change in fault dip, as suggested by the focal mechanisms, a discontiuity between en echelon fault segments, or possibly the the intersection of N-S and E-W faults.

The November and March earthquakes occurred seaward of the junction between recently slipped and locked segments of the plate boundary, represented by the rupture zone of the great 1964 Alaska earthquake to the northwest and the Yakataga seismic gap to the north. The recent earthquakes appear to have occurred in response to a stress field with an axis of least compressive stress closely aligned to the NW direction of relative plate motion, and a subhorizontal, SW-NE-trending axis of greatest compressive stress. We infer that these orientations reflect interaction between an extensional stress regime seaward of the 1964 rupture zone and a compressional regime associated with the Yakataga seismic gap. Geodetic observations from 1980-1986 (Savage and Lisowski, 1988) reveal that the gap area is being compressed approximately in the direction of relative plate velocity, consistent with a locked plate boundary. These recent earthquakes represent failure and possible fragmentation of the oceanic plate seaward of the locked Yakataga seismic gap, possibly presaging a reconfiguration of the plate boundary that will eventually detach the Yakutat block, which is colliding with the North Amercian plate, from the Pacific plate. Dislocation modeling (J. C. Savage, personal comm., 1988) suggests that the recent Gulf of Alaska earthquakes should have perturbed only slightly (by an amount comparable to the maximum solid earth tidal strain and less than half of the measured annual strain accumulation) the strain field within the northern part of the gap, where a major earthquake would most likely initiate. A gap-filling event is therefore not considered less likely as a consequence of the Gulf earthquakes.

3.) Development of PC-based event recorders has continued. Software modifications have been made to the the PCELOG (PC Event Logger) currently operating in Yakutat. During the period September 23, 1987 through March 17, 1988, waveforms from more than 1200 triggers were recorded by the PCELOG, of which 695 have been saved for analysis. About 95% of the saved events are earthquakes; the remainder consists of station calibrations and other signals such as glacial activity.

For more sophisticated processing, a fast digital-signal-processing (DSP) auxiliary board made by Symmetric Research in Seattle is being programmed to handle computation-intensive processing in near real time. In a configuration based on a PC/XT computer with an external A/D board, the DSP Event Logger (DSPELOG) is currently able to record signals from 16 (expandable to 32) channels. For each channel, when a potential event is detected by an STA/LTA algorithm, an FFT is calculated to discriminate among various types of signals on the basis of frequency content. This technique has proved to be quite sensitive for detecting particular non-seismic signals of interest such as automatic calibration signals from the remote seismic instrumentation and trigger signals from co-located stong-motion accelerographs. The FFT should also help in identifying earthquakes and classifying them in terms of local or teleseimic origin. A time-domain technique using least-squares correlation has also been developed to detect in real time square-wave signals that indicate gain-ranging in the seismic amplifier.

## References

Savage, J. C. and Lisowski, M., 1988, Deformation in the Yakataga seismic gap, southern Alaska, 1980-1986, Journal of Geophysical Research, v. 93, (in press).

## Reports

Page, R. A., Stephens, C. D., Lahr, J. C., and Fogleman, K. A., 1987, the transition between the Aleutian and Wrangell Wadati-Benioff zones, southern Alaska, EOS, v. 68, p. 1456.

Fogleman, K. A., Stephens, C. D., and Lahr, J. C., 1988, Catalog of earthquakes in southern Alaska for 1985, U. S. Geological Survey Open-File Report 88-31, 112 p.

Page, R. A., Fogleman, K. A., Stephens, C. D., and Lahr, J. C., 1988, State of stress in the subducted Pacific plate beneath Prince William Sound, southern Alaska, Seismological Research Letters (abs, in press).

Stephens, C. D., Lahr, J. C., Page, R. A., and Fogleman, K. A., 1988, The northern Gulf of Alaska earthquakes of 17 November (6.9 $M_s$) and 30 November (7.6 $M_s$) 1987: rupture of the Pacific plate south of the Yakataga seismic gap, Seismological Research Letters (abs, in press).

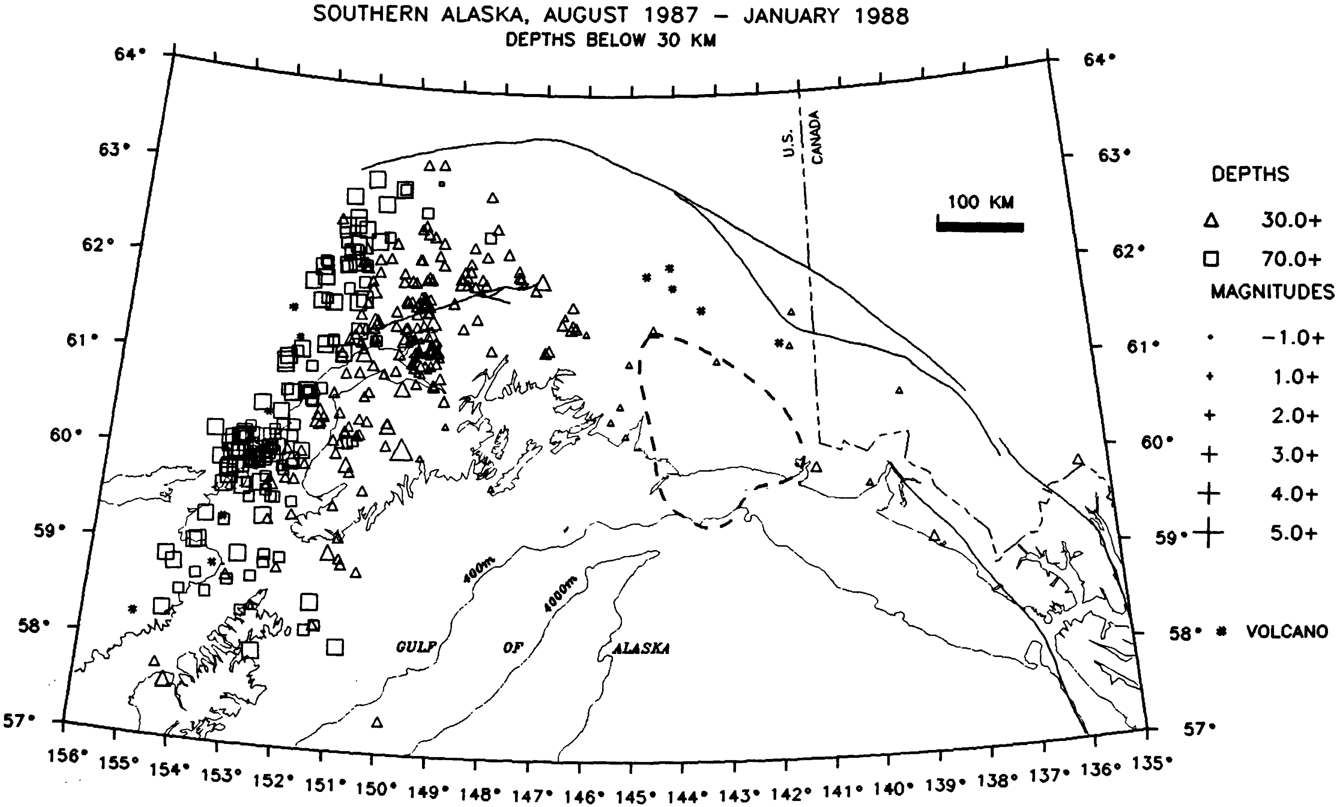

Figure 2: Epicenters of 398 earthquakes deeper than 30 km located using the USGS seismograph network for the period August 1987 - January 1988. See Figure 1 for details about magnitudes and for identification of map features.

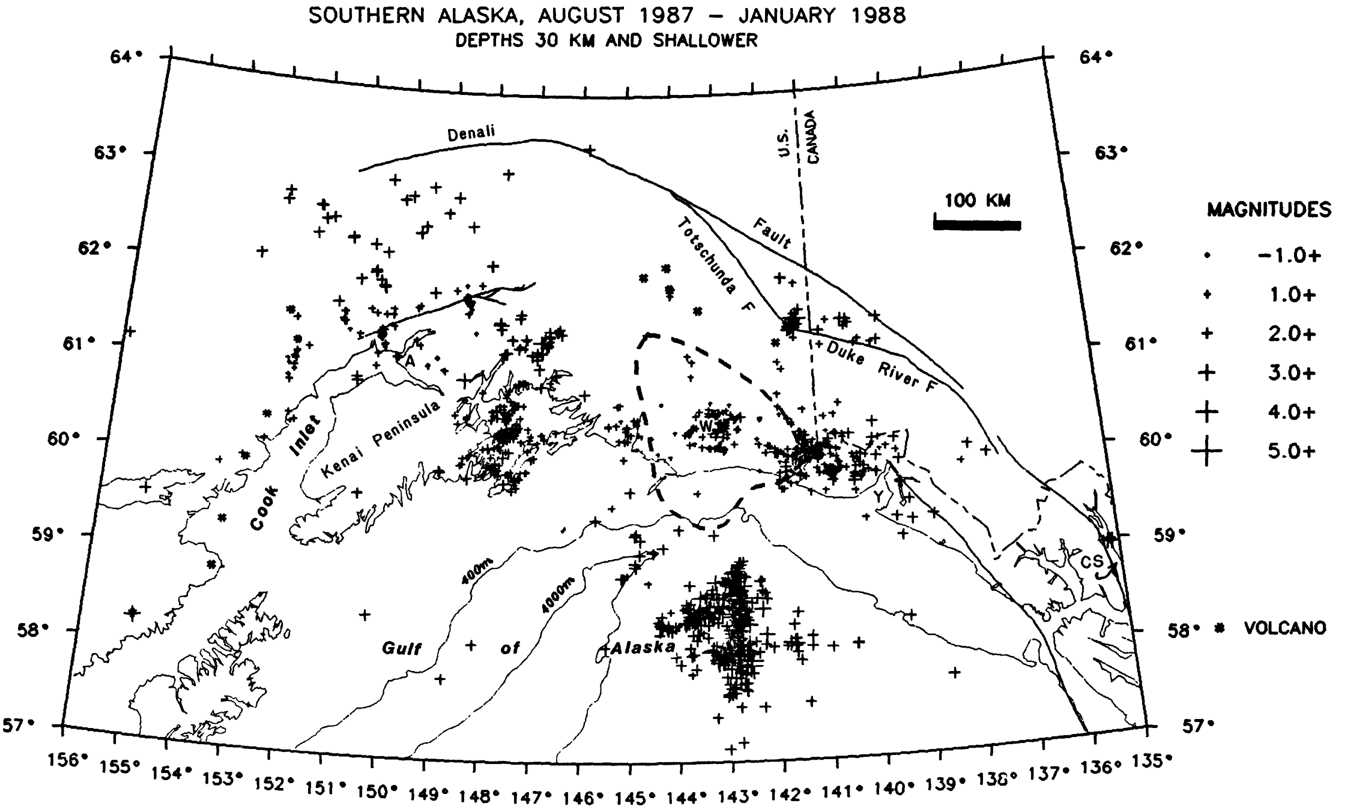

Figure 1: Epicenters of 1,182 earthquakes located at depths of 30 km and shallower using the USGS southern Alaska seismograph network for the period August 1987 - January 1988. Magnitudes are determined from coda duration or maximum amplitude, and events of magnitude 3 and larger are generally about one magnitude unit smaller that the corresponding teleseismic $m_b$ magnitude. The lowest magnitude level to which data is processed varies across the network due to uneven station spacing and changes in processing criteria. Heavy dashed contour outlines inferred extent of Yakataga seismic gap. Abbreviations are: A - Anchorage, CS - Chatham Strait, W - Waxell Ridge, Y - Yakutat Bay.

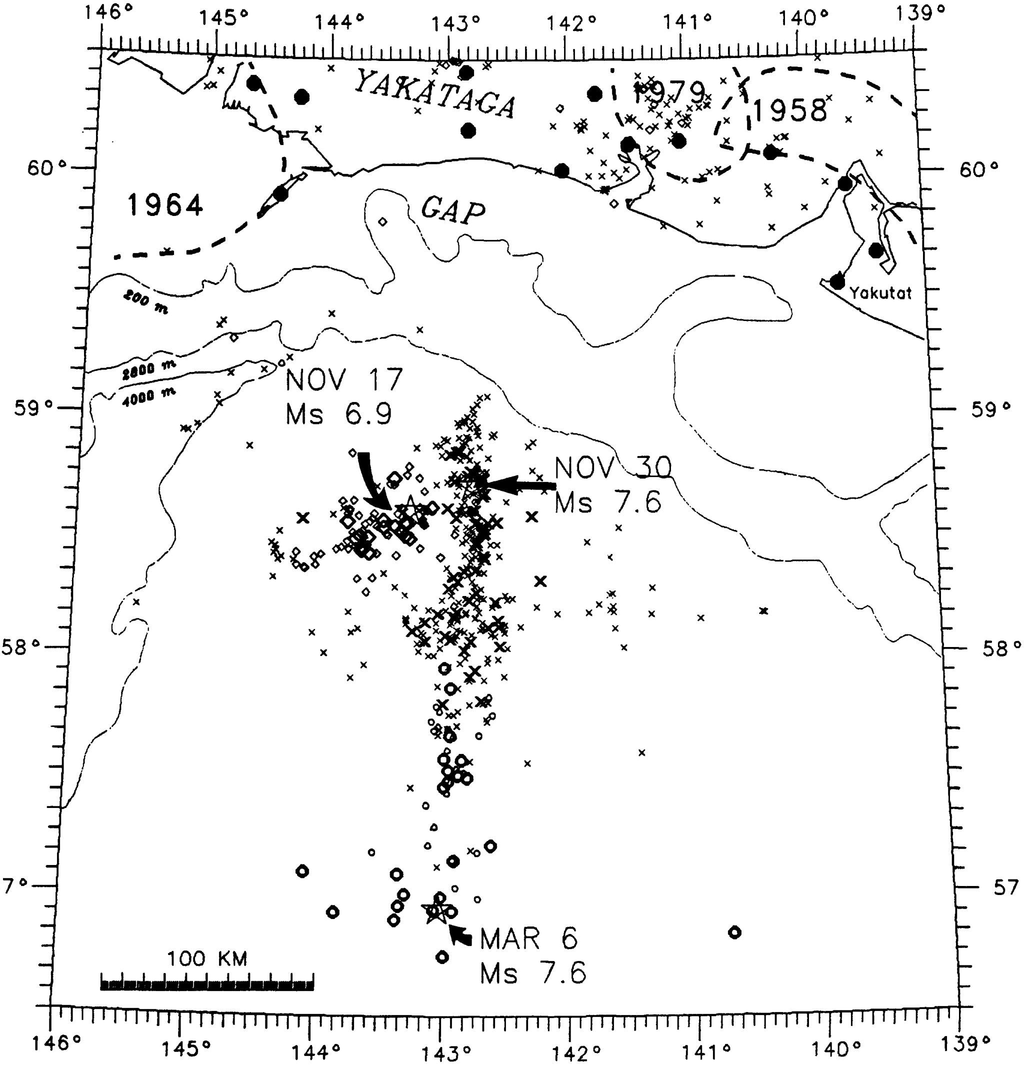

Figure 3: Aftershock epicenters for the three recent northern Gulf of Alaska earthquakes (stars). Symbol type indicates time of occurrence after each mainshock as follows: diamond - November 17, 1987 , X - November 30, 1987, circle - March 6, 1988; larger, heavier symbols are used for shocks within 6 hr of each mainshock. Data is incomplete after January, 1988, and includes selected events through March 26. Heavy dashed contours outline aftershock zones of large plate boundary earthquakes after 1900. Solid circles indicate locations of seismograph stations.

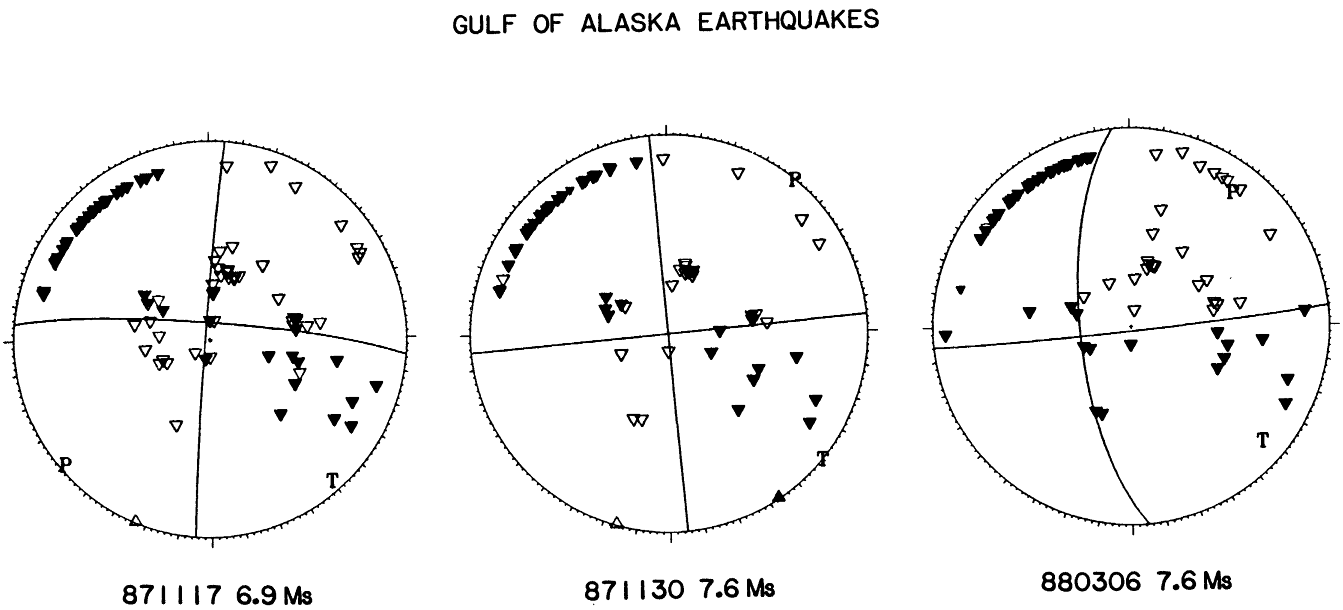

Figure 4: P-wave first motion polarities for the three recent large northern Gulf of Alaska earthquakes. Solid symbols are used to indicate compressions, open symbols for dilatations. Triangle pointed up indicates upward angle of emergence; pointed down indicates downward angle of emergence. Both long-period teleseismic and short-period regional data are shown; regional data are plotted with angles of emergence greater than 74° and appear near the outer edges of the equal area, lower hemisphere plots. Regional data for the November 30 shock are from the 4.5 $m_b$ initial event (see text) which obscured later arrivals. The preferred slip planes based on aftershock distributions are the E-W-trending plane for the November 17 shock, and the N-S-trending planes for the November 30 and March 6 shocks.

# Seismic Data Library

9930-01501

W. H. K. Lee
U. S. Geological Survey
Branch of Seismology
345 Middlefield Rd., MS 977
Menlo Park, California
(415) 329-4781

This is a non-research project and its main objectives is to provide access of seismic data to the seismological community. The Seismic Data Library was started by Jack Pfluke at the Earthquake Mechanism Laboratory before it was merged with the Geological Survey. Over the past ten years, we have built up one of the world's largest collections of seismograms (almost all of them on microfilm) and related materials. Our collection includes approximately 4.5 million WWNNS seismograms (1962 - present), 1 million USGS local earthquake seismograms (1966-1979), 0.5 million historical seismograms (1900-1962), 20,000 earthquake bulletins, reports and reprints, and a collection of several thousand magnetic tapes containing (1) a complete set of digital waveform data of the Global Digital Seismic Network (Data Tapes), and (2) a complete set of digital archive data of Calnet (CUSP archive tapes).

# Northern and Central California Seismic Network Processing

9930-01160

Fredrick W. Lester
Branch of Seismology
U.S. Geological Survey
345 Middlefield Road M/S 977
Menlo Park, California 94025
(415) 329-4747

## Investigations

1. In 1966 a seismographic network was established by the USGS to monitor earthquakes in central California. In the following years the network was expanded to monitor earthquakes in most of northern and central California, particularly along the San Andreas Fault, from the Oregon border to Santa Maria. In its present configuration there are over 350 single and multiple component stations in the network. There is a similar network in southern California. From about 1969 to 1984 the primary responsibility of this project was to manually monitor, process, analyze, and catalog the data recorded from this network. In 1984 a more efficient and automatic computer-based monitoring and processing system (CUSP) began online operation, gradually replacing most of the manual operations previously performed by this project. For a more complete description of the CUSP system see the project description "Consolidated Digital Recording and Analysis" by S. W. Stewart.

   Since the introduction of the CUSP system the responsibilities of this project have changed considerably. The main focus of the project now is that of finalizing and publishing preliminary network data from the years 1978 through 1984. We also continue to manually scan network seismograms as back-up event detection for the CUSP system. We then supplement the CUSP data base with data that were detected only visually or by the other automatic detection system (Real-Time Processor, RTP) and digitized from the continuously recording analog magnetic tapes. Project personnel also act as back-up for the processing staff in the CUSP project.

2. This project continues to maintain a data base for the years 1969 - present on both a computer and magnetic tapes for those interested in doing research using the network seismic data. As soon as the older data are finalized they are exchanged for preliminary data in the data base.

3. For nearly two decades this office monitored earthquakes in Yellowstone National Park and vicinity. The data from these earthquakes have been collected and processed, and more than 6000 events have been located for the time period 1964 to 1981. These data are currently being used to produce a map of epicenters for the region. This map will compliment the recently published catalog of earthquakes for 1973 to 1984 covering the same area.

## Results

1. Figure 1 illustrates nearly 6000 earthquakes located by this office for northern and central California during the time period October 1987 through March 1988. The largest earthquake to occur was a M5.0 shock that occurred on February 28, 1988 near Hollister. It was accompanied by a few small aftershocks. There were no other earthquakes that were magnitude 5 or larger for this time period and there were no other large or significant sequences of earthquakes.

2. Final processing of data for the second half of the calendar year 1982 is complete and those data are ready for publication, as are the data from the Lake Shasta area for 1981-1984. It is expected that all these data will be published by this summer.

3. Since June 1986 this project has been involved in a combined effort with personnel from many different projects. The first purpose of this group endeavor has been to collect all available seismic data pertaining to the more than 150,000 earthquakes that the USGS has located in northern and central California, mainly from 1969 to the present. Those data will then be combined, checked for errors and omissions, reprocessed as necessary, and finalized for publication. It is estimated that reprocessing will take six months to one year, which is much less time than would be necessary for this project working alone. Personnel in this project will be responsible for coordinating much of this group effort. To date all but a small portion of the data have been collected, had gross errors corrected, and have been rerun through the location program.

4. For the time period October 1987 through March 1988 there were from 0 to 7 events per day missed by the CUSP automatic detection system, with an average of 2.7 missed each day. These were added to the existing CUSP data base from the back-up magnetic tape and processed using standard CUSP processing techniques. Most of the earthquakes that were missed occurred in northern California, north of latitude 39 degrees. This is a particular problem in the north because of telemetry noise that exists on those circuits. To avoid producing an abnormally large number of false triggers in the detection system the trigger thresholds are often set higher than normal and therefore some of the real events are missed by the automatic system.

5. Quarterly reports were prepared on seismic activity around Monticello Dam, Warm Springs Dam, the Auburn Dam site and, New Melones Dam for the appropriate funding agencies.

6. The maps of earthquake epicenters for Yellowstone Park and vicinity is now undergoing final review and revisions. It is expected to be completed by later this spring.

## Reports:

Pitt, A. M., (in press), Maps showing earthquake epicenters (1964-1981) in Yellowstone National Park and vicinity, Wyoming, Idaho, and Montana. U.S. Geological survey, Miscelaneous Field Studios Map, MF-2022, scale 1:250:000.

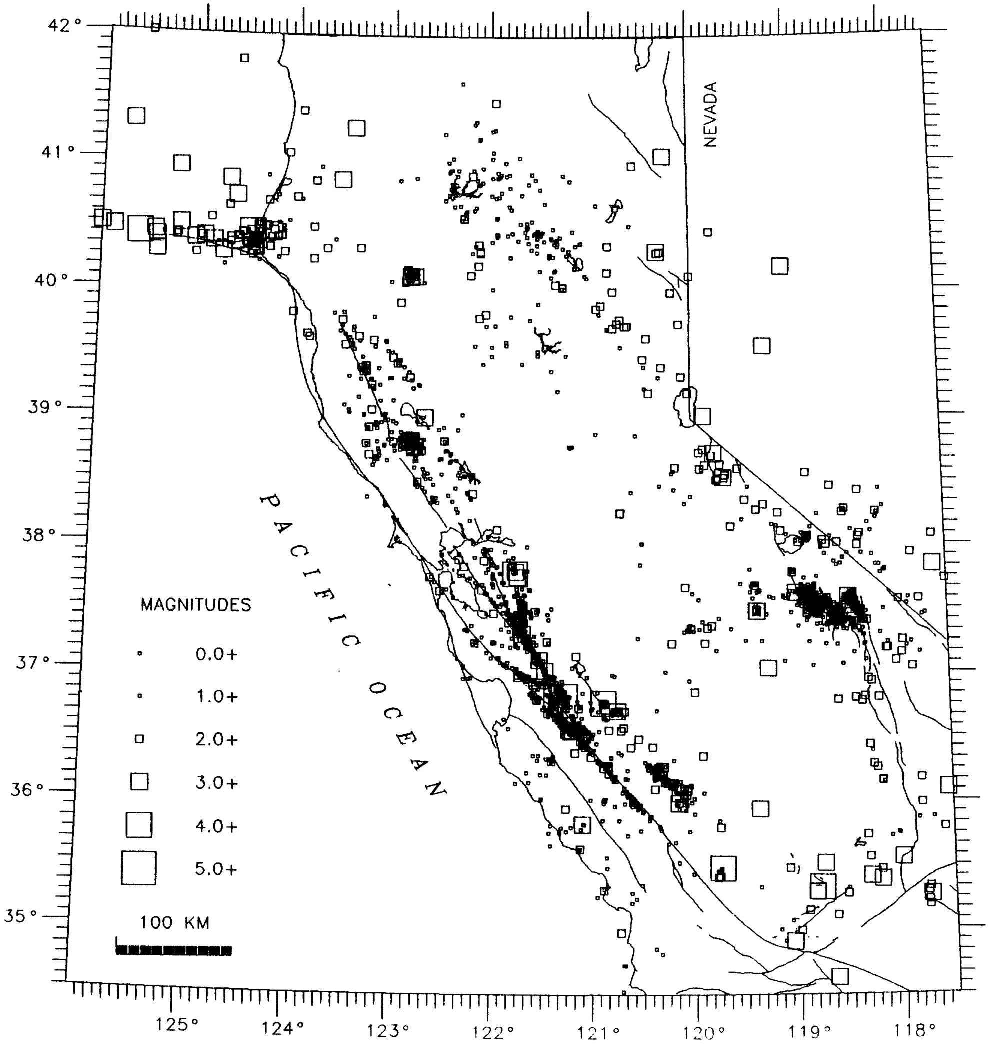

Figure 1. Northern and central California seismicity October 1987 - March 1988

# WESTERN GREAT BASIN-EASTERN SIERRA NEVADA SEISMIC NETWORK

*USGS Cooperative Agreement 14-08-0001-A0262*

Principal Investigators: M. K. Savage and W.F. Nicks
Seismological Laboratory
University of Nevada
Reno, NV 89557
(702) 784-4315

## Investigations

This contract supported continued operation of a seismic network in the western Great Basin of Nevada and eastern California, with the purpose of recording and locating earthquakes occurring in the western Great Basin, and acquiring a data base of phase times and analog and digital seismograms from these earthquakes. Research utilizing the data base was performed under USGS contract 14-08-0001-G1524 and is reported elsewhere in this volume.

## Results

### *Development of the network*

Figure 1 shows the network as of April 29, 1988. Three vertical-component analog stations that had been dropped from the network in 1976 and 1984 were reoccupied to increase coverage to the east of the Mono Lakes area. The 3-component, broadband, digital station at Battle Mountain is on-line again, connected by a radio relay instead of the telephone line that was cut off in February 1987. We are beginning the process of expanding and updating our digital network and our recording facilities. We will replace our existing 11/34-11/70 processing system with a system developed by the USGS and Caltech based on a microvax cluster, the CUSP (Caltech-USGS Seismic Processing system). The system will allow simultaneous acquisition, in an event-triggered mode, of digital and analog stations. The system is being configured for the recording of a large number of digital stations, so that the CUSP data base will eventually comprise all data being recorded at UNR. We are adding 6 new wide-band digital stations in Southern Nevada. In addition, we will begin receiving 40 stations (of which 16 will be recorded at any one time) from the Southern Great Basin network that is operated by the USGS-Golden. The microvax system is operating and awaits installation of the CUSP system for the process of expansion to continue.

### *Seismicity during report time*

From October 1, 1987 through March 31, 1988, the University of Nevada Seismological Laboratory located 2355 earthquakes (Figure 2). Of these events, 611 events were magnitude 2 or greater, 60 events were magnitude 3 or greater, and 1 had magnitude greater than 4 (4.2, located north of Warm Springs, Nevada, outside the network coverage). As usual, most activity was associated with the Long Valley Caldera area (in particular, the Chalfant aftershock area), and the Mono Lakes area. Activity in the state of Nevada continued to be higher than in 1985, the first year in which the present analysis system was in place; the network coverage was substantially the same during both periods. In one half year, there were 327 events located in Nevada, compared to 554 during all of 1985. 210 of these were over magnitude 2, compared to 271 in all of 1985, and 25 were greater than magnitude 3, compared to 19 in all of 1985.

More detailed monthly reports of seismicity can be obtained by contacting the laboratory. The bulletin for 1983-1984 is in press, and that for 1984-1987 is near completion.

# Stations
March 1988

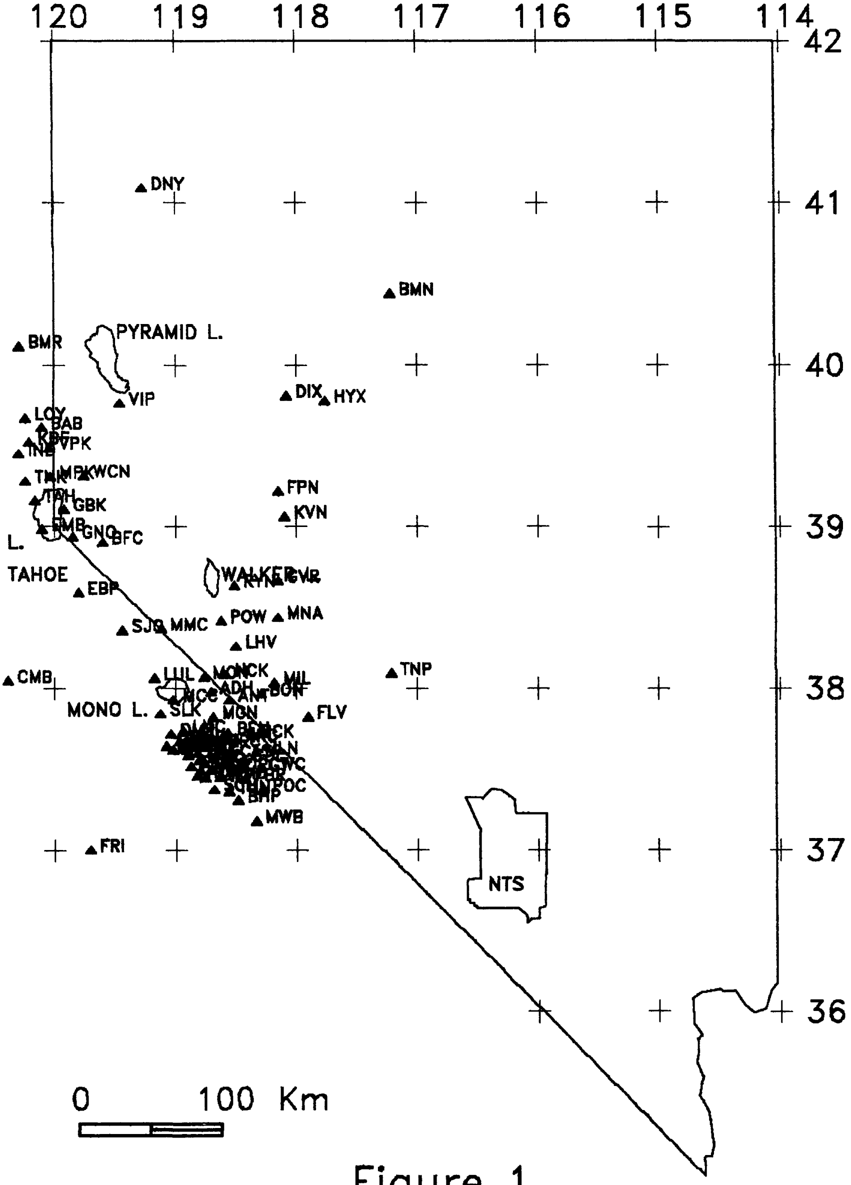

Figure 1

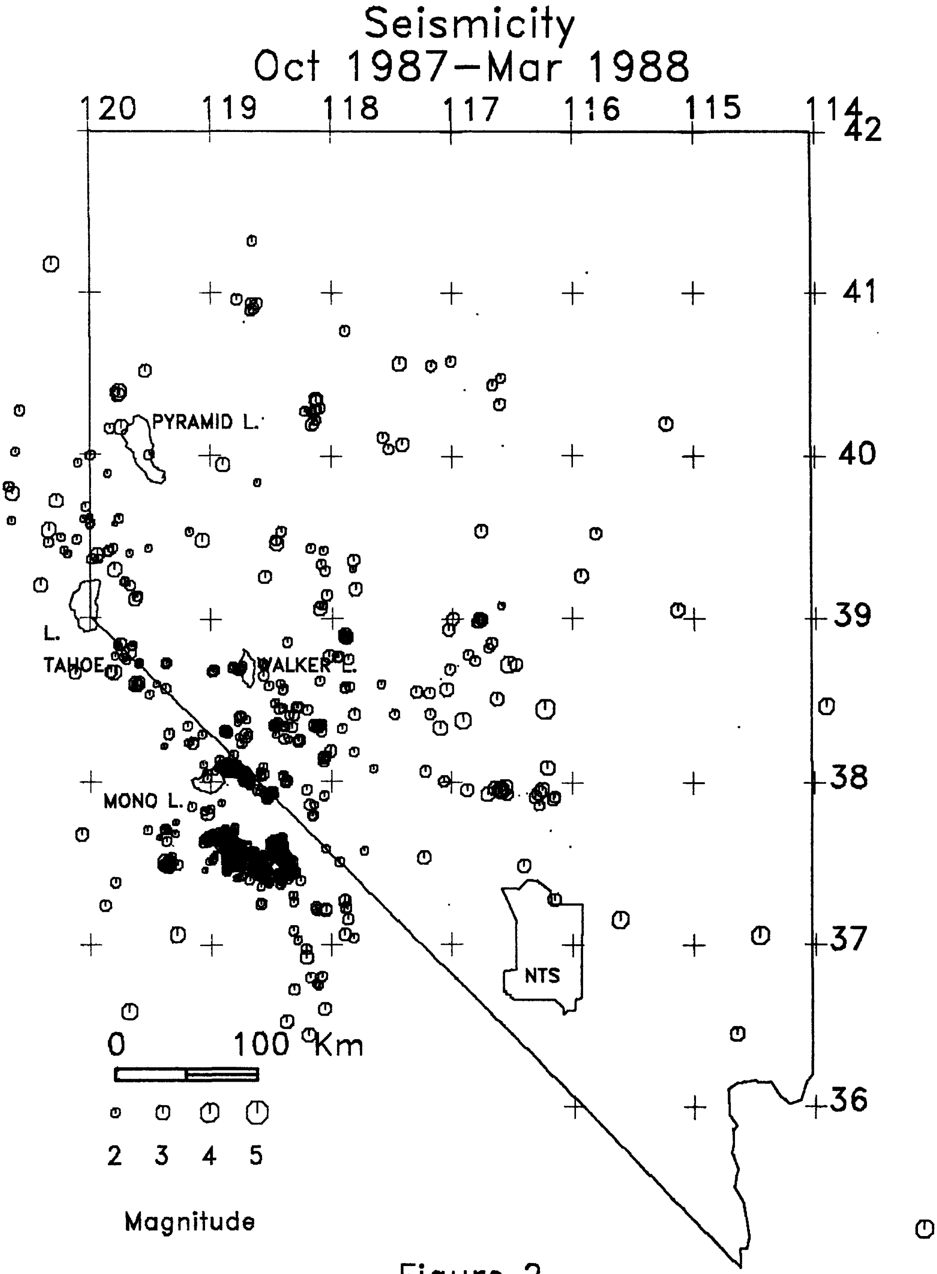
Seismicity
Oct 1987–Mar 1988
120
119
118
117
116
115
114
42
41
40
39
38
37
36
PYRAMID L.
L.
TAHOE
WALKER L.
MONO L.
NTS
0
100 Km
2
3
4
5
Magnitude

Figure 2

5. November 27, 1058 UTC. 36.84°N, 83.09°W: felt (V) at Bledsoe and Jeff Kentucky. Felt (IV) at Baxter and Putney, Kentucky and Dryden, Pennington Gap and St. Charles, Virginia. Felt in Clay, Harlan and Perry Counties, Kentucky and in Lee and Wise counties, Virginia. md=3.5 (CERI).

6. Five aftershocks have been recorded from the June 10, 1987 (2348 UTC) event which was located at 38.70 °N, 87.95°W, $m_{Lg}$(10Hz)=5.2(SLM).

*Acknowledgements*

The cooperation of the Center for Earthquake Research and Information, National Earthquake Information Service, and the University of Kentucky is gratefully acknowledged for providing station readings, magnitude data, and felt information. The results reported were supported by the Department of the Interior, U. S. Geological Survey, under Contract 14-08-0001-A0263 and the U.S. Nuclear Regulatory Commission under Contract NRC-04-86-121.

*References*

Central Mississippi Valley Earthquake Bulletin, Department of Earth and Atmospheric Sciences, Saint Louis University. 1987 Nos. 53 and 54.

PDE Preliminary Determination of Epicenters, Monthly Listings, U.S. Geological Survey, 1987

CERI Quarterly Seismological Bulletin, Center for Earthquake Research and Information, Memphis State University. 1987, Vol. VIII, Nos. 3,4.

# Regional Microearthquake Network in the Central Mississippi Valley

14-08-0001-A0263

William V. Stauder and Robert B. Herrmann
Department of Earth and Atmospheric Sciences
Saint Louis University
P.O. Box 8099 Laclede Station
St. Louis, MO 63156-8099
(314) 658-3131

## *Investigations*

The purpose of the network is to monitor seismic activity in the Central Mississippi Valley Seismic zone, in which the large 1811-1812 New Madrid earthquakes occurred. The following section gives a summary of network observations during the last six months of the year 1987.

## *Results*

In the last six months of 1987, 67 earthquakes were located and 25 other nonlocatable earthquakes were detected by the 42 station regional telemetered microearthquake network operated by Saint Louis University for the U. S. Geological Survey and the Nuclear Regulatory Commission. Figure 1 shows 67 earthquakes located within a 4° x 5° region centered on 36.5°N and 89.5°W. The magnitudes are indicated by the size of the open symbols. Figure 2 shows the locations and magnitudes of 50 earthquakes located within a 1.5° x 1.5° region centered at 36.25°N and 89.75°W.

In the last six months of 1987, 104 teleseisms were recorded by the PDP 11/34 microcomputer. Epicentral coordinates were determined by assuming a plane wave front propagating across the network and using travel-time curves to determine back azimuth and slowness, and by assuming a focal depth of 15 kilometers using spherical geometry. Arrival-time information for teleseismic P and PkP phases has been published in the quarterly earthquake bulletin.

The significant earthquakes occurring in the last six months of 1987 include the following:

1. July 7, 1919 UTC, 36.04)deN, 89.80°W: felt in the Charleston Missouri area. $m_{bLg}$=3.6 (NEIS).

2. August 31, 1712 UTC. 38.30°N, 89.68°W: felt (IV) at Lenzburg and St. Libory. Felt (III) at Coulterville. $m_{bLg}$=3.1 (SLM)

3. September 29, 0004 UTC. 36.84°N, 89.21°W: felt (V) at Wolf Island and Wyatt, Missouri. Felt (IV) at Arlington, Bardwell, Columbus and Lovelace, Kentucky. Also, felt in parts of Missouri, Illinois and Kentucky. $m_{bLg}$=4.5 (NEIS).

4. October 14, 1549 UTC. 37.05°N, 88.78°W: felt (V) at West Paduach, Kentucky. Felt (IV) at Bandana, Burna, Hickory, Hampton, Kevil, Lovelace, Lowes, Melber, Milburn, Paduach and Symsonia, Kentucky. Felt in parts of Kentucky, Illinois and Missouri. $m_{bLg}$=3.8 (NEIS).

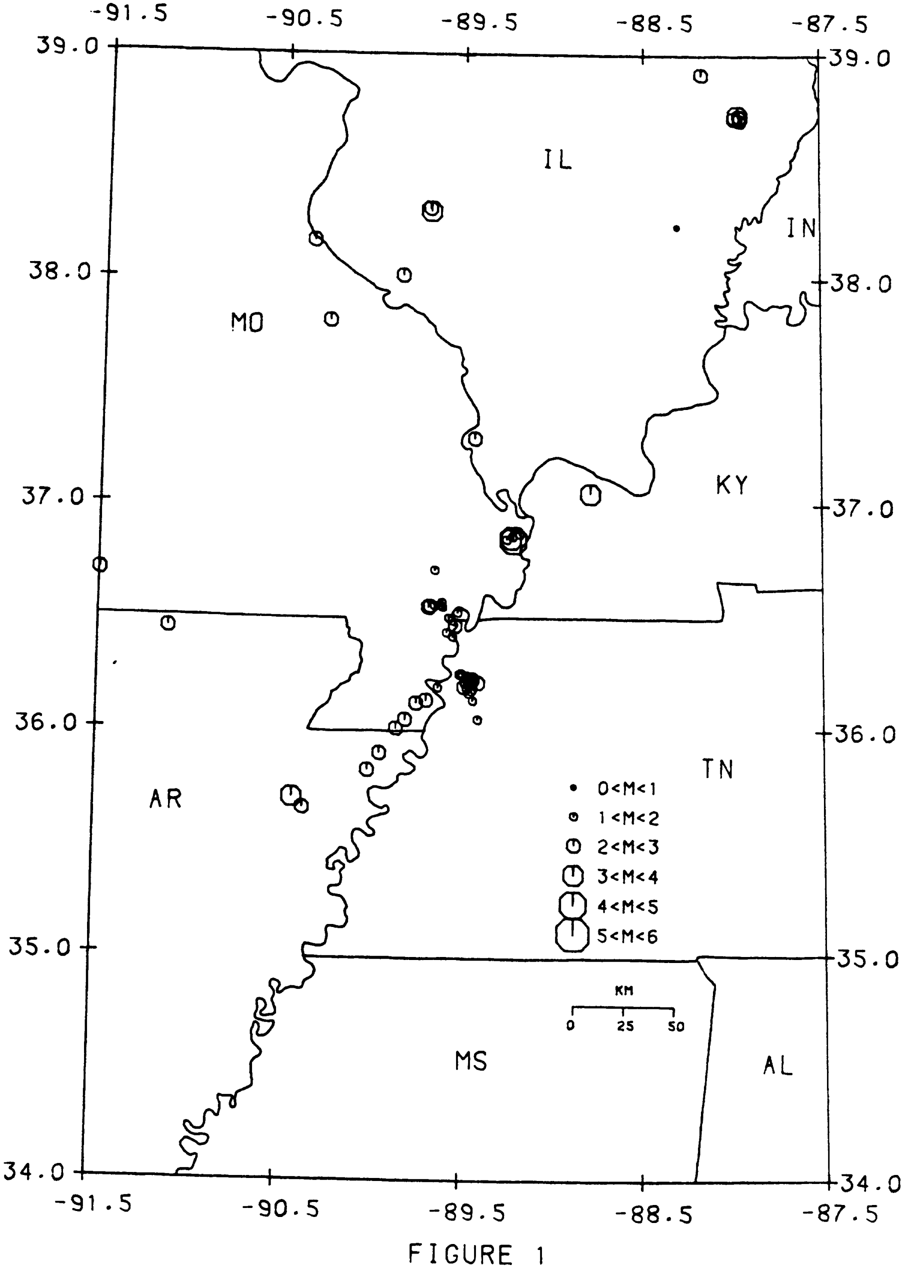

FIGURE 1
CUMULATIVE EVENTS 01 JUL 1987 TO 30 DEC 1987
LEGEND ▲ STATION ◎ EPICENTER

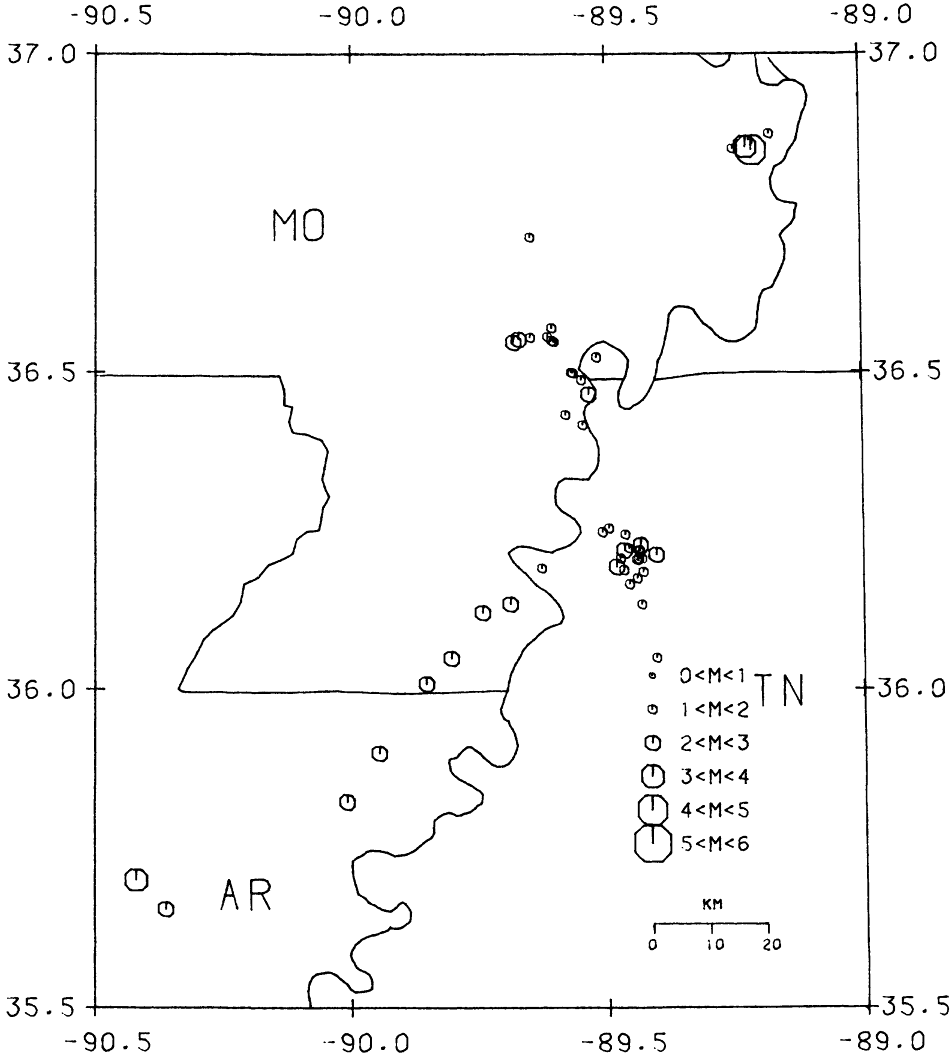

FIGURE 2

CUMULATIVE EVENTS 01 JUL 1987 TO 30 DEC 1987

LEGEND . △ STATION ○ EPICENTER

# Consolidated Digital Recording and Analysis

9930-03412

Sam Stewart
Branch of Seismology
U. S. Geological Survey
345 Middlefield Road, Mail Stop 977
Menlo Park, California 94025

## Investigations

This project is responsible (1) for operating, on a routine and reliable basis, a computer-automated system that will detect and process earthquakes occurring within the USGS Central California Earthquake Network (also known as CALNET), (2) for maintaining and developing software relevant to automated processing techniques, including analog-to-digital conversion and processing of events from analog magnetic tapes, and (3) for making the data available for research purposes on a timely basis. Presently, the signals from about 490 seismic instruments (including hi-gain vertical seismometers, lo-gain 3-component seismometers, force balance accelerometers and dilatometers) are telemetered to a central recording point in Menlo Park. One PDP 11/44 computer system is dedicated to online, realtime detection of earthquakes and storing of the digitized waveforms for later analysis. A second PDP 11/44 computer is dedicated to offline timing, processing and archiving of the waveform data. The DEC VAX/750 operated by the Branch of Seismology is used for final processing and archiving of the earthquake data. This computer is used by the research staff to obtain our data for research purposes. The total processing hardware/software systems used by the three DEC computers is known generically as the 'CUSP' system. The system was conceived of, designed and developed by Carl Johnson while in Pasadena. It has been modified considerably by Peter Johnson, Bob Dollar and Sam Stewart to meet the specific needs of Menlo Park.

## Results

1. The CUSP system processed approximately 5200 earthquakes detected online during the period October thru March. This is a lower seismicity level than usual. In addition, a few thousand noise events that were detected had to be examined and deleted from the system as well. In addition, we are reviewing and cleaning up older data, using programs and techniques that were not available to us when the system first started in January 1984.

2. We are in the process of upgrading the CUSP hardware and software to meet the needs of other CUSP sites, to make our own operations more efficient and versatile, and to replace aging hardware and related software (including operating systems).

Two DEC VAXstation 2000's and one DEC VAXstation 3200 were ordered, along with graphics software. These will replace the two 11/44 systems, the RSX11-M+ operating system, and the two Tektronix 4014 interactive graphics terminals. When this transition is finished, we will only be supporting one operating system (VMS) instead of two, and one unified version of online and offline CUSP software, instead of three.

Carl Johnson (the author of CUSP), Peter Johnson and Bob Dollar are developing a 'consolidated' version of CUSP software that will be the core system used in Menlo Park, Pasadena, and at HVO. It is the system that will be distributed to other sites wanting to use CUSP.

3. Since April 1984 the CUSP system has generated nearly 2000 Archive tapes of digitized waveforms. These tapes are recorded at 6250 bpi density, usually on 2400 foot reels. To make these data more easily available to non-CUSP programs, the PHASEOUT program was modified to provide, in ASCII format, all data necessary to read and demultiplex selected files on the Archive tapes. Mary Allen and Bruce Julian have successfully read these Archive tapes into UNIX-based systems. The PHASEOUT program was further modified to produce ASCII phase and related data from the CUSP and RTP data sources to contribute to the primary database for the new ASCII catalog being developed by the Seismology Branch.

4. Bob Dollar has developed a realtime digital data acquisition and analysis system for use in the Parkfield Digital Seismic Experiment. The system is designed around a DEC MicroVAX computer, the DEC VMS operating system, and the CUSP database/processing system. It has been benchmarked at a thruput rate of 102,400 samples per second. As used at Parkfield, it samples up to 116 sensors each at a rate of 500 samples/second. The software was designed to be easily adaptable to monitoring larger networks (such as the Central and Southern California seismic networks, and to digitizing from analog tapes.

## Reports

Dollar, R., and P. Johnson, 1988, "The Parkfield Digital Seismic Experiment: Realtime high frequency data acquisition and analysis system", (Abs). Earthquake Notes (in press).

Johnson, Peter, 1988. "Basic VMS Block I/O and Related Concepts", (Abs). Presented at DECUS 1988 Western Regional Conference, San Francisco, March 24-25, 1988.

MacGregor-Scott, Nan, and Allan Walter, 1988, Crustal velocities near Coalinga, California modeled from a combined earthquake/explosion refraction profile. Bull. Seis. Soc. Am. (accepted for publication).

# Seismic Monitoring of the Shumagin Seismic Gap, Alaska

USGS 14-08-0001-A0260

John Taber
Lamont-Doherty Geological Observatory of Columbia University
Palisades, New York 10964
(914) 359-2900

## Investigations

Seismic data from the Shumagin seismic network were processed to obtain origin times, hypocenters, and magnitudes for local and regional events. The processing resulted in files of hypocenter solutions and phase data, and archive tapes of digital data. These files are used for the analysis of possible earthquake precursors, seismic hazard evaluation, and studies of regional tectonics and volcanicity (see Analysis Report, this volume). Yearly bulletins are available starting in 1984.

## Results

The Shumagin network was used to locate 833 earthquakes in 1987. The seismicity of the Shumagin Islands region for this time period is shown in map view and cross section in figure 1. The largest event in this period in the region occurred on 6/21/87, had a $M_s$ of 6.2, and was located south of the network at 54.04N, 162.46W (obvious cluster on seismicity map). The event was felt up to 300 km away. Over 140 aftershocks have been located, the largest having an $m_b$ of 5.5. Not including the aftershock sequence of the June event there were 21 events over magnitude 4. The largest of these earthquakes was an $m_b$ 5.1 event on 5/2/87 that was felt (intensity V) in Sand Point. Otherwise the overall pattern over this time period is similar to the long term seismicity. Concentrations of events occur at the base of the main thrust zone and in the shallow crust directly above it. The continuation of the thrust zone towards the trench is poorly defined. West of the network (which ends at 163°) and the June sequence, the seismicity is more diffuse in map view and extends closer to the trench. All but three of the 21 located events larger than magnitude 4 that were not aftershocks of the June event occurred in this western region. Below the base of the main thrust zone (~45 km) the dip of the Benioff zone steepens. Part of the double plane of the lower Benioff zone is evident near 100 km depth.

The network is capable of digitally recording and locating events as small as $M_l$=0.4 with uniform coverage at the 2.0 level. Events are picked and located automatically at the central recording site in Sand Point, Alaska and the results, along with subsets of the digital data, can be accessed via telephone modem. Onscale recording is possible to ~$M_s$=6.5 on a telemetered 3 component force-balance accelerometer. Larger events are recorded by one digitally recording accelerometer and on photographic film by 11 strong-motion accelerometers.

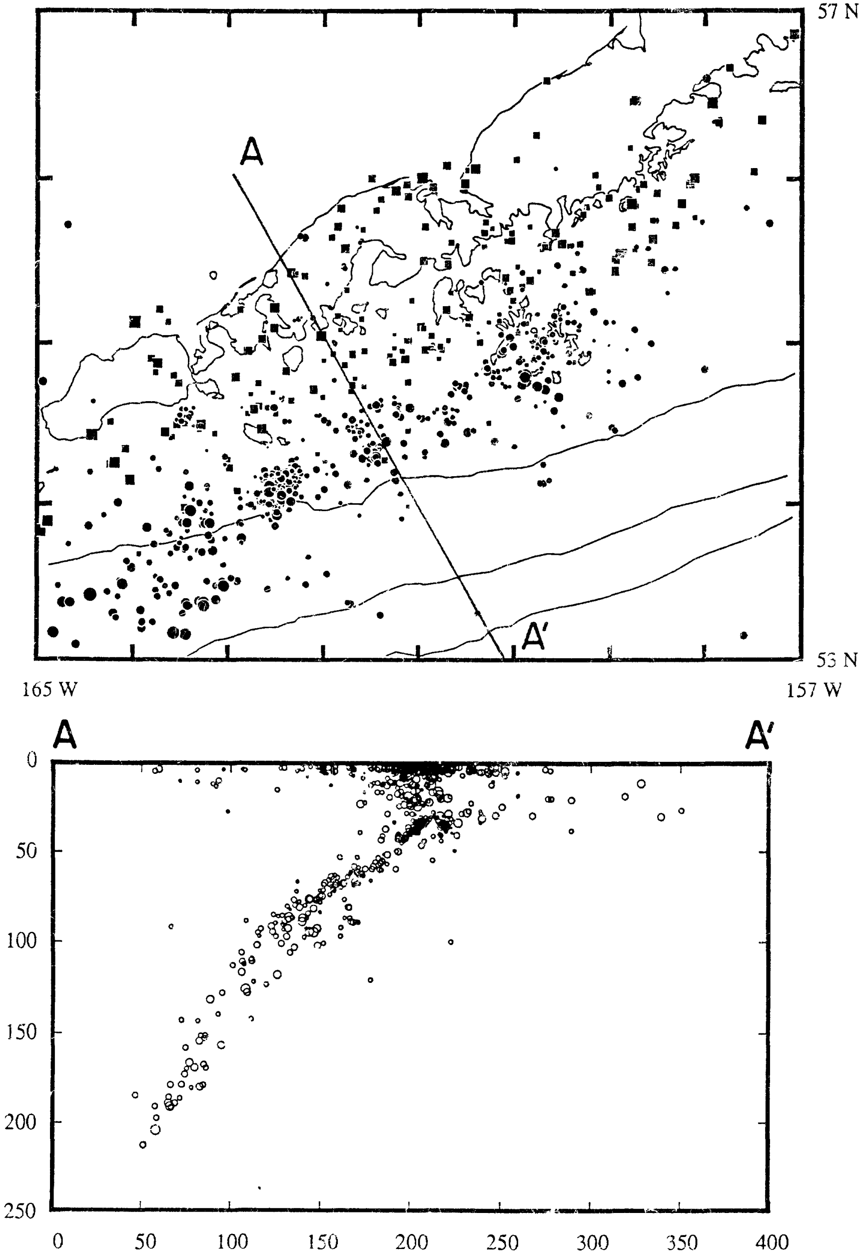

Figure 1. Top: Seismicity recorded by the Shumagin seismic network during 1987. Squares are events deeper than 50 km. Bottom: Cross section of seismicity projected along the line A-A' in the upper figure.

# Earthquake Hazard Research in the Greater Los Angeles Basin and Its Offshore Area

#14-08-0001-A0264

Ta-liang Teng
Thomas L. Henyey
Egill Hauksson

Center for Earth Sciences
University of Southern California
Los Angeles, CA 90089-0740
(213) 743-6124

## INVESTIGATIONS

Monitor earthquake activity in the Los Angeles Basin and the adjacent offshore area.

## RESULTS

### The 1987 Los Angeles Basin Seismicity

During 1987 the ($M_L$=5.9) Whittier Narrows earthquake sequence dominated the Los Angeles basin seismicity (Figure 1). In addition, two small swarms occurred on February 8 and 26 near the northern end of the Newport-Inglewood fault. Eleven earthquakes of $M_L \geq 3.0$ occurred in the greater Los Angeles basin in addition to the Whittier Narrows sequence.

The preliminary seismological results from the Whittier Narrows sequence are described by Hauksson et al. (1988). The main shock epicenter was located 3 km north of the Whittier Narrows, at the northwestern end of the Puente Hills (Figure 1). The spatial distribution of the hypocenters of the main shock with its aftershocks, as well as the focal mechanism of the main shock, indicate that the causative fault is a gently dipping thrust fault with an east-west strike, located at depths from 11 to 16 km. The largest aftershock ($M_L$=5.3) occurred on October 4, 1987 and was located 3.0 km to the northwest of the main shock's epicenter. A low rate of aftershock activity, with less than 10 events per week, was recorded during November and December, 1987.

Two earthquake swarms occurred near the north segment of the Newport-Inglewood fault on February 8 and 26 with 6 and 5 events of $M_L \geq 2.0$, respectively. This activity was followed by a $M_L$=3.1 event on March 28, which showed a reverse faulting focal mechanism (Figure 2). Two other events of $M_L \geq 3.0$) occurred near the NIF showing normal (July 8) and strike slip (December 1) motion, similar to the focal mechanisms reported by Hauksson (1987). Four events of $M_L \geq 3.0$) were recorded in the South Bay area near the City of Long Beach. This sequence that began May 29 with a $M_L$=3.1 event was followed by a $M_L$=3.2 event on June 8 and culminated with two events on July 8 and 9 of $M_L$=3.6 and 3.3, respectively. Three events (August 28, October 24 and November 29) occurred offshore to the west of the Los Angeles basin. In summary, during 1987 eleven earthquakes of $M_L \geq 3.0$ occurred in the greater Los Angeles basin in addition to the Whittier Narrows sequence.

## PUBLICATIONS

Hauksson, E., Seismotectonics of the Newport-Inglewood Fault Zone in the Los Angeles Basin, Southern California, Bull. Seism. Soc. Amer., 77, 539-561, 1987.

Hauksson, E., T. L. Teng and T. L. Henyey, Near-Surface Attenuation of Waveforms of Local Earthquakes: Results from a 1500 m Deep Downhole Seismometer Array, Bull. Seism. Soc. Amer., 77, 1883-1904, 1987

Hauksson, E., L. M. Jones, T. L. Davis, L. K. Hutton, A. G. Brady, P. A. Reasenberg, A. J. Michael, R. F. Yerkes, P. Williams, G. Reagor, C. W. Stover, A. L. Bent, A. K. Shakal, E. Etheredge, R. L. Porcella, C. G. Bufe, M. J. S. Johnston, E. Cranswick, The 1987 Whittier Narrows Earthquake in the Los Angeles Metropolitan Area, California, Science, 239, 1409-1412, 1988.

Hauksson, E., and L. M. Jones, The July 1986 Oceanside ($M_L$=5.3) Earthquake Sequence in the Continental Borderland, Southern California, submitted to Bull. Seism. Soc. Amer., 1988.

## REPORTS

Hauksson, E., Seismotectonics of the Newport-Inglewood Fault Zone and the 1933 Long Beach Earthquake ($M_L = 6.3$) in the Los Angeles Basin, southern California. Seism. Res. Letters, 58, 14, 1987.

Hauksson, E., T. L. Teng, T. L. Henyey, M. Robertson, J. K. McRaney and L. Hsu, Earthquake hazard research in the Los Angeles basin and its offshore area, Annual Technical Report submitted to the U.S. Geological Survey, March 1988, 90 pp.

Hauksson, E. and L. M. Jones, The July 1986 Oceanside Earthquake Sequence ($M_L$ = 5.3) in the Continental Borderland, southern California, EOS Trans., Amer. Geophys. Union, 68, 1361, 1987.

Hauksson, E., L. M. Jones and L. K. Hutton, The 1987 Whittier Narrows Earthquake in the Los Angeles Metropolitan Area, California: Overview, Locations and Seismotectonics, EOS Trans., Amer. Geophys. Union, 69, 259, 1988.

Hauksson, E., Seismicity, Anticlines and Thrust Faults in the Los Angeles Basin: Implications of the Whittier Narrows Earthquake, submitted to the spring SSA meeting 1988.

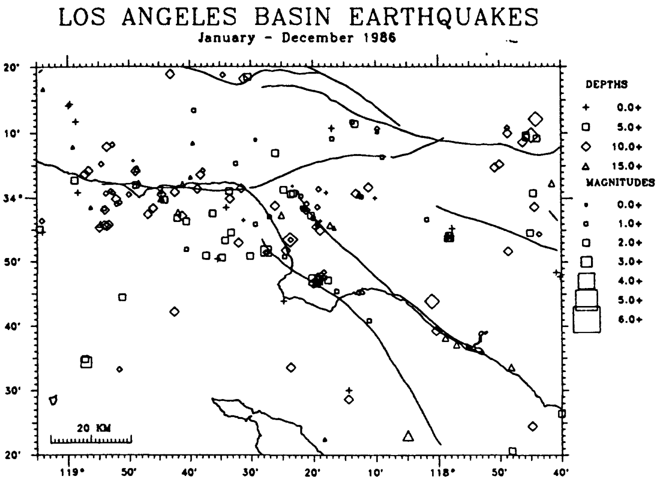

FIGURE 1. Los Angeles basin seismicity 1986 (Top) and 1987 (Bottom)

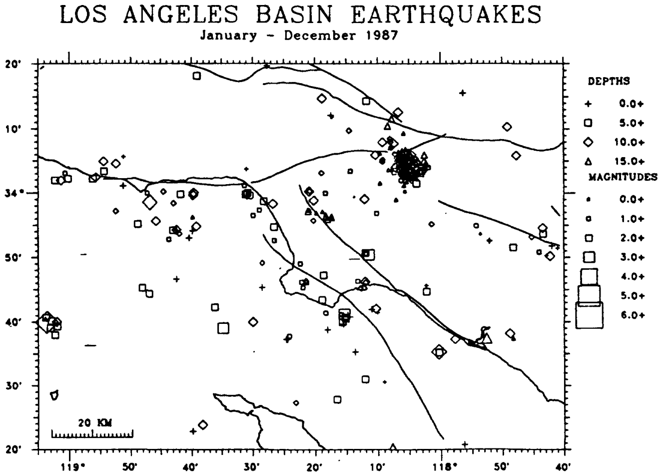

# LOS ANGELES BASIN EARTHQUAKES

## focal mechanisms for M>2.9 earthquakes 1987

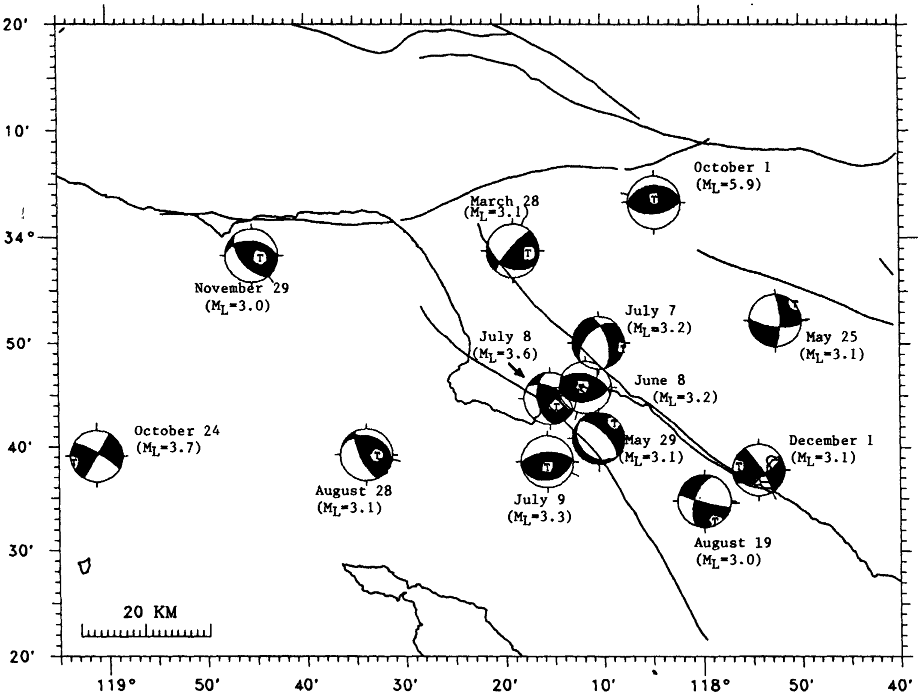

FIGURE 2 Focal mechanisms of $M \geqslant 3.0$ earthquakes reported during 1987 in the Los Angeles basin.

# Field Experiment Operations

9930-01170

John Van Schaack
Branch of Seismology
U. S. Geological Survey
345 Middlefield Road MS-977
Menlo Park, California 94025
(415) 329-4780

## Investigations

This project performs a broad range of management, maintenance, field operation, and record keeping tasks in support of seismology and tectonophysics networks and field experiments. Seismic field systems that it maintains in a state of readiness and deploiys and operates in the field (in cooperation with user projects) include:

a. 5-day recorder portable seismic systems.
b. "Cassette" seismic refraction systems.
c. Portable digital event recorders.

This project is responsible for obtaining the required permits from private landowners and public agencies for installation and operation of network sensors and for the conduct of a variety of field experiments including seismic refraction profiling, aftershock recording, teleseism P-delay studies, volcano monitoring, etc.

This project also has the responsibility for managing all radio telemetry frequency authorizations for the Office of Earthquakes, Volcanoes, and Engineering and its contractors.

Personnel of this project are also responsible for maintaining the seismic networks data tape library. This includes processing daily telemetry tapes to dub the appropriate seismic events and making playbacks of requested network events and events recorded on the 5-day recorders.

## Results

### Seismic Refraction

The seismic cassette recorders were deployed for a calibration shot for the recorders used in the Whittier Narrows after shock study. Twelve hundred pounds of explosives were fired 100 feet underground at the epicenter of the Whittier Narrows Earthquake. Environmental impact statements are being prepared for experiments in Alaska, Arizona and Nevada. Preliminary work has been done on the experiment to be conducted in New York, Vermont, and Maine during September 1988. Project personnel made a trip to Kenya, Africa for a preliminary survey of a proposed refraction-reflection seismic line.

### Portable Networks

Six 5-day recorders were deployed near Westmoreland CA. to augment the network for aftershock studies of the Westmoreland Earthquake for a period of 2 weeks. After shocks were also recorded by 8 recorders following the Whittier Narrows Earthquake for a period of 3 weeks.

# Geothermal Seismotectonic Studies

9930-02097

Craig S. Weaver
Branch of Seismology
U. S. Geological Survey
at Geophysics Program AK-50
University of Washington
Seattle, Washington 98195
(206) 442-0627

*Investigations*

1. Continued analysis of the seismicity and volcanism patterns of the Pacific Northwest in an effort to develop an improved tectonic model that will be useful in updating earthquake hazards in the region. (Weaver)

2. Continued acquisition of seismicity data along the Washington coast, directly above the interface between the North American plate and the subducting Juan de Fuca plate. (Weaver, Zollweg, UW contract)

3. Continued seismic monitoring of the Mount St. Helens area, including Spirit Lake (where the stability of the debris dam formed on May 18, 1980 is an issue), Elk Lake, and the southern Washington-Oregon Cascade Range (north of Newberry Volcano). The data from this monitoring is being used in the development of seismotectonic models for southwestern Washington and the interaction of the Basin and Range with the Oregon Cascades. (Weaver, Zollweg, Grant, Yelin, UW contract)

4. Study of Washington seismicity, 1960-1969. Earthquakes with magnitudes greater than 4.5 are being re-read from original records and will be re-located using master event techniques. Focal mechanism studies are being attempted for all events above magnitude 5.0, with particular emphasis on the 1962 Portland, Oregon event. (Yelin, Weaver)

5. Detailed analysis of the seismicity sequence accompanying the May 18, 1980 eruption of Mount St. Helens, including about 500 deep earthquakes (>3 km) that occurred prior to May 18. Earthquakes are being located in the ten hours immediately following the onset of the eruption, and the seismic sequence is being compared with the detailed geologic observations made on May 18. Re-examination of the earthquake swarms that followed the explosive eruptions of May 25 and June 13, 1980, utilizing additional playbacks of 5-day recorder data. (Weaver, Zollweg, Norris, UW contract)

6. Study of earthquake catalogs for the greater Parkfield, California region for the period 1932-1969. Catalogs from the University of California (UCB) and CalTech (CIT) are being compared, duplicate entries noted, and the phase data used by each reporting institution are being collected. The study is emphasizing events greater than 3.5, and most events will be relocated using station corrections determined from a set of master events located by the modern networks. (Meagher, Weaver, with Lindh, Ellsworth)

7. Study of estuaries along the northern Oregon coast in an effort to document probable subsidence features associated with paleosubduction earthquakes (Grant).

*Results*

1. The distribution of earthquake hypocenters for events greater than magnitude 3.5 located by the USGS network (Figure 1A) for the years 1970-1986 for the greater Parkfield area (from the southern end of Bear Valley to the northern edge of the Transverse Ranges and on the east to the foothills of the Great Valley and extending westward to the Pacific Ocean) shows three main areas of seismicity: 1) earthquakes are located east of the San Andreas fault at Coalinga, 2) along the fault near Parkfield, and, 3) a diffuse band of earthquakes about 30 km wide is along the coast.

We are testing the hypothesis that a relocation of the historical events, estimated to be greater than magnitude 3.5, will show a distribution similiar to that reported by the USGS. After removing duplicate entries from the earthquake catalogues of the University of California (UCB) and CalTech (CIT) for the time period 1932-1969, a total of 235 quakes was compiled; the reported epicenters are scattered throughout the region (Figure 1B) in comparsion to the concentrated epicenters from the USGS catalogs. For the events shown in Figure 1B, we have assembled phase data files from the microfilmed phase data from CIT and UCB. We have augmented the phase data collection by re-reading seismograms of questionable readings; in some cases new readings have been obtained. All of the events have been relocated (Figure 1C) using station corrections calcuated with respect to the 1975 Parkfield earthquake. The best located quakes (Figure 1D) have been relocated using 7 or more P readings, have a RMS less than 1.5 sec., a gap less than 230 degrees and the closest recording station less than 180 km.

For our best locations, the epicentral distribution is very similar to the USGS locations. In addition to tightening the distribution within our study area, the relocations have resulted in moving 30 events ourside of the study area; most of these events have been relocated into the Bear Valley area adjacent to the north (compare Figure 1B & 1D).

2. Subsurface stratigraphy in tidal marshes along the Salmon and Nehalem Rivers in northern Oregon record at least one episode of sudden submergence that was probably caused by large thrust earthquakes on the Cascadia subduction zone. Along the Salmon River, both core samples and streamcuts are characterized by fine-medium sand grading up into sandy-silt and silt, and gradually (over several centimeters) becoming very organic-rich, so that the upper part of the unit consists of peat or muddy peat with an abrupt upper contact. These peaty units vary from several up to about 10 cm in thickness and are, in some cases, overlain by a fine-medium sand unit. This sand unit ranged (where present) from a trace up to approximately 10 cm in thickness and was overlain by silt and silty-sand grading up into the present marsh surface. Along the Nehalem River, the tidal-marsh subsurface stratigraphy is similar to that of the Salmon River with the difference that there is no 'packet' of sand lying in direct contact over the peaty horizon. Instead, the peaty horizon is abruptly truncated and overlain by organic-poor silt or sandy-silt grading upward into the modern marsh surface.

At both the Nehalem and Salmon Rivers, the subsurface stratigraphy is interpreted to represent the sudden lowering of a high marsh environment into an unvegetated tidal flat as a result of a large thrust earthquake on the Cascadia subduction zone. The fine-medium sand 'packet' that lies on top of the peaty unit along the Salmon River shows a distribution that thins both up the valley and away from the river channel; this distribution indicates a seaward source and is interpreted as resulting from a tsunami generated by the rupture process.

Preliminary radiocarbon dating of the peaty horizons and preserved plant rhizomes both above and below the peat yields an approximate age of peat burial of 300-400 years before present at both the Nehalem and Salmon Rivers. This age is consistent with the age of the youngest buried unit at several sites on the Washington coast to the north. If the subsidence at the Salmon and Nehalem Rivers was coincident in time with subsidence in southwestern Washington, the 240 km extent of the down-dropped zone indicates that an earthquake of magnitude 8.5 could have generated these features.

3. A Masscomp 5600 computer system has been installed at the University of Washington to both collect digital seismic data from the UW seismic network and eventually to handle the routine analysis of that data. The event-detection system is currently operating in a test mode, and is running parallel with the existing DEC 11/34 on-line computer that handles data collection.

*Reports*

Grant, W. C. and Weaver, C. S., Seismicity of the Spirit Lake area: Estimates of possible earthquake magnitudes for engineering design, in *The formation and significance of major lakes impounded during the 1980 eruption of Mount St. Helens, Washington, U. S. Geological Survey Professional Paper,* edited by R. L Shuster and W. Meyer, (still in press).

Weaver, C. S. and G. E. Baker, Geometry of the Juan de Fuca plate beneath Washington: Evidence from seismicity and the 1949 South Puget Sound earthquake, *Bulletin of the Seismological Society of America, 78,* 264-275, 1988.

Guffanti, M. and C. S. Weaver, Distribution of late Cenozoic volcanic vents in the Cascade Range (USA): Volcanic arc segmentation and regional tectonic considerationsr, *J. Geophys. Res., 93,* (in press), 1988.

Yelin, T. S., Magnitude and cumulative moment release estimates for earthquakes in Washington and northern Oregon, 1960-1984, *Bull. Seism. Soc. Amer.,* (submitted).

Grant, W. C., and D. D. McLaren, Evidence for Holocene subduction earthquakes along the northern Oregon coast, (abs), *EOS, Trans. Am. Geophys. U., 68,* 1239, 1987.

Weaver, C. S. and S. R. Walter, Influence of backarc tectonics on the seismicity distribution of the Cascade Range, (abs), *Earthquake Notes, 59,* in press, 1988.

Grant, W. C. and C. S. Weaver, Earthquake hazards in southwestern Washington, (abs), *Earthquake Notes, 59,* in press, 1988.

Yelin, T. S., Tectonic setting, relocation, and revised focal mechanism of the 6 November 1962 Portland, Oregon, earthquake, (abs), *Earthquake Notes, 59,* in press, 1988.

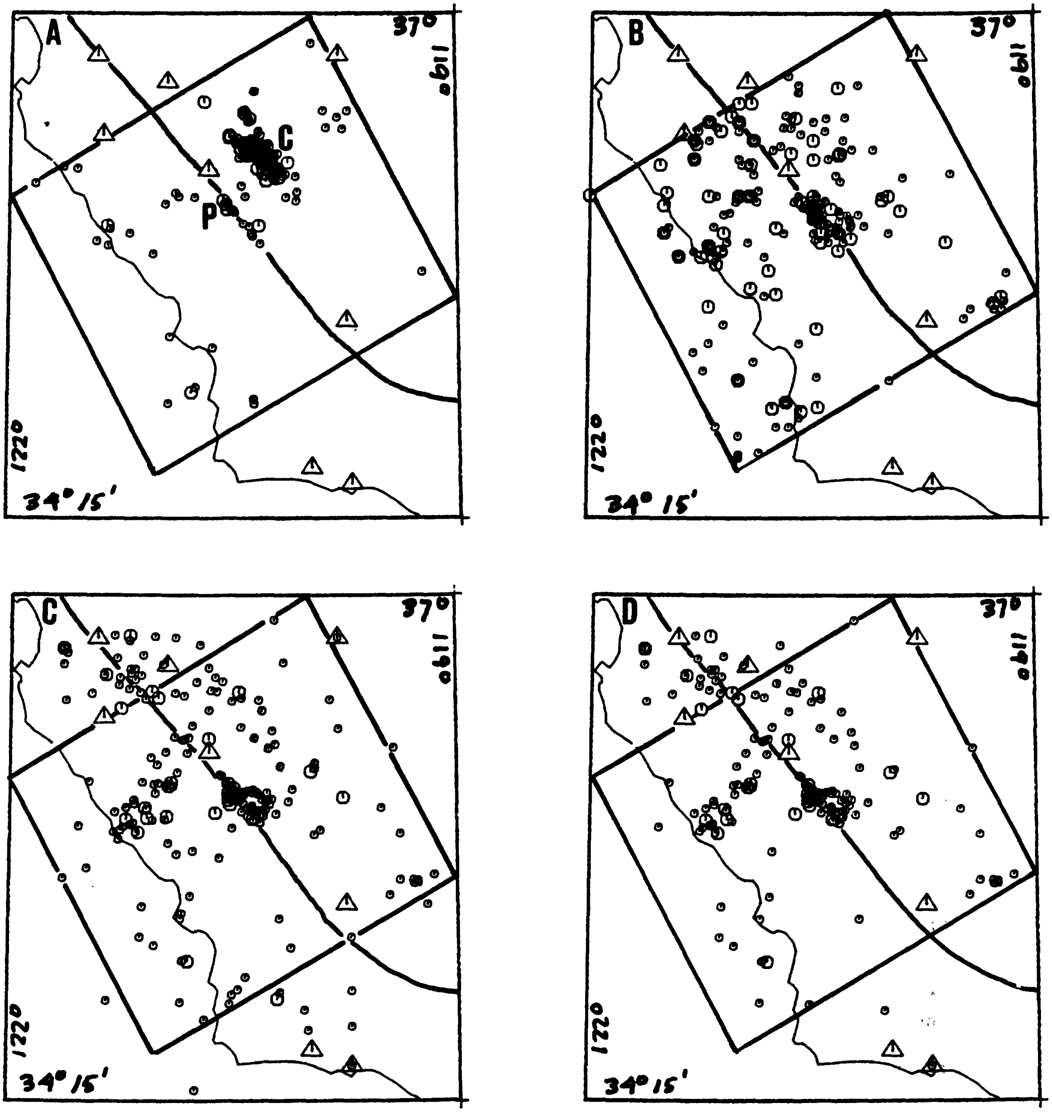

Figure 1. Earthquake epicenters (magnitude ≥ 3.5) in the vicinity of Parkfield, CA. Box outlines study area, triangles are seismic stations in operation at some time from 1932-1969, solid line is San Andreas fault, P is Parkfield, C is Coalinga.

A) U.S.G.S. locations, 1970-1986, 196 events.
B) UCB and CIT locations, 1932-1969, 235 events.
C) relocations, 1932-1969, 235 events.
D) best relocations, 1932-1969, 167 events.

# Strong Ground Motion Data Analysis

9910-02676

J. Boatwright, M Andrews, and L. Wennerberg
Branch of Engineering Seismology and Geology
U. S. Geological Survey
345 Middlefield Road, MS 977
Menlo Park, California 94025
(415) 329-5609, 329-5607, 329-5659

## Investigations

1. Recording and analyses of the aftershock sequence from the November 24, 1987, Superstition Hills, California, earthquake.

2. Theoretical investigation of the earthquake rupture process, with application to locating subevents of a complex rupture process.

3. Modeling the high-frequency acceleration radiated by extended seismic sources.

## Results

1. 12 GEOS digital event recorders were deployed at 21 different sites in the epicentral area of the Superstition Hills earthquakes. The sites included a liquefaction array on the floodplain of the Alamo River, three of the stations of the El Centro Accelerograph array, and five other permanent strong motion accelerograph stations. Approximately 400 aftershocks, whose magnitudes ranged from 1.0 to 4.6, were recorded during the two week deployment. The analyses of these recordings are presently divided into two distinct efforts: 1) The recordings of the aftershocks are being collated to determine a complete set of Green's functions for modeling the mainshock rupture process. The apparent complexity of the body-wave propagation in the area, particularly for seismic sources at shallow depths (< 3 km) indicates that exploiting the aftershock recordings to obtain Green's functions is far efficient than trying to determine a sufficiently detailed (3-dimensional) velocity model. 2) The topological amplification of Superstition Mountain is being investigated, using an array of five instruments deployed on the flanks of the mountain as well as co-sited with the strong motion instrument at the top of mountain. This strong motion instrument recorded a peak acceleration of 0.86 G from the largest of the two main shocks.

3. An inversion procedure for locating the subevents of a complex earthquake rupture process has been developed, which following the theoretical work of Boatwright (1988). The complex rupture is decomposed into the rupture of a set of discrete subevents. The slip associated with the stress release of the subevent is calculated by modeling the subevent as an asperity. To model the subevent radiation, aftershock recordings are causally filtered to enhance their low frequency content. The method of inversion incorporates positivity constraints for the stress drops of the subevents.

The set of subevents is determined inductively, where the amplitudes of the subevents are resolved iteratively each time a new subevent is added to the solution. A statistical test for the reduction of variance is used to limit the number of subevents. This inversion procedure is presently being applied to a set of accelerograph recordings of the 1976 Friuli, Italy, earthquake sequence.

2. The theory derived by Boatwright (1982) has been extended to analyze the acceleration radiated by extended faults. In contrast to kinematic treatments, where the source excitation is obtained from the distribution of the slip velocity multiplied by the radiation pattern, in the high-frequency analysis, the source excitation is obtained from the distribution of the dynamic stress drop multiplied by a high-frequency radiation pattern which incorporates directivity and crack diffraction effects. By specifying the approximate rupture history, the high-frequency analysis yields an envelope for the radiated acceleration. The method has been tested using a computer model of a 3-D dynamic rupture (Boatwright and Quin, 1986). The technique is presently being applied to accelerograph recordings of the 1980 Irpinia, Italy, earthquake.

## References

Boatwright, J., 1982, A dynamic model for far-field acceleration, Bulletin of the Seismological Society of America, v. 72, p. 1049-1068.

Boatwright, J., 1988, The seismic radiation from composite models of faulting, Bulletin of the Seismological Society of America. v. 78, p. 489-508.

Boatwright, J. and H. Quin, 1986, The seismic radiation from a 3-D dynamic model of a complex rupture process, Earthquake Source Mechanics, Geophysical Monograph 37, Maurice Ewing Series, v. 6, S. Das, J. Boatwright, and C.H. Scholz, Eds., American Geophysical Union, Washington, D.C., p. 97-109.

## Publications

Andrews, M.C., C. Dietel, T. Noce, E. Sembera, and J. Bicknell, Preliminary analyses of digital recordings of the Superstition Hills, California, aftershock sequence, abstract submitted to Earthquake Notes, 1988.

Boatwright, J., A dynamic decomposition of the earthquake rupture process, abstract submitted for the American Society of Mechanical Engineers, Symposium of the Mechanics of Earthquakes.

# Comparative Earthquake and Tsunami Potential for Zones in the Circum-Pacific Region

9600-98700

George L. Choy
Stuart P. Nishenko
William Spence
Branch of Global Seismology and Geomagnetism
U.S. Geological Survey
Denver Federal Center
Box 25046, Mail Stop 967
Denver, Colorado 80225
(303) 236-1506

## Investigations

1. Prepare detailed maps and text of comparative earthquake potential for west coasts of Mexico, Central America and South America.

2. Prepare detailed maps and text of comparative earthquake potential for the southwest Pacific.

3. Conduct investigations of the historic repeat-time data for great earthquakes in the northern Pacific Ocean margin.

4. Develop a working model for the interaction between forces that drive plate motions and the occurrence of great subduction zone earthquakes.

5. Compile tsunami data for the circum-Pacific and the corresponding seismic source zones.

6. Develop methods for the rapid estimation of the source properties of significant earthquakes.

7. Develop methods for improving significance and accuracy of determining probability of earthquake recurrence.

## Results

1. The probabilistic work for northern Mexico has been completed and published in three papers by Nishenko and Singh in 1987. Two regions have the highest probabilities for the recurrence of large earthquakes within the next two decades: the central Oaxaca gap and the Acapulco-Marco gap. With the occurrence of the catastrophic earthquake of September 19, 1985, the Michoacan seismic gap now has a very low probability for recurrence of a great earthquake within 20 years. Mendoza and Hartzell (1988) have studied the source characteristics of the earthquake. A study of aftershocks of the great 1979 Colombia earthquake has been accepted for publication (Mendoza, 1987). The study of this event in the context of the great 1906 and 1958 earthquakes will help the probabilistic assessment for the recurrence of great earthquakes in this region. The probabilistic work for the west coast

of Chile has already been done. Choy and Dewey (1987) have studied earthquake characteristics and seismotectonics associated with the great thrust earthquake of March 1985 near Valparaiso. The study of this earthquake is particularly important because Nishenko has concluded that the moment released since the turn of the century in this area is only about one-third of the moment of the great 1906 earthquake. The southern third of the Valparaiso zone is still at high risk.

2. Drs. Nishenko and McCann have identified three areas of high seismic hazard in SW New Britain, San Cristobal and the central Tonga arc. Data collection and analysis should be finished by late spring 1988.

3. Data on the occurrence of great earthquakes and tsunamis from the Queen Charlotte Islands to the Aleutian Islands have been collected, and the evaluation of probabilistic recurrence is being conducted by Drs. Nishenko and Jacob.

4. An evaluation of the ridge-push and slab-pull forces in the context of stresses that lead to great subduction zone earthquakes has been completed (Spence, 1987). An important conclusion is that specific parts of a subducting plate may be monitored for precursors to seismic gap-filling earthquakes.

5. Several tsunami catalogs have been gathered prior to compilation of a comprehensive tsunami catalog. In cooperation with NOAA, Dr. Nishenko has designed a form for systematically gathering and analyzing tsunami data. Currently, there is no uniform approach for this data acquisition.

6. We have incorporated algorithms into NEIC operations that now permit the analysis of broadband data for all earthquakes with magnitude greater than 5.8. Broadband data are now being used routinely to increase the accuracy of reported parameters such as depth and radiated energy. Choy and Boatwright (1988) are developing a method for determining maximum expected acceleration levels from teleseismic data. These estimates will fill the void caused by the lack of near-field recording in regions of high seismic risk.

7. Drs. Nishenko and Buland have completed a paper to improve the methodology of determining the probability of earthquake recurrence.

## Reports

Choy, G. L., and Boatwright, J., 1988, Teleseismic and near-field analysis of the Nahanni earthquakes in the Northwest Territories, Canada: Bulletin of the Seismological Society of America (submitted).

Choy, G. L., and Dewey, J. W., 1988, Rupture process of an extended earthquake sequence: Teleseismic analysis of the Chilean earthquake sequence of 3 March 1985: Journal of Geophysical Research, v. 93, p. 1103-1118.

Mendoza, C., and Hartzell, S. H., Inversion for slip distribution using GDSN waves--North Palm Springs, Borah Peak, and Michoacan earthquakes: Bulletin of the Seismological Society of America (in press).

Nishenko, S. P., and Buland, R. P., 1987, A generic recurrence interval distribution for earthquake forecasting: Bulletin of the Seismological Society of America, v. 77, p. 1382-1399.

Nishenko, S. P., and Singh, S. K., 1988, The Acapulco-Ometepec, Mexico earthquakes of 1907-1982--Evidence for a variable recurrence history: Bulletin of the Seismological Society of America (in press).

Nishenko, Stuart P., and Singh, S. K., 1988, Conditional probabilities for the recurrence of large and great interplate earthquakes along the Mexican subduction zone: Bulletin of the Seismological Society of America (in press).

Spence, William, 1987, Slab pull and the seismotectonics of subducting lithosphere: Reviews of Geophysics, v. 25, p. 55-69.

# Earthquake Hazard Investigations in the Pacific Northwest

14-08-0001-G1390

R.S. Crosson
Geophysics Program
University of Washington
Seattle, WA 98195
(202) 543-8020

## Investigations

The objective of this research is to investigate earthquake hazards in western Washington, including the possibility of a large subduction-style earthquake between the North American and Juan de Fuca plates. Improvement in our understanding of earthquake hazards is based on better understanding of the regional structure and tectonics. Current investigations by our research group focus on the configuration of the subducting Juan de Fuca plate, differences in characteristics of seismicity between the overlying North American and the subducting Juan de Fuca plates, determination of regional stresses through analysis of earthquake focal mechanisms, and modeling of lateral velocity variations in the shallow crust. Research during this contract period concentrated on the following topics:

1. Tomographic inversion of earthquake travel times to determine 3-D velocity structure at Mount St. Helens.

2. Investigation of focal mechanisms of crustal earthquakes in western Washington, and implications for regional tectonic stresses.

## Results

1. As part of a larger investigation of 3-D seismic velocity variations in western Washington, we have recently completed a concentrated study of the Mt. St. Helens region. This region is important because of the possible shallow earthquake hazard associated with the St. Helens seismic zone (SHZ), the eruptive potential at Mt. St. Helens, and the abundance of earthquake sources. It provides an excellent testing ground for our technique of using earthquake sources in tomographic inversion. Approximately 17 thousand source-receiver pairs were used in the data processing to obtain a "picture" of the velocity (expressed as slowness) variation throughout the St. Helens region. Figs 1a and 1b show an example inversion result for a layer 2.0 to 4.0 km depth (a) along with the earthquake epicenter plot (b) for those events used. The volcano is near the center of the plots, and the treeline contour is drawn. Light colored regions are higher velocity, and dark regions are lower velocity. The SHZ itself is relatively low velocity and there appears to be a fundamental change in this character (or bend) about the latitude of Mt. St. Helens. High velocity regions NNE and NW of the volcano correspond to known plutons. The relatively high velocity directly beneath the cone may indicate a solidified residual magma conduit. We suspect that the currently active magma chamber lies immediately to the north with a small associated low velocity anomaly. Further refinement of this technique may provide greater structural resolution. A manuscript by J.M. Lees and R.S. Crosson is currently being completed for publication.

2. We have completed initial work on stress inversion using focal mechanism data (M.S. Thesis by Li Ma). This work is based on analysis originally done by McKenzie (1969) and developed into a formal inversion method by Gephart and Forsyth (1984). The objective is to find the range

of acceptable stress models (orientation plus ratio of principal stresses) which satisfy the focal mechanism data within specified misfit criteria. Fig. 2a shows an example of a set of P axes for 76 earthquakes in the Puget Sound region. We ask if a single stress model can give rise to this distribution, and if so, what is the range of allowable orientations? Fig. 2b shows the distribution of allowable σ1 and σ3 axes (σ1 as pluses, σ3 as squares) that are compatible with the focal mechanisms at the 90% confidence interval from the Gephart and Forsyth analysis. We conclude that NS compression with largely easterly extension is the dominant regional tectonic stress in the Puget Sound region. There is no evidence from our analysis that stress coupling between the North American and Juan de Fuca plates across the Cascadia subduction zone modifies the stress in this location. Preliminary results from the Mt. St. Helens region suggest that in spite of significant rotation of the mechanism P axes to the northeast, NS compression may be the best fitting stress model there also. By comparison, earthquakes in the subducted Juan de Fuca plate beneath western Washington indicate an entirely different, much more complex stress distribution. We interpret these results to indicate that east of approximately 123.5 W. longitude, the effects of coupling between the continental and subducted plates, if it exists, is not observed from focal mechanism observations.

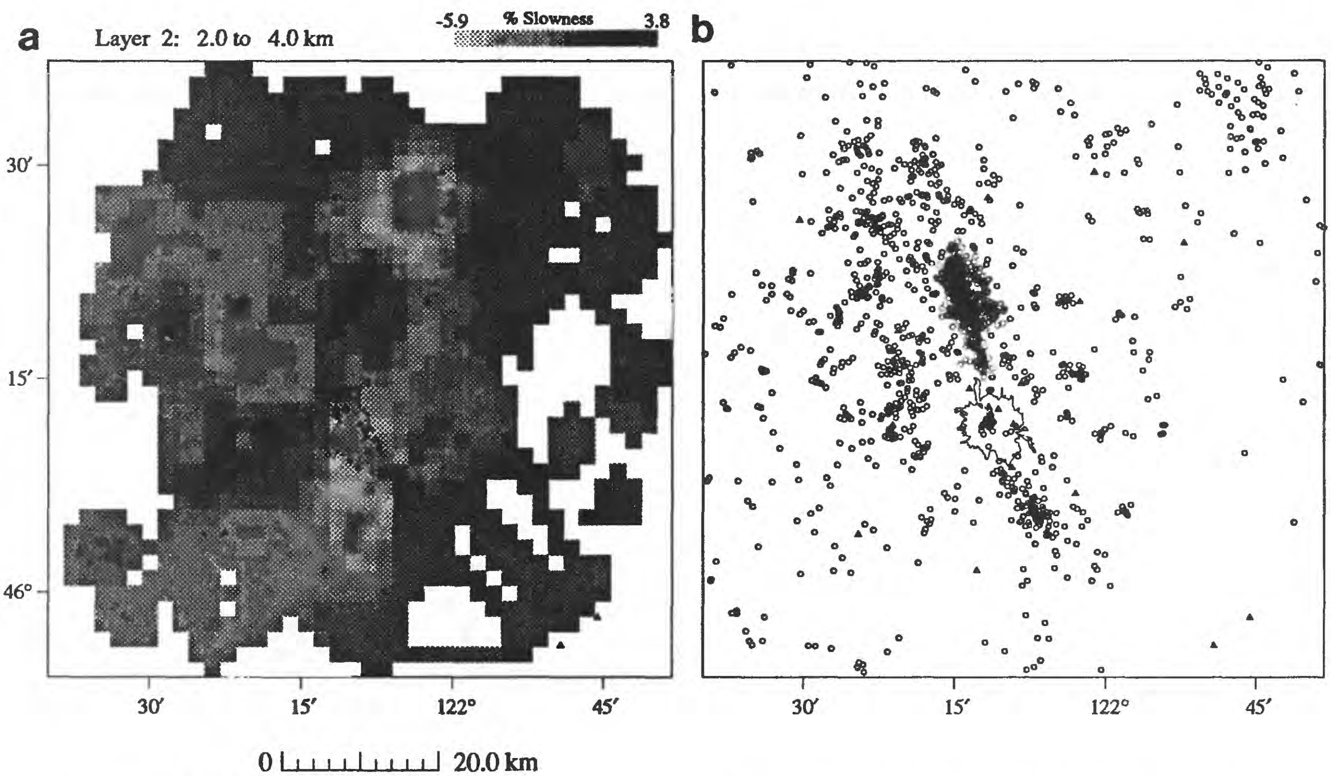

**Figure 1. 1a)** Result of tomographic inversion for a layer from 2 to 4 km depth in the Mount St. Helens area. Map view of percent slowness perturbation from initial constant slowness of .185 sec/km.
**1b)** Epicenters of earthquakes used in the inversion.

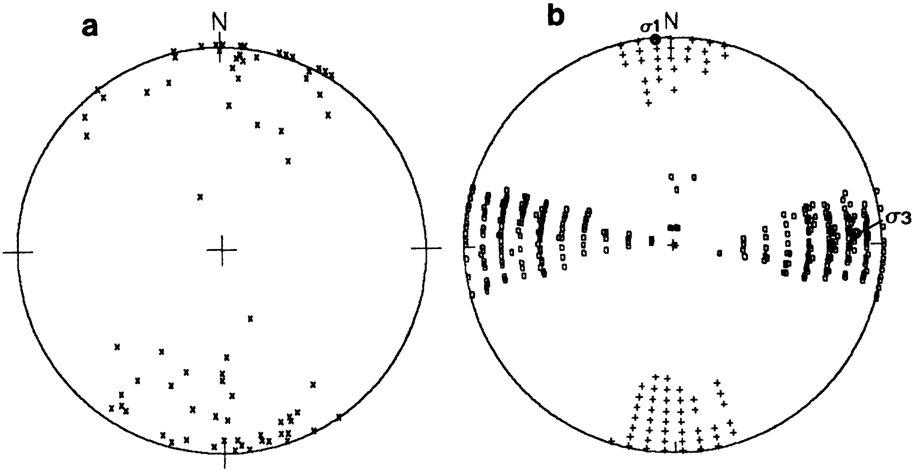

**Figure 2. 2a)** Composite lower-hemisphere equal area plot of P axes from 76 focal mechanisms determined for shallow earthquakes in western Washington.

**2b)** Best-fitting greatest and least principal stress directions σ1 and σ3 for shallow western Washington earthquakes. Additional σ1 and σ3 directions within 90% confidence limits are plotted. Azimuth and plunge of the best fitting greatest principal stress axis are σ1 = 356°, 1°, while best fit for least principal stress are σ3 = 86°, 18°.

## Articles

Lees, J.M. and R.S. Crosson, 1988 (in preparation), A tomographic inversion fro the 3-D velocity structure at Mount St. Helens using earthquake data.

VanDecar, J.C. and R. S. Crosson, 1988 (in preparation), Determination of teleseismic relative phase arrival times using multi-channel cross correlation and least squares.

Ludwin, R. S., S.D. Malone, R.S. Crosson, 1988 (in press), Washington Earthquakes 1983, in U.S. Earthquakes, National Earthquake Information Service.

Ludwin, R. S., S.D. Malone, R.S. Crosson, 1988 (in press), Washington Earthquakes 1984, in U.S. Earthquakes, National Earthquake Information Service.

Ludwin, R. S., S.D. Malone, R.S. Crosson, A.I. Qamar, 1988 (in press), Washington Earthquakes 1985, in U.S. Earthquakes, National Earthquake Information Service.

Ludwin, R. S., S.D. Malone, R.S. Crosson, A.I. Qamar, 1988 (in preparation), Washington Earthquakes 1986, in U.S. Earthquakes, National Earthquake Information Service.

Ludwin, R. S., C.S. Weaver, R.S. Crosson, S.D. Malone, 1988 (in preparation), Seismicity in the Pacific Northwest, in Decade of North American Geology, published by Geol. Soc. Am.

## Reports

Univ. of Wash. Geophysics Program, 1988, Quarterly Network Report 87-D on Seismicity of Washington and Northern Oregon

Univ. of Wash. Geophysics Program, 1988 (in preparation), Quarterly Network Report 88-A on Seismicity of Washington and Northern Oregon

## Abstracts

VanDecar, J.C. and R. S. Crosson, 1987, Automated Determination of Teleseismic Relative Phase Arrival Times using multi-channel cross-correlation and least squares, EOS, V. 68, p. 1359.

Lees, J.M., 1987, Tomographic inversion of local earthquake travel time data for lateral velocity variation in western Washington, EOS, V. 68, p. 1374.

Ma, Li, R.S. Crosson and R.S. Ludwin, 1988 (in press), Regional tectonic stress in western Washington from focal mechanisms of crustal and subcrustal earthquakes, Seismol. Research Letters, V. 59, p. 16.

## Thesis

Ma, Li, 1988, Regional Tectonic Stress in Western Washington from Focal Mechanisms of Crustal and Subcrustal Earthquakes, M.S. Thesis, University of Washington.

# EARTHQUAKE LIQUEFACTION: SOUTH CAROLINA, VIRGINIA, WASHINGTON

9950-03868
Stephen F. Obermier
Branch of Geologic Risk Assessment
MS 926, National Center
Reston, Virginia 22092
(703) 648-6791

9510-01343
Gregory S. Gohn
Branch of Eastern Regional Geology
MS 926, National Center
Reston, Virginia 22092
(703) 648-4382

## Investigations

A search was continued for liquefaction features in the vicinities of Charleston, southeastern South Carolina, and Savannah. In the Charleston area, the search was for 1886 features whose source sands could be tested to back-calculate shaking severity of the 1886 earthquake and to determine geologic and engineering controls on surficial development of liquefaction. In areas far from Charleston, the search was for pre-historic liquefaction features.

Six sites of 1886 liquefaction were tested in the field (using cone penetration or standard penetration tests) by researchers from Virginia Polytechnic Institute; many sites with no liquefaction were also tested.

Geologic and structure contour maps were drafted for the Summerville, Summerville NW, Ridgeville, and Pringletown 7.5 minute quadrangle.

## Results

In extreme eastern Georgia, near Savannah, no liquefaction features have been discovered. Thus, it would appear that the possibility of strong Holocene earthquake shaking in that area is quite low.

The liquefaction caused by the 1886 earthquake that was farthest from the epicentral region developed only in exceptionally loose sands. This implies that far from the epicenter, exceptionally low near-surface accelerations produced many of the liquefaction-related earthquake effects.

A manuscript has been completed which describes characteristics of earthquake-induced liquefaction features and characteristics of nonseismogenic features that might be confused with the earthquake-induced features. These characteristics are described in both the coastal setting of South Carolina and fluvial setting of the New Madrid seismic zone.

## Reports

Obermeier, S. F., Weems, R. E., Jacobson, R. B., and Gohn, G. S., in press, Liquefaction evidence for repeated Holocene earthquakes in the coastal region of South Carolina, New York Academy of Sciences.

Weems, R. E., Jacobson, R. B., Obermeier, S. F., and Gohn, G. S., 1988, New radiocarbon ages from earthquake-induced liquefaction features in the lower coastal plain of the Carolinas, Geological Society of America Abstracts with Programs, Southeastern Section, v. 20, no. 4, p. 322.

# Magnitude Stability and Detection Changes in the California Seismicity Catalogs

**14-08-0001-G1314**

R. E. Habermann
School of Geophysical Sciences
Georgia Institute of Technology
Atlanta, Georgia 30332[1]

It has become clear that systematic changes in magnitudes in local and teleseismic catalogs are a major barrier to studies of changes in seismicity rates which may occur as precursors to earthquakes. The emphasis in this study has shifted away from the California catalogs primarily because of the on-going U.S.G.S. effort at correcting the magnitudes in those catalogs. The main task now involves evaluating temporal stabiltiy of magnitudes in Central America and Mexico, the Aleutians, and South America and re-examining possible precursors which have been reported prior to recent large earthquakes in those areas. We have made substantial progress on the first aspect of this study using several approaches.

## Maximum Liklihood Magnitude Comparisons.

Several authors have recently re-computed magnitudes for a large number of teleseismic events in the ISC catalog using the maximum liklihood technique developed by Ringdal. This technique incorporates station corrections as well as considering the fact that a given station with known noise levels did not report the event. The magnitudes which result from this re-calculation are probably more consistent than the original magnitudes which are determined as simple averages.

The existence of the re-calculated magnitudes allows one to compare them with the original magnitudes in order to assess the temporal consistency of the originals. Figure 1 shows comparisons of these two types of magnitudes for the three regions we are presently studying. South America and the Aleutians both show sharp decreases in magnitude difference of about -0.15 during 1975. This suggests that the original magnitudes increased by that amount at that time. The picture for Mexico and Central America is somewhat more complex. Both regions show general increases in magnitude throughout the period studied. The amount of these increases is between -0.2 and -0.25.

Interpreting these changes in magnitude difference strictly as changes in the original magnitudes may not be justified because of some possible problems in the assumptions of the maximum liklihood technique. The principal assumptions are that the network used for the magnitude determinations does not change through time and that a single value is appropriate for the station correction. It is well known that the first assumption is incorrect, the network changes drastically as a function of time. The validity of the second assumption is also questionable.

Figure 2 shows the biases for station EUR as a function of time for the regions we are examining. These biases clearly show temporal variations in all regions. This station reports a substantial number of magnitudes for all of these regions (), so the assumption that a single number describes the biases well could certainly introduce time-dependent systematic errors in the magnitudes. In addition to the temporal dependence of bias, we have found a clear linear dependence of bias on the station magnitudes. In most cases the slope of this relationship is positive.

**Constant Networks.**

It has been customary to explain changes observed in catalogs by calling on changes in the network which is used to create the catalog, particularly in the absence of clear proceedural changes. In order to examine this explanation we have imposed a constant network on the catalogs of these three regions and produced catalogs in which all events are reported by the same stations. Our initial analysis has focused on the VELA arrays and is, therefore, limited to the period 1964 through June, 1969. The most surprizing initial result is that temporal changes in station bias can also occur if a constant network is used. This is particularly true in Mexico and Central America. In the Aleutians and South America the station biases change, but the size of the changes is rather small.

**Other Studies.**

We have done the comparisons of maximum likelihood and original magnitudes in all Gutenberg-Richter regions with more than 1000 events. This analysis clearly indicates regional variations in the behavior of magnitudes. Regions in the southwest Pacific, for instance, show similar patterns with low magnitudes during the late 1970's which recover during 1980. In this case the changes in differences range up to 0.3 units, large enough to seriously affect the results of many seismicity studies in that region.

**Recent Papers.**

R. E. Habermann, (1986). **A test of two techniques for recognizing systematic errors, in magnitude estimates using data from Parkfield, California**, Bull. Seismol. Soc. Amer., 76, 1660-1667.

R. E. Habermann (1987). **Man-made changes of seismicity rates**, Bull. Seismol. Soc. Amer., 77, 141-159.

R. E. Habermann and M. Wyss (1987). **Reply**, Journ. Geophys. Res., 92, 9446-9450.

R. E. Habermann, **Seismic quiescence: past, present and future**, PAGEOPH, in press.

R. E. Habermann (1987). **Precursory seismic quiescence: Past, present and future**, in Proceedings of Conference XXXVII, Physical and Observational Basis for Intermediate-Term Earthquake Prediction, U.S. Geological Survey Open-file Report 87-591, 461-507.

1

---

[1] Present Address: NOAA/NGDC E/GC1, 325 Broadway, Boulder, CO 80302

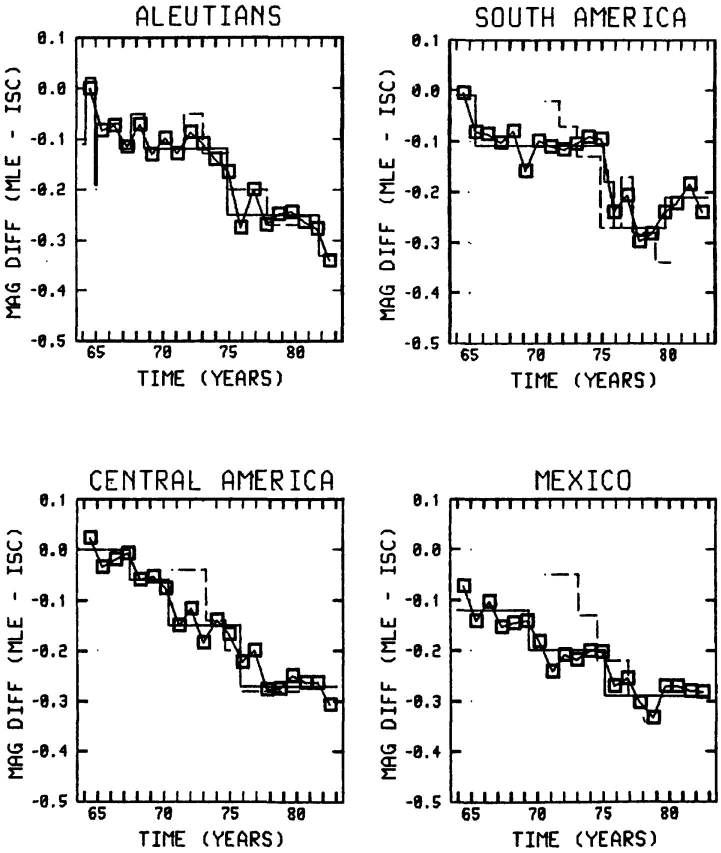

**Figure 1.** Differences between maximum likelihood magnitude estimates (MLE) and original ISC magnitudes for 4 regions. The boxes are the yearly average differences using MLE's by Lilwall and Neary. The solid line is a fit to these data using the genas algorithm for finding the times of change. The dashed line is the fit to the differences using the MLE's calculated by Ringdal. Ringdal's data covers only the 1970's whereas the Lilwall and Neary data extend from 1964 to 1983. The agreement between the changes in these two different sets is usually good.

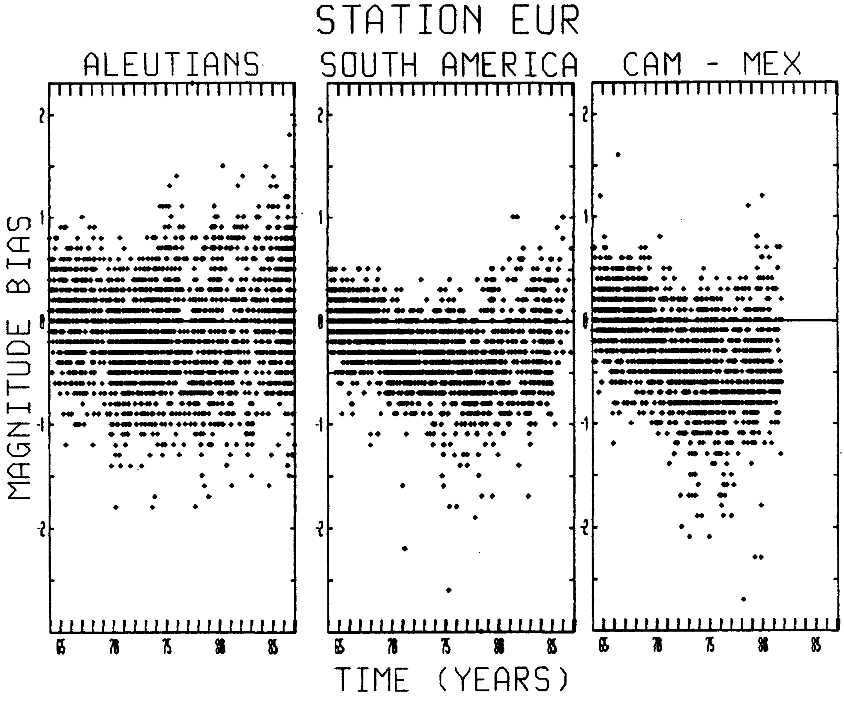

Figure 2. Magnitude bias for the station EUR for three regions as a function of time. Note the clear pattern of change in bias, with negative biases during the 1970's and biases close to 0 during the 1960's and 80's. Note also that the variance of the bias is larger in the Aleutians, making the change less clear.

# Spatial and Temporal Patterns of Seismicity in the Garm Region, USSR: Applications to Earthquake Prediction and Collisional Tectonics

14-08-0001-G1382

Michael W. Hamburger, Gary L. Pavlis,
Mariana Eneva, and William A. Swanson
Department of Geology, Indiana University
Bloomington, Indiana 47405
(812) 335-2934

## Investigations

This program focuses on the highly active collisional plate boundary between the Indian and Eurasian plates in Soviet Central Asia. The Garm region, located between the Pamir and Tien Shan mountain belts (Figures 1 and 2), is characterized by a dense concentration of both shallow and intermediate-depth earthquakes. Since the early 1950's, Garm has been the home of the Complex Seismological Expedition (CSE), whose primary mission is the prediction of earthquakes in the USSR. Beginning in 1975, the USGS, in cooperation with the CSE, has operated a telemetered network nested within a stable CSE network that has operated in the area for over thirty years. The fundamental aims of the present research project are: (1) to elucidate the structures and processes involved in active deformation of the collisional plate boundary, and (2) to examine the temporal variations in seismicity near Garm, in the form of changing spatial, depth, and stress distribution of microearthquakes that precede larger events. The data base for this study includes the combined resources of the global, regional, and local seismic networks.

## Results

*Seismicity data.* All work reported here is based on the compilation of earthquake catalogs from five distinct sources: (1) *Historical earthquake catalogs,* including all events of $M_S \geq 6$, have been compiled from a variety of historical and instrumental sources. (2) *Global seismicity catalogs* are from the ISC and PDE bulletins and their precursors. (3) The *Soviet regional catalog* (from "Earthquakes in the USSR," Acad. Sci. USSR), which covers an area of approximately 15° by 25° and includes nearly 30,000 events since 1962, has been compiled in collaboration with D.W. Simpson (Lamont-Doherty Geol. Obs.). (4) The *CSE network* covers an area of about 2° square surrounding Garm, and has recorded over 70,000 events since the early 1950's. Arrival times and event locations for the period 1969-1987 have been made available as part of the US-USSR exchange. (5) The *USGS network* provides the most precise spatial information for an area about 1° square over the highly active Peter the First Range.

Our work during this period has focused on completion of earthquake catalogs, and obtaining refined hypocentral locations from the two local networks at Garm. We have augmented the regional catalog data reported earlier by addition of over 9000 events for the periods 1962-63 (contributed by D.W. Simpson) and 1981-1983 (entered from the new catalog "Earthquakes in Central Asia and Kazakhstan", obtained through the Tadjik Institute of Seismology). Thus, we now have a 22-year catalog for the Central Asian region, complete for magnitudes greater than 3 (and for some subsets to the magnitude 2.5 level). Regional network earthquake locations for central Tadjikistan are shown in Figure 2. The 18-year, 50,000+ event CSE catalog and associated arrival time data (over 500,000 station-arrival times) have been decoded from a Soviet tape and are now being used for earthquake location and velocity inversion studies. As an example of the quantity and resolution of the CSE network data, one year of earthquake locations is presented in Figure 3a. Earthquakes were relocated by the single-event location program HYPOELLIPSE (Lahr, 1984), using a simple three-layer velocity model (see below). The earthquake distribution is extremely nonuniform in space, and well defined earthquake clusters and lineations of seismicity can be distinguished from background activity. In addition, we have gathered all available arrival time data for the USGS network at Garm, and have located over 1600 events in the Peter the First range. This new catalog expands the existing data base (reported by Pelton and Fischer, 1981) by a factor of ten. The USGS locations (Figure 3b) provide additional constraints on spatial distribution of seismicity near Garm. For example, an extremely well defined cross-strike feature (oriented parallel to the plate convergence vector) is evident at basement depths, possibly segmenting the major northeast-striking folds and faults in the Peter the First Range.

*Velocity structure.* In order to improve the accuracy of earthquake locations and depths in the Garm area, we require a realistic approximation of the velocity structure beneath the Garm networks. Velocity models estimated by Soviet seismologists have generally been obtained using forward modeling techniques with earthquakes as sources (*e.g.*, Bune *et al.*, 1960; Kulagina *et al.*, 1974), and provide little constraint over detailed upper crustal structure. Pelton and Fischer (1981) first obtained a one-dimensional velocity model under the Peter the First range using an inverse technique. They used arrival time data from a subset of a catalog for the period 1975-1976 for their study. We expanded on their work by applying the same algorithm (Roecker and Ellsworth's VELEST), but using a greatly increased data base. Preliminary hypocenter locations for well recorded events in the CSE network (1981) and the USGS network (1975-1982) were obtained using Pelton and Fischer's (1981) velocity model. These events were graded and subsets of well constrained events chosen for subsequent inversion for velocity structure (Figure 2). Using VELEST, we inverted these arrival time data for the simultaneous estimates of hypocentral parameters, P velocity structure, S velocity structure, and station corrections. The hypocentral parameters for the well constrained subset events (within each of the networks), along with the corresponding phase data, were used as the input for VELEST. Simultaneous adjustments of hypocenter and model parameters are made to obtain a 'best' least squares fit to the data. This procedure was repeated for numerous inversion tests using different initial velocity models, layer parameterizations, damping parameters, and so on.

For most of the CSE data inversions the crustal velocity structure was parameterized by three-layer models. The velocities of the lower two crustal layers converged (within the standard deviation of the associated model parameter) to yield a simpler two-layer model estimate (Figure 4a). On this basis, we used a two-layer parameterization of the upper crust for subsequent testing and earthquake locations. The USGS network data inversions proved to be most stable using the two-layer results from the CSE tests as input models . Subsequent tests with the USGS data involved using the CSE model estimate as an initial velocity configuration and varying the layer thickness. The resulting models produced consistent velocities; the model with an 8 km-thick surface layer had the 'best' overall statistics (Figure 4b). The final velocity models for both the USGS/CSE and CSE networks are reasonable, based on the following criteria: (1) the upper crustal model velocities (5.4 - 6.4 km/sec) are geologically reasonable, and do not support Pelton and Fischer's unusually high-velocity (7.7 km/sec) midcrustal layer; (2) the obtained S-models corroborate the P-models by yielding Vp/Vs ratios that are reasonable (1.7 - 1.8); (3) both the data variance and RMS have been decreased by about 50 percent; (4) the standard tests of credibility provided by the inversion program indicate that resolution was high (> 0.98) and the standard deviation was low (< 0.10 km/sec) for each model parameter. There are of course significant deficiencies with the velocity inversion technique, but we believe the velocity model and station corrections obtained provide a reasonable first-order model to proceed with the earthquake relocations.

*Space-time seismicity patterns.* The high level of seismic activity in the Central Asian region (Figure 2) has led us to consider more rigorous methods of analyzing spatial and temporal seismicity patterns. Our previous reports have described techniques for identification and characterization of nonrandomness in the spatial and temporal distribution of earthquakes (Eneva *et al.*, 1987; Eneva and Hamburger, 1987; 1988). The approach compares the observed distributions of distances and time intervals among all possible pairs of events with the distributions that would be expected were the events distributed in a uniform fashion within the active seismic zones. Our previous work examined various subsets of earthquakes within the India-Eurasia plate boundary zone, at various spatial scales, magnitude ranges, and tectonic settings. In virtually all cases, the seismic activity displayed a marked tendency to cluster in both space and time. The obvious question remains, however, to what degree this tendency can be explained by the occurrence of tightly grouped sequences of aftershocks and swarms.

To address this question, we have developed a reliable technique for removing aftershocks and swarms from an earthquake catalog. The approach is also useful for distinguishing these "unusual" earthquake sequences from the "normal" background activity. Our approach is based on comparison of observed rates in isolated space-time windows with average rates of seismic activity. "Excess" events are removed from windows of unusually high activity, but with three important considerations: (1) we use the average rate for a particular portion of the seismic zone (rather than the entire seismic zone) for calculating the background activity, (2) we do not remove all the events from a high-activity window (i.e., the background activity for that area is left in the catalog), and (3) we do not restore all such windows to identical rates of seismic activity. For this purpose, we use a "double random" approach to remove clustered events from the catalog. The entire seismic zone is broken up into arbitrary spatial and temporal windows. An initial average rate of activity is assigned to each *spatial* unit by calculating the mean from the rates in all the *temporal* units associated with that area. The anomalous time intervals (defined as those windows whose rate is outside the 95% confidence limits about the average rate) are dropped from consideration, and a new average rate is calculated. This procedure is iteratively applied until all rates in the remaining time intervals fall within the 95% confidence limits. The procedure is repeated for all spatial units. Thus, a final average rate is assigned to each unit, believed to represent best the background activity. The space-time windows in which seismic rates exceed the 95% confidence limits are identified as intervals from which events have to be removed. The number of events that should remain in such windows is randomly generated using a normal distribution around the average rate. The particular events to be removed are then randomly chosen (hence the name "double random"), with the exception that the largest event from such windows (*i.e.*, the mainshock) is not removed. The success of this technique is demonstrated by the "raw" and "declustered" space-time diagrams presented in Figure 5. Our preliminary results indicate that the marked spatial clustering of events persists even when aftershocks and swarms are excluded from consideration, while the temporal clustering disappears when aftershock/swarm sequences are excluded.

## References

Bune, V.I., and others, 1960, Methods of detailed study of seismicity [in Russian], *Trudy Inst. Fiz. Zemli, 9,* 31-68.

Eneva, M., G.L. Pavlis, and M.W. Hamburger, 1987, Discrimination of non-random features in the space-time distribution of earthquakes [abstract], *Seis. Rss. Lett., 58,* 96.

Eneva, M. and M.W. Hamburger, 1987, Space-time seismicity patterns within the Gissar-Kokshal and Tadjik Depression seismic zones, Soviet Central Asia [absract], *EOS, Trans. AGU, 68,* 1868.

Eneva, M. and M.W. Hamburger, 1988, Spatial and temporal patterns of earthquake distribution in Soviet Central Asia: Application of Pair Analysis Statistics, to be submitted to *Bull. Seism. Soc. Amer.*

Kulagina, M.V., A.A. Lukk, and V.K. Kulagin, 1974, Block structure of the earth's crust in Tadjikistan [in Russian], in *The Search for Earthquake Precursors in Prediction Polygons,* Moscow, Nauka, pp. 70-84.

Lahr, J.C., 1984, HYPOELLIPSE/VAX: A computer program for determining local earthquake hypocenter parameters, magnitude and first-motion pattern, *U.S. Geol. Surv. Open File Rept. 84-519,* 60 pp.

Pelton, J., and F.G. Fischer, 1981, An earthquake catalog and velocity model for the USGS Peter the First Range seismic array, Tadzhikistan, USSR, *U.S. Geol. Surv. Open-File Rept. 81-1150,* pp. 221-246.

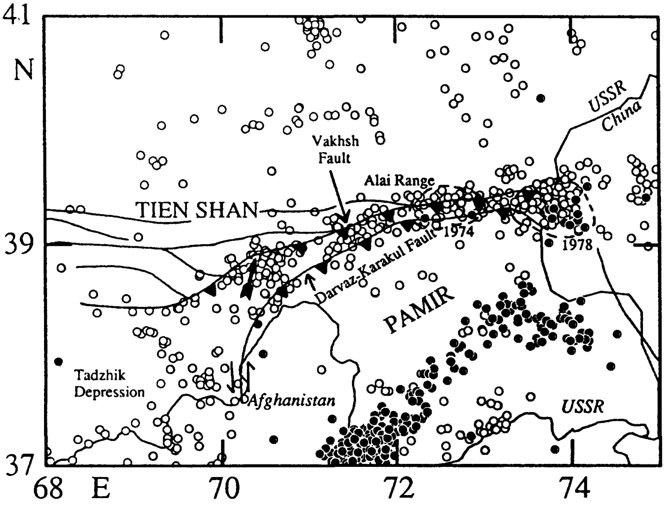

Figure 1. Teleseismically located earthquakes and active faults of the Garm region. Earthquakes recorded from 1964-1984 and located by ≥ 20 stations, are from the ISC catalog. Open circles represent earthquakes at ≤ 70 km depth; filled circles: h > 70 km. Fault maps are adapted from Keith et al. (1982) and Wesson (1986). Dashed ellipses indicate aftershock zones of 1974 Markansu and 1978 Daraut-Kurgan earthquakes. Heavy arrow shows the location of Garm.

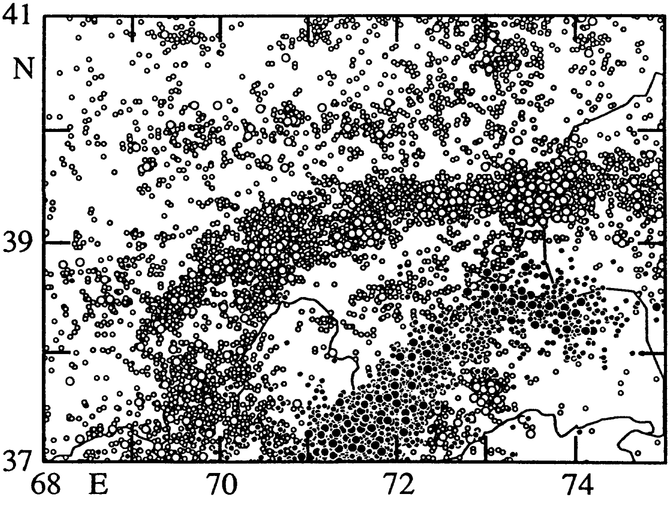

Figure 2. Earthquakes located by the Soviet Regional Network, 1964-1980, classified by magnitude and depth: open circles: h ≤70 km; filled circles: h > 70 km. Small symbols: M ≤ 4.0; large symbols: M > 4.0. We have arbitrarily "randomized" the coordinates of poorly located events on the margins of the seismic network whose position was given in 0.1° increments in order to remove an apparent gridding of epicenters.

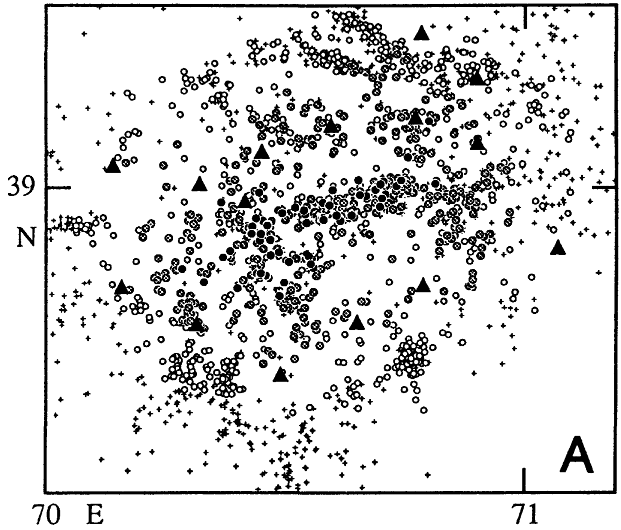

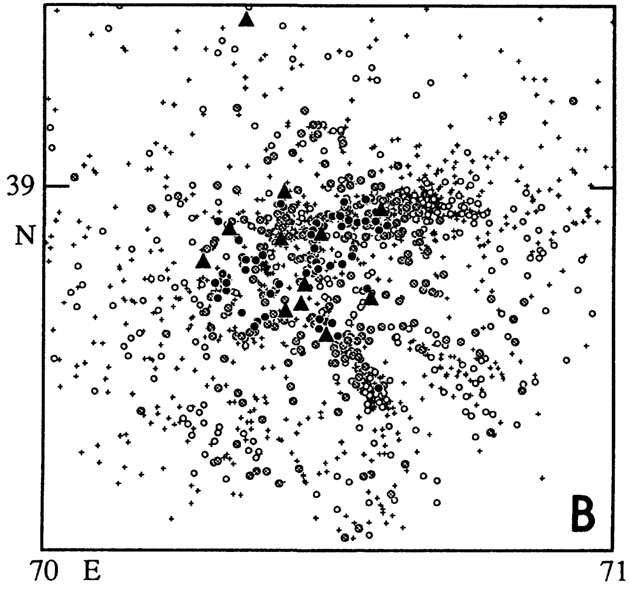

Figure 3. (A) CSE network and relocated events based on 1 year of arrival time data. (B) USGS network and all events for 1975 - 1982. In both figures, eathquake symbols represent location quality: filled circles = 'A' events; shaded circles = 'B' events; open circles = 'C' events; crosses = 'D' events. Filled triangles represent seismic stations.

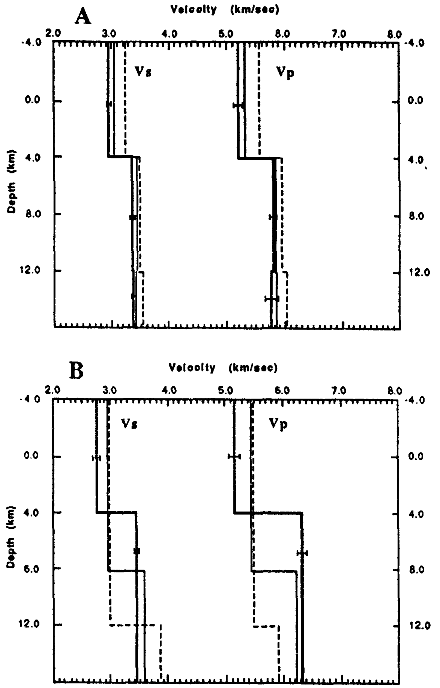

Figure 4. Velocity model estimates using different initial velocity models. (A) Results from 3-layer inversions on CSE network subset. (B) Results from 2-layer inversions on USGS network subset. Associated error bars are included in 'best' estimate (bold solid line) in each figure.

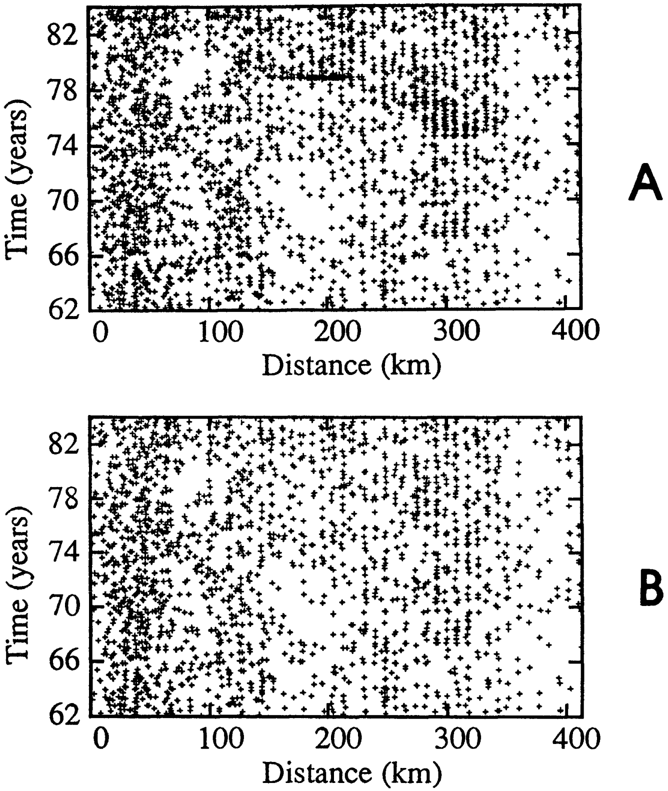

Figure 5. Space-time plots of the Gissar-Kokshal area: (A) all events located by the Soviet regional network; (B) residual catalog after removal of aftershock/swarm sequences. Distance axes are from W to E along the main seismic zone bounding the Tien Shan.

# Analysis of Earthquake Data from the Greater Los Angeles Basin and Adjacent Offshore Area, Southern California

#14-08-0001-G1328

Egill Hauksson
Ta-liang Teng
Center for Earth Sciences
University of Southern California
Los Angeles, CA 90089-0741
(213) 743-7007

## INVESTIGATIONS

Analyze earthquake data recorded by the USC and CIT/USGS networks during the last 12 years in the greater Los Angeles basin to improve earthquake locations including depth and to determine the detailed patterns of faulting in the study region.

Analysis of the July 1986 Oceanside ($M_L$= 5.3) earthquake sequence in the Continental Borderland has been completed.

## RESULTS

An earthquake of $M_L$=5.3 occurred at 32°58.7'N, 117°51.5'W southwest of Oceanside in San Diego County on 13:47 July 13, 1986 (UT) (Figure 1). This main shock was followed by an extensive aftershock sequence, with 55 events of $M_L \geq 3.0$ during July 1986. The epicenters of the main shock and aftershocks are located at the northern end of the San Diego Trough-Bahia Soledad fault zone (SDT-BS) where it changes strike from northwest to a more westerly direction through a left offset or a bend in the fault. The northwest striking SDT-BS is one of three strike-slip fault systems that constitute the Agua Blanca fault system. The spatial distribution of the aftershocks indicates a unilateral 7 -9 km long rupture to the east-southeast away from the epicenter of the main shock. The focal mechanism of the main shock also has an east-southeast striking and south-dipping plane with mostly reverse movement on it. Focal mechanisms of the $M_L \geq 3.0$ aftershocks show both reverse and strike-slip movement (Figure 2). The reverse focal mechanisms indicate that this sequence may have occurred on a thrust fault that provides for a left stepping offset or a bend in the San Diego Trough fault as movement is transferred to the west along the Santa Cruz - Catalina Island escarpment (Figure 3). Some of the aftershocks that are located to the southeast of the main shock and have strike-slip focal mechanisms, indicate activation of the northwest trending San Diego Trough fault. A stress inversion of the focal mechanism data shows that the maximum principal stress determined from the focal mechanisms of the main shock and 22 aftershocks that occurred within 36 hours of the main shock, has an azimuth of S30° W plunging 18°. The maximum principal stress determined from 30 aftershocks that occurred from July 15 to October 2, 1986 has an azimuth of S20° W, plunging 18°. The $\phi$-values (the measure of the relative sizes of the principal stresses) are approximately 0.07 and 0.1, respectively, indicating that the intermediate and minimum principal stress are of similar magnitude. The results of the stress inversion and the focal mechanisms that showed reverse faulting suggest that the Inner Continental Borderland is not a pure-strike-slip tectonic regime but rather a strike-slip mixed with reverse faulting regime. When the 52 aftershock focal of the maximum principal stress, which is largest in the days following the main shock and decreases rapidly with time. The abundance of aftershocks may be related to the large temporal variation in stress orientation that in turn, may have resulted from the small stress drop of the main shock.

## PUBLICATIONS

Hauksson, E., Seismotectonics of the Newport-Inglewood Fault Zone in the Los Angeles Basin, Southern California, Bull. Seism. Soc. Amer., 77, 539-561, 1987.

Hauksson, E., L. M. Jones, T. L. Davis, L. K. Hutton, A. G. Brady, P. A. Reasenberg, A. J. Michael, R. F. Yerkes, P. Williams, G. Reagor, C. W. Stover, A. L. Bent, A. K. Shakal, E. Etheredge, R. L. Porcella, C. G. Bufe, M. J. S. Johnston, E. Cranswick, The 1987 Whittier Narrows Earthquake in the Los Angeles Metropolitan Area, California, Science, 239, 1409-1412, 1988.

Hauksson, E., T. L. Teng and T. L. Henyey, Near-Surface Atttenuation of Waveforms of Local Earthquakes: Results from a 1500 m Deep Downhole Seismometer Array, Bull. Seism. Soc. Amer., 77, 1883-1904, 1987

Hauksson, E., and L. M. Jones, The July 1986 Oceanside ($M_L$=5.3) Earthquake Sequence in the Continental Borderland, Southern California, submitted to Bull. Seism. Soc. Amer., 1988.

Hutton, K. L., L. M. Jones, E. Hauksson and D. G. Given, Seismotectonics of Southern California, Decade of North American Geology Neotectonics of North America, Geol. Soc. Amer. Ser., submitted August 1987.

Saldivar, G. V., E. Hauksson and T. L. Teng, Seismotectonics of the Santa Monica and Palos Verdes Fault Systems in the Santa Monica Bay, Southern California, to be submitted to BSSA, 1988.

Jones, L. M. and E. Hauksson, Preliminary Analysis of the 1987 Whittier Narrows Earthquake Sequence, submitted to Earthquake Spectra, 1988.

## REPORTS

Hauksson, E., Seismotectonics of the Newport-Inglewood Fault Zone and the 1933 Long Beach Earthquake ($M_L$ = 6.3) in the Los Angeles Basin, southern California. Seism. Res. Letters, 58, 14, 1987.

Hauksson, E. and T. L. Teng, Analysis of earthquake data from the greater Los Angeles basin and adjacent offshore area, southern California, Annual Technical Report submitted to the U.S. Geological Survey, March 1988, 60 pp.

Jones, L. M. and E. Hauksson, The Size and Location of the Next Great Southern California Earthquake: Implication of Constant Stress Drops, to be presented at EOS Trans., Amer. Geophys. Union, 68, 1349, 1987.

Hauksson, E. and L. M. Jones, The July 1986 Oceanside Earthquake Sequence ($M_L$ = 5.3) in the Continental Borderland, southern California, EOS Trans., Amer. Geophys. Union, 68, 1361, 1987.

Hauksson, E., L. M. Jones and L. K. Hutton, The 1987 Whittier Narrows Earthquake in the Los Angeles Metropolitan Area, California: Overview, Locations and Seismotectonics, EOS Trans., Amer. Geophys. Union, 69, 259, 1988.

Jones, L. M., E. Hauksson, L. K. Hutton, Spatial Variations in the Locations and Focal Mechanisms of Aftershocks of the 1987 Whittier Narrows Earthquake, Los Angeles County, California, EOS Trans., Amer. Geophys. Union, 69, 259, 1988.

Hauksson, E., Seismicity, Anticlines and Thrust Faults in the Los Angeles Basin: Implications of the Whittier Narrows Earthquake, submitted to the spring SSA meeting 1988.

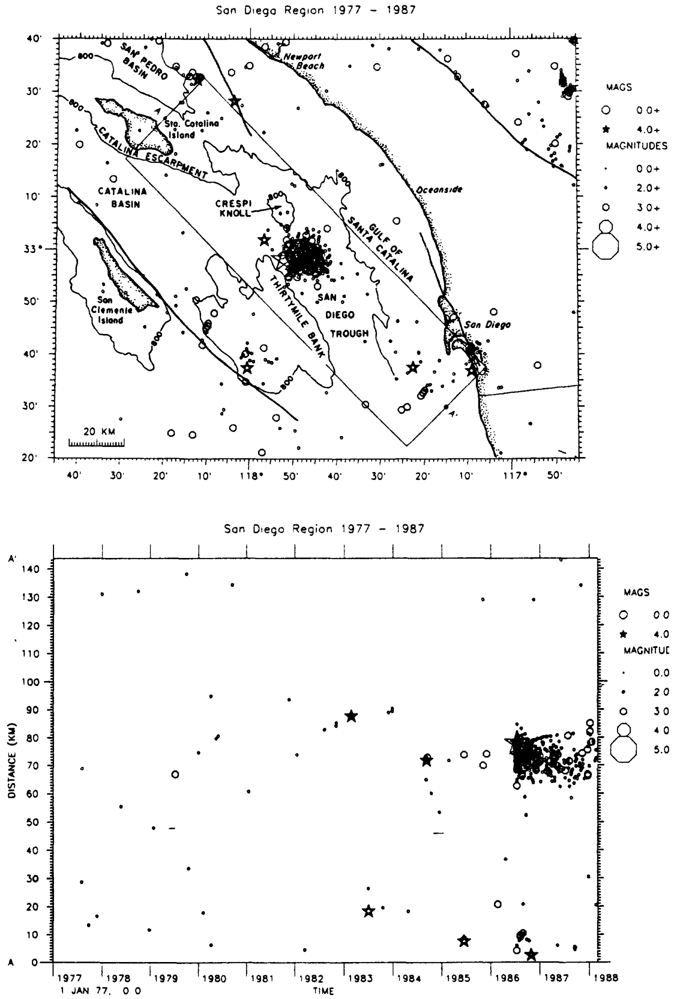

Figure 1. Seismicity from the CIT/USGS catalog in the Inner Continental Borderland and San Diego Region, southern California. (Top) the seismicity from January 1977 to February 1988. The 800 m bathymetric contour is also shown. Earthquakes located within the box A-A' are shown in a time-space plot below. Symbol size is scaled with magnitude and events of $M_L \geq 4.0$ are plotted as stars. (Bottom) time space plot showing level of activity before and after the $M_L$=5.3 Oceanside main shock.

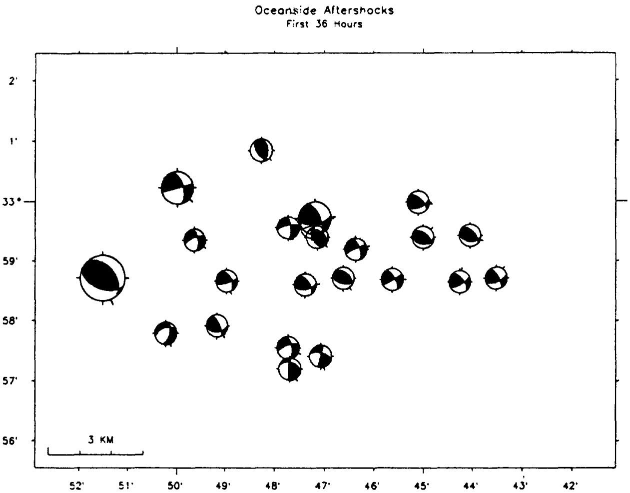

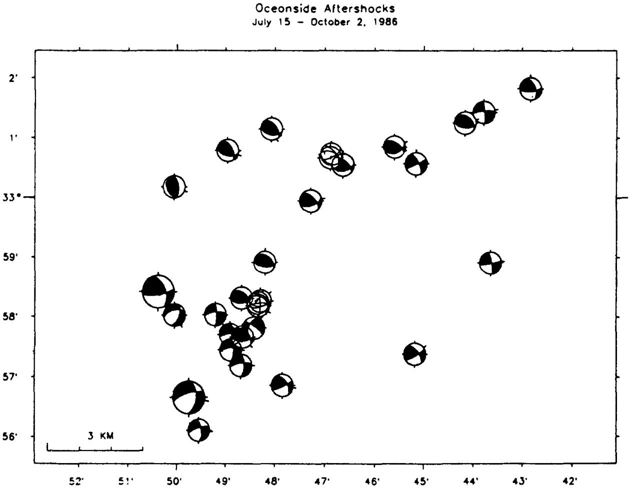

Figure 2. Single-event lower-hemisphere focal mechanisms for the Oceanside sequence. (Top) the main shock focal mechanism and focal mechanism of $M_L \geq$ 3.0 aftershocks recorded during the first 36 hours following the main shock. (Bottom) The focal mechanisms of the main shock and $M_L \geq$ 3.0 aftershocks from July 15 to October 2, 1986.

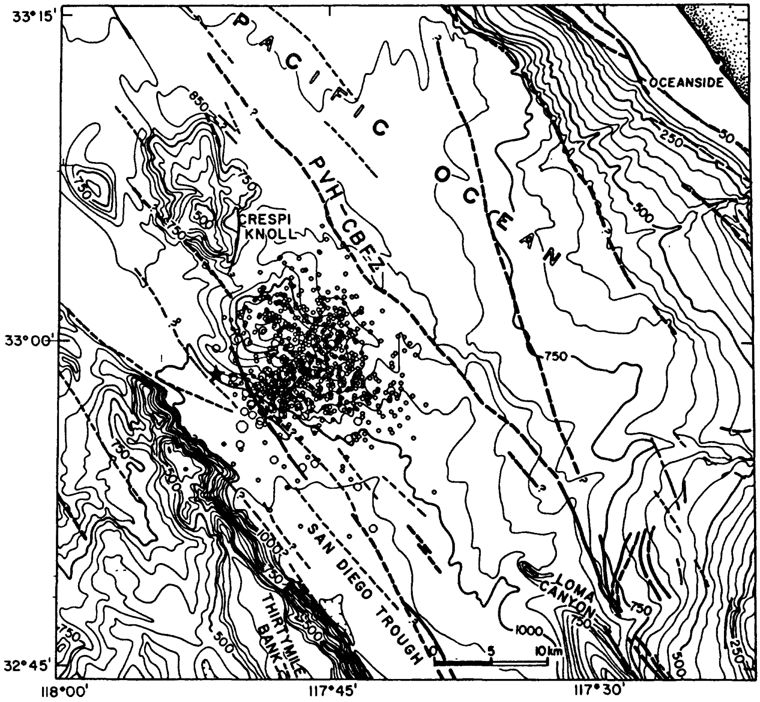

Figure 3. The main shock (shown as a star) and all aftershocks from July 1986 to April 1987 plotted on a bathymetric map of the study area. Offshore faults are from Clarke et al. (1988). PVH-CBFZ-Palos Verdes Hill-Coronado Bank Fault Zone. Faults with known Holocene offsets are plotted as thick lines. Inferred faults are shown as dashed lines.

# Seismic Source Characteristics of Western States Earthquakes

Contract No. 14-08-0001-21912

Donald V. Helmberger

Seismological Laboratory
California Institute of Technology
Pasadena, California 91125
(818) 356-6998

## Investigation

A study on the characteristics of pre and post- 1962 Western U.S. earthquakes is continuing with special emphasis on clusters. The study has begun with well recorded modern events (post-1962) and will proceed to (pre-1962) events later. Four major tasks will be addressed in this funding cycle. These tasks are:

1.) Extended analysis of low-gain recordings of earthquakes occurring in the Imperial Valley and Northern Baja; to fix the depths of main energy release (asperity concentration).
2.) Analysis of body waves at all ranges using direct inversion for fixed earth models, application of the intercorrelation method to measure differences between events and develop master events per region.
3.) Analysis of historic events (pre-1962) using the same methods (masters) but on a more regional basis.
4.) Reassessment of events with sparsely recorded strong motions using more accurate Green's functions computed from laterally varying earth models.

## Results

Although we planned to study historic earthquakes over this funding cycle, we keep having local earthquakes which has side tracked this activity. The most recent set occurring near the Superstition Hills, Imperial Valley, are particularily interesting; and will be reported on at the SSA (88) meeting. An abstract of this talk along with a summary of a recently completed paper on the Whittier event follow:

### a) The November 1987 Superstition Hills Earthquake and Comparisons with Previous Neighboring Events

We compare the teleseismic waveforms of the two November 1987 Superstition Hills earthquakes, subsequently referred to as EQ 1 and EQ 2, with previous events occurring in the region, namely the Imperial Valley and Borrego region. Because of the trade-offs in moment estimates due to upper mantle attenuation estimates and source strength, we have accepted the bodywave moments of $1.1 \times 10^{26}$ for the

1968 Borrego Mountain event and 5 x $10^{25}$ for the 1979 Imperial Valley event based on a relatively large number of investigations. Comparisons of observations at similar stations, as well as forward modeling attempts, yield moment estimates of 1.8 and 8.2 x $10^{25}$ separated by 7.5 seconds. The surface waves of EQ2, for the records that remain visible, appear to be stronger than predicted from the bodywave ratios, which is indicative of a low stress drop expanding rupture. The same set of events is compared on the strong motion records at Pasadena where complex events can be easily identified. The results are compatible with the teleseismic source parameter estimates. In particular, models of the PAS EQ2 record indicate 2 events separated by 7.5 seconds, the same as seen teleseismically. Although the second event is more subdued in amplitude, results imply that the two asperities are located near each other with a brief delay in energy release. Perhaps the first event of EQ2 is the mainevent and the second is an aftershock or the first event is a preshock.

### b) Source Complexity of the 1 October 1987 Whittier Narrows Earthquake

At long periods the Whittier Narrows earthquake can be modeled as a simple thrust event. The best fitting fault plane solution has a strike of 280°, a dip of 40°N and a rake of 98°. The focal depth is 14 km and the moment is $10^{25}$ dyne cm. When the short period data are also considered, the earthquake appears to consist of two events on subparallel faults separated in time by 1.2 seconds. The first has a strike of 250°, dip 30°N and rake 90°, occurred at a depth of 17 km and had a moment of .25 x $10^{25}$ dyne cm. The second source has a focal mechanism identical to that of the best fitting single source, but occurred at a depth of 11 km and had a moment of 1.3 x $10^{25}$ dyne cm. We believe that the Whittier Narrows earthquake was a double event because both short and long period body waves at all distances can be well modeled by a double event, the short period data cannot be modeled as a simple event and the long period synthetics are improved by a double source. The source parameters are well constrained due to the number of stations and phases modeled. Attempts to determine the stress drop were inconclusive due to the difficulty in exactly defining the area of the fault plane. Using the total aftershock area and long period results, we obtain an overall stress drop of 682 bars for the double source. Using the asperity area and the short period results we obtain a stress drop of 608 bars for the first event and 578 bars for the second. We can conclude that this was a high stress drop event even though we cannot get an exact value for the stress drop. Many good, but complex, strong motion records of this event were recorded in the Los Angeles area. The results obtained in this study should be useful as a starting point in modeling the strong motion records.

# Earthquake Source Parameters Using Regional Seismic Network Data: Application to California and Eastern United States

14-08-0001-G1391

Robert B. Herrmann
Department of Earth and Atmospheric Sciences
Saint Louis University
P.O. Box 8099 Laclede Station
St. Louis, MO 63156
(314) 658-3131

## Goals

1. Perform research on the earthquake process in the New Madrid Seismic Zone to delineate the active tectonic processes.
2. Perform more general research relating to the problems of the eastern U. S. earthquake process and of the nature of eastern U. S. earthquakes compared to western U. S. earthquakes.

## Investigations

1. A draft paper on the southeastern Illinois earthquake of 10 June 1987 has been prepared. The paper reviews historical and regional seismicity in the epicentral area, provides a surface-wave based focal mechanism for the main event, and a study of regional tectonics based on an analysis of 10 years of regional seismic network data. A section on aftershock distribution will be provided by co-authors from Indiana University, Memphis State University and the USGS.
2. A paper on the importance of Q corrections for Lg source spectrum estimates is under significant revision. The conclusions are that Lg data can be used to estimate the seismic moment and corner frequency of the source if Q corrections are applied. The results are compatible with short distance S-wave and teleseismic P-wave estimates for the region.
3. A rough draft of a paper on the surface-wave analysis and modeling of strong motion data from the January 31, 1987 northeastern Ohio earthquake.
4. Numerical simulation of long period ground motion at the cities of Chicago, Illinois and Atlanta, Georgia has been performed for a hypothetical $M_W = 7.5$ earthquake in the New Madrid seismic zone. Ground motion response spectra are estimated in the period range of 0.5 - 20 seconds.

# Tectonics of Central and Northern California

9910-01290

William P. Irwin
Branch of Engineering Seismology and Geology
U. S. Geological Survey
345 Middlefield Road
Menlo Park, CA 94025
(415) 329-5639

## Investigations

1. Preparation of a reconnaissance geologic map of the Pilot Creek 15-minute quadrangle, Humboldt and Trinity Counties, California.

2. Compilation of a geologic map of the Klamath Mountains and adjacent areas in northwestern California and southwestern Oregon for purposes of tectonic analysis.

3. Study of distribution of radiolarian-bearing chert deposits in the California Coast Ranges as a possible means of determining regional tectonic dislocations.

## Results

1. The reconnaissance geologic map of the Pilot Creek quadrangle was prepared in collaboration with K. R. Aalto of Humboldt State University and H. M. Kelsey of Western Washington University. The quadrangle straddles the South Fork fault which forms the boundary between the Coast Ranges to the southwest and the Klamath Mountains to the northeast. The Coast Range portion of the quadrangle is composed of South Fork Mountain Schist and Franciscan rocks, and the Klamath mountains portion includes Galice Formation and Rattlesnake Creek terrane. In addition to the South Fork fault, the Coast Range portion of the quadrangle contains other major fault and shear zones including the well-known Grogan fault. The map is planned for an Open -File report and is now in Branch review.

2. Compilation of the geology of the various source maps of the Klamath Mountains (scale 1:500,000) and preparation of the peripheral explanatory material has been completed. The map is planned for publication in the Miscellaneous Geologic Investigations map series and is now in Branch review.

3. Samples of radiolarian chert have been collected from the main exposures of Franciscan rocks in the central and southern coast ranges for the purpose of extending and refining the known distribution of the Lower Jurassic chert. The Lower Jurassic chert, which is the oldest paleontologically dated rock of the Franciscan assemblage, has previously been paid scant attention, but its pattern of distribution may possibly provide important information relating to large tectonic dislocations of the Franciscan rocks on either side of the Salinian block. The study is in collaboration C. D. Blome and M. J. Rymer. Progress has been slowed by a delay in processing of the chert samples.

## Reports

Mankinen, E. A., Irwin, W. P., and Gromme, C. S., 1988, Paleomagnetic results from the Shasta Bally plutonic belt in the Klamath Mountains province, northern California: Geophysical Research Letters, v. 15, no. 1, p. [illegible]6-59.

Schweickert, R. A., and Irwin, W. P., 1988, Extensional faulting in the southern Klamath Mountains, California: Submitted to Tectonics.

04/88

# Seismicity Patterns and the Stress State
# in Subduction-Type Seismogenic Zone

Grant Number 14-08-0001-G1368

Carl Kisslinger
Cooperative Institute for Research in Environmental Sciences
Campus Box 449, University of Colorado
Boulder, Colorado 80309-0449
(303) 492-6089

Research during November, 1987 to April, 1988 was focused on the following tasks: (1) a re-examination of the teleseismic seismicity prior to the May 7, 1986 Andreanof Islands earthquake as one means of verifying the quiescence in the local data on which the prediction of a strong earthquake in this region had been based; (2) investigation of the distribution of the aftershocks in space and time in order to relate this activity to the pre-event patterns and the details of the rupture processes during the main shock; (3) search for changes with time of seismic velocitites, Q, and earthquake characteristics by the analysis of earthquake doublets.

## Teleseismic Seismicity before May 7, 1986

During the prediction phase preceding the May 7 earthquake (1983-1985), the seismicity distribution in the region monitored by the Adak network, as manifested by the teleseismic solutions in the PDE reports, had been examined in an attempt to verify that the quiescence that was seen in the local data set was genuine. The use of the PDE catalog for this purpose is limited by inherent problems. First, the number of events within small geographical regions in short time intervals is small, so that statistically significant variations in occurrence rates can rarely be isolated. The number is further reduced by the need to apply a lower magnitude cutoff to the catalog in order to obtain a homogeneous data set. Another difficulty for this particular application is the systematic mislocation of PDE hypocenters in the central Aleutians because of plate effects that are neglected in the routine location procedure. An approximate correction for mislocation had been made in the earlier work. A third problem is the standard uncertainty in the magnitudes routinely determined, which is ± 0.3 to 0.4 units. The conclusion of the earlier analysis was that the teleseismic data did not contradict the strong quiescence seen in the Center subregion of the Adak zone, but that these data alone did not establish a rate change that would have been accepted as an anomaly in the absence of the local network data.

As part of his study of the seismicity and seismotectonics of the central Aleutians, E.R. Engdahl, USGS, carefully relocated all events from January, 1964 through April, 1987 for which adequate teleseismic data exist. His methods remove the plate effects and have produced the most reliable catalog for this region that is likely to be available for a long time. In addition, he introduced a method for improving the screening of events by size in which the reported body wave magnitude and the number of stations reporting the event are combined. An analysis of the number-of-stations vs. magnitude data, some of which was done as part of this project, showed that a criterion requiring both a magnitude greater than or equal to 4.3 and a minimum of 15 reporting stations yielded a catalog with a reliable minimum magnitude of 4.6. Similar combinations can be used to establish higher cutoffs, for example 4.7 and 75 stations gives a real cutoff of 5.0.

His revised catalog, with the new locations and a cutoff of 4.6 as defined above, was analyzed according to the same subregions used in the original prediction experiment. The inherent problem of small numbers remains, of course. The results, shown in Figure 1, again show a marked decrease in activity in the Central region, but not in the adjacent subregions. This catalog, which covers the Aleutian arc from 179.5 ° W to 172 ° W, permitted an examination of the behavior of seismicity in the eastern part of the May 7, 1986 rupture. This part of the seismic zone is not monitored by the network. As seen in Figure 1, the activity levels in the eastern part of the zone are lower than in the region near Adak. The West Atka subregion contains the epicenter of the May 7 mainshock. The complete cessation of activity at magnitude 4.6 and greater from mid-1981 to late 1984,and the increase in activity rate up to the time of the mainshock is seen. There is no suggestion of quiescence in the teleseismic data in the part of the rupture zone east of the epicentral region.

## Aftershocks of the May 7, 1986 Earthquake

The time and space distribution of the aftershocks has been analyzed from both the Engdahl teleseismic catalog and the local data for the first seven days after the event. This analysis has revealed a number of interesting features which will be described in a paper by Engdahl, Billington, and Kisslinger that is in the last stages of preparation. The teleseismic sequence fits the Modified Omori relation well out to the beginning of March, 1987, as seen in Figure 2. The decay constant, p, is 0.880 when the entire aftershock zone is included.

The segments of the fault east and west of the epicenter were also analyzed separately (Figure 2, lower part) . For the segment west of the epicenter, the part monitored by the local network, p=0.831. However, the eastern segment, with a late surge in March - April 1987 excluded, had a much higher decay rate, 1.12. This is also a normal value, but the substantial difference in the two parts of the rupture plane indicates a difference in either the fault zone properties or the stress distribution following the main shock. Most of the moment release in the event occurred in the western segment. In March and April, 1987, a surge of activity at the easternmost extremity of the rupture zone, apparently a late extension of the aftershock zone. caused the sequence to rise significantly above the rate predicted by the Modified Omori fit.

Both the early local data and the teleseismic sequence show a concentration of aftershocks in the Center region. This is the segment of the thrust zone that was by far the most active in the microearthquake catalog prior to mid-1982, that showed the sharpest and most persistent quiescence, and where the greatest moment release took place during the main event. A physical connection of quiescence, earthquake occurrence, and pattern of moment release is strongly suggested. It is not possible with existing data to resolve the locations well enough to determine if these aftershocks actually took place on the surface of rupture of the main event or in the material on either side of this surface, as has been suggested by others.

The results demonstrate the value of the frequency -linearized - time plot for isolating intervals of activity that depart from the Modified Omori relation. With many hundreds of events to examine, this tool helps identify groups of particular interest.

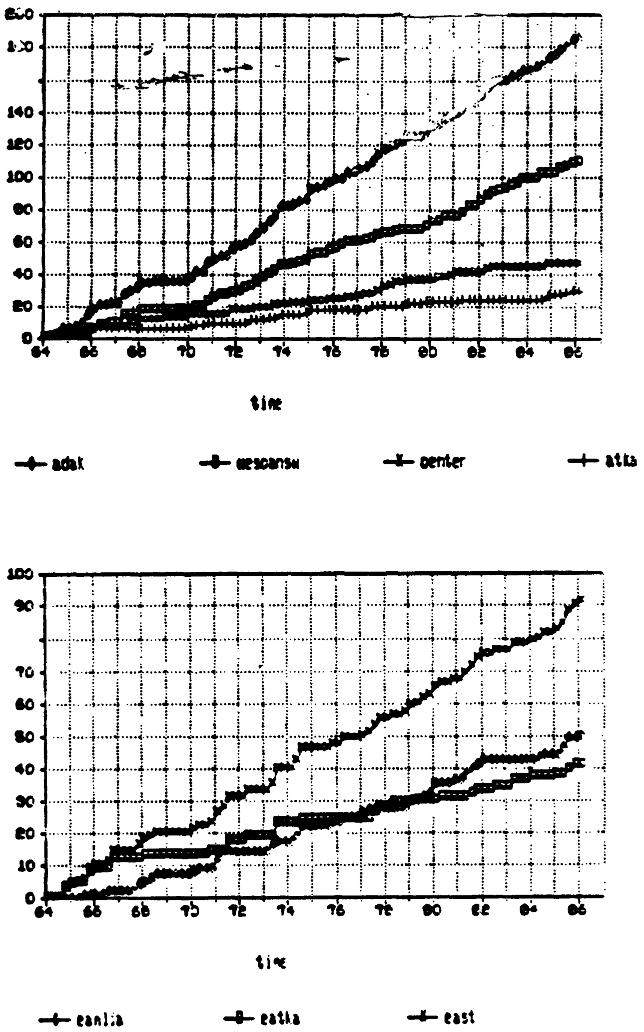

Figure 1. Cumulative number of independent earthquakes (swarms and aftershocks removed, 1964 - May 6, 1986. Engdahl revised catalog, $m_b$ – 4.7, depth less than 100 km.

Top: Adak zone, 174.82 - 178.46 ° W (260 km), the segment monitored by the Central Aleutians Network. Subregions are: Wescansw = 176.50 - 178.46 ° W (140 km), Center = 175.38 - 176.50 ° W (80 km), Atka 174.82 - 175.38 ° W (40km).

Bottom: East zone, 172.0 - 174.82 ° W (197 km). Subregions are:

Eatka = 173.5 - 174.84 ° W (92 km), Eamlia = 172.0 - 173.5 ° W (105 km)

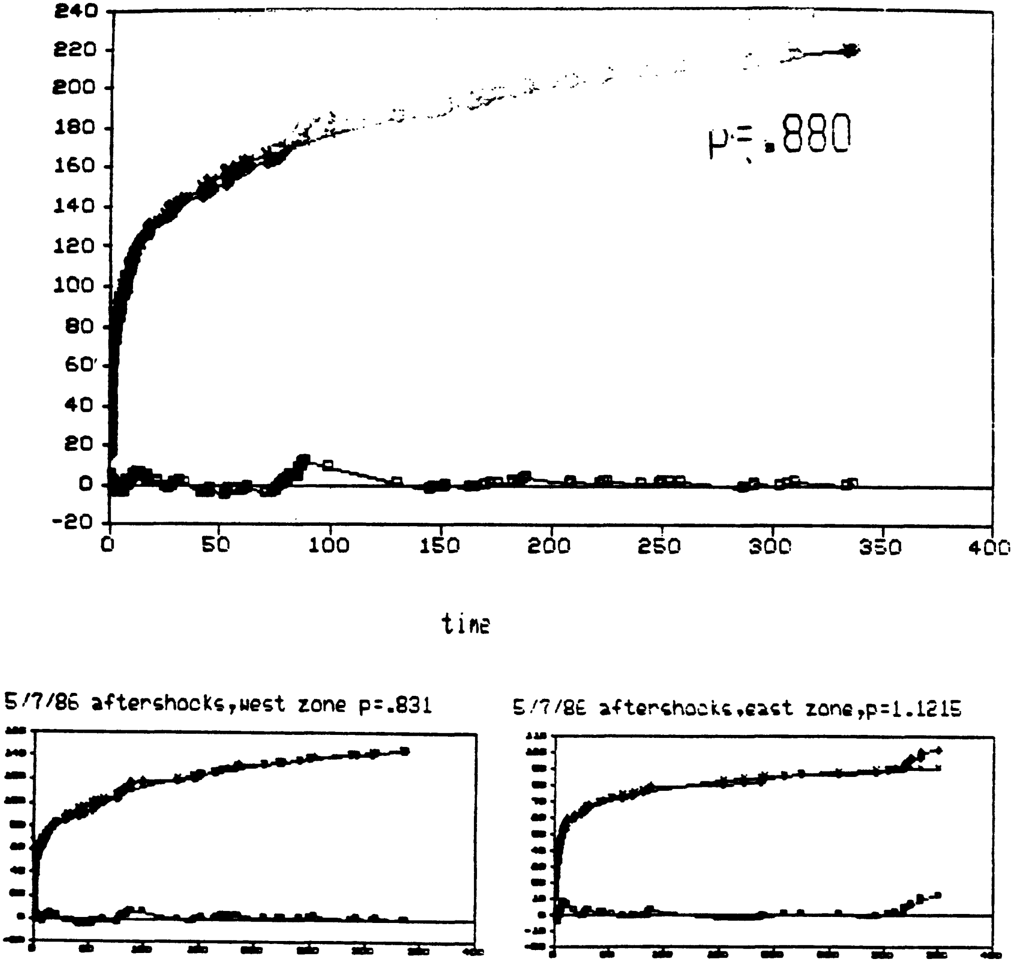

Figure 2. Cumulative number of aftershocks of the May 7, 1986 earthquake vs. time, to the end of April, 1987. Time in days after the main shock. The best fitting Modified Omori curve, with the p-value is also plotted, along with the departures of the data from this curve. $m_b \geqslant 4.6$, depth less than 100 km. From Engdahl revised catalog.

Top: Data for the whole zone, 173.86° W to 178.5° W.

Bottom: data for the segments of the aftershock zone west and east of the epicenter of the mainshock. The data for the eastern segment were analyzed with out the surge of activity at the eastern boundary in March-April, 1987, but these events are plotted to show the marked increase above the projected rate.

## Analysis of Earthquake Doublets

The first objective of this study is to determine if the change in the stress distribution resulting from the May 7, 1986 earthquake caused detectable changes in seismic wave velocities. In particular, we are looking for anisotropic velocity changes that may have been caused by the changes in deviatoric stress or by crack formation. M. Biot and A. Nur have shown that a change in stress can cause velocity anisotropy.

If two earthquakes occur at or very close to the same location, the seismograms produced by them at any one station should be identical except for amplitude if there are no changes in properties along the propagation path between the times of the two events. Such pairs are called doublets. Velocity changes between the events will cause a relative expansion or contraction of the time intervals between arrival of phases on the seismograms. The measurement of these relative time differences provides a very accurate method of detecting velocity changes. The availability of digital seismograms for many hundreds of earthquakes that have occurred in the region affected by the May 7 earthquake provides an opportunity to make these measurements.

The necessary software has been assembled and the method tested. The major source of error was found to be long-term speed variations in the magnetic tape record/playback system. Although negligible for most seismological analyses, this time drift, usually of the order of tens of milliseconds over many months, is well within the threshold of detection by this method. A correction can be made for this drift, because the time code recorded with the seismic data is subject to the same drift (absolute time as read on record is not affected). After processing to remove the different pulse widths used to encode day, hour, and minute, the seconds pulses on the time code channels of the two seismograms to be compared are cross-correlated and the relative time drift due to tape speed variations measured. After the time drift is removed from the data, time differences between corresponding phases in a doublet can be interpreted as due to physical changes in the medium that have occurred between the times of the two events.

In order to reduce the large data base available to manageable numbers of event pairs, attention has been directed to four small rectangular areas, shown in Figure 3. The areas were selected because they experienced either dense concentrations or an absence of aftershocks of the May 7 mainshock. The identification of doublets is a time-consuming task. Suitable doublets have been identified in one of the areas. An example of the seismograms from one doublet is given in Figure 4, along with the time delays remaining after the drift correction has been applied. Events occurring close in time are beng analyzed to test the resolution and stability of the method. Other pairs widely separated in time, in some cases both before the main shock, in other cases spanning the mainshock, will be analyzed. In this way both velocity changes that may have preceded the mainshock and those that may have resulted from it will be sought.

## Publication

Kisslinger, C., An Experiment in Earthquake Prediction and the 7 May 1986 Andreanof Islands Earthquake, *Bull. Seism. Soc. Amer., 78:* 218-229, 1988.

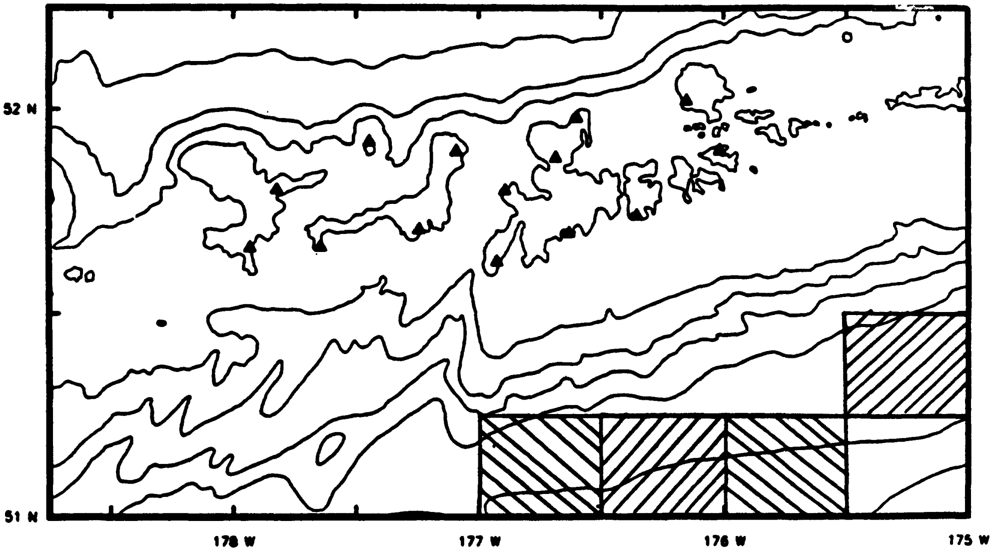

Figure 3. Map of the Adak seismic zone, showing the four areas selected for the doublet analysis.

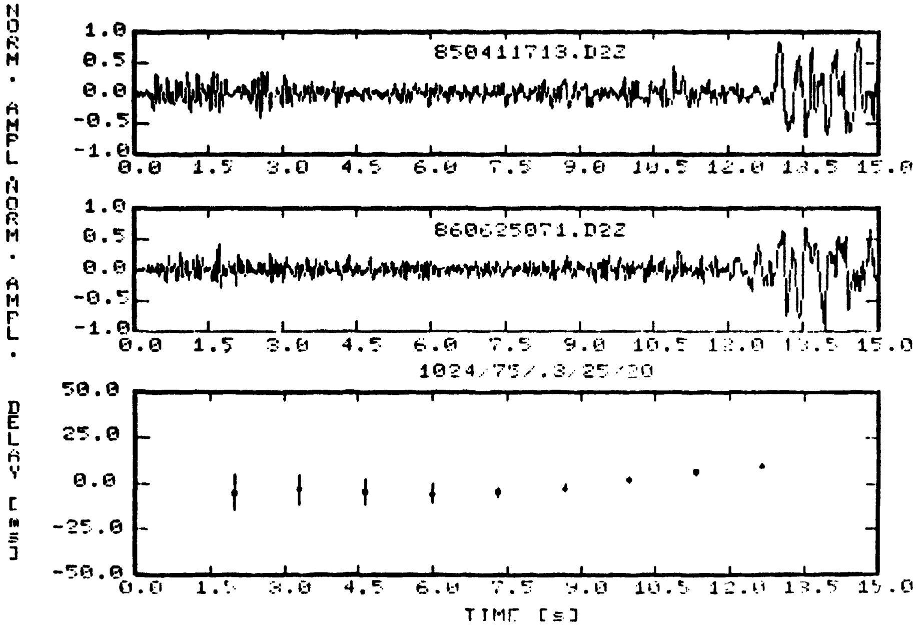

Figure 4. Two events at the same location, one before and one after the May 7, 1986 earthquake.

From top to bottom: the vertical component seismograms at station AD2 from an event on April 11, 1985; the same for an event on June 25, 1986; the calculated delay times as a function fo running time along the seismograms. The delay times have been corrected for long-term tape speed variations.

# Seismological Field Investigations

9950-01539

C. J. Langer
Branch of Geologic Risk Assessment
U.S. Geological Survey
Box 25046, MS 966, Denver Federal Center
Denver, CO 80225
(303) 236-1593

## Investigations

1. Laramie Mountains, Wyoming, postearthquake study--local investigation of aftershocks resulting from the $m_b$ 5.4 earthquake of 18 Oct 84.

2. Study of Q along the Wasatch Front, Utah.

## Results

1. Forty-seven aftershocks, one regional event, and two local blasts were located from data obtained during eleven days of portable instrument operation surrounding the main shock ($m_b = 5.4$; $M_O = 1.1 \times 10^{24}$ dyne-cm; 42.375° N. lat., 105.20° W. long.; depth >21 km). Eighty-seven percent of the aftershocks fit in a tight pattern roughly 3 1/2 km long by 3 km wide. Their focal depths are between about 21 and 25 km. Using the above aftershock volume measurements and $M_O$ gives an estimated maximum fault displacement of about 35 cm and a stress drop for the main shock of about 140 bars. Focal mechanisms (main shock and single-event solutions for the aftershocks) indicate east-northeast right lateral strike slip or north-northwest left lateral strike slip on near-vertical fault planes. The "T" axes are subhorizontal, striking roughly N. 25° E.

2. A data set of 108 digitally recorded earthquakes that occurred during 1984-1985 in northern Utah has been processed to evaluate the geometric and anelastic attenuation parameters that control short-period peak amplitudes south along the Wasatch Front. The earthquakes were detected and recorded by the University of Utah seismograph network and the data processing was conducted by Stan Brockman at the USGS facility in Golden. We applied a technique similar to that used by Rogers and others (1987) in determining Q for the southern Great Basin, but our preliminary results are vastly different. The southern Great Basin Q model is reported by Rogers and others (1987) as $Q(f) = 774\ f^{0.04}$ (essentially no frequency dependence, $3 \leq f \leq 10$ Hz); our indicated Wasatch Front Q model is approximately $Q(f) = 110\ f^{0.69}$ ($1.0 \leq f \leq 10.0$ Hz) which is reasonably consistent with what Chavez and Priestly (1986) determined for the Great Basin as a whole, $Q(f) = 206\ f^{0.68}$ ($0.3 \leq f \leq 10.0$ Hz), and very close to Nuttli's (1986) model ($Q(f) = 139\ f^{0.6}$) for the Great Basin.

## References:

Chavez, D.E., and Priestley, K.F., 1986, Measurement of frequency dependent $L_g$ attenuation in the Great Basin: Geophysical Research Letters, 13, 551-554.

Nuttli, D.W., 1986, Yield estimates of Nevada Test Site explosions obtained from seismic $L_g$ waves: Journal of Geophysical Research, 91, 2137-=2151.

Rogers, A.M., Harmsen, S.C., Herrmann, R.B., and Meremonte, M.E., 1987, A study of ground-motion attenuation in the southern Great Basin, Nevada-California, using several techniques for estimates of $Q_s$, log $A_o$, and coda Q: Journal of Geophysical Research, 92, 3527-3540.

## Reports

Langer, C.J., Powers, P.S., Johnston, A.C., and Bollinger, G.A., 1987, The magnitude 5.1 Olney, Illinois, earthquake of 10 June 1987: Preliminary results from locally recorded data [abs.]: Seismological Research Letters, 58, p. 100.

Langer, C.J., Powers, P.S., Johnston, A.C., and Bollinger, G.A., 1987, The Olney, Illinois, earthquake of 10 June 1987--A preliminary report: U.S. Geological Survey Open-File Report 87-623, p. 1-23.

# Hayward Fault

9910-04191

J. J. Lienkaemper
Branch of Engineering Seismology and Geology
U.S. Geological Survey
345 Middlefield Road, MS 977
Menlo Park, California 94025
(415) 329-5642

## Investigations

Determine slip rates and earthquake recurrence intervals on the Hayward fault. Compare geologic surface-slip rate to historic creep rates and geodetically determined deep-slip rate. Analyze effects of structural complexity and fault segmentation upon how recurrence may be inferred from slip rate.

## Results

1. Trenching near Fremont Civic Center 1986-1987 yielded a slip rate of 5.5 ± 0.5 mm/yr for the the last 8040 yr from an offset buried channel unit. Manuscripts for open-file release of the data are now completed and in review [Borchardt et al., 1987; Borchardt et al., 1988a; Borchardt et al., 1988b]. Laboratory results on paleomagnetic samples have not arrived yet.

2. Offset cultural features near the Fremont trench site indicate creep rates of 5.3 to 5.4 mm/yr over the last 2 to 3 decades in the central part of the Niles alluvial cone. Thus it appears that long-term slip rate and creep rates are equal here. The Hayward fault makes a right jog of a few hundred meters across this area. To the south, cultural features indicate creep rate of ~9 mm/yr since ~1920 (Lienkaemper and Borchardt, unpub. data, 1987). This greater creep rate (i.e. 9 > 5.5 mm/yr) may reflect the full rate of slip on the Hayward fault below seismogenic depths. It thus appears the right jog across Niles Cone either acts as a barrier to slip or causes deformation to distribute in some unknown way. South of Warm Springs district in Fremont no Quaternary fault zones or fold structures have been identified that seem to be either independently or collectively capable of 9 mm/yr geologic slip rate. Preliminary geomorphic and structural inspection of the Mission Fault suggests minor slip rate despite its distinct subsurface connection to both Calaveras and Hayward faults as observed in microseismicity.

3. A potential 18-km-long gap in high creep rate exists on the Hayward fault in the Oakland area. We have identified minor creep in the Knowland Zoo area, but search northward to the Caldecott tunnel reveals no distinct evidence of creep. We intend to begin rigorous monitoring of creep in the Oakland gap (?) in co-operation with other projects and agencies this year to determine if surface slip actually lags behind the 5.5 mm/yr observed along most of the Hayward fault. If creep is nil in this segment, then this area becomes one of the most likely places in the S. F. Bay Region to experience a large, damaging earthquake.

## Reports

G. Borchardt, J. J. Lienkaemper, D. P. Schwartz, 1987, Holocene slip rate of the Hayward fault at Fremont, California (abstract): *EOS Trans. AGU, 68,* 1506.

G. Borchardt, J. J. Lienkaemper, K. Budding, and D. P. Schwartz, in review, Holocene slip rate of the Hayward fault, Fremont, *California: Calif. Div. Mines Geol. Open-File Report.*

G. Borchardt, J. J. Lienkaemper, and D. P. Schwartz, in review, Soil development and tectoturbation in a catena produced by Holocene downwarping along the Hayward fault, Fremont, California: *California: Calif. Div. Mines Geol. Open-File Report.*

# San Andreas Fault Slip Near Cholame, California

9910-04192

J. J. Lienkaemper
Branch of Engineering Seismology and Geology
U.S. Geological Survey
345 Middlefield Road, MS 977
Menlo Park, California 94025
(415) 329-5642

## Investigations

1. Surface slip along the San Andreas fault near Parkfield, California.
2. 1857 slip on the San Andreas fault near Cholame, California.

## Results

1. We completed the Parkfield slip manuscript [*Lienkaemper et al.,* in review]. Surface slip in characteristic Parkfield earthquakes reaches ~35 cm in the central segment of the 1966 rupture, and is ~15 cm both north of Middle Mountain and south of Gold Hill. We present a dislocation model of the entire ~44-km-long by ~13-km-deep 1966 rupture surface. We infer a long, narrow asperity near 5~7 depth between Middle Mountain and Gold Hill from 1966 aftershock distribution, and use our surface-slip data to constrain slip beyond the asperity. Slip on such an asperity of 65 ± 10 cm fits coseismic geodetic line-length changes well. This amount of slip can be reloaded on the asperity at deep-slip rates of 30 ± 5 mm/yr in a 21.9-yr Parkfield earthquake cycle. The inferred size of the asperity 2.7 km by 26.4 km gives a moment 1.4 x $10^{25}$ dyn-cm in good agreement with long-period teleseismic moments.

2. Two large southern California earthquakes occurred in late 1987: Whittier (Los Angeles County), Oct. 1, $M_s$5.6, and Superstition Hills (Imperial County), Nov. 24, $M_L$6.3. Several weeks were spent in field investigation, analyzing and reporting these events during a period that had been scheduled for completing field investigations in Cholame.

Results of a detailed reconstruction of an especially distinct (in 1966) stream channel probably offset in 1857 were reviewed for publication [*Lienkaemper and Sturm,* in revision]. I presented a summary of the overall 1857 slip investigation [*Lienkaemper,* 1987]. My conclusions remain essentially unchanged since reported in the last semi-annual report. I believe 1857 slip between Cholame and Bitterwater Valley probably averaged 6 ± 2 m. Preservation of channel offsets is generally poor. Nevertheless, it is clear that 1857 slip here was greater than the 9 m observed in Carrizo Plain, but most probably larger than the 3-4 m slip plateau of *Sieh and Jahns* [1984]. This 3-4 m slip was the basis of *Sieh and Jahn's* forecast of a M7 Cholame earthquake to accompany the next moderate Parkfield earthquake. Although, I believe such a large event is possible; my slip data suggest that its likelihood cannot be considered either large or distinct.

## Reports

Lienkaemper, J. J., 1987, 1857 slip on the San Andreas fault southeast of Cholame, California (abstract): *EOS Trans. AGU, 68,* 1345.

Lienkaemper, J. J., and T. A. Sturm, reviewed, Reconstruction of channel offset in 1857(?) on the San Andreas fault near Cholame, California: Bull. Seismol. Soc. Am. [in revision].

Lienkaemper, J. J., W. H. Prescott, and J. D. Sims, in review, Surface slip along the San Andreas fault near Parkfield, California: *J. Geophys. Res.*

## References

Sieh, K. E., and R.H. Jahns, 1984, Holocene activity of the San Andreas fault at Wallace Creek, California: *Bull. Geol. Soc. Am., 95,* 883-896.

# EARTHQUAKE LIQUEFACTION: SOUTH CAROLINA, VIRGINIA, WASHINGTON

9950-03868
Stephen F. Obermier
Branch of Geologic Risk Assessment
MS 926, National Center
Reston, Virginia 22092
(703) 648-6791

9510-01343
Gregory S. Gohn
Branch of Eastern Regional Geology
MS 926, National Center
Reston, Virginia 22092
(703) 648-4382

## Investigations

A search was continued for liquefaction features in the vicinities of Charleston, southeastern South Carolina, and Savannah. In the Charleston area, the search was for 1886 features whose source sands could be tested to back-calculate shaking severity of the 1886 earthquake and to determine geologic and engineering controls on surficial development of liquefaction. In areas far from Charleston, the search was for pre-historic liquefaction features.

Six sites of 1886 liquefaction were tested in the field (using cone penetration or standard penetration tests) by researchers from Virginia Polytechnic Institute; many sites with no liquefaction were also tested.

Geologic and structure contour maps were drafted for the Summerville, Summerville NW, Ridgeville, and Pringletown 7.5 minute quadrangle.

## Results

In extreme eastern Georgia, near Savannah, no liquefaction features have been discovered. Thus, it would appear that the possibility of strong Holocene earthquake shaking in that area is quite low.

The liquefaction caused by the 1886 earthquake that was farthest from the epicentral region developed only in exceptionally loose sands. This implies that far from the epicenter, exceptionally low near-surface accelerations produced many of the liquefaction-related earthquake effects.

A manuscript has been completed which describes characteristics of earthquake-induced liquefaction features and characteristics of nonseismogenic features that might be confused with the earthquake-induced features. These characteristics are described in both the coastal setting of South Carolina and fluvial setting of the New Madrid seismic zone.

## Reports

Obermeier, S. F., Weems, R. E., Jacobson, R. B., and Gohn, G. S., in press, Liquefaction evidence for repeated Holocene earthquakes in the coastal region of South Carolina, New York Academy of Sciences.

Weems, R. E., Jacobson, R. B., Obermeier, S. F., and Gohn, G. S., 1988, New radiocarbon ages from earthquake-induced liquefaction features in the lower coastal plain of the Carolinas, Geological Society of America Abstracts with Programs, Southeastern Section, v. 20, no. 4, p. 322.

# EARTHQUAKE RESEARCH IN THE EASTERN SIERRA NEVADA- WESTERN GREAT BASIN REGION

Contract 14-08-0001-G1524, October 1987

W.A. Peppin, M.K. Savage, U.R. Vetter, J.N. Brune, and K.F. Priestley
Seismological Laboratory
University of Nevada
Reno, NV 89557
(702) 784-4975

## Investigations

This program supports continued studies with research focused on: (1) seismicity in proposed seismic gaps; (2) magmatic processes in Long Valley Caldera; (3) relocations of Mammoth Lakes earthquakes; (4) focal mechanisms and stress distribution: (5) analysis of digital waveforms. Some of the new results are described below.

## Results

### *Seismicity in and near seismic gaps*

Several investigators, beginning with A.S. Ryall and R.W. Wallace have identified two regions along the west-central Nevada seismic zone as likely locations for the next major western Great Basin earthquake (**Figure 1**). One of these, the *Stillwater gap*, lies between the rupture zones of the 1915 Pleasant Valley and 1954 Dixie Valley - Fairview Peak earthquakes; the other, the *White Mountains gap*, lies between the rupture zones of the 1932 Cedar Mountain and 1872 Owens Valley earthquakes. Previous reports have discussed the White Mountains gap and quantified specific features upon which the next major event is likely. **Figure 1** shows a map of recent seismicity together with outlines of the historic ruptures and the locations of the seismic gaps. Of note is the recent burst of activity within the Stillwater gap, wherein very few earthquakes have been previously observed. This pattern suggests a possible impending earthquake following the pattern observed by Ryall (1977 BSSA p 512). A microseismicity study is planned for this region in the summer of 1988 to attempt to characterize this renewed seismicity in detail. This seismicity was part of a general increase of seismicity throughout Nevada in 1987.

The pattern of seismicity preceding the 1986 Chalfant sequence suggested impending activity within the White Mountains Gap; three-component digital event recorders were deployed right over the sources of the two principal early shocks. A shallow cluster of activity near the town of Mina, Nevada, during July and August of 1987, also generally within the White Mountains seismic gap and the Walker Lane, was similar to the foreshocks of the Chalfant sequence, and digital instrumentation was again deployed in anticipation of a larger event, which was not forthcoming. However, the added instrumentation improved the hypocentral determinations and focal mechanisms of the Mina swarm, which should provide a better understanding of the tectonic involvement of the Walker Lane structure. Manuscripts have been submitted on this work (see below).

A field experiment was conducted in the vicinity of Station SLK to determine apparent velocity and particle-motion characteristics of a pre-S phase seen at that station. A small-dimension array was set up and the phase was seen for three earthquakes. Very precise timing calculations now underway will be reported at the spring SSA meeting. Preliminary results indicate that: (1) the phase has characteristics characteristics similar to those reported by Zucca and others (1987, BSSA p 1674), and (2) the phase cannot be a deep reflection

# Discrimination of Space-Time Clustering in Central California Earthquake Sequences

14-08-0001-G1533

Gary L. Pavlis, Michael W. Hamburger, and Mariana Eneva
Department of Geology, Indiana University
Bloomington, IN 47405
(812) 335-5141

## Investigations

This report reflects work on a newly supported NEHRP research project to investigate spatial and temporal distribution of earthquakes in four seismically active areas in central California. The project is an extension of a previous study of the earthquake distribution within the area of the 1984 Morgan Hill, California aftershock sequence. A technique based on pairs of earthquakes is used to quantitatively evaluate the nonrandomness in the spatial and temporal distribution of earthquakes. The present project features an investigation of the finer-scale spatial clustering of the events in this area, as well as a similar study in the areas of: 1) the 1979 Coyote Lake aftershock sequence; 2) the 1983 Coalinga aftershock sequence; and 3) the creeping segment of San Andreas fault near Hollister, characterized by high microearthquake activity (Figure 1). This will allow comparisons to be made of seismicity patterns in similar and contrasting tectonic settings.

## Results

*Pair Analysis Method.* We use distributions of earthquake pairs to study nonrandomness in spatial and temporal distribution of seismic events. A related approach, called the method of second-order moments, has been applied by Kagan and Knopoff (1980) and Reasenberg (1985). Pair analysis allowed us to show that the spatial distribution of the aftershocks of the 1984 Morgan Hill earthquake is nonrandom (Eneva and Pavlis, 1985), as well as to quantitatively evaluate the degree of this nonrandomness (Eneva and Pavlis, 1986). We have been applying similar ideas in the study of the seismicity in Soviet Central Asia (Eneva et al., 1987; Eneva and Hamburger, 1987).

Our work on the 1984 Morgan Hill aftershock sequence (Eneva and Pavlis, 1988) examined the nonrandomness in the spatial and temporal distribution of earthquakes in the Morgan Hill area by comparing observed distributions of interevent distances and times with simulated expected distributions. Figure 2 schematically shows the principle of this evaluation in space. The observed distribution of distances between events (Figure 2A) is compared with the expected distribution of distances between randomly distributed points (Figure 2B), the simulation being done using a uniform distribution of point coordinates within the study area. When the expected distribution is subtracted from the observed, a residual distribution is obtained (Figure 2C) that shows the departures in terms of residual number of pairs. The dotted lines indicate the tolerance limits, which we used to estimate the statistical significance of the differences between observed and expected distributions of pairs; deviations within the tolerance limits are not considered to be significant. Distributions of time intervals between events are similarly used to evaluate nonrandomness in temporal distribution of earthquakes. Residual distributions of number of pairs, such as those shown in Figure 2C, were obtained for different magnitude intervals and time periods and served as a basis to estimate the degree of nonrandomness in terms of relative number of events. These estimates are represented by the so-called c-functions (Eneva and Pavlis, 1988) that describe the departures from uniform distribution (Figure 3). We found that a short-distance clustering (distances < 7 km) occurs in both preshock and aftershock periods. This feature is more pronounced after the mainshock and for the events of larger magnitude. A long-distance nonuniformity was also observed (distances > 11 km) during the preshock and early aftershock periods, but gradually disappears in the late aftershock sequence. In time, there is no indication of any significant nonrandom pattern in the preshock distribution. However, the distribution of time intervals between aftershocks, although dominated by the classic power-law decay, suggests the existence of characteristic time intervals increasing with magnitude and time.

*Acquisition of Data.* This is a new project and much of our efforts to this point have been directed at gathering the necessary data. With the help of Paul Reasenberg from USGS we now have precise location data from the 1979 Coyote Lake and 1983 Coalinga aftershock sequences. In addition we have acquired routine earthquake location estimates for the entire CALNET and USGS southern California catalogs through 1986. These will be used in the study of seismicity in the Hollister area. We have also been using relocated data from Morgan Hill area for the period 1978-1986.

*Development of New Algorithms.* We are currently working on an algorithm that will allow us a greater flexibility in the random generation of earthquake catalogs. Our previous work was limited to outlining an arbitrary rectangular frame around the study area. In the case of Morgan Hill we showed (Eneva and Pavlis, 1988) that as long as the width of the modeling rectangle is within reasonable limits, the final estimates of spatial nonrandomness are not greately affected. However, this may not be valid in other seismically active areas of different configuration and can become a serious problem when quantitative comparisons between different areas are made. With the new algorithm we will be able to simulate the locations of earthquakes within areas of irregular shape, which will reduce the arbitrariness of the expected distributions being used.

A technique for identifying earthquake clusters in a catalog was also developed. It differs from other methods in that it uses randomly generated rates of seismic activity and a random choice of the events to be removed as clustered. By employing the following procedures, some deficiencies associated with previous methods are avoided: (1) we assign an individual average rate to each portion of the seismic zone, rather than calculate a single average rate for the entire zone; (2) we do not remove all the events from a high-activity window, but leave in the catalog a certain number of earthquakes, corresponding to the background activity; (3) we do not restore the activity in all such windows to identical rates, but the background rate in each window is randomly generated using a normal distribution, with the average rate as a mean. Further, the events to be removed are randomly chosen, excluding the largest earthquakes. We are currently working on combining our technique with the declustering method described by Reasenberg (1985). This may allow us to overcome the shortcomings of each of the two approaches.

## References

Eaton, J. P., Regional seismic background of the May 2, 1983 Coalinga earthquake, in *Mechanics of the May 2, 1983 Coalinga Earthquake, U. S. Geol. Surv. Open-File Rep. 85-44*, ed. by M. J. Rymer and W. L. Ellsworth, 44-60, 1985.

Eneva, M., and M. W. Hamburger, Space-time seismicity patterns within Gissar-Kokshal and Tadjik Depression seismic zones, Soviet Central Asia, *EOS, Trans. Amer. Geophys. Union, 68*, 1368, 1987.

Eneva, M., and G. L. Pavlis, Application of pair analysis statistics to aftershocks of the 1984, Morgan Hill, California, earthquake, *J. Geophys. Res.*, in press, 1988.

Eneva, M., and G. L. Pavlis, A study of space-time patterns in the 1984 Morgan Hill earthquake aftershock sequence: An event pair analysis, *EOS, Trans. Amer. Geophys. Union, 66*, 972, 1985.

Eneva, M., and G. L. Pavlis, Quantification of space-time irregularities in aftershocks of the 1984 Morgan Hill, California, earthquake, *EOS, Trans. Amer. Geophys. Union, 67*, 314, 1986.

Eneva, M., G. L. Pavlis, and M. W. Hamburger, Discrimination of non-random features in the space-time distribution of earthquakes, *Seis. Res. Lett., 58*, 96, 1987.

Kagan, Y., and L. Knopoff, Spatial distribution of earthquakes: the two-point correlation function, *Geophys. J. R. Astr. Soc., 62*, 303-320, 1980.

Reasenberg P., Second-order moment of central California seismicity, *J. Geophys. Res., 90*, 5479-5495, 1985.

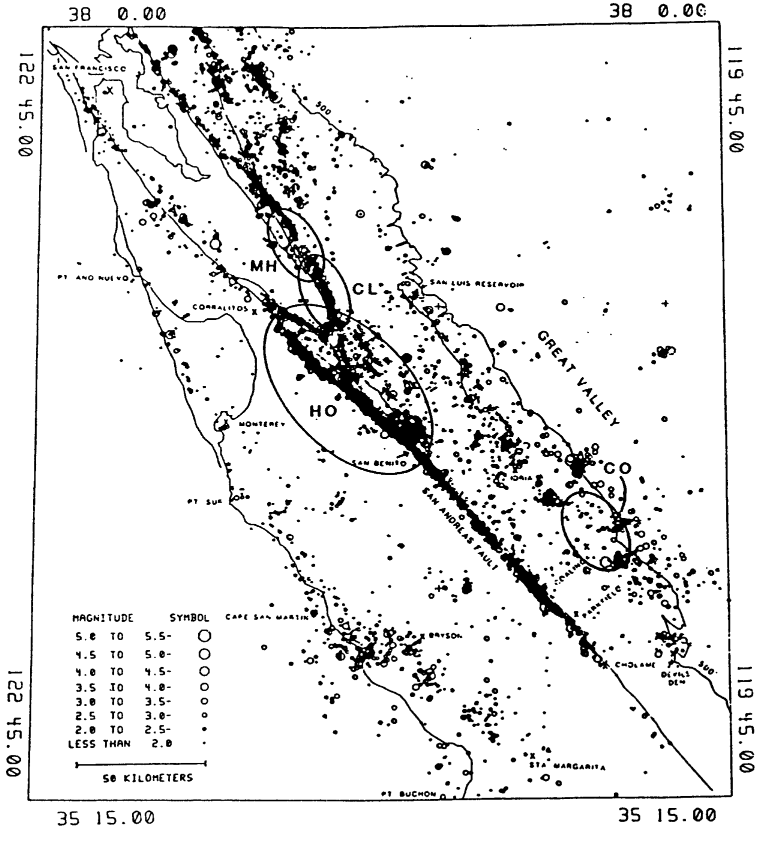

Figure 1. Epicentral map of California, $M_L \geq 1.5$, 1972-1983. Ellipses indicate the approximate areas of study in the project: MH = 1984 Morgan Hill sequence; CL = 1979 Coyote Lake sequence; HO = microearthquakes near Hollister; CO = 1983 Coalinga sequence. Adapted from Eaton (1985).

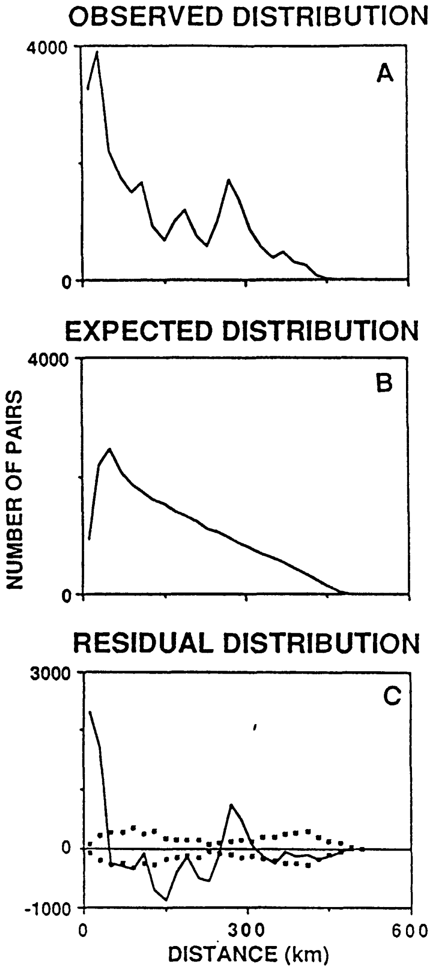

Figure 2. Example of pair analysis method. Frequency distribution of pairs: (A) observed distribution of interevent distances; (B) expected distance distribution, obtained as an average from a number of uniform random simulations of earthquake coordinates; (C) residual distribution, obtained by subtracting the expected distribution from the observed. Dotted lines denote the tolerance limits, measuring the statistical significance of departure from the expected distribution.

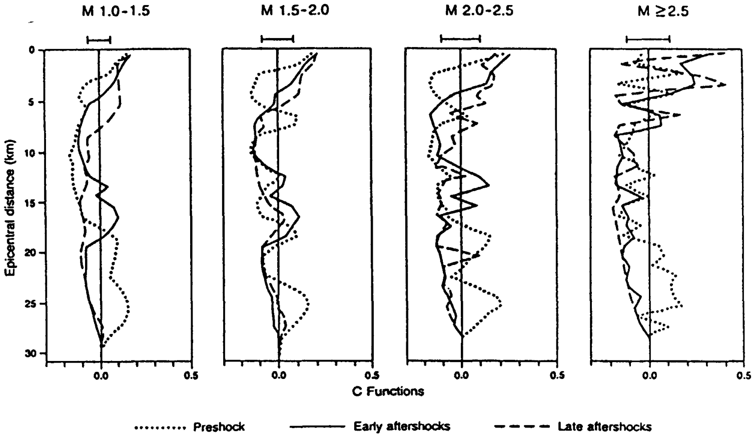

Figure 3. Departures of observed distributions of epicentral distances from expected distributions (c-functions). Each frame corresponds to the magnitude interval indicated and shows results for three time periods: preshocks (6 years before the main event); early aftershocks (first 5 months of the sequence); late aftershocks (the subsequent 18 months). The bars at the top show the average widths of the tolerance intervals.

# Mountain Run Fault Zone of Virginia

9510-03680

Louis Pavlides
Branch of Eastern Regional Geology
U.S. Geological Survey
National Center, MS 928
Reston, Virginia 22092
(703) 648-6925

## Investigations

Mapping within the Mountain Run Fault Zone (MRFZ) indicates that the Everona Limestone occurs almost exclusively on the northwest side of and at the foot of the phyllonite-mylonite scarp of the MRFZ. Furthermore, the Everona Limestone consists of a discontinuous series of lenses rather than being a continuous stratigraphic layer as previous mapping by others has portrayed it. Some limestone lenses contain internal complex folds whereas other lenses are charaterized by homoclinal layering. Poorly exposed lenses of ironstone also occur close to the Everona Limestone. Both the ironstone and limestone lenses are included within the True Blue formation (informal name) that lies between the MRFZ and the Catoctin Formation (Precambrian Z) to its northwest. The True Blue terrane is interpreted to be the continental margin deposit of a back arc sea (see technical summary for 1986 and Pavlides, in press). Also, scattered in random fashion within the True Blue, are outcrops of argillite and chert which may be exotic blocks rather than stratigraphic lenses. At one place a boudinaged siliceous mylonite layer is interpreted to have formed from chert. The new information on the True Blue suggests it may be an olistostromal-tectonic melange, in contrast to the metavolcanic and ultramafic block-bearing melanges to the southeast of the MRFZ described recently (Pavlides, in press) as comprising the Mine Run Complex.

## Reports

Pavlides, Louis, in press, Early Paleozoic composite melange terrane, central Appalachian Piedmont, Virginia and Maryland: its origin and tectonic history, in Horton, J.W., Jr., and Rast, Nicholas, eds., Melanges and olistostromes of the U.S. Appalachians: Geological Society of America Special Paper 228, p. ____.

from an extensive magma body as suggested by those authors. Data taken are shown in **Figure 2**..

Following previous work by Vetter on regional directions of stress from focal mechanisms which showes a clockwise rotation by 28° from Mammoth Lakes in the west to Chalfant Valley in the east, the method of Gephart and Forsyth (1984) was used to estimate principal stress directions of the best fitting stress tensor. At the 95% confidence level, this method shows overlap of the Mammoth Lakes, Round Valley, and Chalfant sequences (**Figure 3**). The method also shows good agreement between earthquake populations near Mono and Walker Lakes, with a significant clockwise rotation relative to Mammoth Lakes (Vetter, 1988.)

### Reports published or submitted during this period.

Cockerham, R.S., Smith, K.D., and K.F. Priestley, Spatial and temporal patterns in the 1984 Round Valley, California, earthquake sequence, *submitted to Bull. Seism. Soc. Am.*, 1988.

Corbett, E.J. The University of Nevada seismographic network, *U.S. Geol. Survey Open-file Rpt. 88-XXX, in press*, 90-101.

Peppin, W.A.. Exotic seismic phases recorded near Mammoth Lakes and their use in the delineation of shallow-crustal (magma?) anomalies. *PAGEOPH, 125*, 1009-1023, 1987.

Peppin, W.A., and Delaplain, T.W.. Pre-S observations at station SLK, NW of Long Valley Caldera, California. 1. Characterization of the observations. *submitted to Bull. Seism. Soc. Am.*, 1988.

Peppin, W.A., Honjas, W., Delaplain, T.W., and U.R. Vetter. The case for a shallow-crustal anomaly (magma body?) near the south end of Hilton Creek fault, California, *submitted to Bull. Seism. Soc. Am.*, 1988.

Peppin, W.A., Honjas, W., Vetter, U.R. and M.R. Somerville. Precise master-event locations of the 1978 Wheeler Crest, California earthquake, *submitted to Bull. Seism. Soc. Am.*, 1988.

Priestley, K.F., and J.N. Brune, Spectra scaling for the Mammoth Lakes, California earthquakes, *submitted to Geophys. J. Roy. Astron. Soc.*, 1988.

Priestley, K.R., and K.D. Smith, The 1984 Round Valley, California Earthquake Sequence. *submitted to Geophys. J. Roy. Astron. Soc.*, 1988.

Savage, M.K., X.R. Shih, R.P. Meyer, and R.C. Aster, 1988. Shear-wave anisotropy of active tectonic regions via automated shear-wave polarization analysis, *Tectonophysics*, in press.

Savage, M.K. and R.P. Meyer, 1988. Comment on: "Apparent stresses, stress drops, and amplitude ratios of earthquakes preceding and following the Hawaii $M_S$ =7.2 main shock, by F.R. Zuniga, M. Wyss, and M.E. Wilson. *Bull. Seism. Soc. Am.*, submitted.

Smith, K.D., and K.F. Priestley, The Foreshock Sequence of the 1986 Chalfant, California Earthquake. *Bull. Seismol. Soc. Am., 78*, 172-187, 1988.

Smith, K.D., W.R. Walter, R.R. Castro, K.F. Priestley, and A.R. Anooshepoor, Earthquake clustering near Mina Nevada, July and August 1987. submitted to Cenozoic faulting in the Southern Great Basin, *symposium held at the University of Nevada-Reno*, fall 1987.

Smith, K.D., J.N. Brune and K.F. Priestley, Seismic Energy, Spectrum, and the Savage and Wood Inequality for complex Earthquakes, *submitted to the Proceedings of the Hundredth Aniversity of the Berkeley Seismograph Station*, 1988.

Vetter, U.R. Characterization of regional stress patterns in the western Great Basin using grouped earthquake focal mechanisms, *Tectonophysics*, in press, 1988.

Walter, W.R., J.N. Brune, K.F. Priestley, and J. Fletcher, Observations of high frequency P-wave earthquake and explosion spectra compared with $\omega^{-3}, \omega^{-2}$ and Sharpe source models. *J. Geophys. Res.* in press, 1988.

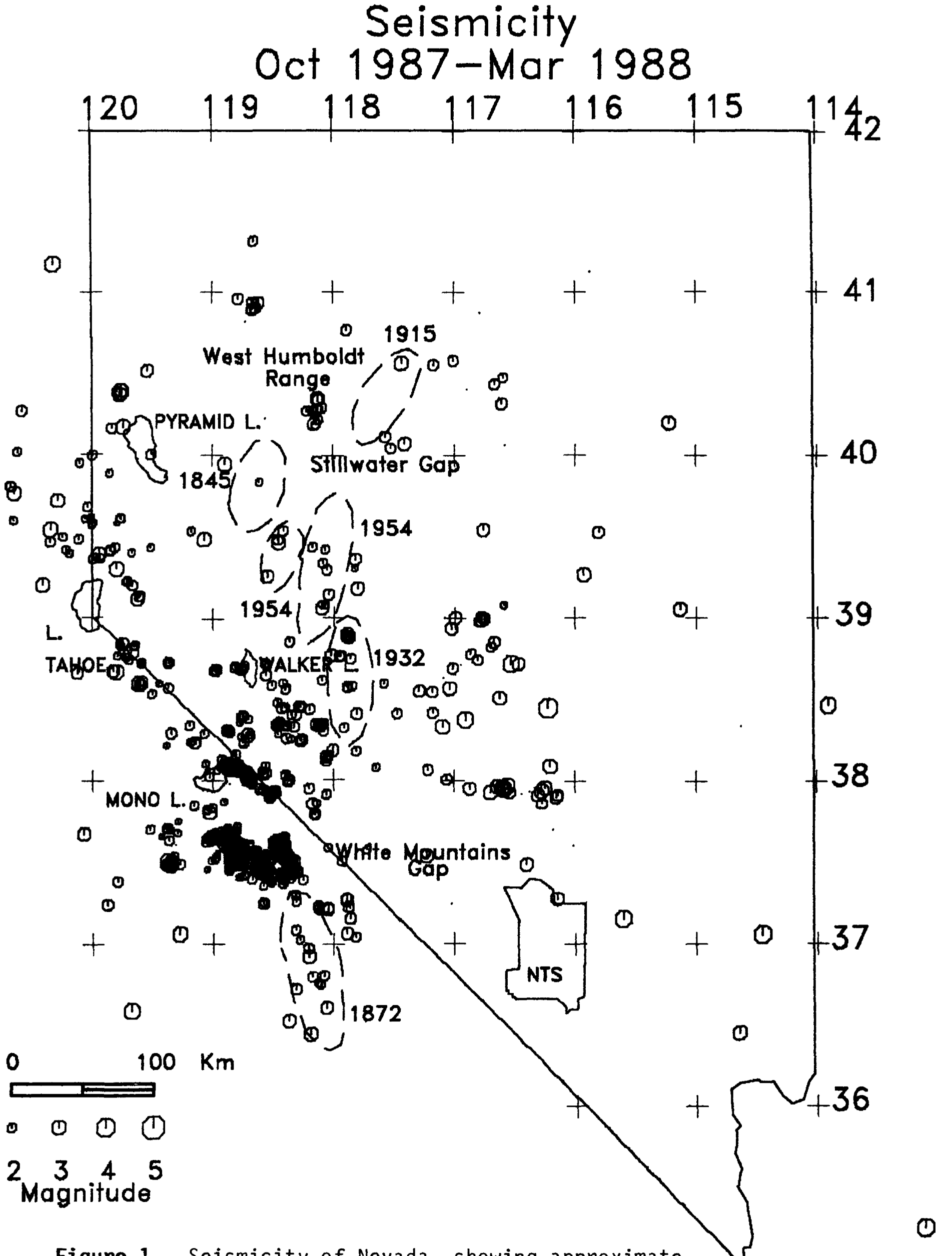

**Figure 1.** Seismicity of Nevada, showing approximate rupture zones of large historic earthquakes, seismic gaps between rupture zones, and the West Humboldt Range, where seismicity began appearing for the first time in 1986.

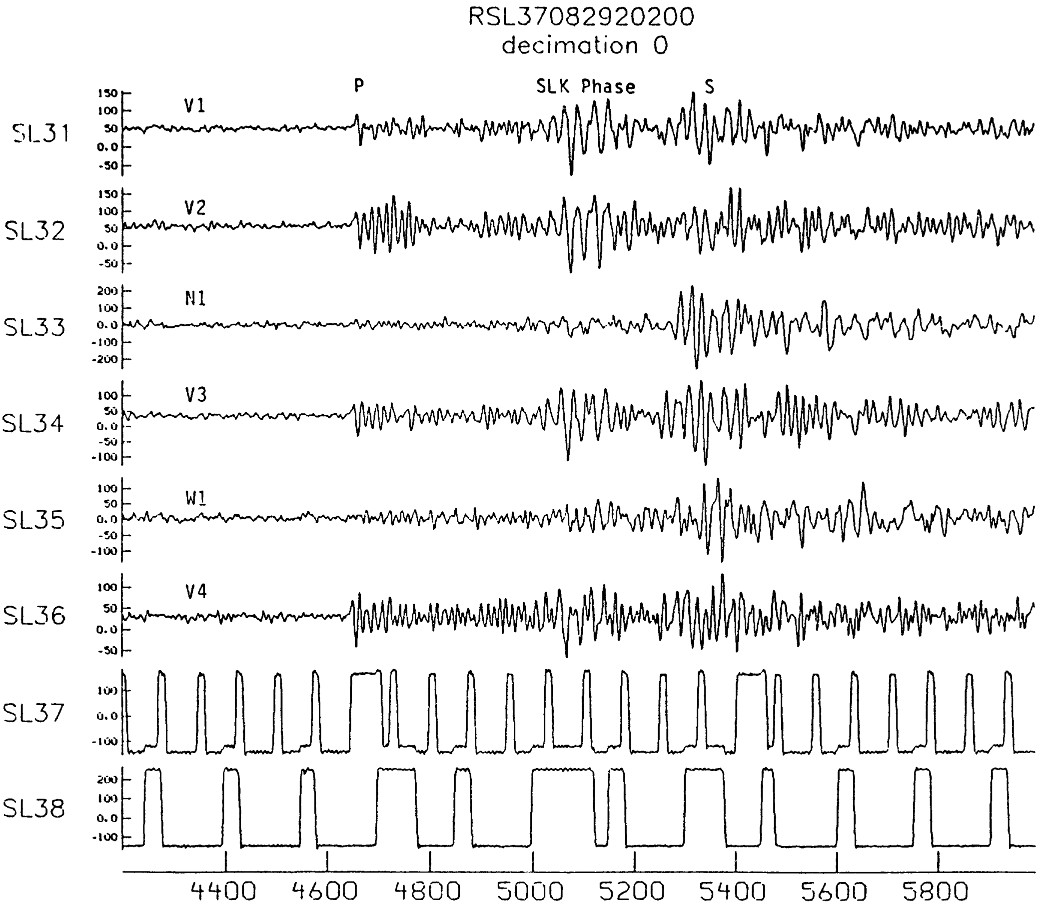

**Figure 2.** Observations on a mini-array near the SLK station for the earthquake of 29 August 1987 at 2020 GCT, showing P, S, and the SLK phase. Traces V1, N1, and W1 are three- component observations showing that the SLK phase is seen dominently on the vertical component (ordinate scale in equivalent digital counts). Traces V2, V3, and V4 are vertical component observations from three other stations within 100 meters of station V1, showing phase coherency for the SLK phase (surprizingly, more than for the P and S phases themselves). Four other mini-arrays were deployed at the same time, and data for these has not yet been worked up.

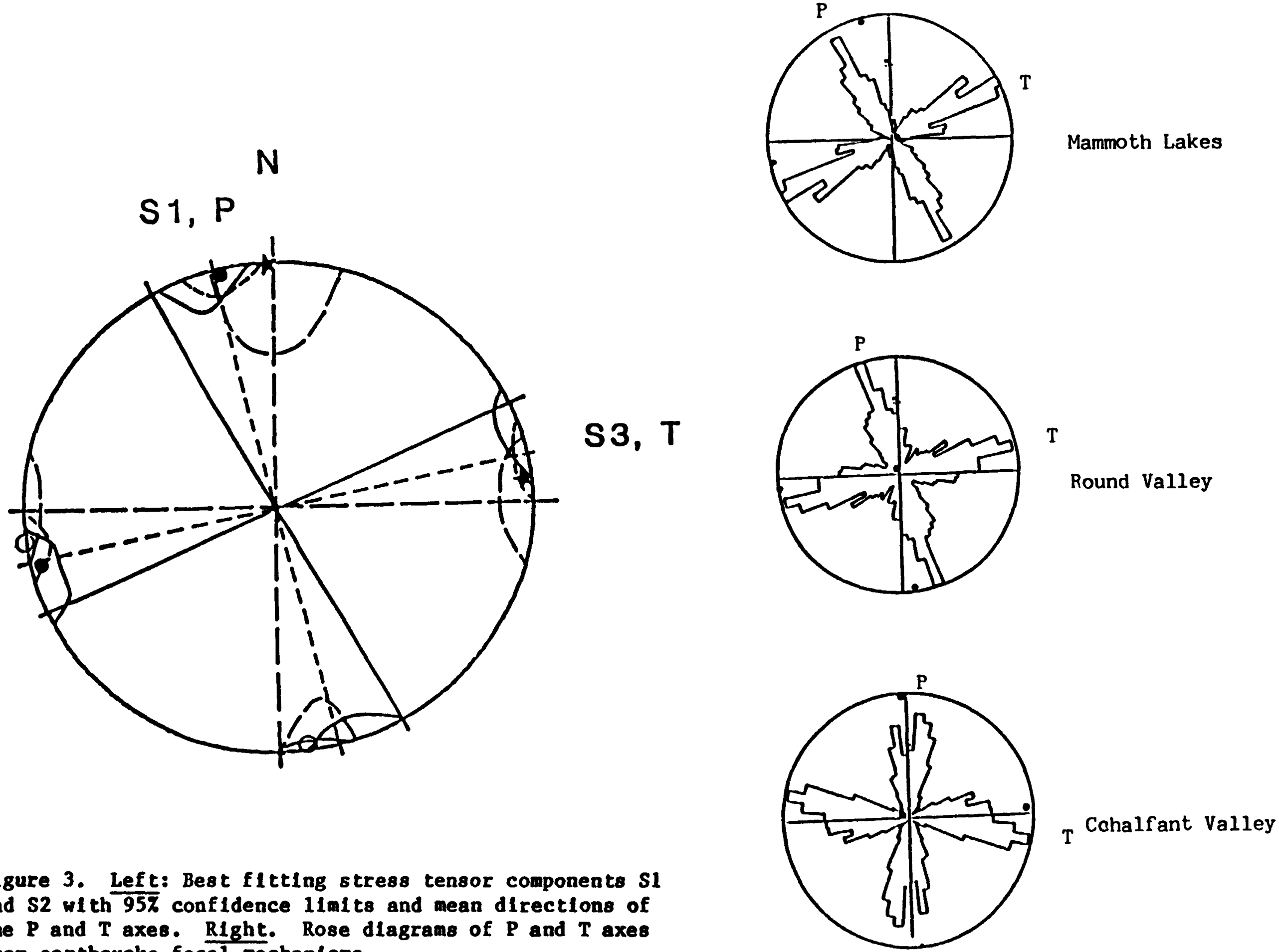

Figure 3. <u>Left</u>: Best fitting stress tensor components S1 and S2 with 95% confidence limits and mean directions of the P and T axes. <u>Right</u>. Rose diagrams of P and T axes from earthquake focal mechanisms.

Mamoth Lakes: ———, ●  Round Valley: ----, o
Chalfant Valley — — —, *

# Detailed Geologic Studies, Central San Andreas Fault Zone

9910-01294

James A. Perkins
John D. Sims
Branch of Engineering Seismology and Geology
U.S. Geological Survey
345 Middlefield Road, MS 977
Menlo Park, California 94025
(415) 329-5647 or (415) 329-5653

## Investigations

1. Continued studies of late Quaternary movement along the Calaveras and Paicines faults.

2. Calibrate fault scarp degradation dating techniques to alluvial deposits.

3. Detailed mapping of active faults and alluvial deposits along a 60-km-long reach of the San Benito River.

## Results

1. Continuing investigations of the Calaveras and Paicines faults concentrate on two study sites: the Windfield Ranch along the Calaveras fault and the Roberts Ranch along the Paicines fault. Previous trenching and geomorphic studies at Windfield Ranch suggest that the Calaveras fault here has averaged about 9 mm/yr during the last 14 ka. Stratigraphic correlations of San Benito River alluvium suggests a slip rate of 9 mm/yr for the Paicines fault at the Roberts Ranch. Additional age data are necessary to confirm the slip rate along the Paicines fault. Trenching studies failed to recover sufficient carbonaceous material to use the radiocarbon dating method. Attempts are underway to apply thermoluminescence dating to the displaced alluvium (with Steve Forman).

2. Numerous alluvial deposits along the San Benito River are displaced by the Calaveras or Paicines faults, but the age of the deposits is unknown. Calibration and application of fault scarp degradation dating techniques to these displaced alluvial deposits may provide multiple slip rates for the Calaveras and Paicines faults. This part of the project received low priority during the reporting period. If thermoluminescence dating is successfully applied to the San Benito River alluvium, then scarp degradation studies will continue.

3. Field work on detailed mapping of active faults and alluvial deposits along the San Benito River between the towns of Tres Pinos and San Benito is complete. Field data were recompiled during the reporting period.

## Reports

None

04/88

# Basement Tectonic Framework Studies
# Southern Sierra Nevada, California

9910-01291

Donald C. Ross
Branch of Engineering Seismology and Geology
345 Middlefield Road, MS 977
Menlo Park, California 94025
(415) 329-5650

## Investigations

1. Continued compilation of data and preparation of report on the chemical traits and trends of the granitic rocks of the southern Sierra Nevada.

2. Determination of magnetic susceptibilities on most collected granitic samples from the southern Sierra Nevada and preparation of summary tables and graphs to characterize the data.

3. Planning for final check of the northwest corner of the field area in the White River and Woody 15' quadrangles, southern Sierra Nevada.

4. Collating chemically analyzed samples from the granitic rocks of the southern Sierra Nevada for submission to the archives of the Smithsonian Institution.

## Results

1. Completion of report on the chemical traits and trends of the granitic rocks of the southern Sierra Nevada (now in technical review). These rocks show no surprising chemical characters -- they are on average calcic, but near the calcic-alkalic field and not too dissimilar from other granitic suites of the region.

2. Magnetic susceptibility of granitic rocks in the southern Sierra Nevada shows a marked zonation. The Sierran tail and the area north to about lat. 35°30' N is magnetically very "quiet" with average values of granitic units from 0-40 s.i. x $10^{-5}$. Further north, average values range up to 2,000 s.i. x $10^{-5}$. The right-lateral offset of the basement caused by movement on the White Wolf-Breckenridge-Kern Canyon fault zone is reflected grossly by the distribution of magnetic susceptibility values, with higher readings generally extending further south on the east side of the fault zone. Further magnetic susceptibility studies are in progress to refine this picture (or dissolve it!)

3. Magnetic susceptibility measurements on a limited number of samples from the Salinian block reference collection, show generally low readings (30-50 s.i. x $10^{-5}$) with the exception of the La Panza Range where readings are much higher (700-1,600 s.i. x $10^{-5}$). Limited hot spots in the Santa Lucia Range are as high as 1,600 s.i. x $10^{-5}$. These generally low read-

ings confirm earlier petrographic studies which showed metallic opaque minerals were generally rare or absent in the Salinian block. These readings also point to a "magnetic affinity" between the northern and central Salinian block and the Sierran tail area. Carrying speculation one step further, a long suspected porphyritic correlative of the La Panza Range granitic rocks, east of the San Andreas fault, in the Thermal Canyon area near Palm Springs, has values of around 2,000 s.i. x $10^{-5}$. This would also support a cross-fault match of about the same magnitude as a match of the north central Salinian block and the southern Sierra Nevada. These speculations, based on very limited samples, at least suggest that further magnetic susceptibility studies may yield useful, and easily acquired, data for basement rock correlations.

## Reports

Ross, D.C. 1988, Specific gravity data from granitic rocks of the southern Sierra Nevada, California: U.S. Geological Survey Open-File report 88-72, 37 p.

# Salton Trough Tectonics and Quaternary Faulting

9910-01292

Robert V. Sharp
Branch of Engineering Seismology and Geology
U.S. Geological Survey
345 Middlefield Road, MS 977
Menlo Park, California 94025
(415) 329-5652

## Investigations

1. Field investigation for surface faulting -- Whittier Narrows, California, earthquake of October 1, 1987 (with several others).

2. Field investigation of surface faulting -- M6.2 and M6.6 Superstition Hills earthquakes of November 24, 1987, in the Salton Trough of southern California (with many others).

3. Additional trenching of young faults in the San Andreas zone near Bombay Beach (with M. Rymer).

## Results

1. A two-day search for surface faulting in the region around the Whittier Narrows was fruitless. In checking the Whittier fault, the Raymond Hill fault, the Norwalk fault(?), and other nearby previously mapped fault structures, we found only a few cracks that we interpret to represent downslope motion of pavements and poorly consolidated alluvial material.

2. This pair of earthquakes (Elmore Desert Ranch earthquake on 23 November local time, followed by the Superstition Hills earthquake about 12 hours later) were associated with widespread surface faulting of principally left-lateral type in the northern part of the Superstition Hills and with right-lateral movement along 28 kilometers of the Superstition Hills fault zone. Surface movements were also triggered on parts of two nearby faults -- the northern half of the Imperial fault and the southern part of the Coyote Creek fault. Surface fault mapping and and displacement measuring programs were initiated, and many individuals both within and outside of OEVE participated in data gathering.

   Right-lateral surface movement on the traces of the Superstition Hills and Wienert strands of the Superstition Hills fault zone grew rapidly during the second event. The growth of these displacements is being documented by remeasurement at progressively extended time intervals, and this effort will continue, probably for several years. Maximum horizontal offsets of about 0.8 meter were recorded by February 1988 at sites on the Superstition Hills trace that showed about 0.5 meter during the second day following the earthquake. The maximum horizontal movements found on the Wienert strand grew from about 0.1 meter to 0.3 meter over the same time interval.

At least 132 conjugate surface faults, both northwest-trending right-lateral and northeast-trending left-lateral, were activated at the surface in a 16 km (east-west) by 10 km (north-south) area lying northeast of the Superstition Hills fault zone. These faults showed principally small and locally discontinuous surface movements (maximum about 0.1 meter); these surface displacements apparently were coseismic and have not grown since. It is unknown with which event they may have been coseismic.

3. A new trench across a previously excavated fault trace has revealed a complex multi-stranded zone of strike-slip faulting in lake beds older than 300 years. It is highly likely that these traces are the San Andreas fault or at least strands within the zone. Reasons why the active San Andreas trace has not been definitely pinpointed in the Bombay Beach area relate to: (i) the complexity of shearing in the highly deformed Pleistocene sediments exposed there; (ii) the apparent absence of surface displacement there during historic movements triggered on other sections of the fault; (iii) the widespread concealment of fault traces by a veneer of deposits laid down during the late stand(s) of Lake Cahuilla. These trenches show fault traces in deposits that are intermediate in age and that are themselves mostly concealed by the youngest lake beds. This trenching investigation will necessarily be extensive.

## Reports

Budding, K.E., and Sharp, R.V., 1988, Surface faulting associated with the Elmore Desert Ranch and Superstition Hills, California, earthquakes of 24 November 1987 [abs.]: Seismological Society of America, Annual Meeting, Honolulu, Hawaii, May, 1988.

# Seismotectonic Framework and Earthquake Source Characterization (FY88) Wasatch Front, Utah, and Adjacent Intermountain Seismic Belt

14-08-0001-G1349

R.B. Smith, W.J Arabasz, and J.C. Pechmann*
Department of Geology and Geophysics
University of Utah
Salt Lake City, Utah 84112
(801) 581-6274

## Investigations

1. Suppressed earthquake clustering in the Wasatch Front region.
2. Seismotectonics of the 1987-1988 Lakeside, Utah, earthquakes.
3. Elastic wave propagation and site amplification in the Salt Lake Valley from normal faulting earthquakes.

## Results

1. The University of Utah earthquake catalog between 1962 and 1985 for the Utah region has been analyzed for the identification of independent main events and for the hierarchical clustering of secondary events. The methodology has been developed by D. Veneziano and co-workers at M.I.T., and it effectively handles both spatial nonhomogeneity and nonstationarity in seismic sequences. Based on collaborative work with D. Veneziano, analysis of 3,003 events of M2.0 and greater shows that earthquake clusters in the Utah catalog have highly variable spatial configurations and space-time extent. Also, the clustering pattern displays a remarkable paucity of secondary events, relative to the number of main events, in a well-instrumented area between roughly 40.0°N and 41.5°N (Figure 1, left). This area encompasses the most active segments of the Wasatch fault. The sparse clustering observed here is not simply explainable by lack of main-shock occurrences. Eight independent main shocks of $M_L \geq 4.0$, including shocks of M5.2 and M5.7, occurred during the sample period of Figure 1 (left) in the region where first-order clustering is absent.

As a further test of sparse clustering near the Wasatch fault, data were scrutinized for the time period *after* the start of automated digital recording on January 1, 1981. Figure 1 (right) shows 15 main shocks ($M_L \geq 3.5$) that occurred in the Wasatch Front area between 1981 and 1987. Corresponding to each main shock, a string of numbers (from left to right) indicates the number of secondary events differing in size from the main shock by 2.0 units or less, the number of secondary events (in parentheses) above a uniform threshold of M1.5, and the main-shock magnitude ($M_L$). Clustering based on automatic event detection tends to be minimal for earthquakes occurring where major clustering (identified by ellipses) had earlier

---

*H.M. Benz, E.D. Brown, and T. Zhang also contributed significantly to the work reported here.

been absent. Two good examples of main shocks occurring close to the Wasatch fault and having very few or no apparent dependent events are: (a) a shock of M3.9 in February 1981 (40°19'N, 111°44'W) that had no detected aftershocks of M1.5 or greater, and (b) a shock of M4.3 in October 1983 (40°45'N, 112°00'W) that had only two aftershocks of M1.5 or greater. Main shocks located where major clustering had earlier been identified generally (but not in all cases) tend to have many aftershocks. Suppressed earthquake clustering has been suggested to be a precursory phenomenon (e.g., in the Anza seismic gap). In the case of the Wasatch Front area, multiple hypotheses are being considered that relate to heterogeneity of rock strength, mode of seismic slip, and time-varying deformational state.

2. During September 1987-March 1988, an earthquake sequence which included shocks of $M_L$4.8 and 4.7 on September 25 and October 26, respectively, and a total of 8 events of $M_L \geq 3.8$, occurred beneath a desert basin west of the Great Salt Lake (see Figures 1 and 2 of the summary report for our companion network operations award, this volume). Wood-Anderson seismograms indicate nearly identical magnitudes for the two largest earthquakes but a factor of two to five larger moment for the first. The shocks were the largest in the Utah region since a $M_L$6.0 main shock in 1975. Significant aspects of the 1987-88 sequence included: foreshock activity, proximity ($\Delta$ = 7–12 km) to a major pumping facility completed in early 1987 to lower the level of the Great Salt Lake, a strike-slip focal mechanism for the $M_L$4.8 main shock (Figure 2), and the lack of a clear association with late Quaternary surface faults.

Despite constraints on accessibility to the epicentral area, the stations of the regional seismic network ($\Delta > 60$ km) were supplemented with local stations—initially four portable seismographs and later up to four telemetered stations ($2 < \Delta < 25$ km) that have operated continuously since October 7, 1987. Well-located aftershock foci concentrate along a NNW-trending zone 4-6 km long, parallel to one of the nodal planes for the focal mechanism of the $M_L$4.8 event (Figure 3). Three-dimensional interpretation of the seismicity pattern awaits results of further hypocentral refinement, but focal depths appear to predominate in the 4 to 10 km depth range. Despite coincidental timing and proximity of the earthquakes to major pumping activity at the surface, the case for induced seismicity is weak.

3. For a two-dimensional velocity model of the Salt Lake Valley, we calculated the valley's seismic response to simulated vertically-incident plane waves and to waves generated by normal-faulting earthquakes on the basin-bounding Wasatch fault. The plane wave source response is simulated using the finite difference method while the seismic response of slip along the Wasatch fault is calculated using the finite element method. The vertically incident plane wave response of the basin was investigated in order to understand wave propagation effects due to relatively simple radiation patterns. Additionally, the plane wave model is appropriate for comparing synthetic site amplifications with observed site amplification studies in the Salt Lake Valley (Hays and King, 1984; King *et al.* 1987). Recording nuclear

explosions from southern Nevada across the Salt Lake Valley, Hays and King (1984) showed that the spectral amplification within the Salt Lake Valley can exceed 10 times that measured at hard rock sites, immediately adjacent to the basin. While they attribute the site amplification, measured over the frequency band 0.3-5.0 Hz, to the near-surface unconsolidated/consolidated alluvial fill contact, our synthetic results suggest that in the frequency band 0.3-1.5 Hz at least one-half the site amplification can be attributed to deeper basin structure.

Synthetic seismograms from the vertically incident plane waves predict that both margins of the Salt Lake Valley will produce large amplitude Rayleigh wave phases. In contrast, simulations of earthquakes on basin bounding, normal faults show that Rayleigh waves are predominantly produced on the fault-bounded edge of the basin. Additionally, investigation of synthetic seismogram spectra shows that spectral amplification is localized near the fault trace and falls off rapidly away from the fault. These results have important implications for understanding and using site amplification measurements derived from nuclear explosions or teleseismic events.

## Reports and Publications

Pechmann, J.C., W.P. Nash, J.J. Viveiros, and R.B. Smith (1987). Slip rate and earthquake potential of the East Great Salt Lake fault, Utah, *EOS, Trans. Am. Geophys. Union 68,* 1369.

Veneziano, D., Y. Shimizu, and W.J. Arabasz (1987). Suppressed earthquake clustering in the Wasatch Front region, Utah, *EOS, Trans. Am. Geophys. Union 68,* 1368.

Westaway, R. and R.B. Smith (1987). Strong ground motion parameters for normal-faulting earthquakes, *EOS, Trans. Am. Geophys. Union 68,* 1348.

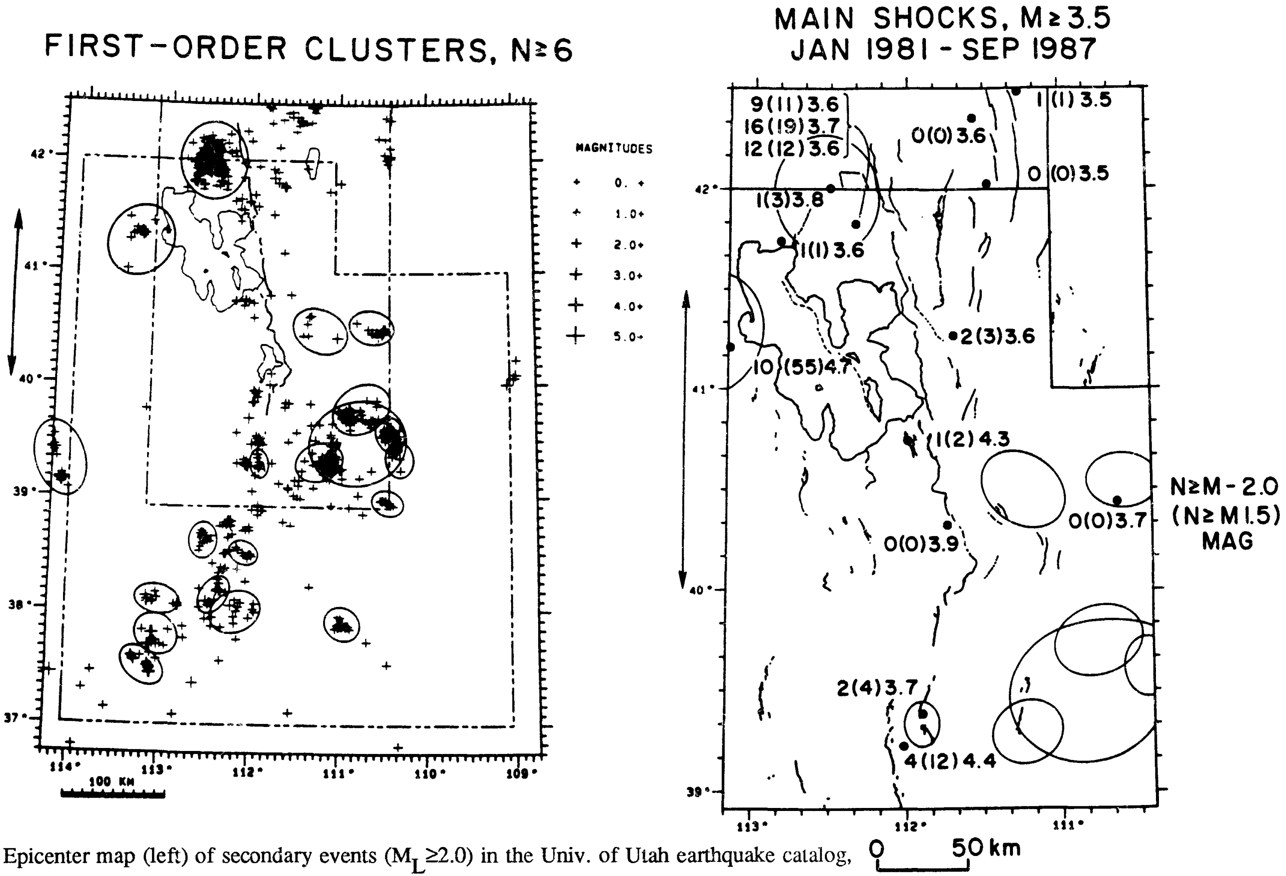

Figure 1. Epicenter map (left) of secondary events ($M_L \geq 2.0$) in the Univ. of Utah earthquake catalog, July 1962-December 1985, from a cluster-analysis study of Veneziano and Shimizu (1987). Clusters of 6 or more secondary events are circumscribed. Map of Wasatch front study area (right) showing cluster locations from map on left together with location of main shocks of M3.5 or greater since beginning of digital network recording in January 1981 and counts of associated secondary events (explained in text).

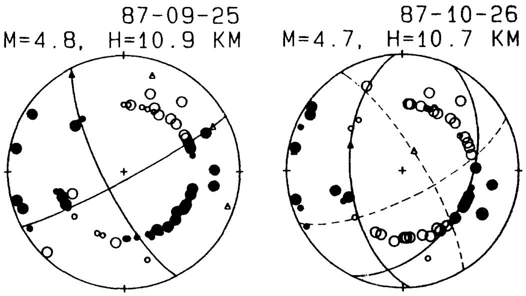

Figure 2. Focal mechanisms for the two largest events in the Lakeside sequence: the September 25 mainshock ($M_L$ 4.8) and the $M_L$ 4.7 aftershock on October 26. These are lower-hemisphere projections, with compressions shown as solid circles and dilatations as open circles. Small circles indicate readings of lower confidence. The triangles show slip vectors and P and T axes. For the aftershock, the solution shown in solid lines is our preferred focal mechanism. An alternative solution (dashed) similar to that of the $M_L$ 4.8 event can be fit to the data if we disregard two weak dilatational first motions read from paper records for Boise State stations located more than 340 km northwest of the epicenter.

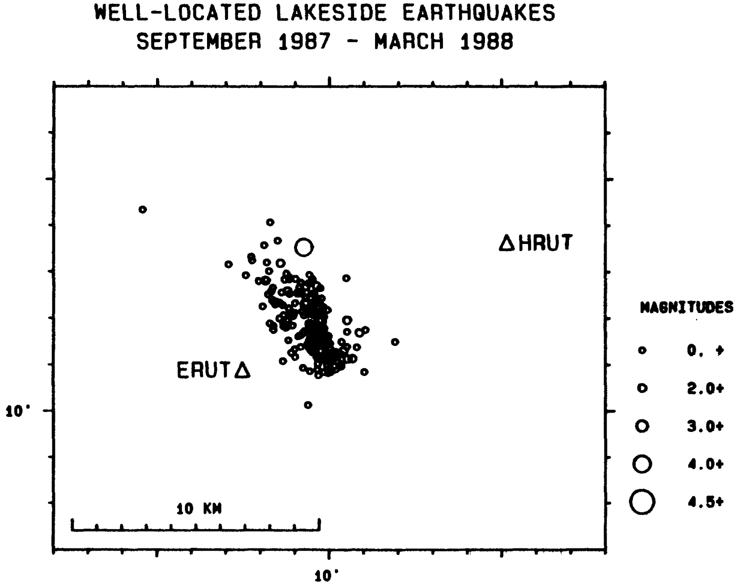

Figure 3. Map view of 182 well-located aftershocks (gap ≤180°, dmin ≤15 km, and nwr ≥8 readings) that occurred from September 26, 1987, through March 31, 1988. The NNW trend of the aftershock zone is parallel to a nodal plane of the mainshock focal-mechanism (see Figure 2). The two closest portable telemetry stations are shown as triangles.

# Northeast Cross Faults, Detachments, Crustal Blocks and Strain Partitioning in Southern California: A Search for Changes in Seismicity and Focal Mechanisms Precursory to Major Earthquakes

USGS 14-08-0001-G-1096

Lynn R. Sykes and Leonardo Seeber
Lamont-Doherty Geological Observatory of Columbia University
Palisades, New York 10964
(914) 359-2900

Objective: For the past 5 years we have been studying the detailed distribution of earthquakes, focal mechanisms, rotations of small crustal blocks, N.E.-striking cross-faults, the existence of shallow-angle detachment faults and premonitory changes before large earthquakes along the southern San Andreas and San Jacinto faults in southern California. Sixteen papers have been written on this work. Major emphasis has been given to the large tectonic knot centered near San Gorgonio Pass and to 2 recent earthquakes near the southern end of the Salton Sea. Little of the present seismic activity occurs on the major throughgoing faults themselves. Instead much of it is situated on secondary structures such as cross-faults and detachments. Seismicity in the months before the 1986 North Palm Springs earthquake appears to be concentrated on a detachment fault that determined the lower limit of the rupture. Secondary cross-faults at the two ends of the rupture were active during the aftershock sequence. Preliminary work involves using relocated hypocenters and single-event focal mechanisms to examine precursory changes in three regions near the San Jacinto and southern San Andreas faults that contain prominent cross-faults and detachment faults. A small earthquake associated with a magnitude 6 event on a cross-fault near the southern end of the Salton Sea that was a short-term precursor to a larger event in 1987 on the Superstition Hills fault. A temporal sequencing of activity along NW and NE trending conjugate faults of the Brawley zone has been identified and will be examined in detail. Future changes in activity on the next cross fault to the north of the one that ruptured in 1987 could be a precursor to a larger event that would rupture the southern San Andreas. We have developed computer programs to automatically determine hundreds of focal mechanism solutions of high quality so as to examine in detail the hypothesis that the San Andreas is a weak fault.

Data Acquisition and Analysis: For the past 5 years we have concentrated a great deal of our efforts in studying the major tectonic knot in the vicinity of San Gorgonio Pass.

Early Results: We initially chose a segment of the San Andreas fault near San Gorgonio Pass (SGP) for detailed study since it is characterized by high seismicity and it may control the behavior of this fault in southern California. In the Area chosen the San Andreas fault takes a compressional (left) step as well as a compressional bend. As a consequence the complex tectonics of that area are dominated by north-south shortening. Sykes and Seeber (1985) postulate relatively high strength for this portion of the fault and call it a major tectonic knot. Failure of this segment of the San Andreas fault zone would likely result in a great earthquake that would rupture as far north as Tejon Pass or as far south as the Salton Sea.

Nicholson et al. (1986a,b) found that although this area is unusually seismogenic, very few earthquakes were occurring in the upper 5 km or could be directly associated with any of the major branches of the San Andreas fault itself. Instead, they identified an active system of relatively short left-lateral faults striking northeast. This pattern of deformation, in conjunction with an unusual set of earthquake mechanisms involving both normal and reverse faulting, suggested a series of blocks confined between the major faults and undergoing clockwise rotation as a result of regional right-lateral shear.

Recent Results: In our initial studies we used effectively composite fault-plane solutions. We are now developing a series of algorithms that determine fault-plane solutions for single events, and then display the results in a variety of forms, each emphasizing different aspects of the kinematics. These algorithms do not differ in fundamental ways from several previous ones but they are designed to handle and display large quantities of data.

Williams et al., (1988) examined focal mechanisms for many small earthquakes and relocated hypocenters of large numbers of earthquakes in the vicinity of the southernmost San Andreas fault in the northern Salton Trough and the eastern Transverse Ranges of southern California. The San Andreas fault itself in that region is essentially quiescent at the microearthquake level, and nearly all of the earthquakes during that period occurred on secondary structures to the northeast of the San Andreas fault. Focal mechanisms in that region involve either strike slip or normal faulting with a common horizontal T axis. An abrupt boundary between contemporary stress provinces occurs at the east side of San Gorgonio Pass where the strike and complexity of the San Andreas and heat flow change dramatically. This may be associated with a two mode rupture pattern for the southern San Andreas with large events (magnitude 7-7 1/2) that rupture only the Salton Trough portion of the fault and larger events that rupture the tectonic knot near San Gorgonio Pass, as well.

Pacheco and Nabelek (1986, 1988) studied the source processes of three moderate-size California earthquakes: the $M_L$=5.9 event near North Palm Springs, the $M_L$=5.3 shock located offshore from Oceanside and San Diego, and the $M_L$=6.2 event in the Chalfant Valley. The centroidal source parameters were estimated by inversion of teleseismic P and SH waves. The North Palm Springs earthquake involved right-lateral strike slip with a sizable component of reverse faulting that is consistent with the uplift of the region to the north of Banning fault and with many of the focal mechanisms in the area. The mechanism for the mainshock determined from short-period P waves was nearly pure strike slip and on a a fault plane striking more northerly than that determined from longer-period waves . Its strike rotated more westerly and involved a larger component of thrust faulting as rupture progressed westward along the curving Banning fault. The long-period thrust mechanism for the earthquake offshore of Oceanside was quite unexpected since short-period data from onshore stations that sampled only a small part of the focal sphere indicated a strike-slip mechanism. The presence of this event and its thrust mechanism require a re-evaluation of the contemporary tectonics of the southern California borderland and the tsunami potential of the region.

Portions of the San Jacinto fault zone consist of multiple strands with intervening crustal blocks that have rotated appreciably during the past 1 million years (Bogen and Seeber, 1988). We are investigating an active portion of the southern San Jacinto fault and its adjacent secondary faults (Petersen, 1987). Phase data from 1981 to 1986 were used to redetermine hypocenters and then to delineate structural trends. Inversion of long-period data for the Borrego Mountain earthquake indicate that a significant release of seismic moment occurred about 12 seconds after the mainshock, most likely on a secondary fault. We plan to continue making careful relocations of events and to obtain revised focal mechanisms for other portions of the San Jacinto fault zone in an effort to understand the interaction among crustal blocks, cross faults and main strands of faults.

## Publications

Bogen, N. L., and L. Seeber, Late Quaternary block rotation within the San Jacinto fault zone, southern California, submitted for publication, 1988.

Hudnut, K., P. Williams, K. Sieh, and L. Seeber, Geomorphic Evidence for a Pre-Historic earthquake on the Superstition Mountain fault, Southern California (abstract). EOS, Trans, AGU, 68, 1369, 1987.

Nicholson, C., L. Seeber, P. Williams, and L.R. Sykes, Seismicity and fault kinematics through the eastern Transverse Ranges, California: Block rotation, strike-slip faulting and shallow-angle thrusts, J. Geophys. Res., 91, 4891-4908, 1986.

Nicholson, C., L. Seeber, P.L. Williams, and L.R. Sykes, Seismic deformation along the southern San Andreas fault, California: Implications for conjugate slip and rotational block tectonics, Tectonics, 5, 629-649.

Pacheco, J., and J. Nabelek, Source mechanisms of three moderate southern California earthquakes of July 1986 (abstract), EOS, Trans. AGU, 67, 1091, 1986.

Pacheco, J., and J. Nabelek, Source mechanisms of three moderate California earthquakes of July 1986, submitted to Bull. Seismol. Soc. Am., 1988.

Petersen, M.D., L. Seeber, and K. Hudnut, Importance of transverse features along the southern San Jacinto fault zone, California (abstract), EOS, Trans, AGU, 68, 1507, 1987.

Seeber, L., and C. Nicholson, Block rotation along the San Andreas fault system in California: Long-term structural signature and short-term effects in the earthquake cycle, in preparation, 1988.

Seeber, L., J. G. Armbruster, P. Williams, and L. R. Sykes, Faults antithetic to the San Andreas delineated by seismicity in the San Gorgonio Pass of southern California (abstract), EOS, Trans. AGU, 67, 1200, 1986.

Seeber, L., J. G. Armbruster, M. Tuttle, Secondary faults associated with the 7 July 1986 Palm Springs earthquake rupture on the San Andreas fault (Abstract), Seismol. Soc. Am., Santa Barbara, 1987.

Seeber, L., and J. Armbruster, Secondary faults as agents for segmentation of the master strands in southern California (abstract), IUGG Conference, Vancouver, Canada, Aug. 17-22, 1987.

Sykes, L. R., and L. Seeber, Great earthquakes and great asperities, San Andreas fault, southern California, Geology, 113, 835-838, 1985.

Williams, P., S. Fagerson, and K. Sieh, Triggered slip of the San Andreas fault after the July 8, 1986 North Palm Springs earthquake (abstract), EOS, Trans. AGU, 67, 1090, 1986.

Williams, P., L. R. Sykes, C. Nicholson, and L. Seeber, Seismicity and state of stress, eastern Transverse Ranges, California: Implications for seismic potential of the southern San Andreas fault, submitted to J. Geophys. Res., 1988.

# Microearthquake investigation of the Kaoiki fault zone, Hawaii

14-08-0001-1G1529

Clifford H. Thurber
Dept. of Earth and Space Sciences
Stae University of New York at Stony Brook
Stony Brook, NY 11794-2100
(516) 632-8218

Objective: The seismically active Kaoiki fault zone lies between the Hawaiian volcanoes Mauna Loa and Kilauea, and is thought to be an expression of the horizontal compressive forces induced by the growth of the two volcanoes. A detailed investigation of the 1983 Kaoiki earthquake sequence has been initiated, and the relation of this sequence to two previous earthquake sequences (1974, 1962) is being examined in order to improve our understanding of the seismotectonic setting of this active fault zone.

Data Analysis: The first three months of work on this project has concentrated on an initial examination of hypocenters and focal mechanisms determined using standard layered crustal models for the region.

The 1983 main shock (M=6.7) has been modeled previously as a strike-slip event with a dip-slip component, with the presumed fault plane oriented at about N 45° E. The aftershocks delineate three separate zones of faulting, each of which has both strike-slip and thrust mechanisms. Two of the zones have the same orientation as the main shock fault plane, and the third is orthogonal to it (see Figure 1). The thrust events concentrate in the depth range of 10 to 12 km, apparently confirming the existence of a subhorizontal detachment beneath Kaoiki similar to that beneath the south flank of Kilauea. Strike-slip events range in depth from the near surface to about 10 km. They outline the boundaries of two distinct crustal blocks that form the Kaoiki fault zone. Their relative motions can be determined from analysis of focal mechanisms. Both blocks are being displaced seaward along the detachment zone.

Wyss (Science, 234, 1986) has claimed that the frequent moderate-sized earthquakes in the Kaoiki fault zone are recurring events with a repeat time of about 10 years. In order for this claim to be valid, the same zone of rupture must be responsible for all the events. However, comparison of the hypocenter locations for the 1983, 1974, and 1962 sequences reveals that the latter two events ruptured the same zone along the boundary between the two crustal blocks forming the Kaoiki fault zone, while the 1983 activity concentrated along the boundaries between the Kaoiki blocks and the adjacent volcanic blocks. There is very little overlap in the aftershock distributions of the 1983 versus the 1974 and 1962 sequences. Thus Wyss' claim of a recurrence pattern and his prediction of the next event (M~6 between July 1993 and October 1996) should be reexamined.

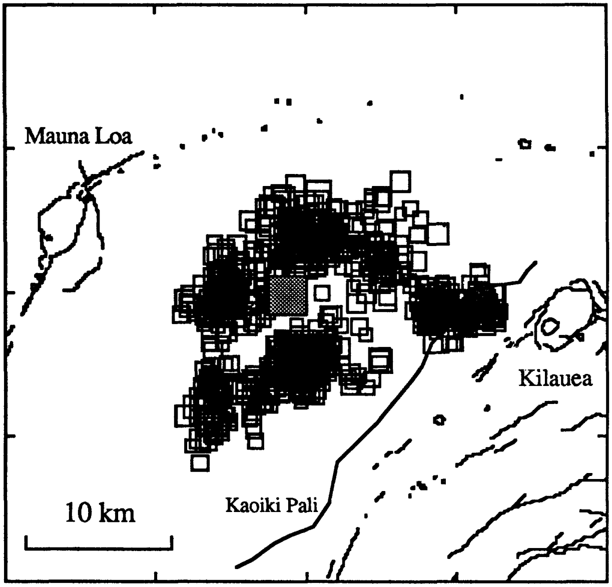

Figure 1. November 1983 Kaoiki earthquake sequence. The main shock (M=6.7) is shaded. Note the three distinct zones of activity. The main shock was primarily a strike-slip event, with one fault plane parallel to the adjacent aftershock activity. The aftershocks mechanisms are a mixture of strike-slip and low-angle-thrust events.

# DEVELOPMENT OF A PREDICTION MODEL FOR A POSSIBLE KAOIKI MAINSHOCK

14-08-0001-G1325

Max Wyss
CIRES/Dept. of Geological Sciences
University of Colorado
Boulder, CO 80309-0449
(303) 492-5642

## Investigations

(1) Macroseismic locations of historic Kaoiki earthquakes.

(2) Relationship between magnitude and extent of felt areas for Hawaii.

(3) A proposed model for the 1868 great Kau earthquake.

(4) Seismic quiescence before the January 1982 Hilea mainshocks.

(5) Moment-magnitude relation for Hawaii

## Results

(1) In collaboration with personnel of the Hawaiian Volcano Observatory we have compiled a catalog of macroseismic data for Hawaiian earthquakes from 1912 to 1983. By comparing the pattern of intensity distribution for historic mainshocks that might have been located in or near the Kaoiki area with those of recent mainshocks with instrumentally determined epicenters we identified additional Kaoiki mainshocks. The calibration set of macroseismic maps consisted of those of the 1941, 1951, 1962, 1974 and 1983 Kaoiki earthquakes. For the period 1912 through 1939 there were 7 candidates for possible Kaoiki sources in the $M > 5$ range. Five of these were most likely not located in the Kaoiki area, instead they were associated with the Mauna Loa, Kilauea and the Hilea areas.

Of the remaining two events the macroseismic pattern of 2 November 1918 was very similar in extent and distribution to that of the 1962 and 1983 Kaoiki mainshocks. It was concluded that the 1918 mainshock was located in the Kaoiki area and had a magnitude of about 6.1. The other possible Kaoiki mainshock occurred on 25 May 1930, but its magnitude was smaller (about 5) and its intensity distribution was not well defined. Although the pattern was similar to that of the 1974 ($M=5.5$) mainshock, the macroseismic data did not allow a definite association with the Kaoiki or the Kilauea area. Our interpretation of this event as a Kaoiki mainshock is based on the observations by T. Jaggar, Director of HVO at the time, who did not consider this a possible Kilauea event, but attributed it to the Kaoiki area.

After reviewing all the available eyewitness reports on the effects of the 1868 great Kau earthquake it was concluded that this mainshock was centered in Hilea but that it also ruptured the Kaoiki area.

It was previously proposed that the Kaoiki mainshocks occur at regular intervals of about 10 years with every second event having a magnitude $M > 6$ with the other magnitudes $M < 6$ (Wyss, 1986). The search for historic earthquakes in the Kaoiki area was carried out to test the above hypothesis. Extrapolating the known sequence back in time, mainshocks were expected near 1930 and 1919. During the period for which macroseismic data were available (1912 through 1939) the only two Kaoiki mainshocks found occurred in 1930 and 1918. This observation supports the idea that Kaoiki mainshocks occur at intervals of approximately 10 years. In addition the occurrence time of the great Kau earthquake, that ruptured the Kaoiki area, also fits a time expected for a Kaoiki rupture based on extrapolation. It is concluded that the observations support the proposal of regular occurrence of the Kaoiki mainshocks.

(2) A relationship between the extent of the felt areas of given intensity and the magnitude of Hawaiian earthquakes was needed because the attenuation of seismic waves below and near the island of Hawaii appears to be stronger than in the contiguous United States. Based on 9 earthquakes for which instrumental magnitudes were available we estimate the following relationship between magnitude and intensity VI and V areas

$$M = \log ( A(VI) ) + 2.63$$
$$M = \log 1.16( A(V) ) + 1.34$$

These relationships are proposed for Hawaiian earthquakes in the range $5.4<M<8.1$. This relationship indicates that the felt areas in Hawaii are smaller for a given magnitude than in California. Based on these relationships and additional macroseismic data for subcrustal earthquakes we estimated magnitudes for 14 historic Hawaiian earthquakes.

(3) The proposed model for the great Kau earthquake of 2 April 1868 was finalized. It is estimated that its magnitude was approximately 8 and that its rupture area included all of Hawaii's SE coast, Kaoiki, and Hilea, abutting Mauna Loa's south-west rift zone. Evidence was found that suggests that the accelerations in the meisoseismal area were larger than 1 g.

(4) Seismic quiescence appears to have preceded the January 1982 mainshocks in the Hilea area of Southern Hawaii. The two mainshocks of 21 January 1982 plus the aftershocks added up to an equivalent magnitude of 5.6. The rupture area had a radius of about 5 km. The significance of the 46 weeks quiescence scored not very high on the $\beta$-test, but it was unique in the area during 14 years of data, except for one period of known low reporting during the aftershock sequence of the large 1975 Kalapana earthquake. It is concluded that for earthquakes in Hawaii with $M \geqslant 5.5$ precursory quiescence may be detected if this phenomenon occurs and if conditions are favorable, that is if the local seismicity rate is high and if the catalog contains small events reported homogeneously.

## Publications

Zuniga, F.R., M. Wyss and F. Scherbaum, A moment magnitude relation for Hawaii, *Bull. Seis. Soc. Am.,* 78, 370 - 373, 1988.

Wyss, M., A proposed source model for the great Kau, Hawaii, earthquake of 1868, *Bull. Seis. Soc. Am.,* in press, 1988.

Wyss, M. and R.L. Kovach, Comments on "A single force model for the 1975 Kalapana, Hawaii, earthquake" by H.K. Eissler and H. Kanamori, *J. Geophys. Res.,* in press, 1988.

Wyss, M. and Z.-X. Fu, Precursory seismic quiescence before the January 1982 Hilea, Hawaii, earthquakes, Bull. Seis. Soc. Am., submitted, 1988.

Wyss, M. and R. Koyanagi, Macroseismic maps for earthquakes in Hawaii, 1968 to 1983, in preparation, 1988.

# Geologic studies for seismic zonation of the Puget lowland

Brian F. Atwater
Branch of Western Regional Geology
University of Washington AJ-20
Seattle, Washington 98195
(206) 442-2927    FTS 399-2927

## INVESTIGATIONS AND RESULTS

Preparation of reports concerning the results summarized for this project in Volume 25 of the Summaries of Technical Reports (USGS Open-File Report 88-16).

## REPORTS

[Published between October 1987 and March 1988]

Atwater, B.F., Hull, A.G., and Bevis, K.A., 1987, Aperiodic Holocene recurrence of probably coseismic subsidence in southwestern Washington: EOS (Transactions, American Geophysical Union), v. 68, p. 1469.

# DATING MARINE TERRACE DEFORMATION NORTH OF THE MENDOCINO TRIPLE JUNCTION

Contract No. 14-08-001-G1332

Glenn W. Berger and Don J. Easterbrook

Dept. of Geology
Western Washington University
Bellingham, WA 98225

## OBJECTIVES

This project began February 15, 1987. The objective is to date eolian and waterlaid sediments by thermoluminescence (TL) methods (eg. Berger, 1986), and thereby establish the chronology of observed uplift and displacement features in the area of the Mendocino triple junction in Humboldt County, northern California (eg. Carver et al., 1986). The applicable range of TL dating, a few hundred to several hundred thousand years, spans the inferred time of deformation in the area. Paleomagnetic measurements are also being made at each site to screen sediments that would be too old for TL dating and to look for the ~100,000 year-old Blake event in terrace deposits.

## PROGRESS TO DATE

We traveled to Humboldt County in late February, 1987 to collect samples with the assistance of Drs. Burke and Carver of Humboldt State University. Sediments for thermoluminescence and paleomagnetic measurements were collected at the mouth of the Mad River, Table Bluff, Centerville Beach, and Trinidad Head. Fifteen samples were selected for TL analyses: two "zero-age" samples to check zeroing assumptions under specific depositional conditions, two Holocene dune sands to check zeroing assumptions for older dune sand, one late Holocene clay to check zeroing for older clay, three pre-Holocene unknown-age dune sands, two unknown-age marine estuarine clays, and five unknown-age marine shoreline clay-silt-sand deposits.

## PALEOMAGNETIC ANALYSES

Seven localities associated with recent tectonic movement in the Arcata area were sampled for paleomagnetic measurements. The purpose of the paleomagnetic sampling was (1) to screen sites which might be too old for thermoluminescence dating, and (2) look for evidence of the ~100 ka Blake event in terrace sediments believed to be about that age. The localities which were sampled are listed below:

Southport Quarry
Table Bluff
Centerville
Upper Patricks Point
Lower Patricks Point
Hilltop terrace

Experimental paleomagnetic measurements were carried out on samples from each locality to determine the nature of the magnetic remanence and to establish the best demagnetization level for the bulk of the samples. All paleomagnetic measurements were made on a Schonstedt spinner magnetometer and Schonstedt demagnetization equipment at the Western Washington University paleomagnetic laboratory.

Examples of the paleomagnetic data are listed below for each of the localities sampled:

### Southport Quarry

Samples were collected from silt/clay lenses interbedded in sandy gravel which has been folded into an anticline whose flanks dip about 20 degrees. The gravel is believed to represent a beach environment. All samples showed normal polarity, suggesting that the sediments were deposited during the Brunhes Polarity Chron. Samples for thermoluminescence dating were also collected.

## Table Bluff

Samples for thermoluminescence dating and paleomagnetic measurements were collected from silt interbedded with sandy gravel near the top of the section. Additional samples of paleomagnetic measurements were collected from another silt unit near the base of the section about 50 feet beneath the upper silt. All of the samples showed normal magnetic polarity.

## Centerville

Two parallel profiles of samples for paleomagnetic measurement were sampled in silt interbedded with marine sand and gravel. All samples showed normal magnetic polarity.

## Patricks Point

Two levels of marine terraces are tilted northward along sea cliff exposures over a mile long. Samples for thermoluminescence dating and paleomagnetic measurements were taken from sediments exposed in the sea cliffs. Samples were collected from silty clay interbedded with dune sand high in the section and from marine silty clay near the base of the cliffs. All paleomagnetic measurements showed normal polarity.

## Hilltop Terrace

Samples of terrace sediments were collected from Hilltop terrace for paleomagnetic measurement. The sediments are believed to be about 100 ka and provide a possible site to look for the Blake reversed event within the Brunhes Polarity Chron. All samples showed normal magnetic polarity.

The paleomagnetic measurements for these sites all show normal magnetic polarity, indicating that they are younger than 730 ka and are therefore within the probable range of TL dating. No evidence of the Blake Event was found at any of the sites.

## TL-RELATED ANALYSES

Data essential for calculating the ionizing radiation dose to the TL samples have been measured (potassium, uranium, and thorium concentrations) for all but three samples. One of these was chosen for TL measurement only, whereas the two others are presently being processed. Potassium has been determined by atomic absorption analysis and uranium and thorium by thick-source alpha particle counting. TL measurements are now in progress. Thus far, radiation sensitivity, anomalous fading, and optical bleaching tests have been performed on about three-quarters of the samples, and final TL readout (partial-bleach method) has been completed for four samples. Preliminary data suggest that the collected dune sand represents good material for TL dating and that the beach sand also has "well-zeroed" TL mineral clocks. The remainder of the TL analyses are proceeding.

Feb. 23, 1988.

# Frequency and Magnitude of Late Quaternary Faulting, Sierra Nevada, California

14-08-0001-G1334

Peter W. Birkeland and Margaret E. Berry
Department of Geological Sciences
University of Colorado
Boulder, Colorado, 80309
(303) 492-6985

## Investigation

The project is designed to study the history of late Quaternary faulting along a portion of the eastern escarpment of the Sierra Nevada, California. The work entails 1) study of the glacial stratigraphic sequences in valleys where deposits have been offset by faulting, and 2) study of the fault scarps which cut these deposits. Most of the work has been done in the areas around Bishop, McGee (S), Pine, and McGee (N) Creeks. Objectives of this work are to determine a time frame for faulting, in particular frequency of faulting and amounts of offset associated with displacement events, and from these data calculate rates of offset. As discussed previously (Summaries of Technical Reports volume XXV), two trenches were excavated for the study: one located in the Bishop Creek area on a Tahoe or pre-Tahoe moraine, and the other in the McGee (N) Creek valley on a Tioga recessional moraine. Work on the project during the past six months has included continued laboratory analysis of soils and sediments collected in the Bishop Creek trench, and the dating of materials collected in the McGee (N) Creek trench.

## Results

1) Grain-size analyses have been completed for samples collected in the Bishop Creek trench. Particle-size distribution of the <2-mm fraction of the soils show a slight build up of clay in soils developed upslope of the fault relative to those developed in the fault-scarp colluvium, and a slight fining of grain size in the more distal colluvium relative to the proximal colluvium. In general, soils developed in the colluvium have a more uniform particle-size distribution than do those developed in till. This latter characteristic of the colluvial sediments is similar to what we see in the McGee (N) Creek colluvium. Data obtained from the Bishop Creek trench exposure suggest that faulting produced multiple surface ruptures rather than a single break. Much of the fault displacement probably occurred prior to extensive weathering of the clasts. This interpretation is suggested because boulders both in the till and in the fault-scarp colluvium are highly grussified.

2) Five sediment samples collected for thermoluminescence (TL) dating from distal colluvium within the McGee (N) Creek trench have been analyzed. TL age estimates determined thus far are encouraging; ages are progressively older with depth in the profile. In addition, similar ages are obtained for sediments sampled laterally within the trench. Although interpretation of the results is not final, the preliminary data indicate that faulting began <25,000 years ago, and that deposition of the colluvial wedge continued into the Holocene.

3) Four wood and charcoal samples found at various sites within the McGee (N) Creek trench have been submitted for 14C dating by accelerator mass spectrometry. Age estimates for these samples should provide some constraints on the timing of colluvium deposition, as well as a broad check on TL age estimates obtained for the sediments.

# Surface Faulting Studies

9910-02677

M.G. Bonilla
Branch of Engineering Seismology and Geology
U.S. Geological Survey
345 Middlefield Road, MS 977
Menlo Park, CA 94025
(415) 329-5615

## Investigations

1. Preparation of reports.
2. Field investigation of earthquakes.
3. Variation in fault displacement along trace.

## Results

1. Changes were made in reports on a) the smallest earthquake magnitude associated with coseismic surface faulting, and b) the appearance of active faults exposed in exploratory trenches.

2. Participated in mapping liquefaction effects and surface faulting associated with the November 1978 Superstition Hills earthquakes.

3. In collaboration with W.R. Thatcher, began study of variation in fault displacement along faults that have had surface rupture in historical time. Among the factors considered are slip estimated by both geologic and geodetic methods, and the distribution of the seismic energy released in the earthquake. Preliminary results were presented by Thatcher at the "Workshop on fault segmentation and controls of rupture initiation and termination" that was held March 7-9, 1988.

## Reports

Bonilla, M.G., 1988, Minimum earthquake magnitude associated with coseismic surface faulting: Association of Engineering Geologists Bulletin, v. 25, no. 1, p. 17-29.

Bonilla, M.G., in press, Faulting and seismic activity, Chapter 10 in Kiersch, G.A., ed., The heritage of engineering geology--the first hundred years: Geological Society of America Centennial Special Volume CSV-3.

# Sedimentological Analysis of Postulated Tsunami-Generated Deposits from Great-Subduction Earthquakes Along Washington's Outer Coast

14-08-0001-G195

Joanne Bourgeois
Dept. of Geology
University of Washington
Seattle, Washington, 98195
(206) 545-2443

OBJECTIVE: It has been suggested by several workers that tsunamigenic subduction earthquakes, similar to the 1960 and 1964 events of Chile and Alaska, have occurred along the Cascadia Subduction Zone. Recently, on the southern coast of Washington at Willapa Bay, geologic evidence for very rapid subsidence of coastal wetlands has been discovered. The evidence consists of several layers of supratidal and forest peat which alternate with beds of estuarine mud (Fig. 1). Three of these formerly emergent surfaces are overlain by a thin layer of sandy-silt interpreted by Atwater as the residual deposits of tsunamis that overran freshly submerged coastal platforms. The purpose of this study is to determine if these sands were deposited by tsunamis or by some other mechanism.

Approach: There are several mechanisms by which fine sand and silt could be deposited on a submerged coastal platform: 1) (landward-directed) surges generated by a tsunami wave train, 2) seiching generated by subsidence due to an abrupt down-dropping of the coastal platform; 3) (landward-directed) flooding from storms; or 4) (seaward-directed) flooding of tidal channels and/or migration of tidal channels. Our approach is to consider the potential of each mechanism to transport sediment over salt marsh surfaces. We will accomplish this by conducting detailed field measurements, grain size analyses, and petrography, and then generating a sediment-transport model for the deposition of these layers.

WORK IN PROGRESS: To date our work at Willapa Bay has focused on the sandy unit overlying the youngest buried wetland surface. Already, we have conducted regional (Willapa Bay) and detailed local mapping of this sand layer, sampled for petrographic and grain-size analyses, and described the unit from cut-bank outcrops.

Field Work: This unit comprises laminae of sandy silt alternating with mud, capped by a distinctive couplet of two thin laminae, which we have correlated regionally in Willapa Bay and northward to Gray's Harbor (Fig. 2). We have completed an isopach map of the sandy unit along the Niawiakum River (Fig. 3), which shows that the unit thins in the upstream direction, and that it is thicker on the downstream sides of point bar/wetland surfaces than on the upstream sides. This pattern exists on other tidal channels also and is a key to locating the layer, as surfaces than on the upstream sides. This pattern exists on other tidal channels also and is a key to locating the layer, as well as to its interpretation.

Grain Size Analysis: We have begun grain-size analyses of the sandy unit from the Niawiakum River. Two important preliminary results are 1) the grain sizes of the basal sandy lamina fine in the upstream direction; and 2) the lamina contains a high proportion of silt and clay sizes, evidence for rapid deposition of sediment from suspension, rather than tractional deposition in an upper-plane-bed regime, wherein we would expect little if any clay to be deposited.

Petrography: Thin sections of the sandy unit, and of samples from modern sand flats, mud flats, and tidal channels are presently being prepared. Petrographic analysis will be used to determine the sediment source of the sandy unit.

PRELIMINARY CONCLUSIONS:

1) The event depositing the sandy unit was of at least regional scale (Willapa Bay to Grays Harbor), as indicated by correlation of the lamina couplet.

2) The depositional event was composed of several pulses, as indicated by the alternating laminae of sandy silt and mud, and the sediment of each lamina was deposited from suspension.

3) The event was landward-directed, as indicated by upstream thinning and fining of the unit, as well as by its distribution over the point bar/wetland surface.

4) Seaward channel flooding or migration of tidal channels could not have produced this pattern of sand distribution; we have not yet eliminated any of the pulsing, landward-directed processes, i.e., tsunami, seiche and tide-modulated storm surge.

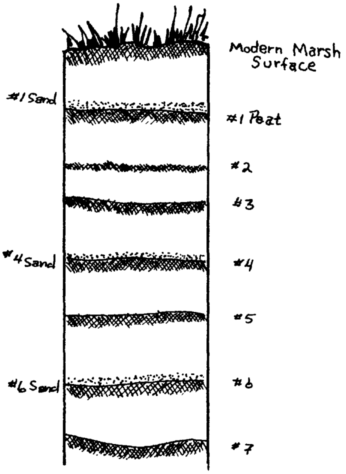

FIGURE 1. Generalized stratigraphic section of Holocene sediment at the Niawiakum River in Willapa Bay showing all identified peaty layers (representing buried surfaces) and sandy units. The section is compiled from cores made by Atwater and Grant (1986). The sandy units are labeled to coincide with their corresponding peats.

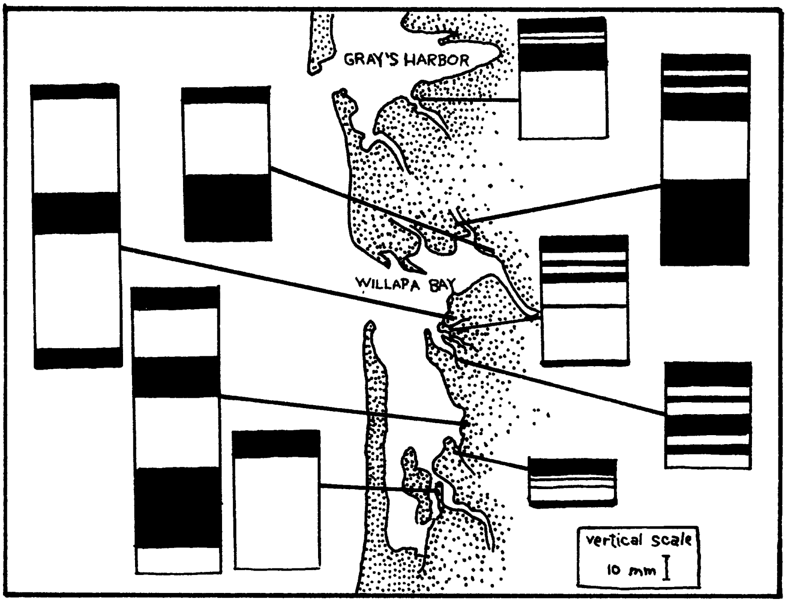

Figure 2

Figure 2. Map of Willapa Bay and Gray's Harbor showing the regional distribution of the sandy unit and correlative nature of the couplet. The small insets represent the micro-structure of the unit at each locality (White = sand; Black = mud). Two patterns of sedimentation have be found 1) thicker laminae of sand (left side of diagram) occurring at sites more exposed to the bay and 2) thinner laminae, including the couplet, found at sites more protected from the bay.

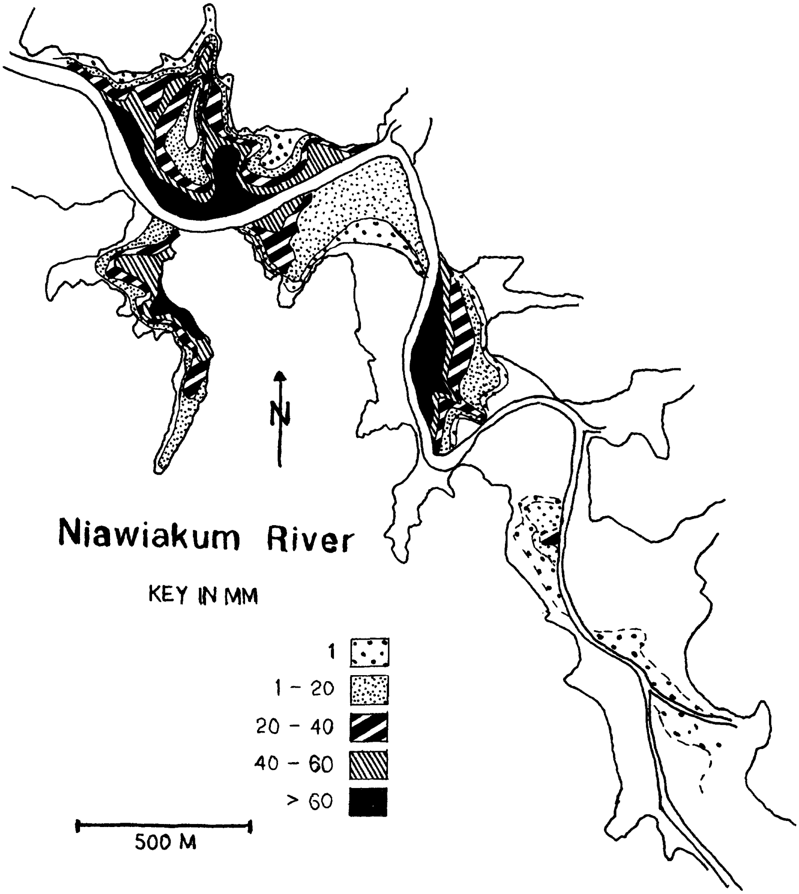

Figure 3. Isopach map of #1 sand (overlying the youngest buried wetland surface) at the Niawiakum River in Willapa Bay as compiled from tidal-channel outcrop and approximately 200 cores. The map shows two trends of sediment distribution: 1) thickness of #1 sand is greatest at the channel mouth, measuring >60 mm and thinning to <1mm about 3 km upstream, and 2) thicker accumulation of sand occurs on the downstream side of point bar/marsh surfaces than on the upstream sides.

# Northern San Andreas Fault System

9910-03831

Robert D. Brown
Branch of Engineering Seismology and Geology
U.S. Geological Survey
345 Middlefield Road, MS 977
Menlo Park, California 94025
(415) 329-5620

## Investigations

1. Continuing research and compilation of data on Quaternary deformation in the San Andreas fault system, for a planned volume summarizing current geologic and geophysical knowledge of the fault system.

2. Research and review of work by others on the tectonic setting and earthquake potential at Diablo Canyon Power Plant (DCPP), near San Luis Obispo, California. Activities are in an advisory capacity to the Nuclear Regulatory Commission (NRC) and are chiefly to review and evaluate data and interpretations obtained by Pacific Gas and Electric Company (PG&E) through its long-term seismic program.

3. Serve as chairman of Policy Advisory Board, Bay Area Earthquake Preparedness Project (BAREPP). A joint project of the State of California and the Federal Emergency Management Agency, BAREPP seeks to further public awareness of earthquake hazards and to improve mitigative and response measures used by local government, businesses, and private citizens.

## Results

1. Completed paper entitled Quaternary deformation of the San Andreas fault system; received review comments.

2. Continued reviews of geologic and geophysical data related to DCPP and provided oral and written review comments to NRC. Coordinated USGS review and data acquisition efforts related to DCPP.

3. Provided informal oral and written data, analysis, and recommendations to BAREPP and other Policy Advisory Board members on geologic, seismologic, and management issues relating to earthquake hazard mitigation in California.

## Reports

None.

04/88

# Characteristics of Active Faults

9950-03870

Robert C. Bucknam
Branch of Geologic Risk Assessment
U.S. Geological Survey
Box 25046, MS 966, Denver Federal Center
Denver, Colorado 80225
(303) 236-1604

## Investigations

1. Study of neotectonic deformation in the vicinity of Seattle, Wash.

## Results

1. The current U.S. Geological Survey program to evaluate earthquake potential in the Puget Sound region is focused on an area that has not had a large earthquake in historic time. There is a critical need to document and carefully evaluate any evidence that would demonstrate that large earthquakes have occurred in the region in the geologically recent past (for example, during Holocene time). Such information would significantly strengthen inferences of earthquake potential that are based on the historic record of relatively small earthquakes and on general analyses of the tectonic setting of the region.

   This study is focused on developing an understanding of the nature of Holocene deformation in central Puget Sound that is likely to be the result of large prehistoric earthquakes. Knowledge of the details of such deformation will provide a basis for estimating the size and frequency of occurrence of earthquake events that might be expected to occur in the Seattle area.

   Several sites in the Seattle area show evidence of late Quaternary deformation likely to be associated with one or more major earthquakes. At one of these sites on southern Bainbridge Island (site no. 40 of Gower and others, 1985), Jim Yount has found evidence for several meters of uplift within the last few thousand years. The uplift is expressed as a well-defined raised marine terrace and by a somewhat irregular surface cut on bedrock several meters above sea level. The uplift appears to be the result of a sudden event, possibly associated with an earthquake. A similar feature occurs at Alki Point in west Seattle, but is less conspicuous due to urban construction. The work to be undertaken in this study will focus on defining the extent and nature of this deformation to provide a basis for estimating the size of earthquakes that might be expected in the Seattle area.

Conspicuous evidence of recent uplift is restricted to a relatively small area in which bedrock outcrops. To better define the age and extent of the area of this deformation, the stratigraphic record in marsh deposits in the Kitsap Peninsula area will be evaluated using the general approach developed by Brian Atwater for his studies of deformation along the Pacific Coast of Washington.

## Reference Cited

Gower, H.D., Yount, J.C., and Crosson, R.S., 1985, Seismotectonic map of the Puget Sound region, Washington: U.S. Geological Survey Miscellaneous Investigations Map I-1613.

# Late Quaternary Slip Rates on Active Faults of California

9910-03554

Malcolm M. Clark
Branch of Engineering Seismology and Geology
345 Middlefield Road, MS 77
Menlo Park, CA 94025
(415) 329-5624, FTS 459-5624

## Investigations

1. Recently active traces of Calaveras fault zone at Tres Pinos Creek and San Felipe Creek, California (K.K. Harms, J.W. Harden, M.M. Clark).
2. Recently active traces of Owens Valley fault zone, California (Sarah Beanland, Clark).
3. Post-earthquake investigations at Whittier Narrows, California (Oct., 1987) and Superstition Hills, California (Nov.-Dec., 1987) (Clark, Harms).

## Results

As in several other structural valleys of the Walker Lane belt, Owens Valley has independent, subparallel, and active normal and strike-slip faults. In Owens valley they are the Independence fault (the Sierran Range-front fault), and the mid-valley Owens Valley fault. Both are at least 90 km long and have records of Holocene slip; they lie 5-15 km apart. In late Quaternary time the Independence fault shows normal slip only, and at an average rate of about 1 mm/yr; the Owens Valley fault shows dominantly strike slip at an average rate of about 2 mm/yr.

Northwestward from Owens Valley along the Sierran range-front, in contrast, strike-slip faulting is absent near the range-front, but the maximum late-Quaternary slip rates of the range-front normal faults rise to about 2 mm/yr, 20 times greater than the range-front slip-rate in Owens Valley, and about equal to the strike-slip rate there.

Clark and K.W. Hudnut (Lamont-Doherty Geological Observatory) found discontinuous new surface ruptures along a 5-km length of the central break of the 1968 rupture of the Coyote Creek fault on 28 and 30 Nov., 1987, after the Superstition hills earthquake. This possibly triggered slip was right lateral, 15 mm maximum; most measurements were <10 mm. A small vertical component was probably present but could not be measured precisely. Total length of the new ruptures was about 3 km. These ruptures are present on three separate quasi-continuous segments of the main fault plus one segment of a secondary fault. The longest segment followed the NE side of Ocotillo Badlands for nearly 2.3 km. The new ruptures were limited to parts of the central break that showed both large afterslip and large cumulative right lateral and vertical components of slip during and after 1968. All these places have Holocene scarps. The longest segment of new ruptures coincides with zone of most persistent post-1968 fracturing and slip (5-8 yr.). The north break of 1968, which had the largest horizontal slip then (380 mm), locally significant vertical components, Holocene scarps, but no reported afterslip, did not rupture in 1987. The south break also did not rupture in 1987, even though it is the closest of the three 1968 breaks to the epicenter of the Superstition Hills earthquake. Although the south break did have significant afterslip following the 1968 earthquake and evidence for rupture in the period before that earthquake, it lacks Holocene scarps, had no 1968 vertical vertical component, and had the smallest right slip of the three 1968 breaks (80 mm).

Apparently large coseismic slip, afterslip, and vertical components of slip in the past are important in determining where nonseismic or triggered slip occurs along this part of the Coyote Creek fault.

Reports:

Clark, M.M., and Hudnut, K.W., 1988, New slip along parts of the 1968 rupture of the Coyote Creek fault, California [abs.]: Seismological Society of America, 83rd annual meeting, Honolulu, Hawaii, in press.

# SUBSURFACE STUDY OF THE LATE CENOZOIC STRUCTURAL GEOLOGY OF THE LOS ANGELES BASIN

14-08-0001-G1371

THOMAS L. DAVIS
DAVIS AND NAMSON CONSULTING GEOLOGISTS
1545 NORTH VERDUGO ROAD ROOM 09
GLENDALE, CA 91208

818-507-6650

## I. Objectives:

A. Detection of blind thrusts in the Los Angeles basin.

B. Determination of geometry, kinematics, slip and slip rate of thrust faults within the Los Angeles basin.

C. Objectives are obtained by the construction of retrodeformable cross sections. Cross sections integrate surface mapping, oil well data and other subsurface data.

## II. Results:

A. Central Los Angeles basin cross section has been revised with new paleontological data from the Repetto Hills, additional well data and seismic characteristics of the 1971 San Fernando earthquake (M=6.4). The structural solution for the area north of the Raymond Hill fault has undergone minor revision (see NEHRP Technical Reports, v. XXV, p. 150, cross section A-A') and is as follows: The Verdugo-Eagle Rock fault is interpreted to have 2.9 km of dip-slip which is the minimum amount required to thrust crystalline basement over Miocene strata along a 30 degree thrust ramp (Lamar, 1970; Weber et al, 1980). The main strand of the Sierra Madre thrust system is assumed to have a ramp dip of 30 degrees based on surface mapping of the system (Crook et al, 1987), connecting the location of surface rupture of the 1971 San Fernando earthquake to the hypocenter, and the distribution of aftershocks above the hypocenter (Whitcomb et al, 1973). The revised structural interpretation places 2.9 km of dip-slip on the Sierra Madre thrust system which is the minimum amount required on a 30 degree dipping thrust to produce the range front topographic relief of about 1.5 km.

The mainshock focal mechanism for the San Fernando earthquake and distribution of aftershocks below the hypocenter show that the dip of the thrust must increase to 52 degrees near the hypocenter. This steepening with depth of the fault surface is interpreted to be a 50 degree dipping ramp below the thrust flat associated with the intersection of the main Sierra Madre thrust and the Verdugo-Eagle Rock thrust. The hypocenter location of the 1983 Coalinga earthquake (M=6.7) was probably located in a structurally similar position at the top of the thrust ramp (Namson and Davis, 1988) which may indicate a relationship between changes in thrust geometry and fault locking.

These revisions place 6.5 km of dip-slip on the combined Verdugo-Eagle Rock and Sierra Madre faults at depth. About 0.7 km of slip is lost in upper plate deformation associated with a deep-level thrust ramp. The revised convergence rate across the Los Angeles basin is 11 mm/yr.

B. Subsurface mapping in the Whittier Narrows area shows that the Whittier Narrows Earthquake of Oct. 1, 1987 and aftershocks were confined to a zone of north to northwest trending faults that cross-cut the Elysian Park anticlinorim (Figure 1). Many of the afterhocks had right-lateral slip focal mechanism with fault surfaces parallel to the north to northwest trending faults (Hauksson et al, 1988; L. Jones, personal communication). Growth relationships shown on surface mapping (Daviess and Woodford, 1949) and from well data indicate these faults were originally active during late Miocene and early Pliocene. One possible explanation for the present-day activity and kinematics of these faults is they are reactivated as tear faults in the upper plate of the Elysian Park thrust which was the cause of the main shock. Regional subsurface mapping suggests that the Whittier Narrows area has a higher concentration of the cross-cutting faults than regions to either side. This may indicate that the earthquake and aftershocks were confined to a structurally complex and weakened area along the Elysian Park thrust.

C. Papers published, in press and submitted during last 6 months:

1. "Seismically active fold and thrust belt in the San Joaquin Valley, California" by Namson and Davis (1988).

2. "The 1987 Whittier Narrows Earthquake in the Los Angeles Metropolitan area, California" by Hauksson et al (1988).

3. "Structural transect of the western Transverse Ranges, California: Implications for lithospheric kinematics and seismic risk evaluation" Namson and Davis (in press).

4. "Application of retrodeformable cross sections to seismic risk evaluation of the Los Angeles basin and the Whittier Narrows Earthquake (M=5.9) of October 1, 1987" by Davis and Yerkes (submitted).

D. Work in progress:

1. Presently constructing a retrodeformable cross section from Santa Monica northward to the epicentral region of the 1971 San Fernando earthquake.

2. Presently constructing subsurface structure contours maps of the northern margin of the Los Angeles basin. These maps will assist with the structural analysis and identify areas of possible fault segmentation.

3. M.Lagoe, University of Texas, is doing a biostratigraphic analysis of well cuttings from the deep portion of the central Los Angeles basin. This work will assist cross section construction and provide detailed age control on active structures.

4. Advisor for Kurt Haydens's master's thesis on the subsurface of the Elysian Park area, California State University Long Beach.

## III. References:

Crook, R. and others, 1987, Quaternary geology and seismic hazard of the Sierra Madre and associated faults, western San Gabriel Mountains, in, Morton, D.M., and Yerkes, R.F., Recent Reverse Faulting in the Transverse Ranges, California: U.S. Geological Survey Professional Paper 1339, 203 p.

Daviess, S.N., and Woodford, A.O., 1949, Geology of the northwestern Puente Hills, Los Angeles County, California: U.S. Geological Survey Oil and Gas Investigations Preliminary Map 83, 1:12,000.

Davis, T.L., and Yerkes, R.F., submitted, Application of retrodeformable cross sections to seismic risk evaluation of the Los Angeles basin and the Whittier Narrows Earthquake (M=5.9) of October 1, 1987: Geology.

Hauksson, E., and others, 1988, The 1987 Whittier Narrows Earthquake in the Los Angeles Metropolitan area, California: Science, v. 239, p. 1409-1412.

Lamar, D.L., 1970, Geology of the Elysian Park-Repetto Hills area, Los Angeles County, California: California Division of Mines and Geology Special Report 101, 45 p.

Namson, J.S., and Davis, T.L., 1988, Seismically active fold and thrust belt in the San Joaquin Valley, central California: Geological Society of America Bulletin, v. 100, p. 257-273.

Namson, J.S., and Davis, T.L., in press, Structural transect of the western Transverse Ranges, California: Implications for lithospheric kinematics and seismic risk evaluation: Geology.

Weber, F.H., and others, 1980, Earthquake hazards associated with the Verdugo-Eagle Rock and Benedict Canyon fault zones, Los Angeles County, California: California Division of Mines and Geology Open File Report 80-10 LA, 174 p.

Whitcomb, J.H., and others, 1973, San Fernando Earthquake series, 1971: focal mechanisms and tectonics: Review of Geophysical and Space Physics, v.11, no.3, p. 693-730.

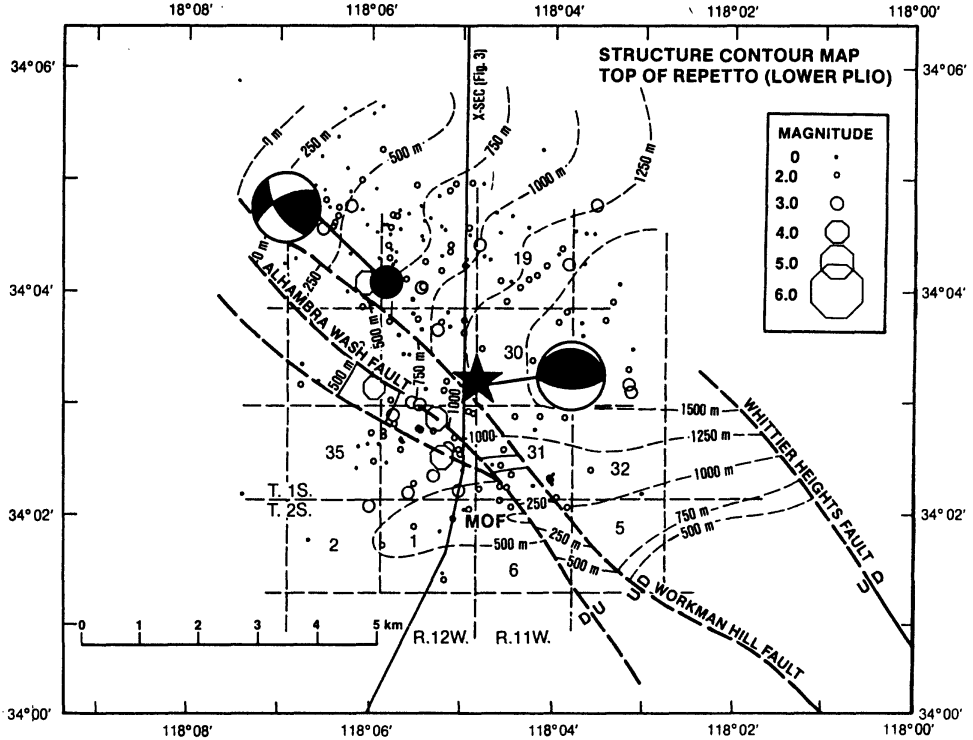

Figure 1. Structure contour map on the top of the lower Pliocene showing the concentration of seismicity within the zone of north to northwest trending high-angle faults. See text for interpretation. Focal mechanisms and aftershocks from L. Jones, USGS.

# Very Precise Dating of Prehistoric Earthquakes in Southern California using Tree-Ring Analysis

USGS 14-08-001-G1329

Gordon C. Jacoby
Lamont-Doherty Geological Observatory
of Columbia University
Palisades, New York 10964
(914) 359 2900

Objective: The objective is to investigate the late holocene history of active faults in southern California, the San Andreas fault in particular. This objective is to be achieved by analyzing growth changes in annual rings of trees growing in the fault zone region. Trees on or very near the fault are compared to trees growing at some distance from the fault. This information is then used to determine precise (to the year) date(s) of, and thus intervals between, major surface-rupturing earthquakes.

Field Sampling: Over 100 trees have been sampled for the purposes of this research. About 70 trees have been sampled in the vicinity of Wrightwood, California(Figure 1). Species are primarily Jeffrey pine (*Pinus jeffreyi*) with some White fir (*Abies concolor*), and Incense-cedar (*Libocedrus decurrens*). To the northwest of Wrightwood 30 Pinyon pine (*Pinus monophylla*) were sampled and northwest of Palmdale, near Three Points (Figure 1), 20 California white oak (*Quercus lobata*) were sampled. All the sampling of living trees was done by coring which is nondestructive, doing no permanent injury to the trees. Several slabs were cut from stumps or previously cut trees.

Analyses: All the samples were mounted, surfaced, dated, and individual ring widths were measured. The dating established the precise date of each individual annual growth ring. Some of the extremely drought-stressed trees and those disturbed by human activities in recent years (post-1900) were not dated. The dating identified locations of missing rings and any false rings. All tree samples were visually inspected for any significant growth disturbances. Plots were made of each radius of all disturbed trees. Undisturbed trees were used to develop chronologies of undisturbed tree growth for two species in the region; Jeffrey pine and California white oak. These chronologies were plotted and used to compare the growth of the disturbed trees to determine the areal extent and severity of the disturbances. See Figure 2.

Results: Unequivocal disturbances were found in nine trees along a 12 kilometer extent of the San Andreas fault near Wrightwood, California. The date of the disturbance based on tree-ring information alone is between the growing seasons of 1812 and 1813 (1812/13 is used herein to mean between the growing seasons of 1812 and 1813). Six of the nine trees also show some evidence of disturbance by the documented 1857 earthquake. The ring-width pattern showing the effects of the 1857 event is similar but usually not as severe as the earlier earthquake.The tree-ring information alone is interpreted as indicating movement along the San Andreas fault. All the disturbed trees are within 20 meters of the fault, The ring-width disturbances are precisely synchronous to year and even season, the pattern is different from any effects of drought in undisturbed trees in the region, and the pattern is similar to that produced by the 1857 event. Alternative interpretations such as fire, disease, or ice storm cannot explain the patterns in space and time of growth disturbances.

Only preliminary analyses have been made of the samples collected from the areas to the northwest of Wrightwood. Immediately to the northwest of the discussed area are some samples collected near Jackson Lake (at star on inset of figure 1). One tree on the fault trace shows possible disturbance that dates to 1812/13. The collection of cores from the site called Caldwell Pinyon is of little help thus far in defining possible earthquake disturbance. Many of the trees are so stressed by drought that there are missing rings in 1813 and 1857, when there were severe droughts in southern California as well as large earthquakes. In the few trees near the fault from this site it is so far impossible to identify any disturbances that are clearly not attributable to the effects of drought. Analysis of these specimens is continuing.

Examination of the cores from the oak trees to the northwest of Palmdale, near Three Points (Figure 1), has likewise not produced a clear, nonclimatic, disturbance signal. Even in the 1857 and following annual rings there is no unequivocal disturbance-induced ring-width change, although the 1857 event is documented to have ruptured the ground surface in this area. More detailed analysis of these specimens is ongoing.

We have reviewed the published historical information on earthquakes in the early 1800's for this area and also the paleoseismological information from other studies. Historical information supports the interpretation of a large earthquake on 8 December 1812 being a possible San Andreas earthquake. Earlier interpretations placed the epicenter nearer the coast but this was because almost all the reports of shaking came from coastal missions. There were no literate peoples in the interior to record effects of earthquakes during that time.

The paleoseismological record, based on trenching and dating of sediments, indicates a major earthquake at Pallett Creek with a carbon-14 date compatible with the tree-ring dated event. There is evidence of a similar event near Frazier Park (Figure 1) but a faultline tree in the same area shows no disturbance. Efforts are underway to reconcile the conflicting evidence from this area.

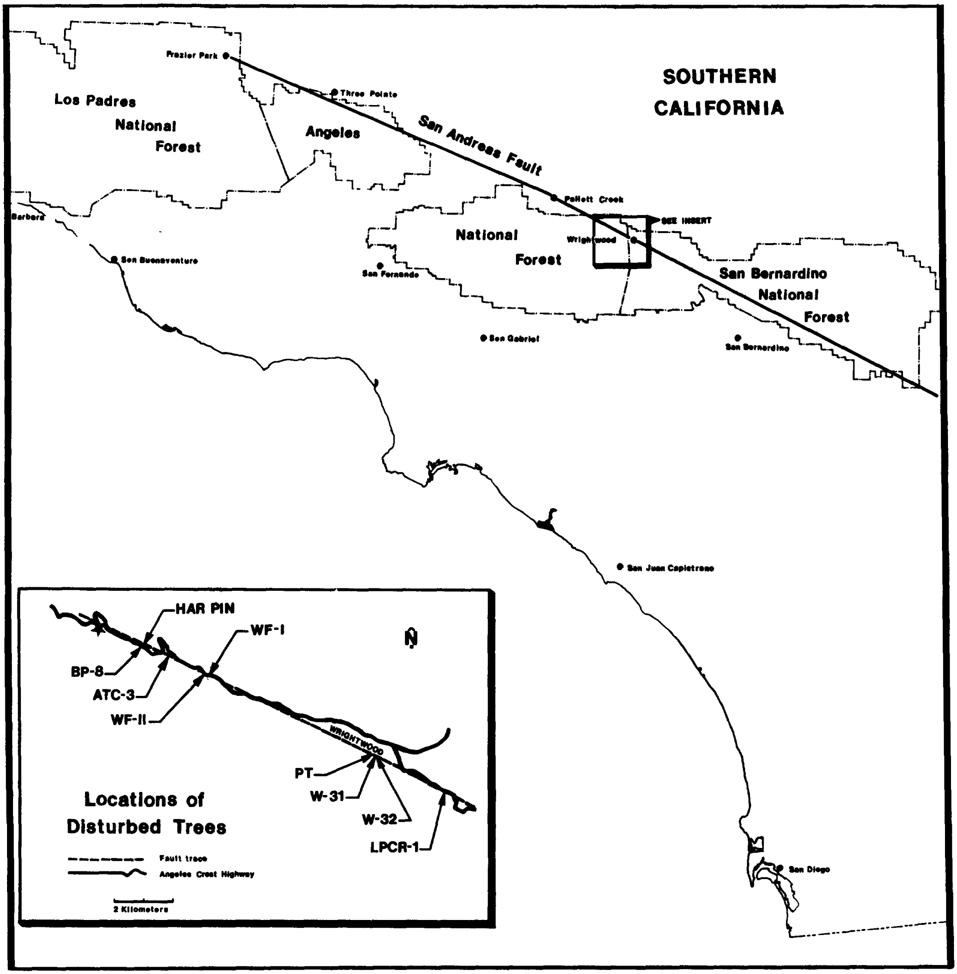

Figure 1: Map of southern California study area. Inset shows location of disturbed trees. Star in upper left is where additional disturbed tree may be located. If confirmed, rupture zone will be extended about two kilometers. Oaks described in text are near Three Points.

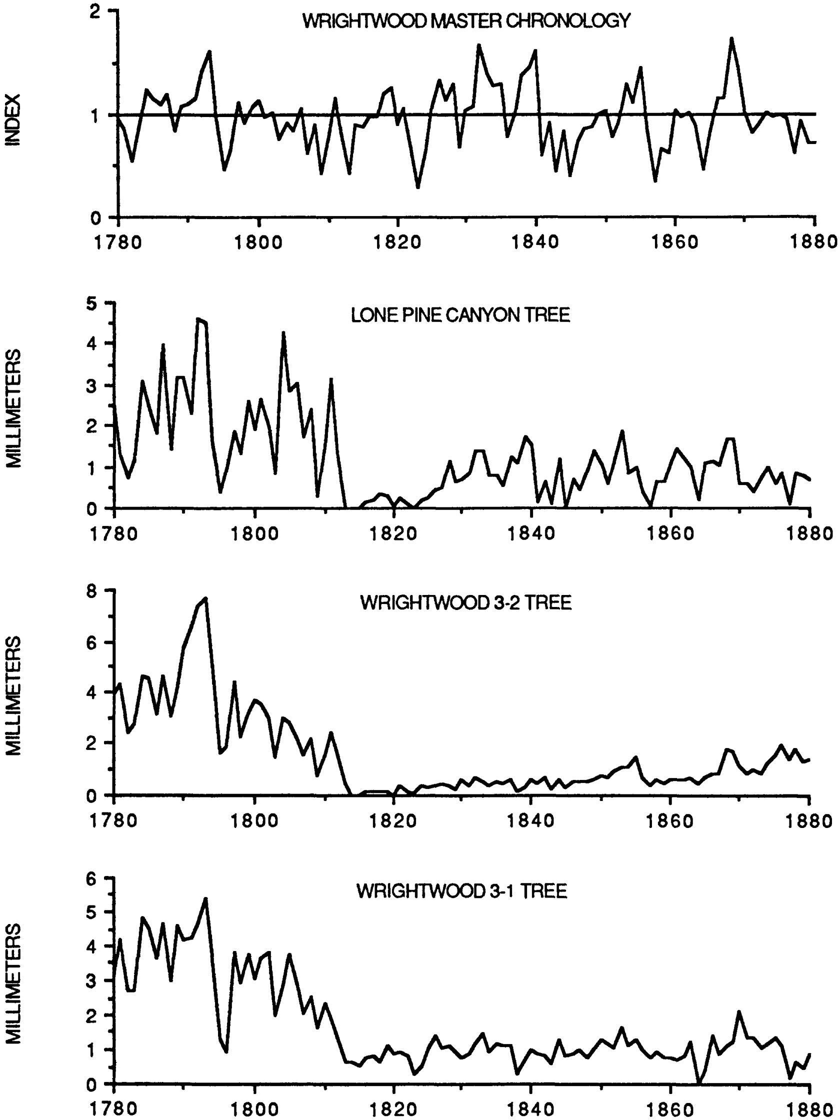

Figure 2: Radial Growth Plots. Top plot represents average growth of Jeffrey pine in the Wrightwood area when only influenced by climate. Lower three plots are ring widths for the three most disturbed trees found along the fault. Two of them had no radial growth at their bases for a few years after the earthquake. Horizontal axes are years.

# Quaternary Tectonic Framework and Earthquake Hazard in Fold-and-thrust Belts of the Western Transverse Ranges, California

14-08-0001-G1496

Edward A. Keller
Department of Geological Sciences
University of California
Santa Barbara, California 93106
(805) 961-4207

Objective: Investigate the earthquake hazard and tectonic framework that produces fault slip and crustal shortening across the western Transverse Ranges. The research involves testing the hypothesis that faulting and folding, with the exception of strike-slip on faults such as San Andreas and Big Pine faults, are mostly near the range fronts, and the interior highlands are experiencing rapid uplift as a block. Uplift of the interior occurs as a result of co-seismic thrust faulting on the edges of the range. Geomorphic response of uplift in the central highlands is reflected by erosion.

Investigations and Results: The first six months of work on this project have been focussed toward better understanding of relative tectonic activity in the Frazier Mountain area. Refinement of the Frazier Mountain soil chronosequence by $^{14}C$ dates provides an improved Late Quaternary chronology for the area. Study of stream terraces coupled to soil chronology suggests a downcutting rate of approximately 2 mm/yr in the Hungry Valley area on the eastern flank of Frazier Mountain. The high erosion rate is comparable to the uplift rate of 4 mm/yr at the San Emigdio front further north. At Little Cuddy Valley on the northwestern flank of Frazier Mountain, a segmented alluvial fan with progressively younger soils on fan segments in the downfan direction indicates that the Frazier Mountain area is experiencing rapid, uniform uplift, and responding by rapid downcutting and erosion. That is, the geomorphic history suggests that differential vertical uplift on reverse faults at Frazier Mountain is not occurring. Rather the mountain is responding to regional uplift.

# Repeatability of Fault Rupture Segments and Earthquake Potential

14-08-0001-G1527

Peter L.K. Knuepfer
Julianne M. Turko
Department of Geological Sciences
and
Center for Study of Natural Hazards
State University of New York
Binghamton, NY 13901
(607) 777-2389

Objective: Large, long faults break in segments rather than in one complete rupture. This appears to be true not only for faults at plate boundaries, but also for interior faults like the normal faults of the Basin-Range province. Two specific aspects of this apparent segmentation of faults can be investigated using geologic data: characteristics of the end-points of segments (i.e. defining segment lengths) and repeatability and independence of individual segments on a fault. The present study focuses on normal faults to examine the characteristics of surface fault rupture segments, especially the repeatability of termination points of ruptures. The primary study area is the Lemhi fault in east-central Idaho, which is east of the Lost River fault that ruptured in 1983 and displays segmented behavior. Our field studies concentrate on recognizing the extent of individual prehistoric rupture events and test whether the 1983 Borah Peak rupture is "characteristic" of other faults in the region. Ultimately we hope to document the segmentation history of the Lemhi fault and compare our results with the work of other scientists on the Lost River fault. We also are continuing ongoing work on the geologic and geometric properties of the terminations of historical surface ruptures from around the world. In this study we are examining the geologic nature of rupture end-points as reflected in surface geology in order to assess the potential of predicting segmented behavior from surface observations.

Accomplishments to Date: The project formally started eight weeks ago, and at this stage we have established our plans for field work in summer and continued to review data we obtained prior to commencement of this project. Our specific accomplishments follow.

1. Summer 1988 field work will concentrate on the Lemhi fault, Idaho. Our work this summer will include completion of data gathering for scarp morphologic studies that we began in 1987. Our principal efforts will involve trenching at as many as four sites along the Lemhi fault. These sites are chosen to maximize the likelihood that we can recover datable material, but they also are chosen to yield the most relevant data to constrain boundaries of rupture segments we have inferred from our preliminary analysis of scarp data (see below).

2. Analysis of historical faulting events has concentrated on examining end-points of ruptures irrespective of whether they acted as nucleation points or not, and comparing the characteristics of end-points with features ruptured through by each of the rupture events. We plan to expand the data

set by analyzing more earthquakes (currently at about 100) and examining the nucleation points of those events that are well enough recorded. Preliminary results of the work we had accomplished prior to this contract, and our first results under this contract, were presented at the U.S. Geological Survey NEHRP meeting on Fault Segmentation in March 1988.

Discussion of Results: We include a brief summary of our analysis of fault-scarp studies along the Lemhi fault. These studies have enabled us to define a tentative segmentation history to the fault, although our additional scarp studies and trenching this summer are critical data for finalizing these interpretations. These results are being presented at the GSA Rocky Mountain Section Meeting (Turko and Knuepfer, 1988).

We have used linear and nonlinear diffusion equations to model the degradation and estimate the relative ages of late Quaternary fault scarps along the Lemhi fault. The age of the youngest displacement varies along the fault, and the scarps allow us to tentatively define as many as nine rupture segments for the most recent events, using cluster analysis and significance tests of differences in relative ages (Figure 1). Multiple-event scarps, defined by relative scarp age, surface offset, and relative age of offset surface, show less distinct patterns of fault segmentation. However, the boundaries between some of the segments that we can distinguish differ from the boundaries between the single-event segments. This may suggest a variation in the rupture history of the fault, especially in the persistence of segment boundaries. The boundaries between the single-event segments display a variety of characteristics. Some boundaries occur at prominent geologic or geometric features, such as a bend in the range front, branching of the active fault into two main traces, or at the edge of a late Cenozoic low-angle slide block. Other boundaries, however, occur where no range bends, fault bends, or other features are obvious. Furthermore, many prominent structural and geometric features, such as a major drainage divide within the down-faulted basin and km-scale discontinuities in the range front, occur within segments. We conclude that not all segment boundaries on normal faults are marked by obvious geologic or geometric characteristics, nor do all prominent fault discontinuities, bends, and structural complexities form segment boundaries.

## REFERENCE:

Turko, J.M., and Knuepfer, P.L.K., 1988, Late Quaternary segmentation of the Lemhi fault, east-central Idaho [abs.]: Geological Society of America Abstracts with Programs, v. 20, p. 472.

FIGURE 1
Preliminary segmentation model for the Lemhi fault, Idaho

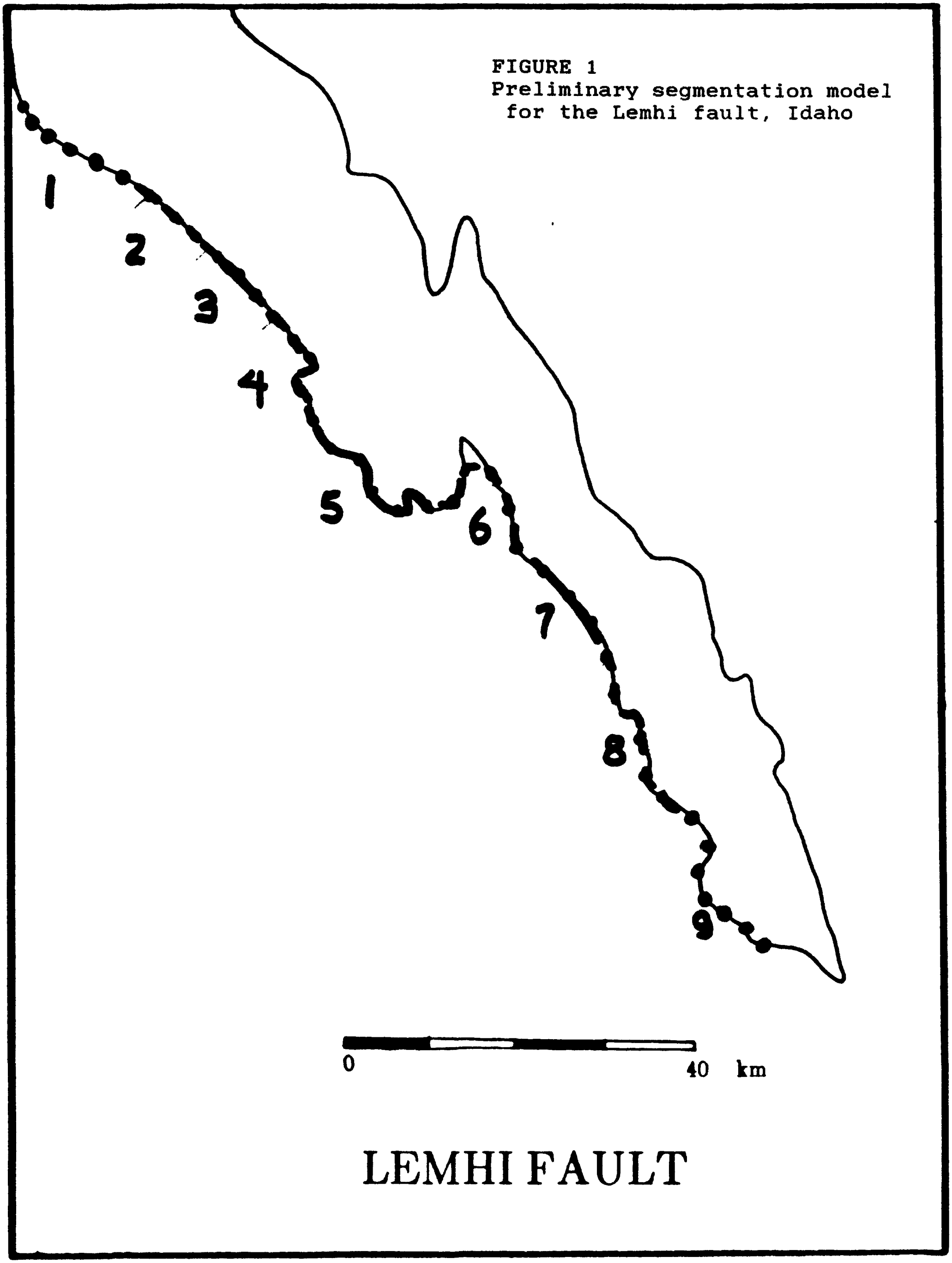

# Coastal Tectonics, Western United States

9910-01623

Kenneth R. Lajoie

Branch of Engineering Seismology and Geology
U.S. Geological Survey
345 Middlefield Road, MS 977
Menlo Park, California 94025
(415) 329-5641

## Investigations:

1. Age and deformation of Pleistocene marine strandlines and sediments in the Los Angeles Basin.
2. Paleoclimatology, tephrochronology, and paleomagnetism of the Paoha Island sediments, Mono Basin, California.
3. Paleomagnetic secular variation recorded in the Wilson Creek beds, Mono Basin, California.
4. Post-earthquake investigations, Superstition Hills, California.

## Results:

1. As we reported previously, there is no clear geomorphic expression of surface faulting in the Newport-Inglewood structural zone (NISZ) southeast of Signal Hill. This relationship might lead to the interpretation that activity in the zone dies out to the southeast. However, there is abundant geomorphic evidence of very young doming in this area, which indicates that deformation is very recent and actually might be progressing southeastward in the zone.

   The Signal Hill dome is expressed geomorphically by Signal Hill (100 m high). Linear scarps on the flanks of the Hill were most likely produced by vertical displacement across the Cherry Hill and Northeast Flank faults that bound a horst at the crest of the dome. Fossil marine shells from beds capping Signal Hill yield an amino-acid age estimate of 200 ka, which yields an average uplift rate of 0.53 m/ka.

   The Seal Beach dome, which lies 2 km southeast of the Signal Hill dome, is expressed geomorphically by the southern part of the Long Beach mesa and the Seal Beach mesa. The marine beds capping these low (25 m) mesas probably correlate with the 200 ka beds at the crest of Signal Hill. If so, the average uplift rate at the crest of the dome was 0.125 m/ka. The broad late Pleistocene (150-15 ka) channel of the San Gabriel River cuts across this dome, indicating that the recorded deformation occurred after 150 ka. If so, the avergae uplift rate was 0.17 m/ka.

The La Bolsa dome (or anticlinal nose), which lies 2 km southeast of the Seal Beach dome across the Los Alamitos gap, is expressed geomorphically by the Bolsa Chica and Huntington Beach mesas. The marine beds capping these low (15-23 m) mesas also probably correlate with the 200 ka beds capping Signal Hill. If so, the average uplift rate at the crest of this broad dome was 0.12 m/ka. The broad, late Pleistocene (150-15 ka) erosional channel cuts across this dome, indicating the recorded deformation in the last 150 ka, which yields an uplift rate of 0.15 m/ka. However, a warped alluvial terrace graded to the 125 ka(?) marine strandline on the southeastern side of Huntington Beach mesa yields a lower uplift rate of 0.07 m/ka, which suggests that deformation is slowing. Interestingly, the La Bolsa and Seal Beach channels are antecedent across structural highs, whereas the intervening Los Alamitos channel crosses the NISZ in a structural low.

The Baldwin Hills dome in the northern part of the NISZ appears to be older than the domes discussed here in the southern part, suggesting that deformation is progressing southeastward along the zone.

2. Alternating beds of diatomite-rich and diotomite-free lacustrine silt Paoha Island beds exposed on Paoha Island in Mono Lake, California, record Pleistocene lake-level fluctuations in Mono Basin, a closed hydrographic basin on the east side of the Sierra Nevada in central California. A tentative correlation of these fluctuations with sea-level fluctuations has been confirmed by tephrochronology and paleomagnetic data. Chemical data on two tephra layers analyzed by A. Sarna-Wojcicki correlate a 1 cm ash layer in glacial silts with a tephra-layer from the Cascades found in a deep-sea core where it is dated at about 290 ka. These glacial silts had been tentatively correlated with isotope stage 8, which is dated at about 305-260 ka. Also, geomagnetic data indicate this tephra layer is reversed. If the age assigned to the tephra layer is correct, this reversal probably is the Biwa II event, which is tentatively dated at 280 ka.

3. Seven meters of lacustrine silt (Wilson Creek beds) dated at 36-12 ka ($^{14}$C by S. Robinson) in Mono Basin record the last glacio-lacustrine highstand in Mono Basin. The Mono Basin paleomagnetic excursion is recorded in strata dated at 28-27 ka. Paleomagnetic secular variation (PSV) data from the entire section (S. Lund, J. Liddicoat) indicate that the excursion was followed by a distinctive but diminishing periodic vector waveform with a repeat time of 3-4 ka. The PSV pattern, which clearly indicates the excursion was the initial pulse that resonated for at least 15 ka, gives valuable insight into the core-dynamo process that produces the earth's magnetic field.

4. Two moderate earthquakes occurred in the Superstition Hills of southern California in November, 1987. A small group of geologists from the Branch of Engineering Seismology and Geology, under the leadership of R. Sharp, mapped the extensive ground rupture that occurred along previously mapped faults (R. Sharp) cutting unconsolidated and highly deformed Pleistocene lacustrine silts and clays. The first earthquake (M6.2; November 23, 5:53 p.m.) occurred on one of several northeast-trending secondary (conjugate) faults, and the second (M6.6; November 24, 5:53 p.m.) occurred on the main northwest-trending Superstition Hills fault. Up to 60 cm of right-lateral coseismic slip occurred on the main fault and up to 12 cm of left-lateral

slip occurred on the secondary faults. Two weeks after the earthquakes up to 30 cm of afterslip had occurred on the main fault, but none was measured on the secondary faults. At the ground surface most of the secondary faults are discontinuous. Many fault segments become bedding-plane faults and disappear into tight folds.

## Reports

None.

# Coastal Tectonics in the Pacific Northwest

9910-04190

Kenneth R. Lajoie

Branch of Engineering Seismology and Geology
U.S. Geological Survey
345 Middlefield Road, MS 977
Menlo Park, California 94025
(415) 329-5641

## Investigations:

Our previous amino-acid data on fossil shells from the Oregon coast suggested that the erosional platform exposed in the sea cliff at Cape Blanco is 40 ka old. More recent general data from the large Saxidomous shells reveal interesting results that imply this platform may be much older (85-105 ka), which is consistent with geologic data in the region. Unfortunately, our previous data (D/L of leucine) cannot be compared with our current data (aloisolucene/isolucene; A/I) so we are reanalyzing all the localities along the west coast to generate new isochrons. Because A/I values are much easier to obtain than D/L values, the new west coast isochron curves will be based on many more data points. Also, curves for many more species are being constructed. As a result, the correlations and ages of fossil beds along the coasts of Oregon and Washington (and along the entire west coast) will be more firmly established. Hopefully, ESR and new U-series data will calibrate these new curves more precisely.

## Results:

Preliminary conclusions from the general experiments on Saxidomous are as follows:

A. Intra-shell variability: Different structural layers in large, thick, well-preserved Saxidomous shells (both left and right valves) collected in growth position have been analyzed in detail. A/I values within one shell systematically range from 0.15 to 0.53, an age equivalence of 5 ka to 200 ka! Other parameters such as total amino-acid concentration generally follow the same pattern (relative to A/I) seen in shells of different ages. In effect, the A/I value is a direct indicator of amino-acid diagenesis, not age! A/I is an indirect indicator of age only because amino-acid diagenesis progresses with time.

The soft porous part of the outer layer of a shell yields the lowest A/I values (0.12), whereas the hard dense part yields the highest values (0.52); intermediate values (0.3-0.4) from bulk samples of this outer layer are merely averages of the extreme values of the constituent parts. The inner layer, which reinforces the lumbo region, yields consistent intermediate A/I values. In most thick shells, this is the layer sampled for analysis. Interestingly, the most consistent A/I values from various parts of a shell come from uncleaned samples. Because A/I values are different for each layer, removing part or all of one layer in cleaning can seriously change the A/I value of the sample. This experiment has demonstrated the need for consistent sampling and cleaning.

B. Inter-shell variability: Shells of <u>Saxidomous giganteous</u> from several outcrops have been analyzed in great detail. Systematic sampling of left and right valves of numerous shells reveals a distinctive A/I pattern for each shell. Some patterns consist of high A/I values while others consist of intermediate to low values. Consequently, the average A/I value for various shells from one outcrop can range from 0.1 to 0.6 (an equivalent age range of 5 ka to 300 ka), a range similar to that found in a single shell. Interestingly, the A/I patterns and average A/I values roughly correlate with shell size and thickness; small thin shells generally have lower values and large thick shells have high values. The average of A/I values from many shells roughly equals the average value of many analyses from the same shell.

Several theoretical and practical conclusions can be drawn from these extensive data sets.

A. A/I values within one shell or in several shells from the same outcrop follow the same diagenetic pathway as shells of different ages. The lessons drawn from these experiments should improve our age estimates for the few fossil localities along the coasts of Oregon and Washington.

B. Sampling and cleaning procedures must be consistent. Some of our past problems may have stemmed from inconsistent sampling and cleaning.

C. Numerous shells of several species from each outcrop must be analyzed to make reasonable correlations and age estimates. Some of the errors we have made in the past probably result from analyzing only one or two samples of only one or two species.

## <u>Reports</u>

None.

# EPISODIC TECTONIC SUBSIDENCE OF LATE-HOLOCENE SALT MARSHES IN OREGON: CLEAR EVIDENCE OF ABRUPT STRAIN RELEASE AND GRADUAL STRAIN ACCUMULATION IN THE SOUTHERN CASCADIA MARGIN DURING THE LAST 3,500 YEARS.

by

Curt D. Peterson and Mark E. Darienzo
College of Oceanography
Oregon State University
Oceanography ADMIN BLDG 104
Corvallis OR 97331-5503

## Multiple Buried Marsh Horizons in Oregon Bays and Estuaries

Coastal marshes from northern, central and southern Oregon have been cored to 6 m depth to establish late-Holocene records of relative sea level and associated coastal neotectonics. Multiple buried marsh horizons (4-6 in number) have been identified in Netarts Bay (45.5 $^{\circ}$ latitude), Nestucca Bay (45.2 $^{\circ}$ latitude), Alsea Bay (44.4 $^{\circ}$ latitude) and South Slough, Coos Bay (43.3 $^{\circ}$ latitude). The marsh horizons, 10 cm to 1 m thick, have been traced laterally (over 1 km in distance) within individual estuarine systems by stratigraphic correlation of marsh and sediment burial sequences. Burial sequences are generally observed to include 1) vertically rooted or rhizome rich muds grading upward to peaty sediments (marsh layer) which are overlain by 2) barren sands or muds which commonly grade upwards to finely laminated or bioturbated muds. Fresh water diatom assemblages (high-marsh) in some buried marsh deposits are consistently overlain by brackish water diatom assemblages, confirming marsh subsidence and subsequent burial by tidal flat muds. Contacts between marsh layers and overlying burial layers are typically sharp, indicating abrupt subsidence. However, some widely traced contacts are clearly gradational (see later section). Sediment capping layers on top of some buried marsh horizons range from 20 cm to less than 1 cm in thickness and often include internal laminations of sand or mud. The sediment capping layers are wide spread in the lagoonal marsh system of Netarts Bay but are less well developed in fluvially influenced marsh systems of Nestucca and Alsea Bays. Ages of buried marsh surfaces have been estimated by radio-carbon dating of peats in Netarts Bay and indicate approximate ages of local subsidence events:

| Surface | Depth (MSL) | $^{13}$C Adjusted Age (yr BP) |
|---|---|---|
| 1st Buried marsh top | 0.7 | 350+-60 |
| 2nd Buried marsh top | 1.5 | 1220+-60 |
| 3rd Buried marsh top | 1.7 | 1640+-80 |
| 4th Buried marsh top | 2.2 | 1760+-60 |
| 5th Buried marsh top | 4.4 | 3170+-90 |
| 6th Buried marsh top | 5.3 | 3290+-100 |

## Comparitive Salt Marsh Stratigraphies From Subduction and Transform Margins

In an effort to constrain the tectonic mechanisms of coastal marsh subsidence observed in the southern Cascadia Margin we have performed comparison studies of marsh stratigraphy from the San Andreas transform margin near Point Reyes, California (38.2 ° latitude). Marsh cores (9) taken in Tomales Bay (formed within the San Andreas fault zone) contained a maximum of 6 buried marsh horizons extending to a depth of 5 m below the modern marsh surface. However, unlike the buried marsh layers of the Cascadia Subduction zone, the Tomales Bay buried marshes 1) are not widely correlated within the basin and 2) do not have distinctive sediment capping layers on top of the buried marshes even though sand is abundant within the upper basin. Burial of the Tomales Bay marshes appears to have occured by both abrupt and incremental subsidence. The preserved marsh layers and intervening sediments in Tomales Bay show no sign of liquefaction or severe disturbance even though the San Francisco earthquake of 1906 was centered near Tomales Bay.

As a control to the study of marsh sequences in the seismically active San Andreas fault zone, an investigation of marsh development was also undertaken in the Schooner Bay arm of Drakes Estero, located about 5 km due west of the fault zone. Uninterrupted peat accumulation was observed in cores to 8 m depth from this tectonically stable setting on the Salinian Block. Episodic tectonic subsidence in the northern California transform margin is limited to the transform fault zone itself. Significantly, the continuous marsh development in the tectonically stable Drakes Estero also demonstrates that marsh burial by potential fluctuations in eustatic sea-level did not occur in late Holocene time. Since marshes of the Schooner Bay arm have developed in a sediment starved, micro-tidal environment they should have been particularly sensitive to any fluctuations in eustatic sea level that might have influenced marsh development on the U.S. west coast.

The results of the northern California studies are significant in that they demonstrate a southern boundary to the abrupt subsidence style of marsh burial seen in Oregon and Washinton. In addition, the lack of severe sediment disturbance in the seismically active San Andreas fault zone demonstrates that marsh and sediment disruption are not neccessarily produced by catastrophic earthquakes. Little or no disruption of marsh or sediment burial sequences are observed in abruptly subsided deposits of coastal marshes in the southern Cascadia Margin. The lack of apparent sediment disruption in the marsh records of the Cascadia Margin does not argue against recent seismic activity in this subduction zone. Finally, the uninterrupted marsh growth in sediment starved arm of Drakes Estero indicates episodic burial of northern marshes from the Cascadia margin are not produced by late Holocene fluctuations in eustatic sea level but rather are the direct result of vertical tectonic movements.

## Temporal Transitions Between Strain Release and Strain Accumulation

While most of the buried marsh sequences we have observed in the southern Cascadia margin have sharp upper contacts (peat-sediment transitions < 1 cm thickness) some buried marshes show gradational contacts (peat-sediment transitions > 5 cm thickness). One such contact at about 4.4 m depth (MSL) is laterally persistent in Netarts Bay, northern Oregon, as the 5th buried marsh layer (see previous section). This gradual subsidence event (3,170+-90 yrs BP) occurs very shortly after an abrupt subsidence event (3290+-100 yrs BP) but long before the next subsidence event (an abrupt subsidence at 2,040+- 70 yrs BP). Two independent measures of the transition from marsh to tidal flat deposits have been performed on this gradational contact in different core sites. Both dry-weight loss on ignition (a measure of the abundance of peaty material) and a diatom indices of salinity (freshwater assemblage=high marsh, brackish assemblage=low marsh or tidal flat) are shown for one core site below.

| **Depth m (MSL)** | **Loss on Ignition (% Org)** | **Diatom Salinity** |
|---|---|---|
| 3.60 | 5 | Brackish |
| 3.96 | 7 | Brackish |
| 4.20 | 8 | Brackish=Fresh |
| 4.33 | 12 | Fresh>Brackish |
| 4.36 | 24 | Fresh |
| 4.40 | 28 | Fresh |

The more common events of marsh burial by abrupt subsidence in Oregon are clearly related to tectonic strain release while the events of gradual marsh burial appear to be related to tectonic strain accumulation. Interestingly, the transition between the two modes of subsidence (rapid strain release and gradual strain accumulation) can occur over very brief intervals (less than 300 years). Additonal evidence of recent subsidence by strain accumulation might be provided by some recent marshes (Netarts Bay and South Slough) which have well defined erosional scarps 0.5-1m in height. The most recent marshes in Alsea Bay and Nestucca Bay have relatively sharp bases (dense rhizome mats over barren sediment) and have prograded over high-energy tidal flats (sand) that have not previously maintained significant marsh development. The unusually broad coverage of these most recent marshes suggest an initial period of coastal emergence by strain accumulation or by strain release. Finally, close spaced couplets of thin marsh layers of similar age might indicate a futher complexity of tectonic movement. Such sequences are observed in Netarts Bay and possibly indicate abrupt subsidence (marsh burial) followed by emergence (rapid marsh progradation). Additional stratigraphic studies of submergent and emergent marsh sequences in the southern Cascadia Margin are needed to establish the complex tectonic cycles of strain accumulation and strain release that have ocurred along this active-margin during late Holocene time.

## Discrimination of Flood and Tectonic Events in Coastal Marsh Records

Regional climatic mechanisms of potential marsh burial have been investigated on a preliminary basis in endmember marsh systems of the southern Cascadia margin. Flood overbank deposition provides a means by which marsh burial could possibly occur independently of tectonic subsidence in fluvially dominated estuaries of the southern Cascadia Margin. In an effort to identify potential marsh burial by flood deposition, several cores (4-5 m depth) were taken in a flood plain-estuarine marsh of the Little Nestucca River in northern Oregon. Several prominant sand and/or gravel layers 10-30 cm in thickness were observed in an upstream flood plain core site, indicating abundant sand supply to the downstream marsh system. A series of 3-5 buried marsh layers were observed in two core sites 0.5-0.75 km downstream of the upper flood plain site. Although this riverine-marsh environment should have been influenced by major flood events and associated sand supply there are no sand layers associated with the buried marshes or with overlying burial sequences. The buried marshes (10-30 cm thick) have sharp upper contacts and are buried by laminated muds 20-100 cm in thickness.

To test the flood hypothesis more rigorously, a total of 10 marsh cores were taken to depths of 4-7 m in the fluvially dominated upper reaches of Alsea Bay in central Oregon. Several buried marsh layers (10-30 cm thick) are preserved in the upper 3 m of this marsh system and two of the buried marshes are capped by sand layers. Two orientated core transects, both normal and parallel to the major estuarine-riverine channel, showed no evidence of increasing sand layer thickness (1-5 cm thick) with increasing proximity to the channel margin or with increasing distance upstream. A thourough search for evidence of the 1964 flood, estimated to have exceeded the 100 yr flood level for this drainage system, showed no evidence of marsh burial or sand accumulation within the modern marsh. Preliminary indications of the marsh studies in Nestucca and Alsea Bays suggest that mash burial by riverine floods have not occured during late Holocene time in these fluvially dominated basins.

# DISCRIMINATION OF FLOOD, STORM AND TECTONIC EVENTS IN COASTAL MARSH RECORDS OF THE SOUTHERN CASCADIA MARGIN

by Curt D. Peterson and Mark E. Darienzo, College of Oceanography
Oregon State University, Oceanography ADMIN BLDG 104
Corvallis, OR 97331-5503 phone (503)-754-2759

Regional climatic mechanisms of potential marsh burial have been investigated on a preliminary basis in end member marsh systems of the southern Cascadia margin. Deposition by flood or storm surge provides means by which marsh burial could possibly occur independently of tectonic subsidence in some estuaries of the southern Cascadia Margin. In an effort to identify potential marsh burial by flood deposition, selected marsh sites (20 total) were cored to 3-5 m depth in flood plain and estuarine marshes of the Little Nestucca and Alsea Rivers in northern Oregon. Sand deposits are associated with riverine-tidal channels of each bay, providing abundant sand supply to the downstream estuarine-marsh systems. However, vertical sequences of 3-5 buried marsh horizons either 1) lack sand capping layers or 2) are overlain by sand capping layers that show no indication of increasing thickness with increasing proximity to river channel axes or with increasing distance upstream. Preliminary study results indicate that sand largely falls out of suspension upstream of estuarine marshes during maximum riverine floods when ebb flow is backed-up by constricted tidal inlets. Thick burial units of sand (>5 cm thick) are unlikely to be deposited by catastrophic floods on supratidal estuarine marshes. However, close examination of the uppermost meter of marsh deposits in Alsea Bay revealed the presence of at least three distinct mud layers (< 5 cm thick) that are associated with reduced marsh development and which correlate widely in the upper reaches of the bay. Work is in progress to establish whether these mud layers represent flood deposits or minor tectonic events.

Sediment transport and deposition by oscillatory and tidal current flow during storm surge conditions represent other potential mechanisms by which supra-tidal marshes might be buried by excessive sedimentation. Fresh water diatom assemblages in buried marsh horizons of Netarts Bay establish supra-tidal settings for the upper marsh surfaces. Detailed examination of sand capping layers above 3-5 buried marsh sequences in exposed settings of Netarts Bay in northern Oregon, demonstrate a lack of any internal cross-bedding associated with traction current transport under sub-critical flow conditions. Marsh burial sequences in exposed reaches of both bays include sand and silt laminations fining-up to silt and clay laminations between successive marsh layers. The burial sequences, up to 100 cm thick, are too thick to be formed by single storm events and yet they lack alternating sand and mud layers in the upper parts of the sequences which would be expected from deposition by repetitive storm events overprinted on a condition of rising sea level. Neither flood nor storm deposition can account for major marsh burial sequences observed in southern Cascadia coastal marshes without prior tectonic subsidence of marsh horizons to low inter-tidal elevations. The observed fining-up burial sequences represent tectonic subsidence followed by vertical sediment accretion and/or tectonic emergence to supra-tidal elevations.

# The Role of Block Rotation in Wrench Tectonics Along the San Jacinto Fault Zone, Southern California

USGS 14-08-0001-G-1330

Leonardo Seeber and Kenneth W. Hudnut
Lamont-Doherty Geological Observatory of Columbia University
Palisades, New York 10964
(914) 359-2900

April 18, 1988

Superstiton Hills Earthquake Sequence. The relevance to earthquake hazards reduction of block rotation, and our studies of cross-faults, was emphasized by the Superstition Hills earthquake sequence of November 1987. In this sequence, rupture of a left-lateral cross-fault, the newly named Elmore Ranch Fault, preceded rupture of the Superstition Hills Fault, a right-lateral master strand of the San Jacinto Fault Zone. We concentrated our post-earthquake response efforts on identification and mapping of the many northeast-trending faults that had left-lateral surface rupture. Also, we made an intensive study of surface ruptures near the intersections of two of these cross-faults with the Superstition Hills Fault. We are in the process of compiling and analyzing these data in conjunction with Tom Rockwell at SDSU.

Previous Slip on the Superstition Hills Fault. Our excavations of prehistoric Lake Cahuilla shoreline deposits near Imler Road (Figure 1) provide evidence for a previous sudden slip event with total pre-1987 slip of about 55 cm (Figure 2). Recessional shoreline deposits of the latest highstand of Lake Cahuilla showed a total of 55 cm slip on the Superstition Hills Fault between ~1680 A.D. and prior to the November earthquakes. The total slip in mid-March from the November events had reached about 55 cm, but if afterslip continues for the next ten years or so, it is projected that total surface slip from the 1987 event will be about a meter at this site (data from Pat Williams and Harold Magistrale). The previous 55 cm of slip was associated with slumping and collapse into the main fault and into minor strands, providing evidence that the previous 55 cm of slip was probably a seismic event. We are examining the possibility that the previous slip may have been due to the 6-23-1915 or 1-1-1927 Imperial Valley earthquakes located near El Centro. On all aspects of this project, we are collaborating with Kerry Sieh at Caltech, who identified this site and has constrained the age of the latest lake highstand with his work at the Indio site (Sieh, 1985).

Previous Slip on the Elmore Ranch Fault (Preliminary Results). Excavations in recessional shoreline deposits, probably of the latest highstand of Lake Cahuilla, show evidence for previous sudden slip on a strand of the Elmore Ranch Fault (northeast-trending, left-lateral). The slip event also post-dates the Lake Cahuilla deposits and pre-dates the 1987 earthquakes. Evidence for previous slip at this site is slumping and collapse into a pull-apart feature which has total left-lateral offset of about 30 cm. The slip in November 1987 at this site was 7.5 cm left-lateral. It appears that the previous slip at this site occurred in a single event, but the evidence for this is still tentative. A possible interpretation is that, during the past 300 years,the Superstition Hills and Elmore Ranch Faults ruptured in a previous sequence similar to the 1987 sequence.

Other recent accomplishments of our project include identification and mapping of possibly 'triggered' surface slip on the Central Break of the 1968 Borrego Mtn. earthquake rupture zone with Malcolm Clark (USGS), mapping new cross-faults in Ocotillo Badlands, mapping cross-faults and folds in the southeast San Felipe Hills, establishment of an alinement array on one of these faults where possible 'triggered' slip was mapped, additional work on the Superstition Mtn. Fault site at Imler/Huff Road, resurveys of geodetic lines at Clark Lake Radio Observatory and further data analysis, collection of new paleomagnetic samples in the Superstition Hills, further analysis of paleomagnetic data from Borrego Badlands, and mapping of recent structures near Borrego Mountain.

References:

Sieh, K. USGS Open-File Report #86-580, pg. 165

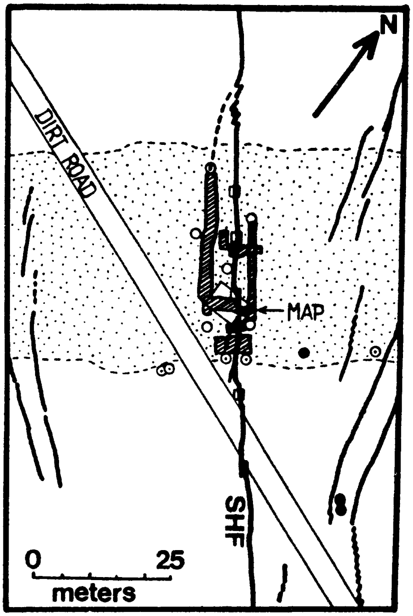

Figure 1. Site map of the excavations near Imler Road on the Superstition Hills Fault (SHF). November 1987 surface ruptures are shown as heavy lines. The ruptures cross the Lake Cahuilla shoreline deposits (stippled area) at this site. Trenches are shown as cross-hatched areas. The location of Figure 2 is indicated by 'MAP' and arrow. Benchmarks of the Caltech alinement array are shown as black dots, and new marks used in this study are shown as open circles. Small squares along the SHF are 'quads' we used to measure afterslip.

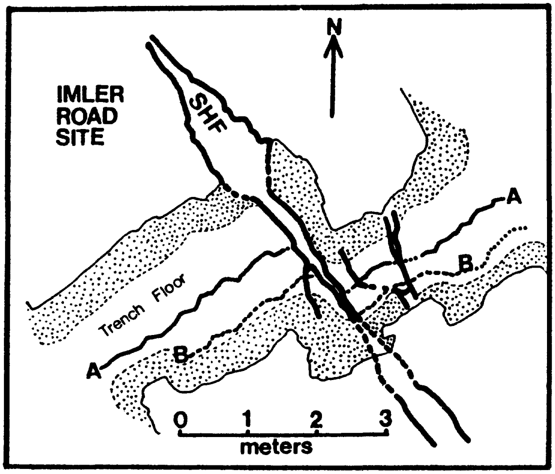

Figure 2. Simplified map of trench exposure of piercing lines A and B, which represent the intersection of foreset beds and the lake-bevelled surface of the Brawley Fm. The sediments forming these piercing lines are stratigraphically constrained to be recessional shoreline deposits from the latest highstand of Lake Cahuilla, and are dated by correlation to Sieh's site at Indio as being deposited at about 1680 A.D. (Sieh, 1985). Total offset of these lines as of mid-March, 1988 is about 110 cm. Of this amount, half occurred prior to the 1987 earthquakes. This previous slip appears to have occurred suddenly, as evidenced by extensive slumping and collapse of post-lake colluvium into the main SHF trace and minor strands prior to the 1987 break.

# EARTHQUAKE GEOLOGY OF THE SAN ANDREAS AND OTHER FAULTS IN CALIFORNIA

Grant number 14-08-0001-G1370

Kerry Sieh
Division of Geological and Planetary Sciences
California Institute of Technology
Pasadena, CA 91125
(818)356-6115

Our work during the past six months involves six separate projects being undertaken as the Ph.D. dissertation work of Marcus Bursik, Ken Hudnut, Sally McGill, Carol Prentice, Stephen Salyards and Patrick Williams.

## Evolution of the Sierra Nevada range front in the Mono Basin and the relationship of range front faulting to volcanism

Marcus Bursik's dissertation on the relationship between range front faulting along the eastern Sierra Nevada and dike intrusion underneath the Mono Craters is almost complete.

His data indicate that dikes, being intruded underneath the Mono Craters in response to crustal stretching, are now accommodating elastic strain that was once accommodated by range-front normal faulting. The section of the range formed near the craters accommodated as much as 1 mm/yr of elastic strain as recently as about 40,000 years ago. For about the past 40,000 years, however, this section of range front has become inactive, even though the range front to the north and south has continued extending at up to 0.9 mm/yr. For the past 30,000 years, dikes have been intruding underneath the Mono Craters. Depending upon the assumptions used to calculate dike intrusion rates, the dikes accommodate the 1 mm/yr of tectonic extension that was previously accommodated by range front faulting.

Extension-direction data coupled with the extension rate data indicate that the Mono Craters may be forming along one of the extensional boundary structures of a pull-apart basin, the other extensional boundary of which is the deactivated range front segment.

Implications of this work range from an increased understanding of the relationship between volcanic and tectonic processes and of slip gaps within fault systems, to ways in which large calderas are related to their tectonic environment.

## Earthquake on the Superstition Hills fault prior to 1987

Ken Hudnut and I have completed excavations of the Superstition Hills fault where it crosses the late Holocene beach berm of ancient lake Cahuilla, near Imler Road. These excavations provided evidence for a previous sudden slip event with total pre-1987 slip of about 55 cm (Figures 1 and 2). Recessional shoreline deposits of the latest highstand of Lake Cahuilla show that 55 cm dextral slip occurred on the Superstition Hills fault after about AD 1680 and before the occurrence of last November's earthquake. This slip appears to have occurred suddenly, as a seismic event, rather than as slow aseismic creep.

This 55-cm value is identical to the total coseismic slip and aftercreep associated with the November events as of mid-March, 1988.

However, if afterslip continues as projected by P.Williams and H.Magistrale (unpublished data) slip associated with the earthquake of 1987 may reach about one meter. Thus, we tentatively conclude that the last prehistoric rupture at this site was appreciably smaller than the rupture of 1987.

This study demonstrates that earthquakes of the magnitude of last November's event (M6.6) have occurred only once in the previous 300 years. The likelihood of another rupture of this fault in the next 100 years can, therefore, be regarded as quite remote.

**Neotectonics of the Garlock Fault**

Graduate student Sally McGill is studying the neotectonics of the Garlock fault. She has studied 1:5000-scale, color aerial photographs of the entire fault and has identified three sites where investigations in progress may reveal the slip rate and the amount of slip and dates of past earthquakes on the Garlock fault. Field work to date has included geologic mapping of a potential slip-rate site near State Highway 14 and measurement of small offsets along a 5-km fault segment just west of U.S. Highway 395 and along a 12-km fault segment in Pilot Knob Valley, within the China Lake Naval Weapons Center.

At the potential slip-rate site near State Highway 14, a channel wall has been offset about 45 meters. Future excavations through a fill terrace within the channel and through colluvium derived from the fault scarp may reveal carbon that would place constraints on the age of the offset.

Near U.S. Highway 395, several gullies and channels are sharply left-laterally offset 8 meters or more, but further study is required to determine whether the latest event on this segment of the Garlock fault involved 8 meters of slip or whether these offset gullies and channels record slip in more then one event.

Along a two-kilometer-long stretch of the fault within Pilot Knob Valley, several gullies and channel walls within young alluvium display consistent offsets of 5 to 5-1/2 meters. Within this stretch no convincing evidence exists for lesser offsets, even though there are even younger fan surfaces that cross the fault in this area that might be expected to show offsets of less than 5 meters if the 5- to 5-1/2-meter offsets were created by more than one event. We thus believe that the latest event on this portion of the Garlock fault probably involved 5 to 5-1/2 meters of left-lateral slip (as well as < 1 meter of down-to-the-south vertical slip).

**Paleoseismic and slip-rate studies of the northern San Andreas and San Jacinto faults**

Radiocarbon analyses of samples collected from excavations across the northern San Andreas fault near Point Arena suggest a maximum late Holocene slip rate of 23 - 27 mm/year. At least six paleoseismic events have occurred at this site since the deposition of a unit that is about 1900 years old. At least four of these events have occurred since the deposition of a unit that is about 1000 years old. Two events (1906 and one prehistoric event) break a unit that contains charcoal that is about 300 to 500 years old. Average recurrence intervals calculated from these observations indicate a maximum average recurrence interval less than 400 years. Division of the newly-determined slip rate into the amount of slip that occurred in 1906 suggests an average interval of about 200 years. This discrepancy may have any of several possible causes; one plausible explanation is that our excavations do not reveal all of the slip events that have occurred in the past two millennia.

Pleistocene marine terraces offset across the San Andreas fault near Point Arena are being studied to provide information on slip rate and deformation over the last several hundred thousand years.

We are awaiting the completion of fission track analysis of zircons separated from an ash collected from the late Pliocene(?) Ohlson Ranch Formation. This unit has been tentatively correlated with deposits offset about 50 km across the northern San Andreas fault, so fission-track ages will constrain the longer-term slip rate of the fault. Samples yielding foraminifera that have been identified by J. Ingle at Stanford University lend support (but not proof) that this correlation is valid.

Studies conducted in cooperation with Steven Wesnousky on the San Jacinto fault in San Bernardino initially suggested a minimum late Holocene slip rate of about 5 mm/yr for that fault. Recently, completion of our study revealed an error in our earlier correlation of units across the fault; A lower minimum rate is now proven. We are awaiting the results of further radiocarbon analyses from samples collected during this study.

**Paleomagnetic studies at Pallett Creek**

During the past six months, graduate student Stephen Salyards continued his analysis of the paleomagnetic rotations he measured at Pallett Creek. These measurements are on samples from a 50-meter-long excavation that cuts perpendicularly across the fault zone. Samples are from two units that bracket the third most recent earthquake at AD 1480 ± 15. Relative to unrotated control groups of samples collected 48 meters from the fault, most of the samples from the transect show clockwise (that is, dextral) rotation. These rotations range up to $40^{o}$.

The most consistent interpretation of these data indicates that dextral rotations within the fault zone totals 14.3 ± 2.5 meters for the past three earthquakes and 8.3 ± 1.0 meters for the past two earthquakes. If one includes offset of piercing points measured across discrete fault planes (Sieh, 1984), about six meters of dextral slip is derived for each of the past three earthquakes. These values give a long-term slip rate of 36 mm/yr for this section of the San Andreas fault (Figure 3). They also indicate that the fault fails with similar slip from one event to the next, even though the interval between events is quite variable.

**Paleoseismic studies along the southern San Andreas fault**

Measurements made recently at Salt Creek by Patrick Williams document a 6.5 m offset and suggest a 7.0 ± 0.25 mm/year average slip rate across the fault at this site since AD 1014 ± 32. 3 of the 6.5 meters occurred rapidly, during an event about 1014 ± 32. Most of the remaining 3.5 meters occurred substantially later, but a precise date for this event is not available.

The slip rate across the San Andreas fault at Salt Creek is a factor of 4 less than a millennial rate determined at the Indio site (Sieh, 1986). One possible explanation for this discrepancy is the occurrence of substantial, unrecognized near-fault deformation at Salt

Creek. Results of the Salt Creek investigation are being prepared for publication in a manuscript entitled Measurement of late Holocene displacements on the southern San Andreas fault at Salt Creek, southeast California.

Measurement of offset geological deposits, man-made structures and records from alignment arrays and creepmeters along two short stretches of the San Andreas fault near Indio and near Salt Creek indicate that low rates of surficial creep have persisted along the southernmost segment of this fault for the past three centuries. This observation indicates that low-level creep is not a one- or two-decade-long precursor to seismic failure of this segment of the fault. The most recent filling of Lake Cahuilla, 310 ± 35 years ago, bounds the age of a 1-m channel offset at the Indio site. Similarly beach deposits of the latest lake Cahuilla, near Salt Creek, are offset 1.2 m. Younger features that have been offset by the fault include a 39-year-old canal offset 68 mm near Indio and an 80-year-old deposit of the Salton Sea offset 150 ± 21 mm at Salt Creek. These and slip-rate data collected over the past two decades suggest that nearly steady creep at rates of a few mm/yr has persisted during the past 300 years. These data are summarized in Figure 4. Results of these investigations are in preparation for publication in a manuscript entitled Behavior of the southernmost San Andreas fault during the past 300 years.

Figure 1. Site map of the excavations near Imler Road on the Superstition Hills Fault (SHF). November 1987 surface ruptures are shown as heavy lines. The ruptures cross the Lake Cahuilla shoreline deposits (stippled area) at this site. Trenches are shown as cross-hatched areas. The location of Figure 2 is indicated by 'MAP' and arrow. Benchmarks of the Caltech alinement array are shown as black dots, and new marks used in this study are shown as open circles. Small squares along the SHF are 'quads' we used to measure afterslip.

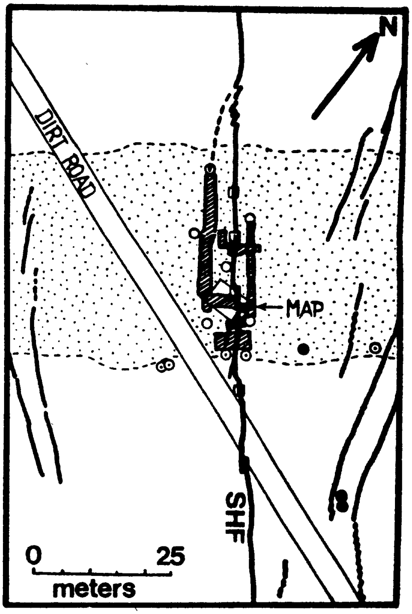

Figure 2. Simplified map of trench exposure of piercing lines A and B, which represent the intersection of foreset beds and the lake-bevelled surface of the Brawley Fm. The sediments forming these piercing lines are stratigraphically constrained to be recessional shoreline deposits from the latest highstand of Lake Cahuilla, and are dated by correlation to Sieh's site at Indio as being deposited at about 1680 A.D. (Sieh, 1985). Total offset of these lines as of mid-March, 1988 is about 110 cm. Of this amount, half occurred prior to the 1987 earthquakes. This previous slip appears to have occurred suddenly, as evidenced by extensive slumping and collapse of post-lake colluvium into the main SHF trace and minor strands prior to the 1987 break.

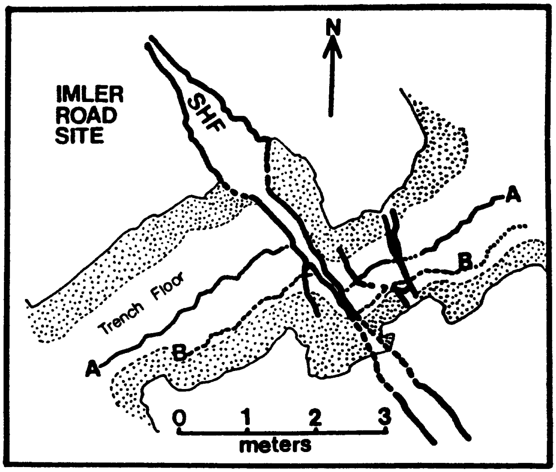

Figure 3.

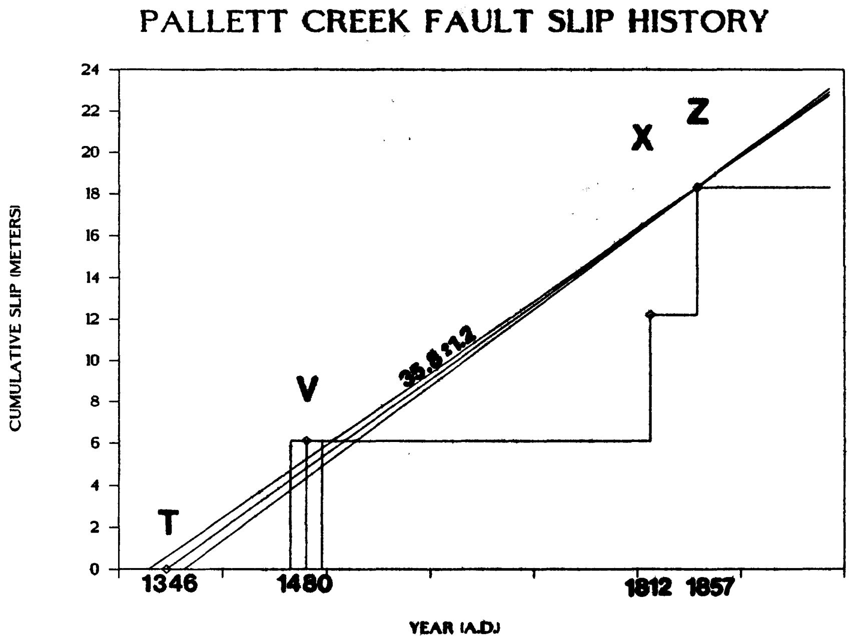
PALLETT CREEK FAULT SLIP HISTORY
CUMULATIVE SLIP (METERS)
24
22
20
18
16
14
12
10
8
6
4
2
0
T
V
35.8±1.2
X
Z
1346
1480
1812
1857
YEAR (A.D.)

Figure 4.

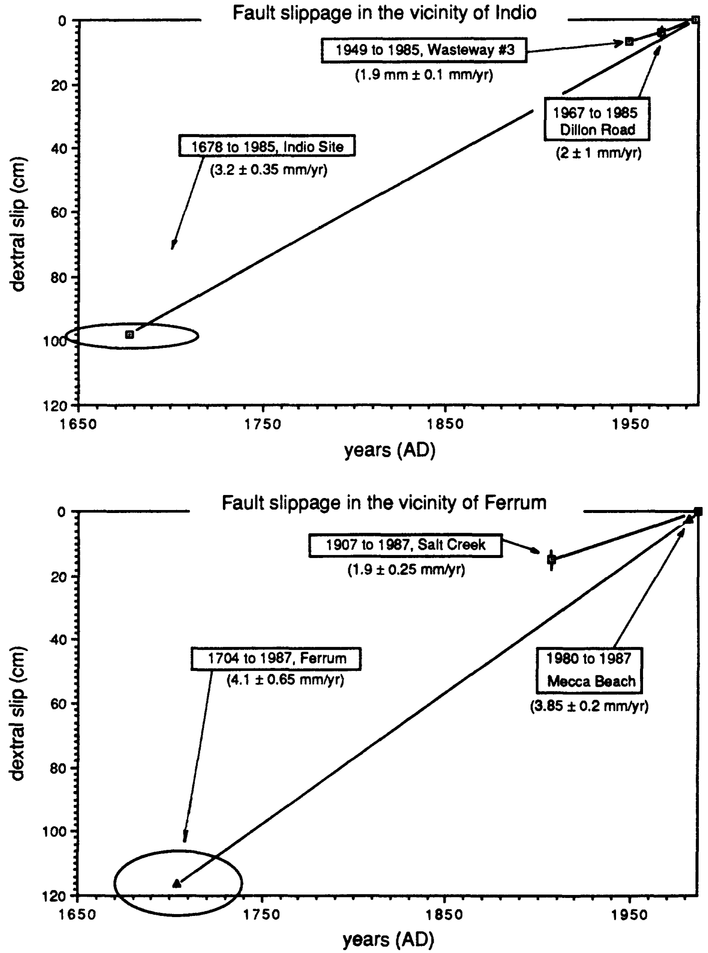
Fault slippage in the vicinity of Indio
1949 to 1985, Wasteway #3
(1.9 mm ± 0.1 mm/yr)
1967 to 1985
Dillon Road
(2 ± 1 mm/yr)
1678 to 1985, Indio Site
(3.2 ± 0.35 mm/yr)
dextral slip (cm)
0
20
40
60
80
100
120
1650
1750
1850
1950
years (AD)
Fault slippage in the vicinity of Ferrum
1907 to 1987, Salt Creek
(1.9 ± 0.25 mm/yr)
1704 to 1987, Ferrum
(4.1 ± 0.65 mm/yr)
1980 to 1987
Mecca Beach
(3.85 ± 0.2 mm/yr)
dextral slip (cm)
0
20
40
60
80
100
120
1650
1750
1850
1950
years (AD)

# DETAILED GEOMORPHIC STUDIES TO DEFINE LATE QUATERNARY FAULT BEHAVIOR AND SEISMIC HAZARD, CENTRAL NEVADA

Contract #14-08-0001-G136

Steven Slaff, Philip Pearthree, William Bull, Karen Demsey,
Julia Fonseca, Suzanne Hecker, and Oliver Chadwick
Department of Geosciences, University of Arizona
Tucson, Arizona 85721
(602)621-6024

## Investigations

The Basin and Range physiographic province has undergone block faulting and rapid extension during late Cenozoic time. Numerous young fault scarps occur throughout the province, and four historical earthquakes of $M_s \geq 7.0$ (Slemmons, 1967) have caused ground-surface rupture in central Nevada, the heart of the Basin and Range. The four rupture zones occur in a belt extending roughly north-south from Pleasant Valley to Cedar Mountain, Nevada. Slemmons (1967) concluded that the recurrence interval of large-magnitude historical earthquakes is considerably less than the late Quaternary average recurrence interval for the Central Nevada Seismic Belt (CNSB). In regard to the spatial and temporal patterns of seismicity, Wallace and Whitney (1984) proposed belt-filling in increments over a few centuries followed by a series of similar bursts of activity in other regions or in localized belts, until the original belt finally becomes active again after thousands of years.

The area of interest is shown in figure 1. The goals of the present study are: (1) to examine the times of occurrence of large-magnitude prehistoric earthquakes in central Nevada; (2) to evaluate the severity of seismic hazards in light of calculated recurrence intervals; and (3) to determine longer-term temporal and spatial faulting patterns and extensional strain rates and to compare them with the historic rates. The methods of investigation include mapping and correlation of faulted and unfaulted late Quaternary geomorphic surfaces and quantification of soil-profile development by using the Profile Development Index (Harden, 1982). Tectonic landform analysis is used to determine relative tectonic activity classes of mountain fronts and their segments (Bull, 1987). Numerical age estimates of fault scarps in alluvial deposits are derived from analyses of surveyed topographic profiles using solutions to the diffusion equation (Hanks and others, 1984).

## Results

Pierce and Colman (1986) demonstrated that for late Pleistocene-age stream terrace scarps in central Idaho, the degradation rate coefficient in the diffusion equation (c*) increases by $1.5 \times 10^{-4}$ $m^2$ with each 1 m increase in scarp height. The degradation rate coefficient also increases with increasing scarp height of pluvial lake wave-cut shoreline scarps (figure 2). For Lake Bonneville, the rate of increase is relatively low, $1.37 \times 10^{-4}$ $m^2$ with each 1 m increase of scarp height. Lake Lahontan shoreline scarps show a higher rate of increase of c*, $3.98 \times 10^{-4}$ $m^2$ with each additional meter of scarp height. For the higher altitude shoreline scarps of pluvial lakes in Grass and Smith Creek Valleys, the rate is $5.79 \times 10^{-4}$ $m^2$. Rate differences result primarily from differences in climate, vegetation, and lithology, which alter the process mix responsible for slope degradation. The data from central Nevada suggest that the dependence of degradation rate on scarp height is stronger under semiarid climatic conditions (Grass and Smith Creek Valleys) than it is under arid climatic conditions (Lahontan shorelines). The grain size distributions of scarp materials evidently may vary from coarse gravel to poorly-sorted coarse-grained deposits containing up to ~50% boulders without significantly affecting the scarp degradation rate. If boulders predominate, the scarp is "armored" and will appear to be younger than it is.

It is difficult to quantify the error ranges of morphometric age estimates because some of the sources of error are inseparable from deficiencies in the model itself (Mayer, 1987). Mayer identifies the principal sources of error as: (1) geologic (differences in lithology, fault characteristics, climate, and the nature of the faulted surface); (2) measurement (limits of the accuracy of surveying instruments, techniques, and surveyors, limited accuracy of graphical representation, and uncertainty of the locations of the present upslope and downslope original surfaces); and (3) model (systematic and random variation in scarp morphology that is unexplained by the diffusion model). The lowest error range achievable with morphometric dating for most fault scarps is probably ±25%. The dependence of $c^*$ on scarp height illustrated in figure 2 (a source of error in the model itself) must be taken into account for a data set that consists of scarps of a small range of offset values. This source of error in the age estimate is minimized if the data include scarps with a large range of offset values, but use of $c^*$ decreases standard deviations as a percent of the mean age estimate for nearly all fault scarp data sets from central Nevada.

## References

Bull, W.B. (1987). Relative rates of long-term uplift of mountain fronts, U.S. Geol. Surv., Open-File Rept. 87-673, 192-202.

Hanks, T.C., Bucknam, R.C., Lajoie, K.R., and Wallace, R.E. (1984). Modification of wave-cut and faulting-controlled landforms, Jour. Geophys. Res., **89**, 5771-5790.

Harden, J.W. (1982). A quantitative index of soil development from field description: Examples from a chronosequence in central California, Geoderma, **28**, 1-28.

Houghton, J.G., Sakamoto, C.M., and Gifford, R.O. (1975). Nevada's Weather and Climate, Nevada Bureau of Mines and Geology, Reno, Nevada, 78 p.

Mayer, L. (1987). Sources of error in morphologic dating of fault scarps, U.S. Geol. Surv., Open-File Rept. 87-673, 302-310.

Pearthree, P.A. (1987). Patterns of Holocene faulting and the rate of extension in central Nevada (abstract), Geol. Soc. Amer. Abstracts with Programs, **19**, 802.

Pearthree, P.A., Demsey, K.A., Fonseca, J., and Hecker, S. (1988). An evaluation of morphologic analysis of pluvial shoreline scarps and young fault scarps in central Nevada (abstract), Geol. Soc. Amer. Abstracts with Programs, Cordilleran section meeting, 220-221.

Pierce, K.L., and Colman, S.M. (1986). Effect of height and orientation (microclimate) on geomorphic degradation rates and processes, late-glacial terrace scarps in central Idaho, Geol. Soc. Amer. Bull., **97**, 869-885.

Slemmons, D.B. (1967). Pliocene and Quaternary crustal movements of the Basin and Range province, U.S.A., Jour. Geoscience, Osaka University, **10**, 91-103.

Wallace, R.E., and Whitney, R.A. (1984). Late Quaternary history of the Stillwater seismic gap, Nevada, Geol. Soc. Amer. Bull. **74**, 301-314.

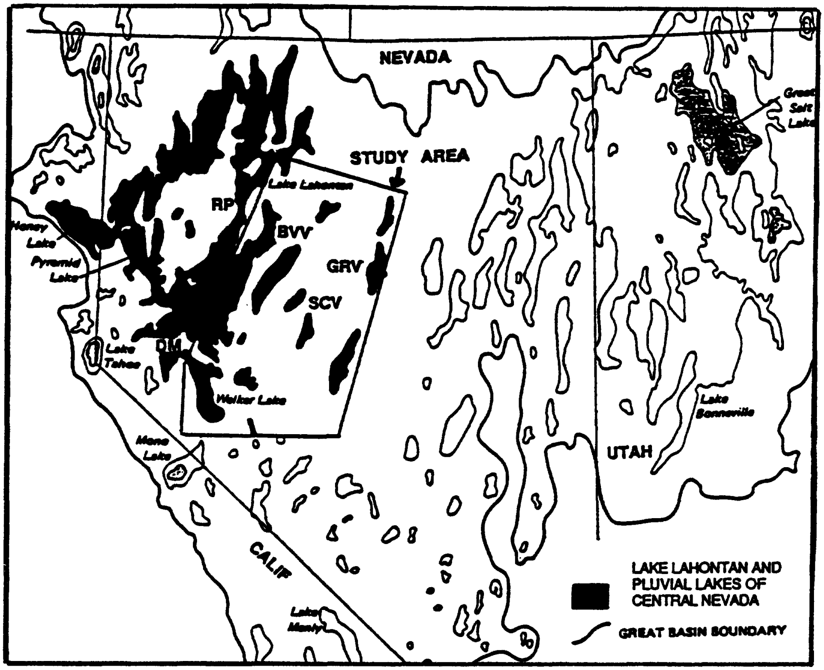

(modified from Houghton et al., 1975)

**Figure 1.** Location of the area of study and the extent of Lake Lahontan and other pluvial lakes of central Nevada. Lahontan shoreline scarps were profiled around Walker Lake, in Buena Vista Valley (BVV), near Rye Patch (RP), and north of the Desert Mountains (DM). Modern climatic conditions at these sites are arid. Shoreline scarp profiles were also collected from pluvial lakes in Grass Valley (GRV) and Smith Creek Valley (SCV), where the modern climate is semiarid.

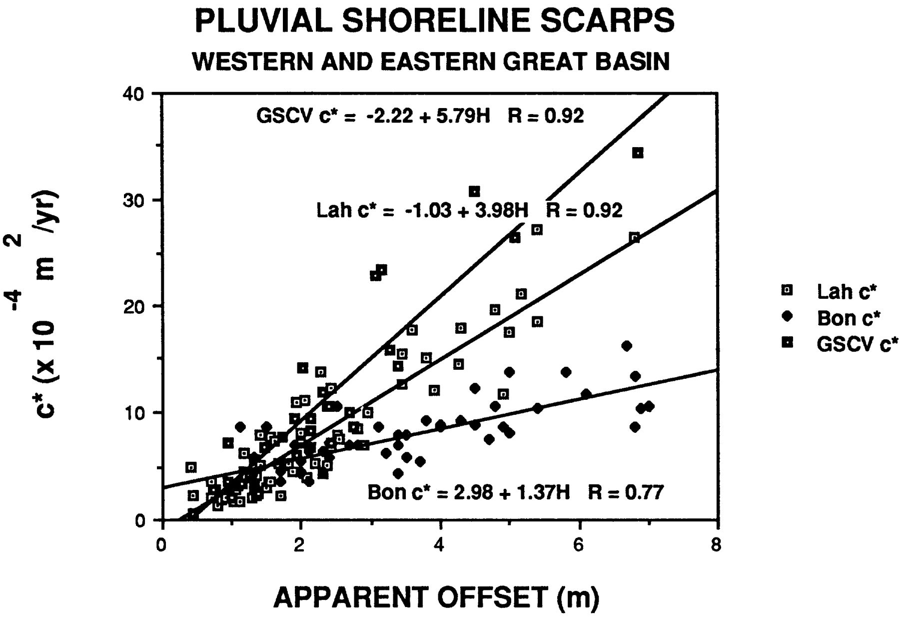

Figure 2. Regression lines showing the dependence of scarp degradation rate coefficient (c*) on scarp height (apparent offset) for pluvial lake shoreline scarps of known ages. Bon = Lake Bonneville, Lah = Lake Lahontan, GSCV = pluvial lakes in Grass and Smith Creek Valleys. The differences in the rates of increase in the value of c* with scarp height for the three data sets is probably controlled by differences in climate, vegetation, and lithology. Lake Bonneville data points from Pierce and Colman, 1986.

# Pilot Study on the Paleomagnetism of Lake Sediments as Indicators of Paleoseismicity and Seismic Recurrence Intervals

14-08-0001-G1514

David B. Stone
Geophysical Institute, University of Alaska
Fairbanks, Alaska 99775-0800
(907) 474-7622

Michael O. McWilliams
Stanford University

James Beget
Department of Geology
University of Alaska
Fairbanks, Alaska 99775

## Objective:

Recurrence intervals for large earthquakes are important to many studies, including hazard assessment, engineering design and simply understanding the tectonic setting of an area. Many direct and indirect techniques are currently employed to determine the recurrence interval, with variable success. The work we will start in summer 1988 is a pilot study to determine the effectiveness of magnetic techniques as an aid to recognizing earthquake signatures in sedimentary records. Although the details of how sediments acquire a depositional remanent magnetization are not well understood, it is clear that the process involves the physical orientation of the magnetic particles in the sediment. It is also clear that if the sediment is liquified, or turned into a slurry by mechanical vibration, that in many cases the magnetic carriers can realign if the ambient field has changed, or improve their alignment if the field direction has remained constant. The work we are planning will test whether the shaking imposed by a known major earthquake has left decipherable magnetic record. We will take cores from Skilak and Hidden lakes on the Kenai Peninsula, Alaska, located within the Mercalli zone VII associated with the 1964 Great Alaskan earthquake (magnitude $M_w = 9.2$). Cores from these lakes should give a sedimentologic and magnetic record of this known seismic event, and should also have a long enough record to cover at least two of the previous large events. The proposed ages of these previous events are based on recent work indicating a recurrence interval of about 400 years for the general area (Combellick, 1986). If the pilot study on Skilak and Hidden lakes is successful, studies on other lakes will be undertaken.

# Central California Deep Crustal Study

9540-02191

Carl M. Wentworth
Branch of Western Regional Geology
U.S. Geological Survey
345 Middlefield Road, MS 975
Menlo Park, California 94025
(415) 329-4950

## Investigations

1. Work continued (Wentworth, Jachens, Fisher) on preparation of a map at 1:750,000 of the surface of crystalline rock beneath the Great Valley of California and adjacent areas. The well file is now essentially complete. Subsurface data have been supplemented by topography (15 second average altitudes sampled at 2 km) to represent the surface of crystalline rock east of the Great Valley.

2. Work is underway with Simpson and Jachens to prepare a regional tectonic interpretation for the region surrounding the Parkfield segment of the San Andreas fault at 1:250,000. Wentworth is compiling a simplified geologic map on a smoothed topographic base prepared by Simpson from the 15-second average altitudes.

3. Participating in discussions about quantitative analysis and use of digital topography and the desirability of obtaining digital elevation models for at least part of the Parkfield region.

# Paleoseismic and Slip-Rate study of the Northern Segment of the San Jacinto Fault Zone in San Bernardino, California

14-08-0001-G1530

Steven G. Wesnousky
Center for Earthquake Research and Information
Memphis State University
Memphis, TN 38152
(901) 454-2007

Objective: To perform a field study of a buried Holocene stream channel that is offset by the San Jacinto fault in San Bernardino, California. Documentation of the total offset and age of the buried stream channel will allow an estimate of fault slip-rate along the northernmost reach of the San Jacinto fault where it traverses the densely populated, rapidly growing, and urbanized area of San Bernardino. Estimates of the average occurrence rate of moderate to large earthquakes along the northern reach of the San Jacinto fault may be based on information regarding the fault slip rate. Such information cannot be gleaned from the short historical record available in this region.

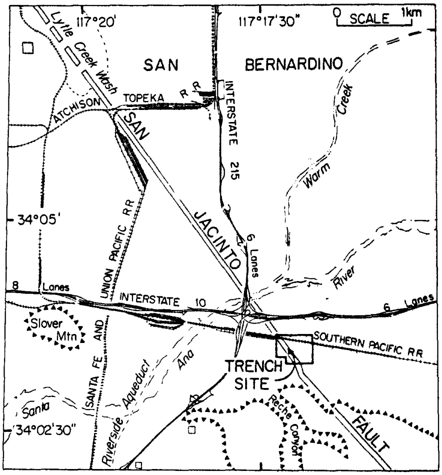

Progress: Work completed at the site thus far indicates that a strand of the San Jacinto fault has offset a buried Holocene stream channel on the order of about 10.5 meters in a right-lateral sense. The buried channel is 1,965 (2 sigma = 134) years old as evidenced by a conventional radiocarbon date on disseminated charcoal collected from the unit. These preliminary observations suggest a slip-rate of about 5.4 mm/yr. However, the result must be interpreted with caution, for we have not ruled out the possibility that a portion of our estimated fault offset is due to the original configuration of the channel rather than solely to movement of the fault. Currently, we have reexcavated the sight and are continuing our investigation in order to remove such uncertainties from our estimate of the offset of the buried stream channel across the fault.

# Convergence Rates Across Western Transverse Ranges

14-08-0001-G1372

Robert S. Yeats and Gary J. Huftile
Department of Geology
Oregon State University
Corvallis, OR 97331-5506
503-754-2484

## Investigations

Huftile (1988) completed his studies of the active, north-verging fold-thrust belt in the Upper Ojai Valley and will soon submit a paper to the American Association of Petroleum Geologists Bulletin. Another paper, "The Ventura Fold Belt and the Oak Ridge Fault, Western Transverse Ranges, California," by R. S. Yeats, G. J. Huftile, and F. B. Grigsby (cf. USGS Open-File Report 88-16, p. 194-195) has been accepted for publication in Geology. A third paper, "Late Quaternary Slip Rates on the Oak Ridge Fault, Transverse Ranges: Implications for Seismic Risk," by R. S. Yeats (cf. USGS Open-File Report 88-16, p. 199-202) has been accepted for publication in Journal of Geophysical Research.

We have acquired two industry seismic lines extending from Santa Clara Valley north to Sulphur Mountain which reveal deep structural data at 5 seconds, permitting us to determine shortening on south-verging structures between the Red Mountain and San Cayetano faults. A third unmigrated seismic line in the Santa Clara Valley east of Santa Paula shows good reflectors to six seconds. 20 traces of this line are being recorrelated to 12 seconds in hopes of mapping the Moho in the center of the Ventura basin.

Gary Huftile, working with Eugene Humphreys of the University of Oregon, is attempting to resolve deep velocity structure of the upper mantle beneath the western Transverse Ranges using seismic tomography.

## Results

A NW-SE trending boundary separates an eastern domain where all late Quaternary displacement on north-verging structures occurs on the Oak Ridge fault and a western domain where late Quaternary displacement has transferred to a decollement in lower Miocene shale. This implies that the Oak Ridge fault near the coast and offshore is now virtually inactive and is being carried passively northward on the active decollement. The active deep Oak Ridge fault below the decollement must be offset southward from the near-surface trace.

The offshore Pitas Point gas field occurs in a broad asymmetric anticline with a steeper north flank. Bryan Grigsby suggested that this anticline is a fault-bend fold related to ramping of the C-3 fault from the Rincon Formation to the Sisquoc Formation.

The new seismic lines provide a solution to the dilemma of why the Red Mountain and San Cayetano reverse faults do not connect but are separated by a region of no south-verging reverse faulting in the Ojai Valley. This intervening region may be characterized by a blind thrust at depth which produces the homocline south of Sulphur Mountain as a fault-bend fold.

Reports

Grigsby, F. B., 1988, Structural development of the Ventura Avenue anticlinal trend at the San Miguelito and Rincon oil fields, Ventura County, California, in Sylvester, A. G. and Brown, G. C., eds., Coast Geological Society Field Guide No. 64, p. 111-124.

Huftile, G. J., 1988, Geologic structure of the Upper Ojai Valley and Chaffee Canyon areas, Ventura County, California: Corvallis, Oregon State University MS thesis, 103 pp.

Huftile, G. J., 1988, Structural geology of the Chaffee Canyon oil field, Ventura Canyon, California, in Sylvester, A. G. and Brown, G. C., eds., Coast Geological Society Field Guide No. 64, p. 125-132.

Huftile, G. J., 1988, Thin-skinned tectonics of Upper Ojai Valley and Sulphur Mountain vicinity, Ventura basin, California (abs.): American Association of Petroleum Geologists Bulletin, v. 72, p. 383

Yeats, R. S., 1987, Late Cenozoic structure of the Santa Susana fault zone: U. S. Geological Survey Professional Paper 1339, p. 137-160.

Yeats, R. S., Lee, W. H. K., and Yerkes, R. F., 1987, Geology and seismicity of the eastern Red Mountain fault, Ventura County: U. S. Geological Survey Professional Paper 1339, p. 161-167.

Yeats, R. S., Calhoun, J. A., Nevins, B. B., Schwing, H. F., and Spitz, H. M., 1988, The Russell fault: An early strike-slip fault of the California Coast Ranges, in Bazeley, W. J. M., ed., Tertiary tectonics and sedimentation in the Cuyama basin, San Luis Obispo, Santa Barbara, and Ventura counties, California: Pacific Section, Society of Economic Geologists and Paleontologists v. 59, p. 127-139.

Yeats, R. S. and Huftile, G. J., 1988, Oak Ridge fault, Ventura fold belt, and the Sisar decollement, Ventura basin, California (abs.): Geological Society of America Abstracts with Programs, v. 20, p. 244.

Yeats, R. S. and Huftile, G. J., 1988, Retrodeformable cross sections and Oak Ridge fault, Ventura basin, California (abs.): _American Association of Petroleum Geologists Bulletin_, v. 72, p. 398.

# On-Line Seismic Processing

9930-02940

Rex Allen
Branch of Seismology
U.S. Geological Survey
345 Middlefield Road, MS 77
Menlo Park, California 94025
(415) 329-4731

## *Investigations and Results*

The Motorola 68020 system that we have had online for several months as a backup for the Parkfield stations has continued to produce very satisfactory results. We are currently preparing a similar system to be used in Southern California to allow online evaluation and response to earthquakes such as the recent Whittier Narrows event. The system being prepared will allow monitoring of a set of about 64 stations or slightly fewer. Like the Motorola system here at Menlo Park it will use only one 68020 processor.

At this point it is neccessary to expand the RTP processing capability to allow monitoring of the nearly 500 analog lines that are telemetered to Menlo Park. Until quite recently we had planned to do this by shifting to a multiprocessor system using as many 680x0 processors as were required. Two developments of late (a sort of good news - bad news combination) have made it more practical to shift to a different strategy.

First, (the bad news), Motorola has decided not to support multiprocessing software under their Versados operating system. Instead they will suggest use of their version of the UNIX system combined with realtime kernels and adaptive software to be supplied by one of several third-party software houses. This has the potential of becoming a much more expensive proposition, and in addition the prospect of the diffusion of responsibility for performance is not appealing.

The good news is that the recently announced Reduced Instruction Set Computers (RISC) from several suppliers make it likely that we will be able to use only one or two extremely powerful RISC processors for the whole CALNET. I am currently evaluating the machines available and developing a benchmark representative of our requirements.

If this does indeed prove a viable alternative it will greatly simplify the task at hand, since we will be able to use the currently running software without needing to adapt to multiprocessing.

Jim Ellis has continued work on the multiproject effort to develop new digital field instruments.

The Mk I RTP's at Menlo Park and at the University of Washington and the University of Utah have continued to operate satisfactorily.

# Crustal Deformation Observatory Part F

14-08-0001-G1355

John Beavan, Douglas Johnson
Lamont-Doherty Geological Observatory of Columbia University
Palisades, New York 10964
(914) 359-2900

## Investigations

We operate a 535 m long-baseline half-filled water tube tiltmeter at Pinon Flat Observatory. This is used in conjunction with a similar instrument operated by the University of California, San Diego, to investigate:

(1) sources and magnitudes of noise affecting the tilt signal;
(2) water level sensor design and reliability;
(3) methods of referencing tiltmeter to depth.

## Results (as of April 30, 1988)

The past 6 months has seen considerable progress with: (1) the installation of new electronics on the PFO tiltmeters that give them 4 times greater resolution and much improved reliability; (2) the installation of new micrometer sensors at the ends of both the LDGO and UCSD tiltmeters that will be used in investigating the residual discrepancy in the long-term signals from the LDGO and UCSD instruments; (3) a start on an independent analysis of the PFO tiltmeter data - all analysis to date has been by the UCSD group.

### *1. Improved sensors*

The LDGO tiltmeter end units and interferometer fringe-counting electronics have been redesigned and several units have been built. The electronics use a Hewlett-Packard quadrature decoder ($\lambda/4$ counter), and an automatic level control that compensates for wide fluctuations in beam intensity and fringe contrast (Figure 1). The new electronics were installed on the existing PFO interferometers in November 1987, and the first month of data is shown in Figure 2. (The subsequent data tape has only just been received by us from UCSD, so more recent data cannot be included in this report).

### *2. Tiltmeter interconnection and micrometer measurements*

Data collected to date from the two tiltmeters suggest that it will be possible to monitor secular tilt changes at much better than the $10^{-7}$/year level with this type of instrument. However, observed differences in long-term tilt rate between the LDGO and UCSD tiltmeters at the $10^{-7}$/year to $10^{-8}$/year level led us to suggest interconnecting the two tiltmeters in order to investigate the source of the discrepancy. The 535 m tiltmeters run parallel about 10 m apart, and both are referenced to approximately 30 m depth, so we would expect nearly identical behavior even in the long term. Possible sources of the discrepancy are the different sensors, different methods of

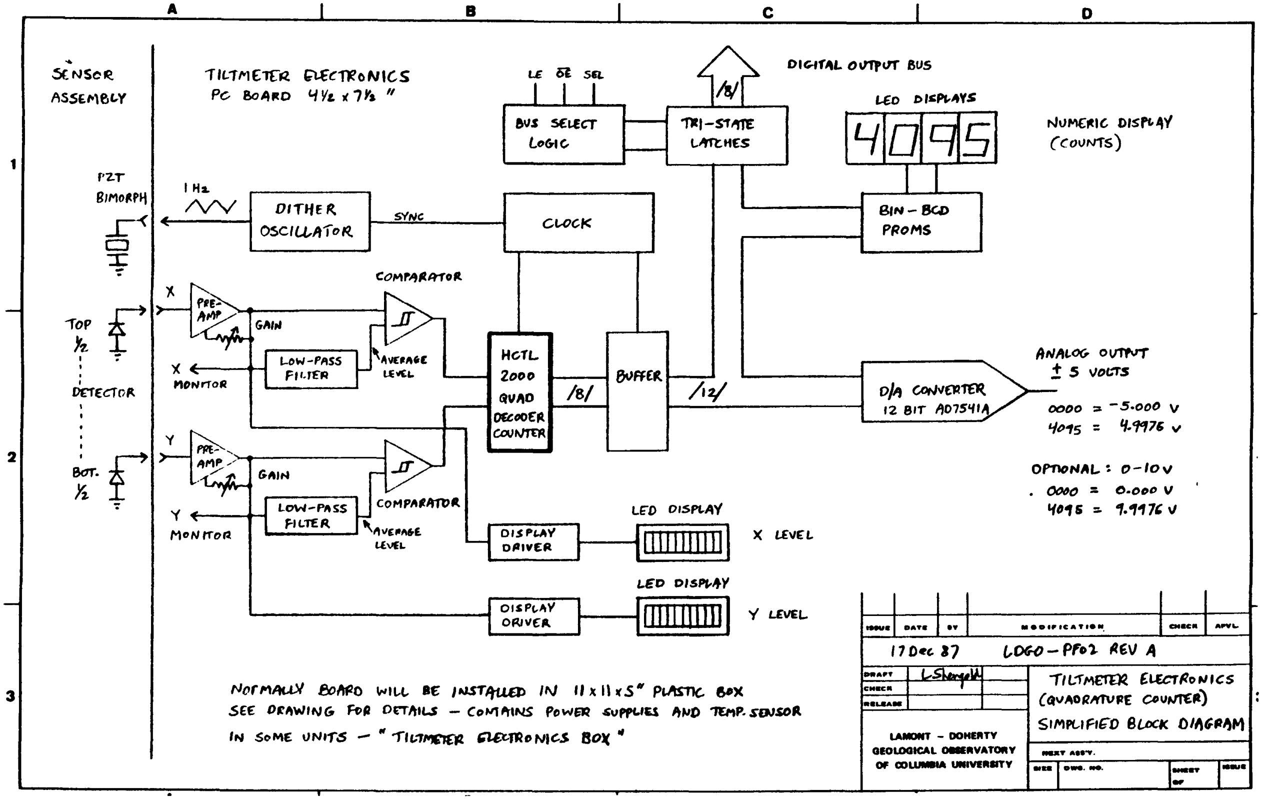

Figure 1. Block diagram of new tiltmeter electronics. Improvements over the old design include the use of a Hewlett-Packard quadrature decoder (HCTL-2000) which includes a digital filter and a "state machine" to eliminate invalid state transitions due to noise, interruptions of optical path, etc. Automatic level control to compensate for changes in laser intensity and/or fringe contrast is accomplished by automatically adjusting the counter's threshold to the average value of light intensity. A triangle wave modulation of the fringe pattern, using a PZT bimorph driven optical retardation plate, permits continuous automatic intensity compensation over a 5:1 range. The sensitivity is improved by use of the aforementioned HP quadrature decoder, which provides quarter-wave fringe counting. This yields a basic sensitivity of 0.238 microns, or 4.4 $10^{-10}$ radians/count in the 535m PFO installation.

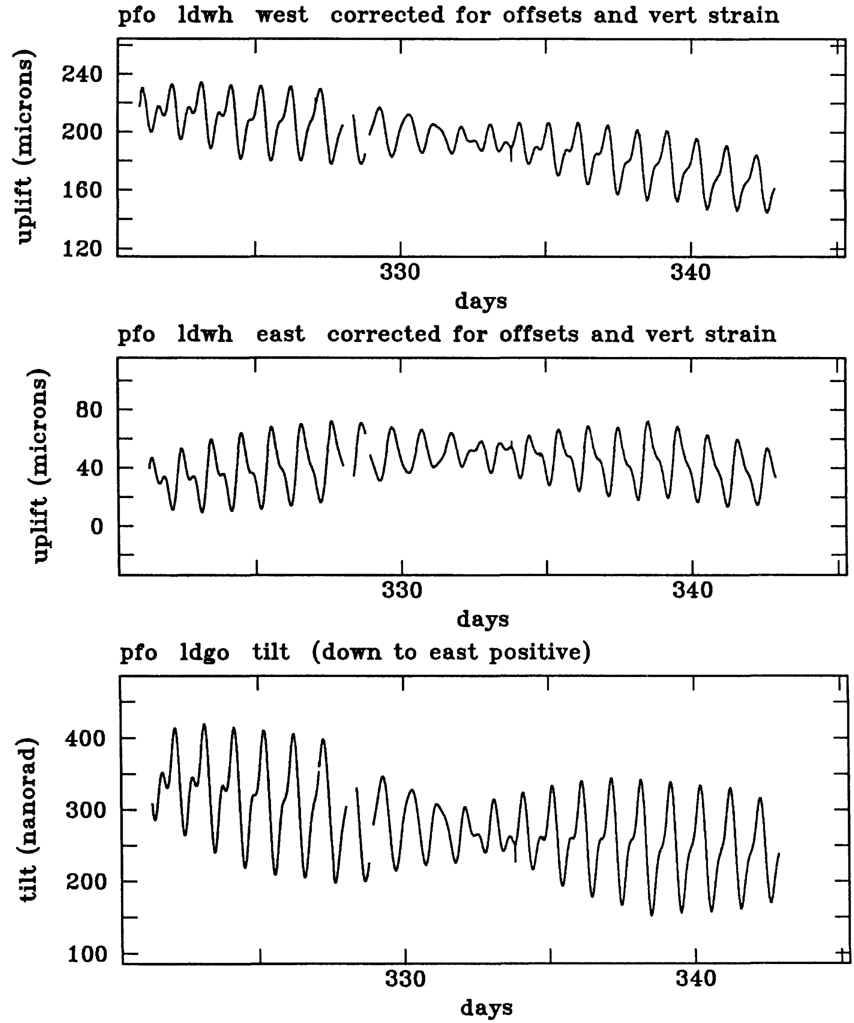

pfo ldwh west corrected for offsets and vert strain

pfo ldwh east corrected for offsets and vert strain

pfo ldgo tilt (down to east positive)

Figure 2. November - December 1987 tilt signals from the LDGO long-baseline tiltmeter at Pinon Flat, since the installation of new tiltmeter electronics. The data have been corrected for vertical strain between the instrument piers and fiducial points at 30 m depth. Non-tectonic offsets on day 328, at the times of the Superstition Hills earthquakes, have been removed from the data. The signal from the Nov. 30 Gulf of Alaska earthquake is visible on day 334.

referencing to depth, and the methods used for filling the inevitable gaps in the data. See USGS Open File Reports 88-16, 87-374 and earlier semi-annual technical reports for more details.

The interconnection was completed in June 1986, with much help from the UCSD group, and micrometer sensors (designed and built by Roger Bilham at the University of Colorado, see Figure 3) were installed on both ends of both tiltmeters by Larry Shengold of LDGO in November 1987. We did not have sufficient funds to install continuously recording sensors, but we believe that periodic readings of the micrometer sensors will be sufficient to resolve the questions about the relative long-term stability of the two instruments. The micrometers have been completely redesigned from those used previously in the LDGO vaults, so that they are easier to read and easier to clean. In tests after installation, three different observers obtained repeatibilities better than ±2 micron, which corresponds to about $\pm 4.10^{-9}$ μrad in the PFO tiltmeter. The micrometers will continue to be read by UCSD personnel at approximately monthly intervals, and results from these readings will be presented in the next semi-annual report..

### 3. *Data Analysis*

The data from the LDGO instrument since the installation of the new electronics are of high quality (Figure 2), and show several interesting features. The signal from the November 30 Gulf of Alaska earthquake is clearly visible on day 334 and it did not cause any loss of count in the interferometers. However, the two Superstition Hills earthquakes of November 24 caused offsets several times greater than the tilt step calculated from dislocation models of the earthquakes, presumably because the interferometer lost count due to ripples on the water surface. These offsets have been edited out of the data plotted in Figure 2. We will put a certain amount of effort into improving the response of the interferometer, perhaps using baffles to reduce rippling, but our main future effort will be to develop an alternative absolute sensor.

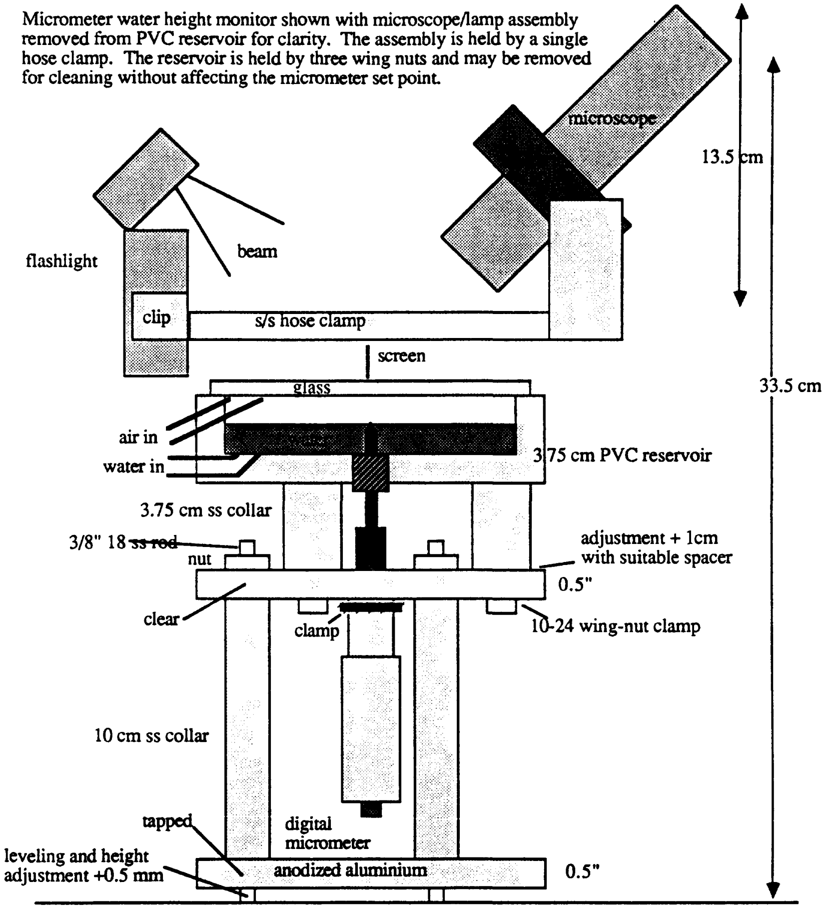

Micrometer water height monitor shown with microscope/lamp assembly removed from PVC reservoir for clarity. The assembly is held by a single hose clamp. The reservoir is held by three wing nuts and may be removed for cleaning without affecting the micrometer set point.

Diameter of baseplate = 6 inches
Total height of micrometer system = 33.5 cm ± ( the angle of the light/microscope pair is adjustabl
Height of water above base = 19 ± 0.5 cm (adjustable + 1.5 cm with suitable spacers)
Operating range of micrometer ± 1cm
Reading resolution ± 1 μm
Reading accuracy ± 2 μm over range of 1 cm.

Figure 3. Schematic of the newly designed micrometer system for measuring absolute height of the water surface to within ±2 μm.

# Crustal Deformation Measurements in the Shumagin Seismic Gap, Alaska

## 14-08-0001-G1379

John Beavan
Lamont-Doherty Geological Observatory of Columbia University
Palisades, NY 10964
(914) 359 2900

## Investigations

1. Nine short (≈ 1 km) level lines are measured approximately annually within the Shumagin seismic gap, Alaska (Fig. 1). Surface tilt data are interpreted in terms of tectonic deformation at the Pacific-North American plate boundary.
2. Five absolute-pressure sea-level gauges are operated in the Shumagin Islands in an attempt to measure vertical deformation associated with the Aleutian subduction zone. A two-component short-baseline tiltmeter is operated at one site.
3. Data from the sea-level and tilt sensors are transmitted to Lamont by satellite in near real time, and are examined for possible tectonic signals. Studies of noise level as a function of frequency are used to determine the relative usefulness of different types of measurement, and to evaluate the minimum size of tectonic signal that will be visible above the noise. Our data are compared with other crustal deformation data from the Shumagin gap.

## Results (as of April 30, 1988)

Sea level gauge locations are given in Figure 1. This report will deal principally with the sea-level data. See USGS Open File Report 88-16 for a recent discussion of the leveling data. We are now able to detect signals of a few cm amplitude over the 100 km range of the sea-level array, and we are confident of the long-term stability of the gauges to better than ±1 cm. The 1976-1987 rates of vertical motion deduced from the gauges are much less than 1 cm/yr.

### *Earthquake Hazard*

Savage and Lisowski (1986) and Savage et al. (1988) have made geodetic strain measurements in the islands from 1980 - 1987, and have reported essentially no horizontal strain accumulation in the plate convergence direction. Their favored explanation for the low strain rates is that subduction is presently accomodated by steady aseismic slip at the plate interface.

Boyd and Lerner-Lam (1988), in a study of turn-of-the-century earthquakes in the Aleutians, recognised a 1917 $M_S$ 7.9 quake along with several large aftershocks, that relocated in the eastern and central section of the Shumagin seismic gap. Boyd et al. (1988) discuss this event in terms of the rupture history and future potential of the Shumagin gap. Assuming a recurrence interval for the eastern portion of the gap of 59 - 70 years, they estimate, using calculations by Nishenko and Jacob (in preparation), that the conditional probability of rupture in the next 20 years ranges between 62% and 96%.

The low measured deformation rates are in sharp conflict with the inferred seismic history if simple models of subduction (e.g., Savage, 1983) are assumed. A possible explanation is that the plate boundary is currently locked, yet the deformation rate is lowered substantially by viscoelastic effects late in the interseismic cycle (Thatcher and Rundle, 1984). This possibility is also considered by Savage et al. (1988), as is the possibility that the low rates may be the result of interaction with neighbouring large quakes. Currently, we just do not understand the disagreement, and we can only hope that further measurements will throw more light on this tantalising scientific problem. Modelling studies, such as those of Stuart (1987), are just beginning to be applied to subduction boundaries, and it is possible that these will also provide illumination of the problem.

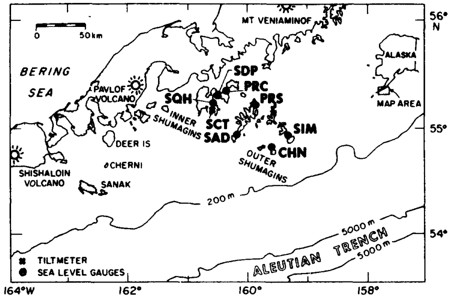

Figure 1. Location of the Shumagin Islands with respect to the trench and the volcanic arc. Depth contours are in metres. The seismic gap stretches from approximately Sanak Island in the west to about 30 km east of the Shumagin Islands. Also shown are the sites of sea-level gauges operated by Lamont-Doherty and by the National Ocean Survey (SDP). Site SAD is no longer operated because of repeated storm damage. All LDGO sites now use Paroscientific quartz pressure sensors, and housings that are substantially improved over those described by Beavan et al. [1986].

The downdip tension presently observed at intermediate depths in the upper plane of the double seismic zone (Hauksson et al., 1984; Taber, pers. comm., 1987) in the Shumagins is thought to indicate a strongly coupled plate boundary above (e.g. Astiz and Kanamori, 1986). However, recent detailed work (Hudnut and Taber, 1987) has shown a pronounced change in the character of the subduction zone about a third of the way along the Shumagin gap. The change is located at the west end of the islands themselves; to the west there is a clear double seismic zone, and to the east an equally clear single zone. Since both Savage's and our deformation measurements are confined to the east of this boundary, this raises the possibility that quite different stress and strain conditions exist to the west. Thus, even if it turns out that the eastern third of the gap is currently aseismic, it is probable that strain is accumulating towards a major earthquake in the western section. This would not be resolvable geodetically given the present geometry of the strain, leveling and sea level networks. With our 1988 funding we hope to install one or two level lines on Sanak, near the western edge of the gap, that will address this problem.

### *Sea level data*

Processed sea level data since 1985 are shown in Figures 2 and 3. Figure 2 shows the low-pass filtered data after tides have been removed. The ≈30 cm annual cycle is well known and is coherent over a wide area (Ingraham et al., 1976). Figure 3 shows the differences between pairs of gauges. An annual cycle of about 4 cm remains, presumably because the amplitude of the annual signal (which is an edge effect due to longshore currents along the coastal shelf), varies as a function of distance from the coast. Nevertheless, the very fact that we can see such signals gives us confidence in the stability of the gauges. We estimate that precursory (or other) signals greater than about 5 cm in relative sea level should be recognisable in our data in near real-time. This corresponds to 0.5 μrad tilt over the baseline of the array. We note that even with the long gaps in data that we have experienced to date, we are still able to derive scientifically valuable results from the sea level data (see Figure 4). We therefore expect even better results as the reliability of the gauges improves.

## Papers published and in press, 1987

Boyd, T.M., J. Taber, A. Lerner-Lam & J. Beavan, 1988. Seismic rupture and arc segmentation within the Shumagin Islands seismic gap, Alaska, Geophys. Res. Lett., 15, 201-204.

Hurst, K.J. and J. Beavan, 1987. Improved sea level monitors for measuring vertical crustal deformation in the Shumagin seismic gap, Alaska, Geophys. Res. Lett., 14, 1234-1237.

McNutt, S.R. & R.J. Beavan, 1987. Eruptions of Pavlof Volcano, and their possible modulation by ocean load and tectonic stresses, J. Geophys. Res., 92, 11509-11523.

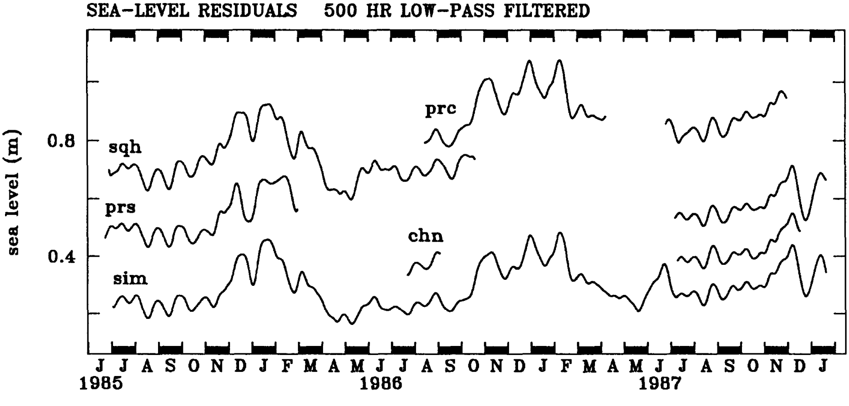

Figure 2. Processed, low-pass filtered sea-level data from 1985 to the end of 1987, from pressure-sensor sea-level gauges that use Paroscientific quartz transducers. The traces show the residual sea level after gaps are filled and tides removed. The curves are offset vertically for clarity. The main signal is the ≈30 cm annual signal due to seasonal circulation changes in the North Pacific gyre.

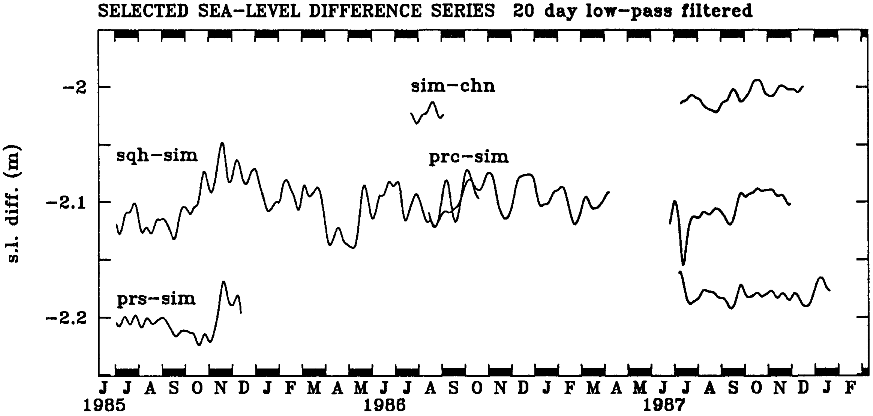

Figure 3. Processed and low-pass filtered sea-level difference data since 1985 from pressure-sensor sea-level gauges that use Paroscientific quartz transducers. The top trace shows the sea level difference between the inner and outer islands (see Fig. 1), where we have overlayed the SQH-SIM and PRC-SIM curves in order to give a more continuous record. PRC and SQH are both in the inner islands, and can be expected to experience similar tectonic and oceanographic signals. The rms noise level is less than 20 mm. The PRC/SQH - SIM trace defines a relative ground uplift at SIM of 2 mm/yr. This is zero within the errors of indexing the gauges to benchmarks, and is consistent with the somewhat longer term 1981-1987 and 1976-1986 estimates given respectively by Table 1, and by Table 5 of Hurst and Beavan [1987].

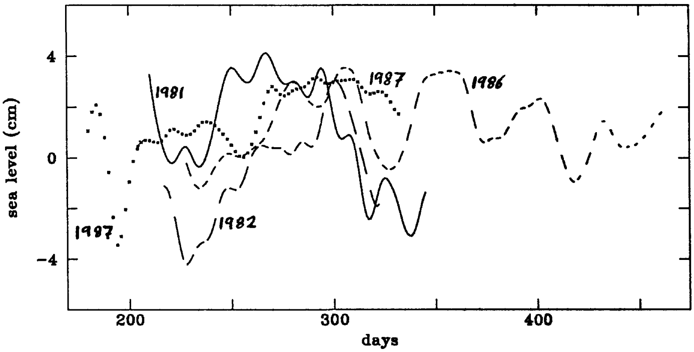

Figure 4. (a) low pass filtered sea level differences between sites PRC and SIM. Upward excursions on the plot correspond to ground uplift at SIM relative to PRC. The data from each year, starting in July, are superimposed. Plotting the data in this fashion and examining the offset of the curves from year to year allows one to estimate the relative vertical motion while reducing the effect of the residual ≈4 cm annual sea level variation. 1983 - 1985 data are corrupted due to drift problems with the ceramic pressure gauges in use at that time. We estimate the 1981-1987 uplift of SIM relative to PRC to be 0.0±0.4 cm/yr. The 1976 data, not plotted here, also show no significant vertical motion between 1976 and 1981 (see Figure 5 of Hurst & Beavan [1987]).

## References

Astiz, L. and H. Kanamori, 1986. Interplate coupling and the temporal variation of mechanisms of intermediate-depth earthquakes in Chile, Bull. seism. Soc. Am., 76, 1614-1622.

Aki, K., 1981. A probabilistic synthesis of precursory phenomena, in Earthquake Prediction, an International Review, Maurice Ewing Series, 4, eds. D.W. Simpson and P.G. Richards, 566-574, AGU, Washington, DC.

Beavan, J., R. Bilham & K. Hurst, 1984. Coherent tilt signals observed in the Shumagin seismic gap; detection of time dependent signals at depth?, J. geophys. Res., 89, 4478-4492.

Beavan, J., K. Hurst, R. Bilham & L. Shengold, 1986. A densely-spaced array of sea-level monitors for the detection of vertical crustal deformation in the Shumagin seismic gap, Alaska, J. geophys. Res., 91:B9, 9067-9080.

Beavan, J., 1987. Crustal deformation measurements in the Shumagin seismic gap, U.S.G.S. Open File Report, 87-374, 207-214.

Boyd, T.M. and A.L. Lerner-Lam, 1988. Spatial distribution of turn-of-the-century seismicity along the Alaska-Aleutian arc, Bull. seism. Soc. Am., in press.

Boyd, T.M., J.J. Taber, A.L. Lerner-Lam and J. Beavan, 1988. Seismic rupture and arc segmentation within the Shumagin Islands seismic gap, Alaska, Geophys. Res. Lett., 15, 201-204.

Gordon, D., 1987. Status report on Alaska and Pacific VLBI measurements, NASA Crustal Dynamics Project Working Group, Oct. 21-23 1987, NASA/GSFC, Greenbelt, MD.

Hudnut, K.W. and J.J. Taber, 1987. Transition from double to single Wadati-Benioff seismic zone in the Shumagin Islands, Alaska, Geophys. Res. Lett., 14, 143-146.

Hurst, K.J. and J. Beavan, 1987. Improved sea level monitors for measuring vertical crustal deformation in the Shumagin seismic gap, Alaska, Geophys. Res. Lett., 14, 1234-1237.

Ingraham, W.J. Jr., A. Bakun & F. Favorite, 1976. Physical Oceanography of the Gulf of Alaska, in Environmental Assessment of the Alaskan Continental Shelf, vol. 2 (Principal Investigators reports, April - June 1976), Environmental Research Laboratories, Boulder, Co, 491-624.

Savage, J.C., 1983. A dislocation model of strain accumulation and release at a subduction zone, J. geophys. Res., 88, 4984-4996.

Savage, J.C., M. Lisowski & W.H. Prescott, 1986. Strain accumulation in the Shumagin and Yakataga seismic gaps, Alaska, Science, 231, 585-587.

Savage, J.C. and M. Lisowski, 1986. Strain accumulation in the Shumagin seismic gap, Alaska, J. geophys. Res., 91:B7, 7447-7454.

Savage, J.C., M. Lisowski, W.H. Prescott and W.K. Gross, 1988. Absence of strain accumulation in the Shumagin seismic gap, Alaska, 1980-1987, J. geophys. Res., in press.

Stuart, W.D. 1986. Forecast model for large and great earthquakes in southern California, J. geophys. Res., 91, 13771-13786.

Stuart, W.D., 1987. Earthquake forecast models (abstract), EOS, 68, 1242.

Thatcher, W. & J.B. Rundle, 1984. A viscoelastic coupling model for the cyclic deformation due to periodically repeated earthquakes at subduction zones, J. geophys. Res., 89, 7631-7640.

# Sources of Errors in GPS Measurements of Crustal Deformation

14-08-0001-G1335

Yehuda Bock, Da-Nan Dong, and Robert W. King
Dept. of Earth, Atmospheric, and Planetary Sciences
Massachusetts Institute of Technology
77 Massachusetts Avenue
Cambridge, MA 02139
(617) 253-7360

Objectives: Understanding the structure and geometry of seismogenic zones is a key element in the prediction of earthquakes. Geodetic measurements contribute to this understanding through the mapping of present-day crustal deformations. Three-dimensional relative-positioning using the Global Positioning System (GPS) appears to be the most accurate and cost-efficient method for measuring crustal deformations over distances of tens to hundreds of kilometers. The objective of our research is to investigate sources of error and optimum analysis techniques for high-precision GPS measurements. Progress in these areas will lead directly to more accurate measurement of deformation in areas of high seismogenic potential.

Investigations undertaken: In December, 1986 and January, 1987, a series of GPS experiments were begun in central and southern California to monitor crustal deformations west of the San Andreas fault (*Agnew et al.*, 1987). In this first campaign, the area of geophysical interest was covered by 15 sites with separations of 35 to 350 km. Five regional (within California) fiducial sites, with separations of 200 to 500 km, were occupied. Sites outside of California at locations in Massachusetts (Westford), Colorado (Platteville), Ontario (Algonquin), and Manitoba (Churchill), providing separations of 1200 to 4200 km, were observing on the same 7-8 hour schedule during this campaign. Thus, the network design provided deliberately for a wide range of inter-station distances (Figure 1), in order to investigate the accuracy with which station coordinates can be recovered using a regional or continental fiducial network. The different scales were also important in studying optimal phase-ambiguity resolution algorithms. The first campaign began with three experiments, each occupying a different subset of sites and each lasting five days. All of the observations were performed with TI 4100 receivers.

In the previous semi-annual report, we reported on the regional orbit relaxation analysis of the first experiment (December 16-20). We have since extended this analysis to the second (December 29 - January 2) and third experiment (January 3 -7). The results of these experiments (*Murray et al.*, 1987b) reinforce our previously reported conclusion: that regional orbit relaxation techniques are a powerful tool for crustal motion monitoring on scales of tens to hundreds of kilometers provided that sufficiently accurate regional fiducial sites are available. In addition, we have performed a detailed network analysis of all the tracking data of the third experiment that includes inter-station separations of 35 to 4200 km. We have studied repeatability of baseline vector determinations as well as their accuracies as compared to independent very-long-baseline-interferometry (VLBI) determinations of the same lines. We report here on the results of the third experiment and on new algorithmic developments in phase-ambiguity resolution.

## Analysis

The GPS phase and pseudorange data were analyzed with GAMIT, the MIT GPS software package. After the preprocessing stage in which we synchronized the station clocks using the pseudorange data and fixed cycle-slips in the phase data, we performed, for each day, a sequence of two simultaneous least-squares adjustments of the phase data. In the first adjustment, we estimated 1) the three-dimensional coordinates for all the sites except three "fiducial" sites (located in California, Colorado and Ontario) which were fixed to their SV3 reference frame values (*Murray and King*, 1988), 2) initial conditions for each of six satellites, 3) a zenith delay parameter for each site for unmodeled atmospheric refraction effects, and 4) an independent set of double-difference phase ambiguity parameters. In addition, we applied tropospheric constraints based on a model of residual tropospheric delay (*Murray et al.*, 1987a). The observables used in the first adjustment were L1 and L2 phases and weighted constraints on residual ionospheric refraction constraints (*Bock et al.*, 1987). The stochastic properties of each observable were modeled by full covariance matrices whose elements are functions of constant and distance-dependent terms (*Schaffrin and Bock*, 1988). For the L1 and L2 phases, the constant terms are related primarily to multipath and residual tropospheric effects, and the distance-dependent terms to remaining uncertainties in the satellite orbits. For the ionospheric constraints, there are no constant terms and the distance-dependent terms are due to the increase in residual ionospheric effects on baselines of increasing length.

The independent set of double-difference phase ambiguity parameters estimated in the first adjustment were generated from the original carrier-beat-phase measurements by means of a mapping based on baseline length and the distribution of phase data (*Dong and Bock,* 1988a). Since unmodeled systematic effects tend to grow with baseline length, so will, in general, the uncertainties in the ambiguity parameters. Therefore, the mapping is designed to construct an independent set of double-difference ambiguities by determining the shortest independent path (no closures) through the network. The double-difference ambiguity parameters are theoretically integers. However, the ambiguity parameters estimated in the first adjustment will be real-valued. Their closeness to integers will be a function of the remaining, unmodeled systematic and random effects in the double-difference phase data. If the correct integer values for these ambiguities can be resolved ("bias-fixing"), the doubly differenced phase measurements are reduced to doubly differenced range measurements. By reducing the number of ambiguity parameters and eliminating their correlations with the other estimated parameters, the uncertainties in the other parameters will be reduced (e.g., *Bock et al.*, 1985).

After the first adjustment, we perform a "bias search" to determine the best-fitting integer values for the ambiguity parameters. This procedure, described in detail in *Dong and Bock* (1988b), is done in a sequential manner starting with those ambiguities with lowest uncertainties (as mentioned above, these are usually from the shortest baselines). By re-estimating the other remaining parameters and their (lower) uncertainties after a new set of ambiguities is resolved, we "bootstrap" the bias-fixing to longer and longer baselines. This bootstrapping is also aided by searching the L2-L1 ("wide-lane") biases with a wavelength of 86 cm and the L1 ("narrow-lane") biases with a wavelength of 19 cm (rather than searching the L1 and L2 biases). This procedure is continued until no more biases can be fixed. Thus, the network design of the third experiment is ideal for this bootstrapping approach since it includes a wide-range of baseline lengths. Similar approaches have also been studied by *Counselman* (1987) and *Blewitt* (1988).

The second simultaneous network adjustment is similar to the first except that 1) the resolvable double-difference ambiguities are held fixed to their best integer values, and 2) the observables fit are the "ionosphere-free" linear combinations of the doubly difference L1 and L2 phases. We refer to this adjustment as an ionosphere-free, biases-fixed solution. That is, once the ambiguities are resolved, we use the observable that is free of first-order ionospheric refraction effects. Except for networks of small spatial extent (less than several kilometers) this second adjustment is optimal for baseline-vector and orbital parameter estimation.

## Results

We analyzed each of the five days of experiment 3 in this manner. We were able to resolve on three days all the double-difference phase ambiguities of the California baselines (35 to 480 km), and on the other two days over 90% of the ambiguities. In addition, we were able to resolve most of the L2-L1 biases for the entire network and 30% of the L1 biases for the longer baselines. In Figure 2, we show the repeatability of the California baselines (weighted rms scatter about the weighted mean) for the ionosphere-free biases-fixed solutions compared to an ionosphere-free biases-free solutions. It is evident that resolving the phase ambiguities results in significantly improved baseline-vector repeatabilities, primarily in the east components.

For the biases-fixed solutions, the repeatabilities in the horizontal components of the baselines are better than 15 mm for baseline lengths up to 500 km. In the well-determined north component and in the length, the repeatabilities are less than 10 mm for baselines up to 300 km. The north component and length show a slight dependence of repeatability on length--about 30 parts per billion. This proportional increase is likely due to errors entering through the satellite orbits. Errors affecting the repeatablities of the orbits include unmodeled non-gravitational forces on the satellites, tropospheric fluctuations at the ficudical sites, and a changing configuration of the fiducial network. Other effects which might degrade the repeatability, such as tropospheric fluctuations at the regional sites, would not depend on baseline length, at least for baselines greater than about 100 km.. Unmodeled signal multipath, which tends to repeat from day to day, and errors in the fiducial site coordinates would effect the accuracy of our results but not the repeatability.

On the last two days of this experiment we were able to estimate the baseline vector between Owens Valley and Mojave (OVRO7114 to GOLDUTEX). This baseline has been accurately determined independently by VLBI measurements (J. Ray and J. Ryan, private communcations, 1988). In Table 1, we compare the VLBI and the GPS determinations of this baseline. We include the two-day mean and uncertainties of the biases-free and biases-fixed GPS results. It is evident that bias-fixing improves the accuracy as well as the precision (repeatabilty) of the baseline-vector determinations.

In summary, we can conclude that with the proper network design and observing conditions, it is possible to measure regional baseline vectors to sub-centimeter accuracy in all three components. We plan to continue our analysis on six GPS campaigns in central and southern California spanning a time interval of three years in order to confirm the long-term repeatability of the GPS technique and to understand the remaining error sources.

## References:

Agnew, D. C., Y. Bock, T. H. Jordan, R. W. King, T. H. Dixon, B. H. Hager, D. D. Jackson, W. H. Prescott, J. L. Stowell, B. E. Schutz, and W. E. Strange, GPS measurements in central and southern California (abstract), *Eos Trans. AGU, 68*, p. 282, 1987.

Blewitt, G., Successful GPS carrier phase ambiguity resolution for baselines up to 2000 km in length (abstact), *Eos Trans. AGU, 69*, 325, 1988.

Bock, Y., R.I. Abbot, C.C. Counselman III, S.A. Gourevitch and R.W. King: Establishment of three-dimensional geodetic control by interferometry with the Global Positioning System, *J. Geophys. Res., 90*, 7689-7703, 1985.

Bock, Y., S.A. Gourevitch, C.C. Counselman III, R.W. King and R.I. Abbot: Interferometric analysis fo GPS phase observations, *Man. Geod., 11*, 282-288, 1986.

Counselman, C.C., III, Resolving carrier phase ambiguity in GPS orbit determination (abstract), *Eos Trans. AGU, 68*, 1238, 1987.

Dong, D.N. and Y. Bock: GPS Network Analysis: Ambiguity Resolution (abstract), *Eos Trans. AGU, 69*, 324, 1988a.

Dong, D.N. and Y. Bock: A demonstration of 1-2 parts in $10^8$ accuracy with network-mode bias-fixing using GPS, in preparation, 1988b.

Murray, M. H., Y. Bock, K. L. Feigl, and J. L. Davis, Assessing the effects of atmospheric error on estimates of relative position obtained from GPS data, Union Symposium on the Impact of GPS on Geophysics, IUGG General Assembly, British Columbia, August, 1987a.

Murray, M.H., Y. Bock, D.N. Dong, K. Feigl, and R.W. King, Initial Analysis of a GPS Network in Central and Southern California (abstract), *Eos Trans. AGU, 68,* 1236, 1987b.

Murray, M.H. and R.W. King, SV3 Coordinates of GPS Receivers, MIT Internal Memorandum, 11 March 1988.

Schaffrin, B. and Y. Bock, A unified scheme for processing GPS phase observations, *Bull. Geod.*, in press, 1988.

Table 1. Comparison of GPS- and VLBI-determined Baseline Vectors between Mojave and Owens Valley ( 246 km )

Differences (GPS - VLBI) in millimeters

| | North | East | Up | Length |
|---|---|---|---|---|
| Biases-free solutions | -31 (13*) | 40 (26) | -18 (28) | -6 (16) |
| Biases-fixed solutions | -11 ( 6) | 10 ( 7) | 4 (27) | -4 (5) |

* Numbers in parentheses are the standard deviations of the baseline components for a one-day estimate of a GPS-determined baseline

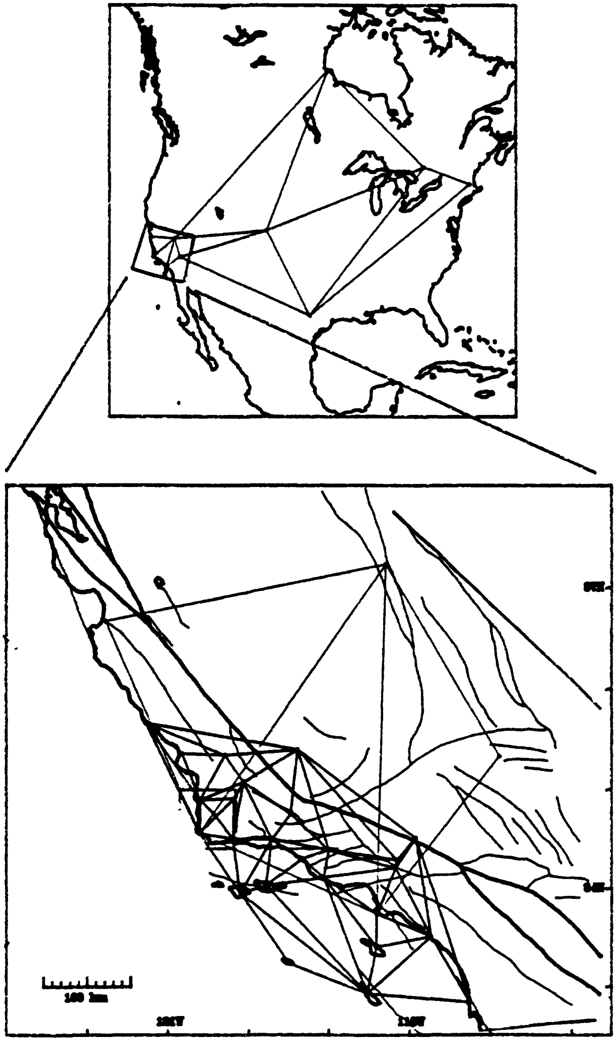

Figure 1. Distribution of stations occupied during the December 1986 - January 1987 GPS experiments, showing the continental and regional networks.

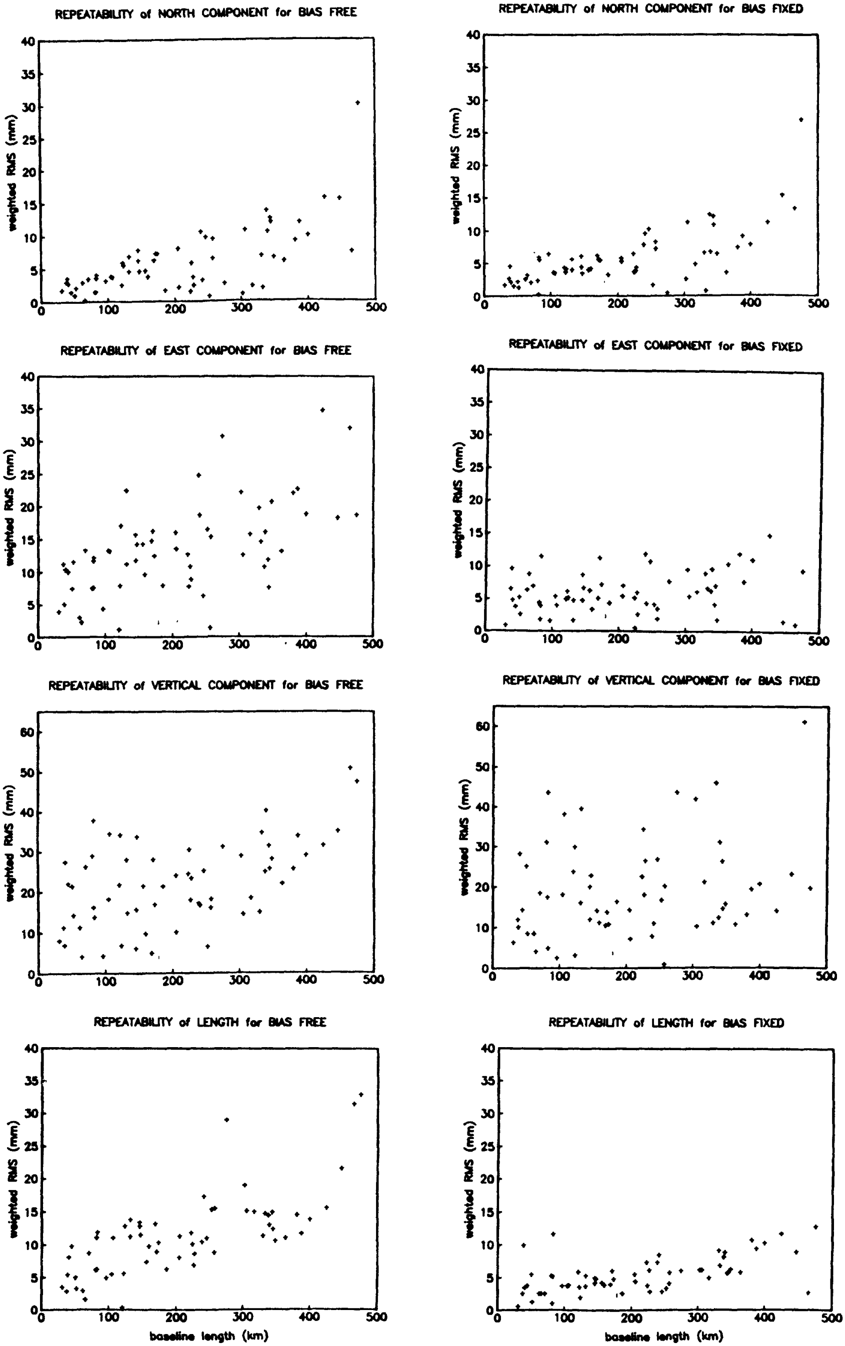

REPEATABILITY of NORTH COMPONENT for BIAS FREE

REPEATABILITY of NORTH COMPONENT for BIAS FIXED

REPEATABILITY of EAST COMPONENT for BIAS FREE

REPEATABILITY of EAST COMPONENT for BIAS FIXED

REPEATABILITY of VERTICAL COMPONENT for BIAS FREE

REPEATABILITY of VERTICAL COMPONENT for BIAS FIXED

REPEATABILITY of LENGTH for BIAS FREE

REPEATABILITY of LENGTH for BIAS FIXED

Figure 2. Repeatabilities of baselines analyzed from experiment 3 (see text). Plots on the left are for solutions in which a bias parameter was estimated for each double-difference combination; plots on the right are for solutions in which double-difference phase ambiguities were resolved (biases fixed at integer values).

# FAULT ZONE TECTONICS

9960–01188

Sandra Schulz Burford
Branch of Tectonophysics
U.S. Geological Survey
345 Middlefield Road, MS/977
Menlo Park, California 94025
(415) 329–4814

## Investigations

1. Directed maintenance of creepmeter network in California.
2. Updated archived creep data on USGS ISUNIX LOW FREQUENCY computer, and provided fault creep information in response to inquiries from both public and private sectors.
3. Continued to establish and survey alinement arrays on California faults.
4. Monitored creepmeter and alinement array data for possible earthquake precursors with primary attention to the Parkfield, California area, site of the USGS–California State earthquake prediction experiment.

## Results

1. Currently 31 extension creepmeters, two contraction meters, and 7 strong–motion creepmeters operate; 25 of the 31 extensometers and all of the strong–motion meters have on–site strip chart recorders. Of the total 40 instruments, 30 are telemetered to Menlo Park (Figures 1, 2).
2. Fault creep data from USGS creepmeter sites along the San Andreas, Hayward, and Calaveras faults have been updated through March, 1988, and stored in digital form (1 sample/day). Telemetry data are stored in digital form (1 sample/ten minutes), and can be merged with daily–sample data files to produce timely data. Fault creep data from a creepmeter (XUB1) and an alinement array (XUB4), located on the site of a proposed dormitory building on the Berkeley campus of the University of California, were provided to the University Regents and Department of Facilities Management, as well as to two geologic consulting firms retained by the University. Data from two alinement arrays near Calaveras Reservoir in central California were provided to the Santa Clara Water District and to a private geologic consulting firm for use in their studies of a proposed housing development in the area. Creepmeter and alinement array data were provided to a California Department of Water Resources project group planning a pipeline across the San Andreas fault south of Parkfield, California.

3. At the request of a private geologic consulting firm conducting an experiment at Parkfield, a 10–monument alinement array was installed in the pasture where the firm has buried pipes in various configurations across the San Andreas fault. A baseline and one repeat survey have been performed and the data provided to the firm.

4. Creep alert criteria written in 1985 for the Parkfield earthquake prediction experiment have been refined by 2 1/2 years' application to real–time incoming data from Parkfield creepmeters, and now (at least) are not over–alerting investigators. One of the most interesting pieces of new data from the cluster of various instruments at Parkfield is a close correlation between changes in water level at a deep well (Wmm3) on Middle Mountain and onset of rapid creep (creep events) at one or both of two nearby creepmeters (XMM1 and XMD1). The well is located approximately 750 m southeast of XMM1 and east of the fault. Since monitoring of the well began in January 1987, one correlation is a 90–day (±4 days) periodicity that began February 1, 1987, between occurrence of large water level drops and onset of creep events at XMM1 and/or XMD1. The fourth such multiple–instrument event occurred even though the well was in the midst of rapid (≈7/ft/day) recharge following heavy pumping on the previous day (Figure 3). A paper describing the data is in preparation (Roeloffs, Evelyn A. and others, Water level changes associated with episodic fault creep near Parkfield, California, in preparation).

## Reports

No papers were published during the reporting period.

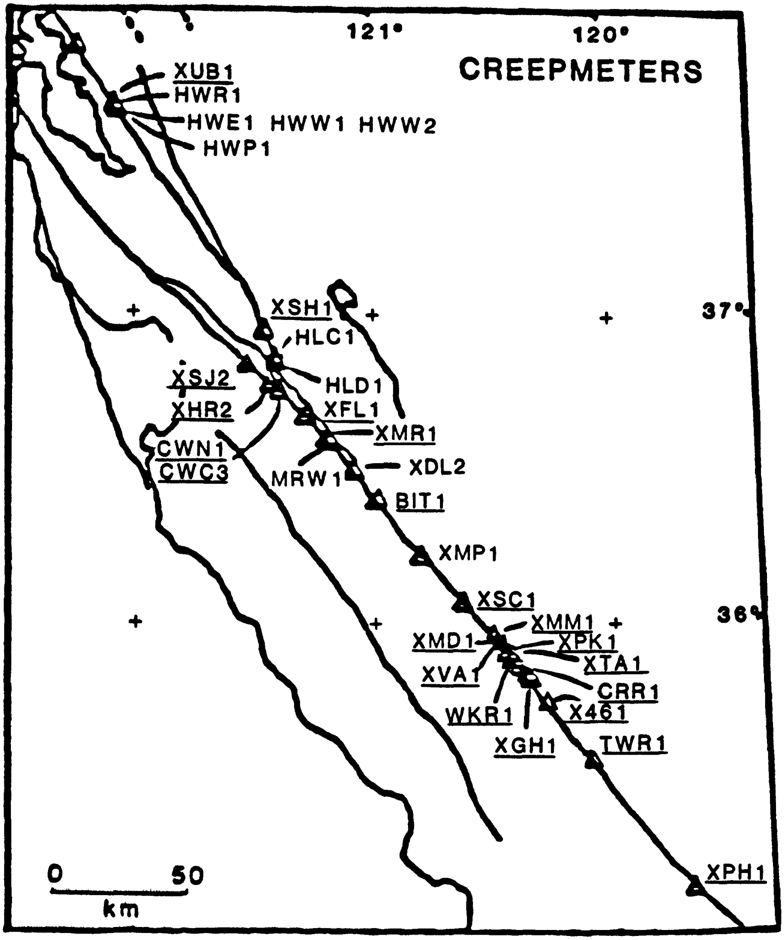

FIGURE 1

USGS creepmeter stations in northern and central California. Instruments with underlined names transmit on telemetry. NOT SHOWN: XRSW, XHSW on the Southwest Fracture near Parkfield (See Figure 2). Strong-motion creepmeters are located in vaults at XMM1, XMD1, XVA1, XTA1, X461, XRSW, and XHSW.

Creep and Alinement : Parkfield, CA

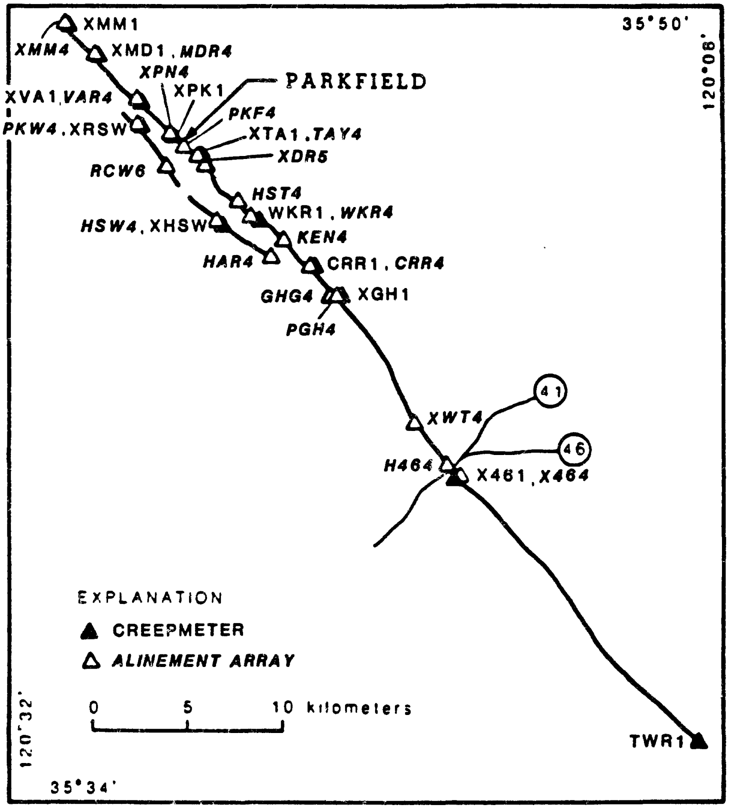

CREEPMETER AND ALINEMENT ARRAY SITES IN PARKFIELD
MARCH 1988

FIGURE 2

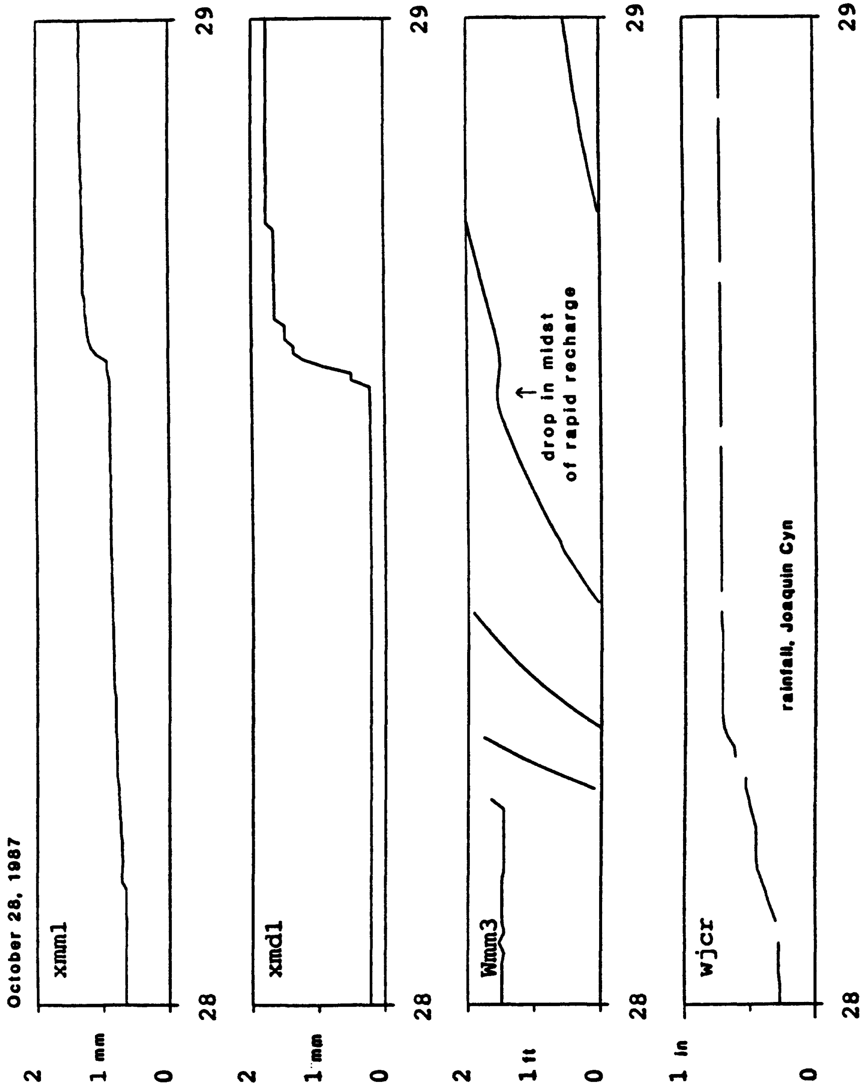
October 28, 1987
xmml
2
1 mm
0
28
29
xmdl
2
1 mm
0
28
29
Wmm3
2
1 ft
0
28
29
drop in midst
of rapid recharge
wjcr
1 in
0
28
29
rainfall, Joaquin Cyn

FIGURE 3

# Remote Monitoring of Source Parameters for Seismic Precursors

9920-02383

George L. Choy
Branch of Global Seismology and Geomagnetism
U.S. Geological Survey
Denver Federal Center
Box 25046, Mail Stop 967
Denver, Colorado 80225
(303) 236-1506

## Investigations

1. Teleseismic estimates of radiated energy and strong ground motion. On a world-wide basis, the relative paucity of near-field recording instruments hinders the prediction of strong ground motion radiated by earthquakes. We are developing a method of computing radiated energy and acceleration spectrum from direct measurements of teleseismically recorded broadband body waves. From our method, the maximum expectable spectral level of acceleration and lower bounds of stress drops can be made for any event large enough to be teleseismically recorded.

2. Rupture process of large- and moderate-sized earthquakes. We are using digitally recorded broadband waveforms to characterize the rupture process of selected intraplate and subduction-zone earthquakes. The rupture processes thus delineated are used to complement seismicity patterns to formulate the tectonic interpretation of the epicentral regions.

3. NEIC reporting services. Broadband data are now being used routinely to increase the accuracy of some reported parameters such as depth and to compute additional parameters such as radiated energy.

## Results

1a. Subduction-zone events. We have compiled the log-averaged P-wave acceleration amplitude spectra from teleseismic data for a set of large, shallow-focus subduction-zone earthquakes. The events range in size from the magnitude 6.2 to 8.1. The acceleration spectra, corrected for frequency-dependent attenuation and the modulation of depth phases, are approximately flat from 10 secs to 2-3 seconds, falling off somewhat at high frequencies. The radiated energies of these earthquakes are proportional to the seismic moments, but the high-frequency acceleration levels are more strongly proportional to the asperity areas than the seismic moments of the earthquakes.

1b. Intraplate events. We have applied our algorithm for the computation of acceleration spectra to a series of shallow intraplate earthquakes. Most of these events are characterized by a flat spectral level at high frequencies but an intermediate slope before an $\omega^2$ fall off at low frequencies. The high-frequency spectral levels of these intraplate earthquakes are the same as the levels of subduction-zone earthquakes with the same seismic moments, although the spectral shapes are different.

2. We have completed a study of the Chilean earthquake of March 1985 and its aftershocks. The main shock was a complex earthquake consisting of three events. The first two events released minor amounts of energy; the major release of energy occurred with the third event that nucleated downdip of the first two events. The size of the early aftershock zone far exceeds the dimension of the major shock; the strong frequency dependence of scalar moment implies that substantial slow slip occurred that was not associated with major energy release.

3. An automated processing package utilizing the method of Choy and Boatwright (1981) and Harvey and Choy (1982) has been implemented and is now routinely obtaining broadband records of displacement and velocity from digital data of the GDSN. The NEIC now uses broadband waveforms to routinely: (1) resolve depths of all earthquakes with $m_b$>5.8; (2) resolve polarities of depth phases to help constrain first-motion solutions; and (3) present as representative digital waveforms in the monthly PDE's. We have developed and implemented a semi-automated package that uses the algorithm of Boatwright and Choy (1986) to routinely compute radiated energy for all earthquakes with $m_b$>5.8. In the Monthly Listings of the Preliminary Determination of Epicenters between April-September 1987, depth phases from broadband data were computed for 27 earthquakes; radiated energies were computed for 36 earthquakes.

## Reports

Boatwright, J., and Choy, G. L., 1987, Acceleration source spectra for large earthquakes in Northeastern North America [abs.]: EOS (American Geophysical Union, Transactions), v. 68, p. 1348.

Choy, G. L., and Boatwright, J., 1988, Teleseismic and near-field analysis of the Nahanni earthquakes in the Northwest Territories, Canada: Bulletin of the Seismological Society of America (submitted).

Choy, G. L., and Dewey, J. W., 1987, Rupture process of an extended earthquake sequence--Teleseismic analysis of the Chilean earthquake sequence of 3 March 1985: Journal of Geophysical Research, v. 93, p. 1103-1118.

# TEMPORAL CHANGES IN SHEAR-WAVE SPLITTING AS THE KEY TO EARTHQUAKE PREDICTION

14-08-001-G1380

**Stuart Crampin**
British Geological Survey,
Murchison House, West Mains Road,
Edinburgh EH9 3LA, Scotland UK
(031) 667-1000

**Background:** The technological advances of the last few years allow three-component digital recording at high enough sampling rates for shear-wave splitting to be easily observed for the first time when the traces are displayed with computer drawn graphics. As a result, shear-wave splitting is now recognized along almost all suitable shear-wave raypaths in the upper 10 to 20 km of the crust. There is rapidly increasing evidence from this splitting that most rocks in the Earth's crust are effectively anisotropic due to an internal structure of stress-aligned fluid-filled inclusions, and that shear-wave motion can be interpreted in great detail in terms of the crack- and stress-geometry within the rockmass (reviewed by Crampin 1987a). These distributions of microcracks and preferentially oriented pore-space are known as *extensive-dilatancy anisotropy* or *EDA*. The observations demonstrate that most *in situ* rocks contain an internal structure of stress-aligned fluid-filled inclusions (*EDA-cracks*) whose geometry can be estimated from three-component shear-wave motion recorded at a distance from the cracked rock.

**Objectives:** Changes in stress before an earthquake are expected to modify the geometry of EDA-cracks and lead to corresponding changes in the behaviour of shear-wave splitting, and it has been suggested that monitoring shear-wave splitting could form the basis for the routine prediction of earthquakes (Crampin 1987b). The importance for predicting earthquakes is that the most direct effect of a change of stress before an earthquake is to alter the strain on the rockmass and modify the geometry of the most compliant parts of the rockmass, and the most compliant parts are the fluid-filled EDA-cracks. Such modifications to the EDA-crack geometry will change the behaviour of shear waves propagating through the rockmass, and the effects should be visible on shear waves recorded remotely.

The objective is to seek temporal changes in shear-wave splitting before and after earthquakes, relate any such changes to the earthquake source process, and improve our understanding of the phenomenon of EDA in relation to stress changes before and after earthquakes.

**Results:** Shear-wave splitting is observed above small earthquakes in the Anza seismic gap on the San Jacinto Fault, Southern California, displaying the effective anisotropy of distributions of parallel vertical fluid-filled EDA-cracks. Only one station (KNW) has arrivals from a wide enough range of azimuths and angles of incidence within the shear-wave window for the behaviour of the shear-wave splitting to be examined in detail. The delays between the split shear-waves in a section of the shear-wave window at this station increase significantly over the three years of records available to Peacock et al. (1988). These changes can be modelled by increasing the aspect ratio ("bowing") of the stress- oriented microcracks. Such bowing is one of the expected (elastic) effects of an increase of stress on a rockmass containing a distribution of fluid-filled inclusions (Peacock et al. 1988; Crampin 1987b).

Since the observations reported by Peacock et al. (1988) further data from the Anza network has been processed by the U.S. Geological Survey. The time taken in processing was the result of the routine location procedure being overloaded by the large number of aftershocks of the $M = 5.9$ North Palm Springs (NPS) earthquake of July 8th 1986, whose epicentre was some 33 km from KNW. Following this earthquake, the shear-wave arrivals within the shear-wave window at KNW show a marked decrease in shear-wave delays in the section of the window that had previously shown the increase (Crampin et al. 1988). The delays returned to approximately the level at the beginning of the three year increase. The data are not sufficient (too few suitable earthquakes as shear-wave sources) to indicate whether the decrease occurs before or immediately after the time of the NPS earthquake, although there is some indication of a levelling-off of the increase shortly before the NPS earthquake (Crampin et al. 1988).

This is the first time that temporal variations in shear-wave splitting have been observed since it was first recognized that crack-induced changes to shear-wave splitting might occur before earthquakes (Crampin 1978). Following Peacock at al. (1988), similar changes were observed in the TDP networks in Turkey (Chen et al. 1987), although they were complicated and no overall pattern of behaviour could be recognized. Recently, behaviour similar to that at Anza has been identified (Booth et al. 1988) before a small earthquake ($M = 3.8$) in the Enola swarm, Arkansas, which was monitored by a digital seismic network for 2½ weeks in June 1982 (Haar et al. 1984).

Note that most of the various other precursors which have sometimes been observed before earthquakes are probably very indirect effects of the stress-induced modifications of these fluid-filled EDA-cracks.

**Conclusions:** The results of Crampin et al. (1988) appear to confirm the suggestion that shear-wave splitting can be used to monitor stress changes before earthquakes (Crampin 1987b). Such temporal changes in shear-wave splitting, as a result of stress-induced modifications to the EDA-crack geometry, are monitoring the most direct effect of the change of stress on the rockmass - the manipulation of the compliant fluid-filled inclusions - and can be interpreted in terms of the three-dimensional anisotropy of the stress-field.

The importance of monitoring shear-wave splitting for earthquake prediction is that the effects of a build-up of stress before a large earthquake can be monitored in as much detail as necessary to predict the earthquake by repeated shear-wave vertical-seismic-profiles (Crampin 1987b). More research is required. In particular, more observations of the behaviour of shear waves before large earthquakes are needed. However, the present technology, and understanding of shear-wave splitting and the behaviour of EDA-cracks, is sufficient to begin establishing procedures for the routine prediction of earthquakes in high-risk vulnerable areas.

**Acknowledgements:** I thank Russ Evans and David C. Booth for their comments on this note. The major part of this research was supported by the Natural Environment Research Council and is published with the approval of the Director of the British Geological Survey (NERC).

**References:**

Booth, D.C., S. Crampin, J. Lovell, and J.-M. Chiu, Observations of shear-wave splitting from an earthquake swarm in Arkansas, *Chapman Conference on Seismic Anisotropy, Berkeley, 1988*, Abstract (1988).

Chen, T.-C., D.C. Booth, and S. Crampin, Shear-wave polarizations near the North Anatolian Fault - III. Observations of temporal changes, *Geophys.J.R.astr.Soc.*, *91*, 287-311 (1987).

Crampin, S., Seismic wave propagation through a cracked solid: polarization as a possible dilatancy diagnostic, *Geophys.J.R.astr.Soc.* *53*, 467-496 (1978).

Crampin, S., Geological and industrial implications of extensive-dilatancy anisotropy, *Nature*, *328*, 491-496 (1987a).

Crampin, S., The basis for earthquake prediction, *Geophys.J.R.astr.Soc.*, *91*, 331-347 (1987b).

Crampin, S., D.C. Booth, R. Evans, S. Peacock, and J.B. Fletcher, Shear-wave splitting as the key to earthquake prediction, *J.geophys. Res.*, submitted (1988).

Haar, L.C., J.B. Fletcher, and C.S. Mueller, The Enola, Arkansas, swarm and scaling of ground motion in the Eastern United States, *Bull.seism. Soc.Am.*, *74*, 2463-2482 (1984).

Peacock, S., S. Crampin, D.C. Booth, and J.B. Fletcher, Shear-wave splitting in the Anza seismic gap, Southern California: temporal variations as possible precursors, *J.geophys.Res.*, in press (1988).

## REPORTS OF RESEARCH PARTIALLY SUPPORTED BY USGS CONTRACTS IN 1986/1987

Booth, D.C., S. Crampin, E.M. Chesnokov, and M.A. Krasnova, The effects of near-vertical parallel cracks on shear-wave polarizations, *Geophys. J.R.astr.Soc.*, *87*, 583-594 (1986).

Bush, I., and S. Crampin, Observations of EDA and PTL anisotropy on shear-wave VSPs, *Expanded Abstracts, 57th Ann.Int.SEG Meeting, New Orleans, 1987*, 646-649 (1987).

Chen, T.-C., D.C. Booth, and S. Crampin, Shear-wave polarizations near the North Anatolian Fault - III. Observations of temporal changes, *Geophys.J.R.astr.Soc.*, *91*, 287-311 (1987).

Crampin, S., Geological and industrial implications of extensive-dilatancy anisotropy, *Nature, 328*, 491-496 (1987a).

Crampin, S., The basis for earthquake prediction, *Geophys.J.R.astr.Soc., 91*, 331-347 (1987b).

Crampin, S., The scattering of shear-waves in the crust, *Pure Appl. Geophys.*, in press (1987c).

Crampin, S., D.C. Booth, R. Evans, S. Peacock, and J.B. Fletcher, Shear-wave splitting as the key to earthquake prediction, *J.geophys.Res.*, submitted (1988).

Crampin, S., and I. Bush, Shear waves revealed: extensive-dilatancy confirmed, *Expanded Abstracts, 56th Ann.Int.SEG Meeting, Houston, 1986*, 481-484 (1986).

Crampin, S. and R. Evans, Neotectonics of the Marmara Sea region of Turkey, *J.geol.Soc., 143*, 343-348 (1986).

Crampin, S., R. McGonigle, and M. Ando, Extensive-dilatancy anisotropy beneath Mount Hood, Oregon, and the effect of aspect ratio on seismic velocities through aligned cracks, *J.geophys.Res., 91*, 12703-12710 (1986).

Evans, R., D. Beamish, S. Crampin, and S.B. Üçer, The Turkish Dilatancy Project (TDP3): multidisciplinary studies of a potential earthquake source region, *Geophys.J.R.astr.Soc.*, in press (1987).

Liu, E. and S. Crampin, Effects of crack anisotropy on cross-hole shooting, *Expanded Abstracts, 57th Ann.Int.SEG Meeting, New Orleans, 1987*, 662-664 (1987).

Peacock, S., S. Crampin, D.C. Booth, and J.B. Fletcher, Shear-wave splitting in the Anza seismic gap, Southern California: temporal variations as possible precursors, *J.geophys.Res.*, in press (1988).

# Analysis of Natural Seismicity at Anza

9910-03982

Joe Fletcher, Art Frankel, Leif Wennerberg, and Linda Haar
Branch of Engineering Seismology and Geology
U.S. Geological Survey
345 Middlefield Road, MS 977
Menlo Park, California 94025
(415) 329-5628 or (415) 329-5612

## Investigations:

1. The purpose of this project is to maintain the 10-station digital array of seismometers at Anza, California, compute source parameters from the digital seismograms, and analyze those source parameters with respect to the generation and propagation of high frequency seismic waves.

2. Investigate the response of the upper crustal rocks at the Anza stations and whether these transfer functions are characterized by amplifications, attenuation, or both. Do these site responses seriously alter estimates of source spectra?

## Results:

1. Processing of the digital seismic data is now complete up through November 24, 1987 with locations, moments, energies, and stress drops for 741 events. Plots of events for the last two years show that events are continuing to occur in the same clusters defined with earlier sets of data. Cluster KN has been the most active with reduced activity at cluster CA (Cahuilla swarm). The block of crust to the northeast of the San Jacinto fault continues to have much less seismicity than the block between the Elsinore and the San Jacinto faults. Televiewer logs obtained from boreholes that were drilled at stations KNW and PFO show much less fracturing at station PFO compared to that at station KNW suggesting a correlation between the high velocity, low fracture densities, and low seismicity. There is a lineation of seismicity extending southeast from the end of a mapped fault trace between Hot Springs and San Jacinto faults. It is somewhat unusual for seismicity to line up along fault trends in contrast to being in the clusters.

2. We analyzed spectra of local microearthquakes recorded by the Anza, California, seismic network to isolate the effects of site response and to investigate the scaling of source parameters for small earthquakes. Spectra of microearthquakes ($M_L<2$; $M_o<10^{19}$ dyne-cm) at Anza have shape characteristics of the receiver sites and are generally independent of the source region. Thus, the site response is a major conditioner of the observed spectral shape. To remove the effects of site response from the spectra of a $M_L \approx 3$ event and isolate its source spectrum, we divided by the spectrum of an adjacent aftershock used as an empirical Green's function event. The spectral ratios indicate that the corner frequencies of small earthquakes ($M_o<10^{19}$ dyne-cm) observed at even the high f max sta-

tions on hard rock are much lower than the source corner frequencies. The spectral ratios are consistent with stress drop remaining constant with decreasing seismic moment, for events with moments as small as $10^{18}$ dyne-cm. An apparent dependence of high-frequency fall-off with seismic moment in the original spectra can also be explained by the effects of site response. The shape of the spectra of microearthquakes at Anza can be largely explained by strong attenuation at shallow depth with a frequency independent Q. Further evidence of low near-surface Q is observed in the anomalous spectra of an unusually shallow earthquake (source depth 1 km) in the network. The spectra from this shallow event are depleted in high-frequency energy at most stations, relative to those of deeper events.

Reports:

Frankel, A., and Wennerberg, L., 198x, Microearthquake spectra from the Anza, California, seismic network: Site response and source scaling: in review.

Fletcher, J.B., Haar, L.C., and Liu, H.-P., 1988, Downhole investigations at Anza: submitted to the Chapman Conference on Seismic Anisotropy, Berkeley, California, May 31-June 4, 1988.

Baker, L.M., 1988, Distriblib: A library for building distributed applications using DECnet/VAX: DECUS, 1988 Western Regional Conference, March 24-25, San Francisco.

Haar, L.C., and Fletcher, J.B., 1988, Amplification and attenuation in the upper crust: Data from two borehole sites at Anza, California: submitted to the Seismological Society of America meeting, Honolulu, Hawaii, May 1988.

# Seismic Waveform
# Analysis Project
# 8-9930-03790

Thomas H. Heaton
Branch of Seismology
525 S. Wilson Avenue
Pasadena, CA 91106

## Investigations

1. Develope methodologies for studying waveform data recorded by the Southern California Seismic Network.
2. Develop a science plan for regional seismic networks.
3. Improvements to teleseismic waveform modeling and inversion codes
    a) Addition of frequency-dependent Minster attenuation operation
    b) Addition of receiver structure effects by Haskell matrix operator.
    c) Addition of GDSN broadband deconvolution response.
4. Development of linearized, iterative least squares inversion program to simultaneously solve for slip amplitude and rupture time on a finite fault.
5. Assist in response to earthquake sequences in Whittier Narrows (1 October 1988) and Superstition Hills (23,24 November 1988).
6. Investigate the nature of displacements produced by body forces in the neighborhood of a boundary between elastic media.

## Results

1) We are continuing to develop the necessary software and documentation to describe the response characteristics of stations in the Southern California Seismic Network. A data base has been developed that fully describes the components for each station in the network. Calibration pulses have been collected for more than ½ of the stations and have been found to correspond reasonably well with theoretical expectations. Three strong motion accelerometers have been added to the telemetered network and their characteristics have been documented. In December 1987, we assisted with the installation of a new high-dynamic-range very-broad-band seismic system (Quanterra-Streckeisen) that is a joint project of the California Institute of Technology, The University of Southern California, The Incorporated Research Institutes for Seismology, and the U.S. Geological Survey. This system records ground

motions in the frequency band from 10 Hz to 0.001 Hz and in the amplitude range from ambient ground noise to 2 g (in excess of 160 db). We have also prepared time-distance plots for waveforms observed on the Southern California Seismic Network for local, regional, and teleseismic earthquake.

2. As a result of a workshop on regional networks that was held in July 1987, we have prepared a seismic plan that describes the current state of regional networks, the types of research currently being conducted, the nature of networks being planned (in particular the National Seismic Network), and the future uses of seismic networks. Strong emphasis is put on practical applications of regional networks. In particular, regional networks could be used for real time response during and immediately following significant earthquake.

3. As part of our work on the inversion of teleseismic body waves to recover the slip history of an earthquake, we have made several improvements to our computer codes. Until recently we have used exclusively a Futterman (1962) operator with constant t* to include the effects of anelastic attenuation on mantle body waves. However, over the past several years it has become clear that higher frequency waves (F > 0.1 Hz) experience less attenuation than lower frequency waves. To account for this difference in attenuation, we have included the frequency-dependent Minster (1978a, 1978b) attenuation operator in our wave propagation code. Receiver structural effects can also be important, particularly at higher frequencies ( f  1.0 Hz). Because we are interested in uncovering ever finer detail in the earthquake source process, it is crucial that we correctly simulate receiver effects. To this end, we have incorporated a Haskell (1953, 1962) matrix operator. (Complexity in the source region has always been accounted for by the summation of generalized rays.) In the inversion of body waves to recover properties of the source, it is necessary to use data with as wide a frequency bandwidth as possible. Until recently this has been accomplished by inverting long-period, intermediate-period, and short-period records simultaneously. However, computer time can be reduced, and a more uniform weighting in frequency content achieved by using broadband deconvolved records as data in the inversion scheme. Therefore, we have included the GDSN broadband deconvolution responses of Harvey and Choy (1982).

4. One of the two major limitations which have surfaced in the inversion of waveform data, is the practical limit on the number of unknowns which may be calculated. Since there is no a-priori detailed knowledge of when a rupture occurred on a finite fault, a straighforward linear parameterization for slip can easily lead to an intractable problem. Therefore, we are exploring linearized iterative methods which solve for rupture time as well as slip.

5. Coordination of field investigations immediately following the M 5.9 Whittier Narrows earthquake (1 October 1987) and the M 6.2 and M 6.6 Superstition Hill earthquakes (23, 24 November 1987) were provided by this project. Rapid deployment of strong motion accelermometers resulted in 2 near-source recordings of the M 6.6 Superstititon Hills earthquake. Numerous briefings on these earthquakes were provided by this project.

6. Exact analytic expression for the displacements that result from point force and force-couple systems embedded within two welded, elastic, Poissonian half-spaces have been developed. We demonstrate that the solution for a vertical strike-slip double couple is continous everywhere (except at the source) as the source is moved across a boundary. However, the solution for a vertical dip-slip double couple jumps everywhere by the ratio of the rigidities as the source is moved across the boundary.

## References

Minster, J.B. (1978a). Transient and impulse responses of a one-dimensional linearly attenuating medium - I. Analytical results, Geophys. J.R. astr. Soc, 52 , 479-501.

Minster, J.B. (1978b). Transient and impulse responses of a one-dimensional linearly attenuating media, - II. A parametric study. Geophys. J.R. ast. Soc, 52, 503-524.

Haskell, N.A. (1953). The dispersion of surface waves in multilayered media, Bull. Seism. Soc. Am., 43, 17-34.

Haskell, N.A. (1962). Crustal reflection of plane P and SV waves, J. Geophy. Res. 67, 4751-4767.

Harvey, D., and G.L. Choy (1982). Broad-Band deconvolution of GDSN data, Geophys. J.R. astr. Soc. 69, 659-668.

Futterman, W.I. (1962). Dispersive body waves, J. Geophys. Res., 67, 5279-5291.

## Reports

Heaton, T.H., D. Anderson, W. Arabasz, R. Buland, S. Hartzell, T. Lay, P. Spudich (1988). National Seismic System Science Plan, manuscript, 80 p.

Stach, L., and T. Wallace (1988). Regional moment-tensor inversion for moderate sized earthquakes in western United States, Earthquake Notes, Vol. 1, in press.

TH(9):1r

# Development of a Kalman Filter for the analysis of GPS data

14-08-0001-G1603

Thomas A. Herring
Harvard-Smithsonian Center for Astrophysics
60 Garden St, Cambridge, MA. 02138
(617) 495-7100

Ojective: Fluctuation of the water-content of the atmosphere is one of the main limiting sources of error in the estimation of relative position using observations of radio signals from the satellites of the Global Positioning System (GPS). Such fluctuations, in fact, may soon be *the* limiting source of error. To reduce this source of error, we are developing a Kalman filter for implementation in programs used for GPS data analysis. The application of Kalman filtering to the analysis of other space geodetic data has yielded, in some cases, severalfold improvements in the precision of the estimates of station heights.

Progress: This grant was recently awarded. So far we have been investigating options for interfacing the Kalman filter analysis software to existing GPS data analysis programs. The two programs we have been studying are those developed at the Massachusetts Institute of Technology (MIT) and the Astronomical Institute of Berne. This latter program is being used by the USGS. By comparing the interfaces which are possible with these two programs, we hope to develop a Kalman filter analysis package that can be implemented in a number of different programs.

# Instrument Development and Quality Control

9930-1726

E. Gray Jensen
Branch of Seismology
U.S. Geological Survey
345 Middlefield Road - Mail Stop 977
Menlo Park, California 94025
(415) 329-4729

## Investigations

This project supports other projects in the Office of Earthquakes, Volcanoes and Engineering by designing and developing new instrumentation and by evaluating and improving existing equipment in order to maintain high quality in the data acquired by the Office.

## Results

Installation was completed on a 35 KVA uninterruptible power supply (UPS) at the Menlo Park office. This UPS will work with the recently installed generator to provide emergency power to real-time data collecting and processing equipment. A 20 KVA generator and a UPS were installed at the Halliburton facility in Parkfield to provide uninterrupted power for the MicroVAX computer which processes digitally telemetered seismic data from the area.

A 2-camera video tape recording system was designed, debugged and installed on the fault in Parkfield. This system records time-lapse images of an array of markers located along and across the fault. A telemetered seismic signal can trigger the cameras to record continuously just before an earthquake arrival. Outdoor lights illuminate the scene at night and precise time information is provided by an LED flashing in the lens.

A MicroVAX-based seismic monitoring system similar to CUSP was installed on a vertical array of over 100 sensors deployed in 1500 m. deep borehole in Parkfield. A set of 120 precision low-noise amplifiers was designed and constructed as an interface between the sensors and the system digitizer. Also the GOES satellite time receiver was modified to provide sampling pulses.

A new version of the clock/power board for the GEOS event recorder was designed and prototyped in preparation for production of 55 new units. A problem, wherein the J120 discriminator output would oscillate at high frequency when installed, was debugged. A solution has been incorporated into new units currently in production. Existing units will be retrofitted.

Five PRS-4 "lunchbox" seismic recorders from EDA were received. They were purchased in order to evaluate their suitability for use in seismic refraction work and other purposes. The preliminary setup software for the recorders was awkward and a new version is pending. Amplifier tests revealed that changes are needed in the front-end gain. The units were recently returned to the factory for upgrades. More conclusive tests will follow.

Almost 1000 multiplexer channels on Tustin digitizers were modified to filter out noise and improve the signal-to-noise ratio. Three 400 Hz. and one 340 Hz. discriminators were added to the CalNet tape digitizing system. This will make playback of signals on these frequencies less complicated. A voltage-limited summing amplifier which protects data on the microwave system from corruption by individual signals was designed and is now being implemented.

As before, much time has been spent augmenting and maintaining the microwave telemetry network. Two radio communications repeaters and a telephone patching system were installed in the Parkfield area. Many CalNet and Parkfield seismic stations were visited for maintenance, repair and upgrading. Also, numerous telemetry radios and seismometers were repaired, adjusted or calibrated.

# Southern California Earthquake Hazard Assessment

8-9930-04072

Lucile M. Jones and Douglas D. Given
Branch of Seismology
U. S. Geological Survey
Seismological Laboratory 252-21
California Institute of Technology
Pasadena, California 91125

## INVESTIGATIONS

### 1. Routine Processing of Southern California Network Data.

Routine processing of seismic data from stations of the cooperative southern California seismic network was continued for the period October 1987 through March 1988 in cooperation with scientists and staff from Caltech. Routine analysis includes interactive timing of phases, location of hypocenters, calculation of magnitudes and preparation of the final catalog using the CUSP analysis system. About 700 events were detected in most months with a regional magnitude completeness level of 1.6 (Fig. 1). Two large earthquakes, the October 1 $M_L = 5.9$ Whittier Narrows earthquake and the November 24 $M_L = 6.0$ Superstition Hills earthquake, occurred during this recording period. Because of the large number of Sueprstition Hills aftershocks, earthquakes in December 1987 have not yet been completely processed.

### 2. Investigation of Southern California Earthquake Sequences.

The $M_L = 5.6$ North Palm Springs earthquake of July 8, 1986, the $M_L = 5.3$ Oceanside earthquake of July 8, 1986, the $M_L = 5.9$ Whittier Narrows earthquake of October 1, 1987, and the $M_L = 6.0$ Superstition Hills earthquake of November 24, 1987 and their aftershocks are being analyzed. Preliminary reports have been completed for all of the sequences. Detailed studies are continuing including determination of focal mechanisms for M $\geq$3.0 aftershocks, inversion of these data for changes in the state of stress, and comparison of the results to the geologic structures to better understand the seismotectonic structure of southern California.

### 3. Characteristics of Aftershock Sequences in California.

Earthquakes in the California catalog from 1932 to 1987 have been grouped into spatio-temporal clusters using Reasenberg's (1985) clustering algorithm. The properties of aftershock sequences including rate of activity, decay rate and b-value have been determined and are compared to the magnitude distirbutions of the clusters and to the seismotectonic region.

### 4. Segmentation of the southern San Andreas fault.

The Mojave segment of the southern San Andreas fault, from Fort Tejon to Cajon Pass, and the Indio segment from Cajon Pass to the Salton Sea are near the end of their respective seismic cycles. If the segments rupture together, a more destructive great earthquake would result than if they fail separately. The slip deficit on these segments, together with the previously observed scaling of rupture length with seismic moment, are analyzed for information about segmentation of the San Andreas in future great earthquakes.

## RESULTS

### 1. Routine Processing of Southern California Network Data.

The projects to upgrade the southern California seismic network are continuing. To increase the accessibility and research potential of the seismic data, a series of semi-annual Network Bulletins have been issued since 1985. These bulletins provide information about how to access data from the network, problems with the data, details of the processing computer systems, and earthquakes in southern California. As part of this project, documentation of past and present station configurations has been compiled. Hardware upgrades of the network have also been undertaken, including the installation of 50 new VCO's in the field for data transmission back to the central recording site. Three new six-component stations (3 high gain and 3 low gain (FBA) components) have also been installed. Preparations are continuing for the installation of a new MicroVAX system for on-line recording of the network data and a RTP (real-time processor) for near-real-time earthquake lcoations. The new systems are expected to be complete by June 1988.

### 2. Investigation of Southern California Earthquake Sequences.

*Oceanside.* The Oceanside earthquake occurred 55 km offshore at 32°58.2'N and 117°52.2'W and was followed by an extensive aftershock sequence with 55 events of $M_L \geq 3.0$ during July 1986. The mainshock and aftershocks are located at the northern end of the San Diego Trough-Bahia Soledad fault zone (SDT-BS) where it changes strike from northwest to a more westerly direction through a left step or bend in the fault. The spatial distribution of the aftershocks indicates a unilateral 7–9 km long rupture to the east-southeast away from the mainshock. The focal mechanism of the mainshock also shows a east-southeast striking and south-dipping plane with mostly reverse motion on it. Focal mechanisms of the $M_L \geq 3.0$ aftershocks show both reverse and strike-slip movement. These data suggest that the earthquake ruptured a thrust fault in the left step of the SDT-BS fault. A stress inversion of the focal mechanism data shows a rotation of the maximum principal stress of 14° that is largest in the days following the mainshock and decreases rapidly with time. The abundance of aftershocks may be related to the large temporal variation in stress orientation that, in turn, may have resulted from the small stress drop of the mainshock. These data suggest that the Inner Continental Borderland is not a pure strike-slip regime but rather a strike-slip mixed with reverse faulting regime.

*Whittier Narrows.* The $M_L = 5.9$ Whittier Narrows earthquake was located at 34° 3.0′N, 118° 4.8′W, at the northwestern end of the Puente Hills, at a depth of 14 ± 1 km. The epicenters of the aftershocks form an approximately circular pattern that is centered at the epicenter of the mainshock, and has a diameter of 4 to 5 km; the hypocenters define a surface that dips gently to the north. The focal mechanism of the mainshock has two nodal planes, that strike east-west and dip 25° to the north and 65° to the south.

The largest aftershock ($M_L = 5.3$) was located 3 km to the northwest of the mainshock's epicenter. In contrast with the mainshock, the focal mechanism of the largest aftershock shows mostly strike-slip movement with a small reverse component on a steeply dipping northwest striking plane. The focus is located at a depth of $12 \pm 1$ km, which is within the hanging wall of the thrust fault and 2 to 3 km above the rupture surface of the mainshock. The locations and focal mechanisms of the two largest and numerous smaller aftershocks define a north-northwest striking, steeply dipping fault, which forms the western edge of the aftershock distribution.The spatial distribution of aftershock hypocenters indicates that this steeply dipping fault exists within both the hanging and the foot wall, and the main shock slip thus may have terminated against this fault.

*Superstition Hills.* The foreshocks, two mainshocks and aftershocks of the Superstition Hills sequence occurred on a conjugate fault system involving the northwest-striking, right-lateral Superstition Hills fault and a previously unknown northeast-striking left-lateral defined by a lineatin of hypocenters extending from the Sueprstition Hills fault to the Brawley seismic zone. The earthquakes have been relocated using data from the Southern California Seismic Network and master event relocation techniques. The first mainshock ($M_L = 5.8$, $M_S = 6.2$), on the northeast trend, and its foreshocks colocate at 33° 4.9′N, 115° 47.7′W, h=10.6 km. Its aftershocks are located on the northeast trend between the Sueprstition Hills fault and the Brawley seismic zone, clustering in time and space. The second mainshock ($M_L = 6.0$, $M_S = 6.6$) is located on the Superstition Hills fault at 33° 0.9′N, 115° 50.9′W, h=1.9 km. The second mainshock initiated 12 hours after the first at a shallow depth where the two aftershock trends join. Epicenters on the northwest trend lie between the Superstition Hills and the Superstition Mountain faults and the extent of aftershocks is not coincident with the extent of surface rupture on the Superstition Hills fault. In general, hypocenters on the northeast trend are deep and hypocenters on the Superstition Hills fault are shallow.

## 3. Characteristics of Aftershock Sequences in California.

Omori's Law (the rate of aftershock activity as a function of time after the mainshock, $N_{perday} = \frac{K}{(t+c)^p}$) and the Gutenberg-Richter magnitude–frequency relation ($N = 10^{-bM}$) have been fit to over 50 aftershock sequences of $M_L \geq 5.0$ mainshocks that have occurred in California over the last 60 years. The average values of $b$ and $p$ for California is approximately 1. These data are being used to develop statistical estimates of the hazard of damaging aftershocks after major earthquakes. Preliminary results suggest significant variation in $b$- and $p$- values with little correlation to tectonic regime.

## 4. Segmentation of the southern San Andreas fault.

A constant ratio of seismic moment to rupture length implies both a constant stress drop and a constant ratio between slip and length. Previously published data on rupture length and slip for strike-slip earthquakes in California have been collected and analyzed. These data show linear correlations between length and moment and between coseismic slip and length, within a factor of 1.5. This correlation predicts that a strike-slip earthquake with 4 m of average slip should rupture a length of 380 ± 130 km. Sieh has shown that the slip deficit at Indio is at least 7.5 m. Even if the average slip in the next event is only half that, the slip-length relation still requires the rupture zone to be twice the length of the 175 km long Indio segment. The slip deficit on the Mojave segment averages 3.2 - 4.5 m, also suggesting that a future earthquake could not be confined to the 175 km of the Mojave segment. Assuming coseismic slip of 4 m and fault width of 12 km, an earthquake on both segments (length = 350 km) would have a seismic moment of $\sim 5 \times 10^{27}$ dynes-cm ($M_w = 7.8$). If the slip deficit is only partially relieved in the next earthquake, then the event could be confined to an individual segment of 175 km length, with a slip of $\sim$ 2 m and a moment of $\sim 1 \times 10^{27}$ dynes-cm ($M_w = 7.3$).

## PUBLICATIONS

Hauksson, E., L. Jones, T. Davis, L. K. Hutton, A. G. Brady, P. Reasenberg, A. J. Michael, R. F. Yerkes, P. Williams, G. Reagor, C. Stover, A. Bent, A. Shakal, E. Etheredge, R. Porcella, C. Bufe, M. Johnston, E. Cranswick, The Whittier Narrows earthquake in the Los Angeles metropolitan area, California, *Science,* **239**, 1409–1412, March 18, 1988.

Jones, L. M., and E. Hauksson, Preliminary analysis of the Whittier Narrows earthquake sequence, *Earthquake Spectra,* in press, 1988.

### Abstracts:

Jones, L. M., and E. Hauksson, 1987, The size and location of the next great southern California earthquake, *Trans. Amer. Geophys. U.,* **68**, 1349.

Hauksson, E. and L. M. Jones, 1987, The July 1986 Oceanside earthquake sequence ($M_L = 5.3$) in the continental borderland, southern California, *Trans. Amer. Geophys. U.,* **68**, 1361.

Hauksson, E. and L. M. Jones, 1988, The 1987 Whittier Narrows Earthquake in the Los Angeles Metropolitan area, California: Overview, locations and seismotectonics, *Trans. Amer. Geophys. U.*, in press.

Jones, L. M., and E. Hauksson, 1988, Spatial Variations in the Locations and Focal Mechanisms of Aftershocks of the 1987 Whittier Narrows Earthquake, Los Angeles County, California, *Trans. Amer. Geophys. U.*, in press.

Given, D. D., and W. D. Stuart, 1988, A fault interaction model for triggering of the Superstition Hills earthquake of November 24, 1987 *Seismol. Res. Letters*, in press.

# State of Stress Near Seismic Gaps

Grant No. 14-08-0001-G1356

Hiroo Kanamori
Seismological Laboratory, California Institute of Technology
Pasadena, California 91125 (818-356-6914)

## Investigations

Use of short-period data for monitoring temporal stress variation.

## Results

Short-period waves contain important information about the state of stress in the rupture zone. In terms of a simple asperity model (e.g. Kanamori, 1981), on the average, the stress drop of earthquakes increases with time before the main shock. The actual situation is probably far more complex than this model predicts. Nevertheless, determination of stress distribution in the epicentral area of major earthquakes is one key to better understanding the earthquake failure process. Continued monitoring of the stress distribution in critical areas is also fundamentally important. Although accurate measurements of earthquake stress drop are difficult, short-period characteristics of source spectra can be used as a good measure of stress drop. Almost all seismic scaling relations predict higher short-period spectral amplitudes for higher stress-drop events for a given seismic moment.

The determination of short-period source spectra is difficult because of the complex source processes and the propagation-path effect. We have gained some experience with short-period spectra obtained from teleseismic short-period and broad-band seismograms (Houston and Kanamori, 1986a, 1986b, Zhou and Kanamori, 1987), and feel that, despite the complexity of the problem, we can determine short-period source spectral amplitudes within a factor of two.

In order to test the method, we have refined the method and made a reconnaissance study. Figures 1, 2, and 3 show the results for the 1986 Aleutian Is. earthquake sequence.

Figure 1 shows the spatial distribution of the events for which source spectra have been determined. Events are numbered chronologically. The main shock ($M_W = 8.0$) is event #12. Figure 2 shows the spectra of the events determined by the method of Houston and Kanamori (1986a). The shaded area is one standard deviation. Stations used for each event are listed in the figure. In order to compare the short- and long-period spectral amplitudes for different events, we show in Figure 3 spectral amplitudes represented by $M_W$. This representation is similar to that used by Zhuo and Kanamori (1987). The dashed line in the figure is drawn as reference. At 1 sec most events occurring before the 1986 main shock exhibit higher spectral amplitudes than events occurring after the main shock. This indicates that the state of stress changed before and after the 1986 main event. At periods longer than 2 sec, no appreciable difference can be detected.

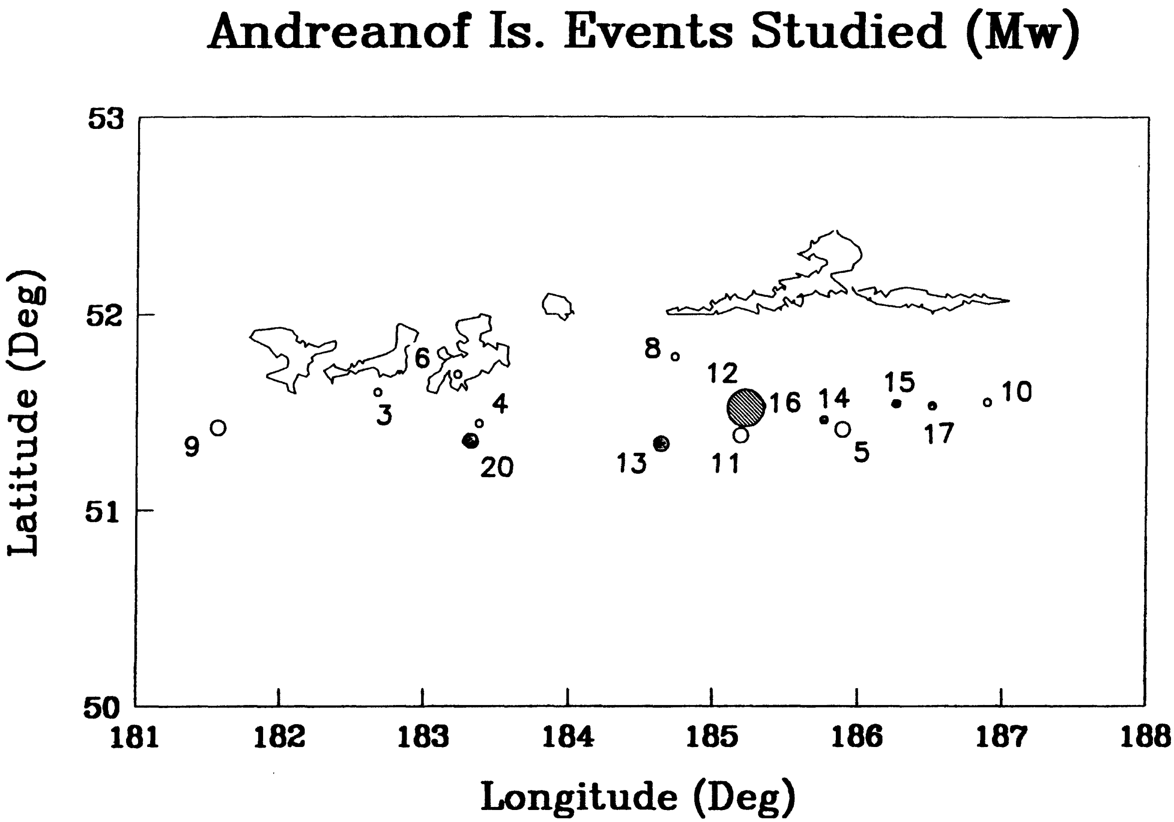

Figure 1.
The locations of the events studied. The events are numbered chronologically. Event #12 is the main event of the Andreanof Is. earthquake sequence. Open and closed symbols indicate events before and after the main shock respectively.

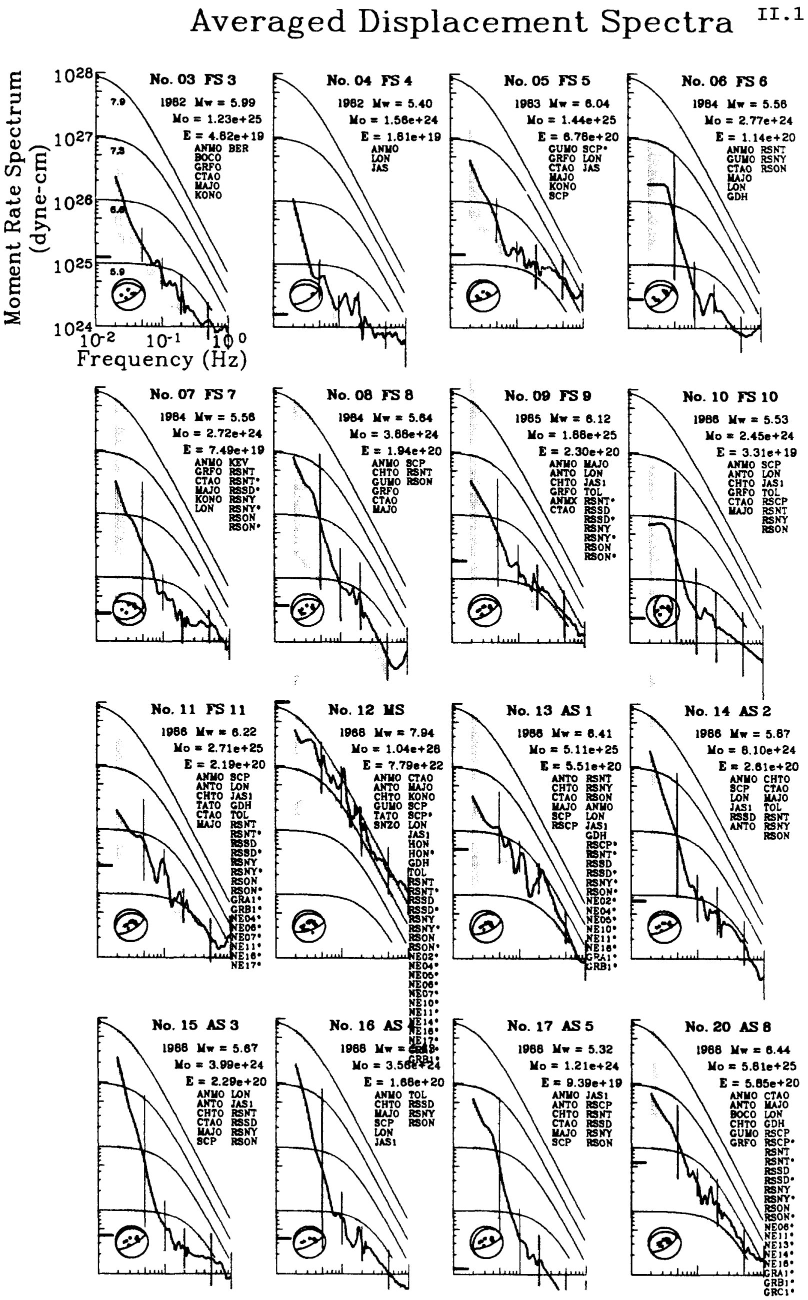

Figure 2.
Moment rate spectra of the events shown in Figure 1. The stations used are listed on each figure.

# Andreanof

## *Spectral Amplitude Comparison*

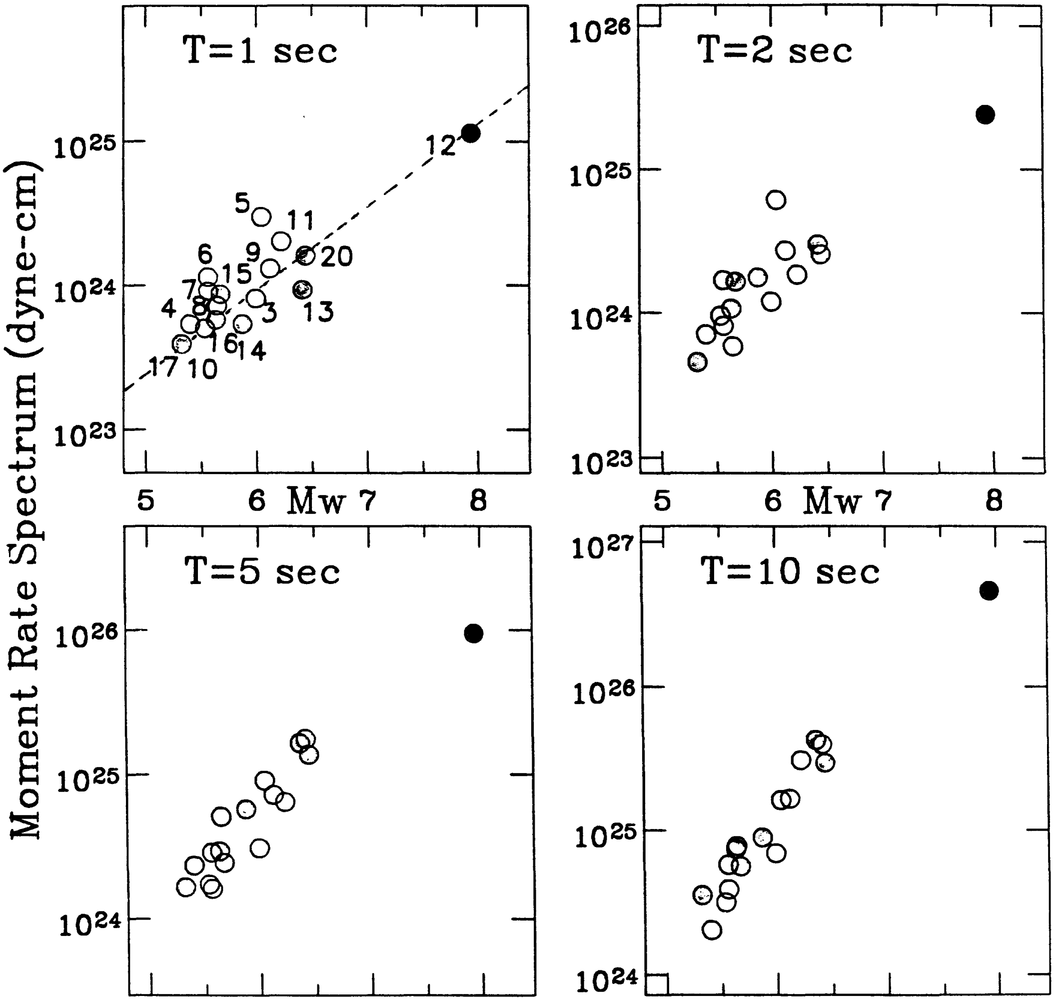

Figure 3.

Spectral amplitudes at 1, 2, 5 and 10 sec as a function of $M_w$. Open and closed symbols indicate the events before and after the main shock, respectively.

For events in different regions, the absolute values of the spectral amplitude at 1 sec cannot be compared with confidence because of the regional variations of attenuation. However, in this study we compare events in the same region and use relative amplitude information as indicators of stress change. Hence, we believe that the differences shown in Figure 3 are real.

**References**

Lay, Thorne, Luciana Astiz, Hiroo Kanamori, Douglas H. Christensen, Temporal variation of large intraplate earthquakes in coupled subduction zones, in press, Physics of the Earth and Planetary Interiors, 1988.

# FAULT MECHANICS AND CHEMISTRY

9960–01485

C.–Y. King
Branch of Tectonophysics
U.S. Geological Survey
345 Middlefield Road, MS/977
Menlo Park, California 94025
(415) 329-4838

## Investigations

[1] Water temperature and radon content were continuously monitored at two water wells in Parkfield, California.

[2] Water level was continuously recorded at six other wells.

[3] Water temperature and electric conductivity were periodically measured, and water samples were taken from most of these wells and two springs in San Jose for chemical analysis.

[4] Radon content of ground gas was continuously monitored at Cienega Winery, California, and at Nevada Test Site.

[5] Migration pattern of historical earthquakes in California is examined.

[6] Volume predictability of volcanic eruptions in Hawaii was studied.

## Results

### Volume predictability of historical eruptions at the Hawaiian volcanoes.

Most major eruptions at the Kilauea and Mauna Loa volcanoes in Hawaii have been approximately volume-predictable (*i.e.,* the volume of a major eruption episode is approximately proportional to the preceding recurrence time interval) since 1920. This observation suggests that the post-eruption magmatic pressure tends to remain constant for long periods of time (several decades), while the pre-eruption magmatic pressure varies with time. The average eruption rates for the individual volcanoes changed (increase for Kilauea and decrease for Mauna Loa) in 1950 when a large eruption occurred at the southwest flank of Mauna Loa, but the combined eruption rate has remained fairly constant during the studied period. This result suggests that both volcanoes tap the same deep magma source, which feeds the magma reservoirs of the volcanoes at a fairly constant rate, though in different proportions.

## Reports

King, C.–Y. (1988). Volume predictability of historical eruptions at the Hawaiian volcanoes (abs.): Letters of Seismological Research, in press.

King, C.–Y. and Scarpa, R., eds. (1988). Modeling of volcanic processes, Friedr. Vieweg & Son, Braunschweig/Wiesbaden pp. 209.

# CALIFORNIA AND HAWAII SEISMICITY STUDIES

Project 9930-03563

Fred W. Klein
Branch of Seismology
U.S. Geological Survey MS 977
345 Middlefield Rd.
Menlo Park CA 94025

## Investigations

The overall objective is to look for long-term seismicity and tectonic patterns in the Northern California and Hawaii earthquake catalogs. The two catalogs are in very different states of self-consistency and usefulness for research, however. Accordingly, the Hawaiian work uses a completely reprocessed catalog and focuses on research. The Northern California effort presently involves cleaning up the raw phase data and developing methods for reprocessing this data into a self-consistent catalog. This reprocessing is necessary before many types of research become meaningful. The emphasis is on applying methods developed for Hawaiian processing and earthquake display to the California catalog.

The Hawaiian seismic investigation consists of a thorough study of earthquake focal mechanisms in the upper mantle beneath Hawaii. The goal is to determine the state of stress, nature of lithospheric flexure and interaction of the volcanic system with the lithosphere. This work includes a detailed study of the vertical magma conduit feeding Kilauea Volcano's shallow (3-7 km depth) magma reservoir. The seismically active conduit extends downward to about 55 km to the top of the magma source region.

The work on the Northern California earthquake catalog is being shared by several colleagues in the branch. This project has assumed responsibility in several areas: (1) Develop a data base of seismic station data including a new systematic set of station codes and apply it to the reprocessing of the earthquake catalog. (2) Develop a computer file system or data base for storing both raw and processed earthquake phase data. (3) Develop and modify the HYPOINVERSE earthquake location program to handle the various tasks needed for Northern California processing. These include archival storage of various data, implementation of a revised coda magnitude procedure, ability to obtain interactive locations in the CUSP processing environment, and use of regionalized crustal and station delay models. (4) Revise the QPLOT geophysical data plotting program as necessary for real-time and other display tasks needed for research, monitoring and reprocessing of seismicity data.

## Results

The research on Kilauea's magma conduit suggests that the earthquakes require external sources of stress and are not simply generated by excess magma pressure, as with rift zone intrusions. Dramatic evidence for an external stress cause is the major drop in earthquake rate following the M=7.2 Kalapana earthquake in 1975. This event thus released stress in the entire volcanic system in addition to the rupture zone in Kilauea's south flank. Seismic gaps occur along the conduit centered at about 5, 13 and 20 km depths. The 3-to-7-km gap is the main magma reservoir, the 13 km gap appears to result from the layer of buried ocean sediments at the base of the volcanic pile, and the 20-km gap is present under the whole island. The latter may be a depth of low or "neutral" stress within the flexing lithosphere. Lateral extension is characteristic of the focal mechanisms within the volcanic pile (above the 13 km gap) and lateral compression occurs just below. Stresses are thus decoupled at the boundary of the volcanic pile with the underlying oceanic crust. Focal mechanisms below 20 km depth are similar to those in Kilauea's south flank and show southward motion of the upper block on a near-horizontal plane. Stresses do not reverse above and below 20 km depth, so this gap is more complex than simply a plane of neutral stress within the flexing lithosphere.

The reprocessing of the Northern California earthquake catalog is underway. Contributions from this project to date include: (1) A data base of seismic stations has been assembled, including assignment of unique 5-letter codes to each station. Several programs use the station data base, including one that converts all of the chaotic station codes in our phase data to the new system. (2) The HYPOINVERSE location program now uses multiple crustal and station delay models assigned to different geographic areas. We have assembled and revised 24 regional models and sets of station delays, and assigned them to different geologic and seismic provinces in California, Nevada and Oregon. The algorithm uses a weighted average technique to combine up to three different models for epicenters near model boundaries.

<u>Reports</u>

Klein, F.W., User's guide to five VAX FORTRAN programs for manipulating HYPOINVERSE summary and archive files: SELECT, EXTRACT, SUMLIST, ARCPRINT and FORCON, U.S. Geological Survey Open File Report, in review, 1988.

Klein, F.W., J.P. Eaton, and F. Lester, Seismic station data for Northern California and surrounding areas, U.S. Geological Survey Open File Report, in review, 1988.

Klein, F.W., Multiple crustal models for earthquake location in Northern California and surrounding areas, U.S. Geological Survey Open File Report, in preparation, 1988.

# Southern California Co-Operative Seismic Network

8-9930-01174

Charles Koesterer
Branch of Seismology
525 S. Wilson Avenue
Pasadena, CA 91106

## Investigations

1. Continuation of operation, maintenance, and recording of the southern California seismic network consisting of 109 U.S.G.S. short period seismic stations and 66 other agency instruments. all of the stations are being recorded onto the CUSP analysis system and 205 stations recorded on FM tape units for back-up of digital recording.

## Results

1. Operation and maintenance of field stations and office recording systems continued with little failure during this reporting period.
2. Replacement of the field AMP/VCO units to the J501 type has been completed on 38 stations.
3. Replacement of discriminators to the new J120 type has been completed on 50 stations.
4. Installation of a new 6 component station at Garvey reservoir, City of Monterey Park, CA., was completed following the October 01, 1987 Whittier Narrows earthquake.

CK(6):lr

# Operation of Borehole Tiltmeters at Pinon Flat Observatory, California and Analysis of Secular and Tidal Tilt

14-08-0001-G1338

Judah Levine
Joint Institute for Laboratory Astrophysics
Campus Box 440
University of Colorado
Boulder, Colorado 80309
(303) 492 - 7785

Objective: To install borehole tiltmeters at Pinon Flat Observatory in Southern California and to compare the records with data obtained from other nearby instruments.

Results: We constructed two completely new systems to replace the tiltmeters that were severly damaged by lightning last November and we made two trips to the site to install them. The axis of one of the pendulums in each borehole is very nearly aligned with the axis of the Long-Fluid Tiltmeter (107 degrees) to facilitate comparisons among the instruments.

The instrument in BOA (the shallower borehole) is working well. The noise level and drift seem to be about the same as the values recorded by the original instrument, although the tiltmeter is still settling down and it is too early to make quantitative comparisons. The instrument in BOB is also working but is somewhat noisier than the one in BOA. We do not yet understand why this is so. The two instruments had comparable noise levels when they were tested in Colorado. We have also completed the construction and testing of a third instrument to be installed in the deeper (400 foot) borehole. We have had some difficulty in finding a driller for this work, but we hope to have the hole drilled shortly.

The tiltmeters in BOA and BOB were aligned using a repaired and re-calibrated alignment rod system. This should remove some of the ambiguities that were present in the previous installation and which limited the robustness of the comparison between our instrument and the nearby Askania.

We are constructing a new alignment system for the deeper borehole, since the alignment rods cannot be used at that depth. The new system will use a notched insert near the bottom of the borehole and a key on the top of the capsule so that the capsule can be lowered into the borehole in only one orientation. The azimuth of the notch will be determined once using a gyro-compass before the instrument is first installed. The notch and key are only intended to align the capsule and will not support the capsule or provide the coupling between the capsule and the casing. The weight of the capsule will still be supported by the hemispherical knob at the bottom and the leaf springs along the sides will press the capsule against the wall of the casing as in the current design.

# Array Studies of Seismicity

9930-02106

David H. Oppenheimer
Branch of Seismology
United States Geological Survey
345 Middlefield Road - MS 977
Menlo Park, California 94025
415-329-4792

## Investigations

1. Assess whether a correpondence exists between fault segment boundaries defined on the basis of geologic surface observations and those defined on the basis of earthquake locations.
2. Continue consolidation and clean-up of phase data of central California Seismic Network (CALNET) from 1969 through present.
3. Continue analysis of digitized seismograms from characteristic earthquake sets in the Stone Canyon/Bear Valley region of the San Andreas fault.
4. Revise algorithms to compute and display fault-plane solutions.
5. Complete manuscript describing fault-plane solutions and stress state at Morgan Hill, California.

## Results

1. Fault segmentation can often be recognized from offsets and bends observed from the mapped surface expression of faults. Frequently, these observations are corroborated by hypocentral patterns which develop over time and during aftershock sequences. However, at two locales southeast of the San Francisco Bay the geologically mapped trace of the Calaveras fault departs from the extrapolation of seismic patterns to the surface. The first locale is the region of the Calaveras fault which ruptured during the 1984 M6.2 Morgan Hill earthquake. The rupture surface is clearly defined by the aftershock activity and shows that this segment of the Calaveras fault is a near vertical plane. However, the mapped surface expression of the fault is offset southwest of the seismic expression of the fault from the point of rupture initiation at the northern end of San Felipe Valley to the southeast end of Anderson Lake. Since there was no unequivocable surface rupture for this earthquake, it is not possible to establish that the mapped fault represents an active strand of the Calaveras fault. In the region of offset there is no surface expression of faulting above the seismically determined fault trace that might support the accuracy of the aftershock locations.

   The second locale is the juncture of the Calaveras and Hayward faults. This segment of the Calaveras fault is immediately north of the Morgan Hill segment. It too is near vertical and planar, but the seismicity and surface expression of the Calaveras fault are coincident. The Hayward fault is southwest of and parallel to the Calaveras fault and is mapped as far south as the Morgan Hill epicenter, but there is no evidence in the geologic surface expression of the two faults that they actually join. However, the earthquake locations clearly demonstrate that the Hayward fault splays from the

Calaveras fault. It is notable that the seismicity departs from the mapped trace of the Hayward approximately 40 km north of the southernmost extent of the mapped fault and approximately 10 km north of an active creep site. Unlike the Morgan Hill segment, the seismicity linking the Calaveras and Hayward faults can be associated with the Mission fault, but there is no reported Holocene movement or creep on the Mission fault.

Inherent in any discussion of earthquake locations is the problem of systematic mislocation due to unmodeled velocity variations. This problem does not appear to be significant in this region, for the following reasons: 1) Seismicity locates beneath the mapped traces of the Calaveras and Hayward faults immediately beyond the regions where the discrepancies are noted, suggesting that the velocity model is appropriate. 2) Were the hypocenters to be severely mislocated, the mislocation would probably manifest itself as a constant offset. However, the relative hypocentral pattern does not mimic the offsets observed in the surface expression of the faults in the above areas. 3) Three-dimensional velocity modelling in the Morgan Hill region by Michael yields hypocentral locations similar to the locations presented here.

These observations indicate that the seismic expression of a fault may not necessarily coincide with the surface expression of a fault. If the seismic data are correctly located, then it is difficult to explain the absence of significant surface rupture above the hypocenters, the presence of pronounced fault features at the surface without any corresponding seismicity below, and the presence of aseismic creep off the "seismic" fault. These observations indicate that caution should be exercised when predicting the location and extent of rupture solely on the evidence provided by the geologic expression of faults.

2. Substantial effort was again devoted to the collection, organization, relocation, archiving, and documentation all the CALNET earthquake data since 1969 (see previous Semi-Annual Report). Main efforts were directed toward the merging of post-1983 RTP and CUSP data augmented with "shadow cards", which describe additional aspects of the phase data. The resulting catalog will contain all known aspects of the data, including coda decay parameters and indices to tapes containing CUSP waveforms. This information will make it possible to access the digital data outside the CUSP environment. Phase data for period 1969–1983 are almost complete, and processing for post-1983 data is commencing. Expansion of the project scope, unforeseen problems, and lack of personnel have delayed completion of this effort.

3. On November 7, 1987, a M3.8 earthquake ruptured a patch of the San Andreas fault which we had previously recognized as a characteristic earthquake source. This is the sixth event to occur on this particular section in the last 55 years, the others occurring in 6/34, 1/42, 11/52, 10/66, and 12/77. The two most recent earthquakes were recorded by CALNET on FM tape. Analogue playbacks of these seismograms appear highly coherent; however, the 87 event seems deficient in the higher frequencies compared to the 77 event. Similar observations were made for a previously analyzed Stone Canyon event pair (65–82) of a different source set. The seismograms from the

77–87 earthquake pair are currently being digitized. Recent efforts have been directed toward the debugging of software (written by C. Aviles and C. Valdes) designed to convert the CUSP-formatted digital records to a format that is more manageable outside the CUSP environment. Once reformatted, this data will undergo cross spectral analysis to determine the stability of this characteristic set's source process.

4. Three years ago Paul Reasenberg and I wrote a program (FPFIT) to compute fault-plane solutions from P-wave first-motion observations. I improved several aspects of the program, such as installing an interactive front-end to set the execution parameters, reading HYPOELLIPSE data formats, correcting a bug that produced spurious multiple solutions, and improving the estimates of the solution uncertainties.
5. This research effort is the result of a collaboration between myself, Paul Reasenberg and Robert Simpson. Our findings were reported in previous Semi-Annual Reports, and our efforts were directed to preparing the manuscript for publication.

Reports

Dietz, L. D., and W. L. Ellsworth, 1987, Cross spectral analysis of repeating earthquakes near Stone Canyon, California, EOS, Tran. Am. Geophys. Union, 68, p. 1349.

Zoback, M. D., M. L. Zoback, V. S. Mount, J. P. Eaton, J. H. Healy, D. Oppenheimer, P. Reasenberg, L. Jones, C. B. Raleigh, I. G. Wong, O. Scotti, and C. Wentworth, New evidence on the state of stress of the San Andreas fault, EOS, Tran. Am. Geophys. Union, 68, p. 1495.

Zoback, M. D., M. L. Zoback, V. S. Mount, J. P. Eaton, J. H. Healy, D. Oppenheimer, P. Reasenberg, L. Jones, C. B. Raleigh, I. G. Wong, O. Scotti, and C. Wentworth, New evidence on the state of stress of the San Andreas fault system, Science, 238, 1105–1111, 1987.

Oppenheimer, D. H., 1988, The geologic and seismic expression of the Calaveras fault, central California: A lack of coincidence, Proceedings of Workshop on Fault Segmentation and Controls of Rupture Initiation and Termination, Palm Springs, CA, March 6–9, 1988.

# "Variations in Electrical Properties Induced by Stress Along the San Andreas Fault at Parkfield, California"

Supported by the U.S. Geological Survey, Department of the Interior
under award number 14-08-0001-G1357

Stephen K. Park and Tien-Chang Lee
Institute of Geophysics and Planetary Physics
University of California
Riverside, California 92521
(714) 787-3438

## Introduction

We have installed an array in Parkfield to monitor variations of resistivity using telluric currents. This array has been recording data of high quality since March 5, 1988. We have used shorter dipoles and thus hope to be sensitive to shallower volumes of rock than the measurements made by Madden in Palmdale and Hollister. Comparison of our data to strain, seismic, geochemical, and hydrologic data will help us better understand the mechanism producing changes of electrical resistivity prior to earthquakes.

## Monitoring Array

The monitoring array (Figure 1) consists of five electrodes which are combined to form eight dipoles. Each electrode appears in three dipoles, and this redundancy helps us isolate sources of noise in the array. Madden has assisted us in developing the techniques for analyzing the data, and we are almost done. We currently use (HR-TF) and (HR-FF) as references and calculate telluric coefficients for the other six dipoles:

$$\text{Dipole} = x(\text{HR-TF}) + y(\text{HR-FF}).$$

Plots of the telluric coefficients $(x,y)$ for the six channels from day 65 (March 5) to day 93 (April 2) are shown in Figure 2. We currently have an unidentified source of noise near Lc or on the telephone line which is degrading the responses of dipoles 2(LC-HQ), 5(LC-TF), and 6(FF-LC). We hope to identify this intermittent source shortly. Our next step is to calculate average coefficients from those in Figure 2 and re-analyze the data with these averages. We can predict the dipolar signals with the references and these coefficients and compare the predictions to the measured signals. The mismatch will give us the variations of resistivity.

## Sensitivity Study

We have completed the telluric-magnetotelluric-resistivity study of Parkfield and are interpreting the data. We originally conducted this survey to determine the electrical structure in Parkfield and around the fault. Our specific goal was to detail the structure in the upper 10 km. The surveys we conducted, however, have yielded structure in the upper 1 km and regional structure at depths of more than 10 km. The data are strongly affected by the Pacific Ocean and the lower crustal structure. We were unable to obtain MT data in the range of frequencies we needed to detail the structure between 1 km and 10 km. Wind noise and small signals combined to degrade data between .1 Hz and 1 Hz. Dave Fitterman (USGS), Dale Morgan (Texas A and M), and I have thus developed an alternative approach to assessing the sensitivity of the array to changes of resistivity. We will transmit electrical current with a dipole which is 1 km long and record the response on our array. This transmitting dipole will be moved around within Parkfield and we will be able to directly measure the sensitivity of the array.

Figure 1 - Map of monitoring array. The heavy black dots are electrodes (FF,LC, TF, HQ, HR) and the lines are our dipoles. The approximate hypocenter of the 1966 earthquake is shown.

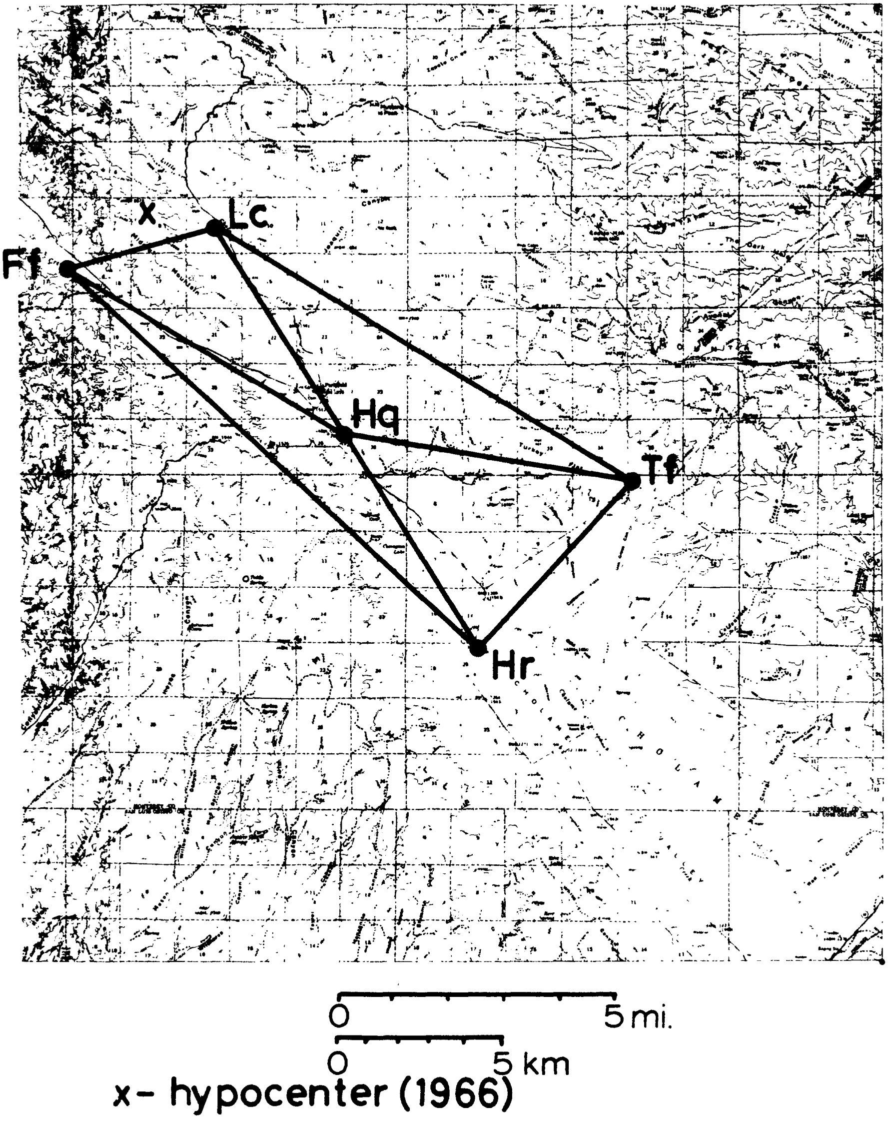

Figure 2 - Telluric coefficients for six dipoles from March, 1988 to April, 1988. Each point represents one day. A scale of 10% is shown in the upper right of the figure. Coefficients are only plotted for days on which the coherency between the predicted and the measured signals was .995 or greater.

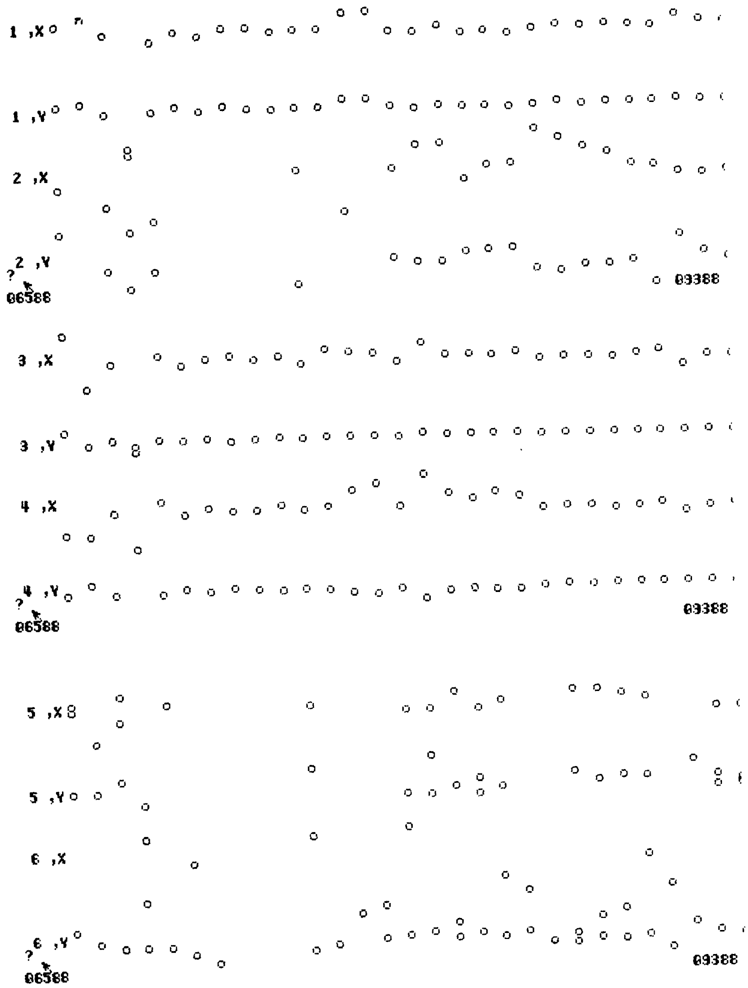

# CRUSTAL STRAIN

9960-01187

W.H. Prescott, J.C. Savage, M. Lisowski, and J.L. Davis
Branch of Tectonophysics
U.S. Geological Survey
345 Middlefield Road, MS/977
Menlo Park, California 94025
(415) 329-4860

## Investigations

The principal subject of investigation was the analysis of deformation in a number of tectonically active areas in the United States.

## Results

### 1. Parkfield GPS experiment

Since early 1986 we have been observing the relative positions (3 components) of four stations in the Parkfield–Middle Mountain area (Fig. 1 and 2). The observations consist of Global Positioning System measurements made approximately monthly. All of these GPS observations were processed using the "Bernese" software package. The observations contained data from both the L1 and L2 GPS frequencies but due to the short distance between stations, no ionosphere correction was included (On these short lines, differences between L1 and L2 are mostly due to random error and interpreting this difference as ionosphere generally introduces error rather that reducing error). Broadcast orbits were used for all processing and all of the integer phase ambiguities were determined, fixed to integers, and eliminated from the solutions. The relative position vectors at each time were resolved into a coordinate system with the x–y plane tangent to an ellipsoid at station 10JDG, and the y axis towards N40°W, parallel to the San Andreas fault in this area. With about 18 months of data, the secular trends in station movement are already very clear. Only the parallel component of 33JDG and Joaquin, the two stations across the fault from the fixed station, exhibits a significant change (Fig. 3). Both 33JDG and Joaquin are moving southeast relative to 10JDG at a rate of 15 ± 2 mm/yr. No convincing deviations from the overall trend are apparent in the plots. No significant deformation was detected in either the normal components or the vertical components. However, the larger errors in the vertical component make this statement much less definitive than it is for the horizontal components. The velocity vectors for the three estimated stations are plotted in Fig. 4. Even with only 18 months of data, fault slip is easily detected. Variations in the rate of fault slip will be difficult to detect (Fig. 3) until the data are quieter. The noise level, about 5 mm in the horizontal components and 20 mm in the vertical component, is probably from the receiver and antenna rather than from some length dependent source like orbit uncertainty.

### 2. Loma Prieta GPS experiment

Since the establishment of a continuous North American Global Positioning System tracking network by a group of institutions in late 1985, it has become possible for GPS users with only a few receivers to carry out high precision observations. We have recently processed data from two GPS measurements of the LP1 to Allison and LP1 to Eagle vectors. Using data from tracking stations at Mojave, California, Westford, Massachusetts, Yellowknife, Yukon Territories, Canada, Richmond, Florida, and Austin, Texas in addition to the locally collected data at LP1, Allison and Eagle, we have computed orbit-improved solutions for the vectors LP1 to Allison and LP1 to Eagle. The processing was done using Bernese software. In addition to the coordinates of Allison and Eagle, we estimated the positions of the satellites over a three day arc, and a tropospheric zenith delay for each station day. The difference between the two observations, 17 September 1987 and 22 October 1987, is shown in these two tables:

Difference in mm between observations on 17 September 1987 and 22 October 1987

| Line | Line Length km | Change Length mm | Change Transverse mm |
|---|---|---|---|
| LP1-Allison | 43.2 | -4.7 | -50.8 |
| LP1-Eagle Un | 31.4 | -1.8 | -26.6 |

Difference in ppm between observations on 17 September 1987 and 22 October 1987

| Line | Line Length km | Change Length ppm | Change Transverse ppm |
|---|---|---|---|
| LP1-Allison | 43.2 | -0.11 | -1.19 |
| LP1-Eagle Un | 31.4 | -0.06 | -0.85 |

For both lines, LP1-Allison and LP1-Eagle, the apparent change in the length was very small, less than 5 mm or about 0.1 ppm. The same is not true of the component of the interstation vector transverse to the length. For both of these lines this transverse component indicated at rotation of the line by about 1 µrad counterclockwise. This apparent rotation may be the result of weak tracking station geometry. For both of these observations, there was only a bare minimum of data from the tracking stations to control the orbits. An experiment in southern California indicates no such orientation problems (see discussion in next section of this report).

## 3. The Mojave-Vandenberg-Palos Verdes GPS experiment

The triangle formed by the sites at Mojave, Vandenberg, and Palos Verdes has been occupied by GPS receivers two or three times per year since June 1986. The distances between these sites are all greater than 200 km (Figure 1), and very accurate orbits are needed to achieve cm-level precision in the estimates of relative position from GPS data. In a manner identical to the analysis for the Loma Prieta network (see above), we have used tracking data from widely separated GPS receivers for the purposes of orbit determination. In addition to the locations mentioned above, we have used GPS data obtained from Haystack (Massachusetts), Churchill (Canada), and Ft. Ord (California). Since Mojave has been a University of Texas tracking station since the autumn of 1986, USGS receivers have not been used to occupy that site since that time.

We have thus far analyzed the data from three epochs. Since the Mojave data for one of these experiments have not yet been obtained, only one baseline of the triangle has three estimates: Vandenberg to Palos Verdes. The estimated components of the vector separating these two sites, in a local geodetic system of coordinates centered at Palos Verdes, is shown in Figure 5. Mean values of 203,021,899.5 mm (east), -92,301,513.9 mm (north) and 3,980,070.3 mm (vertical) have been subtracted from the estimated values.

The repeatability of these components is very good. The worst repeatability (27 mm) is in the vertical component, probably due to atmospheric errors. Since the trajectory of the satellites as seen from the Western United States is nearly north-south , the estimate of the east component of site position is expected to be less precise than that of the north component. This prediction appears to be confirmed in our analysis (10 mm for east vs. 3 mm for north), although another interpretation is possible if we examine the statistics after fitting a line through the results. The estimated rate of the north component is -4 mm/yr (i.e., 4 mm/yr south for Palos Verdes or 4 mm / yr north for Vandenberg), while that of the east component is 23 mm/yr. The RMS residual about the respective best-fit lines is about the same (2-3 mm) for both horizontal components. An eastward motion of about 11 mm/yr for Palos Verdes relative to Vandenberg is consistent with geologic evidence for contraction across the Los Angeles basin. However, our analysis can neither confirm nor reject this hypothesis of relative motion, due to the small number of epochs. Note also that a fairly good straight-line fit can be found for the vertical component of the baseline. However, the estimated rate of uplift of Palos Verdes (or subsidence of Vandenberg) found (41 mm/yr) is too large to be real, and is probably a result of the large error associated with the vertical component. The analysis of future campaigns will add evidence here, also.

### 4. Deformation West of the San Andreas fault near San Francisco, California

Ten years of Geodolite distance measurements of a network including the Farallon Islands (Figure 6) indicate a low rate of deformation west of the San Andreas fault near San Francisco, California. Significant rates of line-length change were observed only in the low-angle, fault-crossing lines Mt. Tamalpais to Pt. Reyes Head and Mt. Tamalpais to Sweeney. No contraction across the San Andreas fault is indicated by the line from Mt. Tamalpais to Farallon. The low average rate of change in the line from Sweeney to Farallon suggests little or no deformation across the San Gregorio fault or any other structure west of the San Andreas fault. Indeed, very little strain accumulation is observed west of the San Andreas fault.

### 5. Horizontal Deformation associated with the Superstition Hills, California, Earthquakes of November 1987

The Superstition Hills earthquakes of November 24, 1987, occurred within a Geodolite network that had been last surveyed in January 1987. The network was resurveyed in early December, 1987. Coseismic (January to December, 1987) line length changes in the epicentral area were as great as 0.5 m. Station displacements (Figure 7) inferred from the observed line length changes suggest both right-lateral slip across the northwest trending Superstition Hills fault and left-lateral slip across one or more northeast trending faults. Only two stations are within 5 km of the surface ruptures: one 5 km southwest of the Superstition Hills fault was displaced $0.37 \pm 0.01$ m in a northwest direction and the other located only 100 m from one of the northeast trending surface ruptures was displaced $0.33 \pm 0.01$ m southwest. A preliminary dislocation model in which the faults' orientations are constrained by the surface ruptures and slip is assumed to be constant from the surface to 10 km depth suggests 1.2 m of right-lateral slip across the Superstition Hills fault and 0.4 m of left-lateral slip across a northeast trending fault. The sparse geodetic data and complex pattern of surface ruptures make the slip estimates very uncertain. The implied seismic moment is $9.3 \times 10^{18}$ Nm, equivalent to a magnitude ($M_L$ or $M_S$) 6.7 earthquake.

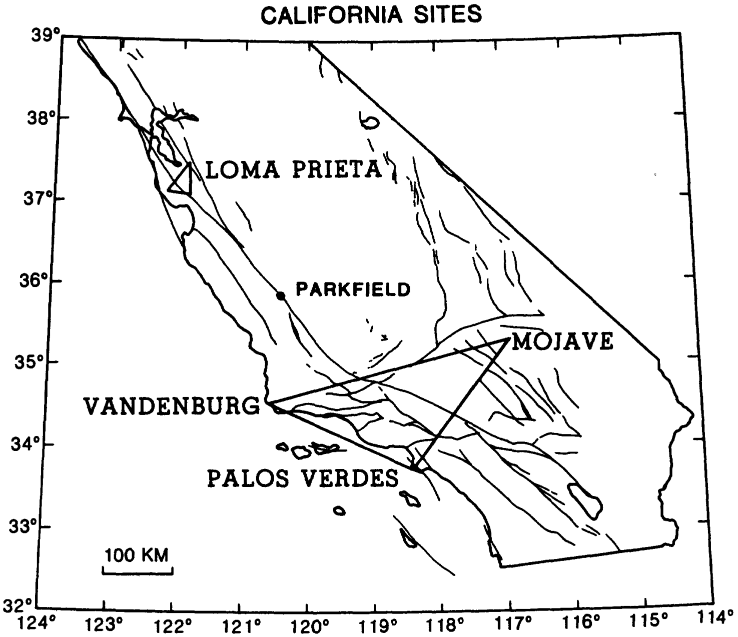

Figure 1. Sketch showing location of three Global Positioning System experiments.

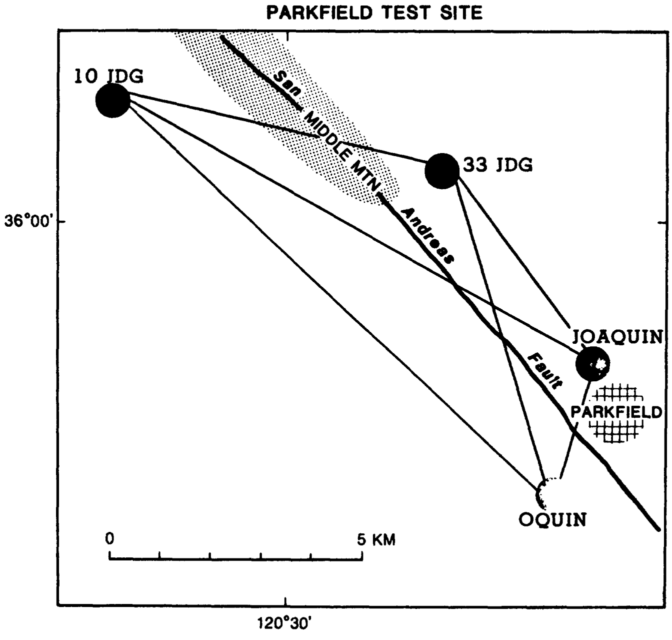

Figure 2. Sketch showing location of stations used in the Global Positioning System experiment at Parkfield.

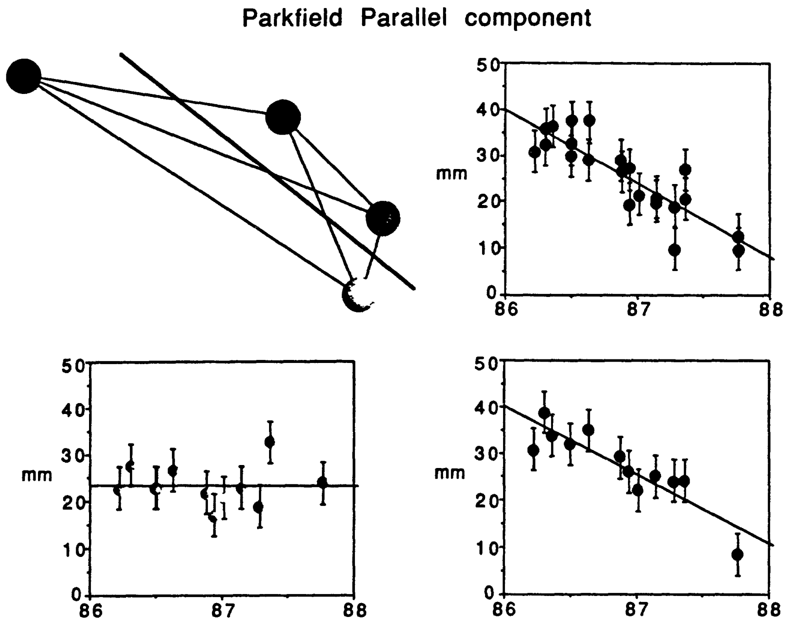

Figure 3. Component of motion parallel to the San Andreas fault as a function of time for the stations in the Parkfield GPS network. Upper left station is fixed; upper right plot is for upper right station, lower right plot for lower right station, and lower left plot for lower left station.

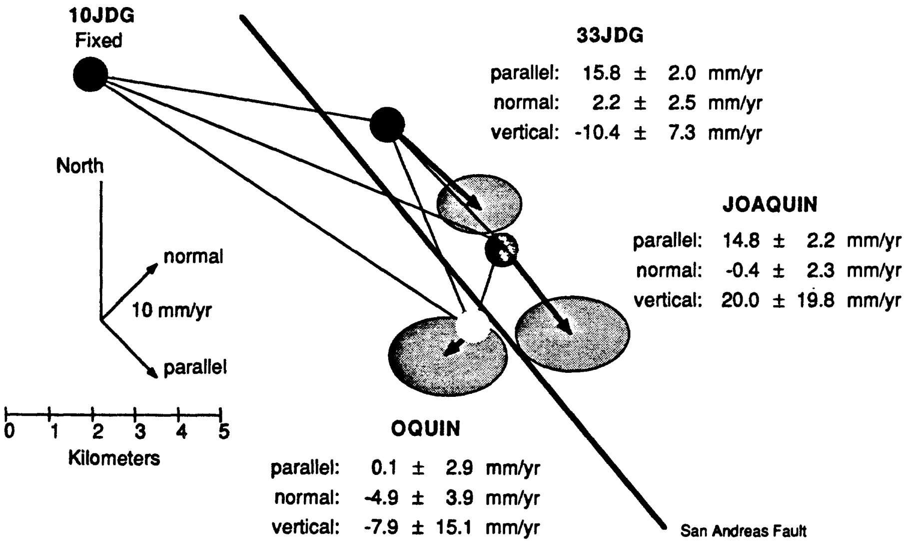

**33JDG**

parallel: 15.8 ± 2.0 mm/yr
normal: 2.2 ± 2.5 mm/yr
vertical: -10.4 ± 7.3 mm/yr

**JOAQUIN**

parallel: 14.8 ± 2.2 mm/yr
normal: -0.4 ± 2.3 mm/yr
vertical: 20.0 ± 19.8 mm/yr

**OQUIN**

parallel: 0.1 ± 2.9 mm/yr
normal: -4.9 ± 3.9 mm/yr
vertical: -7.9 ± 15.1 mm/yr

Figure 4. Vectors indicate the velocity of the stations as determined from GPS observations. Error ellipses indicate 95% confidence level.

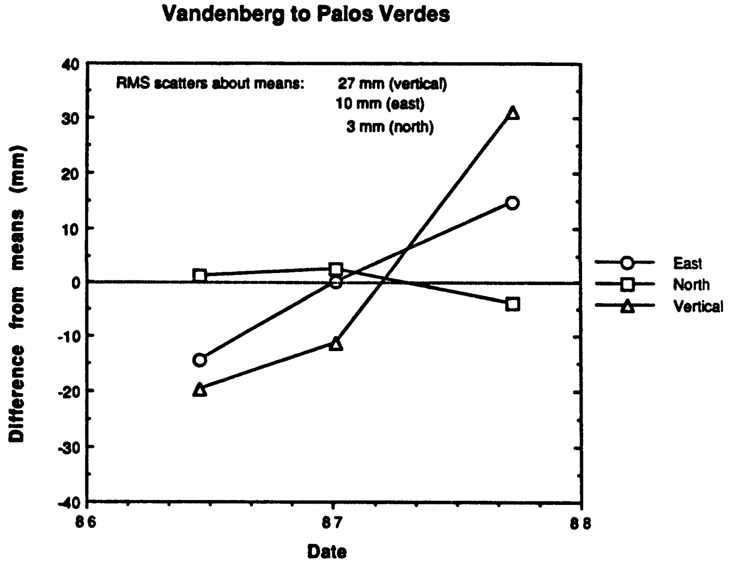

Vandenberg to Palos Verdes

Figure 5. Variation of the components of the vector Vandenberg to Palos Verdes as a function of time.

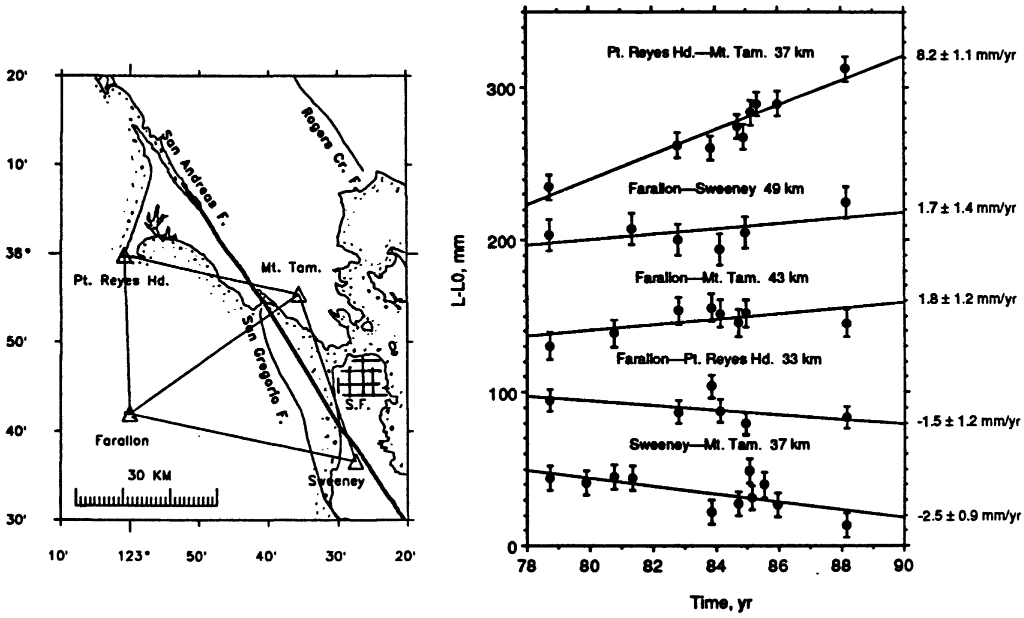

Figure 6. Map of the Farallon Geodolite network (left) and plots of line length as a function of time (right). Error bars are one standard deviation on either side of the plotted points.

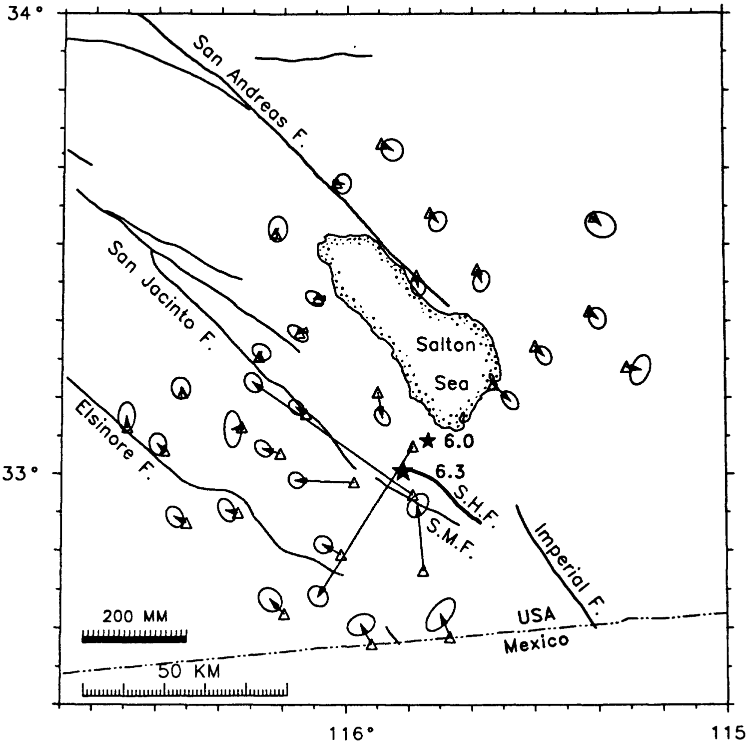

Figure 7. Map of the Salton network showing the January to December,1987 relative station displacements inferred from observed line length changes. The epicenters of the $M_S$=6.0 foreshock and the $M_S$=6.3 mainshock of the November 24, 1987, Superstition Hills earthquake sequence are marked with stars. The displacement solution shown minimizes the component of the vectors perpendicular to the trend of the San Andreas fault excluding stations near the earthquakes. The Superstition Hills fault is labeled S.H.F. and the Superstition Mountain fault is labeled S.M.F. Right-lateral surface rupture was observed across the Superstition Hills fault and left-lateral surface rupture was observed across a number of northeast trending faults located between the Superstition Hills fault and the Salton Sea.

# Seismic Studies of Fault Mechanics

9930-02103

Paul A. Reasenberg
Mark V. Matthews

Branch of Seismology
United States Geological Survey
345 Middlefield Road - MS 977
Menlo Park, California 94025
415-329-5002

## Investigations

1. Analysis of fault-plane solutions for aftershocks of the 1984 (M6.2) Morgan Hill, Ca., earthquake: implications for the faulting geometry and stress field.
2. Investigation of the temporal and spatial variations in seismicity rate in the Kaoiki Seismic Zone, Hawaii, prior to the M 6.6 earthquake of November 16, 1983.
3. Seismicity fluctuations before the 1987 Whitier-Narrows (M5.9) earthquake.
4. Probabilities for damaging aftershocks in California.

## Results

1. Collaboration with David Oppenheimer and Robert Simpson. A summary of our principal results was included in the previous Semi-annual Technical Report volume. We submitted a manuscript describing our findings to J.G.R.
2. Collaboration with Max Wyss. An important factor in the analysis of seismicty rate fluctuations is the influence on the apparent rate imposed by man-made changes in the collection and processing of data for the catalog. An analysis of apparent rate changes in the HVO catalog suspected of having artificial origin was made (by M.W.) We have developed a statistical technique for measuring the spatial distribution of seismicity fluctuations analogous to the beta statistic, which has been used to measure the temporal fluctuations (Reasenberg and Matthews, 1988; Matthews and Reasenberg, 1988). With this tool we investigate the three-dimensional spatial distribution of the extreme seismicity rate fluctuations identified in the time domain.
3. (See Figures) Seismicity rates prior to the Whittier Narrows earthquake were calculated for earthquakes ($M \geq 2.5$) in the entire Los Angeles Basin, the Newport-Inglewood fault zone, and the northern section of the Elsinore fault zone. Aftershocks were removed from the data set by a computer algorithm. The statistical significance of the resulting rate fluctuations in these zones was assessed relative to a null model of stationary Poisson occurrence. The results indicate that there were no significant (n=325; $p > 0.1$) rate fluctuations in the Los Angeles Basin during the 13.5-year interval before the mainshock. In the North Elsinore fault zone, the seismicity rate decreased abruptly from approximately 6.0 eq/yr before 1983 to 2.6 eq/yr from

1983 to the time of the mainshock. This decrease, however, is not significant at the p=0.1 level, owing to the low total number (57) of earthquakes occurring there. Within the Newport-Inglewood fault zone, rate fluctuations were also not significant (n=71; $p > 0.1$) during the 13.5-year interval. These results are consistent with those obtained for other moderate size earthquakes in California. Seismicity rates remained essentially constant during comparable intervals prior to the 1986 North Palm Springs (M 5.9) earthquake, the 1984 Morgan Hill (M 6.2) earthquake, and the 1979 Coyote Lake (M 5.9) earthquake.

4. Collaboration with Lucy Jones. Strong aftershocks pose a significant hazard, particularly to structures already weakened by the mainshock shaking. Assessments of the probability for damaging aftershocks can be useful for guiding decisions involving the management of emergency and other public services, operation of utilities and industrial processes, and the possible use of partially damaged structures. To estimate the probabilities for occurence of damaging aftershocks in given magnitude ranges and time intervals after a given mainshock, we integrate Utsu's four-parameter model for the rate of aftershocks as a function of time and magnitude. We derive an a priori estimate for the model parameters from the distribution of calculated (maximum likelihood) parameter values for major aftershocks sequences in California since 1930. An a posteriori estimate for the model parameters is also obtained by maximum likelihood from the ongoing sequence. A combination of the a priori and a posteriori estimates is used to evaluate the probabilities.

Reports

Oppenheimer, D.H., P.A. Reasenberg, and R.W. Simpson, Fault-plane solutions for the 1984 Morgan Hill, California earthquake sequence: Evidence for the state of stress on the Calaveras Fault, *submitted to* J. Geophys. Res., 64 pp.

Zoback, M.D., M.L. Zoback, V.S. Mount, J. Eaton, J. Healy, D. Oppenheimer, P. Reasenberg, L. Jones, C.B. Raleigh, O. Scotti, and C. Wentworth, New evidence on the state of stress on the San Andreas Fault System, Science, V. 238, 1105-1111, 1987.

Matthews, M.V., and P.A. Reasenberg, Statistical methods for investigating quiescence and other temporal seismicity patterns, Pure and Applied Geophysics, Vol. 126, 1988.

Reasenberg, P.A., and M.V. Matthews, Precursory seismic quiescence: A preliminary assessment of the hypothesis, Pure and Applied Geophysics, Vol. 126, 1988.

Hauksson, E., L. Jones, T. Davis, L. Hutton, G. Brady, P. Reasenberg, A. Michael, R. Yerkes, P. Williams, G. Reagor, C Stover, A. Bent, A. Shakal, C. Bufe, M. Johnston and E. Cranswick, The 1987 Whittier Narrows earthquake in the Los Angeles Metropolitan area, California, Science, Vol. 239, 1988.

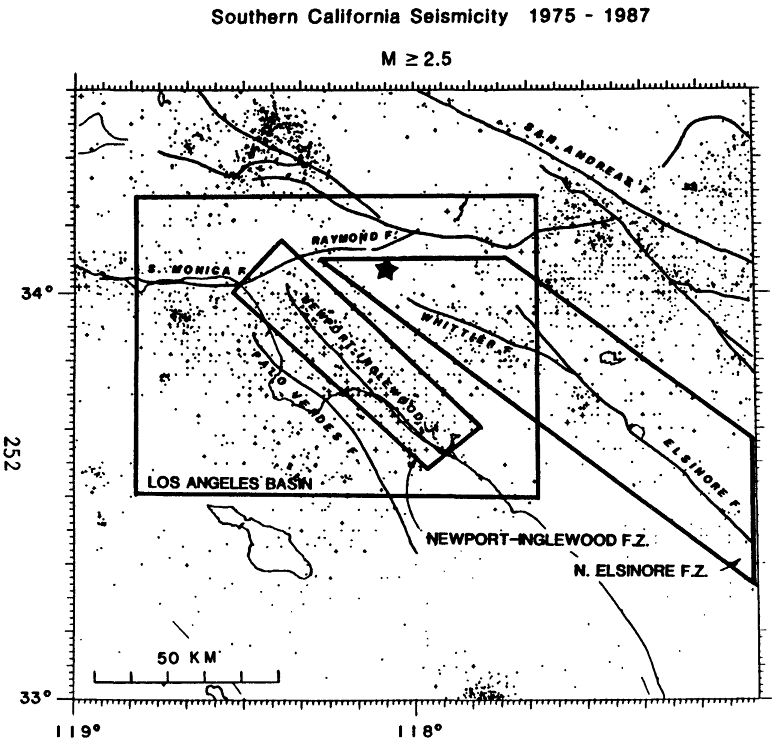

Figure 1. Map of seismicity in southern California, 1975 - 1987.

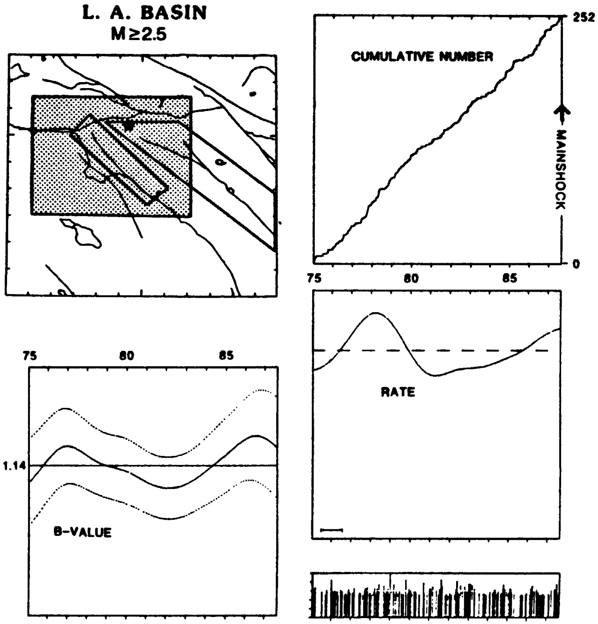

Figure 2. Seismicity fluctuations in the Los Angeles Basin (corresponding to the large rectangular box in Figure 1), prior to the Whittier-Narrows earthquake. Mainshock occured at time corresponding to the right margin in these plots. Fluctuations in b-value (solid curve) and the 90-percent confidence interval for b (dashed curve) and average value of b (solid horizontal line) of 1.14 are shown. Relative fluctuations in seismicity rate (solid curve) are compared to the average rate for the interval (broken horizontal line). None of these fluctuations represents a statistically significant departure from random occurence.

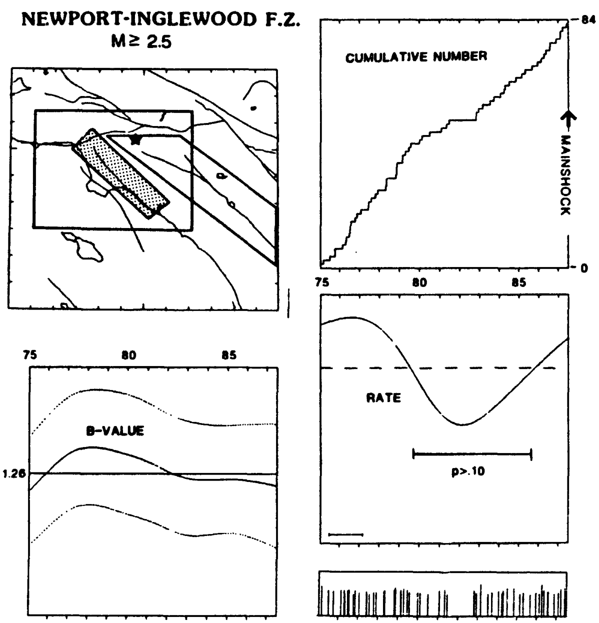

Figure 3. Fluctuations in seismicity in the Newport-Inglewood fault zone (see Figure 1). The low-rate interval in the early 80's is not statistically significant.

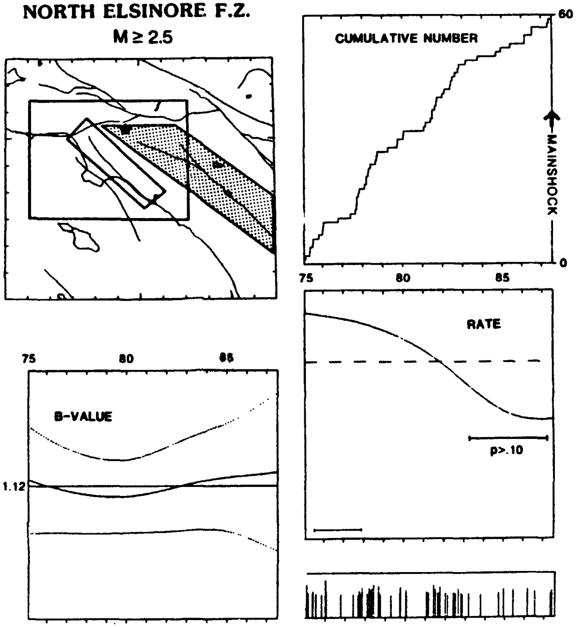

Figure 4. Fluctuations in seismicity in the northern Elsinore fault zone (see Figure 1). The low-rate interval starting in 1983 and continuing up to the time of the mainshock is not a statistically significant departure from random occurence.

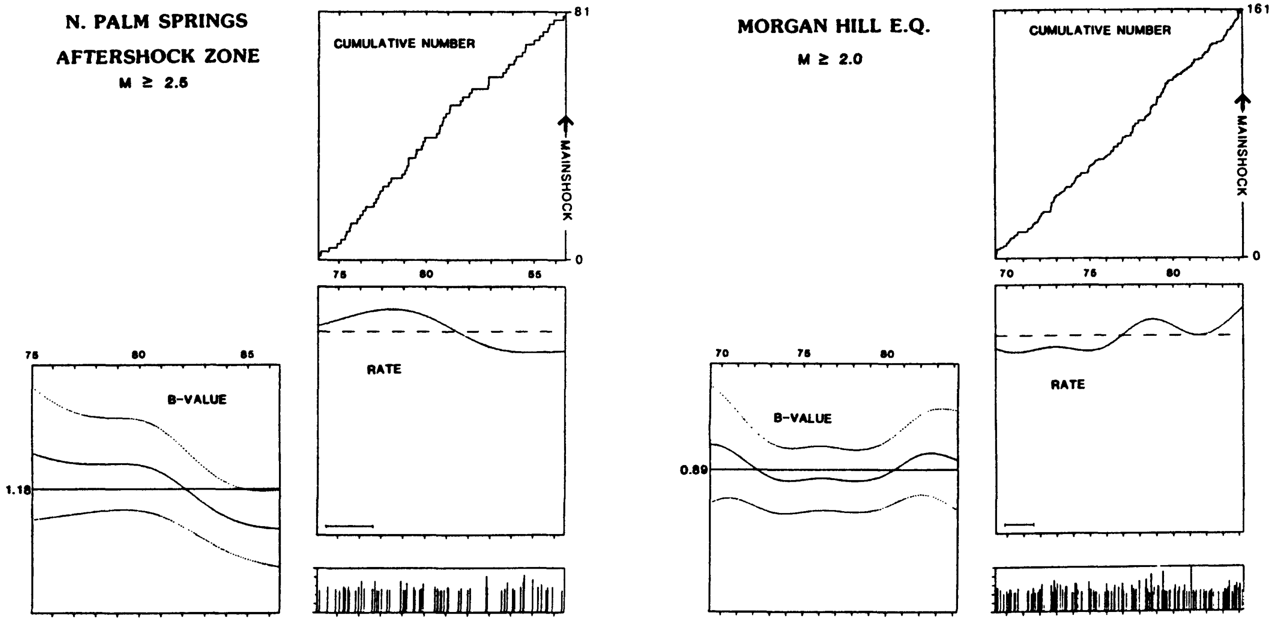

Figure 5. Fluctuations in seismicity in the aftershock zones of the 1986 North Palm Springs earthquake and the 1984 Morgan Hill earthquake. The times of the mainshocks are at the right margins of each plot. Seismicity rates were essentially uniform (constant) during the intervals shown prior to these mainshocks.

# Hydrogen Monitoring (9980-02772)

Motoaki Sato*, Susan Russell-Robinson*, and J. Michael Thompson**
Branch of Igneous and Geothermal Processes
U.S. Geological Survey, *MS/959, Reston, VA 22092;
**MS/910, Menlo Park, CA 94025

(703) 648-6766, FTS 959-6766

## Investigations

Hydrogen ($H_2$) in soil along the San Andreas and Calaveras faults is continuously monitored at a dozen sites by using special fuel-cell sensors and data are telemetered to Menlo Park, CA. Goals are (1) to accumulate valid data, (2) to find patterns of correlation of the hydrogen data with seismic and other geophysical data, (3) to understand the tectonic mechanism of $H_2$ emission along active faults, and (4) to constantly improve the monitoring method.

## Results

### General

Besides maintaining the existing soil hydrogen monitoring sites in good working order, we established a well-water chemistry monitoring station adjacent to the Taylor Ranch creepmeter site and also duplicated soil hydrogen monitors at three sites (one incomplete) in the Parkfield area.

### Parkfield Area

There were two soil hydrogen events in the Parkfield area between October 1, 1987, and March 30, 1988 (Fig. 1). A large peak (2200 ppm) occurred at Gold Hill (H2GH) in mid-October in coincidence with a complex creep event. The $H_2$ level decreased below the baseline immediately after the event and finally recovered to the normal range by mid-November. There were minor changes in early december also at this site.

A minor peak (150 ppm) occurred at Middle Mountain (H2MM) on January 6, 1988. This was the first distinct peak recorded at this site since the 600-ppm peak of February 13, 1987, which preceded by one day an M 5.0 earthquake that occurred 7 km NE of Coalinga. There was an M 4.3 earthquake and several aftershocks about 30 km south of Los Banos on January 7, 1988. The correlation of this earthquake and the small peak at Middle Mountain is not certain on account of the small magnitudes of both events and the considerable distance.

Hydrogen changes became very subdued since mid-January throughout the Parkfield area. The peak at H2M2 in late February was probably an artifact because we replaced an experimental solid-oxidizer sensor with a conventional oxygen-operated sensor on February 24. It normally takes a few days for a new sensor to settle.

## Hollister Area

There were no notable soil hydrogen events throughout this area during the reporting period. No precursory changes were recorded prior to or immediately after the M 5.0 earthquake of February 20, 1988, that occurred near Tres Pinos. This total absence of $H_2$ response was a stark contrast to the large changes recorded along the Calaveras fault prior to the M 5.7 Tres Pinos earthquake of January 27, 1986. The latest quake may possibly be considered as a delayed aftershock of the 1986 earthquake.

## Duplicate Sensors

Duplicate $H_2$ sensors were deployed 50 feet apart at Middle Mountain and Taylor Ranch (new installation). The purpose is to examine how local the soil $H_2$ anomalies are. If two sensors at such a separation distance respond concurrently, the data would become more credible. The sensors are, however, not completely independent: they share the oxygen supply line in series to save on cost and manpower. Installation of the oxygen supply line and cable was completed at the Parkfield (H2PK) site, but the second sensor has not been installed because of difficulty in boring a hole through a gravel layer to 2 m depth.

## Taylor Ranch Geochemical Monitoring Station

The Taylor Ranch well-water chemistry monitoring station has started transmitting data, although a few items may need further improvement. The project is conducted in conjunction with Chi-Yu King's radon monitoring. At present, we monitor conductivity and dissolved $H_2$ and $CO_2$. The monitoring system is completely duplicated, but currently one system is idle because the well does not appear to produce enough water to run two systems simultaneously.

## Publication

Sato, M., Russell-Robinson, S., and Thompson, J.M., 1987, Hydrogen monitoring
in the Parkfield area, central California; EOS, v. 68, p. 1357.

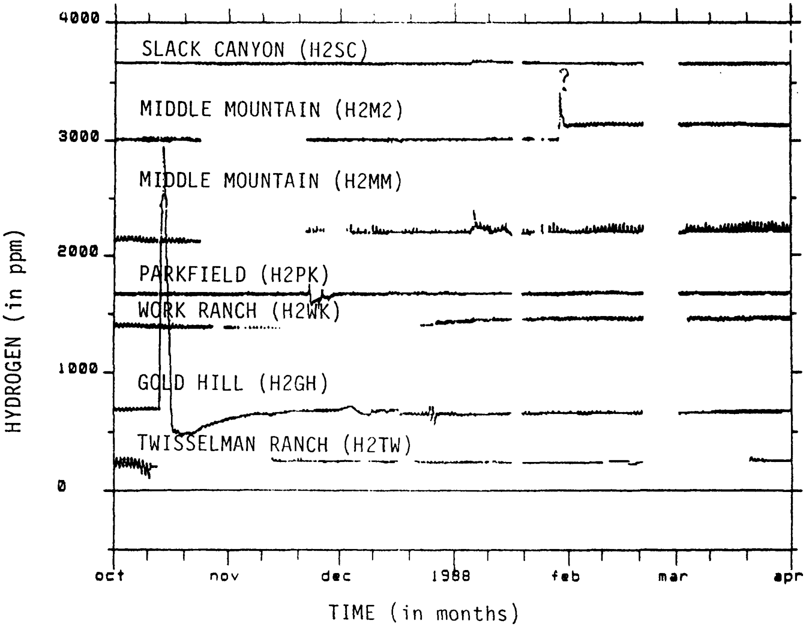

Fig. 1. A composite plot of soil hydrogen data recorded in the Parkfield area from October 1, 1987, to March 31, 1988. The hydrogen scale is relative and approximate. The peak at H2M2 on February 24-26 was probably an artifact because an experimental solid-oxidizer type sensor, which was dysfunctional, was just replaced by a conventional sensor.

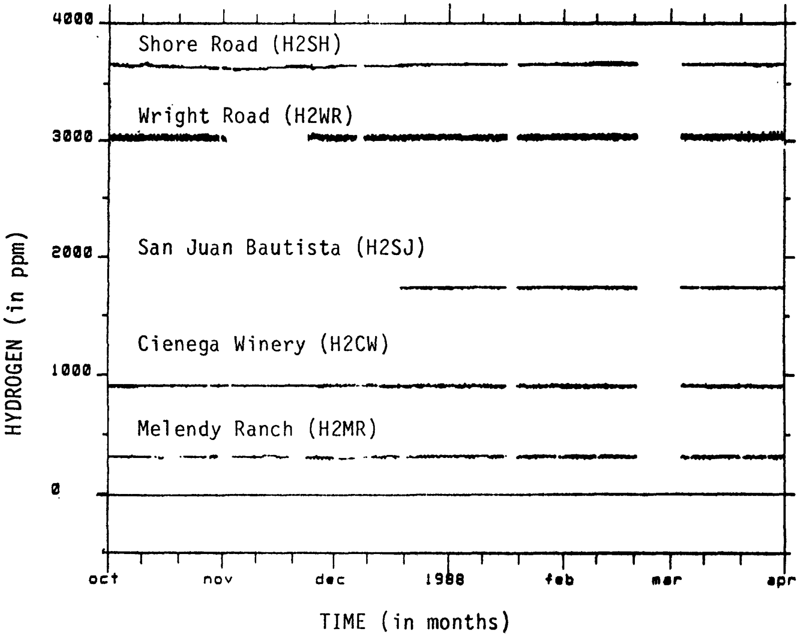

Fig. 2. A composite plot of soil hydrogen data recorded in the Hollister area from October 1, 1987, to March 31, 1988. The hydrogen scale is relative and approximate. Telemetry malfunctioned at the San Juan Bautista site (H2SJ) prior to December 20, 1987.

# Analysis of Seismic Data from the Shumagin Seismic Gap, Alaska

14-08-0001-G-1388

John Taber and Paul Huang
Lamont-Doherty Geological Observatory of Columbia University
Palisades, New York 10964
(914) 359-2900

## Investigations

Digitally recorded seismic data from the Shumagin seismic gap in the eastern Aleutian arc, Alaska, are analyzed for detecting space-time variations in the seismicity, focal mechanisms, and dynamic faulting parameters that could be precursory to a major earthquake expected in this seismic gap. The seismic results obtained from the network data are being integrated with crustal deformation data that are independently collected, with volcanicity data of nearby Aleutian volcanoes, and with teleseismic information to identify basic tectonic processes which may be precursory to a great earthquake.

## Results

As a part of our search for earthquake precursors, we have examined temporal variations in the coda duration-magnitude relation before and after an earthquake sequence that began in October, 1985 using the technique of Sato (1986, 1987). Coda durations were measured for three stations located in the vicinity of the aftershock area (Figure 1). Station CNB is located within the aftershock area at a distance of about 30 km from the main shock epicenter while stations NGI and BKJ are located less than 40 km from the edge of the aftershock area. We analyzed earthquakes in the period between 1982 and June 1987 with $M_L$ between 1.6 and 3.7. No temporal changes were resolvable when all earthquakes with epicenters in the region between 54.5 and 55 N and 159 and 160 W were used. Next, we restricted the data to earthquakes with hypocenters within a region slightly larger than the aftershock area and between 20 and 45 km in depth (Figure 1). For the two more distant stations NGI and BKJ, the data scatter was still too large. However the results from CNB are quite encouraging. To investigate the temporal change in coda duration, we calculated the deviation of the coda duration from a linear regression of coda duration vs amplitude magnitude. This was plotted against the time measured from the main shock (Figure 2). To illustrate the temporal change in coda duration more clearly, we divided Figure 2a into 3 time periods: before the October, 9 mainshock; mainshock through aftershocks of a second event on November 14; and background activity after the entire earthquake sequence. Within each subdivision the selection of time intervals was decided by visual inspection. Figure 2b covers the time period before the October 9, 1985 main event ($M_s$=6.4). From -1200 to -412 days before the mainshock, the average residual is nearly 0 and there is very little scatter in the data. From -412 to -177 days, residuals are almost all positive and the data is scattered little more than in the earlier time interval. From -177 days until the occurrence of main shock, the average residual drops back to nearly 0. Figure 2c covers the first 100 days after the October 9 earthquake. From 0 to 12 days, the scatter of data is very large and the average is negative. From 12 days to just before the November 14 earthquake ($M_s$=5.7) sequence, the residual again become mostly positive. The next time period covers the aftershock sequence of the November 14 earthquake and most residuals became negative. Figure 2d covers the period from the end of the November 14, 1985 earthquake sequence to an earthquake on May 2, 1987 ($M_b$=5.1). Although there are limited data points in this time period, the available data again show positive and negative residual time intervals before the May 2, 1987 earthquake.

Figures 2b-2d show that a positive residual time interval preceded each of the three earthquake sequences in this area. For the October 1985 and May 1987 earthquake, the period of positive residuals is followed by a period of nearly zero residuals. All observed temporal changes are significant at 95% confidence level.

An increase in Q may correspond to the closing of cracks while a decrease in Q may correspond to the opening of cracks (Aki, 1985). Coda Q may therefore be a reliable indicator of the stress in the sampling volume. However there is an inconsistent pattern of change in coda decay observed before large earthquakes. Most of the reported cases of temporal change in coda decay have low coda Q for a period preceding the occurrence of the main shock (eg. Jin and Aki, 1986; Sato, 1986). On the other hand, high coda Q has also been reported before the occurrence of the main shock (eg. Sato, 1987). Recently, Peng et al. (1987) found both high and low Q preceding the Round Valley, California, Earthquake of November 23, 1984. They noted that the low Q values were observed outside the aftershock zone while the high Q values were observed within the aftershock zone. To explain their observation, Peng et al. (1987) invoked the Mogi's doughnut pattern of precursory seismicity (Mogi, 1985). According to Mogi's model, an earthquake induces cracks and the coda Q goes down. Therefore an active area has low Q and the quiescence area has high Q. In the doughnut pattern, the central quiet area has high Q and the surrounding active area has low Q. After the occurrence of the main shock, the aftershock zone in the center of the doughnut will have low Q and surrounding area may become quiet and will have high Q. This model of Peng et al. (1987) seems to explain the apparent inconsistent patterns of temporal coda Q observed. Most cases of low Q prior to the main shock were observed in areas outside the aftershock region where the activity was high at the time while most cases of high Q prior to the main shock were observed in the aftershock area where the activity was low at the time. This model also might explain our observation of temporal change in coda duration before the October 9, 1985 main shock. From 1200 to 400 days prior to the earthquake occurrence the outer aftershock area is very active and we observed a shorter coda duration, as expected. Then from 420 to 190 days before the earthquake, the aftershock area is quiet with only a few small events. For this time period, we observed longer coda durations. From 190 days to 0 days before the main shock, increased activity in the aftershock zone may have opened cracks to produce a shorter coda duration. However, during all three time periods, the very center of the aftershock zone stayed quiet to produce a classical doughnut pattern of seismicity.

## References

Aki, K., Theory of earthquake prediction with special reference to monitoring of the quality factor of lithosphere by the coda method, **Earthquake Prediction Res., 30,** 219-230, 1985.

Jin, A., and K. Aki, Temporal change in coda Q before the Tangshan earthquake of 1976 and the Haicheng earthquake of 1975, **J. Geophys. Res., 91,** 665-673, 1986.

Mogi, K., **Earthquake Prediction**, Academic Press, Orlando, Florida, 355 pp.,1985.

Peng, J.Y., K. Aki, B. Chouet, P. Johnson, W.H. Lee, S. Marks, J.T. Newberry, A.S. Ryall, S.W. Stewart, and D.M. Tottingham, Temporal change in coda Q associated with the Round Valley, California earthquake of November 23, 1984, **J. Geophys. Res., 92,** 3507-3526, 1987.

Sato, H., Temporal change in attenuation intensity before and after the eastern Yamanashi earthquake of 1983 in central Japan, **J. Geophys. Res., 91,** 2049-2061, 1986.

Sato, H., A precursorlike change in coda excitation before the western Nagano earthquake ($M_s$=6.8) of 1984 in central Japan, **J. Geophys. Res., 92,** 1356-1360, 1987.

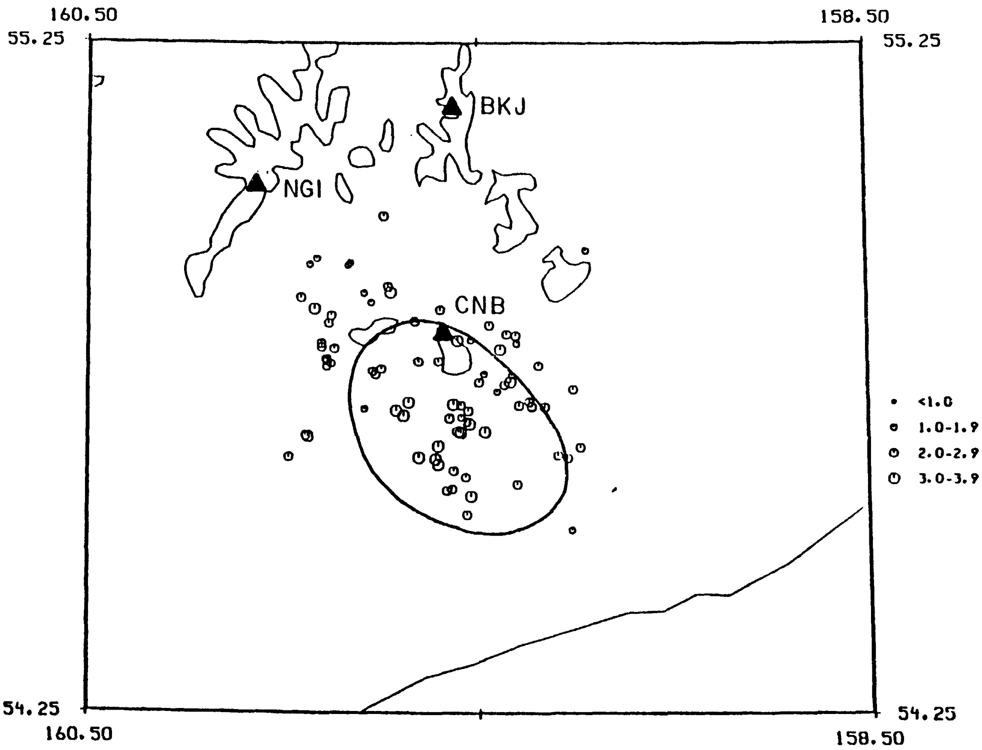

Figure 1. Map showing epicenters of earthquakes used in coda duration analysis. The ellipse marks the outline of the aftershock area of the 1985 $M_s$=6.4 earthquake. Nearby seismic stations are marked by triangles.

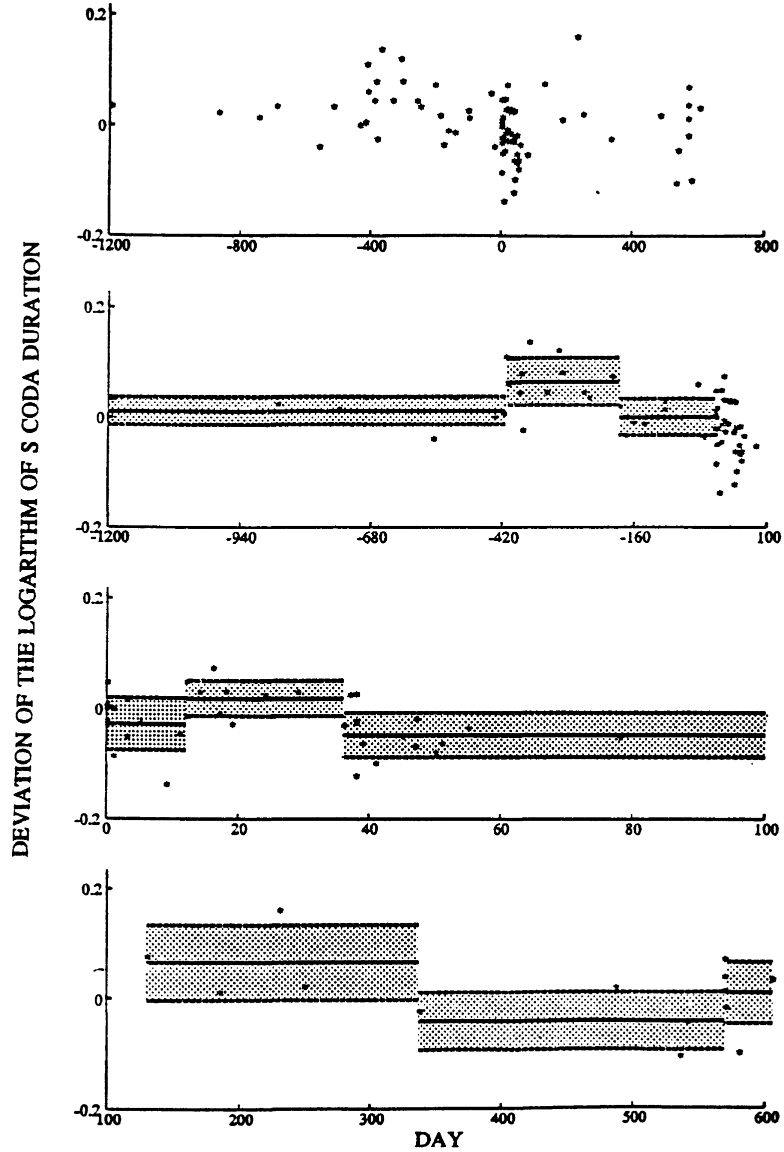

Figure 2. Temporal change in the residual of logarithm of coda duration at station CNB from the linear regression. Figure 2a covers the entire study period. Figure 2b covers the time period before the mainshock on October 9, 1985. Figure 2c extends from 0 to 100 days after the October 9 earthquake. Another moderate earthquake occurred on November 14 during this time period. Figure 2d covers the time period 100 to 600 days after the October mainshock. A third earthquake sequence with a maximum magnitude of $M_b$=5.1 began during this time period on May 2. Shaded area is one standard deviation.

# LATIN AMERICAN EARTHQUAKES AND VOLCANOES

Project #9930-01163

Randall A. White and David H. Harlow
Branch of Seismology
U. S. Geological Survey
345 Middlefield Road, MS 977
Menlo Park, CA 94025
(415) 329-4746

## Investigations:

The eruption of Nevado del Ruiz volcano, Colombia on November 13, 1985 killed about 25,000 people. In cooperation with the Colombian Volcanic Observatory (OVC), we are studying the microseismicity associated with the eruption in order to a) determine how to predict such an eruption in the future and b) model the eruption and subsequent disastrous mudslides.

## Results:

1. High-frequency earthquakes are caused by slippage on fault planes, sometimes induced by magma injection. The hypocenters of well located high-frequency earthquakes are concentrated in a north-south elongated zone of approximately 6 by 10 km that extends southward from about 1 km north of the main crater. Almost all of these events occurred above 7 ±1 km. Within this zone, several distinct source areas generated recurrent swarm activity. A few epicenters are located outside this zone in three principal clusters, up to 15 km from the crater. Depths for these events are less reliable (because they occurred outside the perimeter of the seismic net). One of these these clusters corresponds to an area of hydrothermal activity, another to the nearest major volcano, while the third may correspond to a tectonic fault and/or hydrothermal activity.

Nothing in the distribution of high-frequency earthquake hypocenters indicates the existence of either a small, or a caldera-sized magma body beneath Ruiz. However, the volume of the hypocenters in the elongate zone is small compared with caldera-size struc-tures such as Long Valley, Rabaul, or Campo Phlegri.

The largest swarm of high-frequency earthquakes and largest single earthquake (magnitude 4 1/2) recorded during the 116 days prior to the main eruption, occurred just 5 days before the main eruption.

2. Low-frequency earthquakes are also caused by slippage along fault planes. Many low-frequency earthquakes were recorded and analysis shows that they all originated within the upper 2 km, most from beneath the volcanic edifice as expected, but some from beyond the volcano structure. A likely explanation is that this

seismicity is associated with shallow geothermal systems.

3. Long-period events and volcanic tremor, both periodic and harmonic (continuous), are believed to result from the resonance of fluid-filled conduits induced by pressure transients, with a longer source-time function in the case of tremor. Long-period events were common prior to the eruption of November 13, 1985, and then occurred infrequently until the day preceeding the most recent ash emission on March 22 to 25, 1988. These events suggest that pressurized fluids are present in the system and are responsible for some of the seismic activity. These events are difficult to locate because of their complicated arrivals, but most appear to come from beneath the crater area within the upper 2 km. The reduced displacement for these events is consistent with the shallow ascent of magma beneath the crater.

4. Periodic tremor was recorded during the week preceeding the September 11, 1985 phreatic eruption. Estimates of reduced displacement are consistent with a very small, very shallow source, probably resulting from hydrothermal activity above the ascending magma. Geyser activity apparently began within the crater at about this same time.

5. Harmonic (continuous) tremor occurred principally following the September 11 phreatic eruption and during the three days immediately preceeding the main eruption of November 13. Dominant frequencies were much higher during the September activity.

6. The total energy released by high- and low-frequency earthquakes during the 116 days preceeding the main eruption of was found to be approximately equal to the daily seismic energy released during the two months preceeding the to the May 18, 1980 eruption of Mt. St. Helens. The volume and duration of the Ruiz eruption were also very small compared with that of the Mt. St. Helens eruption. Thus the seismic energy release rate during the couple of months preceeding an eruption appears to scale with the thermal energy release rate during the eruption.

Reports:

White, Randall A., and David H. Harlow, 1987, The San Salvador earthquake of October 10, 1986 - Seismological aspects, and other recent local activity: Earthquake Spectra, V. 3, 419-433.

# Piñon Flat Observatory: A Facility for Studies of Crustal Deformation

14-08-0001-G1178

Frank Wyatt, Duncan Carr Agnew, and
Mark A. Zumberge
Institute of Geophysics & Planetary Physics
Scripps Institution of Oceanography
University of California, San Diego
La Jolla, CA 92093
(619) 534-2411

This grant supports the operation of Piñon Flat Observatory (PFO) by providing 50% the funding needed for running the facility. Matching funds are provided by the National Science Foundation. The work done at PFO includes establishing the accuracy of instruments designed for measuring various geophysical quantities by comparing results from them with data from "reference standard" instruments. This comparison also allows accurate monitoring of strain and tilt changes in the area near the observatory, between the active San Jacinto fault and dormant southern San Andreas fault systems. For only one other site in the U.S. (Parkfield, California), are such reliable records available. All of this effort is intended to foster development of precision geophysical instrumentation. The site it is presently well utilized by a sizeable collection of researchers.

In this report we present data from the laser strainmeters (the operation of which is supported by this grant) for the Superstition Hills earthquakes sequence of November 1987. This sequence produced the most interesting coseismic data in the last several years. The first large event of this sequence was the Elmore Ranch earthquake ($M_s$ 6.2), followed some 12 hours later by the main Superstition Hills event ($M_s$ 6.6), and of course many aftershocks. Seismicity patterns and surface rupture showed two conjugate faults, the Elmore Ranch earthquake being on a fault conjugate to the San Jacinto fault zone with the mainshock on a fault (the Superstition Hills fault) parallel to the main northwest-southeast trending fault zone.

Figure 1 shows the raw data from two of the laser strainmeters at PFO (the third was dismantled at the time for upgrading with optical fiber anchoring). The raw data show the very large dynamic strains, which saturated all instruments at PFO except the strong-motion recorders. To produce the processed data these dynamic strains have been filtered out, and tides and thermal effects subtracted. The results (shown in the upper half of Figure 2, for the NW-SE strainmeter) are dominated by the coseismic offsets, which occur between the arrival of the S-wave and the decay of the coda. The offsets on these and other instruments at PFO are in reasonable agreement with results for a dislocation in a half-space, with seismically-derived parameters used to define the dislocation.

The frequent sampling of these data allows us to look at preseismic and postseismic deformations in some detail, with the best data coming from the fully-anchored NW-SE laser strainmeter. (We dismiss the long-period variations seen in the EW strainmeter records here as being uncorrected monument motion; the records in the lower panel of Figure 2 have had the coseismic steps removed.) Figure 3 shows the NW-SE strain for the time between the two large earthquakes, plotted against the log of the time before the second event's P-arrival—to show the immediately precursive period in more detail. The largest signal during this time is the microseisms, plus some small residual drift in the instrument. We can certainly rule out any anomalous strains during this time above the level of about 3% of the eventual coseismic offset, and for the final 1000 seconds above about the 0.5% level—comparable to the bounds reported by others on precursive strains before other earthquakes in California.

At this stage we have not yet attempted any detailed comparisons with faulting instability models. We are aware that the observed absence of short-term precursive slip is compatible with at least one type of model, since accelerated short-term precursive slip may be concentrated in a small depth range. On the other hand it is hard to believe that the Superstition Hills earthquake was not triggered by the Elmore Ranch earthquake; and given the delay between events some sort of gradually accelerating failure seems like the most tempting model. While they do not rule this out, the PFO data require that it must be small.

The data from the NW-SE strainmeter in Figure 2 also provide bounds on any postseismic slip at depth. In the first 5000 seconds after the event there appears to be about 1.5 n$\epsilon$ strain change—about 10% of the coseismic offset; little strain change is evident after this. Reports that the slip at the surface increased substantially over the next few days can be reconciled with the PFO results by supposing that the slip reflects propagation of deeper slip through unconsolidated material to the surface. Some models of faulting predict postseismic creep on the fault, and this is probably the cause of the afterslip seen in the strain record.

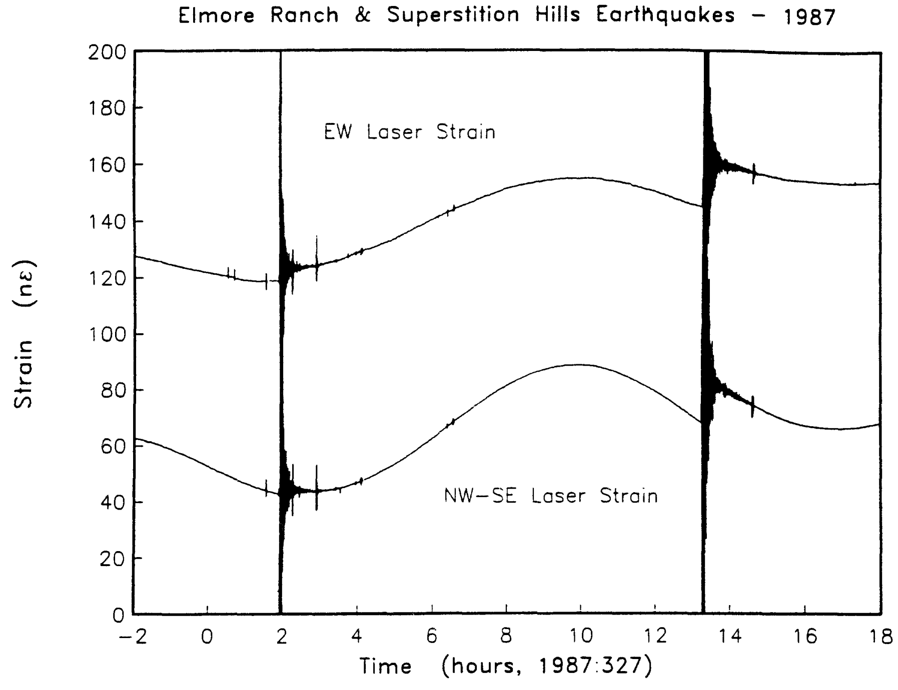

Figure 1.

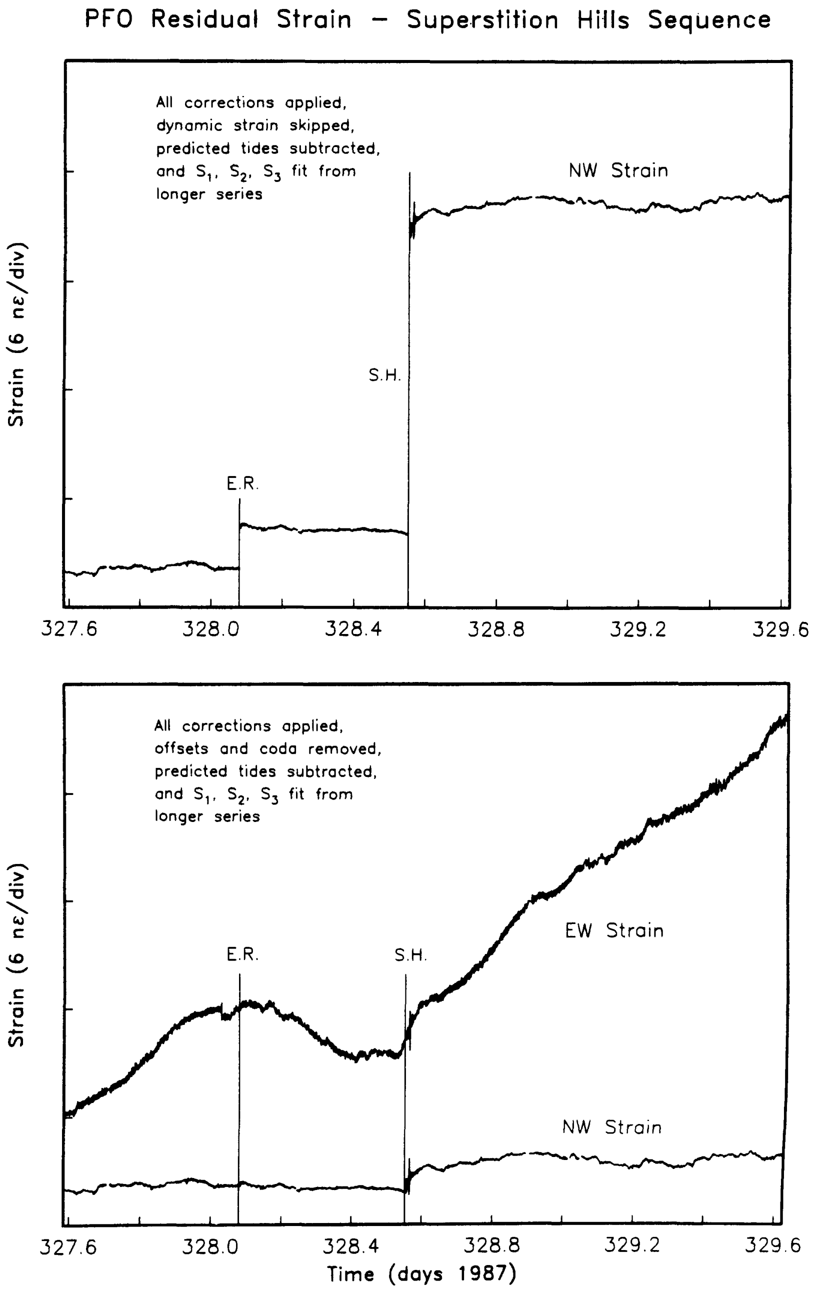
PFO Residual Strain – Superstition Hills Sequence
All corrections applied,
dynamic strain skipped,
predicted tides subtracted,
and $S_1$, $S_2$, $S_3$ fit from
longer series
NW Strain
S.H.
E.R.
Strain (6 nε/div)
327.6
328.0
328.4
328.8
329.2
329.6
All corrections applied,
offsets and coda removed,
predicted tides subtracted,
and $S_1$, $S_2$, $S_3$ fit from
longer series
EW Strain
E.R.
S.H.
NW Strain
Strain (6 nε/div)
327.6
328.0
328.4
328.8
329.2
329.6
Time (days 1987)

Figure 2.

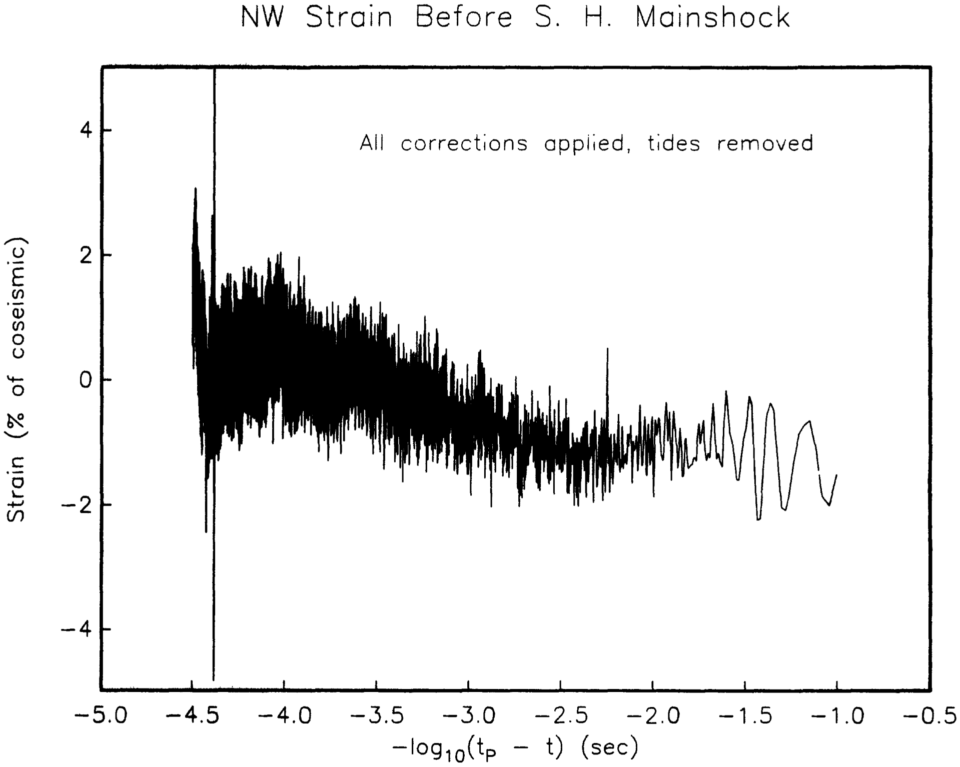
NW Strain Before S. H. Mainshock
All corrections applied, tides removed
Strain (% of coseismic)
4
2
0
-2
-4
-5.0
-4.5
-4.0
-3.5
-3.0
-2.5
-2.0
-1.5
-1.0
-0.5
$-\log_{10}(t_P - t)$ (sec)

Figure 3.

# Piñon Flat Observatory: Cooperative Studies with Outside Investigators

14-08-0001-G1197

Frank Wyatt and Duncan Carr Agnew
Institute of Geophysics & Planetary Physics
Scripps Institution of Oceanography
University of California, San Diego
La Jolla, CA 92093
(619) 534-2411

This grant provides support for our collaborative work with investigators conducting research at Piñon Flat Observatory (PFO) under the auspices of the U.S. Geological Survey. We also provide some direct assistance in the form of (1) research coordination, (2) instrument operation and testing, (3) data logging, (4) preliminary data reduction, and as results become available, (5) data analysis. Part of this program is a cooperative effort (the Crustal Deformation Observatory Project) to evaluate instruments for measuring long-period vertical ground deformation. Most of the studies currently underway are conducted independently, with investigators establishing their own associations to compare results; in the Crustal Deformation Project there is a more formal agreement to share observations.

We list below the research agencies and projects assisted by this grant; all but the first in the list are sponsored by the NEHRP. (The AFGL program is self-supporting, providing valuable tilt data for comparison with the other borehole sensors at the site.)

1. *Air Force Geophysics Laboratory*: The AFGL tiltmeter (normally run at a 25 m depth in an uncased borehole) was returned to the lab in 1987 for refurbishment and recalibration. This is now complete and we expect to reinstall it at PFO in early 1988. (The importance of this measurement is discussed below, with the results from the JILA instruments.)

2. *Cambridge University*: This 535-m center-pressure long-base tiltmeter, seems to have failed late in 1987, apparently due to an electronics problem. We intend to work on it during the coming year, though in its current form this instrument's high thermal-sensitivity makes its usefulness at PFO limited.

3. *Joint Institute for Laboratory Astrophysics*: The two JILA borehole tiltmeters (BOA, in a cased hole 23.5 m deep, and BOB, in a nearby cased hole 35.6 m deep) operated well from the start of 1986 until November 1987 when a lightning strike immediately adjacent to the boreholes destroyed the electronics. The quality of the secular signals produced by these affordable sensors is generally equal to that from the extremely well engineered (and hence expensive) Askania tiltmeter. Analysis, presented at the fall 1987 AGU meeting, has shown that the tides from the two JILA instruments and the colocated Askania tiltmeter differ by 10% in amplitude, and as much as 5% in phase—a most disturbing result for side-by-side sensors. Cross correlation of seismic signals indicate that all three sensors are properly calibrated and responding correctly to higher frequency accelerations. We plan to reinstall all three of these sensors in 1988 (the Askania tiltmeter was also damage by the lightning), together with the AFGL sensor, to resolve further this important issue for earth-tidal studies.

4. *Lamont-Doherty Geological Observatory*: This 535-m Michelson-Gale water-tube tiltmeter has continued to give excellent data, especially since its refurbishment by Larry Shengold (LDGO) in November, 1987. An hydraulic tie between this instrument and the parallel UCSD instrument should serve to identify the source of any discrepancies between these two sensors.

5. *Saint Louis University*: In 1985, Sean-Thomas Morrissey refurbished the three functioning Kinemetrics tiltmeters at PFO. The sensors (in uncased holes at depths of 4.5 m) showed the same behavior after this reinstallation as they had before. We have submitted a paper to *Journal of Geophysical Research*) describing the implications of these data, the most important of which is simply that the upper layers of the ground are too noisy an environment for tectonic strain measurement.

6. *University of California, Santa Barbara*: This precise-leveling project is no longer funded as a specific Crustal Deformation Observatory activity, but is included in the broader program of surveying conducted by Dr. Arthur Sylvester. The UCSB leveling crew (together with the NGS) is now surveying the new class A "bench mark farm" located near the west end of the long fluid tiltmeters.

7. *Carnegie Institution of Washington*: Two of the original three dilatometers at PFO are no longer operating, apparently because of leakage in the cable-head assemblies, which first appears as rapid drift and then degrades the signal. We have installed a wide-band amplifier on the remaining sensor (CIA) to monitor local seismic events and various instrumental effects. A report we are preparing describes a comparison of the results from these instruments with the strains determined by the laser strainmeters, including the barometric response; we believe that a new analysis has enabled us to separate the coupling factors for vertical and areal strain.

8. *University of Queensland*: The Queensland three-component borehole strainmeter, cemented in at a depth of 151 m, has continued to run with virtually no maintenance (except for an occasional back-up battery change). This high-quality instrument has been the focus of a long-term collaborative effort with Dr. Michael Gladwin, the builder of the borehole instrument, to compare the data from it with data from the laser strainmeters.

9. *U.S. Geological Survey – Crustal Deformation*: In the past few years several precise geodetic surveys have been made in the area around PFO. The longest-running is the Geodolite network (part of the larger Anza net) surveyed by the USGS Crustal Strain group of Drs. W. H. Prescott and J. C. Savage. This network (observed since 1973) has given the best values of the secular strain near PFO, serving as the low-frequency constraint on our continuous strain measurements. More recent additions include a 2-color EDM network established by Dr. J. Langbein in the spring of 1986, and a leveling line (with a loop going through PFO) set up by Dr. R. Stein using an NGS contract crew. Both of these new nets have been surveyed annually. We are enthusiastic about this work; the comparison of geodetic measurements and observatory-based results should help us establish the quality of both.

10. *Completed Projects*: We include here several projects that were in operation at PFO earlier, but are no longer being operated (for a variety of reasons). The radon monitor installed by Dr. Mark Shapiro (California Institute of Technology over borehole CIB was removed; it has not been in operation since 1985:74 because of lack of funding. The borehole stressmeters installed by Dr. Bruce Clark (Leighton and Associates) have not been monitored since 1985:174, when recording equipment was removed. Dr. Larry Slater (University of Colorado) visited PFO in late 1984 to remove the liquid from his 2-liquid tiltmeter. The end-vault equipment was removed in January 1985.

# Towards a Widely-Deployable Long-base Tiltmeter: Sensors and Anchors

14-08-0001-G1336

Frank K. Wyatt, Mark A. Zumberge, and Duncan Carr Agnew
Institute of Geophysics & Planetary Physics
University of California, San Diego
La Jolla, California 92093-0225
(619) 534-2411

This proposal supports our work on the design and development of new tiltmeter systems, and for the testing of these new systems against the existing ones at Piñon Flat Observatory. For long-base tiltmeters to be generally useful in measuring crustal deformation, they must be designed to operate without frequent attention, and widely-applicable installation procedures must be devised. Our new instrument incorporates two important features: (1) a self-controlled absolute water-height gauge, and (2) the use of optical fibers in vertical anchoring. We believe flexible optical fibers, cemented into uncased boreholes, will prove a viable means for monitoring the stability of monumentation intended for crustal deformation measurement; the results to date support this view.

Our evaluation program has included installing the new water-height gauge and anchors in a dedicated test vault at PFO so that we could experiment with different optical anchoring schemes in a field setting; extending the fluid-conduit of the original long-fluid tiltmeter to the new vault has allowed us to compare the new and old systems. We correct for any displacements between the new vault (Upl) and the nearer vault of the original tiltmeter (Tau) by assuming uniform tilting. (The extension is only 116 m long and lies close to the azimuth of the original tiltmeter.) We thus use the extension, plus measurements from the old tiltmeter, to give a reference height against to compare the combined new water-height gauge and vertical optical-fiber strainmeter.

Figure 1 presents a schematic of the components at Upl. The granite optics table there holds two systems. One system is a white-light interferometer that records the water-height in the half-filled fluid conduit, measured relative to the top of an invar rod; the rod is free-standing, and cemented to the rock only at its base, 5.4 m below ground surface. The other system is the laser interferometer that keeps a record of the optical path length changes in two taut optical fibers. The protective sheathings of these fibers are cemented in place; one fiber stops at the bottom of the invar (5.4 m) and the other extends to a depth of 35 m, and they are clamped together at the surface. By differencing the fiber signals we may determine the total displacement between the bottom of the invar rod and 35 m. (We do not require that the optical fibers be tied to the water-height gauge or even to the optics table, since the difference is sensitive only to displacements in the interval between their lower ends.) Thus, regarding the invar as stable, we have anchored the fluid level to a depth of 35 m—albeit in two steps; the invar rod is needed as an intermediate step because at shallow depths the temperature coefficient of fiber would create too much noise.

Figure 2 shows the initial results from the new installation, expressed as tilt. The upper two traces are the tilts found by differencing the water-height records from end-vaults Rho and Upl and from the original tiltmeter vaults, Rho and Tau. The records from Rho and Tau are fully corrected for monument motion using the vacuum-path optical anchors; Upl is "anchored" only by virtue of its reference to the short invar rod. The difference between these two tilt signals (shown as the third trace) is remarkably small and sets tight bounds on the true vertical strains to be sensed by the optical anchors at Upl. The odd response in the Rho/Tau record when the extension was first connected to the original tiltmeter is the result of a density contrast with the newly added fluid.

The high stability shown by the "difference" record of Figure 2 shows that two conditions have been satisfied. First, the tilt given by the original tiltmeter can be extrapolated as far as Upl. Second, the newly automated water-height gauge must be working without error. We can also draw two other important conclusions from these records. A water-height gauge and vault designed to be insensitive to displacements within the top few meters of the ground may be adequate for measurements of secular tilt in such locales as PFO; we already suspected this, since other evidence showed that large ground motions there appeared to be confined to the top few meters. And, because only very small displacements ($\approx 10\mu$m) may be occurring beneath the base of the invar rod, this makes the vault at Upl nearly ideal for evaluating the long-term stability of optical fibers—a satisfying result, since this was a primary reason for its construction.

Evidently the prototype water-height gauge, is working quite well. (The many gaps in Figure 2 are the result of other problems: data logging failures and the temporary return of the sensor to the lab for testing.) This device consists of a small platform supported by motorized micrometers and is designed to stay both level (for the optics to remain aligned with the fluid surface) and at a constant height above the fluid. In its final form, the optics would be aligned in the lab (relative to level-sensing tiltmeters attached to the platform) and installed in the field without adjustment. Once turned on, the platform should then automatically find the white-light fringes, at a unique height above the water surface.

Figure 3 shows some early results from the optical fibers. These records are dominated by their nearly identical response to changes in the vault temperature. The step that occurs near day 275 happened a few days after the deep fiber was initially tensioned and is the only instance we have seen of a spurious jump in a fiber record. What little signal remains after their subtraction ("difference") is due to a combination of drift in the fiber, deep temperature variation, and real strain in the depth interval 3.9 m to 33.6 m.

We have studied fiber drift in laboratory experiments; these suggest that the annual fractional change in the length of a tensioned optical fiber is less than $10^{-6}$, and probably closer to $10^{-7}$. This would correspond to a total length change in our deep fiber of 3 — 30 $\mu$m in a year, or a tilt of 0.01 — 0.1 $\mu$rad/yr on a 300 m instrument. (In this regard, fiber anchors should be only as deep as needed to correct for ground instability.)

Temperature fluctuations at depth are another problem we are working on. Common optical fibers have an apparent temperature coefficient of 11.7 $\mu\epsilon$/°C. This is about the same thermal response as the ground's, only in the ground's case the deformations are real, while for the fiber this response is purely an unwanted artifact. The effects on the fiber of the annual ground-temperature cycle can be easily modeled (showing an expected contribution of about 27 $\mu$m for the depth interval 2 to 35 m), but in our application this signal is anticipated to be common to both ends of the instrument and so will cancel. The more serious concern comes from other possible temperature changes at depth, perhaps from variations in ground water flow. We are working on a means to measure the integrated ground temperature along the path of the optical fiber simply by measuring the change in resistance of wire. As different types of optical fiber materials become available we can imagine a far more elegant approach, using the difference in thermal response for two side-by-side fibers.

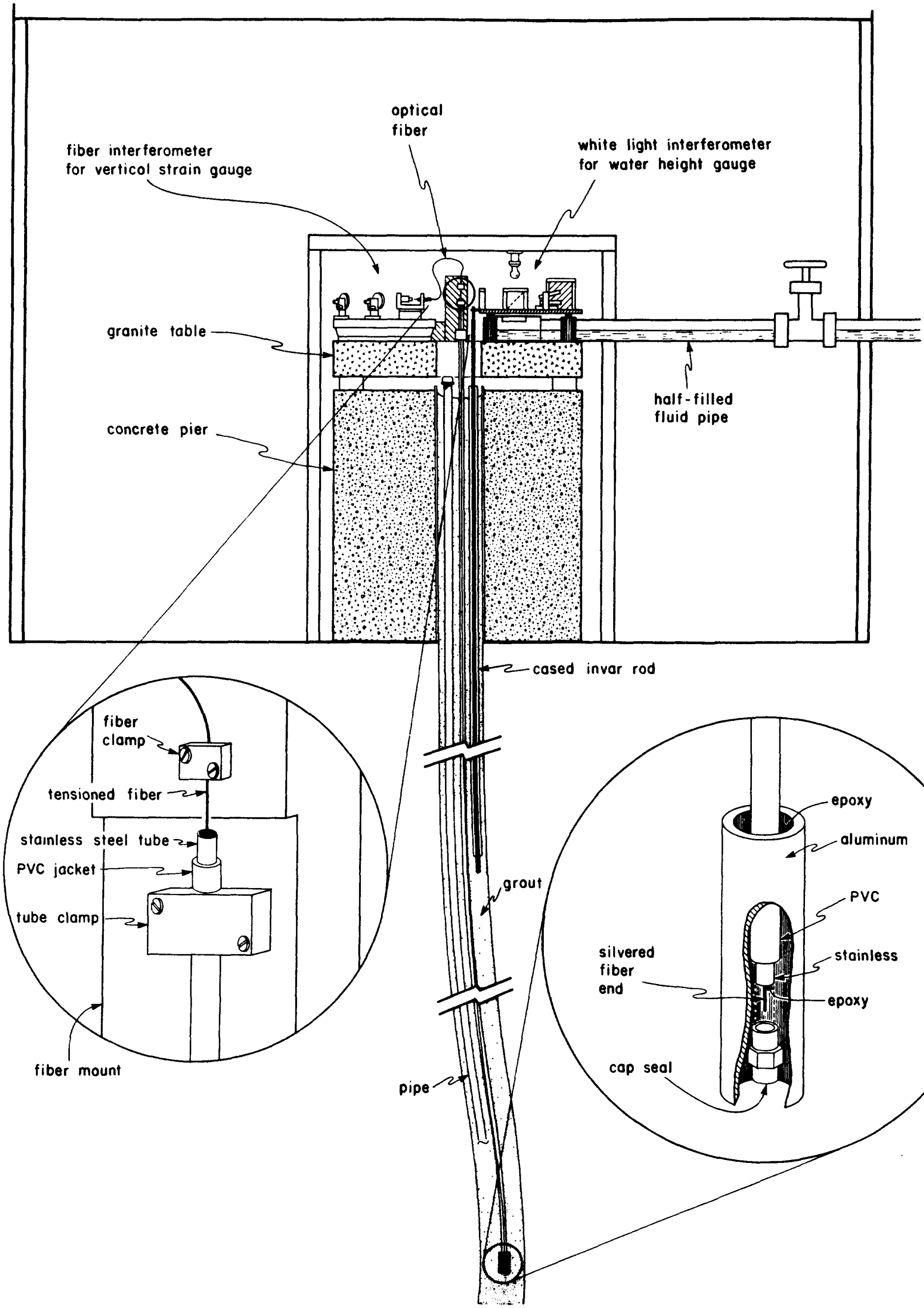
optical fiber
fiber interferometer for verticol strain gauge
white light interferometer for water height gauge
granite table
half-filled fluid pipe
concrete pier
cased invar rod
fiber clamp
tensioned fiber
stainless steel tube
PVC jacket
tube clamp
fiber mount
grout
pipe
epoxy
aluminum
PVC
silvered fiber end
stainless
epoxy
cap seal

Figure 1.

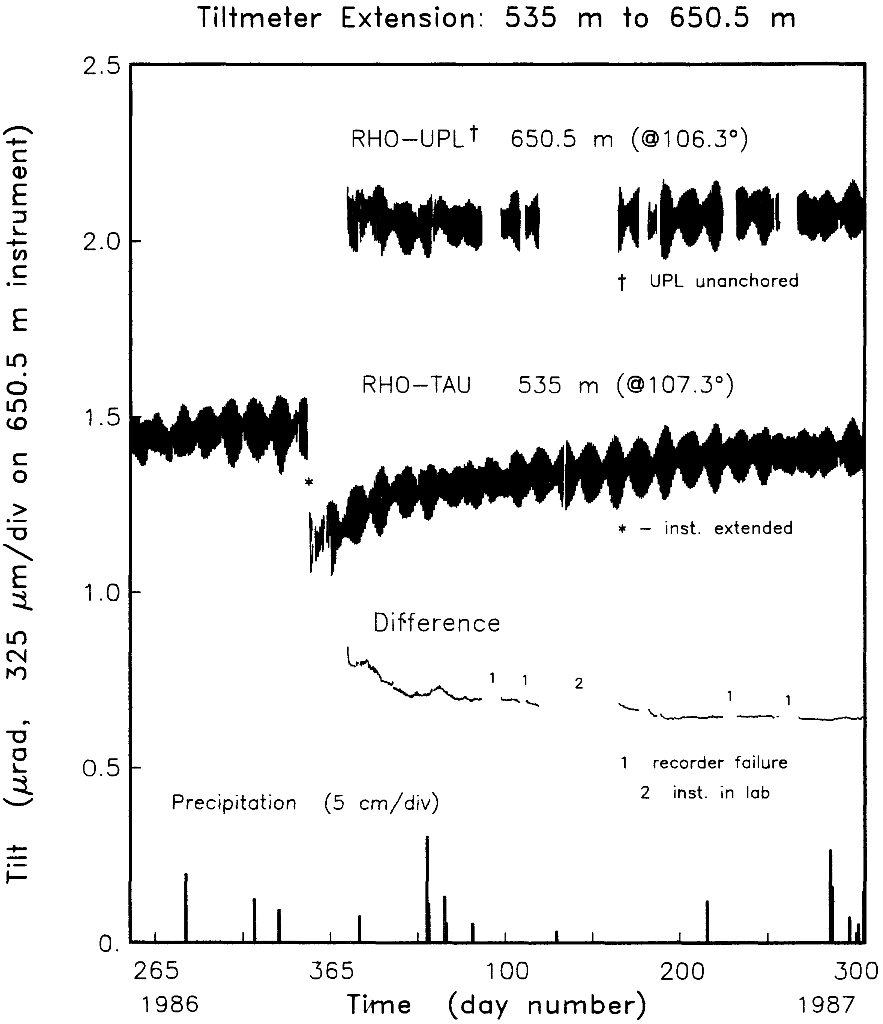
Tiltmeter Extension: 535 m to 650.5 m
Tilt (μrad, 325 μm/div on 650.5 m instrument)
2.5
2.0
1.5
1.0
0.5
0.
RHO–UPL† 650.5 m (@106.3°)
† UPL unanchored
RHO–TAU 535 m (@107.3°)
*
* – inst. extended
Difference
1
1
2
1
1
1 recorder failure
2 inst. in lab
Precipitation (5 cm/div)
265
365
100
200
300
1986
Time (day number)
1987

Figure 2.

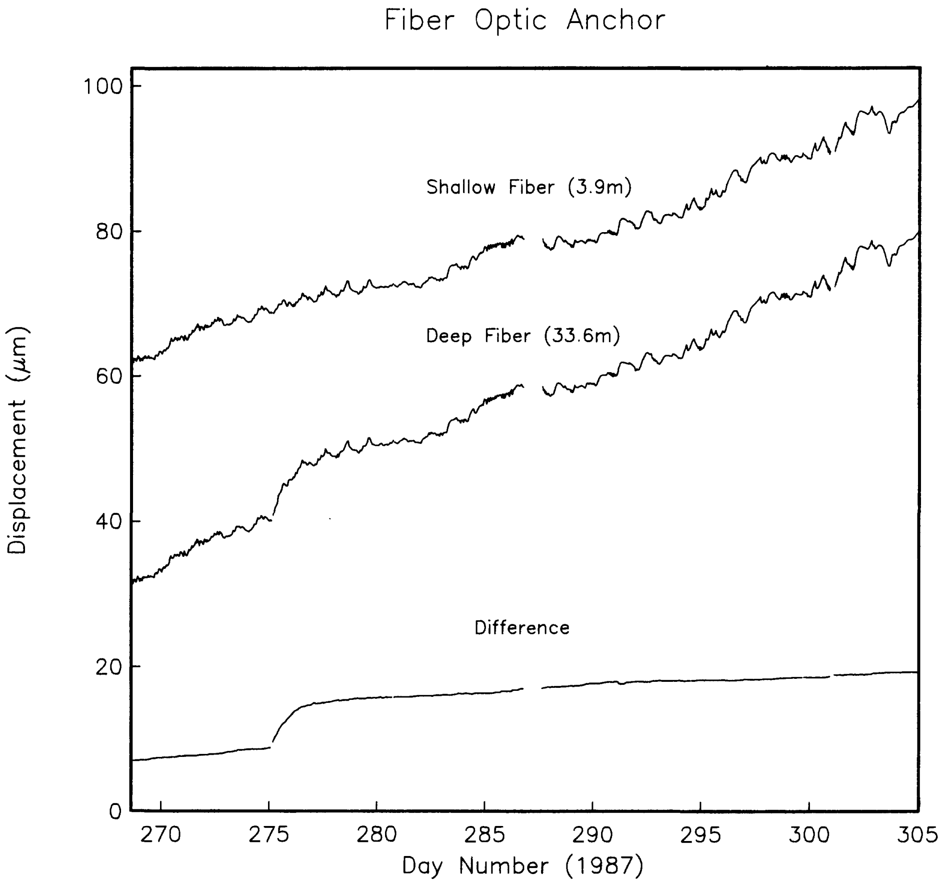
Fiber Optic Anchor
Shallow Fiber (3.9m)
Deep Fiber (33.6m)
Difference
Displacement (μm)
0
20
40
60
80
100
270
275
280
285
290
295
300
305
Day Number (1987)

Figure 3.

# Crustal Deformation Observatory: Part J
# Askania Borehole Tiltmeter

14-08-0001-G1361

Frank K. Wyatt, Duncan Carr Agnew, and Hadley O. Johnson
Institute of Geophysics & Planetary Physics
University of California, San Diego
La, Jolla, California 92093-0225
(619) 534-2411

Walter Zürn
Geowissenschaftliches Gemeinschaftsobservatorium Schiltach
Universitäten Karlsruhe
D-762 Wolfach, Heubach 206, FRG

This grant is the final one in a series of three for installation of an Askania biaxial borehole tiltmeter at Piñon Flat Observatory, and for the analysis of observations from the initial installation at 25 m depth (borehole KUA); records from the final 120-m-depth installation (borehole KUB) will be studied under other funding. This project is part of the overall Crustal Deformation Observatory program to understand vertical deformations (tilts) of the earth's crust. The aims of this project are to:

- Establish techniques (and costs) for emplacing and orienting removable tiltmeters in boreholes of various depths, with special emphasis on developing methods that may be applied at depths of 100 m or more;
- Compare these borehole tilt measurements with those from adjacent tiltmeters, including both long-base surface instruments and other borehole installations. Such comparisons enable us to establish the sources of instability and noise, and test the accuracy of different techniques; and
- Monitor the signals produced by this high-quality borehole instrument to determine the character of near-surface crustal tilt in this tectonically active area.

Our primary task during this period was to design and construct the borehole casing and instrument housing for deep installation, 120 m, and to devise a means to cement the casing in place. The instrument requires a fully cased and dry well bore, vertical to within 3°. The housing includes a forced-alignment device, though, because of budgetary constraints, its orientation is not yet known. Sometime in the coming year we plan to remove the instrument temporarily and log the alignment guide using a gyro compass. This task will serve the additional purpose of investigating the sensor's response to removal and reinstallation: How quickly do the signals return to their previous trends?

The initial records from the 25-m-deep installation are shown in Figure 1. This data set ends abruptly on November 5, 1987, when lightning struck within a 100 m of the borehole and much of the tiltmeter electronics were destroyed. (We are pleased to report that the instrument electronics have been repaired, though it took some time to familiarize ourselves with the inner workings of this well-engineered and complicated instrument.) After a settling in period, the records show tilt rates of 0.23 μrad/yr down to the west (azimuth of 263.8°) and 1.01 μrad/yr down to the south (173.8°), with a annual cycle of approximate amplitude of 0.1 μrad. The EW tilt is only about a factor of 2 larger, and with the same sign, as the tilt determined from the nearly EW long-baseline tiltmeters at the site, which do not show any such pronounced annual response. The NS tilt rate is nearly a factor of 10 larger than the EW long-baseline data, and the geodetically determined strain rates in the area, but is otherwise constrained only by other borehole tilt records from the site; these sensors (operated by the University of Colorado) give generally lower rates. Power spectral analyses show the Askania tiltmeter data to be very low noise. Results from the new, deep installation should testify to the veracity of the secular trends presented here and the quality of our deep emplacement technique.

**Figure 1.**

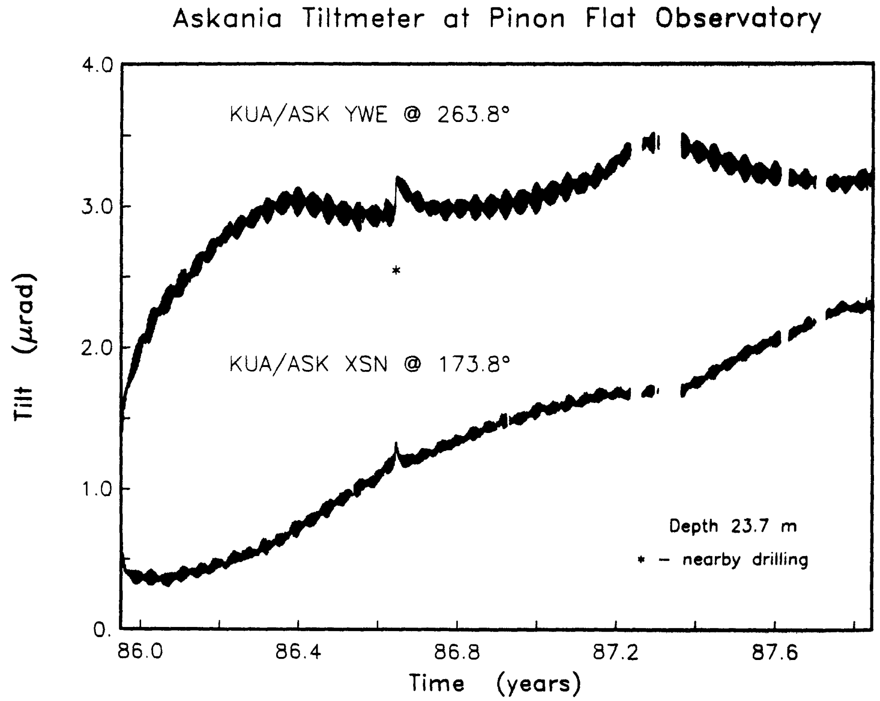

# Creep and Strain Studies in Southern California

Grant No. 14-08-0001-G1177

Clarence R. Allen and Kerry E. Sieh
Seismological Laboratory, California Institute of Technology
Pasadena, California 91125 (818-356-6904)

## Investigations

This semi-annual Technical Report Summary covers the six-month period from 1 October 1987 to 31 March 1988. The grant's purpose is to monitor creepmeters, displacement meters, and alignment arrays across various active faults in the southern California region. Primary emphasis focuses on faults in the Imperial and Coachella Valleys.

During the reporting period, alignment arrays were resurveyed across the San Andreas Banning-Mission Creek (San Andreas) fault at INDIO HILLS, DILLON ROAD, YERXA ROAD, NORTH SHORE, RED CANYON, and THOUSAND PALMS, across the Imperial fault at WORTHINGTON ROAD, HIGHWAY 80 (twice), and TUTTLE RANCH, across the Superstition Hills fault at IMLER ROAD (7 times), across the Coyote Creek fault at BAILEYS WELL (twice), and across the Garlock fault at CAMERON. Nail-file arrays were resurveyed at ROSS ROAD (twice), ANDERHOLT ROAD (twice), and WORTHINGTON ROAD. Creepmeters were serviced at ROSS ROAD (5 times), HEBER ROAD (twice), TUTTLE RANCH (twice), NORTH SHORE (twice), SALT CREEK, SUPERSTITION HILLS, and HARRIS ROAD. Slip meters were serviced at CHOLAME VALLEY, JACK RANCH, and TWISSELMAN RANCH.

## Results

Certainly the most significant observations during the reporting period were those associated with the two Superstition Hills earthquakes of 23 and 24 November 1987 ($M_S$ 6.2 and 6.6), associated with surface ruptures on the left-slip Elmore Ranch fault and the right-slip Superstition Hills fault, respectively, 12 hours apart. Significant observations of creep and slip, or the lack thereof, were made at our various instruments and alignment arrays spanning the nearby Superstition Hills, Imperial, southernmost San Andreas, and Coyote Creek faults

Superstition Hills fault.--The SUPERSTITION HILLS dial-gauge creepmeter across the fault had been read on 29 October, 25 days before the earthquakes. Between 29 October and 12 January 1987, the time of the previous reading, no displacement greater than 1 mm had taken place and, in fact, nothing significant had occurred there since the time of the triggered displacement of 11 mm during the 1979 Imperial Valley earthquake. During the M = 6.6 earthquake on 24 November, the displacement exceeded the instrumental limits, and the creepmeter wire broke. Fortunately, the nearby fault crossing at Imler Road was visited only 3 hrs prior to the M = 6.6 event by James Kahle of the CDMG, and he reported (personal communication) no fresh cracks at that time. Three Caltech graduate students visited the same site about 2 hrs following the earthquake, at which time the fault rupture was obvious, and aftercreep measurements commenced. Nearby, 28 cm of right-lateral displacement was measured at that time, and this had more than doubled to 57 cm by 16 December (Pat Williams and Harold Magistrale, personal communication). Thus, both the co-seismic displacement and post-earthquake creep are well documented, as is the fact that there was no obvious creep 3 hrs before the event. The alignment array across the fault at IMLER ROAD had also been surveyed 25 days before the earthquake and was resurveyed again on both 24 and 25 November. The first resurvey showed a coseismic displacement of 21 to 40 cm, with the larger amount derived from station pairs farthest from the fault (e.g., ±100 m aperture). Subsequent creep, however, all seems to be taking place on the single main trace, and by 28 January, 71 cm of slip had accumulated across the array. Measurements continue.

Imperial fault.--The largest creep event in 3 years occurred on the Imperial fault between 30 October and 2 November 1987, some 21 days prior to the Superstition Hills earthquakes. As recorded by the SMS/GOES creepmeter at ROSS ROAD, two successive creep events totalling 13.4 mm occurred during this period (Fig. 1), and it is particularly significant that a creep episode may have occurred at the same time on the San Andreas fault at SALT CREEK, 75 km northwest (see below). Near the Mexican border at HEBER ROAD, 16.7 mm of slip had occurred on the Imperial fault somewhat earlier, prior to 15 October, although the exact timing was lost due to instrumental failure. The 30 October-2 November creep episode continued farther north from ROSS ROAD for at least 13 km, as is indicated by fresh cracks that were observed as far north as Harris Road during the first week in November by R. V. Sharp (personal communication). At the nearby city of Imperial, 0.8 inches of rain fell on 31 October and 1 November (a rare event), but it seems highly unlikely that this could have triggered a creep event or instrumental response as large and pervasive as that seen at ROSS ROAD and nearby areas. Furthermore, the creep event probably started before the local arrival of the rainstorm.

During the earthquakes of 23 and 24 November, triggered right-lateral slip of 0.2 mm took place during each event at ROSS ROAD, 27 km from the epicentral area. More significantly, however, a large creep event of 7.6 mm took place over a 1-2 day period commencing about 3-1/2 hrs after the $M = 6.6$ event on the Superstition Hills fault (Fig. 2). This is somewhat comparable to the delayed triggered slip on the southern San Andreas fault following the 1986 North Palm Springs earthquake (Williams et al., in press), except that in the more recent 1987 case the two phenomena were on different faults. Also, of course, the post-earthquake creep event on the Imperial fault followed by only 21 days another large creep event, which makes the slip-deficit argument for triggered slip of questionable applicability here. The total slip indicated by the creepmeter at ROSS ROAD between 30 October and 27 November was thus about 21 mm, and it is comforting that the alignment array at HIGHWAY 80, 3 km northwest, also showed 21 mm of integrated displacement between surveys on 27 October and 17 December 1987.

San Andreas fault.--Following installation of the SMS-GOES creepmeter across the San Andreas fault at SALT CREEK in April 1986, no discernable slip had occurred until 30 October 1987, when an apparent right-lateral slip event took place at the same time as the larger creep episode at ROSS ROAD (Fig. 1). If this is an actual tectonic signal, it is very significant, inasmuch as never before have we seen simultaneous creep episodes on two different faults at distances as great as 75 km apart--perhaps reflecting some sort of regional strain episode at depth. Unfortunately, 1.8 inches of rain fell nearby at North Shore during the evening of 31 October and the morning of 1 November (again, a rare event), accompanied by a sharp drop in temperature. We might be inclined to dismiss the alleged signal as weather-induced were it not for the fact that it was simultaneous with the better documented creep episode at ROSS ROAD (Fig. 1). This is obviously a very significant issue to resolve, and studies of the records are continuing at the time of writing this report. Another reason for postulating a deep, regional strain event is that R. V. Sharp independently suggested (personal communication) that the change in the levelling profile across the Imperial fault at Harris Road, remeasured by him shortly following the 30 October-2 November creep event there, could only be explained by a deep-seated strain phenomenon. If this was indeed a regional strain event, it might well have been a significant physical precursor to the earthquakes of November 23 and 24. Arguing against a regional strain event, however, is the fact that no signal was seen on the very sensitive UCSD strain instruments at Piñon Flat (Duncan Agnew, personal communication), although this site is almost 100 km still farther northwest from SALT CREEK.

During the earthquakes of 23 and 24 November, triggered right-lateral displacements of 1.0 and 1.7 mm, respectively, took place at SALT CREEK, 50 km north of the epicentral area (Fig. 3). That these signals were not due solely to instrumental shaking is suggested by the facts that (1) both earthquakes--12 hours apart--recorded signals, whereas this would not be expected if the instrument had been fully "shaken down" during the initial event, and (2) the nearby creepmeter at MECCA BEACH showed an even larger displacement of 6.4 mm. No measurable creep events occurred in this area following the earthquakes.

Coyote Creek fault.--As a result of reports by Ken Hudnut and others that fresh cracks were seen along the Coyote Creek fault shortly after the earthquakes, our alignment array at BAILEYS WELL was resurveyed on 16 December 1987. It is about 25 km northwest of the 24 November epicenter. Fortunately, the same array had been surveyed less than one month before the earthquake, on 28 October. The 12 station pairs showed an average right-lateral slip of 21 mm between the times of the two surveys. This is more than 30 times what would be expected from the average continuing creep rate there and presumably largely represents triggered slip during or shortly following the Superstition Hills earthquakes.

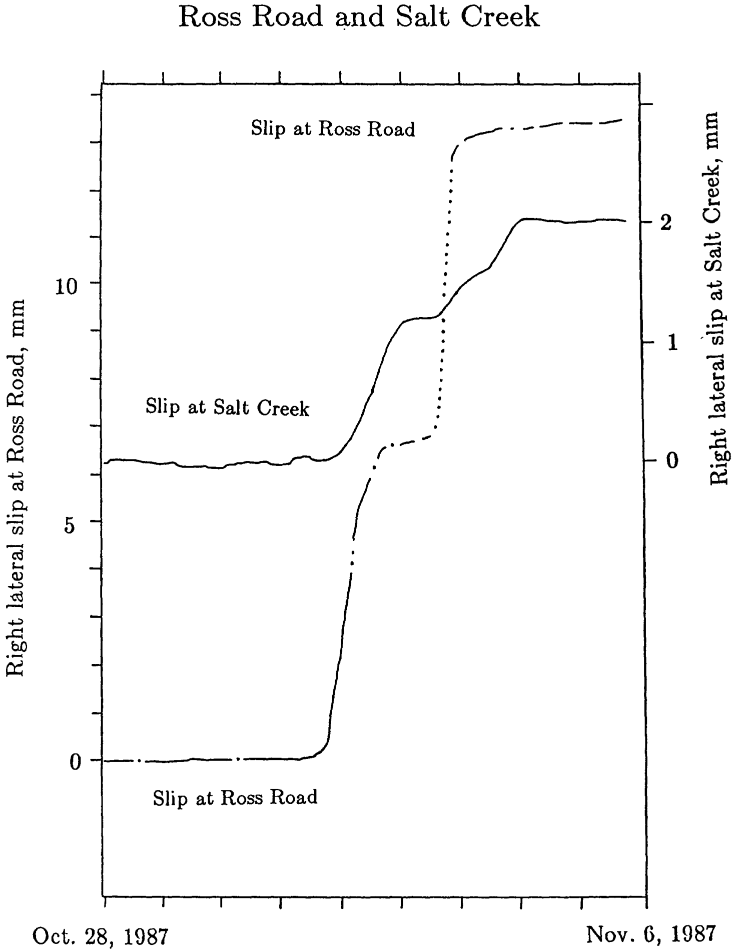

Fig. 1. --SMS-GOES telemetered creepmeter records from ROSS ROAD, on the Imperial fault, and SALT CREEK, on the San Andreas fault, showing apparent simultaneous creep episodes at the two localities, 75 km apart. Dotted lines are our extrapolations during periods of data dropout or instrument recentering. Note different slip scales for the two instruments; the SALT CREEK data have not been corrected for temperature, and corrected slip values will be smaller. This episode occurred about 21 days prior to the M = 6+ Superstition Hills earthquakes of 23 and 24 November 1987 and may represent a regional strain event.

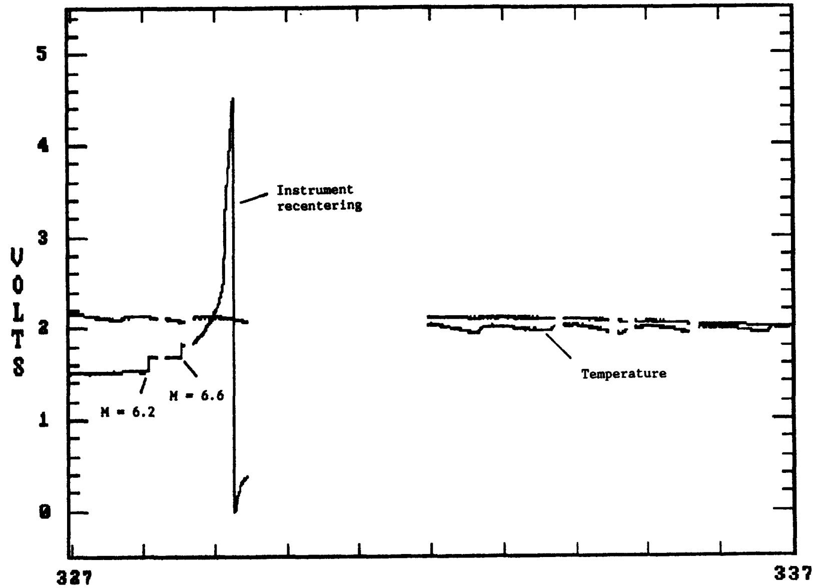

Fig. 2. --10-day creepmeter record from ROSS ROAD showing (1) the two slip events coseismic with the 27-km-distant earthquakes of 23 and 24 November 1987, and (2) the creep event of about 7.6 mm that commenced about 3-1/2 hrs after the second (M = 6.6) earthquake. The data dropout is due to a misunderstanding between Caltech and the USGS, Menlo Park, about scheduling of the SMS-GOES data retrieval over the Thanksgiving weekend.

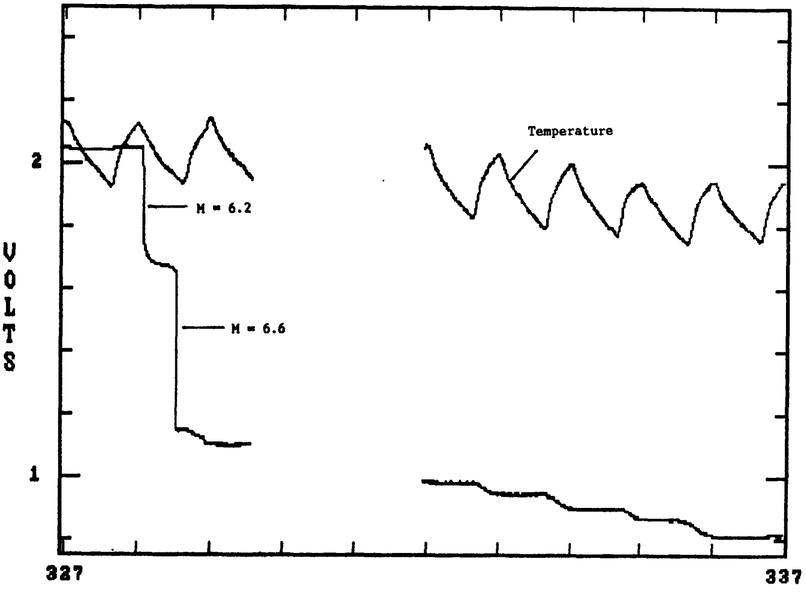

Fig. 3. --10-day creepmeter record from SALT CREEK, on the San Andreas fault, showing the two slip events coseismic with the 50-km-distant earthquakes of 23 and 24 November 1987. Right-lateral displacements are about 1.0 and 1.7 mm. Note vertical scale different from Fig. 2. Data dropout as in Fig. 2.

# Digital Signal Processing of Seismic Data

9930-02101

William H. Bakun
Branch of Seismology
U.S. Geological Survey
345 Middlefield Road, MS 977
Menlo Park, CA 94025
(415) 329-4793
(FTS) 459-4793

## Investigations

1. Continue coordination of the Parkfield prediction experiment.
2. Continue development of procedures to obtain consistent reliable estimates of magnitude and seismic moment for earthquakes in central California using the USGS Central California Seismic Network (CALNET).

## Results

1. The Parkfield prediction experiment is operational. A number of interesting observations have been documented (see attached monthly Parkfield summary reports).
2. A new algorithm that provides improved magnitude estimates has been developed. Station corrections, gain corrections, as well as use of an elapsed time are important parameters in this approach.

## Reports

1. Tucker, B., W. Bakun, W. Ellsworth, C. Real, M. Reichle, and W. Thatcher, 1987, Overview of the joint USGS-State of California Parkfield earthquake prediction fund (abs.), EOS, American Geophysical Union Transactions, vol. 68, no. 44, p. 1345.

2. Bakun, W. H., 1988, Parkfield, California earthquake prediction experiment-a status report (abs.), Earthquake Notes, in press.

3. Bakun, W. H., 1987, Parkfield, California earthquake-prediction experiment-an overview (abs.), EOS, American Geophysical Union Transactions, vol. 68, no. 44, p. 1345.

4. Bakun, W. H., 1988, Historic seismicity of the Parkfield area, Monterey and San Luis Obispo Counties, California Geology, vol. 41, no. 3, p. 61-62.

5. Michaelson, C. A., 1987, Coda duration magnitudes in central California: an empirical approach, USGS Open-File Report 87-588, 55 pp.

# OCTOBER 1987 PARKFIELD DATA REVIEW MEETING
Held Nov. 9 1987

There were no two-color, dilatometer, seismic, or magnetometer alerts during October.

The Gold Hill creepmeter (XGH1) recorded 0.6 mm of right-lateral movement from 10/11-10/17 and an additional 0.9mm of right-lateral movement from 10/17-10/20. The water level rose 1 cm in the Gold Hill well on 10/12, essentially coincident with the beginning of the XGH1 creep surge. A rapid large (>2000 PPM) $H_2$ emission was recorded at the Gold Hill geochemistry site on 10/13-10/17. The close temporal and spatial relationship with the nearby creep and water level changes suggests a tectonic source local to the fault near Gold hill for the $H_2$ emission. Although the $H_2$ emission is extraordinary, its interpretation is uncertain in that comparable Gold Hill creep episodes have not been accompanied by Gold Hill $H_2$ events, and vice versa.

The Middle Ridge (XMD1) and Middle Mtn. (XMM1) creepmeters recorded 1.5 mm and 0.7 mm of right-lateral slip respectively on 10/28, shortly after a 1.3 cm drop in the level of the water in the deep interval of the Middle Mtn. well. In the shallow interval, the water dropped 3.8 cm and recovered in about 6 hours. The water level changes occurred during the recovery of the well from extensive cleanout operations so that the water level changes would likely have been considerably larger if they had occurred after the completion of the cleanout. The simultaneous creep and water well changes conformed to a previously-recognized pattern (90-day period) of similar events that had been used to predict that the events would occur on 11/2, four days later than their actual occurrence. The XMD1 creep triggered a D-level creep alert 10/28-10/31; the superposition of the water well recovery and the water level event precluded the declaration of an associated water level alert.

On 10/10 the water level in the Stockdale Mtn. well dropped by 1/2 foot; a total drop of 14 cm occurred over the next 4 days. Both the tidal and barometric response of the well appeared to increase after the drop.

W. H. Bakun

# November 1987 Parkfield Data Review
## Meeting held Dec. 14, 1987

On 11/17 an M1.8 shock occurred at 11 km depth in MM3, resulting in a D-level seismic alert on 11/17 - 11/20. Save one shock at Simmler, all the Parkfield seismicity since October 1987 has been concentrated at or north of Middle Mtn; this pattern is reminiscent of the 6 months preceding the 1966 Parkfield earthquake.

November was a quiet month for creep with no alerts, despite the onset of winter rains. Reversals in creep direction occurred at VARIAN (XVA1), ROBERSON SW (XRSW), and HEARST SW (XHSW) after the rainy season began.

There were no events of geophysical interest recorded on the borehole strainmeters during November. All strainmeters, including the 3 tensor strainmeters, are fully operational.

There was a level D water well alert on 11/12 - 11/15 due to a 9.4 cm drop in the TAYLOR RANCH well. The anomaly is similar in form to a transient due to a pumping in a nearby well, although no particular nearby irrigation wells have been identified as responsible. The TAYLOR RANCH well will be monitored for geochemical changes, starting before the end of December 1987; pumping tests at 160' depth produce sufficient water volume for continuous monitoring of radon.

There were no two-color geodimeter alerts in November. The line length changes spanning the main fault trace indicated left-lateral slip ranging from 20 mm/yr. near the southend of Middle Mtn. to 6 mm/yr. near Car Hill from late October through November. HP-3808 measurements of the two-color lines have been made so that unambiguous coseismic changes can now be made across the rupture zone of the characteristic Parkfield earthquake.

GPS measurements over the past 18 months of 4 stations near Middle Mtn with no line of sight show secular trends consistent with other deformation data in the area. The lateral resolution is 3-4 mm, comparable to that of single-color laser geodimeter measurement; vertical resolution of the GPS surveys is about 1 cm.

UCSB, UCB, and the USGS have completed installation of the 116 sensor seismic string in the Phillip's Varian A-1 well. All seismic sensors are operational and some VSP data had been recorded. The pore pressure monitor on the Phillip's Varian A-1 well will be installed when the recording trailor is complete, perhaps before the end of December.

W. H. Bakun

# PARKFIELD DATA REVIEW FOR DECEMBER 1987 - MEETING HELD 1/11/88

All Parkfield shocks in December 1987, except for two near Cholame, occurred in or northwest of the Middle Mountain box. There were no seismic alerts.

There were no creep alerts in December 1987. A 0.64 mm right lateral creep event at Middle Mountain (XMM1) on 12/14 and accelerated creep at Slack Canyon (XSC1) on 12/28-12/30 were noteworthy.

A fall and recovery in the water level in the Stockdale Mountain well on 11/29-12/12 should have been declared a d-level alert; the net amplitude for this event was 9 cm, corresponding to 0.2 PPM volume strain. Water level in the deep interval of the Middle Mountain well rose about 4 cm (~0.04PPM volume strain) coincident with the 12/14 XMM1 creep event.

All 10 deep borehole strain instruments, including the 3 tensor strainmeters, operated continuously with high quality data throughout the month. There were no strain alerts.

There were no alerts from the 2-color laser geodimeter network during December 1987

- W. H. Bakun

# JANUARY 1988 PARKFIELD DATA REVIEW - MTG. HELD 2/8/88

Seismic activity at Parkfield was normal with no alerts. Seismic activity was primarily at and north of Middle Mt.; one small shock occurred in MM3.

There was a level-D waterlevel alert due to a 7.2 cm drop in the deep interval of the Middle Mtn. well between 1/28 2346GCT and 1/29 0001GCT. The drop corresponds to 0.07 PPM volume strain. This event is the fifth of a series of similar events, believed to represent right-lateral strike slip over the fault between the XMM1 and XMD1 creepmeters. The intervals between these events are 95, 88, 86, and 92 days. The next event is due on 4/29 ± 5 days; discussions have begun on obtaining additional measurements around the 4/29 time of the next event.

A left-lateral trend at XMD1 beginning on 1/9 technically triggered a D-level creep alert by exceeding 1 mm of movement in 7 days; based on previous winters experience, the XMD1 creep surge appears to be a characteristic rainy season response rather than a tectonic event so that no alert was announced. A right-lateral creep event at XMD1 that exceeded 0.5 mm in the first half hour was observed coincident with the drop of water level in the Middle Mtn. well on 1/28-1/29. While this creep event meets the D-level creep criteria, it was recognized at the time that the creep and rate changes represented the same anticipated tectonic event so that no "extra" D-level alert was declared, thereby precluding escalation by the combination rules to a C-level alert.

There were no borehole strainmeter or magnetometer alerts during January 1988. The Froelich borehole tensor strainmeter is out of service, with recovery expected by Mid-February 1988.

There were no alerts on the two-color geodimeter network during January 1988. The pattern of line length changes appears to be a continuation of the pattern since 10/21/87, except for the onset of rapid extension of lines ESE of Car Hill.

Construction of water well and soil geochemistry monitors in the Parkfield region are progressing rapidly with an emphasis on redundant sensor and recording systems.

W. H. Bakun

# FEBRUARY 1988 PARKFIELD DATA REVIEW - MEETING HELD 3/14/88

Seismic activity at Parkfield was normal, with two D-level seismic alerts. The magnitude 4.6 Antelope Hills shock of 2/22/88 occurred 15 kilometers east of the San Andreas fault near Simmler within the Parkfield alert region, triggering a D-level seismic alert (2/22-2/25). There were several M1 shocks during 2/28-3/2 in the northern corner of MM3 (and at shallow depth northwest of MM3), resulting in a D-level seismic alert from 3/1-3/4. A MicroVax II computer system is now recording the seismic string in the Varian 1-A well.

No unusual activity was observed on the creepmeters during February, despite heavy rainfall on 2/28. There were coseismic steps at XMD1, XVA1, WKR1, and XHSW associated with the 2/22 Antelope Hills shock; the 0.1 mm right-lateral step at XMD1 interrupted its left-lateral trend. Two new alignment arrays, located 1 km each side of XMD1, have been surveyed in preparation for intensive monitoring around the expected time (4/29) of the next northwest-propagating Middle Mtn. creep event.

There were no water level alerts during February. Future analysis of the water level data will be on the LOWFREQ ISUNIX computer rather than on the WRD PRIME computer reflecting the greater reliability of the LOWFREQ ISUNIX. The fluid pressure at the bottom of the VARIAN 1-A well is now recorded near the well head; the available recordings show possible earth tides and the effects of temperature changes on the surface instrumentation. The Varian 1-A fluid pressure data eventually will be transmitted by satellite to Menlo park.

There were no borehole strain or magnetometer alerts during February. Analysis of the strain recorded at Red Hills and Jack Canyon for the 2/22 Antelope Hills shock indicate a seismic moment of $0.8\text{-}1.0\times10^{23}$ dyne-cm. Magnetic field disturbances around 2/22 are due to magnetic storm activity and are not tectonic in origin.

There were no anomalous happenings on the 2-color laser geodimeter network, although the data has been sparse because of adverse weather conditions and a failing laser. (A new laser was installed by L. Slater on 3/13).

There were no geochemistry anomalies observed near Parkfield during February.

- W. H. Bakun

MARCH 1988 PARKFIELD DATA REVIEW - MEETING HELD 4-11-88

The significant events of the month occurred largely in the March 27 - April 4, 1988 period. (The details are reported in the attached 10 April 1988 draft by A. G. Lindh and only a summary will be reported here).

A 1.85 mm right-lateral creep event at XMM1 starting 3/27 2310-2320 GCT and a water level change [rise of 0.6 cm starting 3/27 2316 - 2331 GTC and then a fall of 4.7 cm (0.05 μstrain change) starting 3/28 0001-0016 GCT in the deep interval] in the two levels of the Middle Mountain water well independently triggered a D-level alert from 3/28 - 3/31; Because these two observations were apparently caused by a single tectonic event, i.e. creep at Middle Mountain, the combination rule D+D=C was judged inappropriate so that a D level alert was declared.

On 3/28, a 0.1 μ strain change was noted on the Red Hills dilatometer with a coincident change on the nearby Jack Canyon dilatometer, resulting in a D-level dilatometer alert. The combination rule is appropriate in this care, resulting in a C-level alert.

On 3/31 short-term length change on the POMO and NORE lines resulted in a D-level two-color laser geodimeter alert. Also on 3/31, a M1.9 shock at 11 km depth in MM3 caused a seismic D-level alert. The two-color and seismic alerts combined for a C-level alert, effectively extending the water level, creep and dilameter C-level alert until 4/3/88. The C-level alert was extended until 4/4/88 (Monday a.m.) to give to the Parkfield Working Group time to consider the situations before terminating the alert status. (Shortly after the alerts were terminated, two M 3.5 - M 4.0 shocks near Coalinga reset the alert status to D-level until 4/7/88.)

— W. H. Bakun

C.

A.G. Lindh
10 April 88
Rough Draft

1. Chronology of C level alert at Parkfield, March 27-April 4, 1988. (Observations and alerts as they were actually reported at the time)

   a) Creep and H20 at MM on 27th

   Late Sunday afternoon, March 27th, Kate reported via ISUNIX mail that a level D alert was in effect due to an ongoing creep event at XMM1. This event triggered creep rule D3 (p. 28 Bakun et al., 1987, referred to as BEA hereafter), with more than .5 mm in the first 30 min; this event eventually reached 1.85 mm.

   By midnight Evelyn had reported a simultaneous water level change in both levels at Wmm; she noted that this was different than previous events at this site, since in began with a small upward inflection, followed by a large down-swing, suggesting NW-SE propagation. This also triggered a D alert, by changing more than 0.05 ppm in 24 hours (p. 32, BEA). In a meeting Monday morning, the 28th, the PWG (Parkfield Working Group) decided that these two D alerts would NOT add up to a C, since they so clearly were the result of a since tectonic event; John Filson was so notified by letter.

   b) Dilatometer anomaly South of hiway 46 on 29th

   On Tuesday afternoon (March 30), M.Johnston notified A.Lindh by phone that the two dilatometers south of Hiway 46 had anomalous signals starting at about 00 GMT on the 28th. By strain rule D2 -- a change of 0.1 ppm within 24 hrs. on one instrument, with indications of a simultaneous signal on a second (p. 30, BEA) -- this triggered a D level alert. Combined with the previous D, this resulted in a C alert; Sacramento and Reston were so notified.

   c) Four small earthquakes March 30 - April 1

   Between 0351 GMT on the 30th, and 2139 GMT on the 1st of April, there were four small earthquakes between Gold Hill and Middle Mountain. The third of these, a M1.9 at 847 GMT on the 31st, was within the MM3 box, and thus triggered a D level alert also (Seismic rule D1, p. 26 BEA). This extended the C level alert until 847 GMT on April 3rd. Following the fourth event on the 1st, which was just outside MM3, A.Lindh chose to extend the C alert until 10am (1700 GMT) on Monday, April 4th, to give the PWG time to consider the matter.

   This decision was also based on the two-color alert described below, and the fact that the four small earthquakes progressed linearly from SE to NW at a rate of about 13 km/day, suggesting that the source of the dilatometer anomaly had triggered a deep creep wave along the San Andreas. Although there was no other independent evidence for such a phenomenon, it seemed imprudent to terminate the alert without an opportunity to carefully scrutinize all the data.

d) Two color anomaly on 31st

At 7:40am on the 1st, B. Simpson reported via ISUNIX mail that starting on March 31st, there was a D level alert based on short-term changes in three lines, strengthing the C level alert in effect until the 4th of April.

e) Meeting of the PWG on the 3rd

The PWG met at 10am on the 4th of April to consider the situation. F.Riley showed data from the deep pressure measurement in the Phillips A-1 hole which indicated that within about one hour of the XMM1 creep event on the 27th, that a pressure drop of more than 7 psi had occurred. The pressure subsequently recovered about 90% of its previous value in the next 24 hours. Given that we have been recording this signal less than 30 days, and in light of the unprecidented size of the signal, it was impossible to draw any conclusions. In light of the absence of any further changes, the PWG concluded that the alerts would be considered over at that time.

f) M3.5 eq N of Coalinga

At 2041 GMT on the 4th, four hours after the meeting described above, there was a magnitude 3.7 earthquake north of the Coalinga aftershock zone (Seismic rule D4, p. 26 BEA). This triggered a D level alert which expired on the 7th with no further excitement.

2. Detailed Chronology (Composed after the fact)

| | Date | Time | Event | Figure |
|---|---|---|---|---|
| a) | 880301??-880327 | | NO events south of 36 00 for ??? days, numerous shallow events north of 36 00 | |
| b) | 880315 | (approx) | Resumption slip 2-color shallow near Car Hill | |
| c) | 880327 | (approx) | Gradual changes in sign or rate, at 3 creep meters on Middle Mountain<br>xsc1 increases rate x2<br>xmd1 & xva LL to RL<br>xpk1 RL to LL | |
| d) | 880327 | 2310 | XMM1 1.85 mm creep event | D |
| e) | 880328 | 0000 | Wmm3 0.05 ppm strain related to creep event | D |
| f) | 880328 | 0100 | Phillips (Varian) Deep well -6.6 psi pressure change in about 20-30 min. Amplitude is approx. 50-100 tidal amp. | |
| g) | 880328 | 2100 | Srh 0.2 ppm strain event | D C |
| h) | 880328 | 2100 | Sjc 0.02 ppm " " | |
| i) | 880329 | | Sharp inflection at 4 Middle Mtn creepmeters. All three that changed sign on 27th (XMD, XVA, XPK, see above) clearly start in their new direction within a few hours of one another. | |
| j) | 880330 | 0351 | M0.8 eq near Gold Hill | |
| k) | 880330 | 1534 | M1.0 " " Parkfield | |
| l) | 880331 | | Short term 2-color alert | D C |
| m) | 880331 | 0847 | M1.9 eq in MM3 | D C |
| n) | 880331 | 1650 | Phillips (Varian) Deep Well +0.1 psi event of about 1 hr | |
| o) | 880401 | 0100 | XMD1 0.13 mm creep event (part of gradual increase) | |
| p) | 880401 | 2139 | M1.2 in MM1 | |
| q) | 880404 | 1700 | Meeting Bakuns office, end C (and D) alerts | E |
| r) | 880404 | 2041 | M3.7 & M3.4 eqs north of Coalinga aftershock zone | |

## 3. DISCUSSION

a) Varian block wedged, no seismicity south of 36, much shallow to north.

b) Varian block rotates slightly clockwise, perturbing creep rates, triggering

c) Creep event at XMM1, which triggers

d) small eastward translation of Varian block on Middle Mtn fault, right at bottom Phillips Well, producing enormous pressure change. Pressure change is because geopressure zone at bottom is result of MM fault generated compression beneath an imperiable layer; small motion on fault results in enormous pressure change without surface strains.

e) Jostling of block advances XSC - XVA (NW of Phillips Well)
retards XPK, at south end Varian block,
SE of Phillips Well )
(Check 2-color)

f) Similarly, large strain at Red Hill dilatometer is result of small shallow slip event on Red Hills Fault. This could have been triggered by release of Choke Stone at Middle Mtn, or more likely, both shallow, off San Andreas slip event were triggered by deep slip event. (note that everything to this point has been shallow.)

g) Since Red Hill Block is Choke Stone for southern end Parkfield zone, its motion initiated a small DEEP slip event which propagated to NW on San Andreas, triggering small earthquakes on its way, as well as small creep event at XMD, and small Phillips well event. (Alternatively, earthquakes may have been triggered by a small NW propagating event of EASTWARD translation of Castle Mtn Block.)

h) Eastward propagating slip at base of Castle Mtn Block eventually piles up agains uplifted basement at western edge of San Joaquin Valley, triggering M3.5+ earthquakes north of Anticline Ridge.

i) Plausibility of this model strengthened by previous events:

   1) Creep at XMM and XPK following New Idria EQ in 1982, also small event at Bitterwater Valley following New Idria.
   2) Same creep precedes Coalinga, small earthquakes at New Idria follow, as does creep at XGH?, and swarm at Bitterwater.
   3) Events following Kettleman EQ
   4) Wmm signal preceding M5 (Evelyn)
   5) other C alerts??

4. Figures

   1 a) Map showing eqs, instrument locations, faults, and blocks
   2 b) Two-color strain plot
   3 c) Creep event at XMM and Wmm, pressure at Var1
   4 d) Longer term creep at Middle Mtn creep meters
   5 e) Dilatometer signals at Sjc, Srh
   6 f) Small creep event at XMD, small Phillips A1 signal on 31
   7 g) Space time plot
   8 h) Histograms of alerts
   9 i) Small scale X-section thru Middle Mtn and Anticline ridge

5. Tentative author list

   NOTE TO TENTATIVE AUTHORS:

   My intention is that this will metamorphise into an OFR within 1 week, and into a short article to GRL or ERL within 1 month. Please get in touch with A.Lindh concerning your contributions/reservations, and/or the spelling of your name.

   a) Bakun, W.
   b) Breckenridge, K.
   c) Burford, R.
   d) Burford, S.
   e) Hammon, D.
   f) Johnston, M.
   g) Lindh, A.
   h) Malin.P.
   i) Roeloffs, E.
   j) Simpson, R.
   k) Slater, L.
   l) Wentworth, C.

March 1988

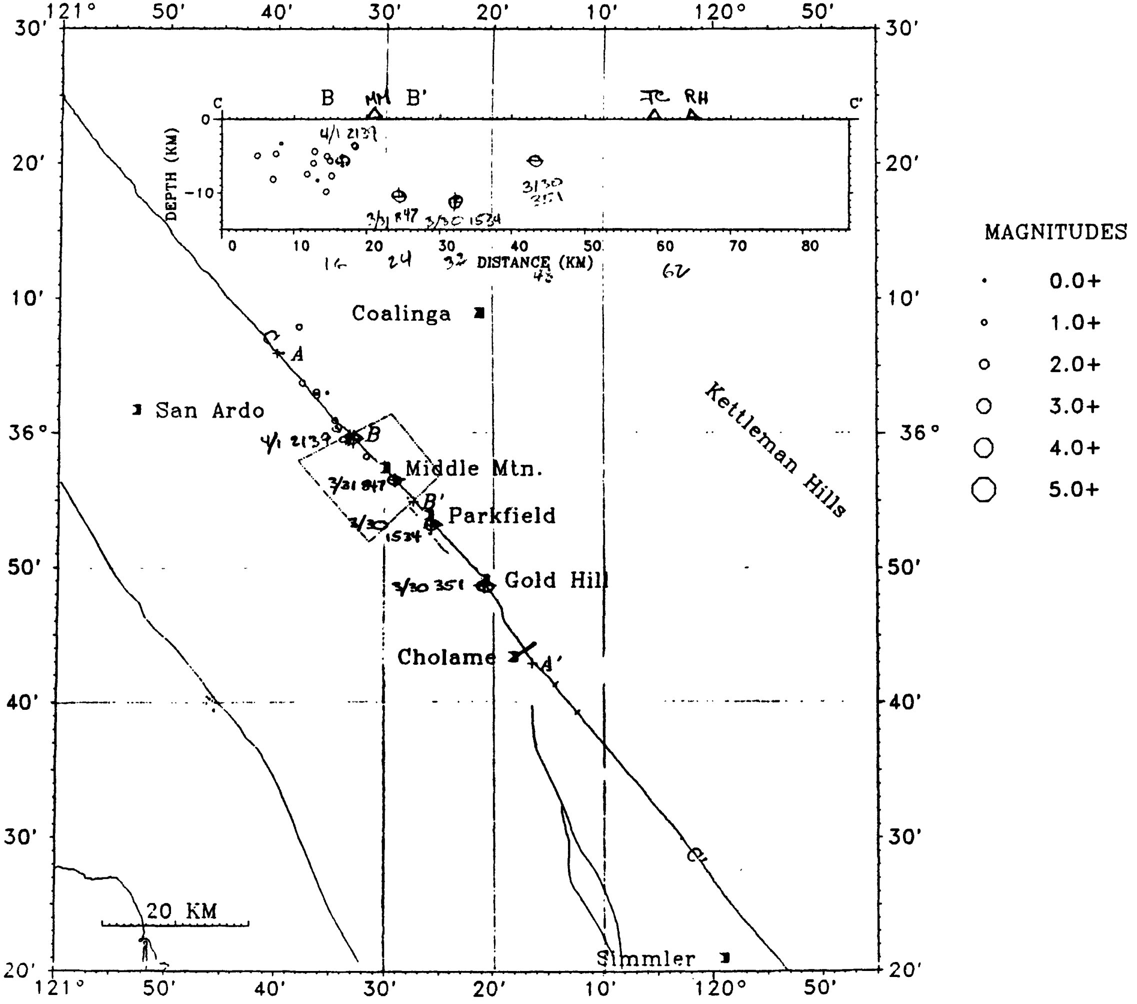

Figure 1

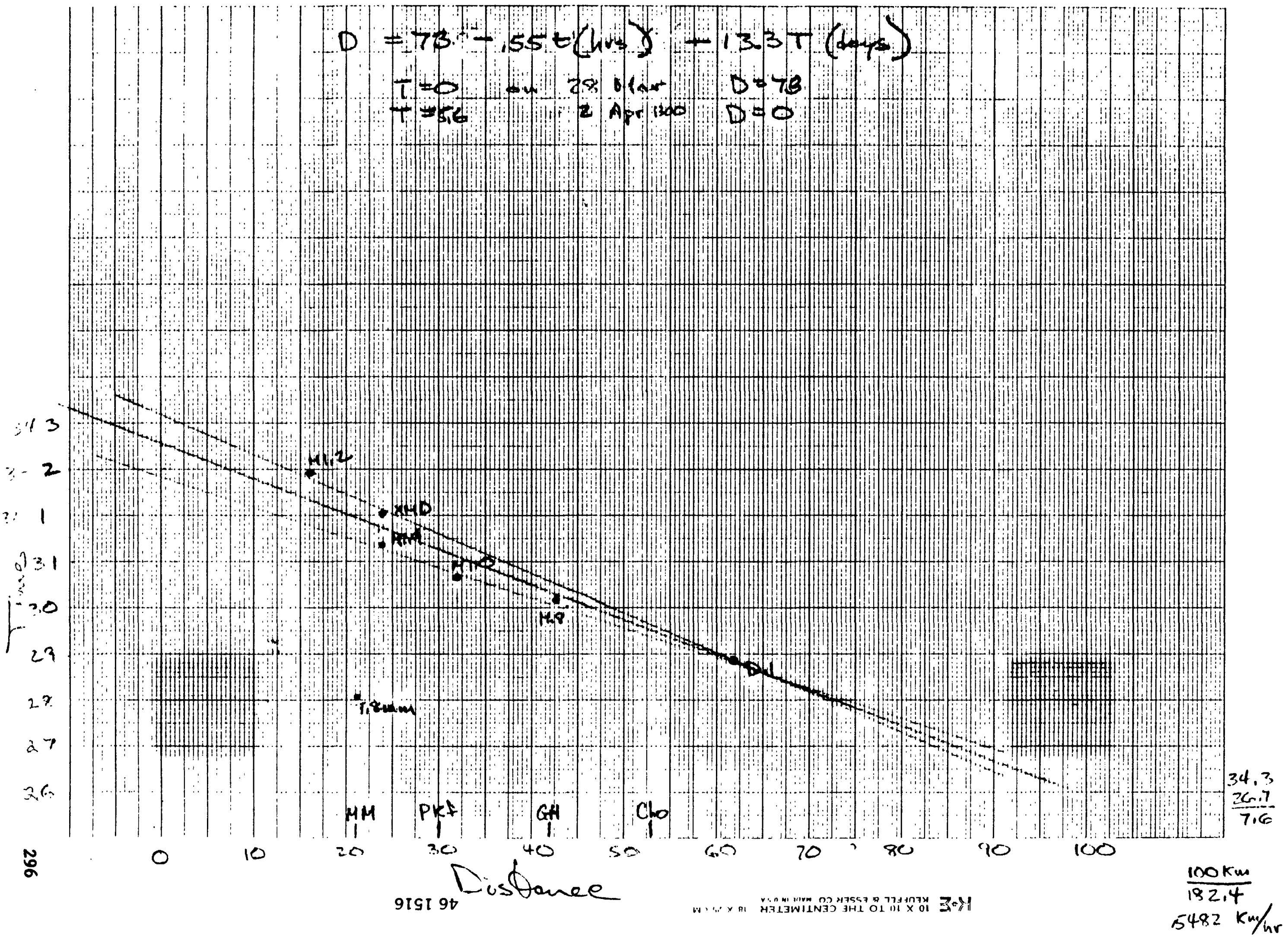
D = 78 - .55 t (hrs) - 13.3 T (days)
T = 0 on 28 Mar D = 78
T = 5.6 2 Apr 1300 D = 0
HI.2
XHD
HM
HI.D
H.8
7.8mm
Time
34.3
3-2
31
31
3.0
29
28
27
26
MM
PKf
GH
Cho
0
10
20
30
40
50
60
70
80
90
100
Distance
34.3
26.7
7.6
100 Km
182.4
5482 Km/hr

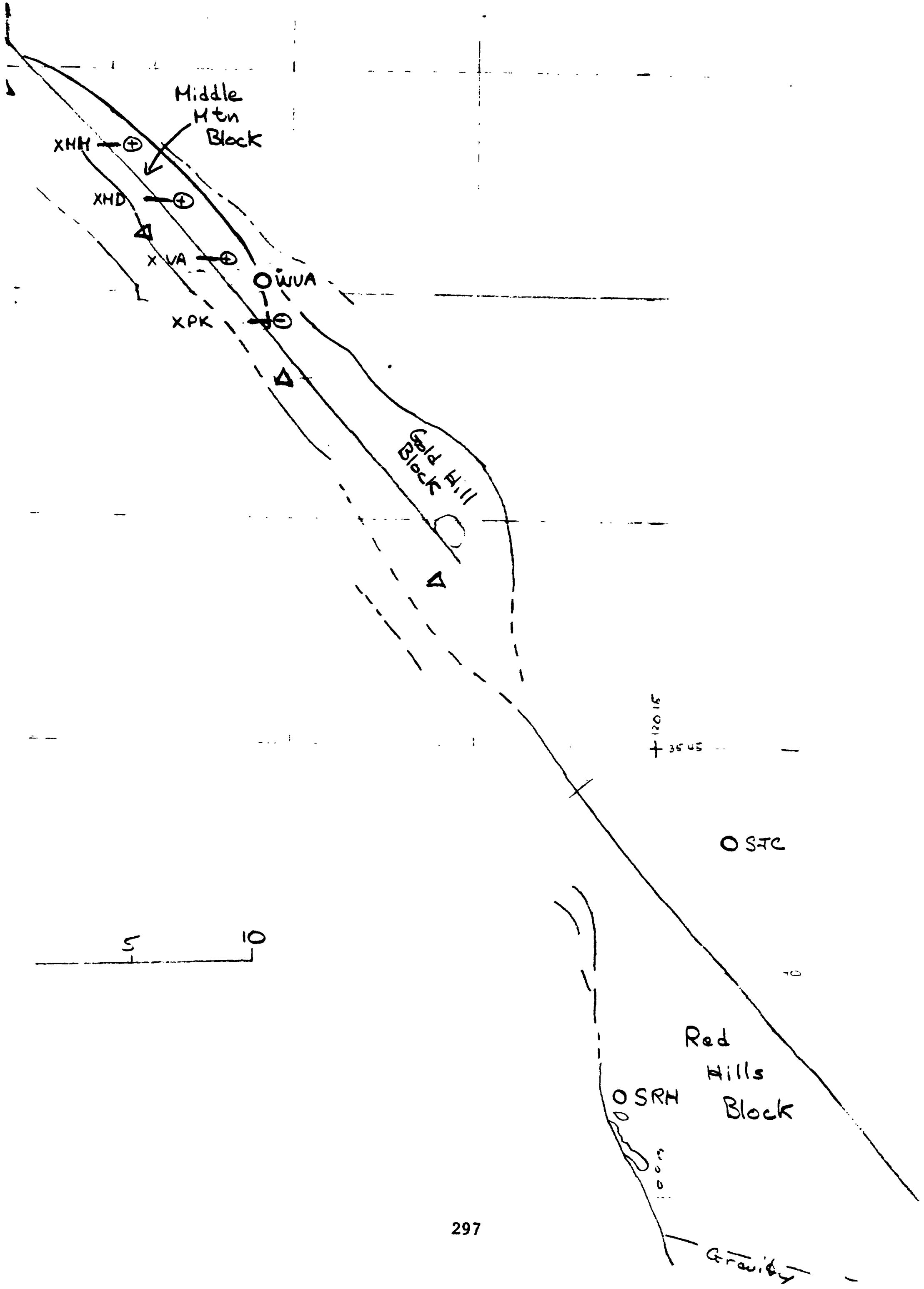
Middle
Mtn
Block
XMM
XMD
X VA
WUA
XPK
Gold Hill
Block
120 15
35 45
SJC
5
10
Red
Hills
Block
SRH
Gravity

# Tectonic Tilt Measurement: Salton Sea

14-08-0001-G1392

John Beavan
Lamont-Doherty Geological Observatory of Columbia University
Palisades, New York 10964
(914) 359-2900

## Investigations

1. Historical water level recordings from three sites around the Salton Sea are being investigated to determine tectonic tilting, taking account of as many noise and error sources as possible.
2. The tectonic tilt so derived is being carefully compared with leveling data from the area.
3. LDGO-designed pressure-sensor gauges at five sites around the sea are being used to measure water level continuously, to investigate noise sources, to determine the level of detectability of tectonic tilt signals in the data, and to measure tectonic tilting.

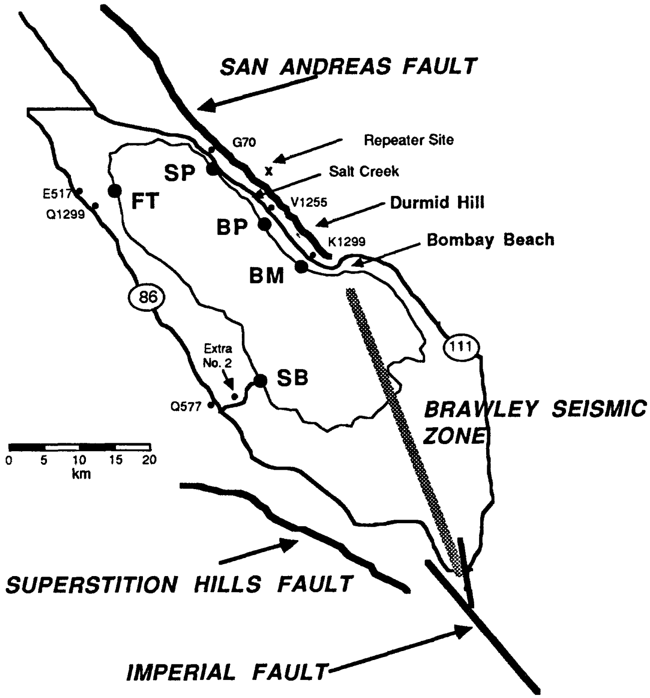

Figure 1. Map of the study region, showing the tectonic setting and the sea-level gauge network. Historical sea-level data have been collected at FT and SB since 1950, and at SP since 1970. Continuous recording pressure gauges have operated at SP since May 1985, at SB since January 1986, at BP since December 1986, and at BM and FT since May 1987. The pressure gauge data are digitally telemetered, via the repeater site shown, to SP. There they are stored on disk, and can be accessed by modem. Datum control of the sea level gauges has been provided by leveling them to nearby NGS benchmarks; clockwise from SP, these are G70, V1255, K1299, Extra No. 2 and Q1299. P. Williams' trenching site across the San Andreas is at Salt Creek. The SB to FT baseline length is 35 km, FT to SP is 14 km.

**Results** (as of April 30, 1988)

We now have a final version of the 1952-87 tilt as recorded by the Salton Sea water level gauges. This follows 1987 leveling between the third gauge (FT) and 1st order benchmarks, in order to check gauge stability. (We leveled to the other two gauges in 1986.) We detected several cm subsidence near FT, which changes the post-1980 tilt history that we reported previously [e.g., *Beavan,* 1987]. However, the pre-1980 tilt is not significantly affected, and our disagreements with the results of *Wilson and Wood* [1980] still stand.

*Gauge Stability*

We searched all the original notes from leveling and gauge maintenance that were provided to us by the gauge operators. Our findings and the corrections made to the data are summarized below. Plots of the correction curves derived from the leveling are shown with the uncorrected water level data in Figure 2.

The corrections to the SB data are as follows: (1) The gauge subsided 3.72 cm between local levelings in 1966 and 1973, and the datum was subsequently raised by 3.72 cm in January 1974. This reset of the datum is clearly recorded in the USGS field notes. We have corrected the observed water level data by assuming that subsidence occurred at a constant rate between 1966 and 1973. (2) Leveling to the SB gauge in 1956 and 1986 shows that the local benchmarks subsided 2.6±0.3 cm between 1956 and 1986 relative to a 3 km distant benchmark in bedrock. We assume the bedrock benchmark remained stable between 1956 and 1986, and correct the data by assuming subsidence of the local benchmarks at a constant rate. Such subsidence is not unreasonable as the local marks are sited on concrete plinths in a swamp that formed as the water level has risen since the 1940's.

Redundancy of staff gauge data at FT prior to 1970, and local leveling at FT in 1956, 1962, 1964 and 1976, show stability of the FT gauge to better than 1 cm prior to 1976. Leveling in 1980, 1984 and 1987 shows an accelerating subsidence of the gauge and the local benchmark array, amounting to about 4 cm since 1980, relative to a benchmark on a 1st order level line ~3 km away. The onset of subsidence coincides with the start of irrigation in the area near the gauge, and we think these events may be causally related. Using the leveling data, the FT water level data can be accurately corrected, provided that the remote benchmarks have remained stable since 1980.

Since installation in 1970, the SP gauge has been stable to ±0.5 cm relative to local benchmarks, after correction for a 9.0 cm offset after January 1980. This was caused when the gauge was moved and was leveled to a benchmark with an inaccurately known height.

*Tilt from Water Level Data*

In order to find the apparent tilt between two water level recording sites, the water level at one site is subtracted from the level at the other. Figure 2 shows the interpolated, uncorrected water level difference between sites FT and SB and the corrections applied to each data set from the leveling. The FT corrections do not significantly affect *Wilson and Wood's* analysis, but the offset at SB in 1974 was not removed by them from the raw data. Our processing of the uncorrected data agrees closely with *Wilson and Wood's* after allowance is made for the stronger smoothing that they adopted. However, when the correction series are added, the resulting water-level difference curve, shown at the bottom of Figure 3, is substantially different. We use this corrected curve to infer the ground tilt. Figure 4 shows the corrected tilt versus time curves for the three water level baselines, after low-pass filtering. The short data gap in 1974 (seen in Figure 2) was filled with a straight line before filtering.

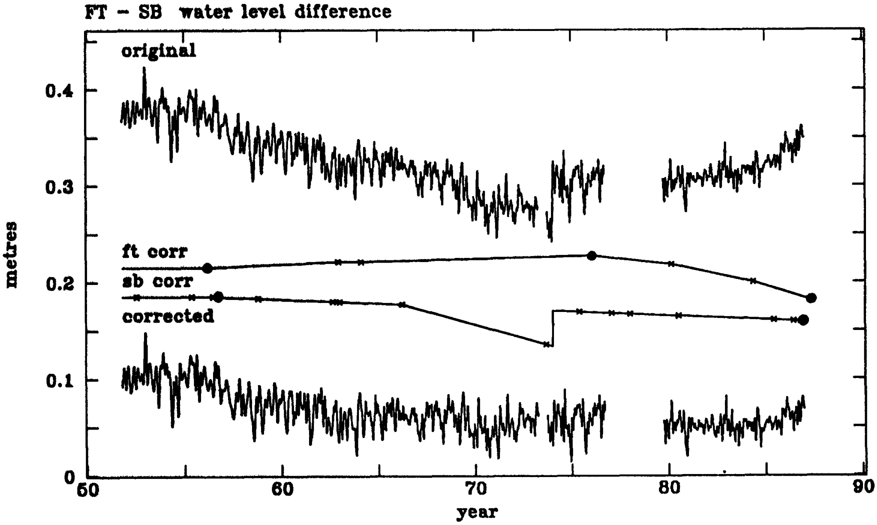

Fig. 2. **(top)** Difference between observed water level records at sites SB and FT. These are obtained by fitting smoothing splines to the unevenly sampled, low resolution raw data, and differencing the resulting evenly sampled series. The obvious step in January 1974 is not tectonic, but is due to a resetting of the SB gauge at that time. This step was left in the data analysed by *Wilson and Wood* and is the cause of the early-1970's tilt reversal that they infer from the data. **(middle)** These two traces show the corrections that should be added to the individual water level series, based on 1956-1987 leveling from the gauges to local benchmarks, and to somewhat more remote 1st order benchmarks. The crosses indicate times of local leveling, and the dots indicate times of remote tie-ins. One major correction is for the resetting of SB in January 1974 when the gauge was found to have subsided with respect to the local benchmarks. We infer that the subsidence was due to sinking of the wooden pier on which the gauge was mounted at the time. To correct the data, we assume that the sinking occurred linearly between the previous leveling in 1966 and the 1973 leveling when it was discovered. The other major correction is due to accelerating subsidence in the vicinity of FT since the late 1970's. This has only recently been quantified by our 1987 leveling to NGS 1st order benchmarks. **(bottom)** The final water level difference estimate after the corrections are added. Note that we have not attempted to decipher the gauge leveling prior to 1956. The curves are offset vertically for clarity. Tick marks on the time axis are at the start of the labelled year.

The data of Figure 4 show down to the south-east tilt from the mid-1950's to ~1970. A high tilt rate from the late 1950's to early 1960's of ~0.2 μrad/yr is followed by a decreasing tilt rate until ~1970. Our analysis indicates that pre-1970 tilting is most likely tectonic, since we cannot explain it in any other way. From ~1970 to ~1985, very little tilt occurred. Since ~1985, some apparent subsidence of FT has occurred. We suspect that this represents slight errors in our correction of the observed subsidence since 1980 at FT, rather than tectonic tilt.

Our different techniques decrease the change in tilt rate that *Wilson and Wood* inferred prior to the 1968 Borrego Mountain earthquake. They claimed an increase in tilt rate from 0.1 μrad/yr to 0.4 μrad/yr in late 1967. Though it is possible to see in the data an increase in tilt rate at this time, many other fluctuations of similar period and magnitude occurred between 1951 and 1987, with no apparent tectonic significance. The datum corrections at SB and FT, particularly the January 1974 correction at SB, cause the tilt reversal reported by *Wilson and Wood* to disappear. They proposed a late 1972 tilt reversal associated with development of the southern California uplift, but our analysis denies this possibility.

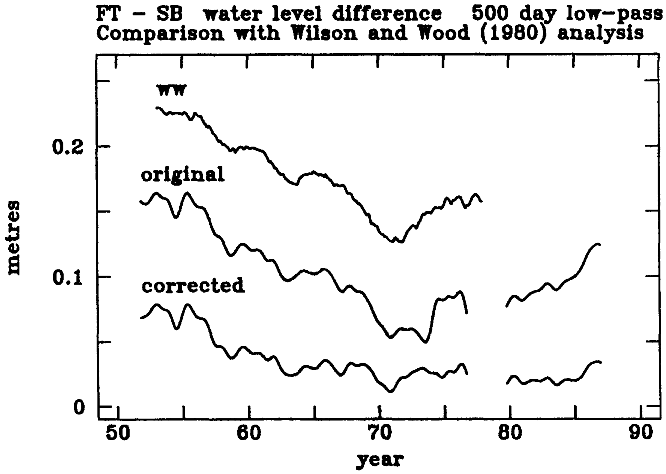

Fig. 3. Water level difference history along the SB to FT baseline. (top) as published by *Wilson and Wood* [1980]. (middle) our analysis of the identical (uncorrected) data set used by *Wilson and Wood.* (Our data extends several more years.) (bottom) our preferred analysis, including the corrections discussed in Figure 2 and the text. The four-month gap in 1973, seen in Figure 2, has been filled with a straight line segment before filtering. The curves are offset vertically for clarity. Tick marks on the time axis are at the start of the labelled year.

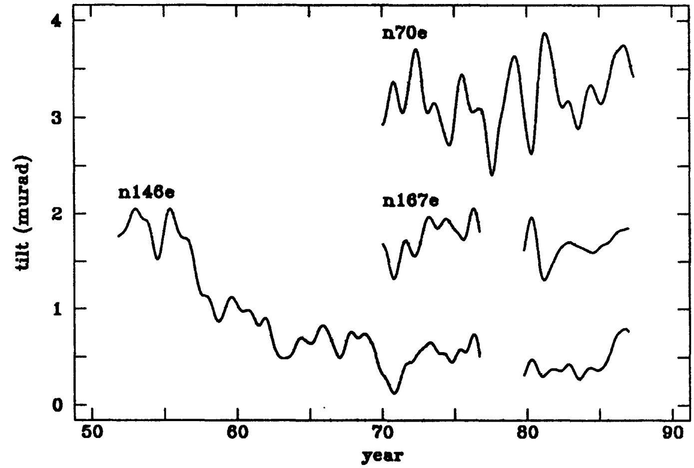

Fig. 4. Ground tilt history deduced from three water level sites around the Salton Sea. The original water level data have been corrected as discussed in the text, filtered with a zero-phase Butterworth low-pass filter with a corner frequency at 500 days, and divided by baseline length to give tilt. The N70°E data are noisier because the baseline is much shorter. Tilt rate on the N146°E baseline is highest in the late 1950's, then decreases from ~0.2 μrad/yr to < 0.1 μrad/yr in the mid-1960's. Since about 1970, there has been no significant tectonic tilt. Apparent tilt since ~1985, indicating subsidence of FT relative to the other two gauges, is probably not tectonic, but rather the result of irrigation-induced subsidence near the FT site. Note that the larger than average noise during 1980 on the N70°E and N167°E baselines results from unusually noisy data at SP. Tick marks on time axis are at start of labelled year.

There were several moderate to large nearby earthquakes during the period of this study; on March 19, 1954 (M=6.2), on April 9, 1968 (M=6.4), on April 28, 1969 (M=5.8), on October 15, 1979 (M=6.6), and on April 26, 1981 (M=5.6). Also, a few months after the end of the data used in this study, the November 1987 Superstition Hills earthquake sequence occurred (M=6.2 and M=6.6). The tilt signal does not appear to be related to these earthquakes.

### *Comparison of Sea Level and Leveling Data*

Repeated leveling data taken over approximately the same baselines as the sea level observations should provide an independent estimate of tilt. Data from leveling surveys in this region have been previously reported [*Wilson and Wood,* 1980; *Castle et al.,* 1984; *Gilmore,* 1986]. We recalculated tilt by linear regression on the observed National Geodetic Survey (NGS) leveling profiles, using data only from surveys that used non-magnetic leveling instruments.

Table 1 shows leveling results from lines on both sides of the Salton Sea. Relative subsidence in the south-east is shown by the west-side levelings in 1956.1, 1969.1, 1974.5, and 1978.2. The tilt rates derived from leveling and sea level differ, with leveling consistently giving higher tilt rates. Both the 1974 to 1976 and the 1976 to 1978 levelings on the east side of the Sea show relative subsidence to the south-east by similar amounts. There is very poor agreement between leveling and sea level derived tilts for this period, with the leveling showing substantially larger tilts. The estimated random error for first order, class II leveling is ≈0.16 μrad for the ≈20 km "west side" leveling profile, and ≈0.13 μrad for the ≈30 km "east side" profile. Therefore, the leveling derived tilts for 1974.3 to 1976.5 are only marginally significant at the 2 sigma level, but the 1976.5 to 1978.2 leveling derived tilts are significant.

If the leveling derived tilts are real, these signals should be seen in the sea level data, as they are well above the noise level in the sea level data (Table 1). The fact that we do not see these tilts leads us to mistrust the larger tilt signals from leveling, even though most of the leveling signals are well above estimated random errors for leveling.

TABLE 1. Comparison of Tilt Derived from Water Level Differences and from Leveling

| | Leveling Derived[1] | | Water Level Derived[2] | |
|---|---|---|---|---|
| Survey Dates | Tilt (μrad) | Correl. Coeff. | N146°E tilt (μrad) | N70°E tilt (μrad) |
| West Side | | | | |
| 68.9-56.1 | -1.5±0.23 | .75 | -1.02±0.15 | |
| 74.5-68.9 | -0.6±0.23 | .47 | -0.23±0.15 | |
| 78.2-74.5 | -1.1±0.23 | .81 | -0.09±0.15 | |
| East Side | | | | |
| 76.5-74.3 | -0.6±0.19 | .85 | 0.18±0.15 | 0.23±0.38 |
| 78.2-76.5 | -1.0±0.19 | .98 | -0.23±0.15 | -0.10±0.38 |

Tilt down towards the south is negative; down towards the east is negative.

[1] Errors are 1 s.d. based on prescribed 1st order leveling errors.

[2] Errors are 1 s.d. estimated from noise in water level data.

If there is localized tectonic tilting or non-uniform tilting outside the sea level gauge network, a discrepancy between leveling and sea level will be seen because the baseline locations are not identical. The "west side" leveling baseline roughly parallels the SB-FT sea level baseline, but is shorter. The "east side" leveling baseline trends about 30° oblique to the SB-FT sea level baseline, and is ≈15 km further NE. Since active faults tend to follow the basin margins in this region, it is also possible that the larger tilts seen by leveling actually result from local tilting near faults. This may be particularly true for the level route on the NE shore of the Salton Sea, as this closely follows the San Andreas fault.

In conclusion, the large leveling-derived tilts deduced from the east-side leveling data may be explained away as local effects. However, the discrepancies between the sea level and west-side leveling, particularly since 1969, point either to errors in the leveling, or to markedly non-uniform tilting.

*Instrumental installations*

The water level data are sampled every 12 minutes, and are digitally transmitted to a central recording site every hour. The system is now accessible by modem and data are transferred to Lamont on a daily basis. This allows us to process the data quickly, and to identify technical problems within a day of their occurrence so that they can be corrected in a timely fashion.

Arrays of local benchmarks and a staff gauge have been installed and measured near all five instruments. These are used to check gauge elevations at every visit, at least once per year. All five sites have also been tied to somewhat more remote benchmarks on the main leveling routes; these ties will be repeated every few years to check the stability of the local array.

The longest water level difference series, between sites SB and SP, is plotted in Figure 5. The large short-term excursions in the difference data, especially in Dec. 1987, are due to very rapid temperature changes in the lake. The effects of temperature and salinity on the difference data are rather unimportant in the long-term (> several weeks) for which these data are most suited [*Beavan,* 1987]. Atmospheric pressure variations have an insignificant effect at periods above a few days. SP and SB difference data from Jan 1986 to Dec 1987 define a tilt rate of 0.1 - 0.2 µrad/yr down towards the south, with an estimated error of about the same magnitude. This is somewhat larger than the 1970-86 rate from the historical data, but it agrees within the errors.

No obvious tectonic signal was associated with the Superstition Hills earthquakes (Figure 6). Dislocation models show that the maximum differential uplift between any pair of sites was only 3 mm. Given the size of the seiche in the sea, it is not surprising that this uplift cannot be unambiguously identified in the sea level signals. However, there may be an indication of a few mm of ground subsidence at SB at the time of the second quake.

The first quake caused up to 10 cm of horizontal NE-SW motion of the sea bed and excited a substantial transverse seiche. The start of Figure 6 shows the normal situation in the Salton Sea, with the 3 hr longitudinal seiche dominant and only a very small component of the 40 minute transverse seiche. The transverse seiche is strongly excited at the time of the first quake.

## References

Beavan, J., 1987. Tectonic Tilt Measurement: Salton Sea, USGS Open File Report, 87-374, 215-222.

Castle, R., M. Elliot, J. Church, and S. Wood, 1984. The evolution of the southern California uplift, 1955 through 1976, U.S.G.S. Prof. Paper, 1342.

Gilmore, T., 1986. Historic vertical displacements in the Salton Trough and adjacent parts of southeastern California, U.S.G.S. Open-File Report, 86-380.

Wilson, M.E. and S.H. Wood, 1980. Tectonic tilt rates derived from lake-level measurements, Salton Sea, California, Science, 207 (11 Jan), 183-185.

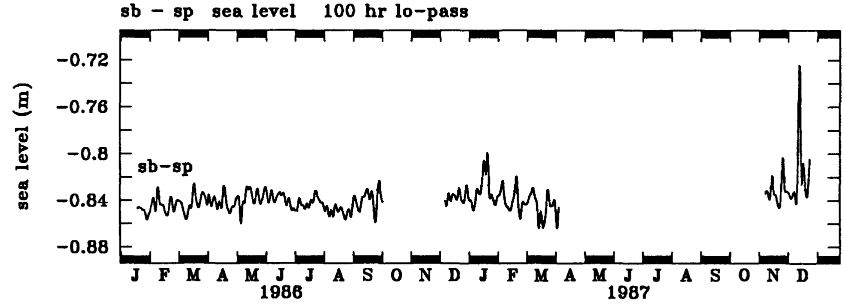

Figure 5. Sea-level difference between sites SB and SP, low-pass filtered with a zero-phase Butterworth filter with corner frequency 0.01 c/hr (≈4 days). Sea level differences typically have rms amplitudes of about 1 cm. The SB-SP data define a ground tilt down to the south of 0.1 - 0.2 µrad/yr. Some large short-term excursions, especially in Dec. 1987, are temperature effects.

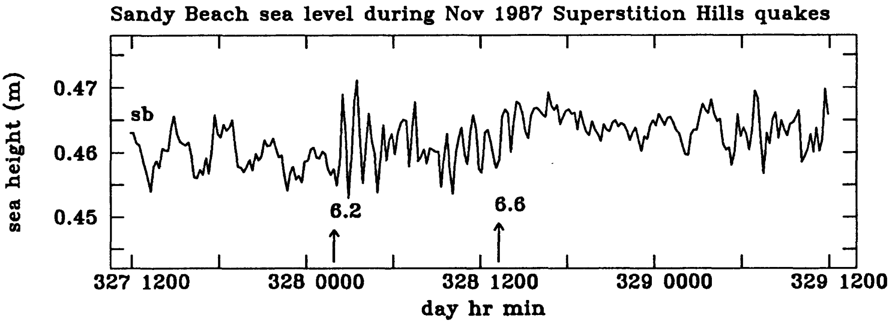

Figure 6. SB record during the November 1987 Superstition Hills earthquakes. SB is the closest station to the earthquakes. Note the record before the earthquake with the ubiquitous 1 cm, 3 hr period, longitudinal seiche, and with a tiny 40 min period transverse seiche superimposed. The first earthquake, with its several cm south-westerly motion of the sea bed, strongly excited the transverse seiche. There is a suspicion of 3 mm ground subsidence at the time of the second quake.

# Earthquake Prediction Research in the Anza-Coyote Canyon Gap

14-08-0001-G1373

Jonathan Berger and James Brune
Institute of Geophysics and Planetary Physics
Scripps Institution of Oceanography
University of California, San Diego
La Jolla, CA 92093
(619) 534-2889

## Introduction

A one-dimensionally varying velocity structure has been found for P-wave velocity and S-wave velocity in the upper 25 km of crust in the Anza region. Station correction terms for P-wave and S-wave velocities show a region in the north and east of the study area where paths are fast and a region in the southwest where paths are slow. The P-wave station corrections are on the order of .15 seconds and the S-wave station corrections are on the order of .3 seconds. The S and P corrections correlate well in sign and relative size, despite the fact that the models differ considerably from a constant $V_p/V_s$ ratio with depth.

## Data

P-wave and S-wave arrival times from the 10 Anza Network stations and 12 of the Caltech SCARLET Array stations were used. The data set consisted of 4472 P-wave arrival times and 2135 S arrivals. The majority of the S picks came from Anza stations since Caltech does not routinely pick S-wave arrivals. Only picks with quality 0 or 1 were included. The data were weighted taking into account the fact that lateral heterogeneity causes variations in traveltimes much greater than the expected picking error of .01 to .05 seconds. The data recorded at each station were weighted by the standard deviation of the residuals at that station, calculated from the starting locations. The standard deviations were typically on the order of .06 seconds for P-waves and .12 seconds for S-waves. These assumed errors turned out to give an accurate description of the residuals that resulted from the final model. P and S velocities at the surface were constrained to be 5.24 ±.02 km/sec and 2.84 ±.02 km/sec respectively, average values for borehole measurements at two of the sites (Joe Fletcher, personal communication).

## Method

The simultaneous earthquake location and velocity inversion follows the method of Pavlis and Booker (1980) and Spencer and Gubbins (1980), where projection of the data onto the nullspace of the earthquake location parameters renders the velocity inversion insensitive to perturbations in earthquake location and reduces the size of the matrix inversion problem. One by one, earthquakes are located using both P and S arrivals, and the derivatives of P-wave traveltime with respect to the 10 P velocity nodes and 22 station corrections are calculated, projected, and accumulated in the perturbation matrix. A similar perturbation matrix is constructed using the S-wave traveltimes. After relocating all the events, the two velocity perturbation matrices are inverted separately. The solution vectors are cast as differences between consecutive model node slownesses, rather than perturbations to model nodes, so exclusion of small singular values in the matrix inversion leads to a smoothed model where the difference between consecutive model node velocities is minimized.

## Results

The final velocity model (Figure 1) and station corrections obtained follow:

| Velocity Models | | | Station Corrections | | |
|---|---|---|---|---|---|
| Depth of node | P vel (km/s) | S vel (km/s) | Station Name | P cor (sec) | S cor (sec) |
| 0.0 | 5.26 | 2.84 | TRO | -0.051 | -0.175 |
| 2.0 | 5.40 | 2.99 | CRY | 0.090 | 0.123 |
| 4.0 | 5.58 | 3.16 | BZN | 0.149 | 0.176 |
| 6.0 | 5.78 | 3.37 | KNW | -0.129 | -0.144 |
| 8.0 | 5.89 | 3.51 | WMC | 0.160 | 0.282 |
| 10.0 | 5.97 | 3.56 | SND | 0.167 | 0.445 |
| 12.0 | 6.01 | 3.58 | PFO | -0.131 | -0.272 |
| 15.0 | 6.03 | 3.59 | LVA | 0.186 | 0.411 |
| 20.0 | 6.04 | 3.59 | RDM | -0.086 | -0.177 |
| 25.0 | 6.04 | 3.59 | FRD | 0.122 | 0.135 |
| | | | PLM | 0.133 | 0.319 |
| | | | COY | 0.014 | -0.019 |
| | | | HOT | 0.080 | 0.151 |
| | | | JUL | 0.118 | -0.075 |
| | | | KEE | 0.017 | -0.046 |
| | | | LAQ | -0.176 | -0.329 |
| | | | OLY | -0.128 | -0.120 |
| | | | POB | -0.146 | -0.150 |
| | | | PSP | -0.215 | -0.318 |
| | | | SMO | -0.029 | -0.143 |
| | | | YAQ | 0.043 | 0.070 |
| | | | VG2 | -0.188 | -0.145 |

The P-wave velocity at depth is significantly different from the velocity obtained using P-wave data alone and not including station corrections (discussed in previous technical report). In that case the P velocity at depth was 6.18 km/sec. The relocated events (Figure 2) show distinctly linear trends that do not necessarily follow the surface trace of the fault. Short rupture segments are obvious running northwest to southeast just south of station KNW, and running almost north-south near station CRY. The cross sections (Figure 3) B—B′ and C—C′ show these features in profile. The depths of events south of KNW range from 15 to 22 km. The events of the Cahuilla swarm near station CRY align at 5 km depth, events below station WMC cluster at about 12 km depth, and events beneath the Santa Rosa Mountains (section D—D′) range from 7 to 17 km depth. It is interesting to note that the depths of the events found with the inclusion of S-wave data are not appreciably different from the depths found inverting with P-wave data alone, demonstrating that the dense array coverage is sufficient to obtain very accurate depths. The calculated error in depth and epicentral location, however, did decrease upon the addition of the S-wave data, as expected. The error in location was .18 km, .43 km in depth, and .04 seconds in origin time. Synthetic experiments show that for events in these three main source areas, the real locations do lie within the calculated errors.

The traveltime residuals show some variation with source area (Figure 4). The most dramatic example occurs in the S-wave residuals at stations SND, WMC and FRD, the Anza stations that are closest to the main trace of the San Jacinto fault. For azimuths that run roughly parallel to the fault trace, the residuals are large and positive, and for the rest of the paths, they are negative. This feature does not show up in the P-wave residuals.

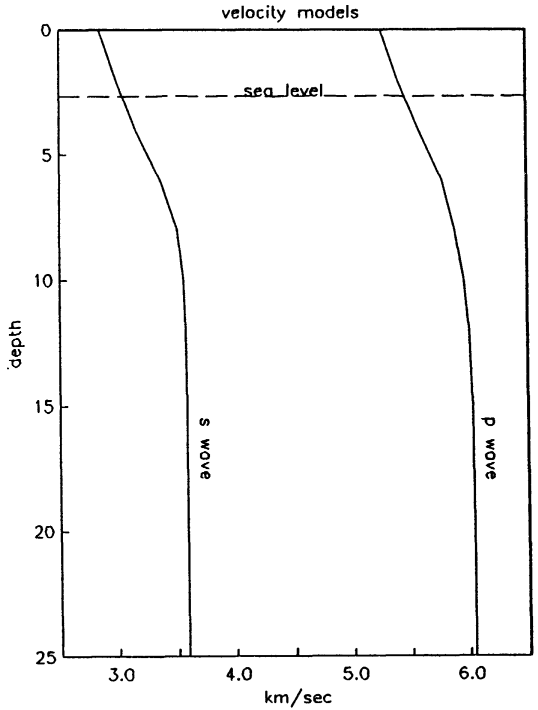

Figure 1. P-wave and S-wave velocity models resulting from the simultaneous inversion.

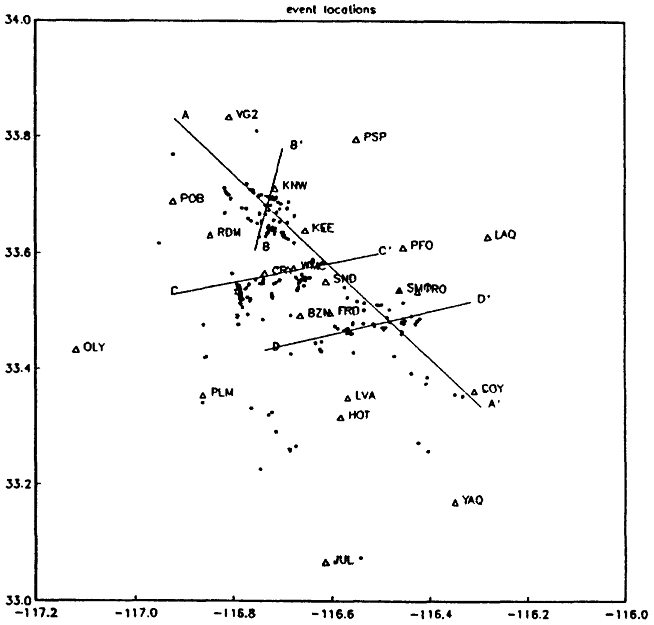

Figure 2. Event relocations using models in Figure 1. Note linear trends south of station KNW and southeast of station CRY. Cross section lines are shown.

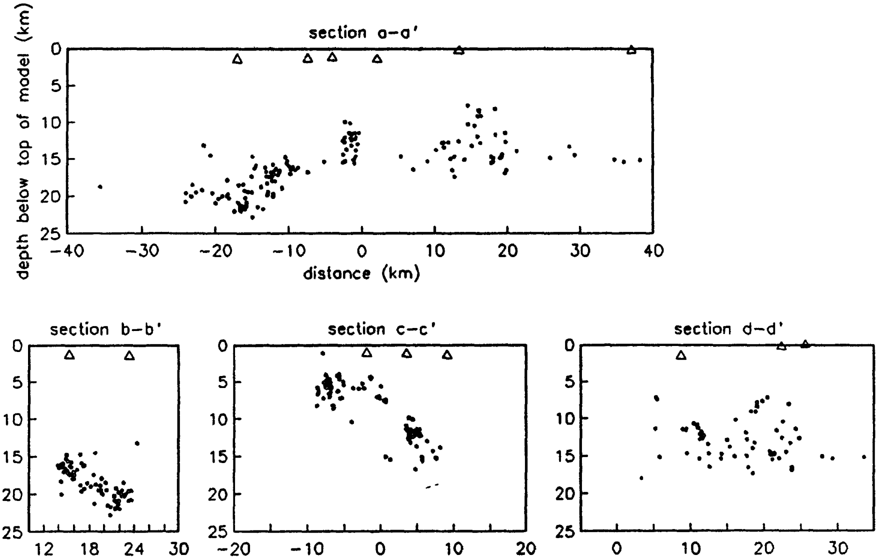

Figure 3. Cross sections showing dipping features of events below station KNW and below station CRY. Note great depth of events below station KNW in section b-b' and at the northwest end of section a-a'. Maximum projection distance is 8 km.

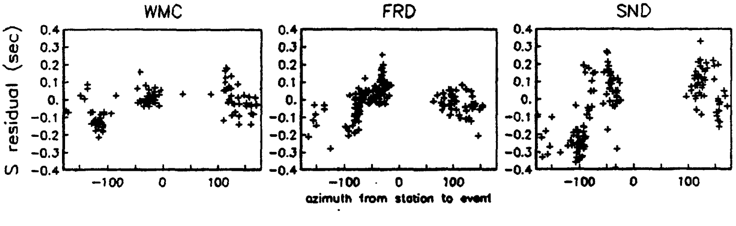

Figure 4. Plots of S-wave traveltime residual versus azimuth from the station to event for three of the Anza stations indicate a significant variation of traveltime depending on the source area. Paths subparallel to the San Jacinto Fault show larger positive residuals than other paths.

The station corrections do not correlate at all with elevation since the topographic effect was removed in the raytracing. It is encouraging that both the P and S velocity station corrections have a similar distribution and that the regions that are fast correspond to large monolithic blocks such as San Jacinto Mountain and slow regions correspond the the shallow sedimentary valley of Anza and the faulted region to the southwest (Figure 5). The features in the traveltime residuals and the large magnitude station corrections will require a laterally varying velocity structure to model accurately.

## References

Pavlis, G. L. and Booker, J. R. The mixed discrete-continuous inverse problem: Application to the simultaneous determination of earthquake hypocenters and velocity structure. *J. Geophys. Res.* **85**: 4801-4810, 1980.

Spencer, C. and Gubbins, D. Travel-time inversion for simultaneous earthquake location and velocity structure determination in laterally varying media. *Geophys. J. R. Astr. Soc.* **63**: 95-116, 1980.

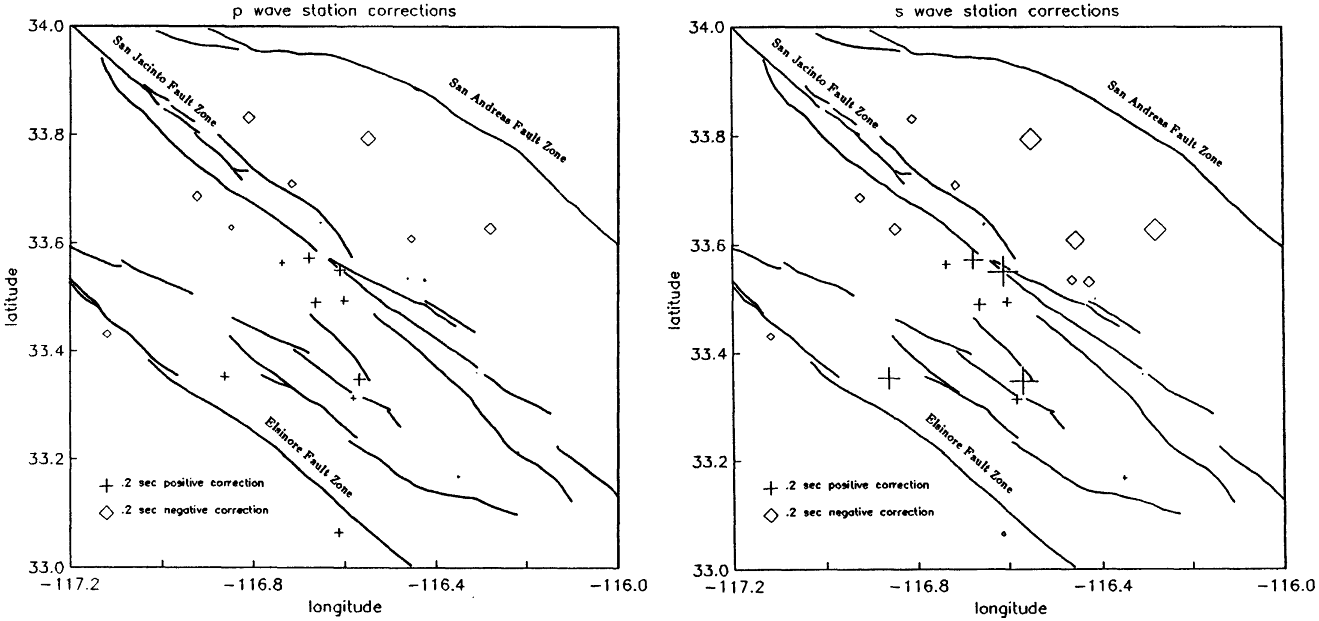

Figure 5. P-wave and S-wave station corrections. Size of symbol is proportional to magnitude of correction. Note dominantly faster region between the San Jacinto and San Andreas Fault Zones. Region between San Jacinto and Elsinore Fault Zones is dominantly slow.

# Acceleration, Velocity, and Volumetric Strain
# from Parkfield GEOS Network

9910-02089

Roger D. Borcherdt, Malcolm J. Johnston, Allan Lindh
Branch of Engineering Seismology and Geology
345 Middlefield Road, MS 977
Menlo Park, California 94025
(415) 329-5619

## Investigations

As part of Parkfield Prediction Experiment install GEOS network to acquire on-scale, broad-band, high-resolution measurements for earthquakes occurring on and near the segment of the San Andreas fault that ruptured during the 1966 Parkfield earthquake. On-scale measurements of ground acceleration for events in the preparation zone are intended for all events larger than magnitude 2. On-scale measurements of pre-, co-, and post-seismic volumetric strain are intended for all events with sensitivities exceeding $10^{-11}$ strain near 1 Hz.

## Results:

1) Installation of a 14 station network surrounding the 1966 rupture zone was completed July, 1987 by T. Noce working in conjunction with project principals, G. Glassmoyer, D. Myren and T. Burdette. Location map for stations is given in figure 1. Five of the stations are configured to record three components of ground acceleration (Kinemetrics FBA-13) together with three channels of volumetric strain (Sacks-Evertson dilatometer; 2 channels in AC coupled mode at 2 gain levels, and 1 channel in DC coupled mode). One of the stations is configured to record three components of ground velocity together with three channels of volumetric strain. Eight of the stations are configured to record three components of acceleration and three components of ground velocity. The signals from the sensors at each of the sites are being recorded with the GEOS programmed to operate in a six-channel, event trigger mode at 200 sps per channel.

2) Locations for the events recorded on the network during 1987 that occurred in the Parkfield-Coalinga area are shown in Figure 1a and those in the Parkfield area in Figure 1b. During 1987 thirty-six earthquakes that occurred within the Parkfield preparation zone were recorded. Ten of them were in the magnitude range 2-2.5 and the rest were smaller.

## Reports

See related projects for list of reports: Borcherdt, 9910-02689; Maxwell and Borcherdt, 9910-03009.

*Figure 1a. 1987*

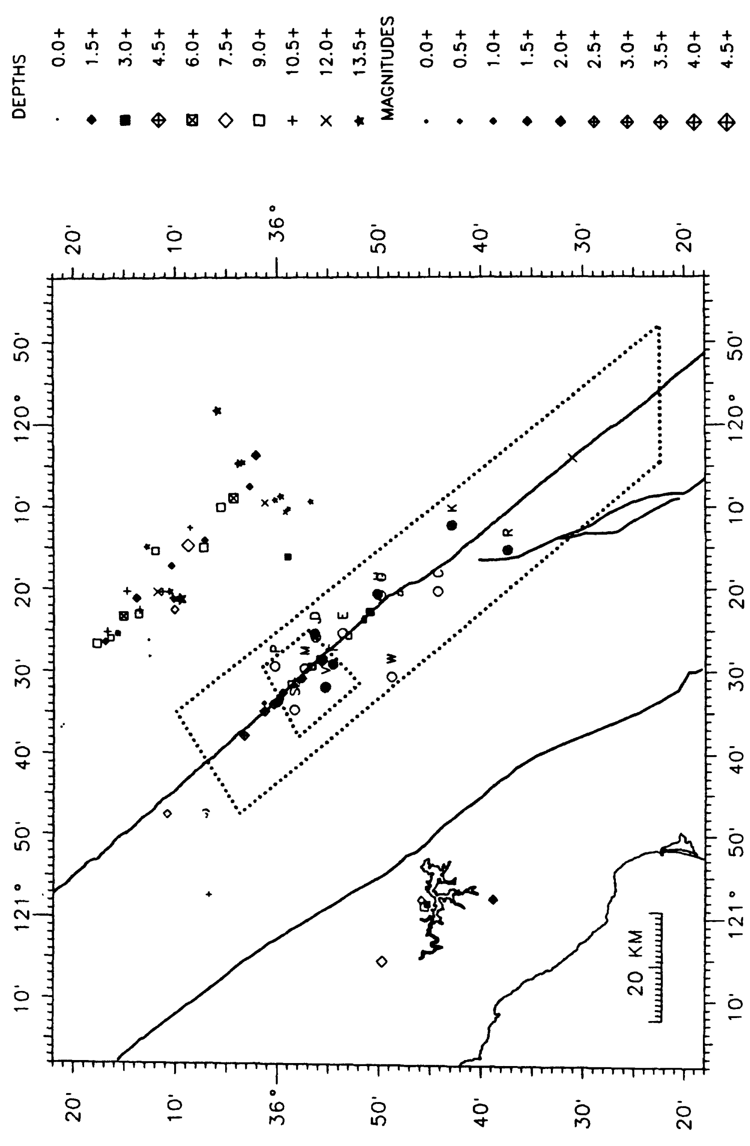

PARKFIELD - COALINGA

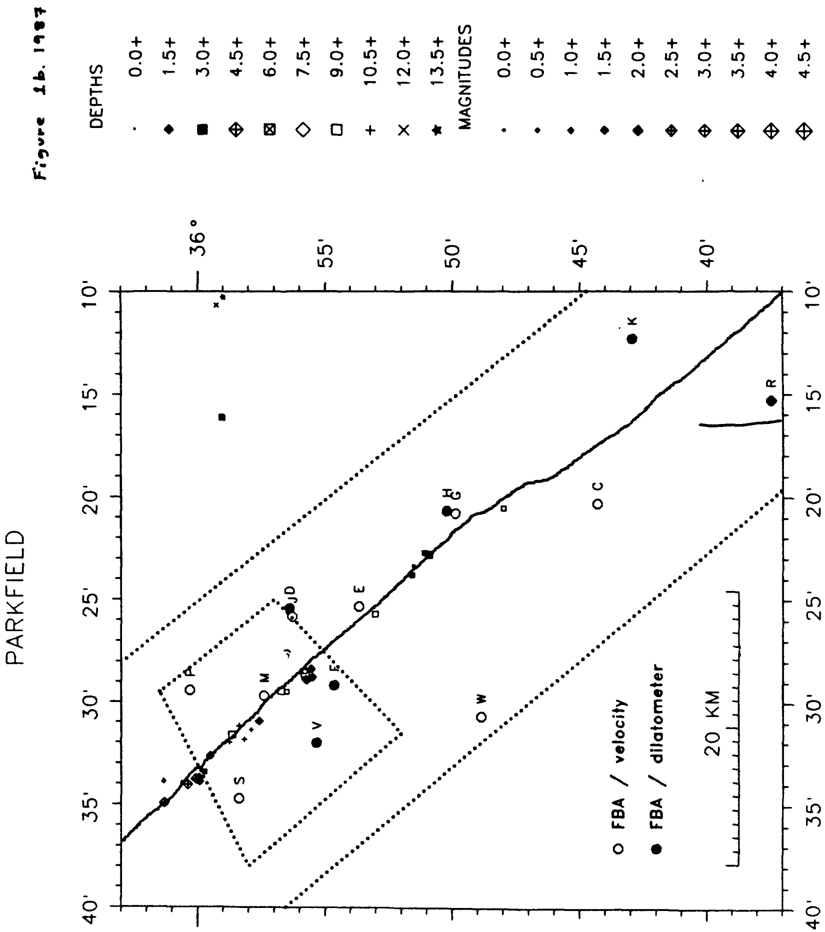

Figure 1b. 1987

# PARKFIELD TWO–COLOR LASER STRAIN MEASUREMENTS

9960–02943

Robert Burford
Branch of Tectonophysics
U.S. Geological Survey
345 Middlefield Road, MS/977
Menlo Park, California 94025
(415) 329–4850

and

Larry Slater
CIRES
University of Colorado
Boulder, Colorado 80309
(303) 492–8028

## Investigations

Operation of the CIRES two–color laser geodimeter at the Car Hill Observatory near Parkfield, California was continued during the period October 1, 1987 through March 31, 1988. Lines to permanent reflector sites that were monitored for length changes during this period are shown in Figure 1. Additional measurements were made occasionally to monumented points without permanent reflectors as well as to reference marks adjacent to the permanent reflectors.

## Results

Plots of detrended length–change histories for the 18 lines to permanent reflector points are shown in Figure 2b. The average rate of length change determined by linear least–squares approximation for each line is given in Table 1. Average station velocities relative to Car Hill for motion constrained to be parallel to the strike of the San Andreas fault zone are also given in Table 1 (negative values denote apparent left–lateral motion).

## Reports

Burford, R.O., Schulz, S.S., and Simpson, R.W., 1987, Retardations in fault creep rates before local moderate earthquakes along the San Andreas fault system, central California: pp. 845–867 in Proceedings of Workshop XXXVIII, v. II, K. Aki and W.D. Stuart, editors, *U.S. Geol. Survey Open–File Rept.* 87–591.

Burford, R.O., 1988, Retardations in fault creep rates before local moderate earthquakes along the San Andreas fault system, central California: in Intermediate-term Earthquake Prediction, W.D. Stuart and K. Aki, editors, Birkhauser-Verlag, Basel, Switzerland.

## Table 1

### Summary of Monitoring Results
### Two–Color Laser Geodimeter Network at Parkfield
### October 1, 1987 through March 31, 1988

| Permanent 2–Color Reflector Sites | Measurements Started | Location Relative to Car Hill | Average Extension Rate, mm/yr | Fault Parallel R.L. Station Velocities |
|---|---|---|---|---|
| 1. Can | 10/09/84 | 5.7 km N03°W | −06.53 ± 0.53 | 8.45 ± 0.68 |
| 2. Nore | 08/13/87 | 1.1 km N44°E | +01.73 ± 0.21 | (36.32 ± 04.41) |
| 3. Table | 10/09/84 | 6.2 km N69°E | +04.51 ± 0.62 | (12.70 ± 1.75) |
| 4. Hunt | 07/28/85 | 2.7 km S72°E | +06.62 ± 0.27 | 7.68 ± 0.31 |
| 5. Mel–S | 10/14/84 | 5.4 km S68°E | +05.51 ± 0.56 | 6.41 ± 0.62 |
| 6. Turk | 07/10/87 | 2.3 km S56°E | +08.17 ± 0.25 | 8.50 ± 0.26 |
| 7. Gold | 04/18/86 | 9.2 km S49°E | +02.90 ± 1.52 | 2.92 ± 1.53 |
| 8. Creek | 06/27/84 | 5.7 km S36°E | −03.58 ± 0.62 | 3.60 ± 0.62 |
| 9. Mason–W | 06/26/84 | 6.3 km S11°W | −04.25 ± 0.55 | 6.95 ± 0.91 |
| 10. Todd | 08/07/85 | 3.7 km S15°W | −18.38 ± 0.39 | 33.30 ± 0.71 |
| 11. Hog–S | 07/25/84 | 5.0 km S62°W | −03.06 ± 0.43 | (−12.64* ± 1.78) |
| 12. Lang | 07/25/84 | 4.1 km N72°W | +02.12 ± 0.35 | 2.44 ± 0.40 |
| 13a. Pomo | 04/29/86 | 5.6 km N51°W | −01.02 ± 0.54 | −1.03* ± 0.55 |
| 13b. Pitt** | 10/09/84 | 5.7 km N47°W | −20.96 ± 1.59 | −21.06* ± 1.60 |
| 14. Mid | 08/23/84 | 5.0 km N43°W | −03.85 ± 0.44 | −3.85* ± 0.44 |
| 15a. Mid–E | 08/21/84 | 4.5 km N35°W | +03.84 ± 0.38 | −3.87* ± 0.38 |
| 15b. Buck | 07/31/86 | 3.1 km N32°W | −07.28 ± 0.31 | 7.38 ± 0.31 |
| 16. Bare | 10/09/84 | 4.8 km N12°W | −05.18 ± 0.42 | 5.97 ± 0.48 |

Note: (*) Indicates apparent left–lateral station movement (column 5)

( ) Fault–parallel projection values in column 5 are unreliable owing to orientation of line nearly normal to fault strike.

(**) Routine measurements discontinued after June, 1986.

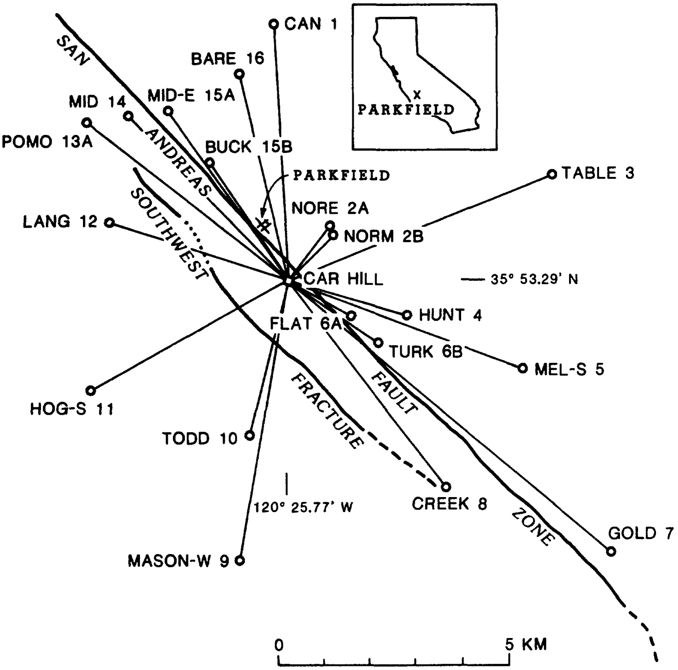

Figure 1. Two-color laser geodimeter network at Parkfield, California.

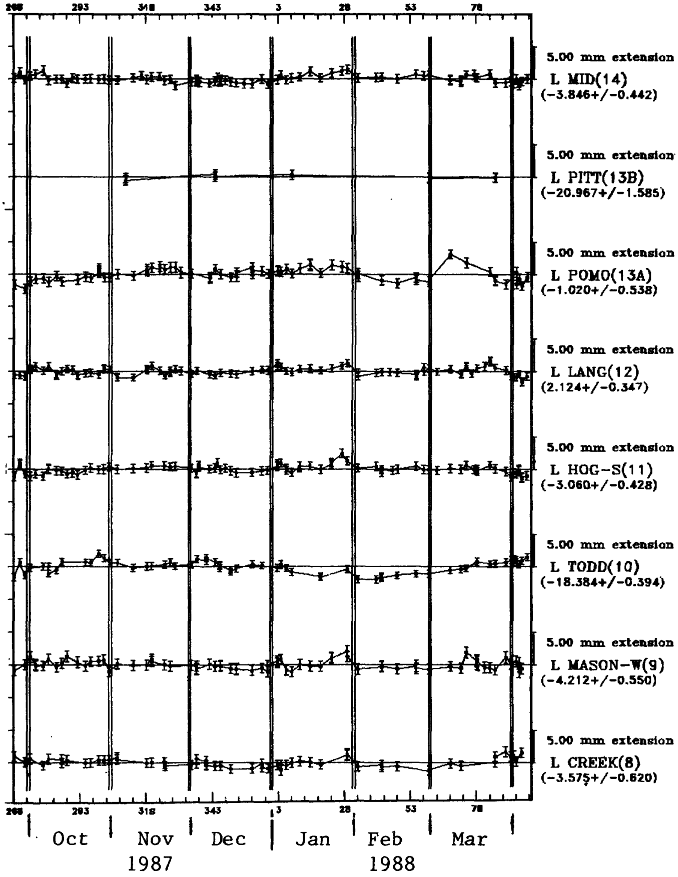

Figure 2a. Detrended 2-color geodimeter data from the Car-Hill Network, Parkfield, for lines terminating in the block southwest of the main San Andreas fault.

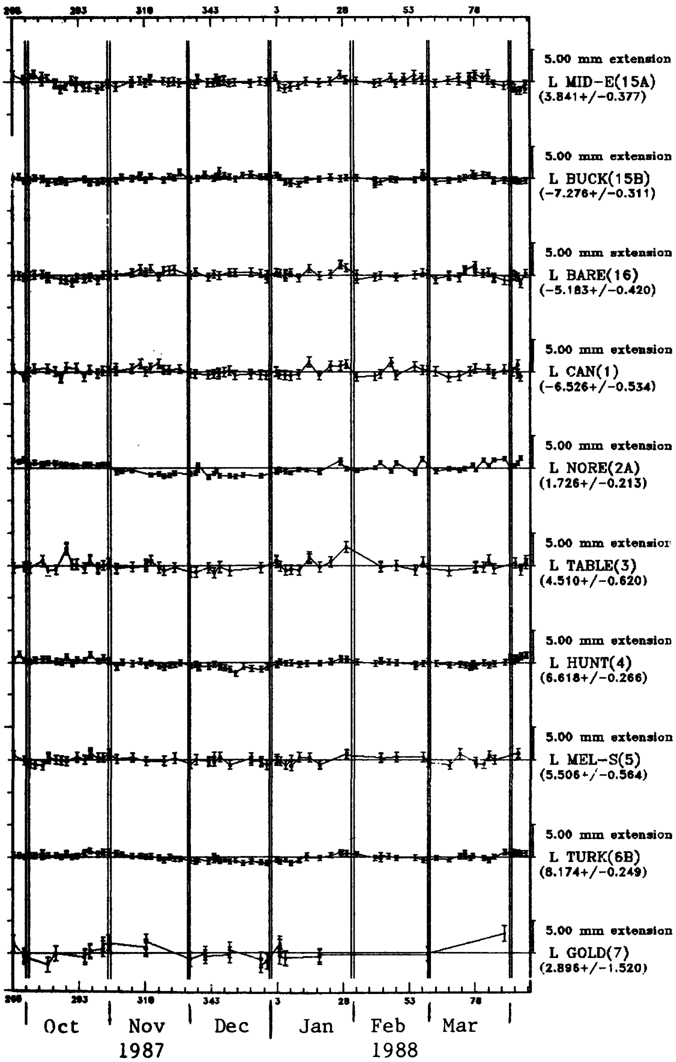

**Figure 2b.** Detrended 2-color geodimeter data from the Car-Hill Network, Parkfield, for lines terminating in the block northeast of the main San Andreas fault.

# Theodolite Measurements of Creep Rates on San Francisco Bay Region Faults

14-08-0001-G1186
Jon S. Galehouse
San Francisco State University
San Francisco, CA 94132
(415) 338-1204

We began measuring creep rates on San Francisco Bay region faults in September 1979. Amount of slip is determined by noting changes in angles between sets of measurements taken across a fault at different times. This triangulation method uses a theodolite to measure the angle formed by three fixed points to the nearest tenth of a second. Each day that a measurement set is done, the angle is measured 12 times and the average determined. The amount of slip between measurements can be calculated trigonometrically using the change in average angle.

We presently have theodolite measurement sites at 20 localities on ten active faults in the San Francisco Bay region (see Figure 1). Most of the distances between our fixed points on opposite sides of the various faults range from 50-275 meters. The precision of our measurement method is such that we can detect with confidence any movement more than a millimeter or two between successive measurement days. We remeasure most of our sites about once every two to three months.

The following is a brief summary of our results thus far.

San Andreas fault - Since March 1980 when we began our measurements across the San Andreas fault in South San Francisco (Site 10), no net slip has occurred. Our Site 14 at the Point Reyes National Seashore Headquarters has also shown virtually no net slip since we began measurements in February 1985. Our Site 18 (not shown on Figure 1) in the Point Arena area has averaged about one millimeter per year of right-lateral slip since January 1981. These results indicate that the northern segment of the San Andreas fault is virtually locked, with very little, if any, creep occurring.

Hayward fault - Since we began our measurements on the Hayward fault in September 1979 in Fremont (Site 1) and Union City (Site 2), the average rate of right-lateral slip is 4.7 millimeters per year in Fremont and 4.2 millimeters per year in Union City (see Figure 2). Since we began measuring two sites within the City of Hayward in June 1980, the average annual rate of right-lateral movement is 4.5 millimeters at D Street (Site 12) and also 4.5 millimeters at Rose Street (Site 13). Since we began measurements in San Pablo (Site 17) near the northwestern end of the Hayward fault in August 1980, the average rate of movement has been about 3.8 millimeters per year in a right-lateral sense. However, superposed on the overall slip rate are changes between some measurement days of up to nearly a centimeter in either a right-lateral or a left-lateral sense. Right-lateral slip tends to be measured during the first half of a calendar year and left-lateral during the second half.

In summary, our data show that since 1979 the average rate of right-lateral movement on the Hayward fault is about 4 to 5 millimeters per year.

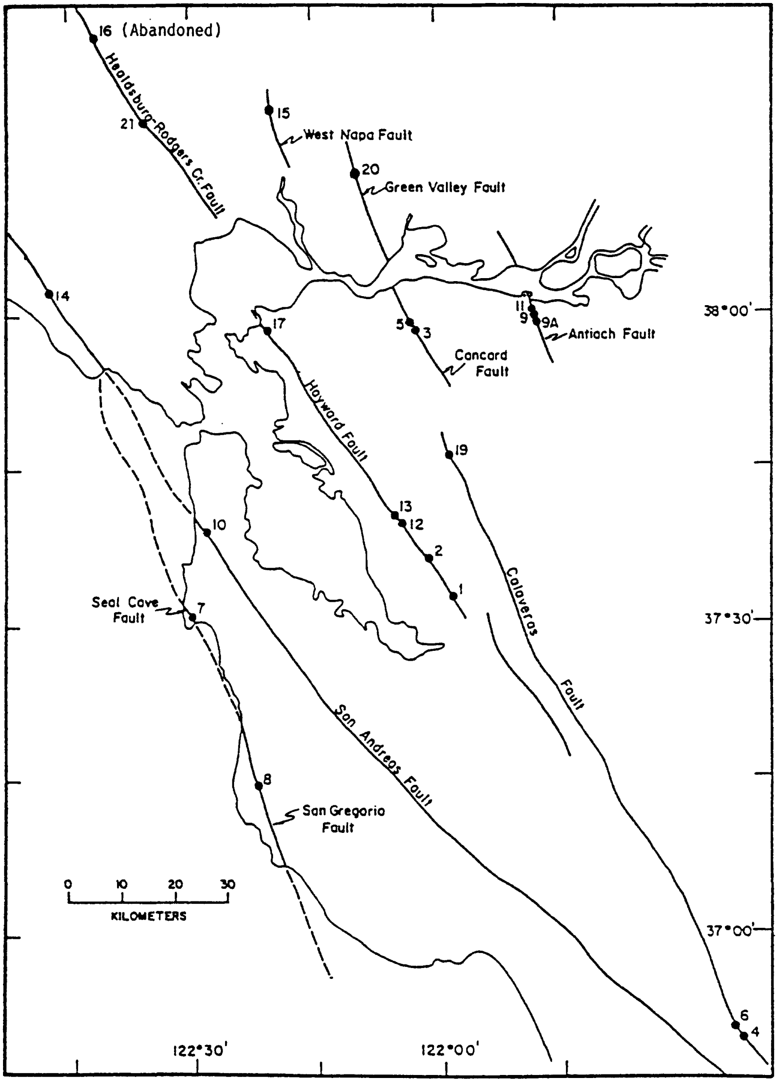

Figure 1. San Francisco State University Theodolite Measurement Sites

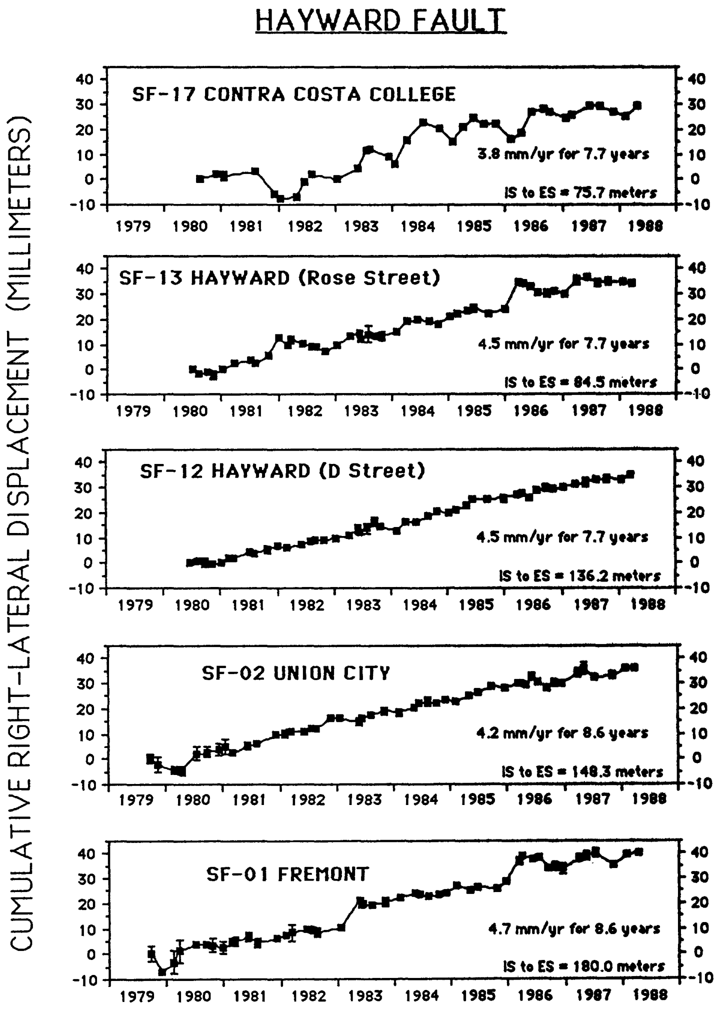

Figure 2. Hayward Fault Displacement

Calaveras fault - We have three measurement sites across the Calaveras fault and the nature and amount of movement are different at all three (see Figure 3). Since we began monitoring our Site 4 within the City of Hollister in September 1979, the average rate of movement has been about 6.6 millimeters per year right-laterally. Slip at this site is episodic, with most times of relatively rapid slip occurring early in a calendar year and little net movement occurring during the rest of the year.

At our Site 6 just 2.3 kilometers northwest of Site 4, the slip is much more steady than episodic. Since October 1979, the Calaveras fault at Site 6 has been moving at a rate of 12.1 millimeters per year in a right-lateral sense, the fastest rate of movement of any of our sites in the San Francisco Bay region.

In contrast to the relatively high creep rates in the Hollister area, our Site 19 in San Ramon near the northwesterly terminus of the Calaveras fault has shown virtually no net movement since we began measuring it in November 1980.

Concord fault - We began our measurements at Site 3 and Site 5 on the Concord fault in the City of Concord in September 1979 (see Figure 4). We measured about a centimeter of right-lateral slip at both sites during October and November 1979. Following this, both sites showed relatively slow slip for the next four and one-half years at a rate of about one millimeter per year. In late Spring-early Summer 1984, both sites again moved relatively rapidly, slipping about seven millimeters in a right-lateral sense in a few months. The rate again slowed to about a millimeter per year for about the next three years, beginnning in late August 1984. Between late November 1987 and late February 1988, the Concord fault moved about eight millimeters right-laterally. Since then the rate has again slowed down. Therefore, it appears that characteristic movement on the Concord fault since at least 1979 is relatively rapid displacement over a period of a few months alternating with relatively slow displacement over a few years. Overall, the average rate of movement since late 1979 is 4.2 millimeters per year of right-lateral slip at Site 3 and 3.4 millimeters per year at Site 5.

Other faults - The Seal Cove fault (Site 7) and the San Gregorio fault (Site 8) have shown very little net slip since November 1979 and May 1982 respectively. However, both sites often show large variations in the amounts and directions of movement from one measurement day to another.

Much subsidence and mass movement creep appear to be occurring both inside and outside the Antioch fault zone and it is probable that these nontectonic movements are obscuring any tectonic slip that may be occurring. Our Site 9A has shown about 1.5 millimeters per year of right-lateral slip since November 1982 and Site 11 has shown about 0.5 millimeters per year of left-lateral slip since May 1980.

Seasonal and/or gravity-controlled mass movement effects are also present at our Sites 16 and 21 on the Rodgers Creek fault. Both sites show large variations from one measurement day to another. Site 16 had to be abandoned in early 1986 because our line of sight became obscured. Net movement had been virtually nil for the previous 5.4 years. Our replacement site on the Rodgers Creek fault (Site 21) has not been monitored long enough for any meaningful rates to be calculated.

## CALAVERAS FAULT

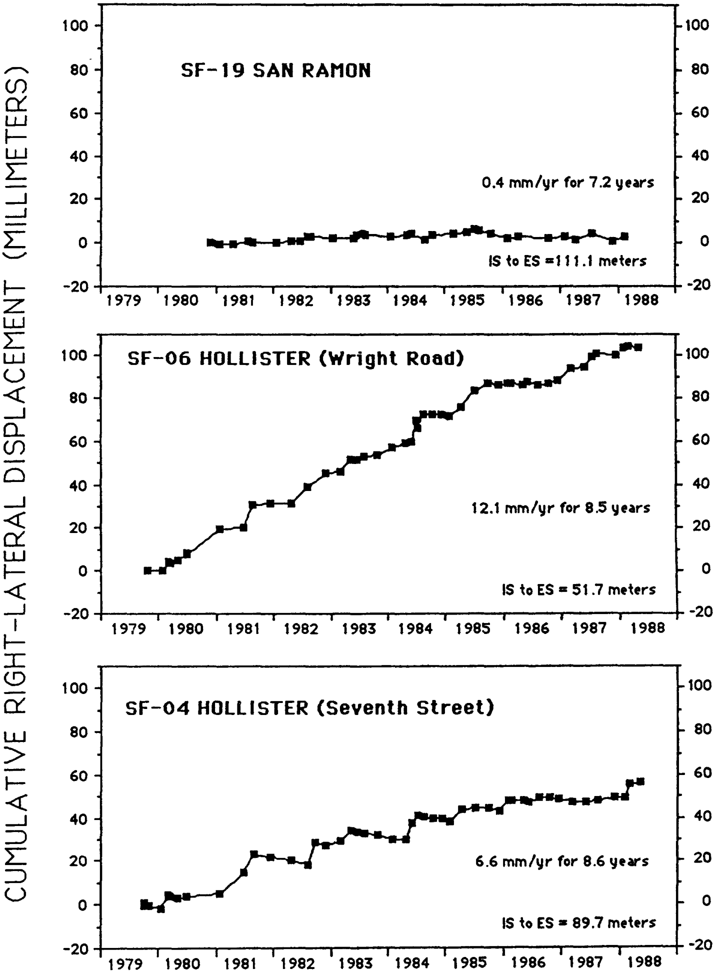

Figure 3. Calaveras Fault Displacement

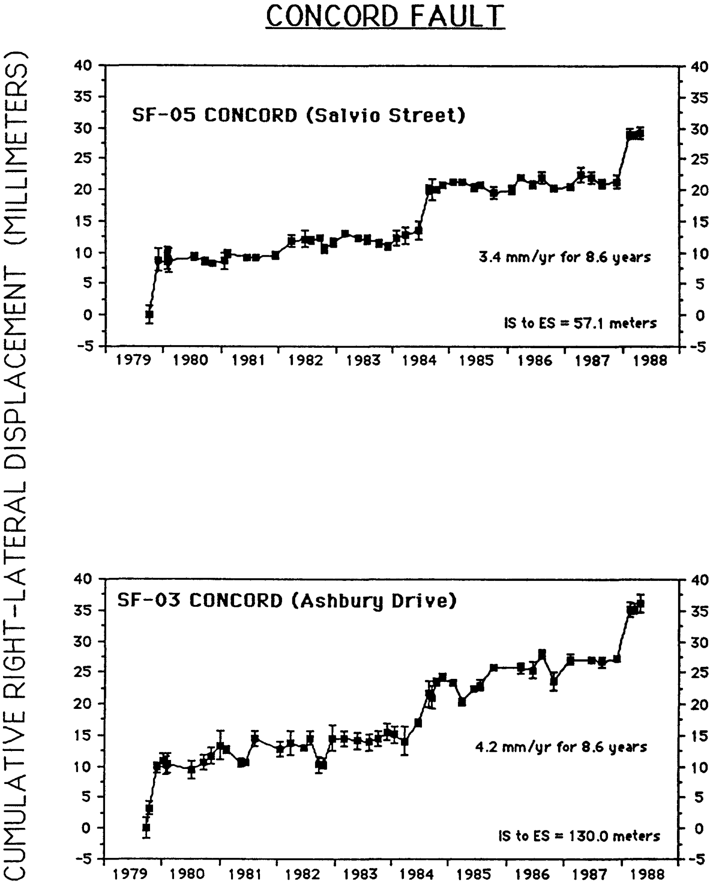

Figure 4. Concord Fault Displacement

Our Site 15 on the West Napa fault also shows large variations, but virtually no net movement has occurred since we began measurements in July 1980.

Since we established Site 20 on the Green Valley fault in June 1984, measurements show right-lateral slip at a rate of about 4.9 millimeters per year. Large variations also tend to occur here between measurement days. Preliminary results suggest that the Green Valley fault may behave similarly to the Concord fault to the southeast, i.e., relatively rapid movement in a short period of time (months) alternating with relatively slow movement for a longer period of time (years). Continued monitoring of the Green Valley fault will help confirm its movement characteristics and rate and help determine if the Green Valley fault is actually the northwestward continuation of the Concord fault.

---

1988 Publication

Galehouse, J. S., 1988, Present-day rates of movement on San Francisco Bay region faults, in Earthquake Prognostics, Hazard Assessment, Risk Evaluation, and Damage Prevention; Vogel, A. and Brandes, K., editors, Friedr. Vieweg and Sohn, Braunschweig/Wiesbaden, pp. 17-28.

1988 Abstract Published

Galehouse, J. S., 1988, Faults of the San Francisco Bay region and the causes of earthquakes, Program of the Earthquake Resistant Structures Seminar Series, San Francisco, California.

# DEEP BOREHOLE PLANE STRAIN MONITORING
# 14-08-0001-G1376

*Michael T Gladwin,*

Department of Physics
University of Queensland
St.Lucia, 4067
AUSTRALIA.

## ACTIVITIES

1. Processing of the data from the five borehole tensor strainmeters installed in California (San Juan and Pinon Flat in 1983, and DonnaLee, Eades and Frolich in 1986) has continued.

2. Instrumentation difficulties with uphole electronics led to some down time at each of the three Parkfield sites, however as of March these have been operating normally, and all five instruments are providing data with good tidal sensitivity.

## RESULTS

1. Sites instrumented in California are shown in figure 1. The 1983 installations are SJT in the north and PFT in the south. The 1986 installations "DLT", "FLT" , and "EDT" are clustered at the southern end of Middle Mountain in the Parkfield region. There are DTM Sack's-Evertson dilatometers in close proximity at each site.

2. The only geophysical signal of interest in the three years at the Pinon site is the North Palm Springs earthquake of July 8, 1986. Several interesting results have been obtained for this event. Location of the event (magnitude 5.9) is shown on figure 1. Processed Pinon Flat data is shown in figure 2. The upper plot is the computed areal strain, and the other two traces represent the two shear components $\Gamma_1$ and $\Gamma_2$.

The results have been corrected for effects of the hole, and represent the implied solid rock result. The dominant exponential curing of the expansive grout with a time constant of order six months is mapped totally into the hydrostatic term, and it is evident that after three years the hydrostatic strain plot has also reached a constant strain rate. This strain rate is evidence of the viscoelastic response of the hole due to the fact that the equivalent inclusion modulus is less than that of the surrounding rock so that a stress gradient surrounds the inclusion.

Figure 3 shows the accumulation of maximum shear strain for this site. It is clear that the constant shear strain accumulation rate indicated in the three years prior to the event is absent in the 2 years since the event. Note that there was no change in the gradient of the hydrostatic data over this time. The post event shear strain rate is now less than 100 n$\varepsilon$ per year, consistent with the long term geodetic rates reported for the area. It could be argued that there has been some change of coupling conditions at the sensor at the time of the event. No such change is evident in the tidal response after the event, and no change in the instrument calibrations have been noted. The orientation of the accumulation of maximum shear observed prior to the event is entirely consistent with failure of the Banning fault (to within 5 degrees) and it is at least plausible that the signal related to this event.

3. There have been no especially significant data from the Parkfield sites. Data for the past five months reduced to Exx, Eyy and Exy components (where x corresponds to East and y to North) are shown in Figures 4, 5 and 6 for these instruments. Maximum shear strain for each of these sites is shown in Figure 7. Despite the significant compromise in installation procedures referred to in the previous report, tidal comparisons between the sites indicate that they are providing useful strain data. Consequently procedures have been developed to provide in near real time a processed version of the tensor strain field for comparison with other instruments. These data sets are provided on a monthly basis for Menlo Park staff responsible for the Parkfield prediction experiment.

4. Hydrostatic and shear components of the San Juan data since installation are shown in Figure 8.

## PUBLICATIONS

Gladwin, M. T., High Precision multi component borehole deformation monitoring. *Rev.SciInstrum., 55*, 2011-2016, 1984.

Gladwin, M.T., Gwyther, R., Hart, R., Francis, M., and Johnston, M.J.S., Borehole Tensor Strain Measurements in California. *J. Geophys. Res. 92*. B8 pp7981-7988, 1987.

Gladwin, M. T. and Hart, R. Design Parameters for Borehole Strain Instrumentation. *Pageoph.,123,* 59-88, 1985.

Gladwin, M. T., Hart, R., and Gwyther, R. L. Tidal Calibration of Borehole Vector Strain Instruments.*EOS, (Trans. Am. G. Un.) 66,* 1057, 1985.

Gladwin, M. T. and Johnston, M.J.S. Strain Episodes on the San Andreas Fault following the April 24 Morgan Hill, California Earthquake. *EOS,(Trans. Am.G.Un.), 65,* 852, 1984.

Gladwin, M.T., and Johnston, M.J.S. Coseismic moment and total moment of the April 24, 1984, Morgan Hill and the January 26, 1986, Quiensabe earthquakes. *EOS,(TransAm.G.Un.), 67, R 308, 1986.*

Gladwin, M. T. and Wolfe, J. Linearity of Capacitance Displacement Transducers. *J.Sc.Instr. 46,* 1099-1100, 1975.

Johnston, M.J.S., Gladwin, M.T., and Linde, A.T. Preseismic Failure and Moderate Earthquakes. *I.A.S.P.E.I.* , Tokyo, August 19-30, S7-65, 35 , 1985.

Johnston, M. J. S., Linde, A.T., Gladwin, M.T., and Borcherdt, R.D. Fault Failure with Moderate Earthquakes. *Tectonophysics.* 144, 189-206, 1987.

Johnston, M.J.S., Borcherdt, R.D., Glassmoyer, G., Gladwin, M.T., and Linde, A.T. Static and Dynamic Strain during and following January 26, 1986, Quiensabe, California, Earthquake. *EOS,(Trans., Am. G. Un.), 67,* 16, 308, 1986.

Johnston, M.J.S., Borcherdt, R.D., Gladwin, M.T., Glassmoyer, G., and Linde, A.T. Static and Dynamic Strain during the $M_L$ 5.9 Banning, California Earthquake on July 8, 1986. *EOS,(Trans. Am.G.Union),68,* 44, 1244 (1987).

Myren, G.D., Johnston, M.J.S., Linde, A.T., Gladwin, M.T. and Borcherdt, R.D. Borehole Strain Array near Parkfield, California. *EOS (Trans. Am.G.Union), 68,* 44, 1358 (1987).

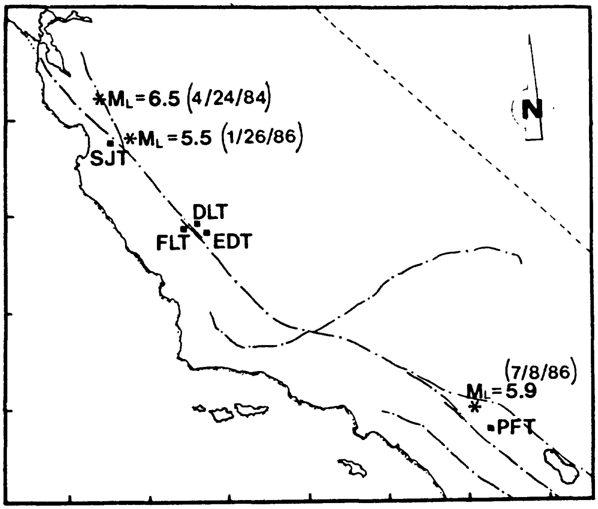

1. Borehole tensor strain sites in California. Sites EDT and FLT include facilities for downhole seismic instrumentation either in the same borehole or in another borehole within 50 meters. Earthquakes which have produced significant signals are shown by the stars.

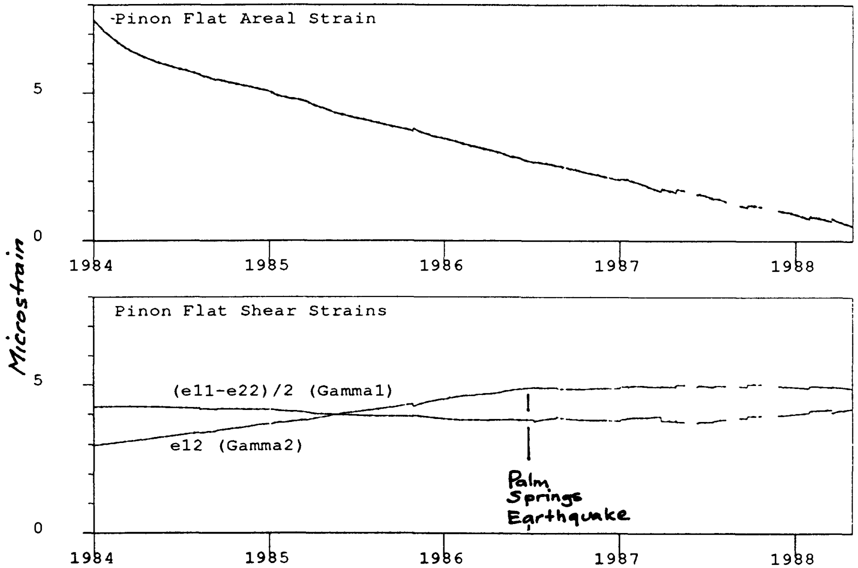

2. Areal and shear strains for the Pinon Flat site since 1983. The only significant change of shear strain gradient over the four and a half years of data occured at the July 8 1986 Palm Springs earthquake.

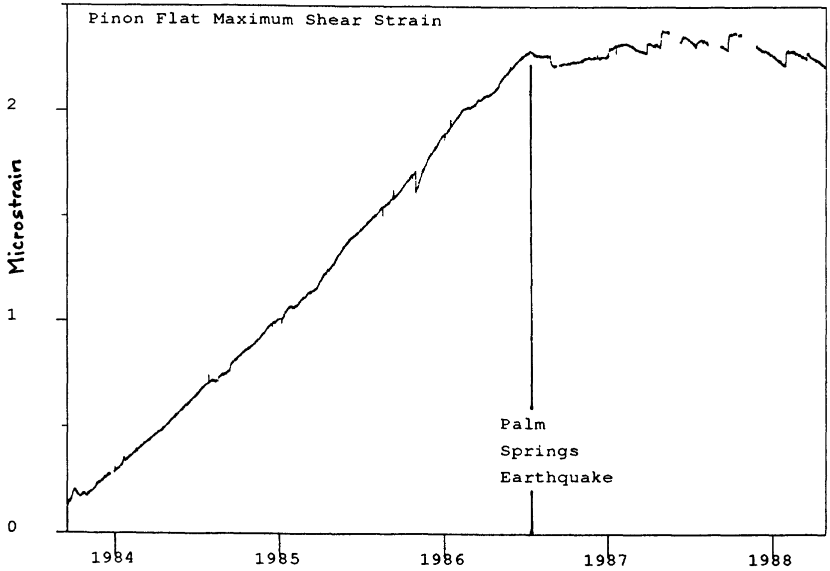

3. Change of shear strain accumulation rate associated with the North Palm Springs event. In the period since the event, the strain rate has reduced to less than 100 n$\varepsilon$ per annum consistent with the long term geodetic average rate for the area. The pre event maximum shear direction is at north 50 degrees West consistent with failure on the Banning fault.

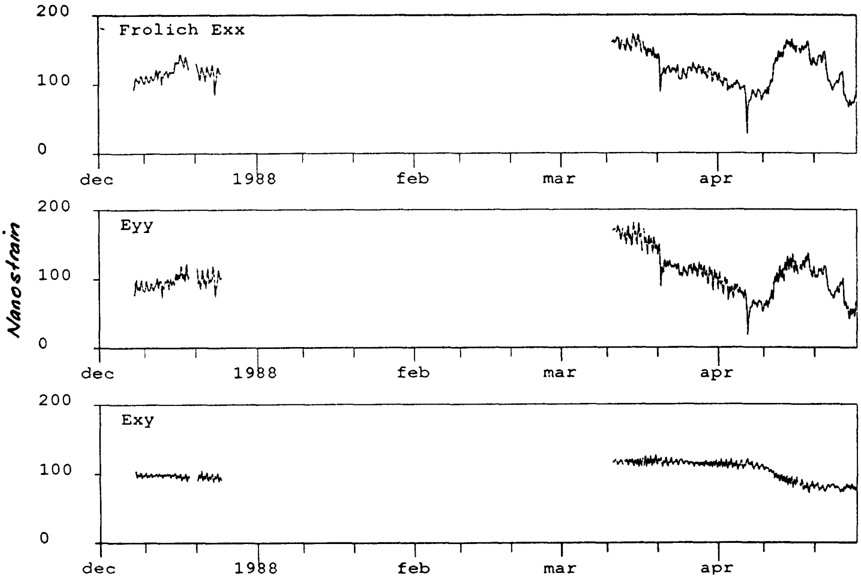

4. Strains Exx Eyy and Ezz for the site FLT since installation. Note that x = East and y = North and that a linear detrend has been removed from the data of Figures 4, 5, 6 and 7.

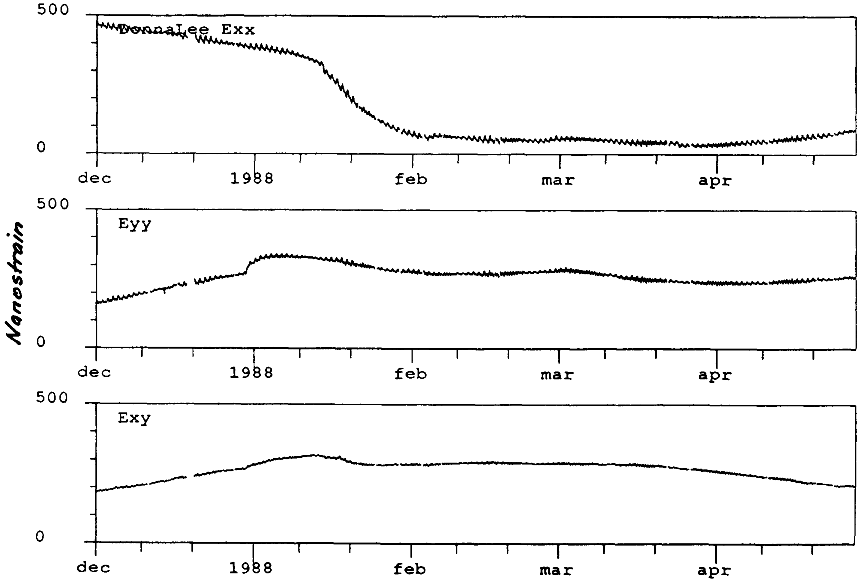

5. Strains Exx, Eyy and Exy for the site DLT since installation. The excursions in Exx and Eyy relate to effective hydrostatic response to atmospheric loading (see Figure 7 for shear response).

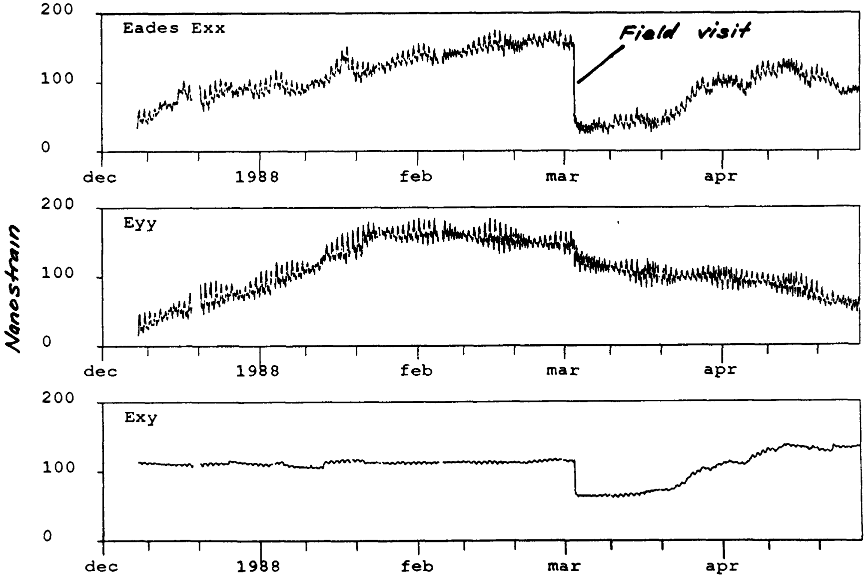

6. Strains Exx,Eyy and Exy at the site EDT. The step on March 2 is due to instrument readjustment during a field visit.

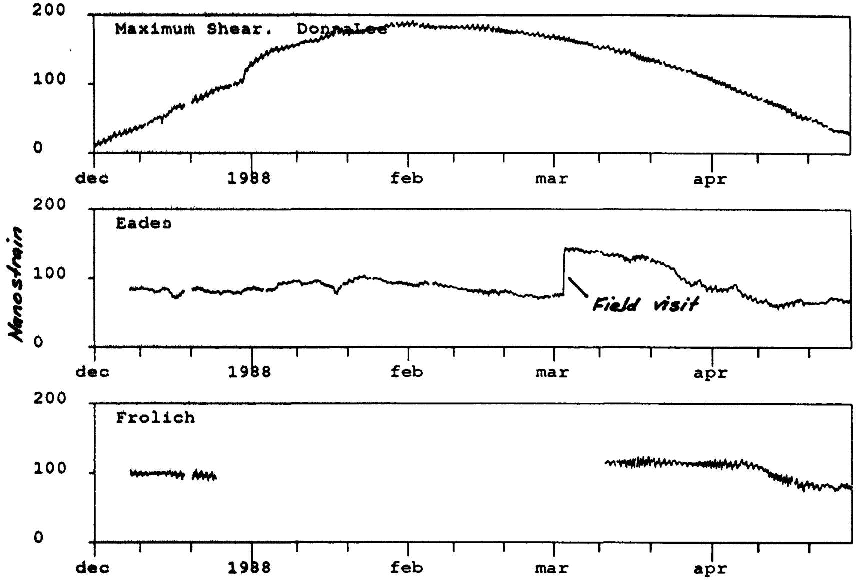

7. Maximum shear strain for the three Parkfield sites over the past five months. Note the absence of significant atmospheric response.

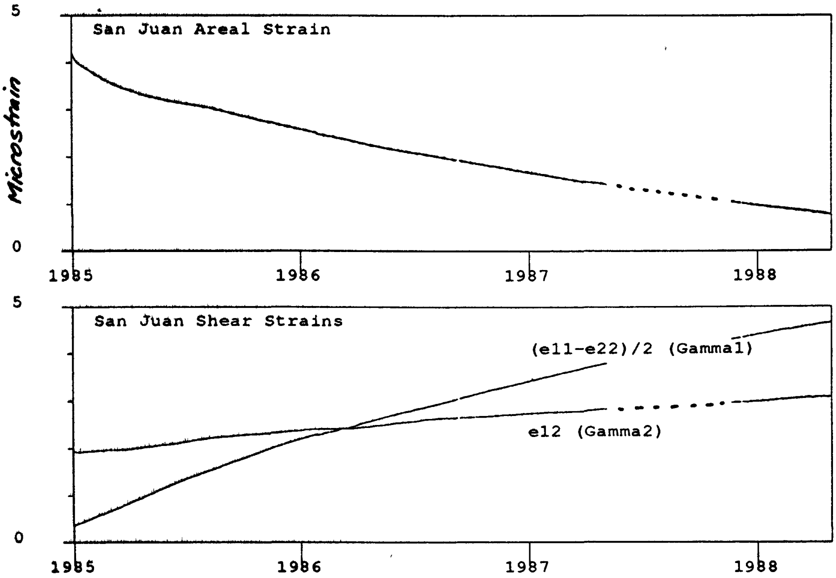

8. Areal and shear strains for the site SJT in Northern California.

# San Andreas Earthquake/Parkfield Geophysics

9380-03074

Robert Jachens, Carter Roberts, Robert Simpson, and Carl Wentworth
U.S. Geological Survey, MS's 989, 977, and 975
345 Middlefield Rd., Menlo Park, CA 94025
(415) 853-8500, x5300

## Investigations

1) Repeat precision gravity surveys were conducted in May 1987 and January 1988 and covered
   a) the southern California high-precision gravity base network
   b) a 100 km-long profile perpendicular to the San Andreas fault and passing through Cajon Pass, and
   c) the two-color laser site at Holcomb Ridge.

   Eleven years of data are now available for most sites in the precision gravity base network.

2) Measured, processed, and began modeling gravity and ground magnetic data along detailed profiles across Cholame Valley southeast of Parkfield.

3) Began modeling aeromagnetic data over Table Mountain, east of Parkfield.

## Results

1) Changes in gravity during the past 10 years at three sites along the "big bend" of the San Andreas fault in southern California were compared with newly processed leveling data from Ross Stein for the same area. Using a gravity change/elevation change relationship of -2 microgal/cm, coincident gravity and leveling data for Cajon Pass and Palmdale show good agreement over the entire period, with only one data pair out of 13 differing by more than the error bars. Equally good agreement is seen at Tejon Pass for two seperate time segments (1978-1982, 1983-1987), but a datum offset appears to have occurred in one of the data sets sometime between May 1981 and May 1983. We will be checking the gravity value at Tejon Pass relative to a number of nearby gravity stations that were last measured in 1978 to determine whether the offset is the result of some local phenomenon that affected only the Tejon Pass station.

2) Gravity models were constructed for five profiles oriented approximately normal to the San Andreas fault and spaced approximately 1.6 km apart. The northernmost profile crosses Cholame Valley at about the location of the Jack (Cholame) Ranch. Hand specimen densities from samples of Franciscan rocks and Salianian block granitic rocks, together with drill hole information provided by John Sims (USGS) were used to constrain the models.

   The gravity models suggest that Cholame Valley is a deep, sediment-filled trough bounded by steeply dipping, nearly parallel faults. Northwest of the place where the surface breakage associated with the 1966 earthquake steps from the northeast side of the valley to the southwest side of the valley, the bounding faults coincide with the active trace on the northeast and the southwest Fracture Zone on the southwest. Southeast of the cross over, the bounding faults coincide with the projection of the active trace on the northeast side of the valley and with the active trace on the southwest side of the valley. The modeling suggests sediment thicknesses of 1.5 km or more along much of the valley, with the greatest thickness present just southeast of the cross-over and then decreasing thickness toward Highway 46. The steep dip on the northeast side is well constrained by the data but the dip on the southwest side is only poorly constrained. Gravity data are sparse northwest of the Jack Ranch but do suggest that the active trace of the San Andreas fault near Gold Hill may dip southwest.

The White Canyon fault located a few km southwest of Cholame Valley is well expressed in the gravity data and the models indicate nearly 1 km of vertical offset of the basement (up to the northeast) at some locations.

# TILT, STRAIN, AND MAGNETIC FIELD MEASUREMENTS

9960–02114

M.J.S. Johnston, R.J. Mueller, G.D. Myren
Branch of Tectonophysics
U.S. Geological Survey
345 Middlefield Road, MS/977
Menlo Park, California 94025
(415) 329–4812

## Investigations

[1] To investigate the mechanics of failure of crustal materials using data from both deep borehole tensor and dilational strainmeters and near surface strainmeters, tiltmeters, and arrays of absolute magnetometers.

[2] To develop physical models of incipient failure of the earth's crust by analysis of real–time records from these instruments and other available data.

## Results

### [1] STATIC MOMENT OF THE OCTOBER 1, 1987, WHITTIER NARROWS EARTHQUAKE FROM BOREHOLE STRAIN DATA

Offsets in the regional strain field, generated by the October 1, 1987, Whittier Narrows earthquake, were recorded on 10 deep–borehole dilational strainmeters and 3 deep–borehole tensor instruments at distances from 46 km to 408 km from the epicenter. Since it had been previously shown that strain offsets recorded on these strainmeters are consistent with those expected from simple elastic dislocation models of earthquakes, the observed offsets were used to estimate the moment of the Whittier event. The best fit to the strain data of a dislocation model (based on the initially seismically determined source mechanism) required a moment of 1.5 to $1.6 * 10^{25}$ dyne–cm. This is consistent with a magnitude 6.1 earthquake. Precursive strain during the previous month is not apparent at the $10^{-8}$ level in the data from the closest instrument ($\Delta = 45.7$ km) but increased dilation occurred following the event.

### [2] EARTHQUAKE STRAIN STEPS, SEISMIC MOMENT AND TOTAL EARTHQUAKE MOMENT

The static strain field generated by an earthquake provides a simpler diagnostic of the seismic source parameters than that derived from spectra of the radiated seismic waves. Co–seismic strain offsets have been recorded for 17 earthquakes since 1982 on clusters of Sacks–Evertson deep borehole strainmeters installed along the San Andreas fault. These strain offsets, which occur only during nearby moderate to large magnitude earthquakes, agree well with, or perhaps slightly exceed, the static strain field steps calculated from simple elastic half–space dislocation models of these earthquakes, scaled by their seismic moment. Since the strain steps result from total fault slip (*i.e.*, the slip contributing to dynamic seismic radiation and any aseismic fault slip), the moment contributing to the step is known as the total seismic moment. Total seismic moment determinations are therefore simply and routinely made from step observations recorded with the present limited strainmeter arrays and earthquake location and focal mechanism data. At particular locations, where the strainmeter clusters are more comprehensive or optimally placed, constraints on other seismic source parameters can be made.

## [3] BOREHOLE STRAIN ARRAY IN CALIFORNIA

A network of 13 borehole dilatometers and 4 borehole tensor strainmeters along the San Andreas fault zone and in the Long Valley caldera has been installed and is being routinely monitored. All instruments are installed at depths between 117–m and 324–m and all are between 1–km and 5–km of the surface trace of the fault. High frequency dilatometer data in the frequency range 0.005 Hz to 100 Hz are recorded on 16–bit GEOS digital recorders with least count noise of less than $10^{-11}$. Low frequency data from zero frequency to 0.002 Hz are transmitted using a 16–bit digital telemetry system through the GOES satellite to Menlo Park, California where they displayed in "almost real time" and continuously monitored with detection algorithms for unusual behavior. Least–count noise on the satellite telemetry system is about $2 * 10^{-11}$ on the high gain channels and about $1.2 * 10^{-9}$ on the low grain channels. Earth strain tides, strain transients of which some are related to subsequent surface observations of fault creep, and numerous strain seismograms from local and teleseismic earthquakes with magnitudes between -1 and 6 have been recorded on these instruments. Strain seismograms are used to calculate the dynamic earthquake moments. Static moments and total earthquake moments are determined from the co–seismic strains and total strain changes observed with larger events.

## [4] DIFFERENTIAL MAGNETOMETER ARRAY IN CALIFORNIA

Continued investigations of total field magnetic intensity measurements and relationships to seismicity and crustal strain along active faults in central and southern California. The network consists of 12 stations of which all are sampled synchronously every 10 minutes and transmitted with 12–bit digital telemetry to Menlo Park, California, through the GEOS satellite. Data are monitored daily with particular attention to the seven stations operating in the Parkfield region of central California.

## [5] CHARACTERISTICS OF SEISMIC WAVES FROM VOLUMETRIC STRAINMETERS

Theoretical descriptions of volumetric and displacement fields for radiated seismic energy predict that simultaneous observations of each on colocated sensors allow determination of 1) the superimposed **P** and **S** radiation fields, and in particular, superimposed **P** and **S** waves reflected at the free surface, 2) angle of incidence and apparent phase velocity based on amplitude ratios and, 3) intrinsic material absorption and characteristics of low–loss inhomogeneous wave fields. Several hundred local, regional and large teleseismic events including the recent Whittier, Chalfant, and North Palm Springs events, have been observed on colocated volumetric strainmeters and seismometers using broad–band high–resolution recorders (GEOS) at fourteen sites near the San Andreas fault, California, and in Long Valley. These observations have been used to determine site and propagation characteristics, earthquake moments, conversion efficiences, long period characteristics, and information during the immediate pre–rupture interval.

## [6] STRAIN AND MAGNETIC FIELD CHANGES ON THE RED RIVER FAULT SYSTEM IN YUNNAN, AND NEAR BEIJING, CHINA

The program of measurement involving arrays of differential magnetometers and intermediate–baseline geodetic nets was reviewed in Beijing and Yunnan in late 1987. These arrays were installed in 1980 and have been surveyed once or twice a year since then. On the basis of seismic recurrence and other evidence, a moderate to large earthquake is expected within the next few years at both the northern end of the Red River fault in Yunnan Province and on the Baboshan fault near Beijing. For the Yunnan data, simple uniform strain models have been fit to the strain data from arrays at Liante and Dengchaun on the northwest extension of the Red River fault. At Liante the primary feature of the data is a uniform well determined negative dilation of about 2 $\mu$strain/a. Negative dilation of 1.2 $\mu$strain is evident also in the Dengchaun data with a marginally significant shear in a direction N60W. Test line data indicate repeatibility in distance measurements during this time to better than 3 mm on a 734 m line. In contrast, the net line length changes are between 10 and 100 mm on lines typically between 4 and 7 km in length. Magnetic measurements in the region of high magnetization on the west side of the fault at Dengchaun show an increase in local magnetic field of up to 2 nT/a over sites on the east side of the fault. In contrast, no significant magnetic changes have occurred in the Liante array. This result is in accordance with tectonomagnetic theory since the absence of regional magnetic anomalies indicate remanent and induced rock magnetization of less than 0.001 A/m. No unusual changes have been seen in the Beijing area.

## [7] CROWLEY LAKE LEVEL MONITORING

Four water level monitoring sites have been installed on Lake Crowley in the Long Valley/Mammoth Lakes region. These stills provide differential water level measurements (tilt) equivalent to 6 independent tiltmeters with baselines of up to 8 kilometers at varying angles to the center of the resurgent dome. Each site has been surveyed into the existing level line routes around the lake. The time constants of the stills are approximately 40 minutes to minimize effects from the primary seiche periods at 18 minutes and 13 minutes, respectively. The water level data, together with water temperature, wind speed, and other parameters, are being transmitted by the low frequency satellite data collection system to Menlo Park at a 2–min sample period. The maximum change in differential elevation that could have occurred during the past year is less than 1 cm (*i.e.,* $< 1$ $\mu$radian).

## [8] FAULT MODELING

A quasi-static dislocation model that allows calculation of strain, tilt, and displacement time histories for a series of interacting faults is being tested. The model deals with the situation where slip on one fault triggers slip on other (up to 400) faults in the region. Various data support the occurrence of this phenomena.

### Reports

Borcherdt, R.D., and M.J.S. Johnston, 1987, A Broad–Band Wide–Dynamic Range Strong–Motion Network near Parkfield, California, USA, for Measurement of Acceleration and Volumetric Strain, *9th World Conference on Earthquake Engineering* (in press).

Myren, G.D., M.J.S. Johnston, A.T. Linde, M.T. Gladwin, and R.D. Borcherdt, 1987, Borehole Strain Array near Parkfield, California, *Trans. Am. Geophys. Un.*, v. 68, p. 1358.

Johnston, M.J.S., R.D. Borcherdt, M.T. Gladwin, G. Glassmoyer, and A.T. Linde, 1987, Static and Dynamic Strain During the $M_L$5.9 Banning, California, Earthquake on July 8, 1986, *Trans. Am. Geophys. Un.*, v. 68, p. 1244.

Borcherdt, R.D., and M.J.S. Johnston, 1987, A High–Fidelity Strong–Motion Network Surrounding the Rupture Zone of the 1966 Parkfield, California, Earthquake, *Trans. Am. Geophys. Un.*, v. 68, p. 1357.

Johnston, M.J.S., A.T. Linde, and M.T. Gladwin, 1987, Static Moment of the October 1, 1987, Whittier Narrows Earthquake from Borehole Strain Data, *Trans. Am. Geophys. Un.*, v. 68, p. 1520.

Hauksson, E., L. Jones, T. Davis, K. Hutton, G. Brady, P. Reasonberg, A. Michael, R. Yerkes, P. Williams, G. Reagor, C. Stover, A. Bent, A. Shakal, C. Bufe, D. Helmberger, M. Johnston, E. Cranswick, 1988, The Whittier Narrows Earthquake in the Los Angeles Metropolitan Area, California, *Science*, v. 239, p. 1409–1412.

Johnston, M.J.S., A.T. Linde, and G.D. Myren, 1988, Earthquake Strain Steps, Seismic Moment and Total Earthquake Moment, *Trans. Am. Geophys. Un.* (in press).

Borcherdt, R.D., M.J.S. Johnston, G. Glassmoyer, and G.D. Myren, 1988, Observations of anelastic free surface reflection coefficients using borehole volumetric strainmeters, *Seis. Res. Lett.* (in press).

# Earthquake and Seismicity Research Using SCARLET and CEDAR

Grant No. 14-08-0001-G1354

Hiroo Kanamori, Clarence R. Allen, Robert W. Clayton
Seismological Laboratory, California Institute of Technology
Pasadena, California 91125 (818-356-6914)

## Investigations

The Superstition Hills, California, Earthquakes of 24 November 1987
Harold Magistrale, Lucile Jones and Hiroo Kanamori

## Results

The November 24, 1987 Superstition Hills earthquakes occurred on a conjugate fault system involving the northwest striking right lateral Superstition Hills fault and a previously unknown northeast striking left lateral feature defined by a lineation of hypo-centers extending from the Superstition Hills fault to the Brawley seismic zone (Figures 1 and 2). Master event locations of Caltech-USGS seismic network data reveal the following. The first mainshock, on the northeast trend, (33°4.9' N, 115°47.7' W, h = 10.6 km, $M_S$ = 6.2, 0154 GMT) and its foreshocks colocate. Events on the northeast trend cluster in space and time, and some aftershocks occur in the Brawley seismic zone. The second mainshock, on the Superstition Hills fault, (33°0.9' N, 115°50.9' W, h = 1.9 km, $M_S$ = 6.6, 1315 GMT) was 122 hours after the first mainshock and initiated at shallow depth where the two trends join. The northwest trend has epicenters lying between the Superstition Hills and Superstition Mountain faults and has a sharp western edge. The extent of the northwest trend aftershocks is not conincident with surface rupture on the Superstition Hills fault. In general, earthquakes on the northeast trend are deep and earthquakes on the northwest trend are shallow. We compare the earthquake distribution to the distribution of crystalline basement rocks defined in the refraction study of Fuis et al., (1982). The earthquake locations and extent of aftershock activity appear to be controlled by the presence of crystalline basement rocks.

## References

Magistrale, Harold, Lucile Jones and Hiroo Kanamori, The Superstition Hills, California earthquakes of 24 November 1987. Submitted to Bulletin of the Seismological Society of America, April 1988.

Ho-Liu, Phyllis, Hiroo Kanamori and Robert W. Clayton, Applications of attenuation tomography to Imperial Valley and Coso-Indian Wells Region, southern California, in press, Journal of Geophysical Research.

Ho-Liu, Phyllis, Jean-Paul Montagner and Hiroo Kanamori, Comparison of iterative back-projection inversion and generalized inversion without blocks: Case studies in attenuation tomography. Submitted to Geophysical Journal, Royal Astronomical Society, December 1987.

# SUPERSTITION HILLS EVENTS

II.2

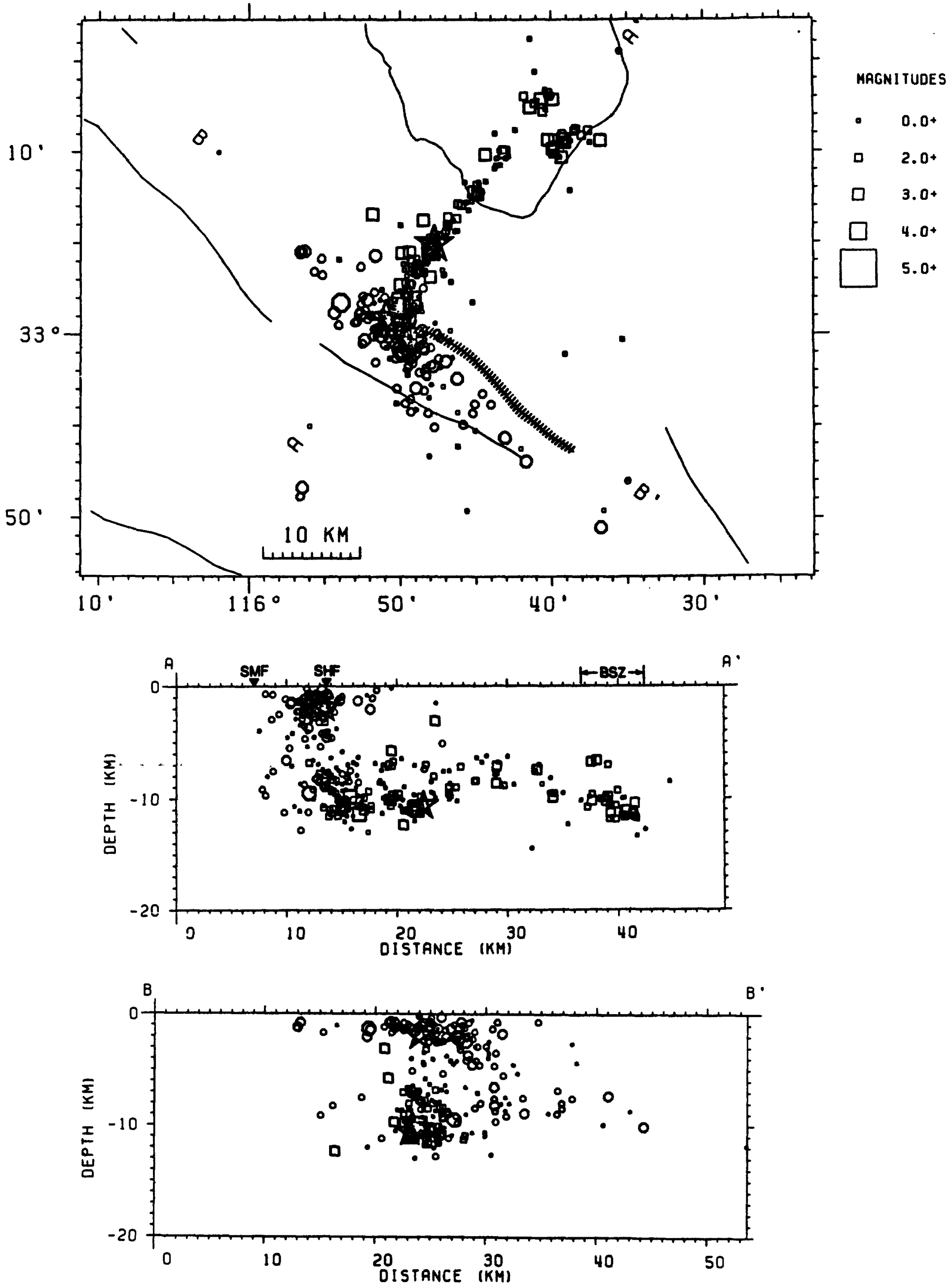

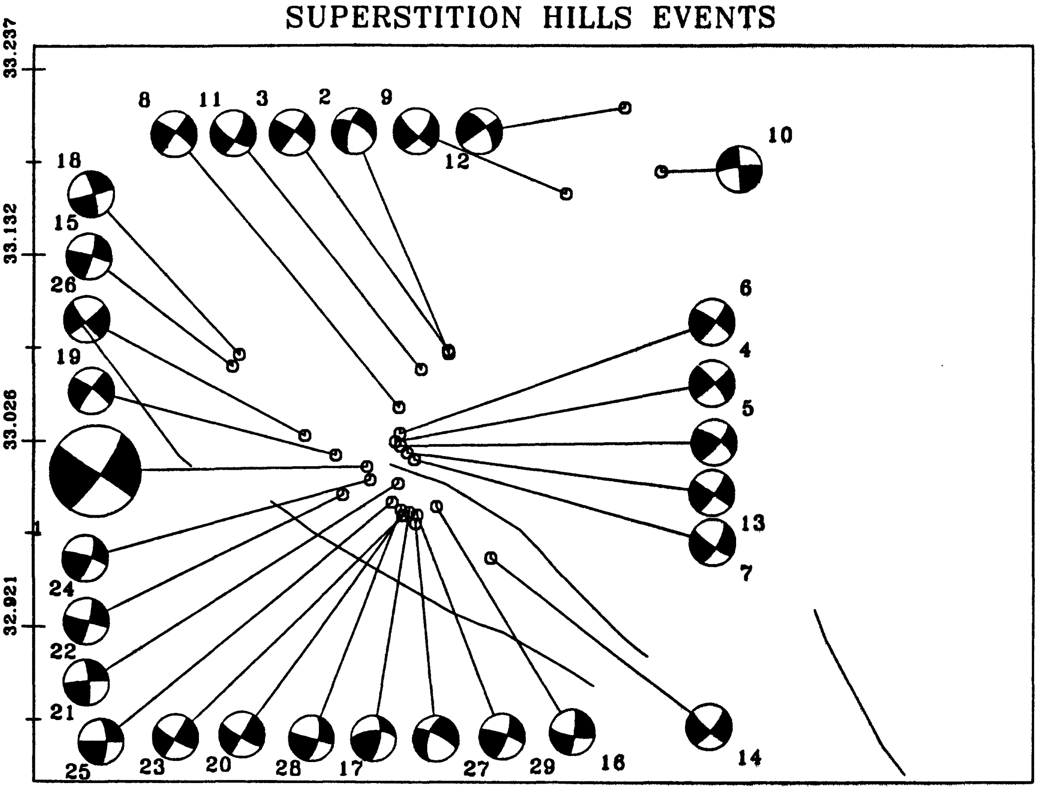

Figure 1. Relocated epicenters of the Nov. 23-24, 1987 sequence. Mainshocks are indicated by "stars". Events before the second mainshock are shown by "squares". Events after the second mainshock are shown by "circles". Hatching shows the approximate extent of surface rupture on the Superstition Hills fault. AA' and BB' are locations of cross section shown below. Cross section AA'is perpendicular to the Superstition Hills fault. All events within 10 km of cross section are projected onto the plane of the figure. Cross section BB' is parallel to the Superstition Hills fault. All events within 10 km of cross section are projected onto the plane of the figure.

Figure 2. Focal mechanisms (lower hemisphere, compressional quadrants "shaded") of some $M_L \geq 3.0$ events. Second mainshock is shown by larger symbol.

# GEODETIC STRAIN MONITORING

9960–02156

John Langbein
Branch of Tectonophysics
U.S. Geological Survey
345 Middlefield Road, MS/977
Menlo Park, California 94025
(415) 329–4853

## Investigations

Two–color geodimeters are used to survey, repeatedly, geodetic networks within selected regions of California that are tectonically active. This distance measuring instrument has a precision of 0.1 to 0.2 ppm of the baseline length. Currently, the crustal deformation is being monitored within the south moat of the Long Valley caldera in eastern California, near Pearblossom, California on a section of the San Andreas fault that is within its Big Bend section and on Middle Mountain near Parkfield, California. Periodic comparisons with the prototype, two–color geodimeter are also conducted near Parkfield, California. These intercomparison measurements serve as a calibration experiment to monitor the relative stabilities of the portable and prototype geodimeters.

## Results

### 1. Instrument intercomparison

In the previous semi–annual report, we stated that the instrument constant for January 1987 (Figure 1) was anomolous. In examining the data and field notes, it appears that the anomolous datum is probably a result of a intermittant connection from the clock to the instrument. This would cause the frequency counters to miss a few beats of the clock and would result in systematically longer distances being observed. The more recent calibration measurements at Parkfield show fairly stable instrument constant for both the portable and observatory based two–color geodimeters. The technique for the measurement of the instrument constant is described by *Langbein et al.* (1987).

### 2. Pearblossom network

Figure 2 shows the results from inferring the strain changes from 7.5 years of line length measurements at Pearblossom, California. Although there have been some minor changes in rate, the secular strain rates are consistent with those originally reported by *Langbein et al.* (1982). Thus, the secular strain rates for a coordinate system oriented parallel and normal to the local strike of the San Andreas fault are as follows:

$$\begin{aligned} \text{areal dilatation} &= -0.070 \pm 0.014 \text{ ppm/yr} \\ E_{11} &= -0.045 \pm 0.008 \text{ ppm/yr} \quad N65^\circ W \\ E_{12} &= \ \ 0.254 \pm 0.005 \text{ ppm/yr} \\ E_{22} &= -0.014 \pm 0.008 \text{ ppm/yr} \quad N25^\circ E \end{aligned}$$

3. Long Valley

We continue to make frequent measurements from our network which uses Casa as the instrument station. The length change appear to be linear in time starting in mid to late 1984. This is in contrast to the high rates that we observed between mid 1983 and mid 1984. Simple modeling of the inflation based upon the two–color geodimeter data implies that the summit of the resurgent dome was uplifted at a rate of 30 mm/yr from mid 1983 to mid 1984 and the rate has subsequently decreased to a steady 13 mm/yr. A similar rate decrease is inferred for slip within the south moat with the slip rate decreasing by a factor of 3 to 4. The slip rate from mid 1983 to mid 1984 is inferred to be 65 mm/yr and from mid 1984 through the present the rate is 20 mm/yr.

4. Parkfield

A computer algorithm has been written to help identify anomolous line–length changes relative to the background noise. Even though the algorithm is written specifically for the observatory based two–color network, it is also applicable to other low frequency data sets. The present algorithm used to identify alerts within the two–color data involves considerable fine tuning of the parameters for each baseline since each baseline shows considerable variation of strain rates over different sampling periods. Specifically, the new scheme involves the idea of a matched filter. We know that the power density spectra for the two–color data has two regimes; for high frequencies, the power density is frequency independent but for low frequencies, the power density is proportional to 1/(f**a) where we assume that a=2. If the power density of the data is known, then the data can be filtered to produce a new time series that looks like white noise with a normal distribution that is characterized by a single variance. Since we know repeatibility or variance of the line–length measurement made over short intervals and the variance of the residual data after a linear trend has been extracted, then it is relatively simple to compute the parameters of the power density spectra which include the break point frequency. Then a high pass filter can be constructed and the line–length data can be convolved with the filter. After filtering and normalizing the data to have a variance equal to one, the data is 'matched' to a function. Initially, we have used box car functions (or running averages) to match with the data and to compare with the variance. Other simple functions including ramp functions and saw tooth functions could be cross correlated with the filtered data. Simple statistical tests verify whether or not a specified interval data is indeed anomolous with its background noise. Currently, the windows use 5, 10, 20, 50, and 100 day averaging. For each baseline, a confidence level can be plotted as a function of time. The confidence level is a measure how anomolous the data is relative to its background variations.

## 5. Principal mode analysis of Long Valley and Parkfield two–color geodimeter data

I have adapted a principal mode analysis scheme to be applied for the frequently measured, two–color geodimeter networks located at Parkfield and in the Long Valley caldera. The results for the Long Valley data yielded deformation patterns both in space and time that could be readily identified with physical sources. The results from the Parkfield network are not so clearcut. Although the primary mode for the Parkfield measurements is consistent with slip on the San Andreas fault, the remaining 3 to 4 significant modes are more difficult to explain using simple tectonic models with deformation wavelength on the order of the network size. With the Parkfield data, only the first or primary mode shows any significant permanent deformation. A simple model to the first mode consists of slip along the San Andreas fault at a rate of 12.5 mm/yr at the center of the network and lateral gradient of 0.64 mm/yr/km. No significant uniform strain is present in the first mode. The other modes show time dependent effects that have periods of roughly one year. Spatially, these modes are difficult to characterize.

The Mammoth data appears to be quite well behaved since each of the 3 primary modes can be easily represented by a linear combination of inflation of the resurgent dome, slip in the south moat, and coseismic deformation associated with the Chalfant Valley earthquake.

### Reports

Langbein, J. and D. Tupper, Deformation of the Long Valley caldera: Besults from 4 years of two–color geodimeter measurements (abs.) *EOS*, v. 68, p. 1246, 1987.

Burford, R.O, J.O. Langbein, L.E. Slater, D.M. Hamann, Deformation within the two–color–laser geodimeter network across the San Andreas fault at Parkfield, CA (abs.), *EOS*, v. 68, p. 1350, 1987.

### Figure Captions

Figure 1. Results from instrument intercomparison at Parkfield. The top plot shows the inferred displacement of the monument used by the portable geodimeter relative to the monument used by the prototype instrument. The lower plot shows the inferred change in length scale of the portable instrument relative to the prototype.

Figure 2. Strain changes inferred from 7.5 years of line–length measurements near Pearblossom, California. Strains are rotated into a coordinate system parallel and normal to the local strike of the San Andreas fault (N65°W).

RELATIVE DISPLACEMENT OF CENTRAL MONUMENTS

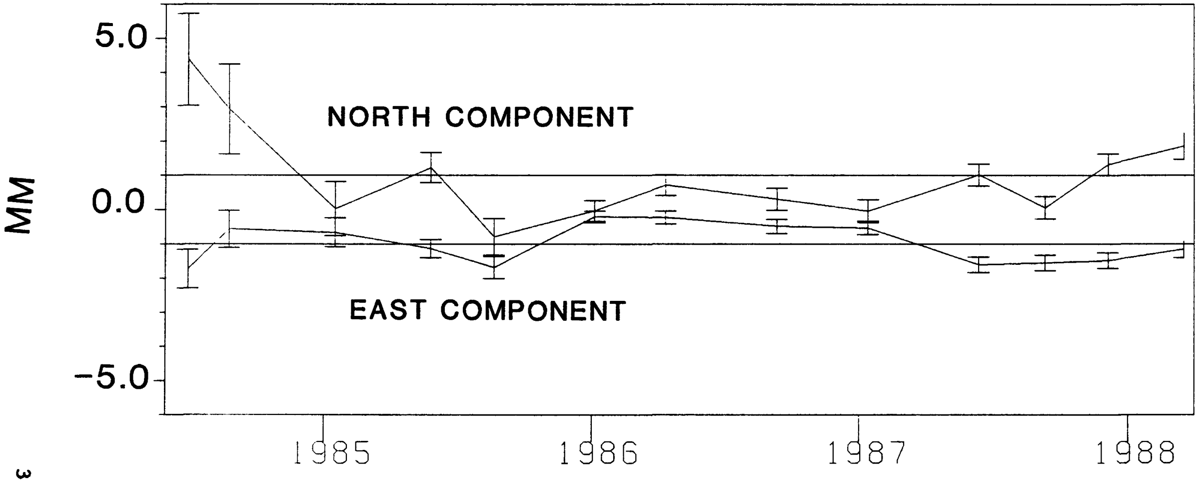

CHANGE IN LENGTH SCALE OF PORTABLE GEODIMETER
RELATIVE TO PROTOTYPE GEODIMETER

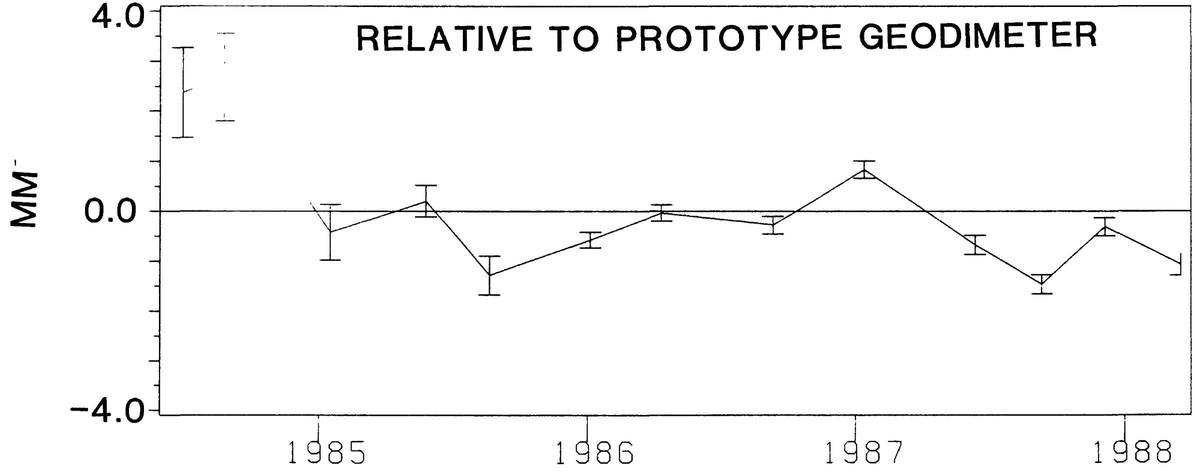

# STRAIN CHANGES AT PEARBLOSSOM

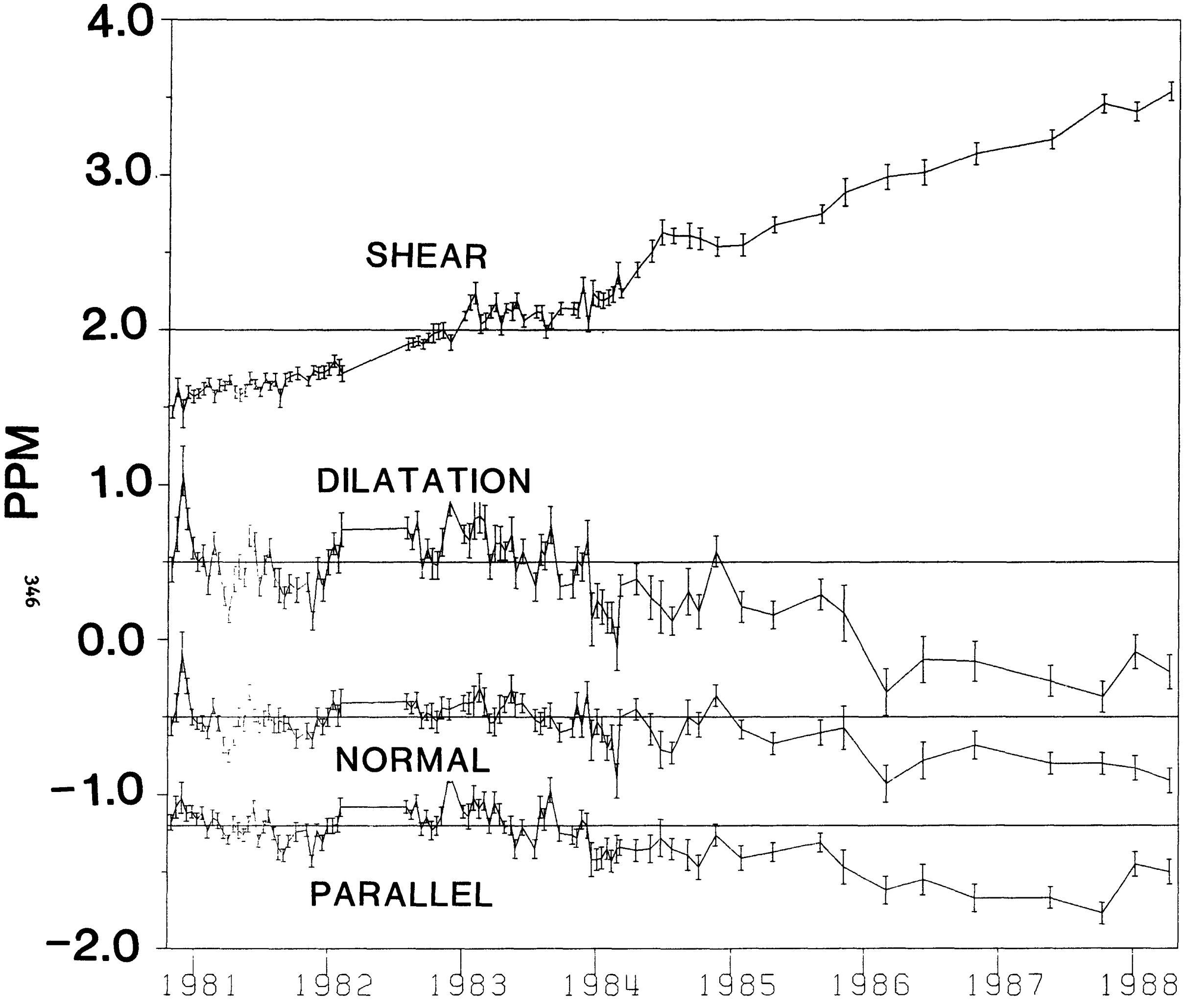

# Microearthquake Data Analysis

9930-01173

W. H. K. Lee
U.S. Geological Survey
Branch of Seismology
345 Middlefield Road, Mail Stop 977
Menlo Park, California 94025
(415) 329-4781

## Investigations

The primary focus of this project is the development of state-of-the-art computation methods for analysis of data from microearthquake networks. For the past six monthis I have been involved in:

(1) A project called "Investigation of signal characteristics of quarry blasts, nuclear explosions, and shallow earthquakes for regional discrimination purposes" for the Defense Advanced Research Projects Agency. The objective is to collect high-frequency seismic data generated by quarry blasts, controlled explosions, and shallow earthquakes, to study their signal characteristics, and to develop a method to discriminate between these three different sources. A telemetered network of 4 stations (eight channels) was installed and operated in the Kaiser Permanente Quarry, and is now being upgraded to 6 stations (5-3 components and 1 vertical component). The purpose of this network is to monitor the quarry blasts more closely. In addition, we will conduct a series of down-hole explosions later this summer.

(2). A collaborative project with Kei Aki and others on coda Q study in California. The objective is to use seismic coda waves recorded by Calnet for investigating the spatial and temporal variations of seismic attenuation. We have extracted a few hundred events from the Parkfield area for the past few years for a coda Q study.

## Results

Two papers were presented at the Fall AGU Meeting in December, 1987. The first paper by Novelo-Casanova et al (1987) is a preliminary report on the temporal variation of coda Q in the Parkfield area. The second paper by Yerkes, levine, and lee (1987) Concerns the contemporary tectonics along the southern boundary of central and western transeverse Ranges, southern California.

I have also completed editing a book (with H. Meyers and K. Shimazaki as co-editors) on historical seismograms and earthquakes of the world.

## Reports

Novelo-Casanova, D. A., Valdes-Gonzalez, C. M., Avileas, C. A., and Lee, W. H. K., 1987. Preliminary Report on Temporal coda wave attenuation in the Parkfield California, area. (Abstract), EOS, v. 68, p. 1349.

Yerkes, R. F., levine, P., and Lee, W. H. K., 1987, Contemporary tectonics along south boundary of central and western Transverse Ranges, southern California, (Abstract), EOS, v. 68, p. 1510.

Yerkes, R. F., and Lee, W. H. K., 1987. late Quaternary deformation in the western Transverse Ranges, U. S. Geological Survey Professional Paper, v. 1339, p. 71-82.

Yeats, R. S., Lee, W. H. K., and Yerkes, R. F., 1987. Geology and Seismicity of the eastern Red Mountain fault, Ventura County, U. S. Geological Survey Professional Paper, v. 1339, p. 161-167.

Lee, W. H. K., Meyers, H., and Shimazaki, K., (Editors), 1988, "Hisotrical Seismograms and Earthquakes of the World", Academic Press, 512 pp.

Lee, W. H. K., meyers, H., and Shimazaki, K., 1988, Introduction to the Symposium on Historical Seismograms and Earthquakes, in "Historical Seismograms and Earthquakes of the Worls", Academic Press, p. 3-15.

Taggart, J. N., Lee, W. H K., and Meagher, K. L., 1988, The U. S. Geological Survey's database of seismic events, in "Historical Seismograms and Earthquakes of the World", Academic press, p. 142-149.

# Parkfield Seismic Experiment

9930-02098

Allan G. Lindh, Catherine M. Poley
John Estrem, and Barry Hirshorn
Branch of Seismology
U.S. Geological Survey
345 Middlefield Road, MS-977
Menlo Park, California 94025
(415) 329-4778

## Investigations

1. Real-time monitoring and analysis of Parkfield seismicity, as part of the Parkfield Prediction Experiment, with special attention given to seismicity near Middle Mountain.
2. Continued work on long-term earthquake probabilities along the San Andreas system.
3. Relocation and spatio-temporal analysis of central California coastal seismicity.
4. Coda-magnitude and "envelope magnitude" study.
5. Daily reprocessing and maintenance of RTP data, with an eye to seismicity changes. Bi-weekly review of station and network performance.
6. Continued work on incorporation of RTP and CUSP data into one database.
7. Monitoring of Parkfield leveling network and analysis of leveling data, as part of the Parkfield Prediction Experiment.

## Results

1. Overall seismicity at Parkfield for the time period 1 April 1987 - 31 September 1987 was normal with 111 events. Activity near Middle Mtn. was slightly higher than normal with 38 events. Seven (7) of these events resulted in seismic alerts (see Figure 1). All (7) were level D; this exceeds the anticipated rate for level D alerts by 4 alerts (see Bakun, this volume).

   Events of interest include:
   (1) On Sunday morning August 15th, 1987 at 9:04 (PDT), a M=2.6 earthquake occurred near Simmler, 40 km south of Cholame (the southern end of the 1966 Parkfield earthquake rupture zone). Four (4) more events occurred there in the following two (2) hours, including a second M=2.6 and a M=2.0 event.
   (2) On September 18th a swarm of 5 M=1-2 earthquakes occurred in a 7 minute span at 6 km depth on the San Andreas fault just north of Parkfield. Four (4) events in 4 hours occurred in the same location on the 19th; single events occurred on the 20th, 21st, and 25th; there were 2 events within 1 minute of each other on the 26th. The swarm nature of seismicity is unprecedented in the detailed recordings of Middle Mtn. seismicity since 1971.

Catherine Poley, with Allan Lindh, Bill Bakun and Sandy Schulz, has completed work on analysing the effects of the 2 May 1983 M=6.7 Coalinga earthquake on the Middle Mtn. section of the San Andreas fault. A paper discussing this work has been published in NATURE.

Events from Parkfield are now being loaded into the VAX750 Parkfield disk for routine analysis of the seismograms.

2. Allan Lindh, using the different approaches used to calculate foreshock probability gains for Parkfield, has extended his study to determine the likelihood that the next characteristic Parkfield earthquake will be a foreshock to a larger earthquake on the southern section of the San Andreas. Efforts continue, to refine the probability estimates of the next characteristic Parkfield earthquake. A paper concerning these questions is in preparation.

3. Catherine Poley, with Allan Lindh and Jerry Eaton, has collected all the phase data from coastal California from San Francisco to the Transverse Ranges. Relocation and analysis of these data are underway and include systematic relocation, focal mechanism determination and stereo-plot projections of the seismicity.

   A subset of this coastal region is the seismicity which occurs in the San Ardo region. The November 24-25 1985 San Ardo earthquake sequence has been studied and is the subject of a paper by Catherine Poley, in press in BSSA.

4. Barry Hirshorn, with Allan Lindh, has derived a magnitude relation for codas measured by the Real Time Picker for earthquakes in central Calif. in the magnitude range of 3 to 6: MZ= -.62 + 2.84*Log (FMP) + .001*DIST + STACOR (1) where FMP is the coda length in seconds (from the P-arrival time), DIST the epicentral distance in km, and STACOR a station term. Coda termination is defined as the time at which the average absolute value amplitude, AAV, on a two second window, falls below 60 mv of amplifier output. The signals used are from CALNET vertical seismometers operated at 48db gain, approximately 32db lower than normal. AAV samples are also saved from the onscale portion of the coda decay, and a straight line fit to them in log-amplitude, log-time space; this results in an estimate of the first derivative of the coda decay, at a single station for a single event, at a specific point in time. We then fit a straight line to these slope-time data, and obtained the relation: dLogA/dLogT = -(1.77 + .011*T) (2) where T is in seconds after the P-wave arrival time. These coefficients provide direct estimates of the a and b parameters in formula (28) of Aki and Chouet (1975). The intercept of 1.77 is NOT consistent with the predictions of their single scatterer model, but can be reconciled with the energy-flux model of Frankel and Wennerberg (1987). A coda decay rate which increases with time is not consistent with a linear Log (coda)-magnitude relation; formula (2) implies that a "correct" coda magnitude relation would have the form: M = A + B*FMP + C*Log(FMP) +... The results of applying this conjecture to our data set will be presented.

5. Allan Lindh meets with John Van Schaak twice a week to review station performance. Barry Hirshorn, in conjunction with reprocessing of RTP data, runs weekly station quality meetings.

6. Successful efforts continue to incorporate RTP data in the CUSP database. RTP data is now reprocessed within the CUSP database.

7. John Estrem continues to keep the leveling network at Parkfield functional, and routine analysis of the leveling data continues. A fault-crossing leveling line has been installed at Gold Hill.

## Reports

Poley, C.M., Lindh, A.G., Bakun, W.H. and Schulz, S.S., 1987, Temporal changes in microseismicity and creep near Parkfield, California, NATURE, v. 327, n. 6118, pp. 134-137.

Jones, L.M. and Lindh, A.G., 1986, Foreshocks and earthquake prediction at Parkfield, California (abs.), EOS Tran. AGU, 66, 982, 1985.

Poley, Catherine M., The San Ardo, California, earthquake of November 24, 1985, BSSA, in press.

Poley, C.M., Eaton, J.P., and Lindh, A.G., 1987, Recent seismicity of the central California region from San Francisco to the Transverse ranges (abs.): Cordilleran section Geol. Soc. Am. Abstracts with Programs, May 1987.

Bakun, W. H., K. S. Breckenridge, J. Bredehoeft, R. O. Burford, W. L. Ellsworth, M. J. S. Johnston, L. Jones, A. G. Lindh, C. Mortensen, R. J. Mueller, C. M. Poley, E. Roeloffs, S. Schulz, P. Segall, and W. Thatcher (1987). Parkfield, California, Earthquake Prediction Scenarios and Response Plans, U. S. Geological Survey Open-File Rep. 87-192.

Borcherdt, R. D., M. J. S. Johnston, A. Lindh, T. Noce, D. Myren, G. Glassmoyer, G. Maxwell (1987). A High-Fidelity Strong Motion Network Surrounding the Rupture Zone of the 1966 Parkfield Earthquake, EOS, 68, p. 1357.

Hirshorn, B., A. G. Lindh, R. Allen, 1987. Real Time Signal Duration Magnitudes from low-Gain Short Period Seismometers, U. S. Geological Survey, Open-File Rep. 87-630, 20 p.

Lindh, Allan G., 1987. Estimates of Long-Term Probabilities for Large Earthquakes Along Selected Fault Segments of the San Andreas Fault System in California, to appear in Proceedings of Earthquake Prediction Symposium, 1988.

Poley, C. M., J. P. Eaton, and A. G. Lindh (1987). Recent Seismicity of the Central California Region from San Francisco to the Transverse Ranges, GSA Abstracts with Program, 19, p. 440.

Poley, Catherine M., and Allan G. Lindh (1987). Parkfield Seismicity: An overview - 1969 to present, EOS, 68, p. 1345.

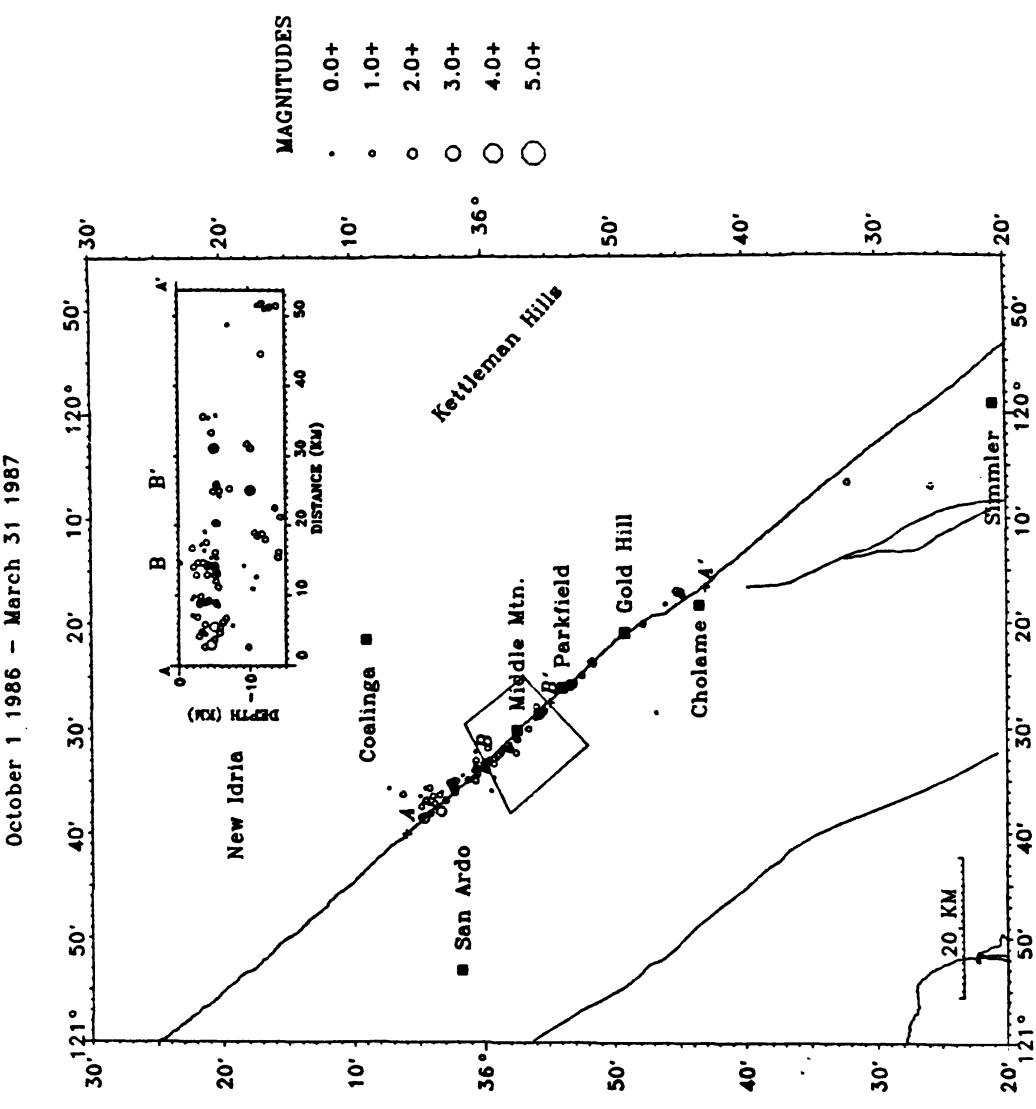

Figure 1. Map of epicentral locations, all magnitudes, from October 1, 1986 thru March 31, 1987. Inset is cross-section along A-A'. The Middle Mtn. region is indicated by the quadrilateral and by B-B' in the inset.

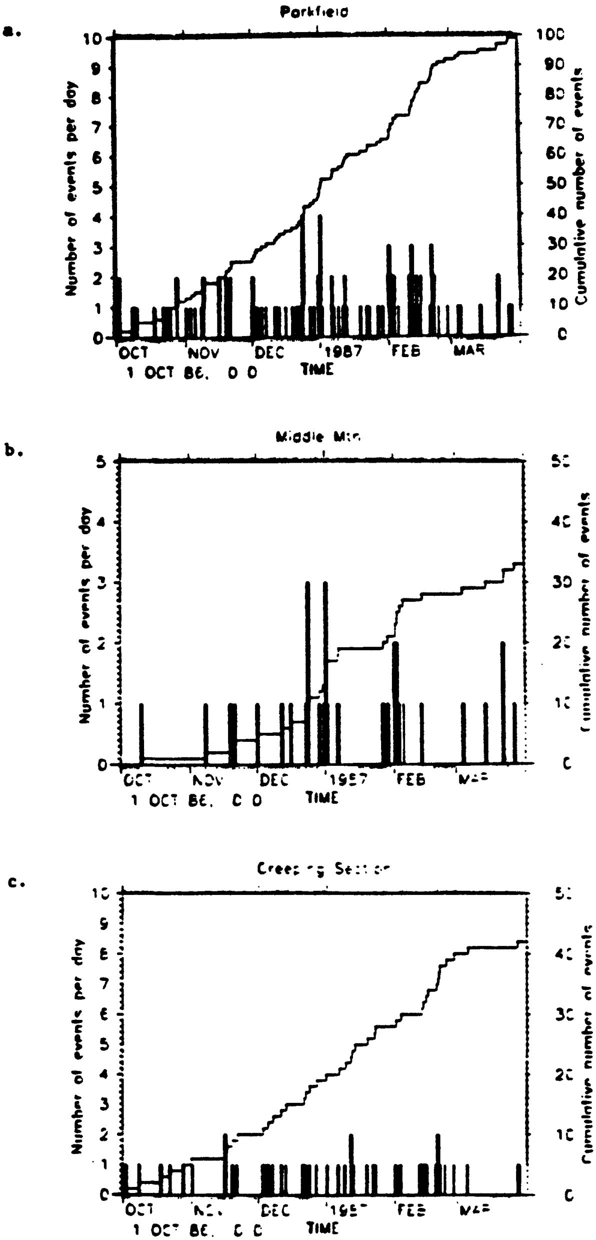

Figure 2. Histograms and cumulative number plots of seismicity, all magnitudes, form October 1, 1986 thru March 31, 1987. a) Parkfield seismicity. b) Middle Mtn. seismicity. c) Creeping section seismicity.

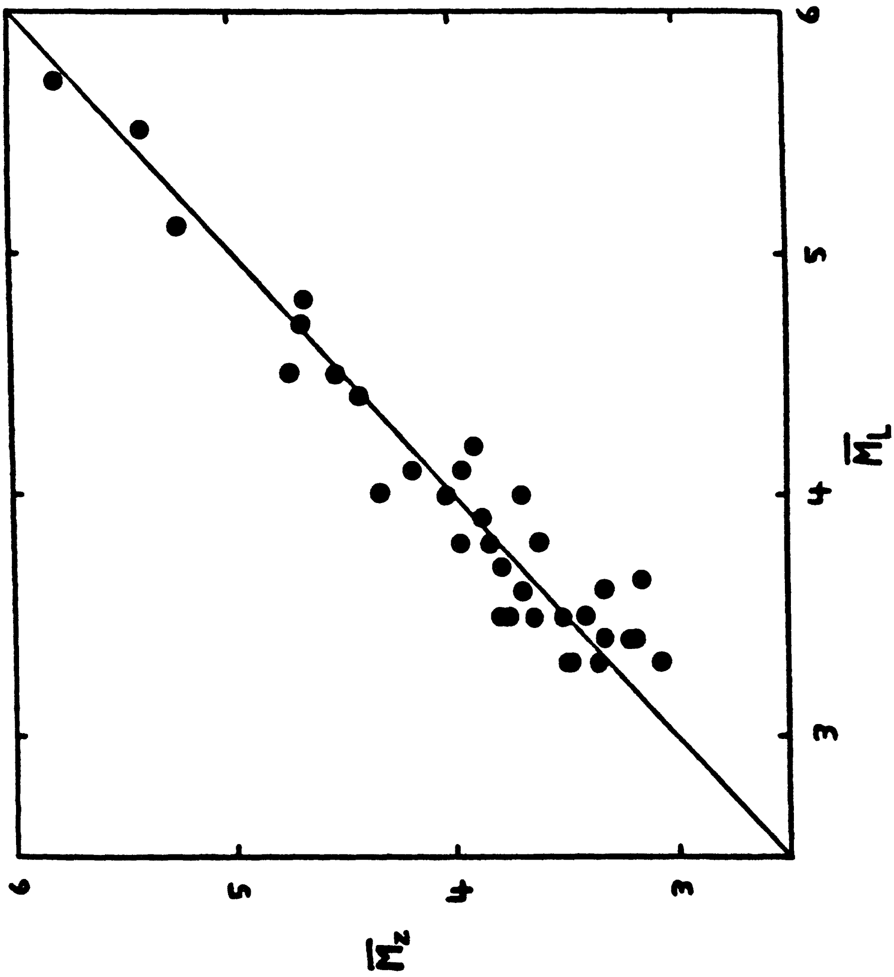

Figure 3. Derived $M_z$ values vs. $M_L$. The slope of the line is 1.00 and the intercept is 0.00.

# SEISMIC WAVE MONITORING AT PARKFIELD, CALIFORNIA

14-08-0001-G1149

T.V.McEvilly, R. Clymer, Wm Foxall
Seismographic Station
University of California
Berkeley, CA 94720
415/642-3977

## Introduction

A program of seismic wave measurements is being carried out using the high-resolution, 3-component, borehole network surrounding the 1966 Parkfield epicenter. The data-acquisition system features digital telemetry with 125 Hz bandwidth and 16-bit resolution, and can operate in external-trigger ( *i.e.,* controlled-source) or event-trigger (earthquake) modes. Earthquake recording began in December, 1986, and routine, controlled-source monitoring began in June, 1987. Considerable effort was also expended through the end of 1987 on acquisition-system improvement and field-site installations. Since the completion of the network in January, 1988, the project has been in a primarily data-gathering mode.

## Investigations

*1) Controlled-source monitoring.* At Parkfield, the nucleation zone is illuminated on a monthly schedule by a shear-wave vibrator operated at eight source sites (Figure 1), generating three shear-wave polarizations at each site. At the Center for Computational Seismology (CCS) at the Lawrence Berkeley Laboratory, data-processing routines are being developed to detect changes in velocity, attenuation, and anisotropy.

*2) Earthquakes.* Local microearthquakes to magnitude approximately -1 are continuously recorded, in cooperation with UC Santa Barbara and USGS. At CCS, development of improved location software is underway. Clusters of events are being analyzed to study failure of very small zones of the San Andreas fault.

*3) Acquisition system improvement.*

## Results

*1) Controlled-source studies.* Beginning in June, 1987, 16 data sets have been acquired at roughly monthly intervals.

At CCS, the basic data-processing software package has recently been changed from DISCO to SierraSEIS. Processing routines for the Vibroseis data (editing, stacking, correlating) developed with DISCO are presently being converted to SierraSeis. Once this is accomplished, a major effort will be expended to bring the basic processing of the Parkfield controlled-source data up to date. In addition, windowing and correlation procedures are being developed within SierraSEIS to reduce, in as automatic a fashion as possible, the huge amount of data being collected to simple plots of a few key waveform parameters.

Figure 2 shows a typical network gather (one source site into all receivers) from the March, 1988 data set. A "time-gather" (one source site into one receiver for all monthly data sets) is shown in Figure 3 for July, 1987 to March, 1988. Portions of the wavetrain remain repeatable out to 16-sec travel time. Also intriguing are the subtle but apparently systematic changes in the shear-wave arrival (just after 4 sec), perhaps explainable by a) near-surface, rainfall-related variations of the source, or b) systematic variations in anisotropy.

2) *Earthquakes.* Since the onset of earthquake recording with the HRSN in December, 1986, the reliability of the acquisition system has been slowly but steadily improved, to the point that, in 1988, there has been little or no "down-time". To date, events detected and on-scale range from approximately $M_c$ -1.0 to $M_c$ 1.6. Local events generally show high signal-to-noise ratio (60 dB at 10 Hz for a $M_c$ 1.3 event), and high bandwidth (usable data to the 125-Hz anti-alias filter).

The most significant microearthquake activity observed within the Middle Mountain zone during 1987 was a cluster of 24 events that occurred between September 18 and October 1 near station FRO. The earthquakes were located using a two-sided velocity model that was developed specifically for the Middle Mountain - Parkfield zone, utilizing data from the Vibroseis monitoring, the Varian well VSP's, and Wadati analysis of the microearthquakes. Figure 4 shows the seismograms from all 24 microearthquakes recorded on the same horizontal component at station VCA. Analysis shows that the small cluster is confined to a half-kilometer-long patch of the fault zone, and contains four distinct types of characteristic earthquakes occurring in four, distinct, non-overlapping volumes. The results imply a relative location accuracy on the order of tens of meters. Thus apparently these data allow the failure process of a small patch of the San Andreas fault to be studied in unprecedented detail. Present efforts are aimed at improving relative locations further by cross-spectral analysis of the characteristic waveforms and use of a master-event technique. The results will be used in an attempt to separate the effects of physical property changes in the medium from changes in hypocenter location.

3) *Instrumentation improvements.* In September, 1987, the acquisition system was returned to the manufacturer for upgrade from 24 to 32 channels. This improvement, with added telemetry equipment purchased by the USGS, allowed full recording of the entire ten-site, three-component network. All installations were made permanent and weatherproof during 1987. The tenth and final instrument, one level of the Varian Well Vertical Array, was brought into service in January, 1988, completing the network.

### Presentations

Foxall, W., and T.V. McEvilly. The Parkfield downhole seismic array: Preliminary analysis of microearthquakes, *EOS, 68,* 1346, 1987 (Presentation at Fall Am. Geophys. Un. meeting).

Foxall, W., and T.V. McEvilly. Microearthquake processes as seen in high resolution with the Parkfield network, in preparation for presentation at Seis. Soc. Am. meeting, May, 1988.

McEvilly, T.V., R. Clymer, J. Durek, and D. Lippert. The Parkfield downhole seismic array: Preliminary results of shear-wave Vibroseis experiment, *EOS, 68,* 1357, 1987 (Presentation at Fall Am. Geophys. Un. meeting).

McEvilly, T.V., and R.W. Clymer. Controlled-polarization shear-wave monitoring at Parkfield, under preparation for presentation at Seis. Soc. Am. meeting, May, 1988.

McEvilly, T.V., T.M. Daley, and R.W. Clymer. Monitoring of anisotropy with VSP surveys and surface array data at Parkfield, CA, in preparation for the Chapman Conference on Seismic Anisotropy in the Earth's Crust, Lawrence Berkeley Laboratory, June, 1988.

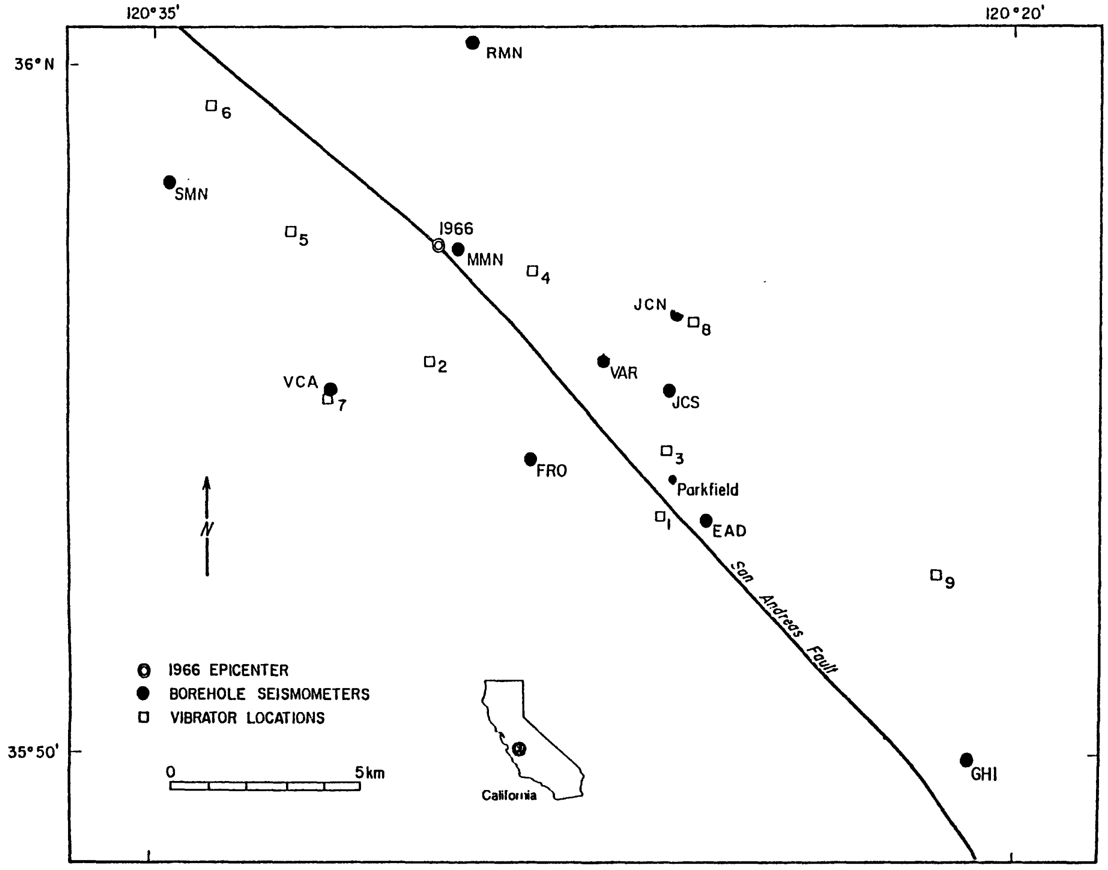

XBL 8712-5130

Figure 1. Parkfield High-Resolution Seismic Network, receiver and vibrator sites.

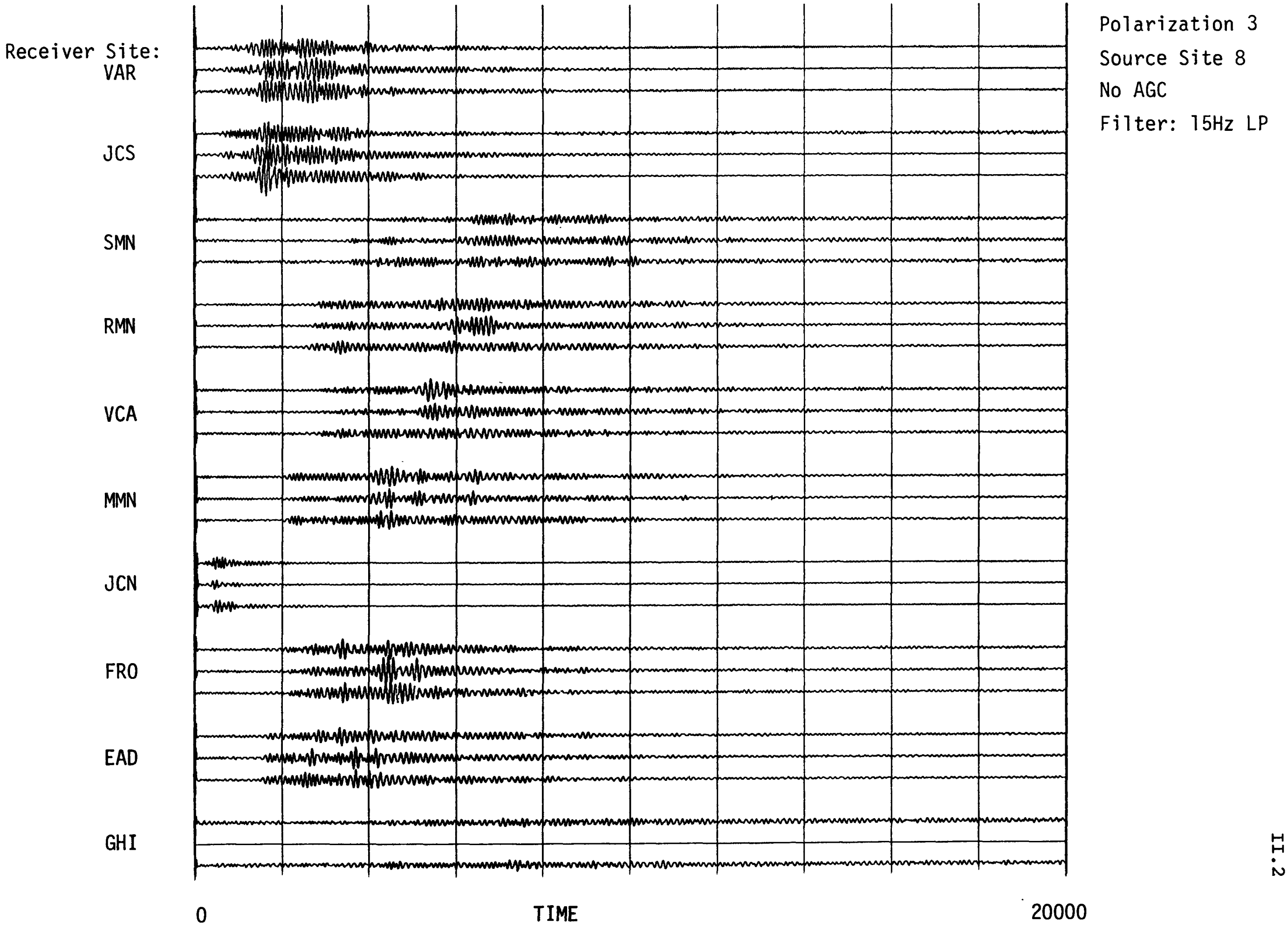

Figure 2. Network gather: Source-site 8 into all receivers. Channels are not uniformly normalized, i.e., this is not a true-amplitude display. (No AGC, 15-Hz low-pass filter applied).

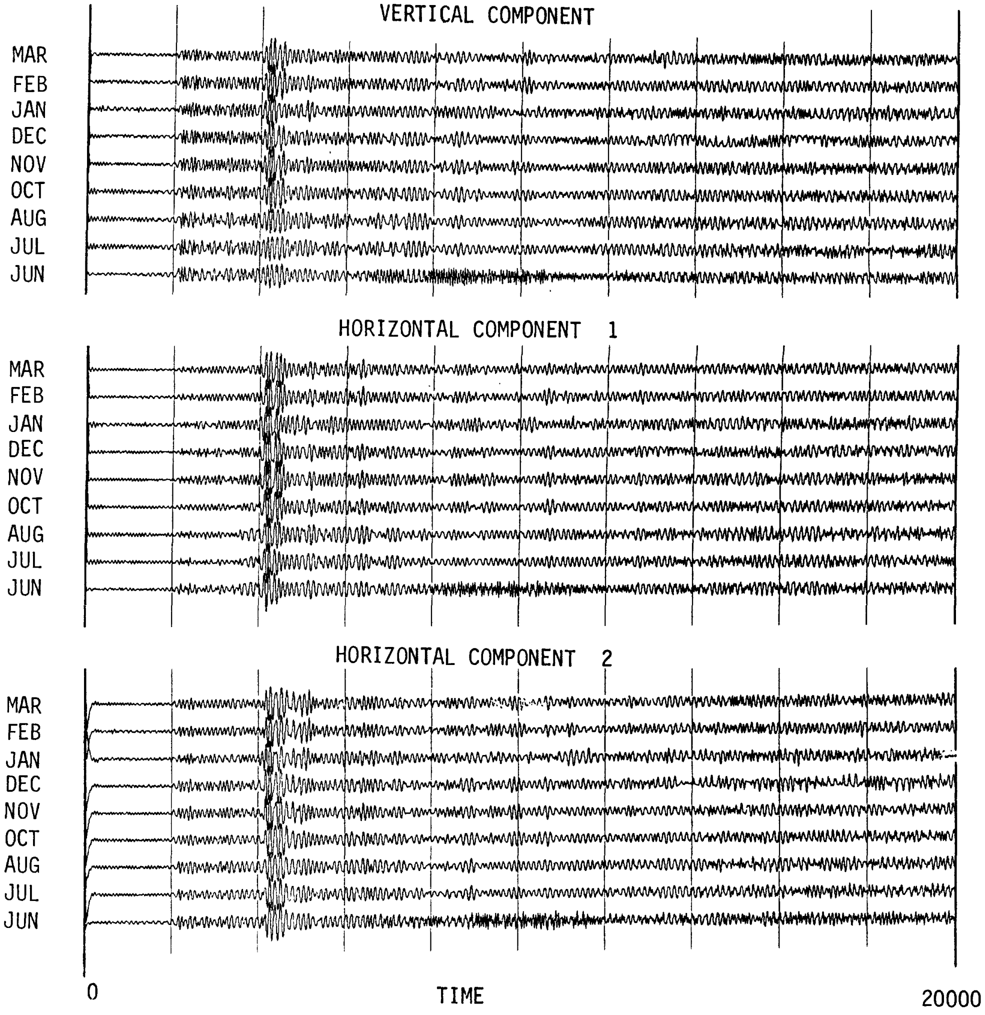

Source Site 8
Polarization 1
Receiver Site: MMN
AGC: 8 sec
Filter: 25 Hz LP

Figure 3. "Time gather": Source site 8 into receiver MMN for all months. Note the subtle and progressive waveform changes in the shear-wave arrival just after 4 sec. The noise on June records is downsweep correlation ghosting. (8-sec AGC and 25 Hz low-pass filter applied.)

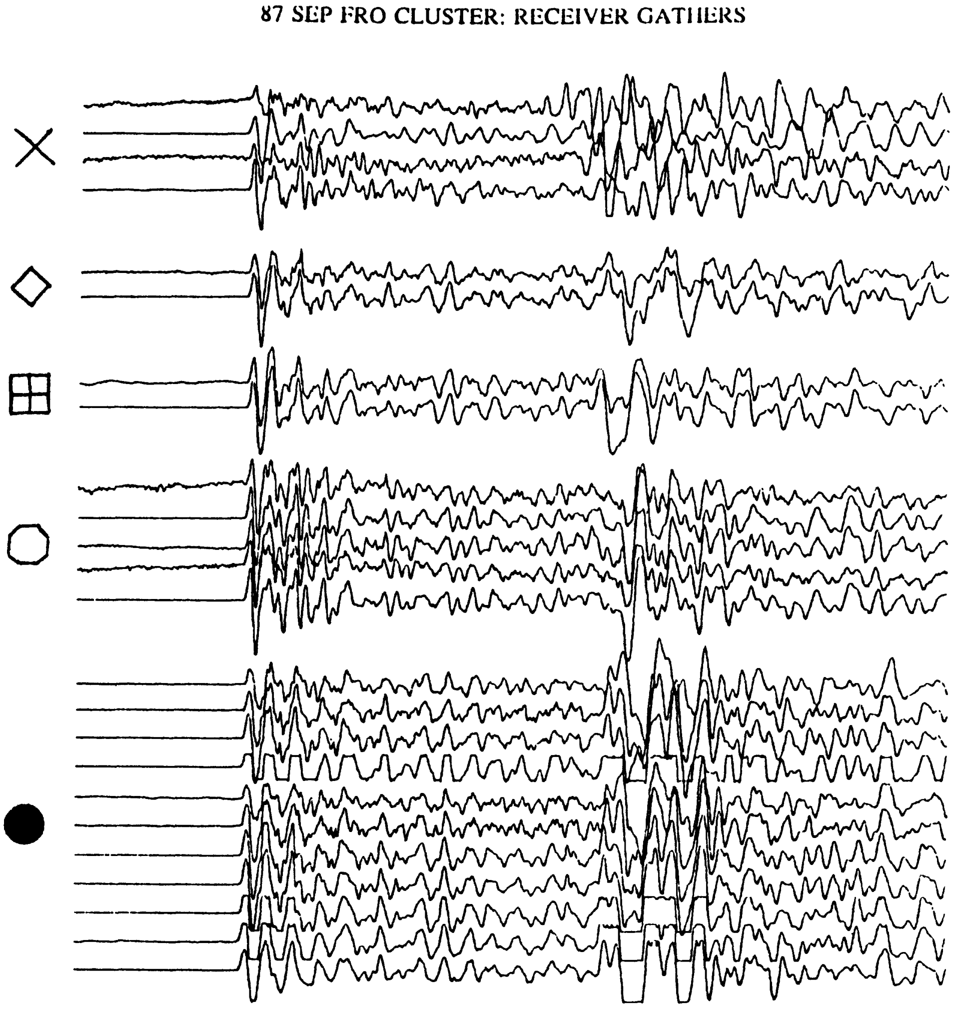

87 SEP FRO CLUSTER: RECEIVER GATHERS

Figure 4. Groups of characteristic microearthquakes in the September 1987 cluster, with symbols used in other figures. Events are arranged chronologically (time progressing upward) in each group. The top group contains the four individual (non-characteristic) events in the cluster. The traces shown are about 2 sec long (S-P is 1 sec).

# SEISMIC STUDIES AT PARKFIELD USING THE VARIAN A-1 DEEP WELL

14-08-0001-G1602

T.V.McEvilly, R. Clymer, T. Daley
Seismographic Station
University of California
Berkeley, CA 94720
415/642-3977

## Introduction

In November, 1987, a vertical array of geophones and accelerometers was installed in the reopened 'Varian A-1' wildcat well at Parkfield. The array, hereinafter termed the Varian Well Vertical Array (VWVA), extends to 1400-m depth at a site 2 km from the San Andreas fault (Figure 1), close to the nucleation zone of the expected magnitude 6 Parkfield earthquake. Several experiments are underway, each of which complements current studies using the Parkfield high-resolution seismometer network (HRSN) to monitor fault zone properties and microearthquake activity.

## Investigations

1) Recording of Vertical Seismic Profiles (VSP) with both compressional and shear-wave vibrators to study details of the wave field and to monitor changes in S-wave anisotropy.

2) Incorporation of VWVA measurements into the ongoing HRSN controlled-source monitoring program, adding the capability for complete determination of the wavefield and more accurate localization of changes in the vicinity of the well. Data will be recorded on a Sercel 338 96-channel acquisition system borrowed from CCG American Services, Inc. The system will be operated in a "piggyback" mode, wherein a signal from an operator at the HRSN recording system will simultaneously trigger that system, the 338, and the vibrator.

3) Non-aliased microearthquake recordings, suitable for beamforming and f-k processing, will be used in conjunction with HRSN microearthquake data to study the failure process at depth with previously unattainable resolution.

## Results

*1) VSP studies.* An initial test of the Varian string was conducted in mid-November, 1987, about a week after installation, to check the status of the receivers, all of which were found to be functioning normally. The test used the UCB shear-wave vibrator in a VSP with two polarizations of shear-waves generated at three offset distances of 100 m, 365 m and 2350 m (Figure 1). Signals from the upper 32 3-component receivers were recorded. The data were then processed to orient the recorded components into the estimated wavefront-based coordinate system of P (Radial), SH and SV orientations, using polarization analysis of the first P-wave arrival. Since SH and SV orientations of the vibrator source were used, a 6-component VSP was produced at each offset (Figure 2).

The near-offset data allow measurement of velocities for vertically traveling P- and S-waves, giving detailed interval-velocity structure. There are also clear indications of deep reflections at 6-10 sec travel time, which will be enhanced with further processing.

The 365-m offset data (Figure 2), in addition to reflections, show evidence of shear-wave velocity anisotropy. There is a 10% difference in travel time between first arrivals on the SV component from the SV source and first arrivals on the SH component from the SH source (Figure 3). The shear wave VSP technique provides a method to investigate causal mechanisms for the anisotropy. (Majer *et al.*, 1987, Daley *et al.*, 1988). Particle motion analysis reveals the direction of dominant shear-wave motion, and the use of various source polarizations and azimuths will allow measurement of the axis of anisotropy symmetry, if one exists. Further, the reflections will be analyzed for evidence of deeper anisotropy. Figure 4 gives the processed particle motion data for the intermediate offset.

A second VSP was performed in January, 1988 at the 365-m source offset after cable tests indicated some of the geophones had failed. This test confirmed the loss of instruments below 1095 m. A third VSP test in Feb 1988 from the three original source locations showed no further loss of instruments. The second and third VSP tests also confirmed the anisotropy observed in the initial test. The remaining well instruments provide enough data to proceed with all the proposed uses of the VWVA, with the original Nov 1987 VSP giving a 'benchmark' data set.

The observation of strong anisotropy in these data sets is encouraging. When the recording system is fully operational (see below), repeated VSP's will be analyzed to detect any temporal changes in waveform parameters that may be associated with the earthquake nucleation process or with changes in stress.

*2) Monitoring studies with VWVA and HRSN.* Two developments, a) additions to the field system of the necessary triggering equipment and of a field stacker to reduce the volume of data, and b) the development of software to demultiplex the 338 data will the allow the beginning of the piggyback experiment in May or June, 1988.

*3) Earthquake data.* Recording and subsequent dissemination of the microearthquake data are the responsibility of the USGS. Recording began in April, 1988 and analysis by a UCB graduate student will begin in May or June.

### References

Daley T. M., Analysis of P- and S-Wave VSP Data from the Salton Sea Geothermal Field, M.S. Thesis, University of California, Berkeley, Ca. *Lawrence Berk. Lab. report*, LBL-24661, Berkeley, Ca., 1987.

Majer, E. L., McEvilly T. V., Eastwood F., and Myer L., Fracture detection using P- and S-wave VSPs at the geysers geothermal Field, *Lawrence Berk. Lab. report*, LBL-20100, *Geophysics*, 53, 76-84, 1988.

### Related Publications and Presentations

Daley, T.M., T.V. McEvilly, and E.L. Majer. Analysis of P- and S-wave VSP data from the Salton Sea Scientific Drilling Project, submitted to the Journ. of Geophys. Res., 1988.

Daley, T.M., T.V. McEvilly, and E.L. Majer. Multiply-polarized, shear-wave VSP's from the Cajon-Pass drillhole, submitted to Geophy. Res. Lett., 1988.

Daley, T.M., T.V. McEvilly, and E.L. Majer. Determination of anisotropy from multi-component VSP's, presentation under preparation for the Chapman Conference on Seismic Anisotropy in the Earth's Crust, Lawrence Berkeley Laboratory, June, 1988.

McEvilly, T.V., T.M. Daley, and R.W. Clymer (1988), Monitoring of anisotropy with VSP surveys and surface array data at Parkfield, CA, presentation under preparation for the Chapman Conference, Lawrence Berkeley Laboratory, June, 1988.

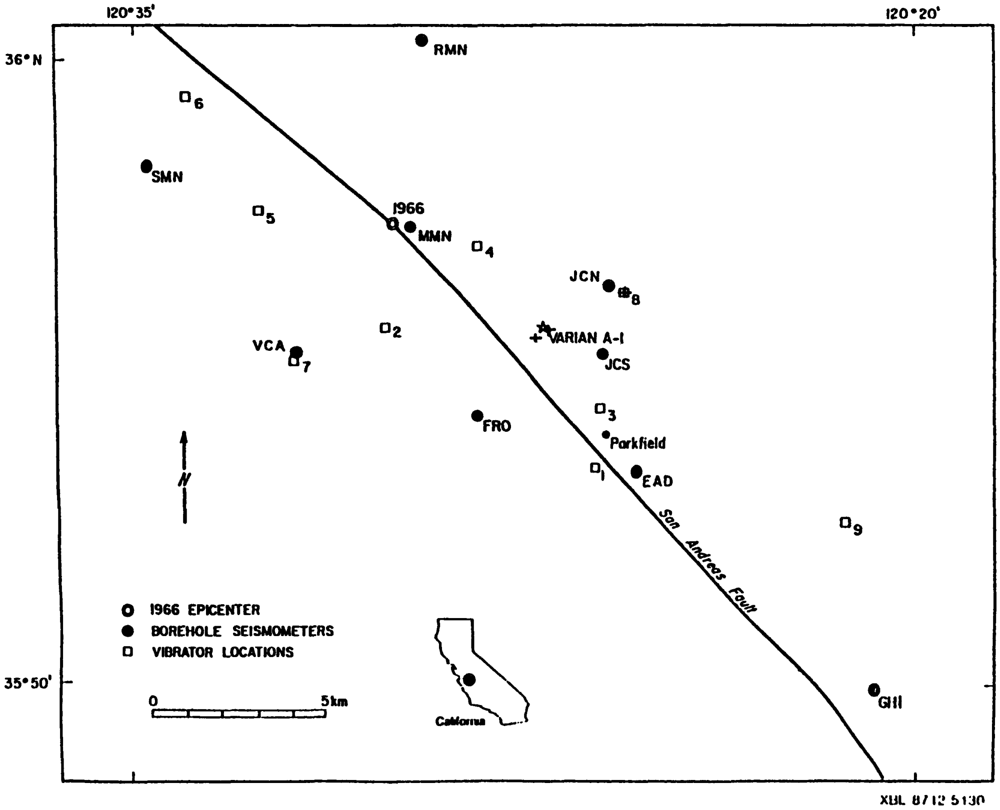

Figure 1. Parkfield network with Varian Well VSP source points shown as crosses near the well (100m), 385m SW of the well, and at monitoring source site 8 near JCN.

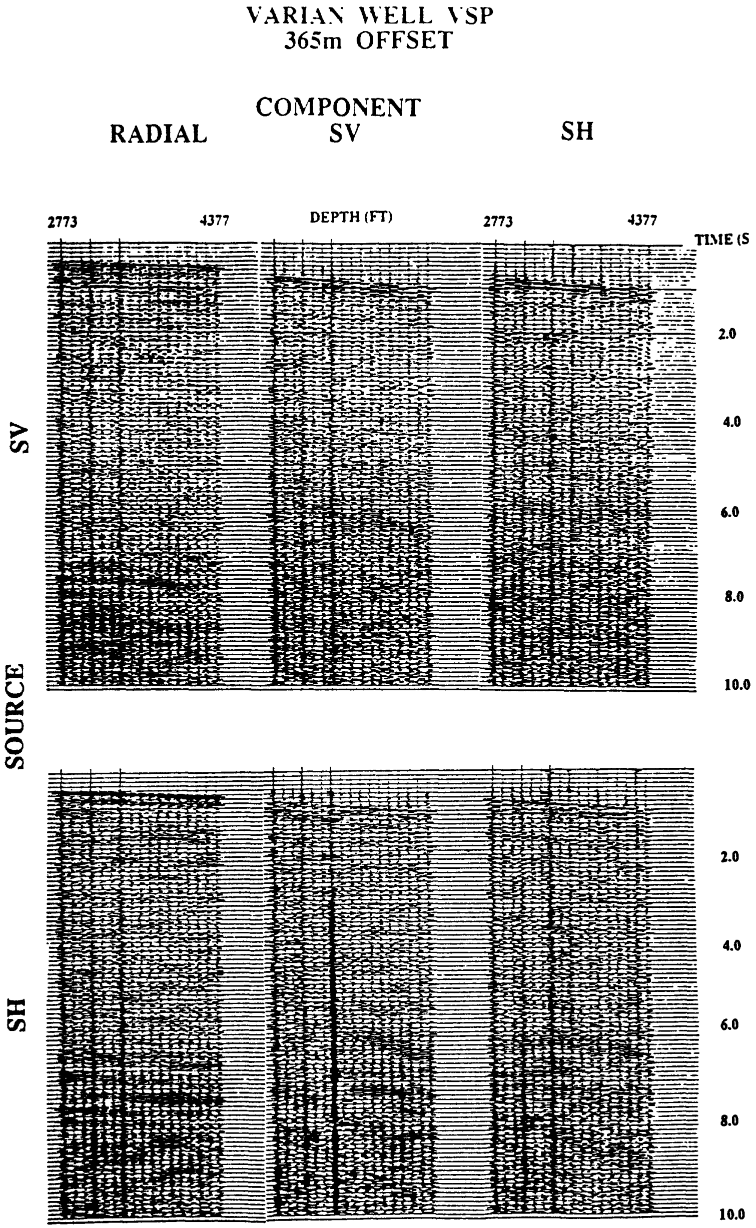

Figure 2. Six-component VSP, after rotation of the original data into radial, SH, and SV components.

# VARIAN WELL VSP
# 365m OFFSET

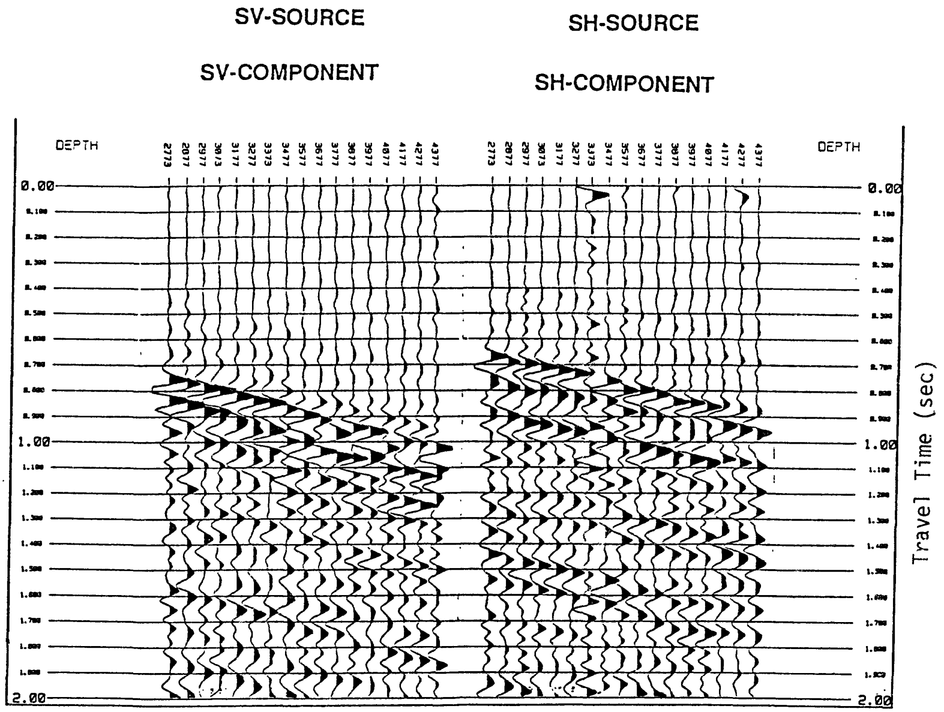

Figure 3. Parkfield Varian well VSP data for 2773-4377 ft depth range, showing S-wave anisotropy.

# VARIAN WELL VSP

# THREE-COMPONENT PARTICLE MOTION

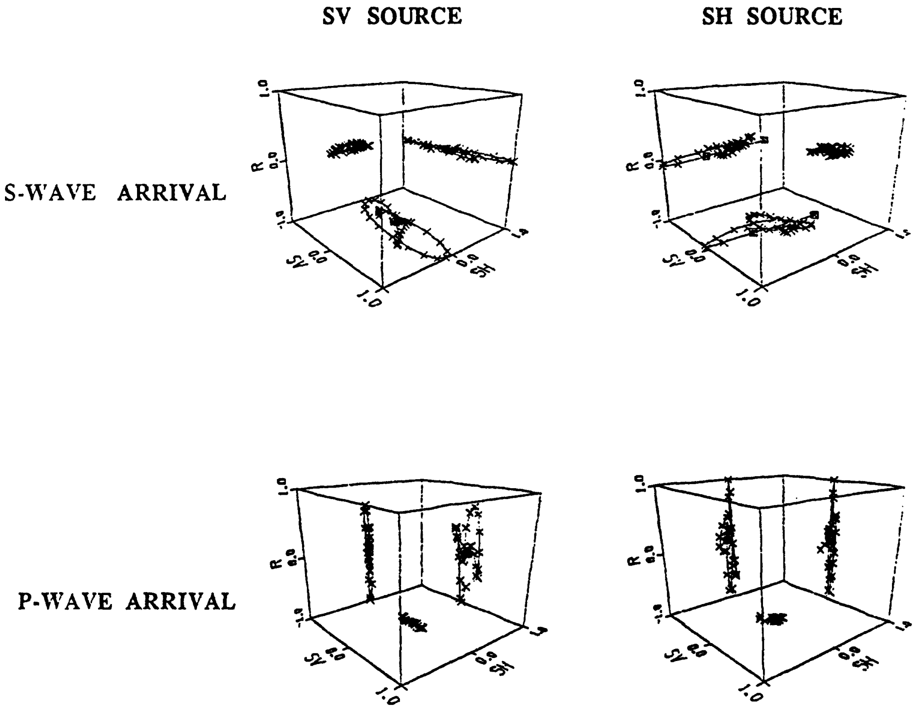

Figure 4. Hodograms for P- and S-waves (direct arrivals) for both source polarizations at 365m offset. Motion shown is at the 662-m level.

# EXPERIMENTAL TILT AND STRAIN INSTRUMENTATION

9960–01801

C.E. Mortensen
Branch of Tectonophysics
U.S. Geological Survey
345 Middlefield Road, MS/977
Menlo Park, California 94025
(415) 329–4856

## Investigations

1. There are currently 110 Data Collection Platforms (DCP's) that transmit a variety of data through the GOES–6 spacecraft to the Direct Readout Ground Station (DRGS) in Menlo Park. Forty of these DCPs transmit data at 10–minute intervals on an exclusively assigned radom channel, which is being utilized under a special agreement with NESDIS. The remainder of the DCPs report at standard 3 or 4–hour intervals as assigned by NESDIS. This system transmits data from all types of low–frequency instruments including dilatometers, creepmeters, strainmeters, water–level meters, magnetometers, tiltmeters, and related measurements.

   A sufficient number of DCPs to replace all of the existing telephone telemetry system have been procured. A system to backup the satellite telemetry system with non–volatile, solid–state memory and dialup or dedicated telephonic communications path is under development. Included in this system will be the capability to lock the DCP timing to a radio time standard. This feature will enable more efficient utilization of the assigned satellite bandwidth.

2. A system to affect emergency communications and routine operational message traffic in the Parkfield area has been implemented. Seven wide–band, digitally–synthesized radios have been delivered and installed – six in field–service vehicles and one at the Car Hill laser observatory. These radios can communicate over the USGS repeater frequency, on commerical mobile radio–telephone frequencies, on the California Emergency Services Radio System, and through the USGS microwave link to the telephone system at Menlo Park. Additional capabilities are available with certain units including access to a large number of local emergency and operational radio nets. It is also planned to establish a capability to link directly to the telephone system locally by installing a phone–patch (already procured) at Car Hill. Equipment to establish a second radio network, with a separate repeater, in the Parkfield area is on order. The purpose of the second network will be to segregate the communications in order to avert saturation of the circuits in the event of heavy operational activity in the area.

3. Networks of tiltmeters, creepmeters and shallow strainmeters have been maintained in various regions of interest in Califorina. A network of 14 tiltmeters located at seven sites monitor crustal deformation within the Long Valley caldera. Other tiltmeters are located in the San Juan Bautista and Parkfield regions. Creepmeters located along the Hayward, Calaveras and San Andreas faults between Berkeley and the Parkfield area are maintained in cooperation with the Fault Zone Tectonics project. A shallow strainmeter is located near Parkfield, while observatory type tiltmeters and strainmeters are sited at the Presidio Vault in San Francisco, and a tiltmeter is installed in the Byerly Seismographic Vault at Berkeley. Data from all of these instruments are telemetered to Menlo Park via the GOES satellite, by phonelines and radio links, or both.

4. A short–haul telemetry system has been assembled from commerically available modules to acquire data from the tiltmeter that monitors rotational changes in the MIDE reflector pier of the two–color laser system at Parkfield.

5. A system for remotely rezeroing and clamping a tiltmeter installed in a deep borehole is being developed, and two deep–borehole tiltmeters are being assembled.

## Reports

Mortensen, Carl E., and Douglas G. Hopkins, 1987, Tiltmeter Measurements in Long Valley Caldera, California, *Jour. Geophys. Res.*, v. 92, p. 13,767–13,776.

# Helium Monitoring for Earthquake Prediction

9570-01376
G. M. Reimer
U.S. Geological Survey, MS 963
Denver Federal Center
Denver, CO 80225
(303) 236-7886

## INVESTIGATIONS

The concentration of helium in soil-gas is being observed to see if a link can be established between variation in concentration and seismic activity. Several sample collecting stations have been established in central California along the San Andreas Fault and are being monitored to establish a data base. Some stations had been in place for 7 years along a traverse from San Benito to Hollister and an interesting correlation between helium decreases and seismic activity was observed. Several of those stations have been moved to near Parkfield and now are the main focus of this monitoring program. A few stations are still in service along the previous traverse but will not be maintained; as they become inoperative or vandalized, they will be withdrawn from the network.

## RESULTS

The initial observations from the Parkfield stations indicate a similar pattern to the San Benito - Hollister network. The seasonal influence on the soil-gas concentrations is evident even after only 6 months of monitoring (Figure 1). The average concentration is higher at Parkfield by about 40 parts per billion as compared to the Hollister - San Benito stations. This is not unusual and is probably due to differences in soil type and the affinity to retain moisture. Alternatively, it could be evidence of greater permeability. A device to measure relative in-situ permeability is being constructed and the question of whether soil moisture or permeability is dominant will be answered during the next site visit. Figure 1 shows the actual helium soil-gas concentrations; they have not been averaged as have the data in previous reports for the San Benito - Hollister stations. As more data are collected, an averaging technique will be utilized and the same method of forecasting seismic activity that had been developed for the northern section of the network will be used for the Parkfield data. That method required an average helium decrease of at least 5 ppb to be observed for a minimum of 2 consecutive weeks. The comparison of the data base from the two areas will provide an excellent test of the validity of the forecasting model. The remaining stations on the northern part of the monitoring network recorded a decrease in helium soil-gas concentrations about 40 days prior to the M=4.5 Tres Pinos earthquake of February 20, 1988. No corresponding decrease was observed for the Parkfield stations.

## REPORTS

None in this semi-annual period.

## SOIL GAS HELIUM CONCENTRATIONS NEAR PARKFIELD, CALIFORNIA

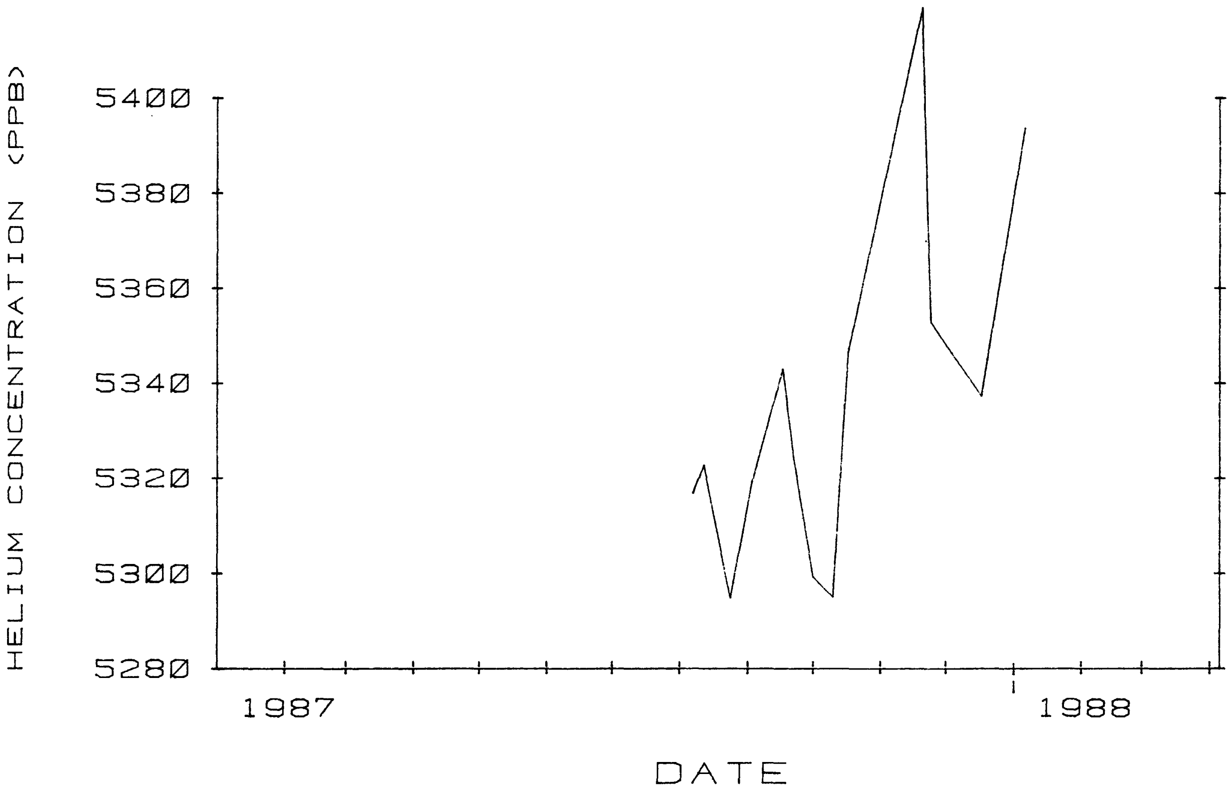

# MECHANICS OF FAULTING AND FRACTURING

9960–02112

Paul Segall and Mark V. Matthews
Branch of Tectonophysics
U.S. Geological Survey
345 Middlefield Road, MS/977
Menlo Park, California 94025
(415) 329–4861

## Investigations

1. Analysis of crustal deformation and the earthquake slip cycle on the San Andreas fault near Parkfield, California.
2. Development of methods for assessing the adequacy of crustal deformation models.
3. Calculation of the effects of non–planar free surface geometry on deformation measurements.

## Results

1. Since 1984 the U.S.G.S. and C.I.R.E.S. have jointly operated a two–wavelength geodimeter near Parkfield. While the average trends in the measurements are consistent with the deformation predicted by the *Harris and Segall* (1987) fault–slip model, the data exhibit large variations about the average trends. If tectonic, these signals can be inverted for time varying fault slip. However, these variations may reflect non–tectonic processes, such as near–surface bench–mark instabilities. Near–surface movements may contain seasonal and/or random walk components.

We have been investigating a class of models of the form

$$y(t_i) = S(t_i) + B(t_i) + \epsilon_i \tag{1}$$

where $y(t_i)$ denotes the measured length of a given baseline at time $t_i$, $S(t)$ is the underlying deformation 'signal', $B(t)$ is a non–stationary stochastic process (Brownian motion) representing local bench–mark instability, and $\epsilon_i$ is random error of the ith measurement.

Initially we considered a simple model in which $S(t)$ is assumed to be linear in time, that is $S(t) = a + bt$. Maximum likelihood estimates of the intercept ($a$), slope ($b$), Brownian motion variance and white noise variance were obtained using methods described more fully below. In this model non–steady tectonic motions are lumped in with random bench–mark motions $B(t)$. The variances of the random errors, however, should be reasonably well determined using this model. We were particularly interested in comparing the random errors in the Parkfield data with those data collected by *Langbein et al.* using the same instrument along the San Andreas near Pearblossom in 1980–1982.

The maximum likelihood estimates of the uncorrelated (white noise) random errors contain a length independent ($0.25 \pm .11$ mm) component and a length dependent component ($0.09 \pm 0.01 \times 10^{-6}$) (Figure 1a). This is indistinguishable from previous estimates of the proportional error of $0.1 \times 10^{-6}$. Our estimates for the Pearblossom data are: $0.28 \pm 0.10$ mm and $0.11 \pm 0.01 \times 10^{-6}$. All the data is shown in Figure 1b, although the fit is to the Parkfield data only. We conclude that random, uncorrelated errors are identical even when the instrument is operated in different tectonic, climatic, and geologic environments, yielding very different data time series.

We are currently attempting to fit models of the form given in (1) with minimal assumptions about the nature of the signal. Presently, we assume only the (interseismic) signal is 'smooth' in time. We incorporate a notion of smoothness into our statistical model by imposing a Bayesian *a priori* distribution on the function $S(t)$. A useful *a priori* distribution for this smoothing problem says that $S(t)$ is an integrated Wiener process with some scale parameter $\lambda$.

Given this prior distribution, (1) may be fit by specifying three scale parameters, $\lambda^2$, the smoothing parameter, and the separate variance parameters of $B(t)$ and $\epsilon$. We are attempting to estimate these three parameters by viewing the 'marginal distribution' of the data as a likelihood function and maximizing it with respect to the three parameters. The maximum likelihood procedure is carried out by casting our model in a state space representation and using the Kalman filter for efficient, recursive evaluation of the likelihood function. Once parameter estimates have been obtained, the Kalman filter may be used again for recursive smoothing of state vector estimates. This yields a 'nonparametric' smooth estimate of the signal – an estimate closely related to and resembling a 'cubic smoothing spline'.

As an example of recursive smoothing with the Kalman filter, we show the decomposition of the data for two baselines, Mid and Mid E, in Figure 2. The data is decomposed into signal (in this case assumed to be linear), Brownian motion, and white noise.

2. Results were described in the previous report. A manuscript on the subject has been submitted to *JGR*.

3. Surface displacements and tilts due to buried deformation sources are influenced by topography. The leading-order corrections due to topography of arbitrary profile $h(y)$, but small slope, are determined for dip-slip faults (edge dislocations) and magma bodies (lines of inflation) in a two-dimensional elastic medium. We assume that the displacements and stresses can be expanded in powers of the characteristic slope, $H/L$, where $H$ and

$L$, respectively characterize the vertical and horizontal length scales of the topography. Approximate free-surface boundary conditions are found by further expanding the stresses in a Taylor series about the horizontal plane $z = 0$. We show that the zero-order (in $H/L$) problem is simply the problem for a fault embedded in a half-space with a plane free surface, the solution of which is well known. The first-order correction due to non-planar topography is equivalent to a distributed shear traction on a half-space, the form of which depends on the topographic profile, $h(y)$, and the horizontal normal strain, $\epsilon_{yy}^{(0)}$, induced on the plane $z = 0$ by the buried source. Further calculation shows that the correction to the vertical displacement field is simply the non-uniform component of the topography multiplied by $\epsilon_{yy}^{(0)}$. The complete vertical displacements, accurate to order $H/L$, are thus

$$u_z(y,h) = u_z^{(0)}(y,0) - h(y)\epsilon_{yy}^{(0)}(y,0)$$

Similar expressions are derived for the horizontal and vertical tilts.

We consider two examples: A normal fault below an idealized basin-and-range profile, and magma chamber below and idealized volcanic topography. For the normal fault the topography and horizontal strain are 'out of phase', so that the topographic correction is smaller than anticipated on dimensional grounds. The principal effect for a fault that breaks the surface is a slight increase in the uplift on the range side.

For the magma chamber the horizontal extension and the topography are 'in phase', leading to a more significant topographic correction (Figure 3). For example, with peak uplift of 100 cm and characteristic slopes of 10° to 20° the topographic correction can be as large as 20 to 40 cm. An expanding magma chamber produces horizontal extension that causes the topography to subside, reducing the peak uplift. For $H/d < 0.3$ (where $d$ is source depth) the effect of topography is to broaden the uplift relative to the maximum uplift. This suggests that, for mild topography, neglecting topographic effects will tend to bias the estimate of source depth toward greater depths. For $H/d > 0.3$, $y = 0$ is a local minimum. Similar double maxima in the vertical displacement field occur for nonspherical sources such as dikes and elongate axisymmetric bodies in the absence of topographic influences. Thus, for this geometry, neglecting topographic effects may bias both the estimated source depth and its shape.

## Reports

Kronenberg, A.K., and P. Segall, Fluid inclusions along healed microcracks and dislocations within a ductile shear zone: implications for fluid access and hydrolytic weakening, *Trans. Amer. Geophys. Union*, 68, p. 1471, 1987.

Matthews, M.V. and P. Segall, The search for temporal variations in buried fault slip on the Parkfield fault segment using two–wavelength geodimeter data, *Trans. Amer. Geophys. Union*, 68, p. 1350, 1987.

McTigue, D.F. and P. Segall, Displacements and tilts from dip–slip faults and magma chambers beneath irregular surface topography, submitted to *Geophys. Res. Letters*, 1988.

Segall, P. and M.V. Matthews, Displacement calculations from geodetic data and the testing of geophysical deformation models, submitted to *Jour. Geophys. Res.*, 1988.

Segall, P., Earthquake potential from analysis of deformation data, *I.U.G.G., XIX General Assembly*, Vancouver, p. 338, 1987.

Segall, P., Observations of interrelated brittle and ductile deformation accompanying faulting in granitic rocks, *Trans. Amer. Geophys. Union*, **68**, p. 1471, 1987.

Segall, P. and M.V. Matthews, Geodetic displacement calculations and the assessment of deformation models, *Trans. Amer. Geophys. Union*, **68**, p. 1243, 1987.

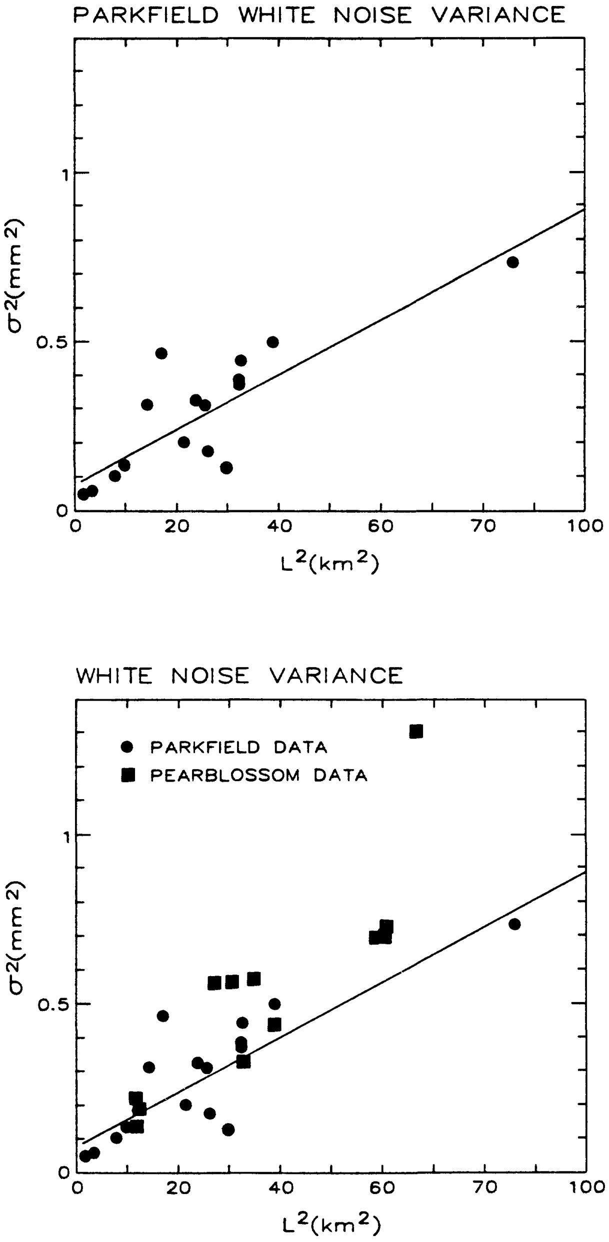

**Figure 1.** Variance of uncorrelated (white noise) measurement errors as a function of baseline length (squared) for two–color geodimeter data.

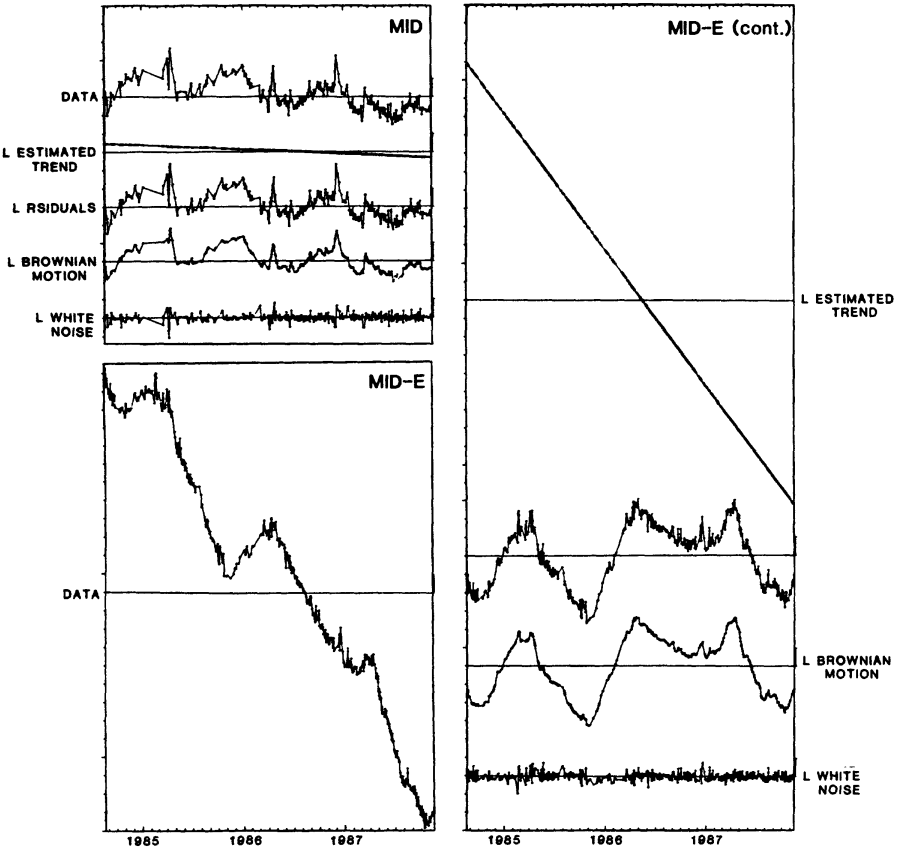

Figure 2. Sample decomposition of Parkfield two-color geodimeter data into linear trend, Brownian motion, and white noise.

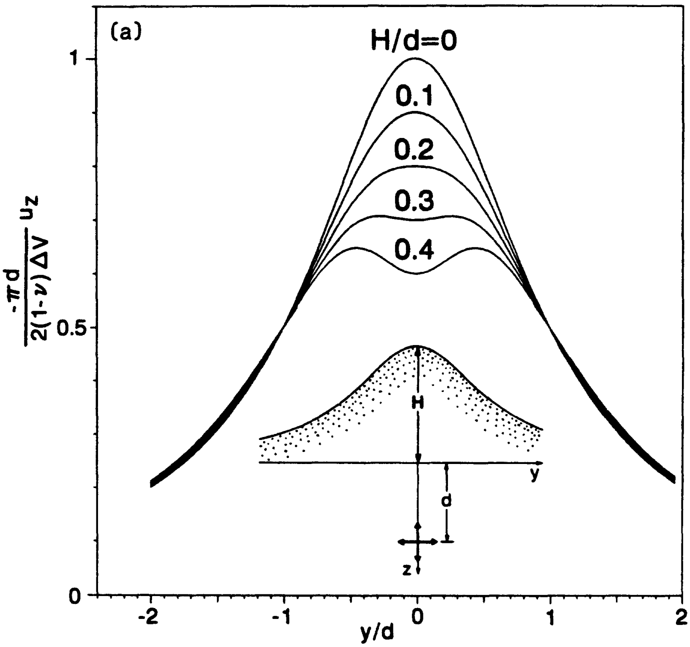

Figure 3. Vertical displacement $u_z$ due to magma chamber beneath a volcano as a function of position $y/d$. $H$ is maximum height of topography, $d$ and $\Delta v$ ae source depth and strength, and $\nu$ is Poisson's ratio.

# LOW FREQUENCY DATA NETWORK

9960–01189

S. Silverman, K. Breckenridge, J. Herriot
Branch of Tectonophysics
U.S. Geological Survey
345 Middlefield Road, MS/977
Menlo Park, California 94025
(415) 329-4862

## Investigations

[1] Real–time monitoring, analysis, and interpretation of tilt, strain, creep, magnetic, and other low frequency data within the San Andreas fault system and other areas for the purpose of understanding and anticipating crustal deformation and failure.

[2] Enhancements to satellite–based telemetry system for reliable real–time reporting and archiving of crustal deformation data.

[3] Compilation and maintenance of long–term data sets free of telemetry–induced errors for each of the low frequency instruments in the network.

[4] Development and implementation of backup capabilities for low frequency data collection systems.

[5] Specialized monitoring, including automated alerts, and display of data relevant to the Parkfield region.

## Results

[1] Data from low frequency instruments in southern and central California have been collected and archived using the Low Frequency Data System. In the six months over four million measurements from approximately 80 satellite platforms have been received via satellite telemetry and subsequently archived by Low Frequency Network computers for analysis. In the same period, more than 60 telephone telemetry channels for field instruments have been monitored, accounting for an additional three million measurements.

[2] The project has operated a configuration of an Integrated Solutions (ISI) V24S computer running under the UNIX operating system, with another ISI serving as data storage backup. A PDP 11/44 and two AT&T PC 7300 computers also have copies of the telemetry data. The ISI has been operational with less than 1% down time. Data from the Network are made available to investigators in real–time and software for data display and analysis is readily available. Tectonic events, such as

creep along the fault, can be monitored while still in progress. Also, periodic reports are produced which display data collected from various groups of instrumentation.

[3] The project continues to use a five meter satellite dish installed in Menlo Park for retrieval of real-time surface deformation data from California and South Pacific islands. The GOES geostationary satellite together with transmit and receive stations make possible a reliable real-time telemetry system. Additional reporting platforms containing waterwell and gas monitoring data are being added to the collection end of the system. Further expansion of the number of platforms monitored is anticipated.

[4] Networking between ISI machines over local area ethernet has enabled creation of a reliable and easily accessed backup facility. Further automated interaction among systems on the network is anticipated to enhance monitoring and analysis of data.

[5] The project continues to take an active part in the Parkfield Prediction activities. New programs to plot low frequency data have been developed for the Parkfield region. These plots can be used to quickly monitor and display ongoing activity. Other software has been written to provide scientists with automated alerts for signals which may indicate anomalous tectonic activity. Kate Breckenridge is the associate monitor for Parkfield creep events, which includes contact via paging system during periods of increased activity. Stan Silverman is the alternate monitor for Parkfield strainmeter data, which also includes contact via paging system for alerts. Also, data collection and computer operations are automatically monitored for normal activity, and project members are paged in the event of problems with either.

[6] The project has continued to provide real-time monitoring of designated suites of instruments in particular geographical areas. Terminals are dedicated to real-time color graphic displays of seismic data plotted in map view or low frequency data plotted as a time series. During periods of high seismicity these displays are particularly helpful in watching seismic trends. The system is used in an ongoing basis to monitor seismicity and crustal deformation in central California and in special areas of interest such as Mammoth Lakes.

# Parkfield Area Tectonic Framework

9910-04101

John D. Sims
Branch of Engineering Seismology and Geology
U.S. Geological Survey
345 Middlefield Road, MS 977
Menlo Park, California 94025
(415) 329-5653

## Investigations:

1. Field investigations of structural and stratigraphic relationships between late Cenozoic sedimentary units and underlying Franciscan and Late Cretaceous units in the Parkfield-Cholame area.

2. Field investigations of late Holocene and historic slip rates in the Parkfield to Carrizo Plain segment of the San Andreas fault.

3. Cooperative research according to the protocols between the USGS and People's Republic of China.

4. Post-earthquake studies of the Whittier Narrows and Superstition Hills earthquakes.

## Results:

1. Filed investigations focused on the Red Hills and White Canyon faults. The Red Hills fault was mapped about 8 km to the north of its previously mapped extent. The fault has young geomorphic features on it in the vicinity of the Red Hills proper and near outcrops of basement rocks. The fault outcrops near Highway 46 in Cholame Creek; at which place the sense of motion on the fault is oblique right lateral. The Red Hills fault is further traced on air photos and by aligned springs north up an unnamed canyon to a projected intersection with the White Canyon fault (see figure).

   The White Canyon fault was mapped about 9 km south of its previously mapped extent. The fault now is demonstrated to extend to the south of Cholame Creek and remains parallel to the San Andreas fault (see figure). Young geomorphic features are common along the White Canyon fault as are springs. Outcrops of the fault are absent but the motion is taken to be right lateral strike slip.

2. A series of quadrilaterals was planned with the consultation of Bob Burford, Sandy Burford, and John Estrem. The first five of these quadrilaterals are installed; one on the White Canyon fault and four on the San Andreas fault in Cholame Valley. Additional quadrilaterals will be installed on the San Andreas fault (5), Red Hills fault (2), White Canyon fault (2), and Gold Hill fault (2), in late April. The quadrilaterals are intended to facilitate the rapid measurement of post-seismic slip following the predicted Parkfield earthquake.

Continued geomorphic studies on the Carrizo Plain yielded a pair of offset streams that are to be trenched. The streams are offset 204 and 162 m respectively. The site is thought to contain a record of multiple offsets over the last 5,000 to 9,000 years.

3. Chinese scientists Wang Tingmei and Li Jialing visited Sims and R.V. Sharp in January and February as part of the USGS/PRC protocols. The Chinese participated in the geomorphic studies on the Carrizo Plain with Sims, post-earthquake investigations of the Superstition Hills earthquake with Sharp and Sims, and trenching of the San Andreas fault near Bombay Beach in the Imperial Valley with Sharp and others.

4. I participated in post-earthquake studies at both the Whittier Narrows and Superstition Hills earthquakes. The Whittier Narrows earthquake had little demonstrable tectonic rupturing although shaking damage was documented.

   The Superstition Hills earthquakes produced striking right-lateral strike-slip movement along the Superstition Hills fault and left-lateral strike-slip movement along numerous conjugate shear faults to the northeast of the Superstition Hills. My mapping of the conjugate shears, especially the Elmore Desert Ranch fault, showed that the fault ruptured preferentially along bedding planes in fold limbs wherever possible. When the fault was forced through the noses of anticlines the rupturing was more diffuse and subject to numerous right steps.

## Reports:

Sims, J.D., in press, Geologic map of the San Andreas fault in the Cholame Valley and Cholame Hills, 7-1/2-minute quadrangles, San Luis Obispo and Monterey Counties, California: U.S. Geological Survey Miscellaneous Field Investigations Map MF-xxx.

Perkins, J.A., Sims, J.D., and Sturgess, S.W., in press, Late Holocene movement of the San Andreas fault at Melendy Ranch: Implications for the distribution of relative plate motion in central California: accepted by the Journal of Geophysical Research.

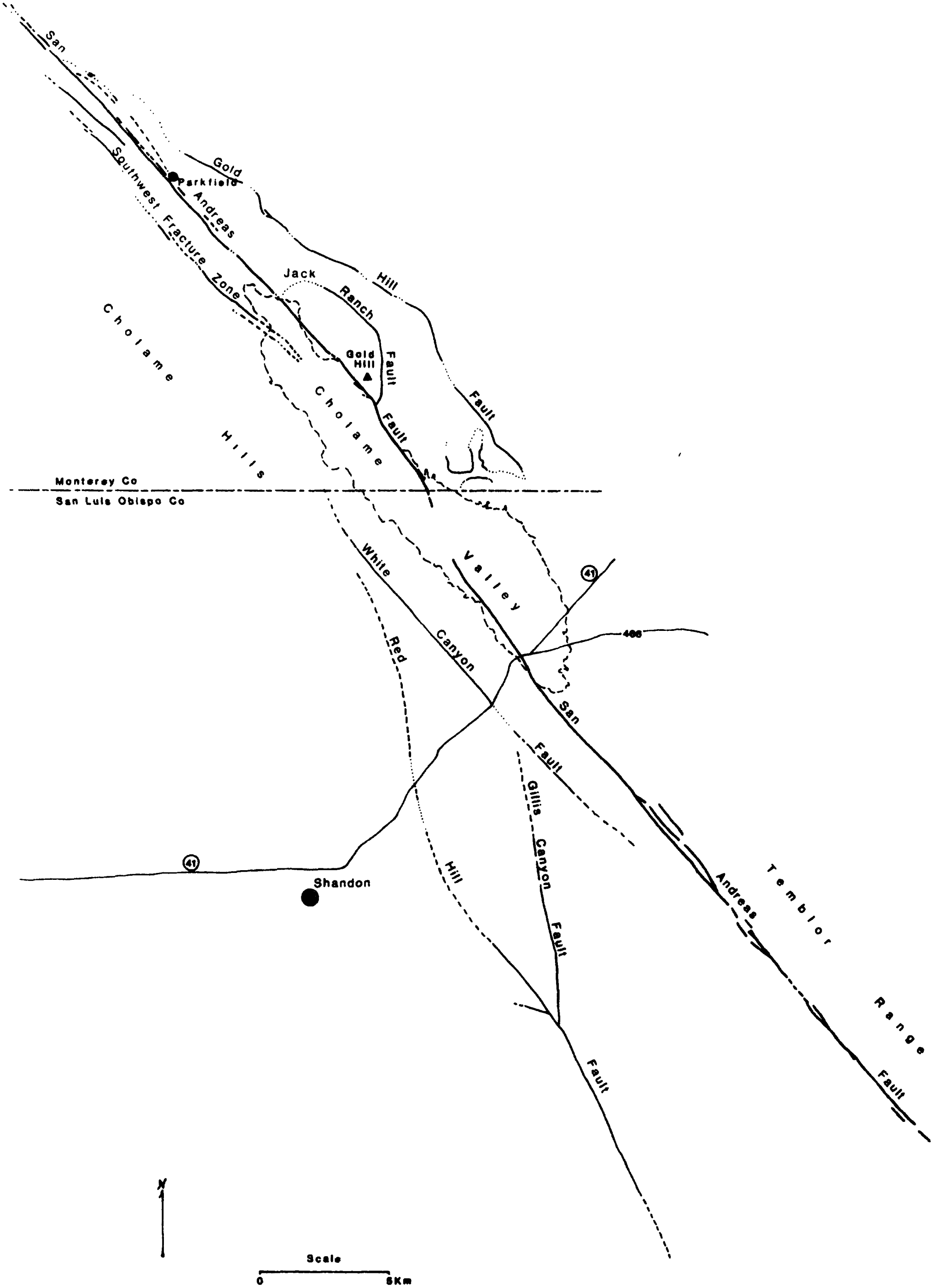
San
Andreas
Parkfield
Gold
Hill
Fault
Southwest Fracture Zone
Jack
Ranch
Fault
Gold Hill
Cholame
Hills
Cholame
Fault
Monterey Co
San Luis Obispo Co
White
Canyon
Fault
Valley
41
466
San
Red
Hill
Gillis
Canyon
Fault
Fault
Andreas
Temblor
Range
Fault
41
Shandon
N
Scale
0
5Km

# Dense Seismograph Array at Parkfield, California

9910-03974

Paul Spudich, Joe Fletcher, and Larry Baker
Branch of Engineering Seismology and Geology
U.S. Geological Survey
345 Middlefield Road, MS 977
Menlo Park, California 94025
(415) 329-5654, (415) 329-5628, or (415) 329-5608

## Investigations

1. Site survey and design of the array (locations of array element).
2. Checkout of Ref-Tek field digitizing units and software design for implementing Anza data acquisition software on a microVAX.

## Results

1. During this period we continued our site survey for the Parkfield dense array. The array will be located on the Work ranch approximately 10 km southwest of the town of Parkfield, California (array coordinates 35°49.0'N, 120°30.2'W). Basement at the site is granite, located at an approximate depth of about 1.5 km. The surface formation is a loosely consolidated gravel and sandstone unit about 500 m thick, overlying more consolidated layers of sandstone and shale. After a reconnaissance trip covering the Work ranch we have tentatively decided to site the array on a ridge that trends north from Work's house for about 3/4 mile and then bends east. Geli et al (1988) suggest that compared to valleys where some spectral components can be filtered out, ridges seem to give a more broad band amplification. The aperture of the array will be between 1 and 1.5 km depending on how far we extend the array to the northeast.
2. The first ten remote digitizing units arrived in late January 1988. We have set up a short network in the lab with all ten elements and so far have been impressed with the ARCnet local area network's functionality. It is straightforward to put together packets in a fortran program on a microVAX that then changes gains, sets time and performs other functions on the remote digitizing units. There have been no resets on the ARCnet controllers in the lab which indicates a certain immunity to noise for the short line lengths being used. We are presently trying to finalize the power system for the field units. We intend to run cable to each site from a central recording site so that the internal batteries will always be trickle charged unless the local power grid fails. A standby uninterruptable power supply will also be capable of providing power for up to four hours.

   At present each field unit has 128 rotating buffers each with 256 words of data. The field units are constantly trying to send data back to the microVAX. The ability of the central recorder to field these packets seems to be the only bottleneck so far. If monitor programs do too much data manipulation the microVAX quickly falls behind and data is lost at the field units. We are presently investigating queing and buffering on the microVAX and how the VMS software compares to RMX.

## References

Geli, L., Bard, P., and Jullien, B., 1988, The effect of topography on earthquake ground motions: A review and new results: Bulletin of the Seismological Society of America, v. 78, p. 42-63.

## Reports

Spudich, P., Baker, L., and Fletcher, J., 1988, The USGS dense seismic array at Parkfield, California: Instrumentation and data analysis: Proceedings of the Second International Workshop on Strong Motion Arrays, Inst. of Earth Sciences, Academia Sinica, Taipei, Taiwan, 16-19 Jan. 1988, Y.T. Yeh, editor.

2 May 1988

# Semi-Annual Technical Report XXVI

Modeling and Monitoring Crustal Deformation
9960-01488

Ross S. Stein and Wayne Thatcher
Office of Earthquakes, Volcanoes, and Engineering
345 Middlefield Road, MS 977
Menlo Park, California 94025

415/329-4840

## Investigations

1. Study of the 1987 Whittier Narrows Earthquake. Conducted releveling in the epicentral region of the 1 October 1987 $M_L$ =6.1 thrust earthquake. The objectives of the geodetic measurements are to gage the fault geometry and slip together with seismic data, and deduce the relationship between the coseismic and long-term deformation at the site to estimate the earthquake repeat time there (Ross Stein and Jian Lin, *Brown University*). Ancillary study of 1982-88 Los Angeles Basin strain from VLBI data in progress (James Davis, Ross Stein).

2. Comparison among geologic, geodetic, and seismologic observations of fault slip, and implications for earthquake mechanics (Wayne Thatcher, Manuel Bonilla).

3. Preliminary investigation of the 1906 Earthquake slip on the San Andreas fault in Offshore northwestern California. No previous estimates of the 1906 slip north of Point Arena have been previously made. Coastal triangulation were used to estimate slip along the northernmost 150 km of the rupture. Values of 4-6 m of slip extending to depths of about 10 km were deduced. (Wayne Thatcher, Michael Lisowski).

## Results

**1. 1987 M=6.0 Whittier Narrows, CA, Earthquake.** We measured 5 cm of coseismic uplift centered on the Whittier Narrows antiform and extending 10-15 km to the north and south, and we interpret this to result from 110±25 cm of dip slip on a thrust fault buried at a depth of 12-15 km. The preseismic elevations were surveyed by Los Angeles County Department of Public Works in 1-2/1986. The National Geodetic Survey re-measured 75 km of the elevations during 10-11/1987 at our request. Additional preseismic leveling in 1975 and extensive recorder well data enable correction for artificial subsidence due to water and oil withdrawal in the epicentral area. Although we cannot distinguish between the deformation produced by either nodal plane of the main shock, the observed pattern of deformation can be adequately modeled by a dislocation in an elastic half space oriented as suggested by the short-period fault plane solution. For a 6x7 km plane (length along strike x down-dip width) dipping 25° to the north, we deduce 110±3 cm of pure thrust slip. This results in a long-period moment of $1.0\pm0.05 \times 10^{25}$ dyne-cm, or a moment-magnitude M=6.0. Davis [1987] argues that a shortening rate of about 1 cm/yr characterizes the fold and thrust belt bounding the northern margin of the Los Angeles Basin. If slip events on the hypothesized thrust fault are no larger than the 1 October 1987 earthquake, then an average repeat time of about 100 years would be consistent with the deduced coseismic slip. Because this rate of earthquake repeat is not observed, the possibility that larger, less frequent earthquakes occur here, or that the slip rate is actually much less, cannot be dismissed [*see Figure 1*].

**2. Fault slip from geologic, geodetic, and seismologic observations.** The spatial distribution of coseismic fault slip provides clues to the mechanics of earthquake strain release and sheds light on the nature and importance of fault segmentation in controlling the strain release pattern. Although the true distribution of slip is not accessible to direct observation, several methods can be applied to recover informative features of its spatial patterns. Earthquake slip distributions obtained by all three methods are typically highly irregular, with maximum slippage often localized in one or a few restricted regions that together comprise only a small portion of the entire rupture plane. The pattern, however, does contain some systematic elements, since rupture has a tendency to initiate towards the ends of the zones of seismic faulting and near or within regions of high coseismic slippage.

## Reports (excluding abstracts)

Stein, R.S., Plate tectonic prediction fulfilled, *Physics Today, 41*(1), S-42 - S-44, 1988.

King, G.C.P., R.S. Stein, and J.B. Rundle, The growth of geological structures by repeated earthquakes: 1, Conceptual framework, submitted to *J. Geophys. Res.*, 1987.

Stein, R.S., G.C.P. King, and J.B. Rundle, The growth of geological structures by repeated earthquakes: 2, Field examples of continental dip-slip structures, submitted to *J. Geophys. Res.*, 1987.

Thatcher, W., and M.G. Bonilla, Earthquake Fault slip estimation from geologic, geodetic and seismological observations: Implications for earthquake mechanics and fault segmentation, *Proceedings of USGS Workshop on fault segmentation and controls of rupture initiation and termination*, in press, 1988.

Lin, J., and R.S. Stein, Coseismic fold growth during the 1987 M=6.0 Whittier Narrows, California, earthquake, to be submitted to *J. Geophys. Res.*, 1988 (special issue on the Whittier Narrows Earthquake).

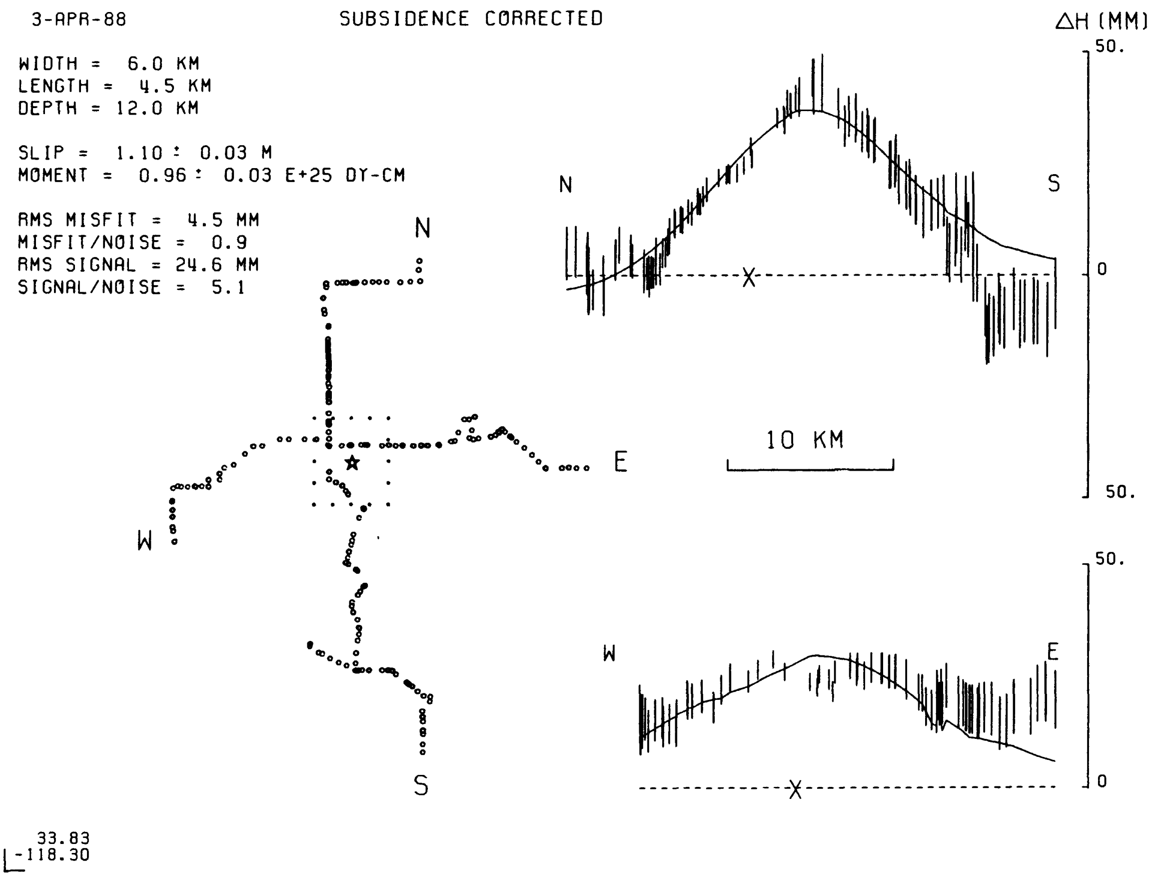

*Figure 1.* Map of leveling network and profiles of coseismic elevation change (vertical lines are ±1σ) with best-fitting model (curves), for 1 October 1987 Whittier Narrows, California, earthquake. Main shock indicated by star; outline of model fault dipping 25° to the north indicated by dotted rectangle; bench marks by open circles. Junction of N-S and E-W line indicated by "X" on profiles. Same scale for map and profiles.

# Nearfield Investigations of Crustal Movements in Southern California

14-08-0001-21997

Arthur G. Sylvester
Department of Geological Sciences, and
Marine Sciences Institute
University of California
Santa Barbara, California 93106
(805) 961-3156

**Objective:** This investigation aims to determine the spatial and temporal nature of nearfield strain accumulation and release, if any, across several kinds of active and potentially active faults in diverse tectonic regions of California. The principal measurement method is precise leveling wherein our reproducibility of single bench mark occupation is 0.5 mm from survey to survey (Sylvester, 1984).

**Activities:** During the six months addressed by this report, we have resurveyed our leveling arrays across the San Andreas in Coachella Valley to determine if the Elmore Ranch and Superstition Hills earthquakes or 23 and 24 November 1987, respectively, perturbed the vertical strain field around the southern end of the San Andreas fault.

The BAT CAVES, NORTH SHORE, AND PAINTED CANYON arrays (Fig. 1) were surveyed in the period 3-7 September 1987 prior to the November earthquakes. We surveyed them again 8-10 December 1987, and found the height changes among all bench marks in each array were negligible (Fig. 2).

Those three arrays, together with MIRACLE HILL, WHITEWATER, and SBVC were surveyed again in the period 20-24 March 1988 to see if the perturbation could have been delayed. The data show that the Durmid anticline grew nearly two millimeters beneath the BAT CAVES array, northeast of the San Andreas fault between our December 1987 and March 1988 levelings (Fig. 3), whereas previous growth of the fold was concentrated southwest of the fault (Fig. 2). The uplift rate is comparable to the annual rate of growth of the anticline in Holocene time of 1-2 mm/yr, which is calculated from geomorphic evidence. Other arrays show no effect.

We also resurveyed the arrays PARKFIELD CROSSTOWN and PITT RANCH across and near the San Andreas fault in the Parkfield area in February 1988. No changes were observed among bench marks in the arrays which differed markedly from those of our last survey in 1986.

**Final Technical Report:** The bulk of our efforts in the last few months has been directed to the compilation of site and measurement data for all of our arrays for the time period from establishment of each array, some of which date from 1970, to the most recent surveys in 1987. The purpose of the endeavor is to present a compilation of principal facts for each of our leveling arrays as a reference for future surveys. The eventual report includes access and trespass information; location and detailed site data exclusive of descriptions of individual bench marks; line graphs comparing noteworthy surveys; and height differences between bench mark pairs for the earliest and most recent good surveys. This report will constitute the Final Technical Report for grant years 1986 and 1987 and may be obtained from the author on request.

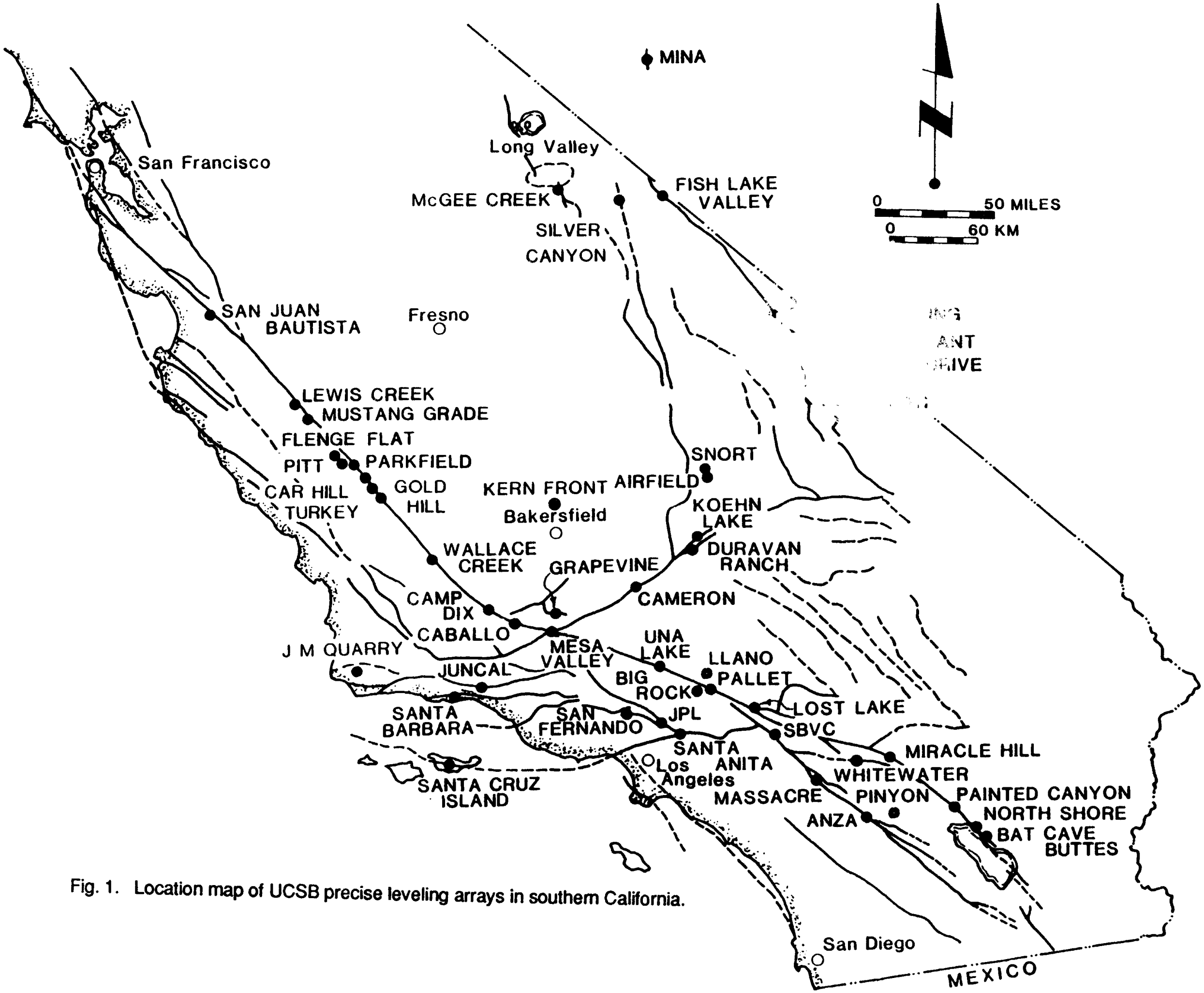

Fig. 1. Location map of UCSB precise leveling arrays in southern California.

Δ BM HEIGHTS - BAT CAVES BUTTE - 1985-1987

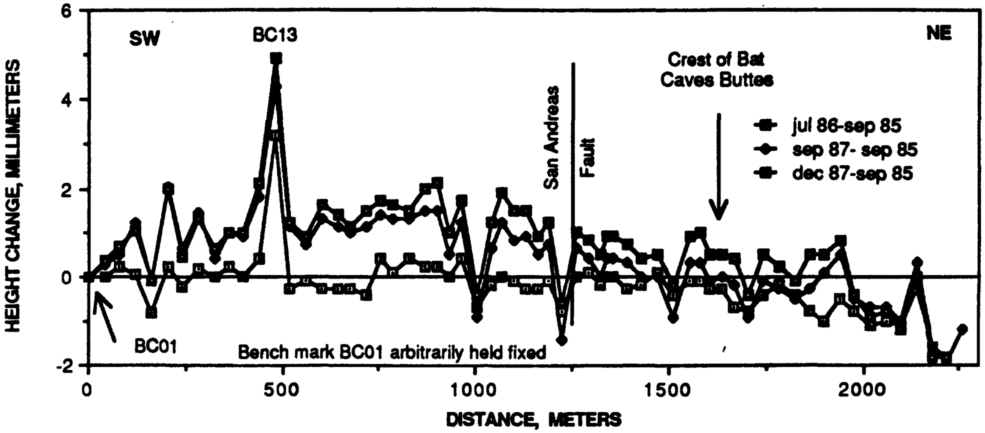

ΔBM HEIGHTS - BAT CAVES - 3 SEP TO 8 DEC 1987

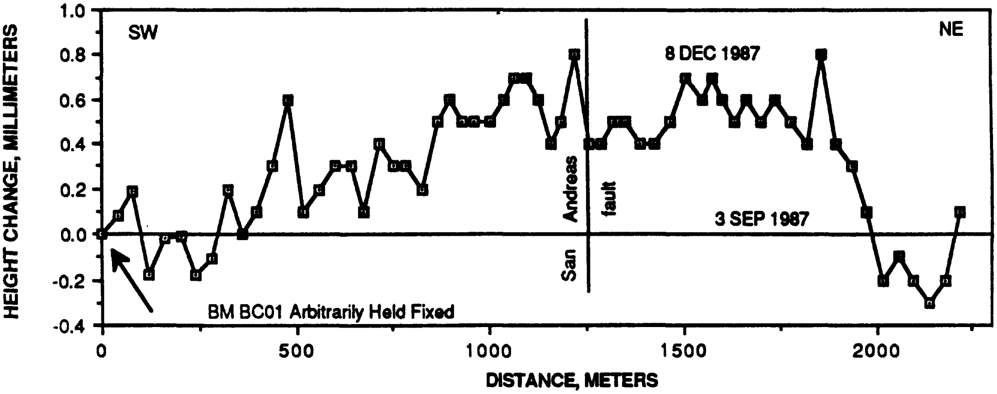

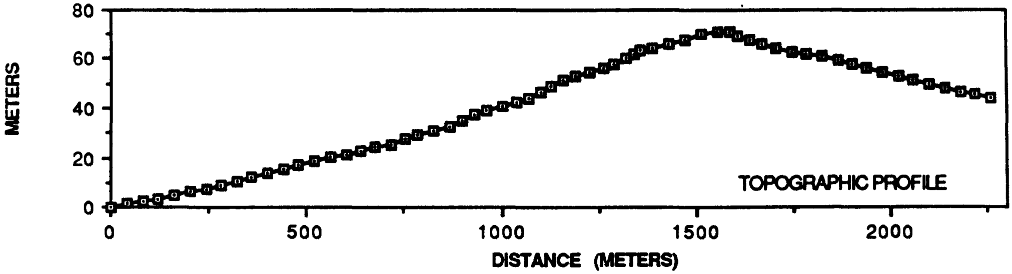

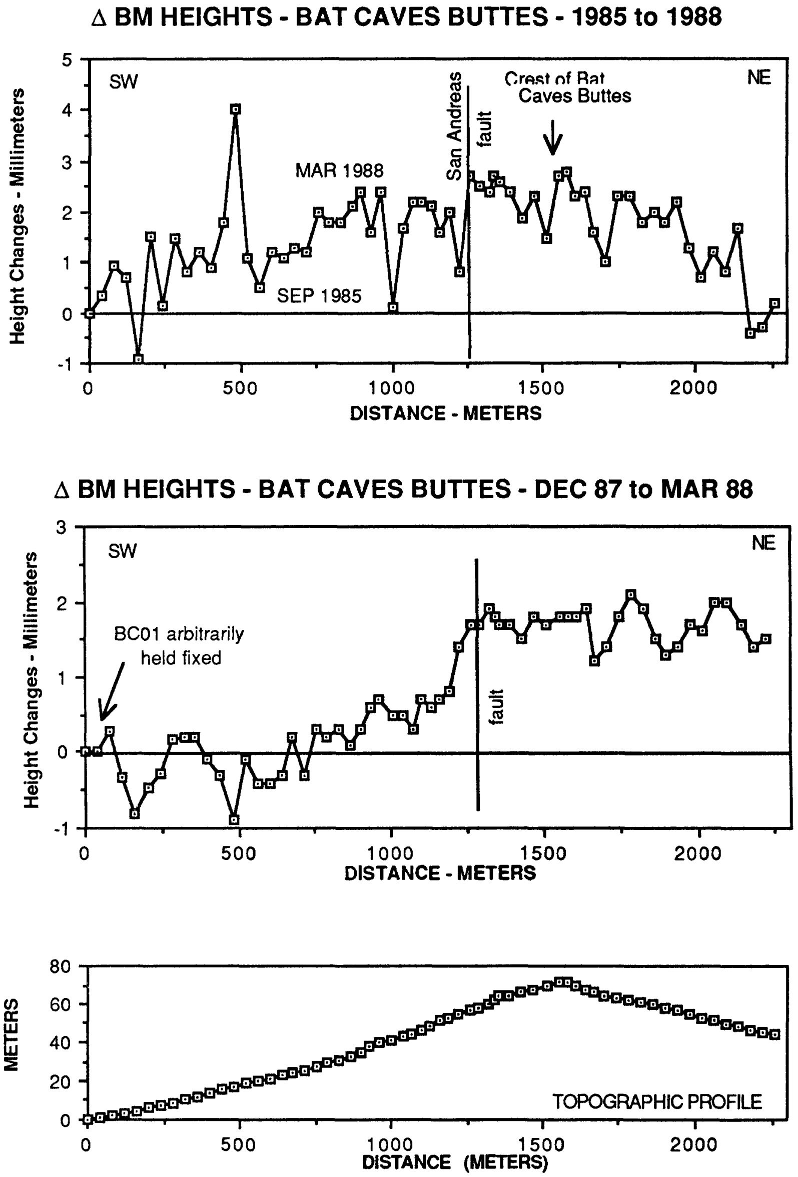

Δ BM HEIGHTS - BAT CAVES BUTTES - 1985 to 1988

Δ BM HEIGHTS - BAT CAVES BUTTES - DEC 87 to MAR 88

**Fig. 3**

# Earthquake Process

9930-03483

Robert L. Wesson
Branch of Seismology
U.S. Geological Survey
922 National Center
Reston, Virginia 22092
(703) 648-6785

## INVESTIGATIONS

1. Analysis of theoretical and numerical models of the processes active in fault zones leading to large earthquakes.
2. Analysis of seismological and other geophysical data pertinent to understanding of the processes leading to large earthquakes.

## RESULTS

Preliminary measurements of the stress orientation at a depth of 2 km in the Cajon Pass Scientific Drillhole, about 3.6 km from the San Andreas fault in southern California, have been interpreted by Zoback, Healy, and others to indicate that the regional orientation of the maximum compression is normal to the fault, and as evidence for a very weak fault. The orientation of the regional maximum compression expected from plate tectonic arguments is about 66 degrees from the strike of the fault. Geodetic data indicate the orientation of maximum compressive strain is about 43 degrees from the strike of the fault, and shows nearly pure right-lateral shear acting parallel to the fault. These apparently conflicting data may be explained in part by a model in which the fault zone is locked over a depth interval in the range of 2-5 to 15 km, but is very weak above and below that interval. An analytic solution for this geometry in an elastic plate predicts orientations of the principal stresses that are nearly parallel or normal to the fault, close to the fault and above and below the locked zone, but an orientation consistent with plate tectonic estimates at depths corresponding to that of the locked interval (Figure 1). This solution does require, however, a few mm/yr of creep at the surface on the San Andreas or nearby subparallel faults, which has not yet been observed.

## REPORTS

Wesson, R. L., Dynamics of fault creep, J. Geophys. Res., in press.

Wesson, R. L., Predicted variation of stress orientation with depth near an active fault: Application to the Cajon Pass Scientific Drillhole, submitted to Geophys. Res. Letters.

Wesson, R. L., Insights into creep, afterslip, and triggered slip from numerical simulation, EOS, Trans. Am. Geophys. Union, 69, 401, 1988.

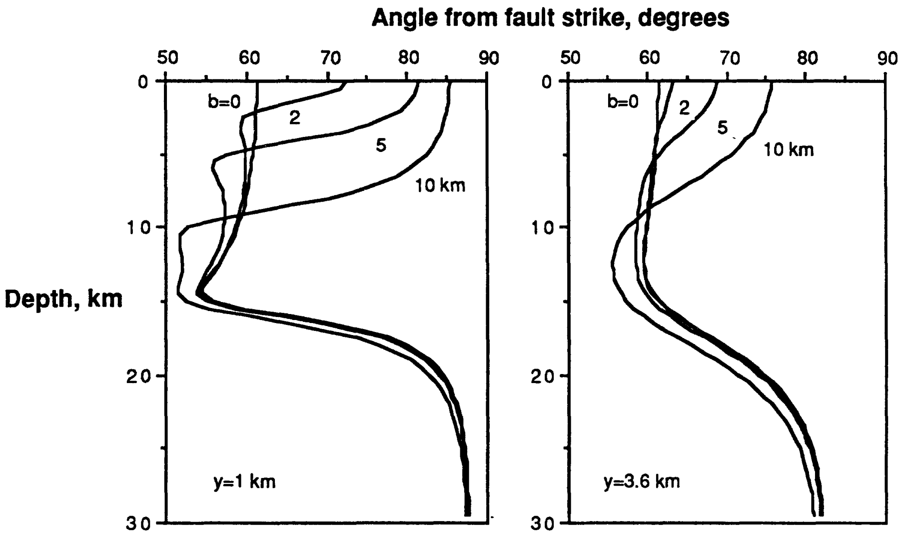

Figure 1. Orientation of the maximum horizontal principal compression relative to the fault strike versus depth for distances y=1 km (left) and 3.6 km (right) from the fault. The elastic plate is loaded by pure shear, with the maximum compression oriented at 66 degrees to the fault strike (N07$^{o}$E). The plate is 30 km thick. Slip is permitted on cuts along the trace of the fault, extending from the upper surface to a depth b (0, 2, 5, and 10 km), and from 15 km to the bottom.

# In-Situ Stress in S. California

14-08-0001-G1604

Thomas J. Ahrens
Seismological Laboratory 252-21
California Institute of Technology
Pasadena, CA 91125
(818) 356-6906

## Investigations:

1. Construct and test a new 6" fully pressurized, and digitally controlled in-situ holographic stressmeter for initial deployment in San Andreas region scientific boreholes. This instrument is expected to measure the complete in-situ stress tensor over a wide range of downhole conditions in zones of solid and deformed rock.
2. Develop analytical and numerical tools to invert holographic interference fringe data taken in several orientations to obtain complete 6-component in-situ stress tensor at depth.

## Results

### 1. Holographic Stressmeter.

A great deal of our experimental effort during the last period has gone into completing construction of the 6" holographic stressmeter apparatus. This 300 lb. instrument consisting of computer controlled mechanical electronic, optical, and hydraulic components is new and is capable of measuring all 6 components of the in-situ stress tensor from uncased fluid filled boreholes to depths of several kilometers. This has never been done before. The new technique should complement the existing hydrofracture method (which, in principle, can determine the orientation and magnitude of the maximum and minimum horizontal stress). We have written extensive software for the operation of the apparatus and its various systems. Important features of the 6" instrument are onboard gas pressurization which maintains the optical cavity used for holographic recording at pressures equal to the mud pressure in the hole, a mud-cake removal and water flushing system, an optical television system for monitoring the borehole wall through filtered, optically-clear, borehole fluid, and the ability to measure in-situ elastic modulus as a function of depth by the indention technique.

In addition to completion of construction and testing of the 6" holographic stressmeter with partial support of DOE, we refurbished a 1981 Schlumberger, Type 7600 logging truck. Power supplies and cable tensioning transducing system has been purchased and is now partially installed.

### 2. Holographic In-Situ Stress Data Analysis.

During the previous period, we have conducted finite element analysis of the deformation around the side test holes in the holographic stressmeter (Smither et al., 1988) to determine the precision which could be obtained with this instrument using the 2-dimensional plate model approximation. This approximation was employed in our previous analysis. The finite element results, demonstrate that the 2-dimensional plate model provides a reasonable approximation to the real rock displacements at radii of greater than 1.3a, where a is the radius of the sidehole. Because the vertical displacements near the edge of the borehole are not taken into account in this model the value of the in-situ stress inferred by comparison calculated to observe interference patterns will tend to give us in-situ stress values which are systematically too high by 10 to 30%.

To overcome this problem, we have calculated the 3-dimensional problem of the surface displacements resulting from the drilling of a deep hole in a prestressed half-space. This is exactly the problem we need to solve within the approximation that the radius of the access drillhole is much greater than the side hole radius and that the depth of the side hole drilled is much greater than its radius. The numerical solution of this problem is outlined in a draft manuscript which we expect to submit to Int. J. Rock Mechanics Min. Sci. (Smither and Ahrens, 1988).

## PUBLICATIONS

1. Analysis and modeling of holographic measurements of in-situ stress, Catherine L. Smither, Douglas R. Schmitt, and Thomas J. Ahrens, Int. J. Rock Mech. Min. Sci., in press (1988).
2. In-situ holographic elastic moduli measurements from boreholes, Douglas R. Schmitt, Catherine Smither, and Thomas J. Ahrens, Geophysics, in press (1988).
3. Displacements from relief of in-situ stress by a cylindrical hole, Catherine L. Smither and Thomas J. Ahrens, draft manuscript.
4. Application of double exposure holography to the measurement of in-situ stress and the elastic moduli of rock from boreholes, Douglas Schmitt, Ph.D. Thesis, California Institute of Technology (1987).

# ROCK MECHANICS

9960–01179

James Byerlee
U.S. Geological Survey
Branch of Tectonophysics
345 Middlefield Road, MS/977
Menlo Park, California 94025
(415) 329–4841

## Investigations

Laboratory experiments are being carried out to study the physical properties of rocks at elevated confining pressures, pore pressure and temperature. The goal is to obtain data that will help us to determine what causes earthquakes and whether we can predict or control them.

## Results

Many of the secondary fault structures developed during triaxial friction experiments have been generally correlated with the structures of natural fault zones. Therefore, any physical differences that can be found between laboratory samples that slide stably and ones that show stick–slip motion may help to identify the cause of earthquakes. We have examined petrographically the run products of many triaxial friction experiments using clayey and quartzofeldspathic gouges, which comprise the principal types of natural fault gouge material. The examined samples were tested under a wide range of temperature, confining and fluid pressure, and velocity conditions.

The clayey and quartzofeldspathic gouges show some textural differences, owing to their different mineral contents and grain sizes and shapes. In the clayey gouges, for example, a clay mineral fabric and kink band sets are commonly developed, whereas in the quartzofeldspathic gouges fracturing and crushing of the predominantly quartz and feldspar grains are important processes. For both types of gouge, however, and whatever the pressure–temperature–velocity conditions of the experiments, the transition from stable sliding to stick–slip motion is correlated with (1) a change from pervasive deformation of the gouge layer to localized slip in subsidiary shears, and (2) an increase in the angle between the shears that crosscut the gouge layer (Riedel shears) and ones that form along the gouge–rock cylinder boundaries (boundary shears). This suggests that the localization of shear within a fault zone combined with relatively high Riedel shear angles are somehow connected with earthquakes.

Secondary fracture sets similar to Riedel shears have been identified at various scales in major strike–slip faults such as the San Andreas of the western United States and the

Luhuo and Fuyun earthquake faults of China. The San Andreas also contains locked and creeping sections that correspond to the stick–slip and stably sliding experimental samples, respectively. We plan to study the physical structure of the San Andreas fault to see if the experimentally observed differences related to sliding behavior can also be distinguished in the field.

## Reports

Moore, D., 1987, Syndeformational metamorphic myrmekite in granodiorite of the Sierra Nevada, California, *Geol. Soc. Am.*, Abstracts with Programs, v. 19, p. 776.

Moore, D., C. Morrow, J. Byerlee, 1987, Fluid–rock interaction and future development in crystalline rock types, *U.S. Geol. Surv. Open-File Report 87-279*, 53 pp.

# PERMEABILITY OF FAULT ZONES

9960-02733

James Byerlee
Branch of Tectonophysics
U.S. Geological Survey
345 Middlefield Road, MS/977
Menlo Park, California 94025
(415) 329-4841

## Investigations

Laboratory studies of the permeability of rocks and gouge are carried out to provide information that will assist us in evaluating whether in a given region fluid can migrate to a sufficient depth during the lifetime of a reservoir to trigger a destructive earthquake. The results of the studies also have application in the solution of problems that arise in nuclear waste disposal.

## Results

Both laboratory and in situ studies indicate that high fluid pressures can lower the strength of fault materials and affect their sliding stability. In addition to the increase in hydrostatic pressure with depth, excess fluid pressures can be generated in the seismogenic zone by time-dependent or tectonically driven compaction of gouges, by fluid expansion during heating, and by metamorphic reactions that generate fluids. These processes become important to the long-term mechanical behavior of the seismogenic zone if the excess pore pressures can be maintained with time, a condition that requires low permeability of the gouge layer and/or the surrounding rocks.

Room temperature laboratory studies of natural clay gouges and comminuted rock flours show that permeability values are between $10^{-19}$ and $10^{-22} m^2$ under conditions of confining pressure and shear stress. These values are within the range where fluid flow can be inhibited through even moderately thin layers of gouge. Surficial crystalline rocks are typically more permeable, around $10^{-15}$ to $10^{-19} m^2$. Ongoing studies of crystalline rocks cored from the Cajon Pass drill hole near the San Andreas fault in California indicate, however, that hydrothermal fluids active near the fault zone can reduce the permeability of the country rock to values as low as that of particulate fault gouge due to the healing of microfractures in the rock. This creates an additional barrier to fluid flow around the fault zone.

High temperature may also act to substantially reduce the permeability of clay gouges, leading to an 'apparent' departure from the effective stress law during deformation. The clay particles become welded together and resemble slate after shearing, causing an increase in the frictional strength and a decrease in permeability. This reduced permeability prevents fluid pressure from equilibrating quickly, thereby creating excess fluid pressures in the gouge layer which affects the deformation behavior of the material. This process is important over long time scales, as well as during earthquakes when frictional heating is significant. The permeability of fault gouges under high temperature is not well studied, but may be an important factor in the seismogenic zone.

### Reports

Morrow, C., and J. Byerlee, 1987, Permeability of core samples from the DOSECC drill hole at Cajon Pass, California, *EOS*, v. 68, p. 1490.

# MECHANICS OF EARTHQUAKE FAULTING

9960–01182

James H. Dieterich
U.S. Geological Survey
Branch of Tectonophysics
345 Middlefield Road, MS/977
Menlo Park, California 94025
(415) 329–4867

## Investigations

1. Laboratory study of fault constitutive properties.
2. Modeling of the nucleation and occurrence of earthquakes.

## Results

1. Laboratory studies were shut down during this period by the asbestos removal project in our building. Some analysis of previous results continued during this period, including cooperative studies with J. Byerlee, of the importance of apparatus effects in conducting fault constitutive measurements; and cooperative study with C. Sammis and R. Biegel of the University of Southern California, of the relationship of gouge particle size distributions and fault roughness on fault constitutive properties.

2. Analytic solutions for the rate of earthquake nucleation events following a stress perturbation have been applied to model the occurrence of aftershocks as a function of time and location. The model assumes that the nucleation process for the initiation of unstable fault slip is governed by stressing history and by rate- and state-dependent constitutive properties as inferred from laboratory fault sliding experiments. In the absence of stressing perturbations, the background seismicity rate is a constant. In applying this model to aftershocks it is further assumed that a main shock event causes a stress step that initiates the aftershocks on adjacent fault segments. The rate of aftershocks at any location on a fault experiencing an increase of shear stress is:

$$\frac{dn}{dt} = \frac{R}{1 + [\exp(-\Delta\mu/A) - 1]\,[\exp(-t/t_a)]}$$

Where, $\Delta\mu$, is the stress step (divided by the normal stress), $A$ is a constitutive parameter and $t_a$ is the duration of the aftershock sequence. From the above relationship, the rate of occurrence of aftershock decays by the familiar $1/t$, then merges with the background rate, $R$. The duration of the aftershock sequence is predicted to be proportional to the earthquake recurrence time, $t_r$:

$$t_a = Ct_r / \ln t_r$$

Values of $C$ fall in the range (0.5 – 1.0) depending upon constitutive parameters. A preliminary sampling of aftershock sequences at least qualitatively supports the prediction that aftershock duration is proportional to recurrence time and suggests the possibility that aftershocks might provide a rough basis for estimating recurrence times in areas where other recurrence data is not available.

The model further predicts that an aftershock zone will show an apparent growth with time. The aftershock rate at some location, $x$, with a stress step $\Delta\mu(x)$, will, at time, $t_s$, merge with the aftershock rates at locations where the stress step was higher.

$$t_s = t_a \exp[-\Delta\mu(x)/A]$$

At the ends of a plane strain, constant stress drop fault, of length $a$, the apparent end of the aftershock zone will be at position $x$ (where $x > a$) at time $t_s$ as given by:

$$t_s = t_a \exp\left\{-\left[\frac{t_r}{t_a}\right]\left[\frac{x}{(x^2 - a^2)^{1/2}} - 1\right]\right\}$$

The various predictions of this model are currently the subject of closer study and comparison with aftershocks in nature. These include the dependence of aftershock rates to the magnitude of the stress perturbation, the relationship of aftershock durations to recurrence time and spreading of aftershocks zones with time.

## Reports

Dieterich, J.H., 1987, Nucleation and Triggering of Earthquake Slip: Effect of Periodic Stresses, *Tectonophysics*, **144**, 127–139.

Dieterich, J.H., 1987, Probability of Earthquake Recurrence with Nonuniform Stress Rates and Time–Dependent Failure, in Physical and Observation Basis for Intermediate–Term Earthquake Prediction, *U.S. Geological Survey Open–File Report*. 87–591, 689–725. Also in press, *PAGEOPH.*

Mikumo, T., Dieterich, J.H., Chen, Y.T., and Kasahara, K., 1987, Introduction to: Mechanics of Earthquake Faulting, edited by R.L. Wesson, *Tectonophysics*, **144**, 1–3.

Biegel, R.L., Sammis, C.G., and Dieterich, J.H., 1987, Frictional Properties of a Simulated Fractal Gouge Layer in Westerly Granite, Abstract, *EOS, Transactions of American Geophysical Union*, **68**, 1478.

Dieterich, J.H., 1988, Growth and Persistence of Hawaiian Volcanic Rift Zones, *Journal of Geophysical Research* (in press).

Yang, X.-M., Davis, P.M., and Dieterich, J.H., 1988, Deformation of a Dipping Finite Prolate Ellipsoid in an Elastic Half-Space as a Model for Volcanic Stressing, *Journal of Geophysical Research* (in press).

# THE PHYSICS AND MECHANICS OF THE BRITTLE-DUCTILE TRANSITION

14-08-0001-G1340

BRIAN EVANS AND JOANNE FREDRICH

*Dept. of Earth, Atmospheric, & Planetary Sciences*
*Massachusetts Institute of Technology, Cambridge*

14-08-0001-G1352

TENG-FONG WONG

*Dept. of Earth & Space Sciences*
*State University of New York, Stony Brook*

### *Objectives*

The physical mechanisms of semi-brittle rock deformation in the Earth are poorly understood and are important in understanding seismogenic faulting and aseismic fault creep. We are conducting an integrated laboratory and observational study of the deformation mechanisms operating during the brittle-ductile transition, the micromechanics of semi-brittle flow, and the effect of variations in pressure, temperature, porosity, and second-phase content on the strength of rocks deformed in the semi-brittle regime. Current work is focusing on the experimental deformation of marble and the theoretical investigation of crack nucleation mechanisms in the semi-brittle regime.

### *Micromechanics of the brittle to plastic transition in Carrara marble*

To study the micromechanics of the brittle to plastic transition, we integrate mechanical measurements of axial stress and strain, volumetric strain, and quantitative stereological characterization of the stress-induced microstructure using optical and transmission electron microscopy on samples of Carrara marble deformed to varying strains at confining pressures spanning the range in mechanical behavior from brittle to plastic.

In the semi-brittle field, deformation mechanisms include microcracking, twinning, and dislocation glide. At constant $P_c$, the density of twins increases with strain. Microcracking occurs along grain boundaries and intragranularly. With increasing pressure ($P_c$), the density of microcracks at constant strain decreases. Stress-induced crack anisotropy also decreases with $P_c$, however, crack anisotropy remains significant for $P_c < 300$ MPa. Slip planes are well developed in some grains in samples deformed at pressures only slightly greater than those at which brittle fracture occurs. Microcracks and voids are observed to initiate at inhomogeneities in twin boundaries, twin terminations, and at the intersection of twin lamallae. High dislocation densities are sometimes observed at crack tips.

The sterological data suggest that the crack or "damage" structure necessary for localization $=f(P_c)$ and that localization is inhibited by the decreased density of cracking, rather than by a critical change in the anisotropy of cracking. An analysis of the energetics of deformation shows that in the semi-brittle field, the energy budget for microcracking is a decreasing function of confining pressure. Qualitative TEM observations indicate that this trend is paralleled by an increase in dislocation activity, although the quantitative measurements of dislocation density show large scatter due to the high dislocation density in the starting material. We conclude that the transition from brittle failure to plastic flow is associated with the decreased contribution of brittle cracking and increased contribution of plastic flow to the total energy budget and that there exists a critical ratio of brittle energy dissipation to total energy dissipation below which localization is not possible. The details of this study are presented in a paper by *Fredrich, Evans & Wong* [1988].

### *Nucleation and propagation of cracks in the semi-brittle regime*

Our experimental results in conjunction with recent studies by other workers have demonstrated that the interaction among dislocations, mechanical twins, and microcracks plays an important role in controlling the semi-brittle deformation mechanism. Stroh's model is often cited in the interpretation of such microscopy observations. A dislocation pile-up against an obstacle such as a grain boundary can induce a local tensile stress which has a maximum at about 70° to the glide plane. The stress concentration can be sufficiently high to nucleate tensile microcracking. *Francois & Wilshaw* [1968] showed by energetic consideration that the nucleation process is not sensitive to pressure.

The stability of the subsequent propagation of a crack nucleated by Stroh's mechanism can influence profoundly the micromechanics of semi-brittle deformation. We are not aware of any theoretical analysis of the propagation behavior under all compressive loading. Our fracture mechaniscs analysis shows that the stress intensity factor $K_I$ can be considered to be the superposition of two opposite components: i) a tensile component due to the dislocation pile-up which is proportional to $nb/\sqrt{c}$ (where n is the number of dislocations with Burgers vector $b$, and c is the half-length of the crack); and ii) a component due to the compressive loading which is proportional to $-\sigma\sqrt{c}$ (where $\sigma$ is the normal stress acting on the crack plane) .

As a crack propagates, c increases and the latter compressive component gradually dominates the crack tip stress field, thus stabalizing the propagation behavior. In a stable mode, the crack gradually takes up a propagation path parallel to the maximum compressive stress. Hence in-plane propagation of a Stroh crack is possible only to a limited extent. We obtain an upper bound on the length $l_c$ for triaxial compression (confining pressure P and differential stress $\sigma_d$) to be:

$$l_c/d = (\sqrt{2}/3)\,(\sigma_d/2-\tau_s)\;/\;(P+.186\sigma_d)$$

where D is the grain size and $\tau_s$ is the glide resistance.

We are currently pursuing this theoretical analysis in two directions. First, numerical computation is performed to analyze the evolution of out-of-plane propagation. Second, cracking induced by mechanical twinning is analyzed by modelling the twinning process as "transformational strain" following the approach of *Kinsman, Sprys & Asaro* [1975].

*Decrepitation and healing of fluid inclusions*

Field observations and experimental studies have documented that fluid inclusion decrepitation nucleates cracking in the semi-brittle regime. Our results on San Carlos olivine and other published data show several systematic trends. First, the decrepitation pressure increases with decreasing inclusion dimension and increasing confining pressure. Second, the length of crack propagation increases as a function of the inclusion dimension. Third, the cracking is usually unstable, emitting an acoustic emission.

We have developed a fracture mechanics model to interpret these observations. Dimension of the flaws on the fluid inclusion surface is assumed to scale as the bubble radius. The crack arrest process is modelled by using a reasonable equation of state for the fluid to evaluate the pore pressure reduction induced by crack volume increase which is then used to determine the decrease in $K_I$. This work has been written up in a paper by *Wanamaker, Wong & Evans* [1988].

*Abstracts and Submitted Papers*

Fredrich, J., Evans, B., & Wong, T.-f., The mechanics of semi-brittle deformation in Carrara marble, *EOS, Trans. Am. Geophys. Un.*, **68**, 1464, 1987.

Fredrich, J., Evans, B., & Wong, T.-f., Micromechanics of the brittle to plastic transition in Carrara marble, submitted to *J. Geophys. Res.*, 1988.

Wanamaker, B., Evans, B., & Wong, T.-f., Fluid inclusion decrepitation (cracking) in San Carlos olivine, *EOS, Trans. Am. Geophys. Un.*, **68**, 1527, 1987.

Wanamaker, B., Wong, T.-f., & Evans, B., Fluid inclusion decrepitation in xenoliths: a fracture mechanics analysis, submitted to *J. Geophys. Res.*, 1988.

Wong, T.-f., Effect of pressure on propagation behavior of microcracks nucleated by Stroh's mechanism, *EOS, Trans. Am. Geophys. Un.*, **68**, 404, 1987.

# High Frequency Seismic and Intensity Data

9910-03793
Jack Evernden and Jean Thomson
Branch of Engineering Seismology and Geology
U.S. Geological Survey
345 Middlefield Road
Menlo Park, California 94025
(415) 329-5627

*Investigations:*

1) Investigating via quantitative modeling of earthquake and explosion spectra the roles of elastic velocity structure, depth of focus and anelastic attenuation on the amplitude and spectral content of both compressional and shear phases ($P_n$, $P_g$, $S_n$ and $S_g$-$L_g$, etc.) as a function of distance.

2) Investigating via large data sets the P-wave spectral content of earthquakes and explosions, the intent being to place in the literature a definitive analysis of this relationship.

*Results:*

1) In EUS-like terrains, the crustal velocity model must be such as to display a $\Delta^{-2}$ fall-off for $P_n$ from 150 to ~2000 km. Modeling has shown such a die-off rate, even at high $Q_\alpha$ values, requires a zone several kilometers thick just above the Moho in which velocity increases by ~0.6 km/sec. There can be no appreciable zone with $P_n > 7.2$ above the Moho (other than the gradient zone), such a model leading to drastic misbehavior of predicted $P_n$ amplitudes in the distance range 150-400 km. A similar but less well-developed velocity increase to that in the EUS-like area above the Moho is required in WUS-like terrain (even with the lower $Q_\alpha$ values) to explain the $\Delta^{-3.5}$ rate of die-off of $P_{7.9}$. Also, explanation of the zero-intercept $P_g$ curve requires a low velocity zone of a few tenths of a km/sec at ~10 km depth in the crust, the velocity increase below that zone being markedly constrained by the requirement to fit observed rates of die-off of $P_g$.

2) The work on 1) has taken much longer than expected, so progress on this phase of the work has been very slow.

3) As a service, we produced intensity maps for the recent southern California earthquakes, the predictions for the Whittier Narrows earthquake agreeing quite nicely with observations. We also generated, and provided to J. Filson, Calcomp plots of predicted earthquakes throughout the USA, illustrating the known facts of intensity vs. rupture length vs. area of occurrence.

Work continues on 1) and 2). We are presently studying the perturbation in published USSR velocity structures required to explain die-off rates and relative amplitudes of $P_g$ and $P_n$ phases. It is certain that a zone of rapid velocity increase above the Moho is required.

*Reports:*

Paper in preparation.

# Field Verification of the New Fracture Pressurization Method for In Situ Stress Determination in Earthquake Prediction Research

14-08-0001-G1517

Bezalel C. Haimson
Geological Engineering Program
University of Wisconsin
1509 University Avenue
Madison, Wisconsin 53706
(608) 262-2563

Objective: A new method of hydraulic fracturing interpretation has been recently proposed which offers distinct advantages over the conventional practice (Cornet and Valette, 1984). The new Fracture Pressurization Method (FPM) is not limited to isotropic rock, vertical drillholes and vertical hydrofracs, and intact zones for testing; it also requires fewer test parameters to be determined. The objective of our program is to verify the applicability and reliability of FPM through a series of field tests in which FPM will be compared with the conventional approach to hydraulic fracturing interpretation.

Field Testing Preparation: The first three months on this project were spent preparing for the field tests. Equipment such as inflatable packers and impression packers have been purchased, and the rest of the equipment updated and readied for the upcoming tests near Waterloo, Wisconsin. An earlier borehole televiewer log has been analyzed for locating test intervals. Both intact and prefractured zones will be tested. The 100 m and 300 m holes near Waterloo are particularly appropriate for these tests because they range in inclination from 0 to 45 degrees, and because the Precambrian quartzite is moderately anisotropic.

# Earthquakes and the Statistics of Crustal Heterogeneity

*9930-03008*

*Bruce R. Julian*

Branch of Seismology
U.S. Geological Survey
345 Middlefield Road - MS77
Menlo Park, California 94025
(415) 329-4797

## Investigations

Both the initiation and the stopping of earthquake ruptures are controlled by spatial heterogeneity of the mechanical properties and stress within the earth. Ruptures begin at points where the stress exceeds the strength of the rocks, and propagate until an extended region ("asperity") where the strength exceeds the pre-stress is able to stop rupture growth. The rupture termination process has the greater potential for earthquake prediction, because it controls earthquake size and because it involves a larger, and thus more easily studied, volume within the earth. Knowledge of the distribution of mechanical properties and the stress orientation and magnitude may enable one to anticipate conditions favoring extended rupture propagation. For instance, changes in the slope of the earthquake frequency-magnitude curve ("b-slope"), which have been suggested to be earthquake precursors and which often occur at the time of large earthquakes, are probably caused by an interaction between the stress field and the distribution of heterogeneities within the earth.

The purpose of this project is to develop techniques for determining the small-scale distributions of stress and mechanical properties in the earth. The distributions of elastic moduli and density are the easiest things to determine, using scattered seismic waves. Earthquake mechanisms can be used to infer stress orientation, but with a larger degree of non-uniqueness. Some important questions to be answered are:

** How strong are the heterogeneities as functions of length scale?

** How do the length scales vary with direction?

** What statistical correlations exist between heterogeneities of different parameters?

** How do the heterogeneities vary with depth and from region to region?

Scattered seismic waves provide the best data bearing on these questions. They can be used to determine the three-dimensional spatial power spectra and cross-spectra of heterogeneities in elastic moduli and density in regions from which scattering can be observed. The observations must, however, be made with seismometer arrays to enable propagation direction to be determined. Three-component observations would also be helpful for identifying and separating different wave types and modes of propagation.

The stress within the crust is more difficult to study. Direct observations require deep boreholes and are much too expensive to be practical for mapping small-scale variations. Earthquake mechanisms, on the other hand, are easily studied and reflect the stress orientation and, less directly, its magnitude, but are often not uniquely determined by available data.

This investigation uses earthquake mechanisms and the scattering of seismic waves as tools for studying crustal heterogeneity.

## Results

### Access to CUSP Digital Data

For several years, the CUSP (Caltech-USGS Seismic Processor) system has been saving digital seismograms for earthquakes in central California, but these seismograms have, as a practical matter, been inaccessible to seismological researchers. The procedure for retrieving the data from CUSP archive tapes has been cumbersome and time consuming, and has required extensive help from the already overburdened CUSP project personnel. During the last six months, with the assistance of David Oppenheimer, Allan Lindh, and the aforementioned CUSP project personnel, we have developed software that makes it relatively easy to read data from the CUSP archive tapes and to convert them to the Lamont-Doherty **AH** (AdHoc) format. There exists a large body of software for manipulating and processing digital signals in this format on modern workstations, which are becoming widely available. We expect the ability to access the existing database of digital seismograms to be very valuable to many projects in the earthquake program.

### Upgraded Computing Facilities

The facilities available to branch projects for scientific computing have become inadequate, so that it often takes days to run some applications programs. During the previous six-month period, Barbara Bekins, the chief of the Seismological Data Processing Project, drew up a plan to begin to remedy this situation, by obtaining several scientific workstations and linking them through a local network to a central file and compute server. As Barbara has been on leave to attend graduate school, it has devolved upon us to carry this plan forward. We are now in the process of purchasing a SUN-4/280 server, which will multiply the processor power available to the branch by several times. Delivery and installation of this server, and its integration into a local network, are planned for this summer.

### Focal Mechanism Inversion

Previous semi-annual reports and Julian [1986] have described a way of using linear programming methods to invert seismic, static strain, and geodetic data to obtain earthquake source mechanisms. For small to medium numbers of observations, the program based on this approach is much faster than alternative methods, but for large data sets, this advantage is lost. This inefficiency results from using a simple but inefficient version of the simplex algorithm. We are now in the process of modifying the program so that it will be equally efficient for large and small data sets.

### Automatic Real-time Earthquake Monitoring

The real-time monitoring of central California seismicity using data from the Allen-Ellis Real-Time Processor (RTP) has continued routinely. No major changes have been made within the last six months.

Work has begun on a new method to detect unusual earthquake activity in real time. The existing method, which compares the numbers of events per day in each region with recent experience, has two disadvantages. First, it only operates once per day, so that many hours may elapse before an unusual occurrence is reported. Second, it can not attach significance levels to its reports; the historical sample does not give the true probability distribution, but merely a sample from it. In particular, it is difficult to interpret activity levels higher that the maximum in the sample.

Therefore, we are trying a new approach, suggested by Mark Matthews, which is based on the non-parametric Wilcoxon rank-sum statistical test. Each event is represented by a single value, which might be its magnitude, or the time since the previous event, for example. The last few events, which are to be tested, are combined with a much larger historical sample, and the combined sample is sorted by the event values. The sum of the ranks (position numbers) of the small sample is then a statistic whose distribution, under the null hypothesis that no changes have occurred, is independent of the underlying physical process. This distribution is tabulated in many statistics books, but unfortunately not for the sample sizes we wish to use. Therefore, we have had to develop a new algorithm, based on the Eulerian theory of partitions of integers, to compute the Wilcoxon statistic for testing a few elements from a large sample. A short paper describing this algorithm is in preparation. The new monitoring method will be incorporated into the routine RTP processing within the next few months.

### Seismological Database Management

At present, the earthquake catalog and other data generated in the real-time monitoring of central California earthquakes are stored in ordinary computer files. This scheme provides no safe way for more than one process to enter or modify data at a time, which makes manual editing of the data awkward and risky. Even worse, it makes impractical many desired improvements to the processing, such as merging data from multiple RTPs, automatically correcting mistakes made by the them, or re-computing and revising earthquake locations and magnitudes using regional earth models. Therefore, we have begun designing seismological database software to manage the real-time RTP data, which we hope will overcome the limitations of ordinary files. The Incorporated Research Institutions for Seismology (IRIS), who have needs similar to ours, have lent us a commercial database management system, DBVISTA, which our work so far indicates is well suited to this application. Currently, we have working a subroutine library that provides a seismologically oriented interface to databases, and programs to store and retrieve earthquake catalogs and associated seismic-wave readings. We expect it to be at least a year before we will be ready to begin using the new software in on-line RTP processing.

### Volcanic Tremor

Most of the work in the last six months has been directed toward understanding chaotic behavior in our model of volcanic tremor. This model, based on nonlinear flow-induced vibration in conduits transporting magmatic fluids, can exhibit chaotic behavior when acoustic resonance in the conduit is taken into account, but not, apparently, without resonance. Most observed volcanic tremor is chaotic in appearance, so it is important to understand chaotic behavior in the model. We currently are concentrating on finding methods for identifying and quantifying "strange attractors" responsible for the model's behavior as well as that of natural tremor, in order to test the model.

# EXPERIMENTAL ROCK MECHANICS

9960–01180

Stephen H. Kirby
Branch of Tectonophysics
U.S. Geological Survey
345 Middlefield Road, MS/977
Menlo Park, California 94025
(415) 329-4847

## Investigations

Direct study of aseismic fault zones in the mantle and lower crustal oceanic crust was the objective of Kirby's participation as staff specialist in Leg 118 of the Ocean Drilling Program to the Atlantis II fracture zone on the SW Indian Ridge.

Further study of anomalously low sliding resistance of olivine under hydrothermal conditions is being made possible by a new miniature pore pressure system under development.

Strain localization is being studied using sawcut samples at pressures and temperatures where, under hydrostatic conditions, sluggish polymorphic phase changes occur. We are studying the role of nonhydrostatic stress and deformation on transformation in the sliding surfaces.

Hydrolytic weakening in quartz depends upon the concentration level which, in turn, is sensitive to the pressure and temperature at which it is equilibrated. We are investigating the solubility of water in quartz using infrared spectroscopy and the ion probe.

## Results

**Aseismic fault zones:** 0.5 km of gabbros and metagabbros were acquired during ODP Leg 118 and this represents the most pristine section of lower oceanic crust (layer 3) ever investigated. In collaboration with Jerry Iturrino of Purdue University, Kirby investigated the velocity structure of the drill core. $V_p$ typically varies from 6.6–7.3 km at atmospheric pressure and several of the shear zones that cut the gabbroic section display $P$-wave velocity anisotropy as much as 11%. This work, as well as ongoing structural petrology of the shear zones, may help determine if ductile fault zones may be detectable using seismic reflection techniques applied to the lower crust of the oceans and continents.

**Alteration weakening of artificial fault zones.** Previous work has shown that hydrothermal alteration of dunite on sliding surfaces reduces sliding resistance well below that associated with dry friction. Those experiments were conducted on low-porosity samples with about 0.1 wt% water in the *undrained* condition. The apparatus is now in place to look at the effect of pore pressure in the shear zone on the sliding resistance and on the extent of hydrothermal alteration. Alteration weakening has potential for explaining why shear stresses along crustal faults appear to be low at shallow to mid-crustal depths.

**Localized polymorphic phase changes and deep earthquakes.** Following up on work reported in a recent discovery paper (Kirby, 1987), Lisa Dell'Angelo has done additional experiments on polycrystalline tremolite. She has discovered that reducing temperature while the samples are under axial load at pressure promotes high-pressure faulting and that high-pressure faulting occurs at lower pressures than suggested by earlier work. More recent work focuses on localization of phase changes along artificial faults in materials expected to undergo polymorphic phase change under conditions expected to favor such transformations.

**Water solubility and hydrolytic weakening in quartz.** Diffusion rates of molecular water in quartz are so slow that it has not been possible to equilibrate a millimeter-scale sample at practical times and temperatures. Two methods are being used to determine the solubility indirectly. A sample has been annealed in $D_2O$ at elevated pressure and temperature, and the surface concentration of deuterium is being measured by an ion probe. The near-surface concentration of deuterium above that required to saturate aluminum substitutional sites is a measure of the molecular water solubility. Second, the solubility may be bracketed by annealing samples with varying initial water concentration and observing whether molecular water has precipitated or not. A suite of quartz samples have been prepared and characterized using Fourier Transform Infrared Spectroscopy.

## Reports

Kirby, S. H., 1987, Localized polymorphic phase transformations in high pressure faults and applications to the physical mechanism of deep earthquakes, *Journal of Geophysical Research,* v. 92, p. 13,789–13,800.

Dell'Angelo, L. and Kirby, S. H., 1987, Strain localization in rocks: phase transitions, mineral reactions and localization on pre-existing faults, *Trans. Am. Geophys. Union,* v. 68, p. 1471.

Wilshire, H. G. and Kirby, S. H., 1988, Dikes, joints and faults in the upper mantle, *Tectonophysics,* (submitted).

# Physical Processes in Shear Zones

14-08-0001-G1509

John M. Logan
Center for Tectonophysics
Texas A&M University
College Station, Texas 77843
(409) 845-0312

Objectives: The purpose of this effort is to elucidate the processes operating in shear zones, and specifically those leading to earthquakes. Although frictional processes have been widely investigated through laboratory experiments the physical processes associated with changes in mechanical behavior are poorly understood. To aid in our understanding we have proposed: 1. To utilize the results of recent studies of halite shear zones to investigate rate dependence and physical process of simulated gouge of calcite deformed in shear.

2. To test our hypotheses that changes of gouge fabric in shear leads to localization of displacement; that along these surfaces changes in area of contact produce negative velocity dependency; and that negative dependency is experimentally related to instability .

Recent Results: The first part of this contract year has been devoted to clarifying the development of simulated fault gouge as it is sheared. The changes in mechanical behavior have been correlated with concurrent changes in fabric of the shear zone and physical processes. Use of black (organically coated) and white calcite has permitted markers to be placed in the shear zone before the experiment. Offset of these markers enables definition of the accommodation of strain within the zone.

In triaxial experiments, compaction with little displacement parallel to the sides of the shear zone occurs with the initial application of differential stress. Fabric elements are defined by R, $R_1$, and P orientations. This compaction proceeds until a critical density is achieved, at which time shear parallel to the interface with the host rock takes place. Now the accommodation of shearing shifts to Y surfaces close to one or both interfaces. The sliding, although initially stable, may become unstable with displacement. At higher normal stress the initial compaction occurs along closer spaced R and P surfaces and is more homogeneously accommodated within the shear zone. The compaction occurs with less displacement parallel to the zone boundaries and stick-slip occurs soon after the Y surfaces form. Y-surfaces are noticeably smoother when they have been the locus of stick-slip sliding as compared with stable slip.

The compaction phase is associated with an initial strain hardening of the differential stress--shortening curve. The ultimate strength is reached during the compaction and strain softening occurs with the formation of the Y surface. Once it is well developed steady-state behavior occurs (i.e. the stress-shortening curve is horizontal) . Stick-slip oscillations may develop if suitable boundary conditions are imposed.

Studies at relatively low confining pressures--about 30 MPa--show an onset of instability with increasing temperature. This occurs at about 300° C. We are presently investigating the processes associated with this shift in behavior.

Now that our understanding of the gouge development is better we are beginning studies of calcite shear zones deformed at different normal stress, temperature and velocities.

# ROCK DEFORMATION

9950-00409

Eugene C. Robertson
Branch of Geologic Risk Assessment
U.S. Geological Survey
MS 922, National Center
Reston, Virginia 22092
(703) 648-6792

## Investigations

Dynamic loading tests of rock samples driven in compression are being made to determine energy absorption by microfracturing, the effects of load level and total strain, the effect of frequency, and the variation of mechanical properties with rock type.

## Results

Samples of granite, basalt, and limestone were tested dynamically in uniaxial compression at frequencies of 1, 0.1, 0.01, and 0.002 Hz to stress levels from 10 to 80 percent of their compressive strengths, corresponding to maximum strains from 5 to 40 x $10^{-4}$ units. Examples of plots are given in Figure 1 of stress-strain hysteresis loops at various loads and frequencies. Unfortunately, the test apparatus had a hydraulic component which increased its compliance such that stress-strain measurements were accurate only to about 5 percent at low stresses, whereas 0.1 percent precision is needed for close comparisons of moduli.

Values of the energy dissipation coefficient, $Q^{-1}$, determined from phase angle measurements of strain and stress, were found to remain essentially constant with frequency for all three rocks at a given stress level. The granite samples were stiff, with E (Young's modulus) about 70 GPa; $Q^{-1}$ decreased from 0.06 to 0.03 from low to medium stress; no finite strain was observed in successive cycles (Fig. 1a). Reliable $Q^{-1}$ values could not be obtained at very low stresses. The limestone samples, on the other hand, were less stiff (E=40 GPa) and had constant $Q^{-1}$ = 0.04 for all stresses (Fig. 1b). The basalt samples, although stiff (E = 65 GPa), had quite high energy dissipation, $Q^{-1}$ = 0.25, at high stresses, although low (0.06) at low stress. Considerable finite strain per cycle was observed in the basalt (Fig. 1c, 1d) and in the limestone (not shown), about 4 x $10^{-5}$ strain units per cycle. This finite strain was fully recovered in the limestone, due to healing by its well-known ductility, but in the basalt samples, healing recovery of the finite strain in basalt was not complete, as incipient fatigue effects were observed. Converting energy absorbed to surface energy of microcracks, 10 percent of each grain's surface was estimated to open up during each cycle in basalt (Fig. 1c). The effect of a high stress range (120 to 250 MPa) in basalt (Fig. 1d) was to decrease $Q^{-1}$ to 0.10, a well-known effect of confining pressure on seismic wave attenuation. Continued, more precise measurements are planned to help explain near-field energy absorption by earthquake and explosion events.

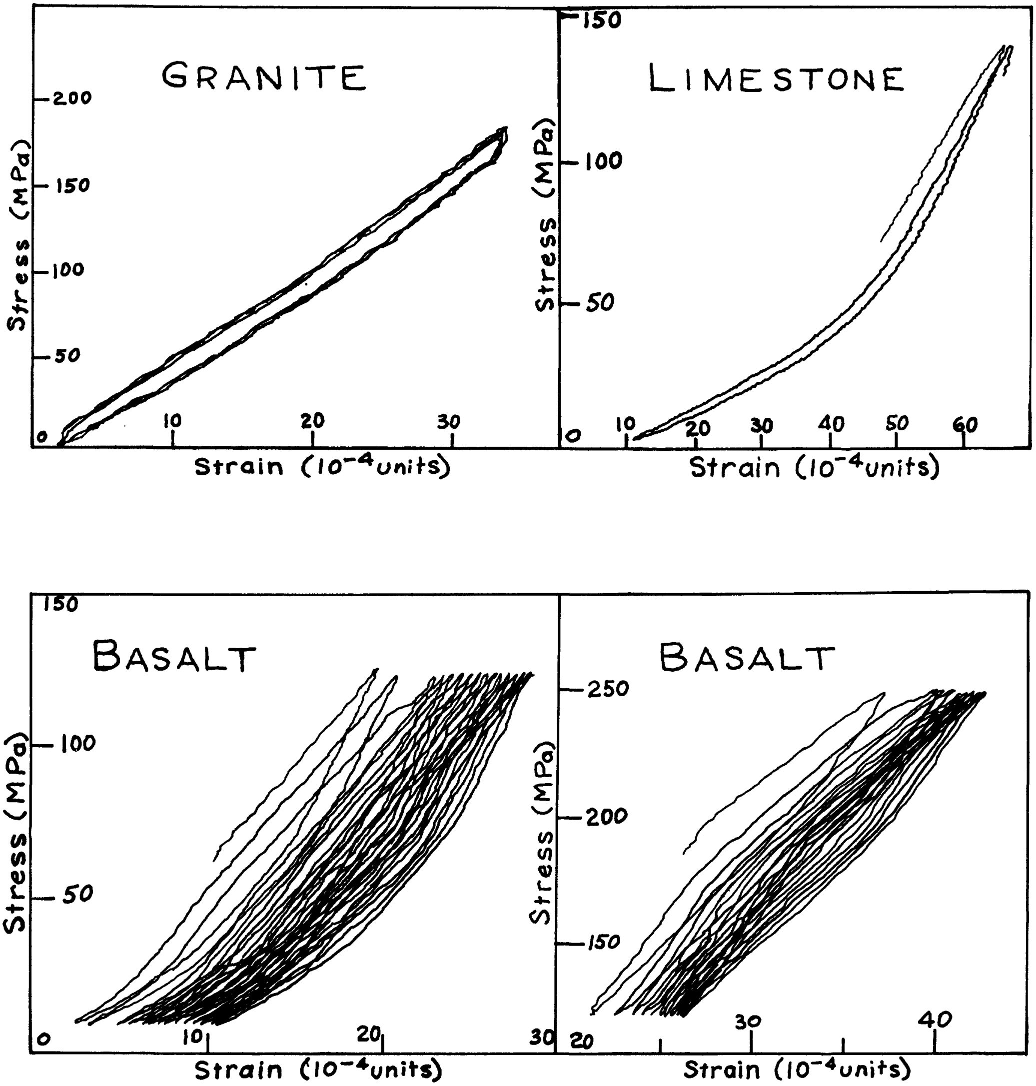

Figure 1. Dynamic compression tests to observe energy dissipation under moderate stresses. a. Granite sample (G-4) freq. = 0.1 Hz, 3 cycles; b. limestone sample (L-5) freq. = 0.002 Hz, 1 cycle; c. basalt sample (B-6), freq. = 1 Hz, 22 cycles; d. basalt sample (B-7), freq. = 0.1 Hz, 11 cycles.

# Accurate Three-Dimensional Calculations for Advancing Slip Zones in the Earth's Crust

(Joint funding with NSF Grant EAR-8707392)

J. W. Rudnicki and L. M. Keer
Department of Civil Engineering
Northwestern University
Evanston, Il 60208
(312)-491-3411

(For period February 1, 1988 to April 30, 1988)

## Objectives

Understanding the mechanism by which slip is transmitted from depth to the surface and along the strike of the fault from freely slipping to locked zones is of great importance for understanding the earthquake process and for possibly anticipating damaging events. A major impediment to more accurate and realistic analyses has been the difficulty of making calculations for three dimensional cracked bodies. We are doing three-dimensional analysis of slip zones (cracks) in an elastic half-space to determine stresses and surface deformations due to the advance of shear faults into locked, or more resistant portions, of the shallow crust. The goal of these studies is to understand and develop theoretical models for the advance of slip zones into and around slip resistant portions of the fault, focussing particularly on the effects of nonuniformities in the advancing slip front. Because of local regions of higher ("asperities" or "barriers") or lower resistance to slip, the slip front may lag behind or move ahead of adjacent regions. Of particular interest is the stability of these perturbations. Are perturbations damped or magnified depending on wavelength, amplitude, etc.? Do segments of the slip front that lag behind adjacent segments catch-up by sudden rapid slip? Will such rapid slip trigger a larger instability?

## Results

During the first three months of the project, which is the period covered by this report, we have concentrated on the refinement and development of our computational procedures and the training of a student to use them. Subsequent work will focus on the application of these procedures to configurations of geophysical interest.

The method of Lee and Keer [1986], developed for tensile crack propagation in bimaterials, has been extended to shear cracks in an elastic half-space. Their method uses the integral representation for a distribution of body force and the elasticity solution for a point force near a bimaterial interface (free surface in the present application). The problem is then reduced to the solution of an integral equation for the unknown crack surface displacements over the two dimensional surface of the crack. Because the method uses the exact asymptotic form of the displacement field near the edge of the crack in discretizing the kernel of the integral equation, the results are accurate. In addition, no unusual difficulties are encountered when the slip zone intersects the free surface.

The procedure of Lee and Keer [1986] has been formulated for interior crack problems or, in other words, isolated slip zones (though of arbitrary shape). Much of our effort during the initial stages of this project has been directed toward formulation of a complementary procedure for exterior crack problems, as needed to treat problems of slip advancing toward a free surface or around an isolated asperity. This is being done using the solution for point loading on the surface of an elastic quarter space. The solution for tangential loading of the surface of an quarter space can, by using symmetry, be used to construct the solutions for an isolated ligament (asperity or barrier) resisting slip on a fault plane in an elastic half-space.

We are investigating two approaches to the quarter space problem. The first follows that of Hetenyi [1970] for the case of normal loading. He assumed uniformly distributed normal stresses to act over small rectangular regions of the free surface fo the quarter space. By using Love's solution for this problem and a reflection scheme, Hetenyi [1970] constructed the solution for concentrated normal loading of the quarter space. This method produced accurate results as long as the load was not too close to the edge of the quarter space.

To avoid the restriction on the location of the applied load, Keer et al. [1983] reduced the problem of an elastic quarter space subjected to either normal or tangential loadings to two uncoupled integral equations by applying a Fourier transform to the Boussinesq potentials in the direction of the edge of the quarter space. The stress and displacement were calculated from these transformed potnetials. Even though this approach is numerically slow, it does not have any restriction on the location of the applied load. Consequently, it can be applied to the shear of two quarter spaces connected by an arbitrarily located, finite size ligament.

These two approaches are presently being implemented numerically and checked for accuracy. A study of the related, but two-dimensional, problem of an elastic quarter plane by Hanson and Keer has been completed.

## References

Hetenyi, M., A general solution for the elastic quarter space, J. Appl. Mech., **37**, 70-76, 1970.

Keer, L.M., J.C. Lee, and T. Mura, Hetenyi's elastic quarter space problem re-visited, Int. J. Solids Structures, **19**, 497-506., 1983.

Lee, J.C., and L.M. Keer, Study of a three-dimensional crack terminating at an interface, J. Appl. Mech., **53**, 311-316, 1986.

Hanson, M.T. and L.M. Keer, Stress analysis and contact problems for an elastic quarter plane, preprint, 1988.

# Heat Flow and Tectonic Studies

9960-01177

John H. Sass
Branch of Tectonophysics
U.S. Geological Survey
2255 North Gemini Drive
Flagstaff, AZ 86001
(602) 527-7226
FTS: 765-7226

Arthur H. Lachenbruch
Branch of Tectonophysics
U.S. Geological Survey
345 Middlefield Road
Menlo Park, CA 94025
(415) 329-4879
FTS: 459-4879

## Investigations:

Interpretation of results from Phase 1 of the Cajon Pass drilling project has been completed. Additional thermal data have been obtained to present depth of ∿11,400'.

Heat-flow studies from the southern California-Arizona Transect (PACE) are up-to-date, and a workshop is being planned for Flagstaff in May.

A summary of permafrost data has been made in the context of global change.

New temperature data from the Alaskan North Slope near Prudhoe Bay have been analyzed to define the gas hydrate stability zone in the region.

## Results:

Cajon Pass. Conventional friction models predict a substantial thermal anomaly associated with active traces of strike-slip faults, but no such anomaly is observed from over 100 heat-flow determinations along 1,000 km of the San Andreas fault. The Cajon Pass well is being drilled to bring deep heat flow and stress data to bear on this paradox. Preliminary heat flows to 1.7 km in the neighboring Arkoma well indicated a positive anomaly of about 30% as would be expected if frictional resistance of the fault were 50 MPa or so, but the Plio-Pleistocene history of the Transverse Ranges, particularly high rates of uplift and erosion, could also explain the anomaly. Preliminary stress results from Cajon Pass and a new interpretation of regional data by Mark D. Zoback and colleagues suggests that the maximum compressive stress near the fault is almost normal to the trace, and hence the resolved shear stress is low and the fault, weak. Although this is consistent with long-standing evidence from low heat flow, vexing questions remain regarding the physics of strike-slip faulting. The heat-flow data show large variability with depth, probably from three-dimensional structure, and an overall decrease from over 90 mW/m$^2$ in the upper kilometer to less than 80 mW/m$^2$ in the lower 300 m with no evidence of advective heat transfer. Whether this decreasing trend is significant and whether it continues downward to the background value (∿70 mW/m$^2$ less the radiogenic heat from overlying rocks) as expected for a weak fault must be verified with data from greater depth.

Permafrost, temperatures, and climate. Temperature profiles in continuous permafrost to depths of a few hundred meters contain a faithful record of change in surface temperature during the past few centuries. When interpreted with heat-conduction theory, this little known source can provide important information on patterns of contemporary climate change. Precision measurements in oil wells in the Alaskan Arctic indicate a variable but widespread warming (typically 2°-4°C) at the permafrost surface during the 20th century. Recent statistical studies of 100 years of weather records from the North American Arctic suggest similar large changes have occurred in the air temperature although they might have started somewhat earlier. The permafrost warming is conspicuous and easily measured, and it is occurring at high latitudes where anthropogenic climatic change is expected to be greatest and first observable. Although permafrost is well-suited to the detection and monitoring of such changes, little is presently known about either the geographic extent or cause of its warming.

Gas hydrate studies. In September 1987, the USGS geothermal logging truck (transported to off-road sites on a Rolligon tractor) was used to log ten wells in the Kuparuk, Milne Point, and Prudhoe Bay oil fields to depths totaling 9,550 m (31,332 ft). The new data permit the construction of a cross section (Fig. 1) of the thermal stability fields for permafrost and methane hydrate (a solid-state ice-like combination of methane and water). Gas hydrates are stable under special conditions of low temperature and/or high pressure; they are of great interest as a possible energy source, a potential hazard in petroleum exploration, and as a source of greenhouse gases during climatic warming.

Even in the restricted area represented by Figure 1, direct temperature measurements reveal systematic changes in the thermal gradients and "freezing-point depression." The isotherms converge to the west (Fig. 1) indicating an increasing thermal gradient both in and below permafrost; this results in a westward thinning of both permafrost and the HSZ. The effects of geographic variations in geothermal gradient can result from corresponding variations in thermal conductivity of the formations or from variation in the rate of heat flow from the earth. There is little doubt that the anomalously great depth of the hydrate stability field at Prudhoe Bay results from the low thermal gradient associated with abundant high-conductivity constituents such as quartz and ice in the porous sands and gravels there.

Reports:

De Rito, R. F., 1988, The effects of weak crust upon the strength of the continental lithosphere (extended abstract): U.S. Geological Survey Circular, in press.

Elders, W. A., and Sass, J. H., The Salton Sea Scientific Drilling Project: Accepted by the Journal of Geophysical Research, March 1988.

Lachenbruch, A. H., 1988, Warming of permafrost in the Alaskan Arctic, in Proceedings of First North American Conference on Preparing for Climate Change, October 27-29, 1987: Climate Institute, Washington, D. C., in press.

Lachenbruch, A. H., Cladouhos, T. T., and Saltus, R. W., 1988, Permafrost temperature and the changing climate: Proceedings, 5th International Conference on Permafrost, Trondheim, Norway, August 1988, in press.

Lachenbruch, A. H., Galanis, S. P., Jr., and Moses, T. H., Jr., A thermal cross section for the permafrost and hydrate stability zones in the Kuparuk and Prudhoe Bay oil fields, 1988, in Galloway, J. P., and Hamilton, T. D., eds., Geologic Studies in Alaska by the U.S. Geological Survey during 1987, U.S. Geological Survey Circular 1016, p. 48-51, in press.

Lachenbruch, A. H., Sass, J. H., Lawver, L. A., Brewer, M. C., Marshall B. V., Munroe, R. J., Kennelly, J. P., Jr., Galanis, S. P., Jr., and Moses, T. H., Jr., 1987, Temperature and depth of permafrost on the Alaskan Arctic Slope, in Tailleur, I., and Weimer, P., eds., Alaskan North Slope Geology: Pacific Section SEPM and Alaska Geological Society, v. 50, p. 545-558.

Lachenbruch, A. H., Sass, J. H., Lawver, L. A., Brewer, M. C., Marshall B. V., Munroe, R. J., Kennelly, J. P., Jr., Galanis, S. P., Jr., and Moses, T. H., Jr., Temperature and depth of permafrost on the Alaskan Arctic Slope: U.S. Geological Survey Professional Paper 1399 (Branch approval, March 1986).

Lachenbruch, A. H., Sass, J. H., Saltus, R. W., Anderson, R. F., and Williams, C., 1987, Thermal regime at the Cajon Pass Research well (abstract): EOS, v. 68, p. 1489.

Langseth, M. G., Lachenbruch, A. H., and Marshall, B. V., 1988, Geothermal observations in the Arctic region: Decade of North American Geology volume, in press.

Pollack, H. N., and Sass, J. H., 1988, Thermal regime of the lithosphere, in Haenel, R., Rybach, L., and Stegena, L., eds., Handbook of Terrestrial Heat-Flow Density Determination (Guidelines and Recommendations of the International Heat Flow Commission), in press.

Sass, J. H., 1987, Salton Sea Scientific Drilling Program: U.S. Geological Survey Yearbook Fiscal Year 1986, p. 55-58.

Sass, J. H., and Morgan, P., 1988, Conductive heat flux in VC-1 and the thermal regime of the Valles caldera, Jemez Mountains, New Mexico: Journal of Geophysical Research, in press.

Sass, J. H., Priest, S. S., Duda, L. E., Carson, C. C., Hendricks, J. D., and Robison, L. C., 1988, Thermal regime of the State 2-14 well, Salton Sea Scientific Drilling Project: Journal of Geophysical Research, in press.

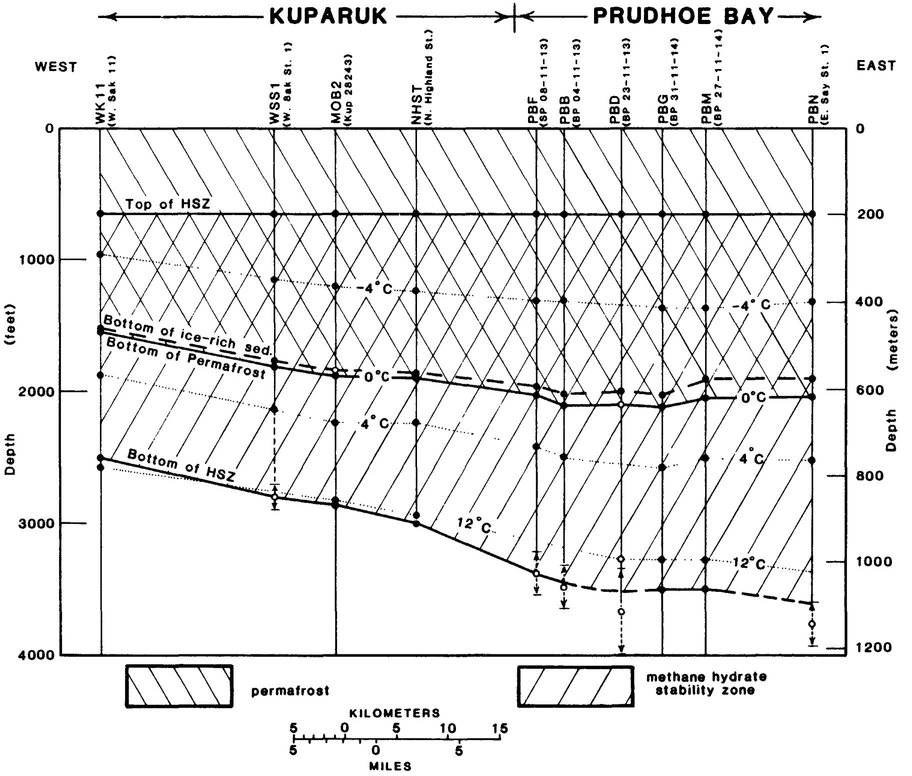

Figure 1. Cross section through Kuparuk and Prudhoe Bay oil fields showing zones of methane hydrate stability (HSZ) and permafrost. Operators' designations for holes in parentheses.

# Fractal Heterogeniety of Faults: Effect of Topography on Friction

14-08-0001-G1366

C. H. Scholz
Lamont-Doherty Geological Observatory
Columbia University
Palisades, N.Y. 10964
(914) 359-2900

*Objective:* Rock friction constitutive laws are now entirely empirical. In order to develop a theory of friction that is quantitative and based on first principles, we are approaching the problem from the standpoint of the micromechanics of rough surfaces in contact. The long range goal will be to be able to predict rock friction directly from knowledge of the topography and physical properties of the contacting surfaces. From this we will gain an understanding of the micromechanics of rock friction so that we will be better able to extrapolate laboratory friction measurements to geological conditions.

*Research progess:* The work done in the last year completes the first stage in our long term plan. This consisted of developing and experimentally verifying a theory for the elastic properties of two rough surfaces in contact under shear loading, no-slip conditions. This work verifies the basic contact theory which will be extended later to predict friction under slip conditions, and also provides an experimental technique, that of measuring the shear and normal compliances of the contact, that can be used in friction experiments to determine the state of the contact as it evolves during slip.

The theory is based on the shear contact theory of Yamada et al (*Wear*, 1978), modified using the results of Brown and Scholz (*J. Geophys. Res.* 1985). The results allow one to calculate the shear and normal compliances of two rough elastic surfaces in contact as a function of normal and shear stress directly from a knowledge of their topographies and elastic constants of the substrate materials. The theory was tested using Westerly granite surfaces. The topography of the surfaces was first measured with a profilometer, providing the necessary imput to the theory. Mechanical measurements were then made in a servocontrolled rotary friction apparatus. Shear and normal compliance were measured as a function of applied load under no-slip conditions for two different surface roughnesses. The results were compared with theory, with excellent quantitative agreement. A preliminary oral presentation of these results was given at the fall 1987 AGU meeting (Yoshioka and Scholz, *EOS*, 68: 1242, 1987) and a more complete report will be given at the 1988 SSA meeting in Honolulu. A manuscript reporting these results is in preparation (Yoshioka, N. and Scholz, C.H., Micromechanics of contact of two rough surfaces, in prep., 1988).

# Systems Analysis of Geologic Rate Processes: Stylized Space-Time Flow Model For California Earthquakes

9980-02798

Herbert R. Shaw and Anne E. Gartner
Branch of Igneous and Geothermal Processes, U.S. Geological Survey
MS-910, 345 Middlefield Road, Menlo Park, CA 94025
(415) 329-5245, 5209

Objectives: Current work concerns general multifractal properties of seismic activity as an approach to quantifying patterns of moment flux, with reference to tectonic earthquakes in California and volcano-tectonic earthquakes and tremor in Hawaii. This report explores possibilities of regional confluences of moment flux in California.

Results: In previous reports we cited several kinds of evidence showing that faults are fractal objects at many different scales of description. This appears to be true of the geometries of fault traces, fault surfaces, and fault sets (e.g. Shaw and Gartner, 1986; Shaw, 1987a); it also appears to apply to the temporal properties of seismic event frequencies (e.g., Shaw, 1987a; Shaw and Chouet, 1987; Shaw and Chouet, 1988). This does not mean that these geometries and processes are described by any one dimension or simple set of dimensions; the fractal geometries at issue are not invariant (rigorous fractal self-similarity probably occurs only in special cases). Evidence suggests, however, that among the infinity of possible local fractal scaling exponents in size-frequency data (including time as a metric as well as spatial distance), there may be ordered sets of finite or continuously varying dimensions. The term singularity spectrum has been applied to this class of fractal objects and has become a new way to characterize the complex dynamical geometries of attractors in phase space (e.g., Shaw, 1987b; Shaw and Chouet, 1988).

Apart from numerical characterization of complex geometries, which is not the subject of this report (cf., Shaw and Chouet, 1988), there is a major qualitative implication that the spatial-temporal properties of seismic instabilities are coordinated over many different scales of length. However, this is a very fuzzy sort of coordination that can be physically likened only to such things as the geometric structures found near the critical conditions of the states of matter or to the transitions between laminar and turbulent flow in fluids. It is this "fuzziness" that hints at the fractal nature of the problems of description and prediction. The fractal character of the problem in turn suggests that if forecasting and(or) prediction are realizable goals of earthquake studies, then one approach is to look for regimes of dynamical states that are analogous to the above types of phenomena and their transitions. The dynamics of the earthquake process is nonlinear and unpredictable in general, but this does not preclude the existence of rigorously ordered states involving local invariances and periodic relationships as special sets within the chaotic regime of unpredictability (cf., Shaw, 1987b).

It would seem that a profitable approach is to investigate the earthquake process on two fronts, one of which is the meticulous search for and description of special structures in space and(or) time, and the other is the attempt to map dynamical fields of behavior analogous to those of thermodynamic phase diagrams and dynamical regimes of fluid motions (e.g., phase portraits). Seismology has made great progress on the first front in special cases of numerous types (as documented in many of the progress reports of NEHRP over the years), and some aspects of the second front are beginning to take shape (e.g., Shaw and Chouet, 1987, 1988; Rundle and Kanamori, 1987; cf., Ryall and others, 1966). The present report describes a conjectural scenario that represents one way the dynamical field approach might be used in a pictorial way to identify some geometrical aspects of the broader regimes of dynamical interactions. Analytical and theoretical tools that might be applied to this second problem are outlined in Shaw (1987b) and Shaw and Chouet (1988).

This scenario concerns the manner in which earthquakes larger than about magnitude 5 have propagated throughout California during historic time (from the year 1800 through October, 1982; see data sources in Shaw, 1987a). Figure 1 is an index map showing 14 subregions within which the numbers of earthquakes were counted at intervals of 5 years. Arbitrary 'benchmarks', shown by triangles, were placed so that tielines between them crossed one or more regions (triangles are named for nearby landmarks, but locations are relevant only in terms of where their centroids plot relative to the coordinates of subregion boundaries). Tielines were numbered consecutively so that their progression moves northwestward from Baja California through coastal and central California to the Oregon border and then swings through eastern California and Nevada and closes in the Mojave desert near the juncture of California, Nevada, and Arizona.

The set of crisscrossing tielines in Figure 1 was treated as though each line was a trip wire that could be broken by a magnitude 5 earthquake that occurred in subregions crossed by that line during a given time interval (this is a crude and nonuniform criterion that could be refined by creating a hierarchy of networks of smaller and smaller equal areas each crossed by symmetrical sets of lines). Only those tielines that remained 'unbroken' during a given time interval were plotted. The results are shown in Figure 2, which also shows the traces of the 1857 and 1906 San Andreas breaks (dotted) and approximate locations of some of the larger historic events (identified by year of occurrence). Despite the uncertainties in documenting older events, it is evident that different areas of the state have been active at different times, and that the activity generally permeated large contiguous regions. For example, activity was dominantly located in more northerly subregions before, during, and after the 1857 San Andreas event (with an easterly excursion prior to the 1872 Owens Valley event), while coastal and southerly subregions were active before, during, and after the 1906 San Andreas event.

The main point of this report is the multiregional nature of activity that is crudely coseismic. However, there are also suggestions of directional propagation relative to three areas of persistent activity, representing regions associated with complex Plate tectonic convergences. One of these is located near Eureka off the California-Oregon coast, another is located in northwestern Nevada, and the third is located in northern Baja California.

The multiregional source phenomenon is illustrated schematically by the inset at the bottom of Figure 2 that shows results of a kinetic model of physical bond failures from Termonia and Meakin (1986, Figure 2). In their model a mosaic of areally disperse small-scale failures coalesces progressively to culminate in a major throughgoing rupture (the trilateral propagation effects noted above in California are analogous to superposition of three such systems oriented generally NW-SE, E-W, and N-S). Termonia and Meakin also demonstrated that the frequency distributions of failures in their model was fractal in character. They estimated a fractal dimension of about 1.27, which is similar to values estimated by Shaw and Gartner (1986) for systems of faults in California (these are statistical averages and do not imply that the geometry is invariant).

If the patterns of tielines in Figure 2 are imagined to include smaller and smaller areas and time intervals, it is suggested that the distributions will come to resemble patterns analogous to those of the inset. In the limit, and over long times, the spatial trajectories of changing patterns in either case increasingly resemble the trajectories of particle motions in a fluid. Lacking the necessary information to complete this picture, however, we make a bold assumption that such trajectories of motion may be mimicked by the changing patterns of the larger earthquakes. That is, using the analogy of vorticity transport in a turbulent fluid, the moment flux associated with the larger earthquakes is analogous to the flux of kinetic energy associated with the larger vortices. Recent studies of the structures of fluid convection at the onset of turbulence suggest that this simile is appropriate to the extent that both types of system can be geometrically described in terms of fractal singularity spectra (cf., Shaw, 1987a,b; Shaw and Chouet, 1987,1988).

The result of this assumption is illustrated schematically in Figure 3, which portrays a fourfold hierarchy of converging foci of seismic moment transport (analogous to a hierarchy of vortex structures). Blank areas and lines with arrows represent the changing patterns of events from about magnitude 5 to 6.5, open circles with dots represent patterns of events with magnitudes from about 6.5 to 7.2, solid dots represent events with magnitudes from about 7.3 to 7.7, and large solid stars represent the three historic events near magnitude 8 (these are uncorrected magnitudes from California Division of Mines and Geology catalogs). Numbers at the left are those of Figure 1, and names at the right represent areas of California where future activity seems most likely based on the generalized trajectories.

In drawing these diagrams it was noted that the present circumstances in California, taken as a whole, are quite different from those that existed prior to any of the three 'great' earthquakes. Activity seems to have been more diffuse in recent decades (perhaps with a generally higher average fractal dimension), even allowing for the poorer documentation of events prior to the advent of seismic networks in the 1920's. Since 1982, localities near coastal southern California, Mojave, Owens Valley, and the eastern Sierra have all had conspicuous events of intermediate magnitudes. "North Central" California, however, has been comparatively quiet, and it will be of interest to notice how seismicity evolves there relative to southern and eastern California.

We conclude that expanding on the concept of singularity spectra in the analysis of interacting spatial-temporal patterns of seismic energy release offers a tool for earthquake forecasting that is analogous to the use of satellite imagery, global networks, and global computer models applied to problems of weather forecasting.

References:

Rundle, J.B., and Kanamori, H., Application of an inhomogeneous stress (patch) model to complex subduction zone earthquakes: A discrete interaction matrix approach, Jour. Geophys. Res., 92, 2606-2616, 1987.

Ryall, A., Slemmons, D.B., and Gedney, L.D., Seismicity, tectonism, and surface faulting in the western United States during historic time, Seis. Soc. Am., Bull., 56, 1105-1135, 1966.

Shaw, H.R., A linguistic model of earthquake frequencies applied to the seismic history of California, U.S. Geological Surv. Open-File Rept. 87-296, 1987a.

Shaw, H.R., The periodic structure of the natural record, and nonlinear dynamics, Eos, Trans. Am. Geophys. Union, 68, 1651-1665, 1987b.

Shaw, H.R., and Gartner, A.E., On the graphical interpretation of paleoseismic data, U.S. Geological Surv. Open-File Rept. 86-394, 1986.

Shaw, H.R, and Chouet, B, Kilauean volcanic tremor as a case study of multifractal attractor dynamics, Abstracts, Symposium on How Volcanoes Work, p. 232, Hilo, HI, January 19-25, 1987.

Shaw, H.R, and Chouet, B., Application of nonlinear dynamics to the history of seismic tremor at Kilauea volcano, Hawaii: Multifractal attractors and singularity spectra, Jour. Geophys. Res., submitted 11 May, 1987; revised 15 March, 1988.

Termonia, Y., and Meakin, P., Formation of fractal cracks in a kinetic fracture model, Nature, 320, 429-431, 1986.

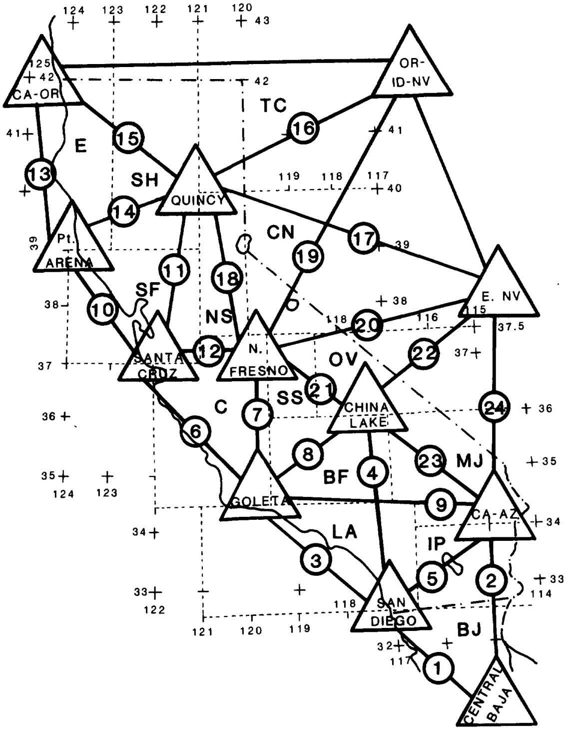

FIGURE 1. Index and "linkage" map of California and environs showing locations of subregions used in this report (from Shaw, 1987a, Figure 14). "Benchmarks" (triangles identified by nearby towns or geographic features) are positioned to approximately straddle subregions (dashed lines demarking 14 areas designated by letter code: E, Eureka; SH, Shasta; TC, threecorners area of California-Oregon-Nevada; SF, San Francisco; NS, northern Sierra; CN, California-Nevada; C, central California; SS, southern Sierra; OV, Owens Valley; BF, Bakersfield; MJ, Mojave; LA, Los Angeles; IP, Imperial Valley; BJ, Baja California). Numbered lines connecting triangles are used as kinematic links to illustrate time variations of regional patterns for events equal to or greater than M = 5 (catalogs compiled by California Division of Mines and Geology; see Shaw, 1987a). Lines between the most northern and northeastern triangles are not numbered because data are not available in the catalogs to evaluate activity near these limits (shown to identify perimeter of "California and environs"); in general, however, central Oregon, southwestern Idaho, eastern Nevada-western Utah, and western Arizona have had relatively low seismicity during historic times (see Shaw, 1987a, Figure 3, Inset B, and Ryall and others, 1966). Events in SH and TC are mostly south of 42$^{o}$ N.; more northerly events occurring offshore in E are referred to either lines 13 or 15. Events in the eastern parts of TC and CN are referred to lines 16, 17, and(or) 19, depending on coordinates.

FIGURE 2. Kinematic linkage maps drawn at intervals of five years (excepting first, and last three) based on index map of Fig. 1 and statistics compiled by Shaw (1987a, Table 2, Figure 18). A "link" is defined as any tieline between benchmarks of Figure 14 that remains "unbroken" by the occurrence of an event of M = 5 or larger in any part of a subregion lying near that line; locations of events having M = 6.7 or larger are shown by year of occurrence. Large events emanate, descriptively, from windows that had prior breaks: e.g., the 1857 San Andreas fault break (dotted) appears to have responded mainly to the northwestern (subregion E) and southern (subregion BJ) sources; the 1872 Owens valley fault break appears to have responded to convergences of northwestern (subregion E) and northeastern (subregion CN) sources; and the 1906 San Andreas fault break (dotted) again appears to have responded to convergences of northwestern and southern source effects (location on the fault may be influenced by relative contributions of northwestern, southern, and northeastern sources). Inset (bottom): Patterns of fractal breaks based on a kinetic model of physical bond ruptures developed by Termonia and Meakin (1986, Figure 2); although no dynamic scaling is implied, areally distributed deformation, fault interactions, and coalescence of rupture foci are analogous (cf., Rundle and Kanamori, 1987). Average fractal dimension of rupture geometry is about 1.27 (similar values for California fault systems were determined by Shaw and Gartner, 1986). The fractal concept suggests that linkage maps describing progressively smaller earthquakes at progressively larger map scales may be statistically similar relative to renormalized singularity spectra (cf., Shaw, 1987a; Shaw and Chouet, 1988). Such maps may be valuable in documenting space-time patterns of migrating loci of fault ruptures over time scales less than 5 years prior to major earthquakes.

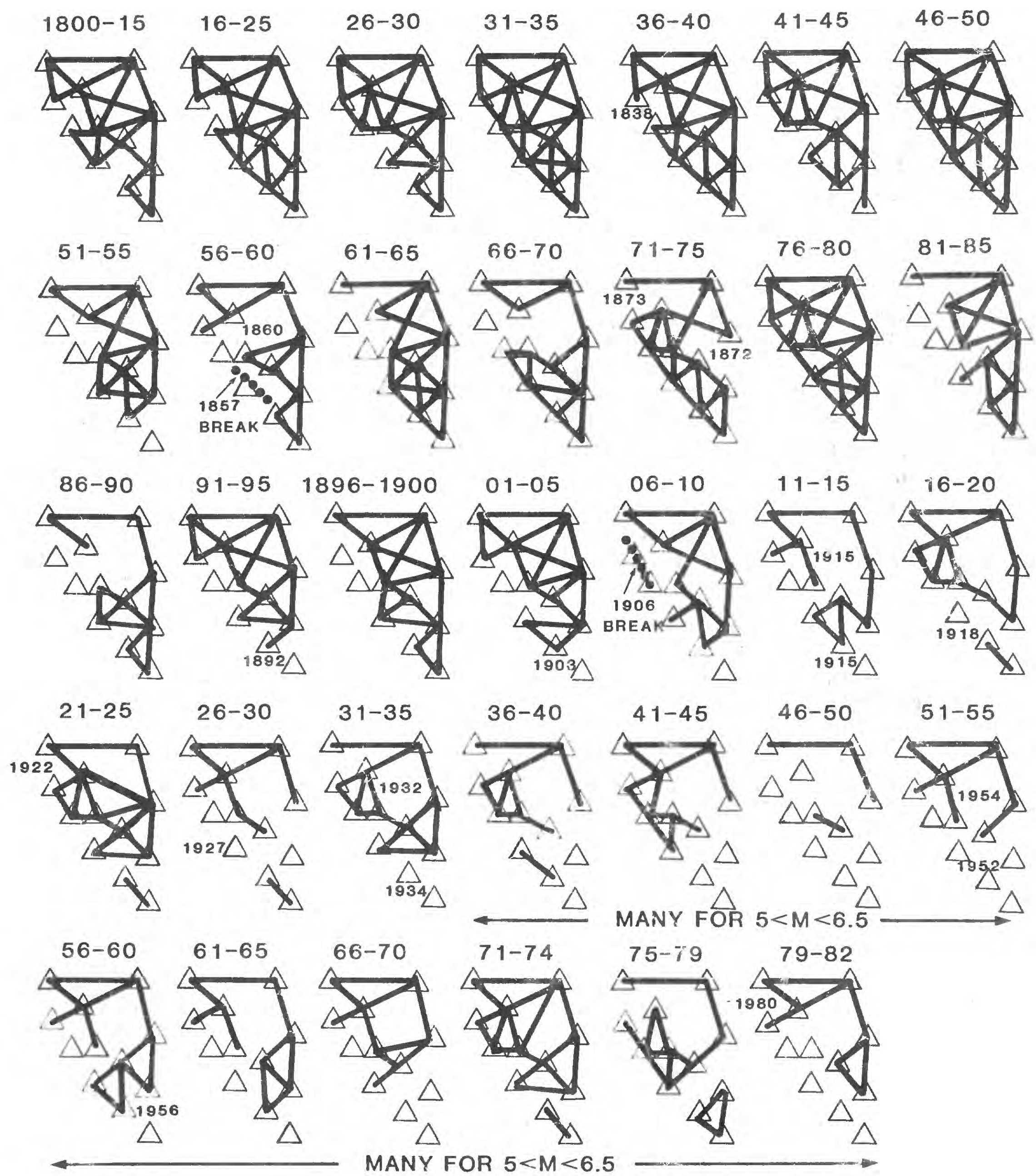
1800-15
16-25
26-30
31-35
36-40
41-45
46-50
1838
51-55
56-60
61-65
66-70
71-75
76-80
81-85
1860
1857
BREAK
1873
1872
86-90
91-95
1896-1900
01-05
06-10
11-15
16-20
1892
1903
1906
BREAK
1915
1915
1918
21-25
26-30
31-35
36-40
41-45
46-50
51-55
1922
1927
1932
1934
1954
1952
MANY FOR 5<M<6.5
56-60
61-65
66-70
71-74
75-79
79-82
1956
1980
MANY FOR 5<M<6.5

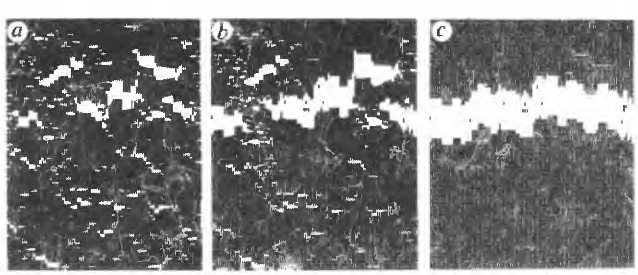
a
b
c

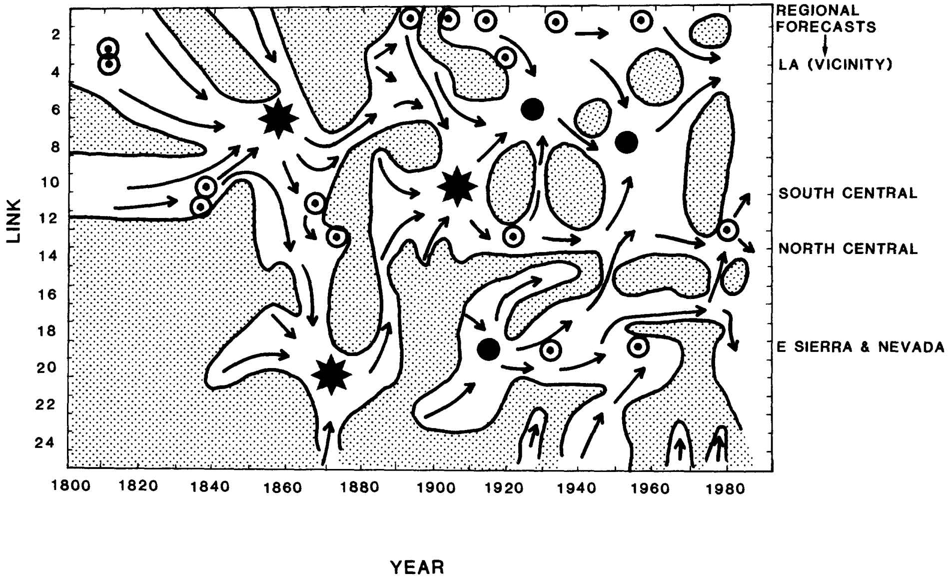

FIGURE 3. Schematic space-time diagram of migrations of seismic activity in California based on patterns in Fig. 2 arranged according to consecutive numbering of tielines in Fig. 1 (other spatial sequences can be plotted by reference to Figs. 1 and 2). Stippled areas indicate areas and times when tielines have not been broken by an event of M = 5 or larger. Seismic energy 'flows' around the stippled areas in manner analogous to vortex lines around rigid obstructions in a fluid; large events represent convergences relative to older ("upstream") trajectories and divergences relative to younger ("downstream") trajectories. Earthquake events are indicated by symbols: M = 8 or larger shown by solid stars, M = 7.3 to 7.7 by solid dots, M= 6.5 to 7.2 by open circles with dots, M = 5 to 6.4 within blank areas (Shaw, 1987a, Table 2 and Fig. 18). Inferences from schematic trajectories for "regional forecasts" shown at right margin (Note: Because two space dimensions are projected onto one space dimension represented by the numbered tielines, such diagrams can be ordered in many ways; trial rearrangements did not change general inferences).

# FAULT PATTERNS AND STRAIN BUDGETS

9960–02178

Robert W. Simpson
Branch of Tectonophysics
U.S. Geological Survey
345 Middlefield Road, MS/977
Menlo Park, California 94025
(415) 329–4865

## Investigations

1. Used cluster analysis to examine the Parkfield two–color laser data for patterns.
2. Assembled gravity, magnetic and topographic data for the Parkfield region.

## Results

1. Cluster analysis can be used to group vectors of observations based on a selected measure of similarity. The end result is a dendrogram or tree–diagram that shows the sequence of clustering (items which are most similar are clustered early in the process) and the degree of similarity. The two–color data were converted to average velocities (mm/yr) over various time windows (*e.g.*, 90 days). It is possible to cluster either the reflectors based on the similarity of their behavior over time, or, transposing the data set, to cluster time intervals based on the similarity of behavior of the various meters in pairs of intervals.

   The results tend to confirm observations already made by Bob Burford. The reflectors tended to cluster into geographic quadrants defined by azimuth of the fault. Even when least–squares trends were removed before velocities were calculated, these quadrant–groupings persisted, suggesting either an azimuthally dependent systematic error, or some geographic coherence to the behavior of the reflectors even after first–order linear trends are removed. Time windows from April to July 1985 (the months before the Kettleman Hills earthquake) generally clustered together and were rather different from other time windows. This suggests that precursory deformation to the Kettleman Hills earthquake was detected by the two–color network. There was also a tendency for winter windows to form one cluster and for summer windows to form another. Thus it appears that cluster analysis may be a useful way to examine two–color data for patterns and as a technique for identifying and characterizing anomalous behavior.

2. As part of a collaborative effort involving Bob Jachens, Carl Wentworth, and John Sims to understand the regional geophysical and geological context for Parkfield, we have compiled and plotted the gravity, magnetic, and topographic data sets for an area about the size of a $1^\circ \times 2^\circ$ quadrangle (see Figures). We are in the process of preparing

derivative maps, models, and cross–sections from these data and the available geologic information. The maps themselves will be made available as Open–File Reports at a scale of 1:250,000. One of the first products will be an interpretative tectonic map of the region. The evidences for fault–normal compression tend to be far more apparent in the data than the effects of strike–slip motion on the San Andreas fault.

## Reports

Oppenheimer, D.H., Reasenberg, P.A., and Simpson, R.D., 1988, Fault–plane solutions for the 1984 Morgan Hill, California, earthquake sequence: Evidence for the state–of–stress on the Calaveras fault, *Journal of Geophysical Research* (in press).

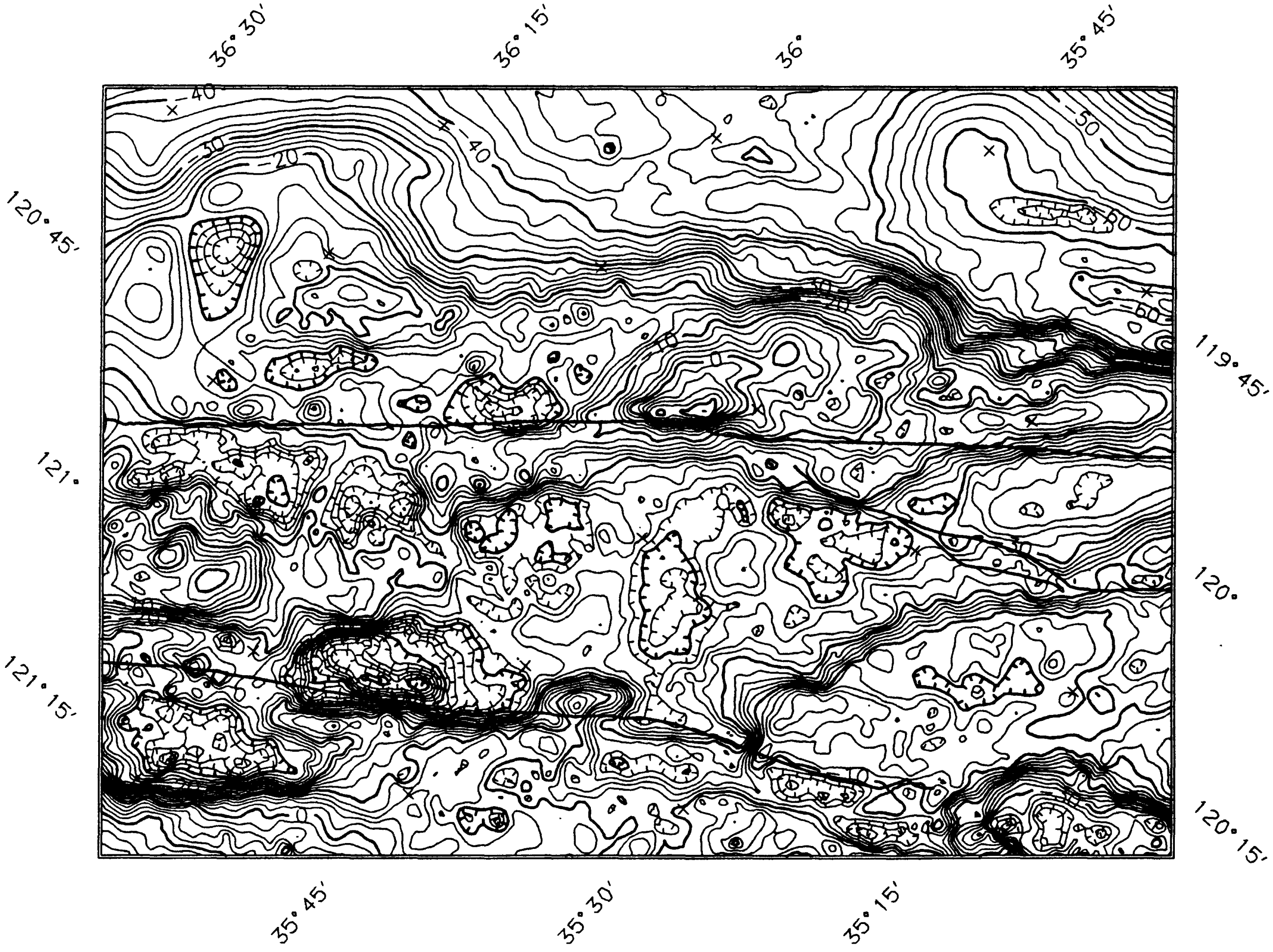

Parkfield Gravity

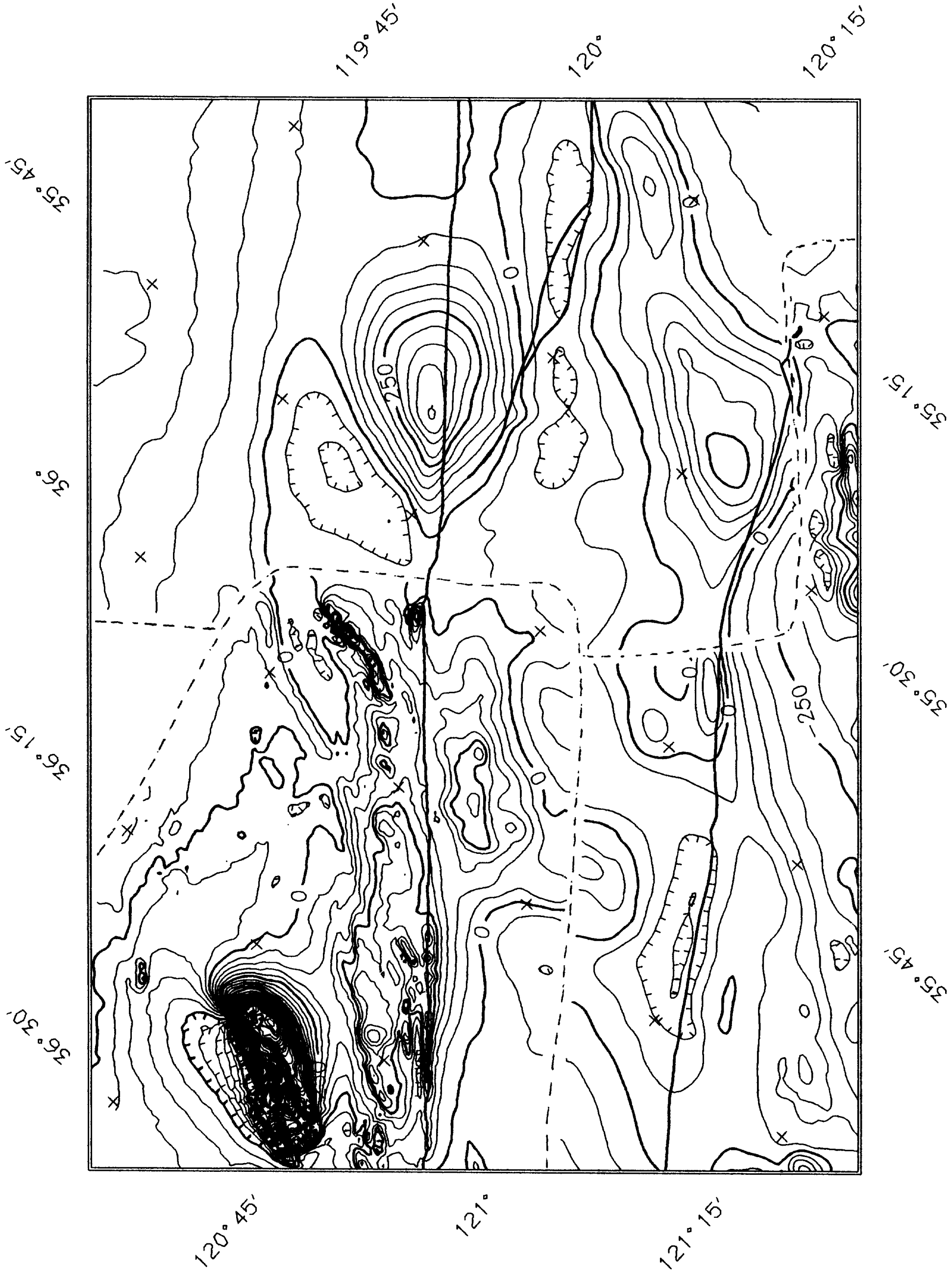

Parkfield Aeromag (50nT)

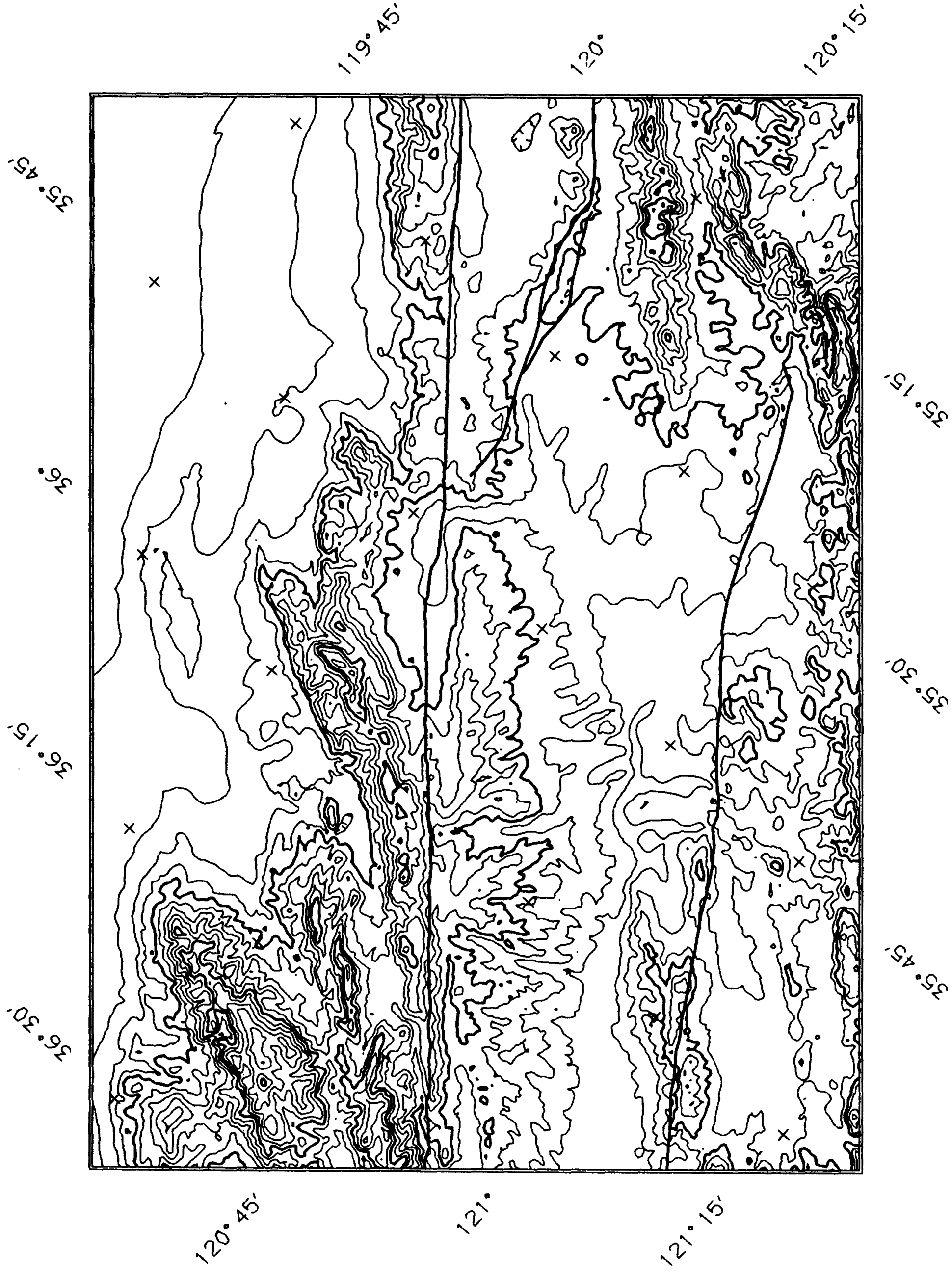

Parkfield Topography

# EARTHQUAKE FORECAST MODELS

9960–03419

William D. Stuart
Branch of Tectonophysics
U.S. Geological Survey
Pasadena, California 91106
(818) 405–7816

## Investigations

Fault Interaction Model for the Superstition Hills, California, Earthquakes

The *M* 6.6 Superstition Hills earthquake last November and its *M* 6.2 foreshock occurred on vertical strike–slip faults which intersected at nearly 90 degrees. The two earthquakes were 12 hours apart. D. Given and I are analysing mechanical models to see under what conditions and in what sense the *M* 6.2 earthquake could have caused the *M* 6.6 earthquake to occur sooner than it might have otherwise. We also are studying the possible triggering of the *M* 6.2 earthquake by precursory slip associated with the *M* 6.6 earthquake.

## Results

We have constructed an earthquake instability model that allows simulation of repeated earthquake cycles associated with failure of brittle patches on vertical strike–slip faults. The model is assembled from parts of earlier related instability models published by various authors. The two new features are pressure dependence of the fault stress–slip law and continuous interaction of aseismic and seismic slip on different faults. Forcing is from steady slip rates applied on faults extending far below the brittle zones.

For application to the Superstition Hills earthquakes the model contains only the northwest trending Superstition Hills fault (for the *M* 6.6 event) and the northeast trending Elmore Ranch fault (*M* 6.2 event). In the simplest model the two faults do not continuously interact. Instead the coseismic stress pulse from the *M* 6.2 event is applied at various times prior to the time that the *M* 6.6 instability would have occurred without the stress pulse. The *M* 6.2 earthquake advances the time of the *M* 6.6 earthquake by about 10% of the time remaining to unpulsed instability. The main cause of the time advance is the decompression of the Superstition Hills fault by slip on the Elmore Ranch fault.

In another, more realistic model, both faults continuously interact, and the times of the two earthquakes depend on initial strengths of brittle patches and their loading history. Because precursory slip to the *M* 6.6 event decompresses the Elmore Ranch fault, the *M* 6.2 event could itself be considered a triggered earthquake, *i.e.,* a premature aftershock. Analysis of the fully interacting fault system is incomplete, but it appears that there is a tendency for earthquakes on the two faults to attract each other in time because of the mutual decompression.

If faults continuously interact in the earth as they do in this and earlier models by others, it makes little sense to think of a particular earthquake triggering another. Instead, one should think of a fault system having the potential to produce two or more earthquakes close in time. The earthquake prediction problem is then to determine from available field data the current and future states of the system, or more concretely, the fault locations and constitutive properties.

## Reports

Aki, K., and W.D. Stuart, eds., Physical and Observational Basis for Intermediate–Term Earthquake Prediction, Proceedings Workshop XXXVII, *U.S. Geological Survey Open-File Report 87-591*, Vols. I and II, 1987.

Given, D.D., and W.D. Stuart, A fault interaction model for triggering of the Superstition Hills earthquake of November 24, 1987, *Seismological Research Letters*, (abstract), 1988.

Stuart, W.D., Forecast Model for Great Earthquakes at the Nankai Trough Subduction Zone, *Pure and Applied Geophysics*, **126** (2–4), 1988.

Stuart, W.D., and K. Aki, eds., Intermediate–Term Earthquake Prediction, *Pure and Applied Geophysics*, **126** (2–4), 1988.

# An Experimental and TEM Study of Cataclastic Flow in Quartzo-Feldspathic Rocks

14-08-0001-G-1363

Jan Tullis and Richard Yund

Department of Geological Sciences
Brown University, Providence RI 02912
(401) 863-1921

## *Investigations*

1. We have determined the P-T locations of the transitions from brittle faulting to ductile cataclastic flow, and from cataclastic flow to dislocation creep, for feldspar aggregates. In addition, we have determined the micromechanical processes associated with these transitions.

2. We have nearly completed work on determining the P-T locations of the transition from brittle faulting to ductile dislocation creep for non-porous quartzite; this material exhibits a very different behavior from that of feldspar aggregates.

3. We have determined the conditions and mechanisms by which porosity induces a transient cataclastic flow in quartz aggregates.

4. We have conducted further TEM investigations of gouge developed in rotary shear friction experiments on granite with simple sliding histories.

## *Results*

### *Brittle-Ductile Transition for Feldspar Aggregates*

In fine-grained anorthosite deformed at $10^{-5}$/sec, brittle faulting occurs at all temperatures tested (20-700°C) at 500 MPa, and at low temperatures (20-200°C) at higher pressure (1000-1500 MPa); cataclastic flow occurs at temperatures of ~300-800°C at 1000-1500 MPa, and dislocation creep occurs >900°C at 1000-1500 MPa (Figure 1). The transitions between these regimes are gradual, and occur over a temperature interval of about 100-200°C.

Cataclastic flow in feldspar involves cracking on the two cleavages and the development of very fine fragments (<0.1 μm) due to their intersection. Although the transition from brittle faulting to ductile cataclastic flow requires modest temperature (>300°C) as well as high pressure (>500 MPa), dislocations are *not* involved in the stabilization of the cracking, as is generally assumed in the metallurgical literature (e.g., Stroh, 1954). New dislocations are first observed in samples deformed at 700°C (at $10^{-5}$/sec). Therefore the role of temperature in crack stabilization is related to the cleavage cracking process itself. Experiments by Atkinson (1984) show a significant expansion of the field of stable crack growth for only a few hundred degrees temperature increase; presumably a similar effect occurs in feldspar. The role of pressure in stabilizing cracking is to inhibit crack opening away from stress concentrations. Thus at modest P and T, distributed stable cracking occurs sufficiently rapidly to prevent the stress from rising high enough to cause unstable crack growth. An illustration of the stability of cracking at >300°C is provided by a sample faulted at 20°C and 1000 MPa, then reloaded at 400°C, where it underwent distributed cataclastic flow with exactly the same stress-strain curve as an originally intact sample.

These experimental results have important implications for the nature of the brittle-ductile transition in the crust. It is commonly assumed that this transition represents the transition from faulting to dislocation creep, in quartz. However, feldspar is volumetrically the dominant phase as well as the stress-supporting matrix phase in granitic rocks, and seems more likely to control the failure of the aggregate. The transition to dislocation creep for feldspar does not occur until ~450°C. We suggest that the macroscopic brittle-ductile transition in granitic rocks in the crust, which occurs at about 300°C, may mark the almost simultaneous transition from unstable to stable cracking in feldspar, and the transition from unstable cracking to dislocation creep in quartz (Figure 2).

It is commonly assumed that the seismic-asesimic transition corresponds to the macroscopic brittle-ductile transition. However, Tse and Rice (1984) have shown that a seismic-aseismic transition would result from a transition with increasing temperature from velocity weakening to velocity strengthening frictional behavior *within* a fault zone such as the San Andreas. There are very few data for the temperature dependence of friction for silicates, but Stesky's (1978) results for Westerly granite suggest the onset of velocity strengthening at ~300°C. Several lines of experimental evidence (from Stesky) suggest that this transition is due to processes occurring in feldspar, not in quartz: (1) dislocations are not observed in quartz until significantly higher temperatures (500°C); (2) the frictional strength of quartzites is higher than that of feldspar rocks; and (3) the temperature of the transition from stick slip to stable sliding in quartzite is significantly higher than it is in feldspar rocks. In addition, our own low temperature experiments on granite, as well as observations of low temperature naturally deformed granites (e.g., Evans, 1984), show that the quartz grains remain undeformed whereas the feldspar grains are crushed. Thus, the seismic-asesimic transition within the San Andreas and similar faults may reflect the frictional properties of feldspar; although we do not pretend to understand the physical basis of the velocity dependence of friction, it is interesting that 300°C is the same temperature at which feldspar aggregates show a transition from unstable to stable, distributed cracking.

### *Brittle-Ductile Transition for Non-Porous Quartzites*

In quartzite, the cataclastic flow regime is limited to a much narrower temperature interval, from 700-850°C at 1000-1500 MPa, for a strain rate of $10^{-5}$/sec. Brittle faulting is observed at temperatures of 20-700°C at 500 MPa, just as for feldspar, but in strong contrast to feldspar it is also observed at temperatures up to 600°C at 1000-1500 MPa. Dislocation creep occurs at >850°C at 1000-1500 MPa.

In quartzite the processes involved in cataclastic flow are very different than in feldspar. New dislocations are first observed at quite low temperature (~300°C) but their mobility is extremely limited, because samples undergo brittle faulting at temperatures up to and including 600°C. Cataclastic flow involves both dislocations and microcracks. Detailed TEM analysis of samples deformed to many different strains at 700°C, 1500 MPa and $10^{-5}$/sec shows that high dislocation densities but no cracks develop at low strain; the lack of climb causes strain hardening, and at ~20% strain one observes cracks and crush zones with extremely fine grain size (<0.1 μm). At ~50% strain some of the very finely crushed regions appear to have undergone grain growth, as the grains appear more uniform in size and somewhat polygonal.

Quartzites thus show very different behavior than feldspar in the brittle-ductile transition. The absence of cleavages means that at low temperatures where dislocation glide and climb are limited, the stress rises much higher and crack propagation is unstable over a much wider range of conditions. At higher temperatures where climb remains limited, dislocation pile-ups generate locally high stresses which nucleate cracks, but these cracks are stabilized in part because the stress decays rapidly away from the pile-ups and in part because the presence of other dislocation arrays and cracks form barriers to continued propagation. Due to the very high stresses required to produce the high dislocation densities, it seems likely that cataclastic flow of this type would be uncommon in nature; instead, pressure solution frequently occurs at these transitional conditions.

### *Effect of Porosity on Brittle-Ductile Transition in Quartzites*

Quartzite with 7% porosity undergoes a transition from brittle faulting to ductile cataclastic flow at room temperature and about 600 MPa (Hadizadeh and Rutter, 1983), whereas non-porous quartzites undergo brittle faulting up to at least 1500 MPa. We have performed additional room temperature experiments on the porous quartzite used by Hadizadeh and Rutter, over a wide range of pressures and total strains, and made SEM and TEM observations of the samples. We find that the cataclastic flow exhibited by the porous quartzites is always transient, and samples develop unstable faulting at ~35% strain.

The onset of cataclastic flow depends on compaction. Pressurization alone causes no compaction of the pores. At low pressure (300 MPa) the differential stress for faulting is less than that for compaction, whereas the reverse is true at higher pressures. Pore collapse involves local intragranular cracking and crushing, which in turn lead to grain boundary cracking, producing cataclastic flow. The maximum compressive stress concentration around a spherical pore is $2\sigma_1 - 0.5\sigma_3$; it appears that compaction is initiated at a critcal value of this stress concentration. Thus an increase of pressure causes this stress concentration to rise faster than the stress required for axial crack nucleation in solid regions.

The termination of cataclastic flow by unstable faulting involves a switch from strain hardening to strain weakening behavior. We observe that this correlates with a switch from compaction to dilatancy, as predicted (although not experimentally demonstrated) by Edmond and Paterson (1972). When a critical dilatancy is reached, unstable faulting results, just as for nonporous quartzites deformed at the same conditions; however, the differential stress required for faulting of the porous quartzites is lower, presumably due to the fact that intragranular cracks do not have to be nucleated, but are already present.

These results are important for understanding the deformation of shallow level porous sedimentary rocks. At modest depth, such units would show distributed cataclastic flow (which would enhance subsequent pressure solution) at fairly low strains, such as those involved in folding. However, in regions of higher strain, unstable faulting would develop, as observed by Aydin and Johnson (1983).

### *Micromechanical Processes in Experimental Fault Gouge*

Previous TEM observations of the gouge developed from initially bare surfaces of granite slid in rotary shear (at a variety of velocities, with a total slip of 376 mm) showed 10–20% amorphous material (some quartz, mostly feldspar). Although the sample exhibited a number of stress drops, our observations of a gradation from amorphous to poorly crystalline to normal crystalline material suggest that the amorphous material is not glass (melt) due to frictional heating. Recently we have examined the gouge from another experimental sample which would not be expected to produce any melt, regardless of the real area of contact, because it was slid at a relatively slow rate (1.0 to 3.2 μm/sec, for a total displacement of 200 μm). This sample also contains amorphous material, which supports our interpretation that it is not glass, but rather results from distortion and eventual destruction of the crystallinity of quartz and especially feldspar, possibly accompanied by gel formation because of the water added to all of these experiments. In order to say more, it will be necessary to make observations from monomineralic aggregates with different, simple sliding histories.

### *Reports*

Hirth, G., and Tullis, J., 1987, The transient nature of cataclastic flow in porous quartzite: Trans. Amer. Geophys. Union, 68, 1464.

Tullis, J., and Hadizadeh, J., in preparation, Transitions from faulting to cataclastic flow to dislocation creep in anorthosite: An experimental study: to be submitted to Tectonophysics.

Tullis, J., and Yund, R.A., 1987, Transition from cataclastic flow to dislocation creep of feldspar: mechanisms and microstructures: Geology, 15, 606-609.

Tullis, J., and Yund, R.A., 1987, The brittle-ductile transition in feldspathic rocks: Trans. Amer. Geophys. Union, 68, 1464.

Yund, R.A., and Tullis, J., in preparation, Micromechanical processes of experimental cataclastic flow in anorthosite: to be submitted to Journal of Structural Geology.

Hirth, G. and Tullis, J., in preparation, The brittle-ductile transition in quartz aggregates: an experimental study of the effects of porosity, pressure, and total strain: to be submitted to Journal of Geophysical Research.

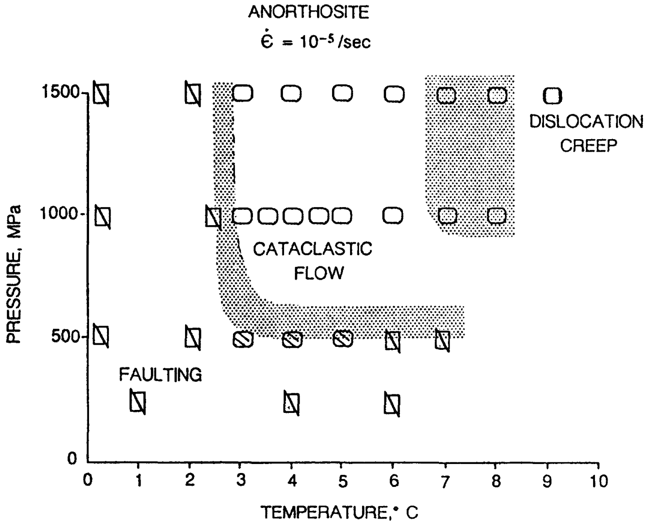

Figure 1. Summary of mechanical data and optical and TEM observations for fine-grained anorthosite cores deformed at a strain rate of 10⁻%/sec, showing transitions from faulting to cataclastic flow to dislocation creep with increasing T and P. The transition regions are shown by the stippled pattern. The transition from faulting to stable, distributed cracking requires moderate T as well as P, but does not involve interactions with dislocations; new dislocations are first observed at 700 C.

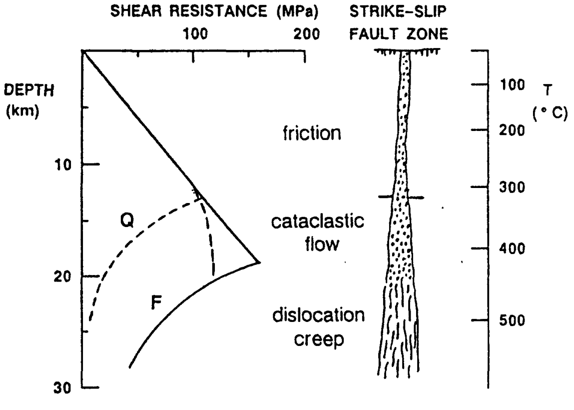

Figure 2. Stress-depth plot for granitic rocks, showing the traditional interpretation of the brittle-ductile transition as corresponding to the transition from faulting to dislocation creep for quartz (short-dashed line). If the volumetrically dominant feldspar controls the aggregate response, the B-D transition observed at 300 C cannot correspond to the transition to dislocation creep (solid line), but may correspond to the transition to cataclastic flow (long-dashed line).

# EXPERIMENTS ON ROCK FRICTION CONSTITUTIVE LAWS APPLIED TO EARTHQUAKE INSTABILITY ANALYSIS

USGS Contract 14-08-0001-G-1364

Terry E. Tullis
John D. Weeks
Department of Geological Sciences
Brown University
Providence, Rhode Island 02912
(401) 863-3829

## INVESTIGATIONS:

1. Our numerical investigation of the temporal and spatial variations in strain and displacement predicted from the model earthquake cycle of Tse and Rice (1986) has been extended to include consideration of the predictability of earthquakes using down-hole strain meters.

2. We continue to investigate the contribution of jacket friction to our measurements of rock friction velocity dependence. We are cooperating with James Dieterich and James Byerlee, both at USGS Menlo Park, to resolve the discrepancies among the various measurements of rock friction velocity dependence.

3. In connection with number 2, we have completed an experiment to measure the velocity dependence of friction of unconfined and unjacketed Westerly granite.

4. We have started a program to measure the temperature rise during high–velocity frictional sliding.

## RESULTS:

1. We have continued our study of the geodetic predictions of the Tse and Rice (1986) numerical model of a strike-slip fault. This study was undertaken in order to determine whether the model predicts any systematic, observable geodetic precursors to earthquakes, how the size and distribution of precursory signals depend on the values of the friction constitutive parameters, and where and how it is best to monitor precursory activity. Simulations of the earthquake cycle were examined with several values of L, ranging from 5 to 80 mm, with near-surface values of **a-b** of -0.0015 and -0.003, and with either zero or 30% dynamic overshoot during the earthquake. Strain changes during the earthquake cycle are largest for the larger values of L and the less negative value of **a-b**. Contrary to our observations for velocity, strain signals are larger near the fault than far away from it. Furthermore, sharp increases in strain rate occur a few minutes to a month before the earthquake (1-500 m away from the fault) for all values of the model parameters. The time scale of the sharp increases in strain rate depends on the model parameters; larger values of L and the less negative value of **a-b** produce larger signals earlier in the earthquake cycle. This behavior is very similar to the behavior observed for velocity. The strain signals are large enough to be detected with a strain meter in the presence of Earth noise for all values of the model parameters except L = 5 mm. In contrast, the sharp increases in velocity that we reported previously would only be detectable for those simulations with L≥60 mm (**a-b** = -0.003) or L=40 mm (**a-b** = -0.0015), using a two–color laser geodimeter with lines extending to 4 km away from the fault (these figures correct an error an earlier report). We have used the model predictions of displacement on the fault throughout the earthquake cycle to calculate the amount of pre– and post–seismic moment release as a function of the model parameters. The predicted moment release prior to and following the earthquake is sensitive to the values of L and **a-b**, but only after the earthquake is the moment release sensitive to dynamic overshoot. The amount of pre– and post–seismic moment release

during any given time interval increases with increasing L and less negative **a-b**. Expressed as a fraction of the co–seismic moment release, the pre–seismic moment release is much smaller than the post–seismic moment release. During the ten minutes immediately preceding an earthquake, the predicted pre–seismic moment release is <<1% of the total earthquake moment for all simulations except those with L≥60 mm (**a-b** = -0.003) or L=40 mm (**a-b** = -0.0015) (Figure 1). The post–seismic moment release within a day of the earthquake ranges from 15 to 75% of the co–seismic moment release, depending on model parameters. This is consistent with the fact that using strain meters remote from a variety of earthquakes, Johnston, et al. (1987) were not able to observe any pre–seismic moment release with a sensitivity of 1–3% but did observe post–seismic moment release of about 50% of the co–seismic value.

2. Our efforts to measure the friction of our sample jackets have two primary goals: To assess the errors that may be contributed by the jackets and to correct for them, and to re-design the jackets to minimize the contribution. A good jacket should have very low friction and very low velocity dependence of its friction. To isolate the contributions from various parts of the jacket and to identify possible replacement materials, we have measured the friction of Teflon, polyethylene, graphite and a proprietary material from Bal Seal Engineering. Of these, Teflon is still the best material, having both the lowest coefficient friction and the smallest velocity dependence. Unfortunately, Teflon has a linear component to the velocity dependence that becomes important at high velocity (Figure 2). These results suggest that our rock friction data needs only a small correction at velocity ≤ 30 $\mu ms^{-1}$. We are now proceeding to the measurement of the friction of various kinds of O-rings, including Teflon-clad O-rings.

3. As Teflon is a major component of our sample jackets, its strong velocity dependence at high velocity has caused us to question our recently published data on the friction of granite at high velocity (Blanpied, et al., 1987). Consequently, we performed an experiment to measure the velocity dependence of granite using an unconfined sample. With no confining pressure, a jacket is not necessary and there are no spurious contributions to the measured friction. The lack of confinement, however, requires low normal stress as rocks have low strength when unconfined (this experiment was run at 10 and 15 MPa normal stress as opposed to 75 MPa for the run reported in Blanpied, et al.). The results of this experiment are shown in Figure 3. In agreement with previous studies, at velocities between 0.01 and 10.0 $\mu ms^{-1}$ the response was velocity weakening. Although the data are poor, there does appear to be a transition to velocity strengthening at high velocity. This occurs at velocities ≥ 1000 $\mu ms^{-1}$, compared to the value of 30 to 100 $\mu ms^{-1}$ reported before.

4. It has been suggested that high temperatures generated by frictional heating may affect the velocity dependence of rock friction at high slip rates. To investigate this possibility, we have begun a study of frictional heating in our experimental samples. Thermistors near the sliding surface will be used to measure temperatures during sliding. Experiments will be conducted at several normal stresses to distinguish changes in velocity dependence due to changing slip rate from those caused by frictional heating. Because our compact sample geometry makes analysis of the thermistor data difficult, we will compare the data to the results of a finite element solution for time-dependent heat flow in our samples.

## REPORTS:

Blanpied, M. L., T. E. Tullis, and J. D. Weeks, Contrasting velocity dependence of granite friction: initially bare surfaces vs. simulated gouge, *Eos, Trans. Am. Geophys. Union, v. 68*, p. 1478.

Lorenzetti, E.A., and T.E. Tullis, 1987, Sensitivity of Geodetic Predictions of a Strike-Slip Fault Model to Variations in Friction Constitutive Parameters, *Eos, Trans. Am. Geophys. Union, v. 68*, p. 1242.

Tullis, T. E., 1987, Progress and problems in understanding rock friction, *Eos, Trans. Am. Geophys. Union, v. 44*, p. 1448.

Tullis, T. E.,.1988, Rock friction constitutive behavior from laboratory experiments and its implications for an earthquake field monitoring program, Pure Appl. Geophys., v. 126, pp. 555-588.

## REFERENCES:

Blanpied, M. L., T. E. Tullis, and J. D. Weeks, 1987, Frictional behavior of granite at low and high sliding velocities, *Geophys. Res. Lett., 14,* pp. 554-557.

Johnston, M.J.S., A.T. Linde, M.T. Gladwin, and R.D. Borcherdt, 1987, Fault failure with moderate earthquakes, *Tectonophysics, v. 144,* pp. 189-206.

Tse, S.T., and J.R. Rice, 1986, Crustal earthquake instability in relation to the depth variation of frictional slip properties, *J. Geophys. Res. v. 91*, pp. 9452-9472.

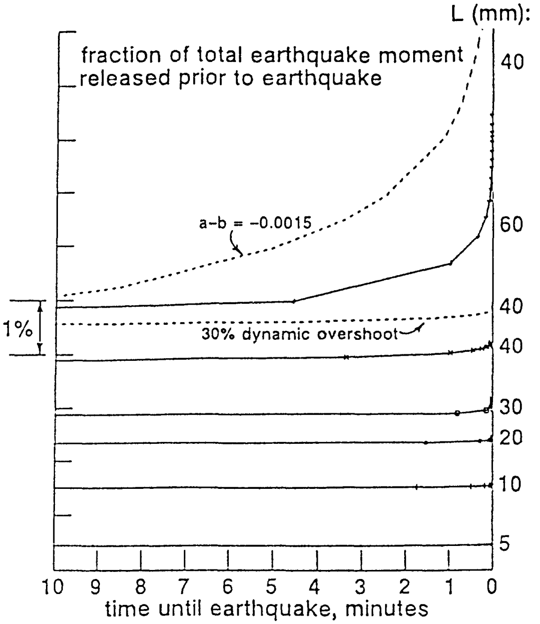

Figure. 1. Predicted pre-seismic moment release during last 10 minutes of earthquake cycle, shown for different values of model parameters used in this study. Except where noted, **a-b** = -0.003 and there is no dynamic overshoot.

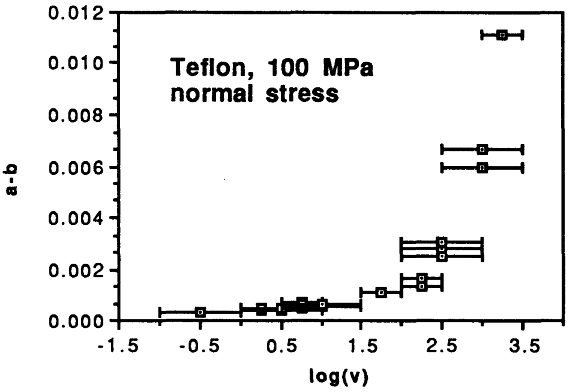

Figure 2. Velocity dependence of Teflon. Horizontal bars indicate the size of the velocity jump used to measure **a-b**; velocities are in $\mu ms^{-1}$. The values are positive, indicating velocity strengthening at all velocities. At velocities over about 30 $\mu ms^{-1}$, a linear component to the velocity dependence causes **a-b** to increase rapidly.

Figure 3. Velocity dependence for frictional sliding of unconfined granite. Horizontal bars indicate velocity jump size, vertical bares indicate the spread of values from noisy data. Because unconfined, there is no need of a sample jacket and there is no contribution to the measured friction from the jacket, as there is in confined experiments. The unconfined strength of the granite limits the normal stress that can be applied to the sample.

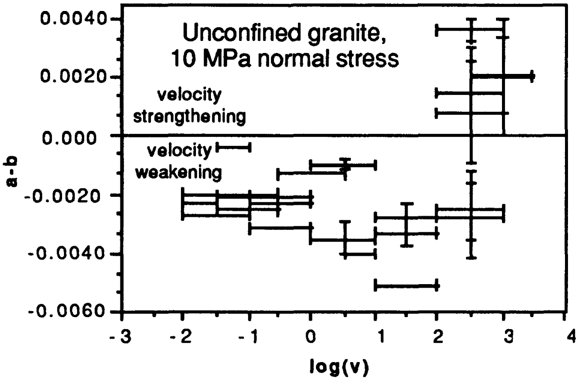

# Deep Hole Desalinization of the Dolores River

9920-03464

William Spence
National Earthquake Information Center
U.S. Geological Survey
Denver Federal Center
Box 25046, Mail Stop 967
Denver, Colorado 80225
(303) 236-1506

## Investigations

This project relates to monitoring the seismicity of the region of the intersection of the Delores River and Paradox Valley, southwest Colorado. The project is a component of the Paradox Valley Unit of the Colorado River Basin Salinity Control Project and is being performed for the U.S. Bureau of Reclamation with support from the Induced Seismicity Program of the U.S. Geological Survey. In this desalinization project, it is proposed to pump approximately 30,000 barrels/day from brine-saturated rocks beneath the Dolores River through a now completed borehole to the Madison-Leadville limestone formation of Mississippian age, some 15,000 feet below the surface. There is a possibility of seismicity being induced by this desalinization procedure, especially in the long term. The project objectives are to establish a pre-pumping seismicity baseline and, during the pumping phase, to closely monitor the discharge zone for possible induced seismicity. If induced seismicity does occur, it should be possible to relate it to formation characteristics and to the pumping pressure and discharge rates.

## Results

A 10-station seismograph network is centered at the location of the proposed injection well. This high-gain network has a diameter of about 80 kilometers, and has been in operation since September 1983. Seismic data are brought to Golden, Colorado, via microwave and phone line transmission. These data are fed through an A/D converter and then through an event detection algorithm. The network has operated at high quality, except for two periods when it was decommissioned by lighting strikes. Analysis procedures have been considerably complicated by a high rate of blasting activity in the region, but means have been developed to distinguish the occurrence of natural earthquakes to good reliability.

Notable regional earthquake activity are a swarm of shallow events (maximum magnitude 3.2) near Carbondale, Colorado, a similar swarm near Crested Butte, Colorado, a magnitude 3.4 shallow earthquake near Blue Mesa Reservoir, Colorado, and a magnitude 2.8 earthquake that was preceded by three events and followed by four events all located about 25 km SE of Grand Junction, Colorado. In the vicinity of the network, the earthquake catalog is complete to about magnitude 2.0, but very few earthquakes have occurred in the immediate vicinity of the proposed injection well. Most of the seismicity in the area of the network is in the shallow crust. However, of the 222 earthquakes located for the period January 1, 1984-June 30, 1987, 46 are in the depth range 10-20 km and 16 earthquakes are deeper than 20 km, with several events in the depth range 30-55 km. These results show that microearthquakes are distributed throughout the crust of the Colorado Plateau, with occasional events in the upper mantle. The shallow and deeper earthquakes follow a diffuse north-south trend, parallel to the eastern boundary of the Colorado Plateau. These results, combined with a lack of historical seismicity at the zone of the Paradox Valley seismic network, indicate that any seismicity induced by deep-well injection near Paradox Valley should be identifiable as such.

Report

Spence, W., and Chang, P-S., 1987, Seismic monitoring in the region of the Paradox Valley, Colorado--Annual Report, July 1986-June 1987: U.S. Bureau of Reclamation, Deep Well Injection Site, Paradox Valley Unit, Colorado River Basin Salinity Control Project, 14 p.

# Regional and National Seismic Hazard and Risk Assessment

9950-01207

S.T. Algermissen
Branch of Geologic Risk Assessment
U.S. Geological Survey
Denver Federal Center, MS 966
Denver, CO 80225
(303) 236-1611

## Investigations

1. Isoseismals were drawn for thirteen historical earthquakes that caused damage-level intensities (MMI≥VI) in the four Wasatch Front counties of Weber, Davis, Salt Lake, and Utah. For each earthquake there was available at least enough intensity information at locatable points for rough isoseismals to be contoured. Four large earthquakes in Sevier County, Utah, in 1901 and 1921 were investigated and isoseismal maps constructed.

2. Loss calculations are proceeding for the Salt Lake City area for several scenarios of large earthquake occurrence on the Wasatch Fault.

3. New initiatives began in the Pacific Northwest. Approximate calculations of probabilistic ground motion associated with the occurrence of a large ($M_w$=8.5) earthquake at two possible locations in the Cascadia subduction zone were undertaken in an attempt to roughly estimate the effects of such an earthquake in the Seattle urban area. The offshore earthquake is assumed to occur at a depth of 20 km. The second earthquake is assumed to occur at a depth of 50 km beneath Puget Sound. In both cases, calcualtions of probable ground motion were made assuming average recurrence times for the earthquakes of 300, 600 and 900 years.

4. Investigations regarding regional segmentation and extensional accomodation in the Great Basin Province were undertaken using a digitized data base of all Quaternary surface faulting in the province. The purpose of the investigation is to provide a regional tectonic framework for young faulting in the province and a stronger tectonic basis for seismic source zones used in probabilistic estimates of the regional ground motion hazard.

## Results

1. For the Sevier County earthuakes in the years 1901 and 1921, intensities assigned in this study were somewhat lower than those of some previous researchers, partly because of the transition from Rossi-Forell to Modified Mercalli intensities, and partly because of a seemingly high assignment of intensity with little supporting evidence. Previously assigned felt areas for three 1921 shocks are in general agreement with those found in this study. However, questions regarding the 1901 felt area cannot be resolved with intensity information presently available. The accounts of the 1901 earthquake's effects are similar to the accounts of the 1921 shocks. However, the 1901 earthquake was also reported felt in Salt Lake City, 220 km to the north. It is not clear whether Salt Lake City should be included as an integral part of the 1901 felt area or treated as an outlying felt report.

The highest historical intensity within any of the four Wasatch Front counties was found to be MMI VII. Davis, Salt Lake, and most of Weber counties were found to be in an area commonly reporting intensity VI. Historic intensities in Utah county have been below the damage level except for the Provo area to the northeast of Utah Lake and the Eureka mining district in the southwest corner of Utah county and adjoining Juab county. Higher intensities in the northern part of the four county-study area are the result of the 1934 Hansel Valley earthquakes and large earthquakes in southern Idaho.

2. Both deterministic (scenario) and probabilistic loss studies are being undertaken. Losses are estimated for scenario earthquakes on the Provo, Salt Lake City and Weber segments of the Wasatch Fault. Earthquakes of magnitude ($M_s$) 7.5, 6.5, and ($M_L$) 5.5 are being simulated on each of the above fault segments. Additionally, an earthquake of magnitude $M_s$=7.5 is being simulated on the west side of the Oquirrh Mountains, approximately 30 km west of Salt Lake City. Probabilitstic expected maximum losses in 50 years are also being calculated with a 10 percent probability of exceedance, using the probabilistic hazard model described in Open-File Report 82-1033, with the seismic source zone for the Wasatch Fault revised in light of the geological research regarding segmentation of the fault. Eight fault segments have been modeled, each having individual recurrence rates for large earthquakes that are based on the new paleoseismic data.

3. The results of preliminary investigations in the Pacific Northwest give only a general idea of the influence on expected ground motion since the subduction zone was only approxiamately modeled. Future work in modeling ground motion in the region will include a careful modeling of all source zones and new attenuation relations. Nevertheless, the results are interesting. A large subduction zone earthquake offshore would not appreciably affect the 50 year acceleration or velocity at Seattle for average recurrence times of 300 through 900 years. The accelerations and velocities (in rock) computed for a 50 year exposure time and 10 percent chance of exceedance at Seattle does not appreciably differ from values shown in the maps of O.F.82-1033. A large subduction zone earthquake at a depth of 50 km beneath Seattle would not appreciably change the 50 year, peak acceleration and velocity at Seattle for an average recurrence time of 900 years but it would approximately double the peak velocity at Seattle for an average recurrence of 300 years. The suggested doubling of the 50 year velocity is only a rough approximation since no entirely suitable attenuation relations are available for such an earthquake.

4. Previously recognized transverse range-tilt domain boundaries trending northwest across the Great Basin are shown to segment and terminate generally north-south zones of Quaternary-Recent normal faulting and juxtapose regions of contrasting ages of latest fault displacements. In at least Quaternary time, these boundaries accomodated differences in extension rates of the brittle crust across them and are therefore termed *extensional accomodation zones*. Depth of the accomodation zones are presently only constrained by the known or inferred depths of Quaternary-Recent faults in the province and the inferred role of the accomodation zones in segmenting the Central Nevada Seismic Zone. Maximum crustal depths of these constraining observations are greatly different on either side of the Great Basin and a growing body of knowledge of late Cenozoic-Recent fault penetration dephs suggests that, in fact, variable depth of the features might reasonably be expected. Future earthquake rupture in a 30 km zone bounded on the south by the 1915 Pleasant Valley surface ruptures and on the north by the northern accomodation zone would serve to complete a belt of Recent fault rupture across the northern extensional domain. A journal paper is presently in revision following internal review.

## Reports

Algermissen, S.T., 1988, Estimation of ground shaking in the Pacific Northwest, *in* Hays, W.W., and Gori, P.L., eds., :U.S. Geological Survey Open-File Report, (in press).

Algermissen, S.T., and Leyendecker, E.V., 1988, Estimation of potential earthquake losses in the Puget Sound, Washington and Portland, Oregon areas, *in*, Hays,W.W., and Gori, P.L., eds.,: U.S. Geological Survey Open-File Report, (in press).

Algermissen, S.T., and Leyendecker, E.V., 1988, Estimation of losses in the Puget Sound area, *in*, Hays., W.W., and Gori, P.L., eds.,: U.S.Geological Survey Open-File Report, (in press).

Leyendecker, E.V., Highland, L.M., Hopper, M.G., Arnold, E.P., Thenhaus, P.C., and Powers, P.S., 1988, Early results of isoseismal studies and damage surveys for the Whittier Narrows earthquake: Earthquake Spectra, Journal of the Earthquake Engineering Research Institute, (in Press).

Thenhaus, P.C., 1988, Site response from distant large earthquakes and issues concerning the earthquake hazard at Bankok, Thailand, *in* Lukkunaprasit, P., Chandrangsn, K., Poobrasert, S., Mahasuverachi, M., eds., Proceedings of the First Workshop on Earthquake Engineering and Hazard Mitigation, November, 1986, Bangkok, Thailand: Southeast Asia Association of Seismology and Earthquake Engineering and The National Earthquake Committee of Thailand, p. 81-104.

Thenhaus, P.C., 1988, Perspectives on the seismic hazard and risk of the New Madrid seismic zone: Central United States Earthquake Consortium, Monograph Series, 67 ms. p. (in press).

# Regional and Local Hazards Mapping in the Eastern Great Basin

9950-01738

R. Ernest Anderson
Branch of Geologic Risk Assessment
U.S. Geological Survey
Box 25046, MS 966, Denver Federal center
Denver, CO 80225
(303) 236-1584

## Investigations

1. Completed text and map dealing with selected Quaternary structures in the Cedar City 1°X2° quadrangle. To be submitted for review by July 15, 1988.

2. Completed text describing the kinematics of extensional deformation in the Caliente, Nev., area. To be submitted for review by June 1, 1988. Work done in cooperation with geologists from the University of Paris.

## Results

Important results from both investigations were included in the previous semiannual report.

## Reports

None.

# Depth to Bedrock Map in the Greater Tacoma Area, Washington

9950-04073

Jane M. Buchanan-Banks
Branch of Geologic Risk Assessment
U. S. Geological Survey
David A. Johnston Cascades Volcano Observatory
5400 MacArthur Boulevard
Vancouver, Washington 98661
(206) 696-7996 FTS 422-7996

## Investigations

Catalogues of locations of the deepest water and oil wells in Kitsap, Mason and Thurston counties were compiled from various data sources and entered in the computer; work began on similar catalogues for Pierce and King counties. The catalogues also contain information on availability of logs of each well, and validity of well location.

## Results

Bedrock outcrops within all counties were compiled on stable base material at 1:100,000 scale. Locations of deepest water and oil wells in Kitsap, Mason, and Thurston counties and some in Pierce and King counties have been compiled, and a draft version of a source map with accompanying bibliographic reference has been prepared.

Within the map area, the Puget Trough is punctuated by bedrock highs in the northwest and southwest parts, and along the eastern edge of the map area. Exploratory oil wells in the eastern part of the area have reached bedrock, while the deepest water well located thus far near the center of the trough was drilled more than 700 m without reaching bedrock. In the southern part of the map area, the till is locally underlain by poorly consolidated Tertiary sedimentary deposits which show no stratigraphic distinction in the logs of the deeper wells to determine the contact between the till and underlying bedrock.

# Geology and Tectonic Evolution of the Western Transverse Ranges

Project Number: 9950-04063
Project Chief: Russell H. Campbell
Address: U.S. Geological Survey
MS 922, National Center
Reston, Virginia 22092
Telephone: (703) 648-6784 (commercial)
FTS 959-6784

Work in the first half of FY 1988 has been restricted to revision of the explanation for the geologic map of the Point Dume quadrangle (1:24,000), subsequent to GNU check in Menlo Park. The preparation of the Point Dume and the eastern part of the Triunfo Pass 7.5° quadrangles (western Santa Monica Mountains) has proceeded more slowly than was anticipated, as the project chief was constrained to work on landslide probability and risk and to BGRA administrative duties. General stratigraphic and faunal charts for the western Santa Monica Mountains are in preparation; however, the earliest possible target for their completion (originally the end of calendar year 1987) is now January, 1989.

Preparations are being made for the compilation of new mapping by USGS, CDMG, and others, at 1:100,000 scale, for the Los Angeles 1° x 30'quadrangle. Compilation, which was expected to begin in FY 1987, is now scheduled to begin as early in FY 1988 as other duties permit.

# Holocene and Quaternary Geologic Studies

9540-03787

Robert O. Castle
Branch of Western Regional Geology
345 Middlefield Road MS 975
Menlo Park, CA 94025
(415) 329-4941

## Investigations

1. Expanded supplementary investigations of anomalous vertical displacements in the Los Angeles Harbor area to include additional southern California tide stations. The chief thrust of this effort lies in the discrimination of vertical displacements (if any) from errors attributable to measurement system failures and variations in the oceanographic-meteorlogic regime between stations.

2. Completed report and revisions on vertical surface displacements along the Newport-Inglewood zone between the Dominguez Hills and Corona del Mar, Los Angeles and Orange Counties, California.

3. Completed report on a revised configuration of the southern California uplift.

## Results

1. Analysis of repeated geodetic levelings along the onshore section of the Newport-Inglewood zone between the Dominguez Hills and Corona del Mar indicate that nearly the entire vertical-displacement field along this zone is attributable to coseismic effects associated with the 1933 Long Beach earthquake or continuing oil-field operations. The only significant exception to this generalization seems to consist of modest down-to-the-south aseismic tilting between Long Beach and Corona del Mar of the order of 0.05-0.10 $\mu$rad/yr.

2. Recently discovered vertical-control data from southwestern Arizona and adjacent parts of California compel major revisions in the configuration of the southern California uplift, both at its culmination and following its partial collapse. These revisions are limited to the southeastern part of the uplift, which is now believed to have projected into northern Mexico. The chief changes consist of: a sharply diminished gradient south of Cottonwood Pass; dramatically reduced tectonic subsidence centering on the Salton Basin; and short-lived uplift of at least 0.2-0.3m at the latitude of El Centro. The required changes are attributable to errors in judgement (mine) and are unrelated to measurement accuracy.

## Reports

Castle, R.O., 1987, Bulge bashing: modern sophistry in action (abs.): EOS, Transactions, American Geophysical Union, v. 68, no. 44, p. 1506.

# Network and Array Analysis of Puget Sound Earthquake 1962-1969

14-08-0001-G1521

W. Winston Chan
Teledyne Geotech Alexandria Labs
314 Montgomery St., Alexandria, VA 22314
(703) 836-3882

## Objective:

Seismic activity of the western Washington region in the 1960's, excluding Mt. St. Helens, appears to be greater than those in 1970's and 1980's when dense local seismic networks were installed in the region. This study will use previously unutilized data from the Long-Range Seismic Monitoring (LRSM) network to study the relationships between aftershocks to the rupture processes of the principal 1965 Puget Sound earthquake. The rupture extent of the mainshock will be delineated and the hypothesis that clusters of aftershocks are found at asperities or at the limits of rupture on the fault plane will be tested. New information will be provided about an earthquake that serves as a model for seismic hazard in the Puget Sound area. A similar analysis will be performed of other events in the Puget Sound area during the 1960's by studying this data set with other existing ones.

## Data Acquisition and Analysis:

(1) The initial two months of this project are devoted to examining the significant events in the western Washington and northern Oregon coast range-Portland area during the 1960's. Figure 1 shows the relative locations between the seismic region of interest and some of the LRSM stations. The following events and their aftershocks are selected to be studied in relationship to the Juan de Fuca plate:

| DATE | REGION | mb |
|---|---|---|
| Oct 11, 1960 | Swift Creek | 4.4 |
| Sep 17, 1961 | Siouxon Peak | 5.1 |
| Nov 6, 1962 | Portland | 5.5 |
| Oct 1, 1964 | Portland | 5.3 |
| Apr 29, 1965 | Puget Sound | 6.5 |

Film records are scanned to identify each individual event and aftershocks at available LRSM stations. Timing of arrivals are made on the film for event location. Additional events in the Seattle-Portland region will be included to supplement the data set in case of poor data quality for the above selected events.

(2) The selected earthquakes are digitized from the analog tapes. Data from all high and low gain short- and long-period three-component channels are digitized. Examples of some of the digitized waveforms on the short-period instruments are

shown in Figure 2. The digital data will be calibrated, quality assured, and archived. Sample spectra will be made to inspect the bandwidths available.

(3) The array and single station data will be deconvolved to far-field displacement at each station using the method of Shumway and Der (1985). The events will be relocated with the revised depth information revealed by the deconvolved data. Moments and corner frequencies will be estimated from the broadband displacement P and S waves. Focal mechanisms will be determined using the deconvolved array and single station data.

(4) P and S spectral ratios of aftershocks of various size ranges will be examined for source scaling relationships of corner frequency and spectral fall-off with moment. The main shock and a subset of aftershocks will be examined for correlation and study. Particular attention will be paid to the location of aftershocks and their potential use as Green's functions of small fault sections.

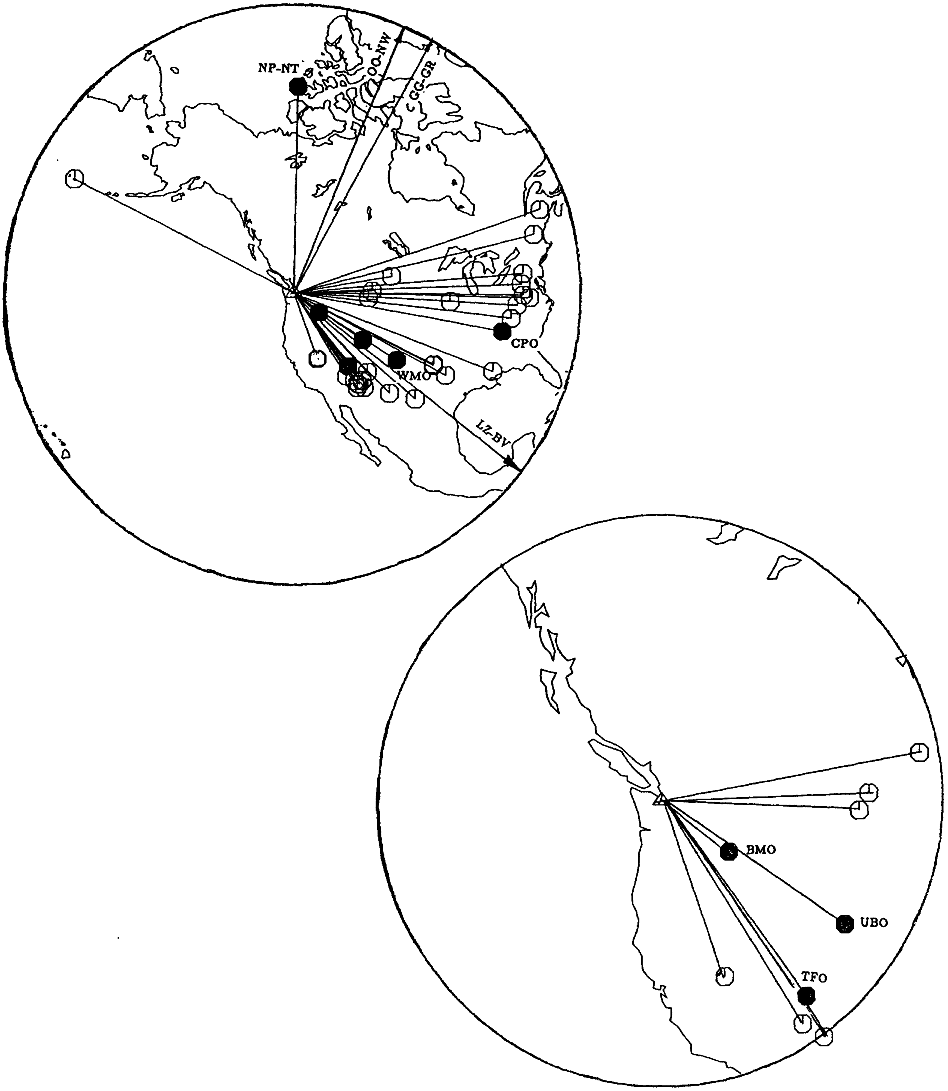

Figure 1. Map indicating the locations of the LRSM stations in North America and the Puget Sound region.

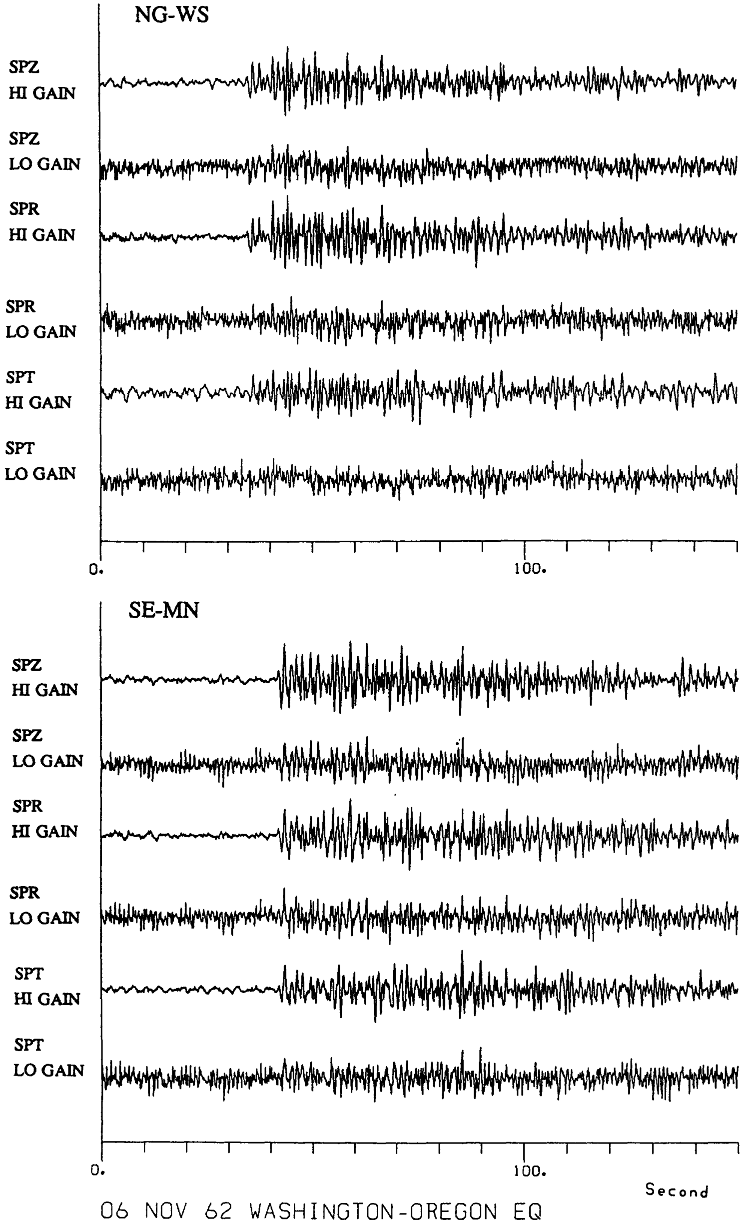

Figure 2. Examples of some of the three-component short-period LRSM data recorded on both the low and high gain instruments SE-MN (Minnesota) and NG-WS (Wisconsin).

# Engineering Behavior Study of Sites Affected by Past Seismic Activity in the Charleston, S.C. Area

14-08-001-G-1348

G. W. Clough
Department of Civil Engineering
Virginia Polytechnic Institute and State University
Blacksburg, Virginia 24061
(703) 961-6637

During the past year, the principal investigator and his students have conducted the first phase of an investigation concerning the seismicity of the Charleston, S.C. area under the auspices of a contract through the 1987 Solicitation for the USGS Earthquake Hazards Reduction Program. The first phase involved preparing for and undertaking a comprehensive field study, and collecting reference materials from existing data files. Working under subcontract to the project, faculty and students at the Citadel in Charleston are assisting in the on site work, and classification of the existing data files. Funding for a second year of this effort is in place, with the intent that this phase concentrate on extending the first year effort, allowing new field sites to be investigated, and returning to some of the original ones to fill gaps in our knowledge.

This research was triggered by findings of workers at the USGS and the University of South Carolina of numerous artifact liquefaction features from the 1886 and earlier earthquakes. These findings have introduced new insights into the seismic history of the Charleston area. The VPI investigations are designed to supplement the earlier work by conducting an engineering study which can assist in quantifying information in a form that will be useful in engineering design. The primary purposes of the research are: (1) Define the behavior of the Charleston sands relative to other standard materials and soil involved in earthquakes elsewhere; (2) Determine parameters for the subsoils which can be used for backcalculations of accelerations that should have caused the observed liquefaction features; (3) Perform analyses which can produce reasonable estimates of the accelerations that did occur at the sites of various liquefaction phenomena, and hence advance our knowledge of the seismic environment of the Charleston area; and, (4) Use the information to extend our understanding of liquefaction phenomena in general.

Preparing for the field work involved adaptation of a in-house designed miniature electric cone penetrometer to a small drill rig, and development of a fully automated microcomputer data acquisition system. Additionally, based on preliminary site visits, a strategy was developed for the sequence of testing. The field studies involved drilling 35 exploratory holes, and conducting 24 electric cone penetrometer probes at sites within the meizoseismal zone of the 1886 earthquake. Standard penetration tests were also performed in a number of holes to complement the cone penetration tests. Finally, data were collected on a large number of commercial borings done in the city limits of Charleston. Approximately 100 laboratory classification tests were performed on soil samples obtained from the field exploration.

The results of the first phase of the field testing are now being assessed. Quality and consistency of the test results appear very good. Figure 1 shows a boring log and test data from the Hollywood site. This site is important because of the presence of a 9000 ft long drainage trench where numerous artifact liquefaction features from the 1886 and other earlier earthquakes have been exposed by USGS researchers. It is of particular interest in that the features from the earlier earthquakes show considerable disruption of the ground, but those from the 1886 event are relatively small. The soil profile in Figure 1 consists of about 3 ft of an overlying stiff organic layer, underlain by 12 to 15 ft of fine sand, followed by a 5 ft layer of soft clay which is in turn underlain by dense sands and clayey sands. The cone and standard penetration data are in agreement, and show that the sand layer is dense in its upper portions, but that it becomes progressively looser with depth. In its lower portions, the sand layer is very loose, with blowcounts of 2 blows/ft, and cone tip resistances of 10-20 kg/ sq cm. The low densities of the sands are of interest since this would suggest that this material is susceptible to liquefaction, and that it has not densified in spite of having been subjected to multiple significant earthquakes and liquefaction events. Superimposed onto Figure 1 are curves showing accelerations at which liquefaction should occur given a Richter magnitude earthquake like that of the 1886 Charleston earthquake. At accelerations as low as 0.2g significant portions of the profile are liquefiable.

At the Hollywood site, holes were drilled and insitu tests performed in a pattern along the trench, and at two locations perpendicular to it. The findings show a consistent soil profile, and similar densities for the soils regardless of location. There is also a consistency in most of the grain sizes of the sands, although in one area the sand is more silty than elsewhere.

At other sites, the findings of the field testing were typically similar to those at Hollywood in that either large or localized areas exist that fit the profile of conditions conducive for liquefaction. Where the sites are situated in the ancient beach ridges that were formed around Charleston, the sands have remarkably consistent characteristics. These sands classify as uniformly graded and fine grained. In the areas affected by alluvial processes such as in Charleston itself, the sands are silty.

Preliminary assessments from all of the information obtained in the first year work are:

1.) Differences in levels of liquefaction features observed for sites within the meizoseismal zone can be explained in terms of differences in thicknesses of non-liquefiable layers above the liquefiable sand layers, and thicknesses of the liquefiable sand layers themselves.

2.) Given the conduciveness of many of the sites to liquefaction, it can be argued that accelerations in the range of 0.2 to 0.3g for the size of the 1886 Charleston earthquake would serve to explain the observed phenomena. These levels are below those generally accepted for this earthquake from seismological evidence. Further work will be done in an effort to understand this discrepancy.

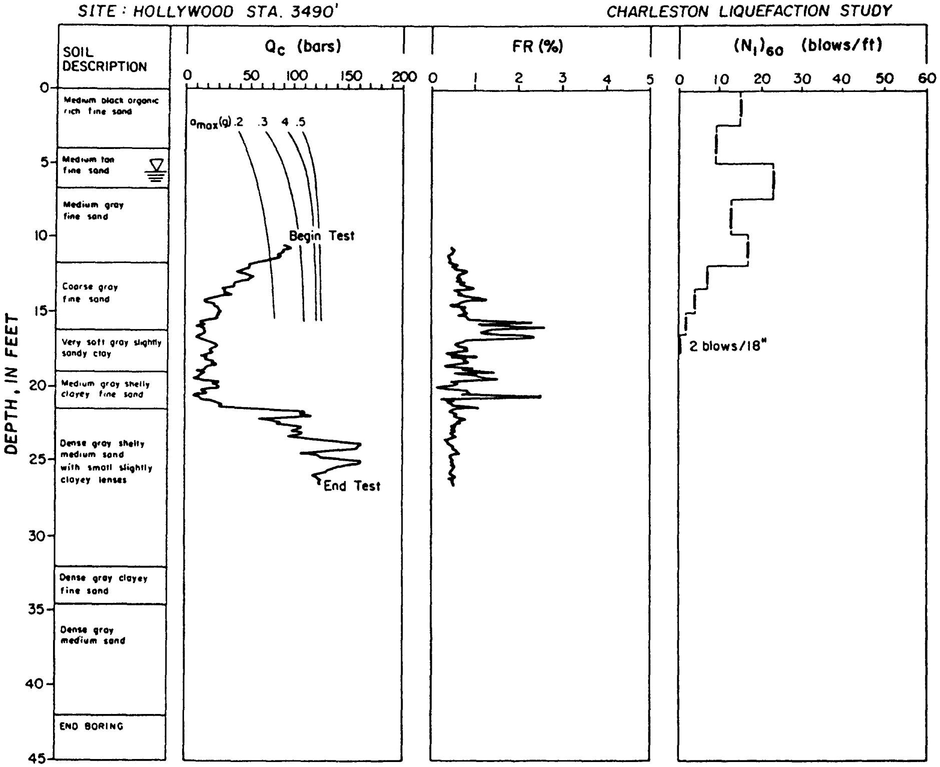

Figure 1. Results of Field Testing and Accelerations Required for Liquefaction at Boring Sta. 3490, Hollywood Site

# EVALUATION OF HOLOCENE SUBSIDENCE EVENTS OF COOK INLET ESTUARINE FLATS NEAR ANCHORAGE, ALASKA, AS A BASIS FOR ASSESSING SEISMIC HAZARDS IN SOUTHCENTRAL ALASKA

14-08-0001-G1582

Rodney A. Combellick and Richard D. Reger
Alaska Division of Geological & Geophysical Surveys
794 University Ave., Suite 200
Fairbanks, Alaska 99709
(907) 474-7147

## Investigations

Borehole drilling with continuous sampling is being undertaken for the purpose of recovering evidence of prehistoric subsidence events associated with major megathrust earthquakes in southcentral Alaska. The program includes drilling into estuarine flats at four sites in upper Knik Arm and two sites in upper Turnagain Arm; radiocarbon dating of buried organic soil layers; and sedimentologic studies for interpretation of paleoenvironment, rate of deposition, and magnitude of subsidence during each event.

## Results

Vegetated estuarine flats in upper Cook Inlet, Alaska, were submerged by regional subsidence and compaction during the great Alaska earthquake of 1964 (Foster and Karlstrom, 1967; Plafker, 1969). Following submergence, intertidal deposition of fine sand and silt buried the preexisting soil and vegetation, and has since nearly restored the Portage Flats, in upper Turnagain Arm, to its pre-1964 level (Ovenshine and others, 1976; Bartsch-Winkler and Garrow, 1982).

In an earlier study (Combellick, 1986), drilling with discontinuous sampling revealed the presence of older peats and organic soils below the 1964 layer in upper Turnagain Arm. The organic layers are each overlain with 2 to 10 ft of fine silty sand, sandy silt, and clayey silt and are interpreted to record prehistoric subsidence events in Turnagain Arm similar to that resulting from the 1964 earthquake. Radiocarbon ages of four of the six organic layers encountered in Turnagain Arm correspond favorably to published radiocarbon ages of elevated marine terraces in the uplift zone of the 1964 event (Plafker and Rubin, 1978). The Turnagain Arm data suggest that recurrence intervals between subsidence events ranged from about 425 to 800 years between 1320 and 4240 radiocarbon years ago. No layers were encountered that would represent events between 1320 years ago and the 1964 event; however, these recurrence intervals must be regarded as maximums because sampling was not continuous. Additional organic layers may exist in the intervals between samples and could provide evidence of more frequent subsidence events.

The current program consists of continuous drilling and sampling at the sites in Turnagain Arm where organic layers were previously encountered, and at four additional sites in upper Knik Arm, about 50 miles to the northwest. The objective is to recover samples of all existing soil layers and to document that the submerged soils can be correlated regionally between basins.

Preparations were made for drilling in March, 1988, when the flats are normally snow covered and frozen. These conditions ensure trafficability for the drill rig and protect the ground surface and vegetation from adverse impact. Four of the six sites are in state game refuges, requiring permits from state land-and-water management and fish-and-game divisions. Permit stipulations prohibit operation in the game refuges when the ground is not frozen and snow covered. Unfortunately, early March brought unusually warm weather to the region, which melted the snow and thawed the ground. Consequently, drilling in the game refuges must be postponed until next winter, probably late November or December, 1988. The Turnagain Arm sites, which are not in state game refuges, will be drilled during the summer of 1988.

## References

Bartsch-Winkler, S., and Garrow, H.C., 1982, Depositional system approaching maturity at Portage Flats, in Coonrad, W.L., ed., The United States Geological Survey in Alaska: Accomplishments during 1980: U.S. Geological Survey Circular 844, p. 115-117.

Combellick, R.A., 1986, Chronology of late-Holocene earthquakes in southcentral Alaska: Evidence from buried organic soils in Turnagain Arm: Geological Society of America Abstracts with Programs, Annual Meeting, v. 18, no. 6, p. 569.

Foster, H.L., and Karlstrom, T.N.V., 1967, Ground breakage and associated effects in the Cook Inlet area, Alaska, resulting from the March 27, 1964 earthquake: U.S. Geological Survey Professional Paper 543-F, 28 p.

Ovenshine, A.T., Lawson, D.E., and Bartsch-Winkler, S.R., 1976, The Placer River Silt--An intertidal deposit caused by the 1964 earthquake: Journal of Research of the U.S. Geological Survey, v. 4, no. 2, p. 151-162.

Plafker, G., 1969, Tectonics of the March 27, 1964 Alaska earthquake: U.S. Geological Survey Professional Paper 543-I, 74 p.

Plafker, G., and Rubin, M., 1978, Uplift history and earthquake recurrence as deduced from marine terraces on Middleton Island, Alaska, in Proceedings of Conference VI, Methodology for identifying seismic gaps and soon-to-break gaps: U.S. Geological Survey Open-file Report 78-943, p. 687-721.

# Portable Digital Seismic Waveform Processing

9950-90636

Edward Cranswick
U.S. Geological Survey
Branch of Geologic Risk Assessment
Box 25046, Mail Stop 966
Federal Center
Denver, Colorado 80225
(303) 236-7492

## Objectives

Research, develop, and apply data acquisition procedures and processing/analysis software of a PDSWP system (see title) designed to obtain the greatest amount of high-frequency (> 1 Hz) information in the shortest period of time from earthquakes and other seismic phenomena recorded by portable digital seismograph systems.

## Background

The essential dual task of the project is the development of software for processing/analyzing high-frequency digital seismic waveform data in conjunction with a scientific research program to investigate both high-frequency seismic sources and the severe signal distortions produced by the near-surface structures of recording sites (*i.e.*, deviations of the site-response greater than an order of magnitude are common in the 6-octave frequency band, 1-64 Hz). Experience has repeatedly demonstrated that the integrity of the complete data acquisition chain — from sensor/site to computer terminal display — is only effectively tested by the rigorous scientific analysis of the data. The software has been sufficiently generalized to process the digital data recorded by a variety of digital data acquisition hardware including six types of PADS (Portable Autonomous Digital Seismographs, see Cranswick, 1987; the instruments are DR100, GEOS, SMR102, NIMBUS, DR200, and MCR600). "Autonomous" denotes that the seismographs are capable of operating independently of any other system: they are battery-powered, maintain their own internal time, and record on their own independent media volumes (tape or solid-state memory). The large number of recorder/sensor/site parameters and the large variation of these parameters from site to site and from study to study necessitates a large amount of software overhead to keep track of this information, but the ability to process the data within real-time+24-hours on a field computer during an on-going field program is a major design criterion (In two field programs, New Brunswick in 1983 and Maine 1984, I operated an earlier and more primitive version of this software — which I had developed at USGS, Menlo Park, based on and in conjunction with the work of many of my colleagues there — on "portable" PDP11/23 and PDP11/73 field computers respectively). The wide and erratic variations of both frequency content and amplitude which are characteristic of high-frequency seismic data are an imperative for developing a portable system to perform digital signal analysis in the field.

## Investigations

### *Scientific Research*

1) Hard-rock-site uphole/downhole records of local seismicity and AE (Acoustic Emission) events related to rockburst activity (Cranswick, Sembera).
2) "The Information Content of High-frequency Seismograms and the Near-surface geologic structure of hard-rock recording sites" (Cranswick).
3) Crested Butte "hard-rock" micro-array (Cranswick).
4) 10 Jun 87 Olney, Illinois earthquake digital dataset (Carver, Williams, Cranswick).
5) 1 Oct 87 Whittier Narrows earthquake digital datasets — 1) DR200 (Bufe, Rogers, Williams, Michael, Cranswick); 2) MCR600 (Bice, Langer, Cranswick).

### *Software/Computer Development*

1) Parallel (high-speed) DR200 playback (Ketchum, Cranswick).
2) Integration of MCR600 data into PDSWP system (Ketchum, Bice, Cranswick).
3) Waveform dataset structure storage/archival (Cranswick, Michael).
4) Digital waveform file structure (Cranswick).
5) Analysis software development (King, Cranswick).
6) Portable microcomputer system (Banfill, Cranswick).
7) PADS data processing/analysis facility (Park, Petkash, Carver, Cranswick).

## Results

### *Scientific Research*

1) Cranswick and Sembera (in press) describe a shallow uphole/downhole hard-rock-site seismic monitoring experiment that was conducted at a site of surficial rock-burst activity which generated acoustic emissions (very small, very local seismic events) with corner frequencies in the kiloHertz range, and several local microearthquakes were also recorded during the field program. These observations demonstrate that the complex effects of near-surface structure of hard-rock are sufficient to produce $f_{max}$ and other related phenomena which are sometimes mistaken as properties of the source.

2) Analysis of the geology of a number of sites by Cranswick (in press) indicates that the overall attenuation of high-frequency ($> 1$ Hz) seismic waves is controlled by the whole-path-Q between source and receiver but the presence of distinct $f_{max}$ site-resonance peaks is controlled by the nature of the surface layer and the underlying near-surface structure. Models of vertical decoupling of the surface and near-surface and horizontal decoupling of adjacent sites on hard-rock outcrop are proposed and their behaviour is compared to the observations of hard-rock site-response. The upper bound to the frequency band of the seismic waves that contain significant source information which can be deconvolved from a site-response or an array-response is

discussed in terms of $f_{max}$ and the correlation of waveform distortion with the outcrop-scale geologic structure of hard-rock sites. It is concluded that although the velocity structures of hard-rock sites, unlike those of alluvium sites, allow some audio-frequency ($> 20$ Hz) seismic energy to propagate to the surface, the resulting signals are a highly distorted, limited subset of the source spectra.

3) I deployed a micro-array for two days, 2-4 Oct 1986, to monitor a microearthquake swarm in the vicinity of Crested Butte, Colorado (Cranswick, 1988). The micro-array consisted of a central three-component sensor, surrounded by three vertical-component sensors deployed in a roughly equilateral-triangular configuration at a radial distance of $\approx 50$ m, and all sensors were mounted directly on the outcrop (see Fig. 1A). Spectral analysis of the P-waves of microearthquakes recorded by the four vertical components (see Fig. 1B) demonstrates that there is a significant variation of site-response across the array. Spectral amplitudes are approximately equal near 5 Hz, but they diverge as frequency increases and exhibit a maximum variation of about 9 dB at 33 Hz (see Fig. 1C). These observations suggest that vertical joints play an important role in decoupling the site-responses of adjacent "hard-rock" sites. Modeling the site-response of the micro-array as a whole with Haskell-model plane-layers implies that near-surface horizontal fractures and/or low-velocity layers (here, a layer of shale) make rigid outcrops of "hard-rock" less coupled to the underlying structure at high frequencies than are the less competent materials of "alluvium" sites.

   I am presently developing software to estimate and remove the respective site-response of the individual array elements. Beam-steering techniques will be applied to the deconvolved signals in attempt to make estimates of the volume and distribution of the source region by a comparison of array records of different microearthquakes using a method of master event location with waveform data.

4) Carver *et al.* (1987) report that over the course of a six-day monitoring period, six PADS's were deployed for various durations at a total of eight stations. We have so far identified 31 earthquakes which have been well-recorded at 1-5 PADS stations. Most of these events are microearthquake aftershocks at epicentral ranges of 5-10 km (depth $\approx 11$ km), but three are larger earthquakes at regional distances — including a magnitude $4.1_{mbLg}$ (NEIS) earthquake which occurred roughly 270 km to the southwest at 164 (Julian Day) 21:17 UTC.

5) DR200 - 5 digital recorders deployed at 13 stations, ~ 30 aftershocks recorded at 1-5 stations (average $\approx 3$ stations/event).
   Preliminary site-response analysis of these data has been presented by Bufe *et al.* (1987), and the phase picks and first motions of 25 events have been included in Hauksson *et al.* (1988).

   MCR600 - 10 digital recorders deployed at 15 stations, ~ 100 aftershocks recorded at 1-8 stations (average $\approx 4$ stations/event).

   We are presently performing tests of the software integrity and hardware calibration and reliability tests of the digital recorders and geophones which generated both the DR200 and MCR600 data.

### *Software/Computer Development*

1) Completed parallel (high speed) playback of DR200 digital recorder. A prototype of this software was functional in late September 1987 which allowed us to rapidly playback, process, and perform preliminary analysis of digital records of aftershocks of the Whittier Narrows earthquake (see "Results: *Scientific Research* #5").

2) In November, following the deployment of MCR600's during the aftershock study of the Whittier Narrows Earthquake, a prototype version of software was completed which converts MCR600 digital waveform data from the original recorder format files written by a playback program into the standard "DR100 Format".

3) Development of standardized data structure for playback, storage, and archival utilizing features of the VAXVMS operating system. During the processing of the Illinois digital dataset and the re-playback of the Anchorage digital dataset, new procedures and conventions for the directory structure of waveform data were established.

4) Further research/development of a new file structure for digital waveform storage (RST Format: Recording System Trigger).

5) Software enhancements to spectral analysis and display techniques.

6) Extensive investigations of and consultations with a professional microcomputer specialist (Mr. Robert Banfill, Small Systems Support) established the feasibility and method of implementing PDSWP software on a portable microcomputer system, but lack of funding prohibited actual software conversion from VAX to PC.

7) In co-operation with the Golden Computer Center and other BGRA staff, a playback/processing facility for PADS data was established which consists of 1 DP260 (DR200 playback unit), 1 graphics terminal, 2 text terminals, and 1 laser printer/plotter for batch processing of waveform plots. We are intending to connect the laser printer/plotter directly to the adjacent microVAX which will reduce the time/plot to approximately 10 seconds.

Publications: 1 Oct 87 — 31 Mar 88

*Papers and Open-File Reports*

Carver, D., R. A. Williams, and E. Cranswick (1987). The Olney, Illinois, Earthquake of June 10, 1987: A Preliminary Report (Section II), *U. S. Geol. Surv. Open-File Rep.* 87-623, 41 pp., 35 figs.

Cranswick, E. and E. Sembera (in press; Director's Approval: 1/18/88). Earthquake site/source studies in the AE/MA domain, *Proceedings of the Fourth Conference on Acoustic Emission/Microseismic Activity in Geologic Structures and Materials*, H. R. Hardy, Jr. and F. W. Leighton (editors), TransTech Publications, 28 pp., 9 figs.

Cranswick, E. (in press; Director's Approval: 2/25/88). The information content of high-frequency seismograms and the near-surface structure of "hard-rock" recording sites, *PAGEOPH*, Special Volume: Scattering and Attenuation of Seismic Waves, ed. R. S. Wu and K. Aki, 21 pp., 13 figs.

Hauksson, E., L. M. Jones, T. L. Davis, L. K. Hutton, G. Brady, P. A. Reasonberg, A. J. Michael, R. F. Yerkes, P. Williams, G. Reagor, C. W. Stover, A. L. Bent, A. K. Shakal, C. G. Bufe, M. J. S. Johnston, and E. Cranswick (1988). The 1987 Whittier Narrows earthquake in the Los Angeles metropolitan area, California, *Science* (in press).

*Abstracts*

Bufe, C. G., A. M. Rogers, and E. Cranswick (1988). Site response information from the Whittier Narrows earthquake and its aftershocks, Special Session on the Whittier Narrows Earthquake, Fall AGU Meeting, San Francisco, Dec 1987.

Carver, D., E. Cranswick, R. Williams (1987). Preliminary analysis of digital seismograms of aftershocks of the June 10, 1987, Olney, Illinois earthquake, *Seismol. Res. Letts.* **58**, no. 4, p. 92.

Cranswick, E. (1988). Microearthquakes recorded by a micro-array at a "hard-rock" site near Crested Butte, Colorado, *American Geophysical Union Front Range Meeting*, Colorado School of Mines, Golden, CO, 11-12 Feb 1988.

Cranswick, E. (1987). PADS/WFPS (Portable Autonomous Digital Seismograph/Waveform Processing System): processing the aftershock dataset of the Olney, Ilinois earthquake, *Seismol. Res. Letts.* 58, no. 4, p. 95.

Cranswick, E. (1987). The role of a portable, audio-frequency (> 20 Hz), small aperture seismic array as part of a national broad-band satellite-telemetered seismograph network, *Seismol. Res. Letts.* 58, no. 4, p. 95.

<u>Background Publications:</u> related to but prior to project start-up

*Abstracts*

Cranswick, E. (1984). Automatic file management and data processing, *International Association of Seismologists and Physics of Earth's Interior*, Committee for Controlled Source Seismology, Meeting at Los Altos, California, Dec 1983, p. 65-66.

Cranswick (1986). Similtaneous single-station estimation of source azimuths and site-response, *Programme and Abstracts*, Annual Meeting of the Eastern Section, Seismological Society of America, Ottawa, Canada, Oct 1986.

Cranswick, E., D. Carver, and G. Patton (1986). The use of gain-ranging in the acquisition of digital seismic data: effects and intepretations, *Programme and Abstracts*, Annual Meeting of the Eastern Section, Seismological Society of America, Ottawa, Canada, Oct 1986.

Cranswick, E., V. S. Deshpande, S. L. Harmsen, C. J. Langer, and D. L. Butler (1987). Procedure of a micro-array experiment on earthquake swarm activity near Crested Butte, Colorado, Annual Meeting of the Seismological Society of America, Santa Barbara, California, Apr 1987.

# VARIATION OF RESISTANT-ROCK SITE-RESPONSE ACROSS A ~100-METER-APERTURE MICRO-ARRAY

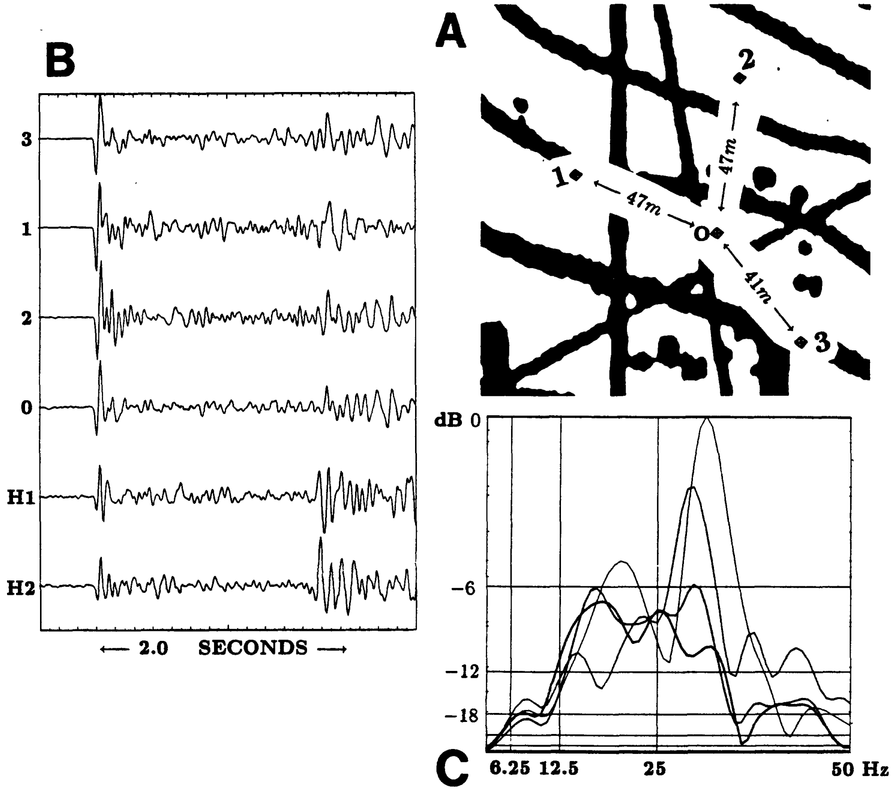

Fig. 1. (A) Plan-view of micro-array which has been superimposed (at the approximate scale and position) on the location of the site which is defined by an enlarged copy of the 1:25,000 topographic map used in the field program (The bold curves are 40 ft contours and the bold straight lines are compass bearings). (B) Micro-array record of a microearthquake. (C) Acceleration spectra of the P-waves on the vertical components plotted on linear-linear axes.

# Quaternary Tectonics of the Wichita Frontal Fault System, Oklahoma

9950-90595

A. J. Crone
Branch of Geologic Risk Assessment
U.S. Geological Survey
Box 25046, MS 966, Denver Federal Center
Denver, CO 80225
(303) 236-1595

## Investigations

1. Continue studies of Quaternary deposits along the trace of the Meers fault in Comanche County to evaluate the history of latest Quaternary displacement on this fault.

2. Digitize and model aeromagnetic data across the Wichita Frontal Fault system in the vicinity of the Meers fault.

3. Reduce gravity data from measurements at 350 stations in the vicinity of the Meers fault.

4. Complete reprocessing of selected COCORP seismic-reflection profiles that cross the Meers fault.

5. Complete the review and evaluation of selected industry seismic-reflection profiles across the Meers fault.

6. Complete publication of proceedings volume from USGS-sponsored workshop on Directions in Paleoseismology.

7. Analysis of stream profile data in area of suspected latest Quaternary deformation west of Pierre, South Dakota.

## Results

1. At two sites where the scarp on the Meers fault has dammed small gullies, pairs of trenches that straddle the scarp provide some constraints on the sense of slip and the time when the scarp formed. Prior to the formation of the scarp, the gullies had eroded small channels into the underlying Post Oak Conglomerate. By realigning the general shape of the bedrock channels on either side of the scarp, we estimate about 5.0 m of left-lateral and a minimum of 0.65 m of vertical displacement at one site, and 3.4-5.1 m of left-lateral and a minimum of 2.1 m of vertical displacement at the second site. These estimates contain large uncertainties because they incorporate some geologically unlikely assumptions about the pre-faulting morphology of the channels, but despite these uncertainties, these estimates are best available information on the sense of late Quaternary slip on the fault. Both estimates indicate a significant component of left-lateral slip on the latest Quaternary. As noted in earlier reports, the radiocarbon ages on soil humus from the basal silt

in the deposits dammed behind the scarp are 1,690±45 yrs B.P. and 1,865±25 yrs B.P. for the two sites, respectively. The ages generally constrain the time when the scarp dammed the gullies.

2. Models of the aeromagnetic data across the Frontal fault system has provided important constraints on structural relationships and lithologic contrasts across the Meers fault in the vicinity of the prominent fault scarp. Previous interpretations (Brewer and others, 1983) have suggested that the Meers fault has a moderate (about 45°) dip to the south similar to the Mountain View fault, another major fault within the Frontal fault system. Models of the aeromagnetic data along profiles across the fault preclude a moderate dip on the Meers fault and strongly suggest that the fault must be nearly vertical to depths of at least 6 km. The models support a moderate southerly dip for the Mountain View fault which is consistent with previous interpretations. The aeromagnetic data suggest splaying of the Meers fault at the northwest end of the Holocene scarp.

3. Field data for about 350 new gravity measurements have been reduced and the locations and new values are being included in the regional gravity data base. The new data are located in areas of poor regional coverage, and were collected and reduced in cooperation with S. L. Robbins (Branch of Petroleum Geology, USGS, Denver). These data include two detailed (≥100-ft spacing) gravity profiles across the Meers fault. Preliminary analysis of these profiles shows an approximately 1-mgal increase in gravity values that coincide with the trace of the Meers fault. The structural and tectonic significance of these increased gravity values is currently unknown.

4. Reprocessing of selected COCORP seismic-reflection profiles that cross the Meers fault has not vastly improved the quality of the record sections. The lines were reprocessed by M.W. Lee, W.F. Agena and J.A. Grow of the Branch of Petroleum Geology, USGS, Denver. The subsurface trace of the Meers fault is difficult to clearly define on the record sections. Only correlated tapes were available for reprocessing which may be part of the reason why reprocessing failed to substantially improve the data.

5. Five 512-fold, industry seismic-reflection lines have recently been released for purchase. In cooperation with personnel from the Branch of Petroleum Geology and the Branch of Sedimentary Processes (USGS, Denver), we have reviewed these data and selected parts of two pertinent lines that can clarify basic structural relationships across the frontal fault system. We have received interim approval to initiate a cooperative purchase of parts of these lines. The purchase agreement will include field tapes that can be reprocessed to enhance pertinent structural details.

6. The proceedings volume of the workshop on Directions in Paleoseismology is published as USGS Open-File Report 87-673. The 456-page volume contains 46 papers that cover a wide range of topics related to paleosesimic studies. The report is divided into the following major categories: (1) Quaternary dating techniques, (2) Recognition of

paleoseismic events in the geologic record, (3) Quaternary slip-rates and coseismic deformation, (4) Modeling fault-scarp degradation-Knowns, unknowns, and perspectives on the problems, (5) The behavior of seismogenic faults, (6) Aspects of seismic-hazard analysis, and (7) The future of paleoseismology- Viewpoints of practitioners and program managers.

7. Analysis of stream profiles and stream orders near Pierre, S.D., indicate stream rejuvenation in the area. Differences in stream-profile shapes indicate maximum rejuvenation on the once-glaciated eastern portion of the study area. Changes in stream slope and sinuosity successfully aided in identifying areas that show recent deformation.

Reports

Crone, A.J., and Omdahl, E.M., eds., 1987, Proceedings of Conference XXXIX-Directions in Paleoseismology: U.S. Geological Survey Open-File Report 87-673, 456 p.

Crone, A.J., 1988, The Meers fault, SW Oklahoma--Evidence of multiple episodes of Quaternary surface faulting: Geological Society of America Abstracts with Programs, v. 19, no. 7, p. 630.

Jones-Cecil, Meridee, Collins, D.S., and Nichols, T.C., Jr., Stream analysis-evidence for rejuvenation near Pierre, South Dakota [abs.]: EOS [Transactions of the American Geophysical Union]. (Director's approval 10/87)

References Cited

Brewer, J.A., Good, R., Oliver, J.E., Brown, L.D., and Kaufman, S., 1983, COCORP profiling across the Southern Oklahoma aulacogen--Overthrusting of the Wichita Mountains: Geology, v. 11, p. 109-114.

# Investigations of Intraplate Seismic-Source Zones

9950-01504

W. H. Diment
Branch of Geologic Risk Assessment
U.S. Geological Survey
Box 25046, MS 966, Denver Federal Center
Denver, CO 80225
(303) 236-1574

## Investigations

1. Relations among seismicity, tectonism, and hydrothermal regime in the southwest moat of the Long Valley Caldera, Calif.

## Results

1. Temperatures in borehole RD08 near Mammoth Lakes, Calif., are within 10 °C of boiling at 1,100 ft. Subsurface boiling and brecciation may have contributed to earthquake swarms in 1980 and 1983 (Urban and others, 1987a, b, c). Steps in precision temperature logs obtained in boreholes RD08 and PLV-1 are remarkably persistent with time. Ratios of gradients are too large to be accounted for by conductive heat transport with normal variations in thermal conductivity. Other heat transport mechanisms must be involved.

## Reports

Urban, T.C., and Diment, W.H., 1988, The thermal regime of the shallow sediments of Clear Lake, California, in Sims, J. D., ed., Late Quaternary climate, tectonism, and sedimentation in Clear Lake, northern California Coast Ranges: Geological Society of America Special Paper 214, p. 207-221.

Urban, T.C., and Diment, W.H., 1987, Repeated precise temperature logs in hot boreholes--One key to understanding the evolution of geothermal systems, in Abstracts of papers, 2nd International symposium on borehole geophysics for minerals, geotechnical, and ground water applications: Minerals and Geotechnical Logging Society, A Chapter at Large of the Society of Professional Well Log Analysts, October 6-8, 1987, Golden, Colorado, p. I.1-I.2.

Urban, T.C., Diment, W.H., and Sorey, M.L., 1987, Temperature and natural gamma-ray logs obtained in 1986 from Shady Rest drill hole RD08, Mammoth Lakes, Mono County, California: U.S. Geological Survey Open-File Report 87-291, 102 p.

Urban, T.C., Diment, W.H., and Sorey, M.L., 1987, Hydrothermal regime of the southwest moat of the Long Valley caldera, Mono County, California, and its relation to seismicity--new evidence from the Shady Rest borehole (RDO8): Transactions, Geothermal Resources Council, v. 11, p. 391-400.

Urban, T.C., Nathenson, Manuel, Diment, W.H., 1987, BPE and BPD--BASIC programs for microcomputers to calculate the local boiling point and the boiling point depth curve for "pure" water: U.S. Geological Survey Open-File Report 87-17, 58 p.

# Evaluation of Liquefaction Potential, Seattle, WA
Award No. 14-08-0001-G1385

W. Paul Grant
Shannon & Wilson, Inc.
1105 N. 38th Street
P.O. Box C-30313
Seattle, WA 98103
(206)632-8020

Objective: Liquefaction during the 1949 and 1965 Puget Sound earthquakes has resulted in substantial damage to buildings, bridges, highways, railroads, water distribution systems, and marine facilities. While total property damage from these historical earthquakes has been estimated at $25 million and $12.5 million, respectively, there is a greater damage potential from future earthquakes considering recent industrial development along low-lying river valleys and the potential occurence of a subduction zone earthquake in the Pacific Northwest. Therefore, it is the purpose of this study to delineate areas of potential liquefaction in the vicinity of Seattle and to evaluate the probability of future liquefaction. This will be accomplished by categorizing soil units within the study region based upon susceptibility to liquefaction. Reports of historical liquefaction in the Seattle area will be documented for future reference. Field investigations consisting of borings with Standard Penetration Tests (SPT) and Cone Penetration Tests (CPT) will be conducted at a total of 4 sites, with 2 sites selected based upon prior reports of liquefaction. The end result of the study will be a liquefaction hazard map for the Seattle area which may be used in land use planning, building development, and planning for disaster response.

Data Acquisition: Data acquisition has focused upon gathering historical reports of earthquake damage in the Puget Sound region and reports of recent and on-going research of regional ground shaking and liquefaction. Attempts at securing Hazard Susceptibility Maps that were previously developed for the Puget Sound Council of Governments were unsuccessful as the available maps were incomplete. Similarly, geologic mapping of liquefaction susceptible materials that has been initiated by James Yount of the USGS has not been completed. Thus, it is likely that we will develop a more simplified grouping of geologic units as compared to Yount's stratigraphic column which included 13 units.

Results: Results of the susceptibility mapping and field studies will be forthcoming, with the final report in November 1988.

# Seismic Hazard Studies, Anchorage, Alaska

9950-03643

A.F. Espinosa
Branch of Geologic Risk Assessment
U.S. Geological Survey
Box 25046, MS 966, Denver Federal Center
Denver, Colorado 80225
(303) 236-1597

## Investigations

1. Preparation of the surficial geologic map of the Anchorage B-7 SE quadrangle has been completed and preparation of the surficial geologic map of the Anchorage B-7 SW quadrangle is in progress. Both maps include extensive introductory texts. Studies of gradients of lateral moraines in valleys that transect both of these quadrangles have aided in making correlations both within these map areas and to type deposits elsewhere in the region as well.

2. Fifteen earthquakes recorded in the seismological field experiment conducted in Anchorage, Alaska, have been edited and are being analyzed. This topic on "Ground amplification studies in areas damaged by the Alaskan earthquake" will be jointly used in the site-response study obtained on different geologic environments with the damage evaluation along 15th and DeBarr Avenues.

3. In cooperation with the Branch of Central Mineral Resources, Denver, results of field investigations of paleoseismicity of the region, based on detailed analyses of emergent tidal sediments and intercalated organic materials, are being evaluated in conjunction with about 30 radiocarbon dates received thus far. A paper intended for publication in the bulletin series is in preparation.

4. Samples at a depth of 155 m from the Anchorage Tikishla Park drill hole (USGS Open-File Report 86-293) have been provided for geochemical analyses in cooperation with the Coal Geology Branch and most data reduction is completed. Previous paleontological work indicates that this drill hole penetrates Tertiary rocks that are substantially deeper than previously thought, and further paleontological analyses have been requested from the Branch of Paleontology and Stratigraphy.

5. Focal mechanism solutions and their distribution in Alaska and the Aleutian Islands for earthquakes which have occurred from 1927 through 1985 have been cataloged. A focal mechanism solution catalog is being prepared for publication.

## Results

1. The surficial geologic map of the Anchorage B-7 SE quadrangle has been submitted to the branch for open-file release and is being revised following technical review.

2. Field observations in cooperation with the State of Alaska, Division of Geology and Geological Surveys were completed for the Anchorage B-7 NE and SE quadrangle areas in sectors previously not investigated because of inclement weather. Thick vegetation and lack of exposures hampered work along the lower margins of major valleys.

3. In cooperation with the Alaskan Geology Branch, helicopter-supported field investigations were undertaken in the Gulkana A-1 quadrangle area, with incidental field observations in the Gulkana B-1, B-3, and Nabesna B-6 quadrangle areas. A long-sought source for the Sanford volcanic mudflow has been identified.

4. Samples at a depth of 155 m from the Anchorage Tikishla Park drill hole have been provided for geochemical analysis in cooperation with the Branch of coal Geology and for paleontological analysis by the Branch of Paleontology and Stratigraphy, and a report has been prepared and accepted for publication in the annual Geologic Studies in Alaska circular.

5. A surficial geologic map of the Nabesna B-6 quadrangle has been prepared by reinterpretation of previously developed material and transmitted to the Branch of Central Mineral Resources for inclusion in the GQ-series map of the area.

6. In cooperation with the Branch of Central Mineral Resources, a report describing the long-sought source for the Sanford volcanic debris flow, discovered in 1987, has been prepared and accepted for publication the annual Geologic Studies in Alaska circular.

Reports

Espinosa, A.F., 1987, Book review; Mecanismo de los terremotos y tectonica, by A. Udias, D. Munoz and E. Buforn; editorial Universidad Complutense, Madrid, 232 p. in Revista de Geofisica (in press).

______1987, Modified Mercalli intensity distribution, seismicity and mode of subduction: Slide collection; Continuing Education Program, EERI, 20 slides.

______1987, Seismicity, tectonic and focal mechanism for the Azores-Tunisia region: Slide collection, Continuing Education Program, EERI, 6 slides.

______1987, Preliminary postearthquake field report; March 5, 1987, Ecuadorian earthquake: U.S. Geological Survey to USAID-OFDA and to Ecuadorian Government, April 3, 1987, 4 p.

______1988, Determinacion de la magnitud local $M_L$ a partir de acelerogramas horizontales en el campo cercano: Universidad Complutense, Facultad de Fisica, Catedra de Geofisica, 30 p.

Espinosa, A. F., and Servando de la Cruz Reina (UNAM, Mexico), 1987, Book review, FUNDAMENTOS DE GEOFISICA, by A. Udias and J. Mezua, Editorial Alhambra, 419 p., in Revista de Geofisica (in press).

Espinosa, A. F., Rukstales, K. S., Biswas, N., and Udias, A., 1988, Focal Mechanism catalog for earthquakes in Alaska and the Aleutian Islands: U.S. Geological Survey Bulletin, 300 p.

Odum, J.K., Yehle, L.A., Schmoll, H.R., Gardner, C.A., and Dearborn, L.L., 1988, Lithological, geotechnical properties analysis, and geophysical log interpretation of U.S. Geological Survey drill holes 1C-79, 2C-80, CW 81-2, and CE-82-1, Tyonek Formation, upper Cook Inlet region, Alaska: U.S. Geological Survey Bulletin.

Richter, D.H., Ratte, J.C., Schmoll, H.R., and Yehle, L.A., Geologic map of the Gulkana B-1 quadrangle, Alaska: U.S. Geological Survey Geologic Quadrangle Map, scale 1:63,360. (In press.)

Richter, D.H., Schmoll, H.R., and Bove, D.J., 1988, Sopurce of the Sanford volcanic debris flow, south-central Alaska, in Galloway, J.P., and Hamilton, T.D., eds., Geologic studies in Alaska by the U.S. Geological Sruvey during 1987: U.S. Geological Survey Circular. (In press.)

Striker, G.D., Brownfield, M.E., Yehle, L.A., and Wolfe, J.A., 1988, Mienralogy and stage assignment of some Tertiary coal from the Tikishla Park drill hole, Anchorage, Alaskas, in Galloway, J.P., and Hamilton, T.D., eds., Geologic studies in Alaska by the U.S. Geological Survey during 1987: U.S. Geological Survey Circular. (In press.)

Updike, R.G., Olsen, H.W., Schmoll, H.R., Kharaka, Y.K., and Stokoe, K.H., 1987, Geologic and geotechnical conditions adjacent to the Turnagain Heights landslide, Anchorage, Alaska: U.S. Geological Survey Bulletin 1817.

Updike, R.G., and Ulery, C.A., 1988, Bedrock geology of the Anchorage (B-7 SE) quadrangle, Alaska: U.S. Geological Survey Map (1 sheet)

# Near-Surface Lithologic and Seismic Properties

9910-01168

J.F. Gibbs
W.B. Joyner

Branch of Engineering Seismology and Geology
U.S. Geological Survey
345 Middlefield Road, MS 977
Menlo Park, California 94025
(415) 329-5631 or (415) 329-5640

## Investigations

Measurement of seismic velocity and attenuation to determine the effect of local geology on strong ground motion and to aid in the interpretation of seismic source parameters.

## Results

1. Analysis of downhole data from Stockdale Mountain, Jack Canyon and Red Hills, all near Parkfield, California, is continuing. Preliminary record sections show good quality data at Stockdale Mountain and Jack Canyon.

2. P- and S-wave velocities were measured (by Tom Fumal and Ed Roth) in a borehole to a depth of 110 m in the Punchbowl Formation near Devil's Punchbowl, southern California, Figure 1.

3. A new three-component 8 Hz downhole geophone has been received and is being fit with an electronically activated clamping mechanism designed by H.-P. Liu and built by R. Westerlund. The new clamping mechanism should improve geophone coupling and enhance data quality.

## Reports

Joyner, W.B., and Boore, D.M., 1988, Measurement, characterization, and prediction of strong ground motion: Proceedings, Conference on Earthquake Engineering and Soil Dynamics II, American Society of Civil Engineers, Geotechnical Engineering Division, Park City, Utah, June 27-30, 1988.

Gibbs, J.F. and Roth, E.F., 1988, A site study near the Parkfield prediction zone in central California: Director's Approval for publication outside the U.S. Geological Survey.

04/88

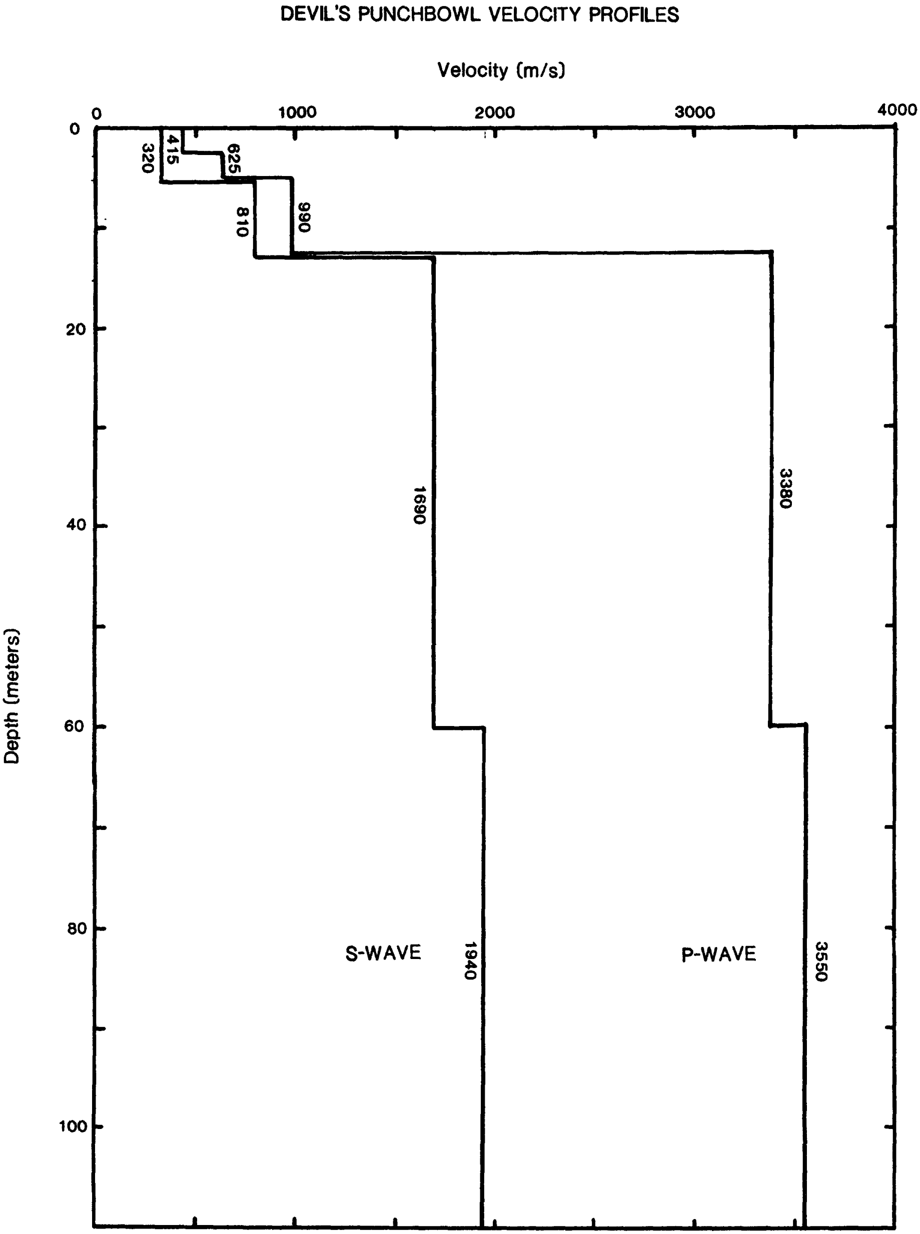

Figure 1. Near-surface velocity profiles determined from borehole measurements near Devil's Punchbowl, California. The Punchbowl formation at this site consists of moderate, well-cemented, well-sorted, coarse-grained sandstone with few joints.

# Soil Development as a Time-Stratigraphic Tool

9540-03852

Jennifer W. Harden
Branch of Western Regional Geology
U.S. Geological Survey
345 Middlefield Road, MS 975
Menlo Park, California 94025
(415) 329-4949

## Investigations

1. Slip-rate studies along the Calaveras Fault near San Felipe Creek: Jennifer Harden, Kathy Harms, Malcolm Clark. See also M.M. Clark, this volume.

2. Quaternary map of San Jacinto Basin and western Riverside County: Jennifer Harden and Cindy Hill.

## Results

1. Soils are being used to date Quaternary surfaces along San Felipe Creek. Time of offset of erosional scarps along the creek can be estimated by ages of the terraces set into the scarps. In addition, the stream appears to have been diverted from a more northwesterly course, and the diversion may be related to fault displacement. Radiometric dates are in agreement with soil ages and will contribute to improved calibration of soils for further studies in the S.F. Bay region. Samples were submitted to contract labs for analysis of particle size, bulk density, dithionite iron and organic carbon.

2. Soil survey data dating back to 1950 was surplused for the western Riverside County. Data are being categorized for completeness of description, quality of location, and general landform type. We will apply the soil development index to soils developed in granitic alluvium and will apply multivariate analysis to the data in order to define alluvial units of different age. Subsequently, we will independently produce a map of different aged alluvial surfaces, based only on geomorphic criteria. Our goal is (1) to test the usefulness of soil survey data in aquiring quantitative information on surficial geology and (2) to provide a regional soil data base for an area that is subject to active tectonism. In addition, much of the area is now developed, which precludes current soils work, but the soil survey was conducted before development of much of the area.

## Reports

Switzer, P., Harden, J.W. and Mark, R.M., 1987, A statistical method for estimating rates of soil development and ages of geologic deposits: a design for soil-chronosequence studies. Mathematical Geology vol. 20, no. 1, p. 49-61.

# Investigation of Seismic-Wave Propagation for Determination of Crustal Structure

9950-01896

Samuel T. Harding
Branch of Geologic Risk Assessment
U.S. Geological Survey
Box 25046, MS 966, Denver Federal Center
Denver, Colorado 80225
(303) 236-1572

## Investigations

1. Processing the 461 km of marine seismic-reflection data acquired from the study of Puget Sound and the Straits of Juan de Fuca, Washington.

2. Processing and interpreting seismic-reflection lines near Parkfield, Calif.

## Results

1. The rough processing of the marine seismic-reflection data acquired from Puget Sound and the Straits of Juan de Fuca has been completed. A number of interesting features are to be found on these cross sections, and interpretations of these lines are now beginning.

2. The Parkfield data have been processed and the report of the findings is being prepared by Kaye Shedlock, Tom Brocher, and Sam Harding.

## Reports

Harding, S.T., and Barnhard, T.P., 1987, Holocene faulting as indicated from marine seismic-reflection survey in Puget Sound Washington: EOS [Transactions of the American Geophysical Union], v. 68, no. 44, p. 1240.

Shedlock, K.M., Harding, S.T., and Brocher, T.M., 1987, The Parkfield shallow-reflection experiment--Structure of the dilational jog southeast of Gold Hill [abs.]: EOS [Transactions fo the American Geophysical Union, v. 68, p. 1345.

# SEISMIC SLOPE STABILITY

9950-03391

Edwin L. Harp
U.S. Geological Survey
Branch of Geologic Risk Assessment
345 Middlefield Road, MS 998
Menlo Park, CA 94025
(415) 329-4891

## Investigations

Efforts were continued to establish reliable values for the concentration of landslides and their geographical limits in terms of a numerical instrumental parameter derived from strong ground motion data. Comparison of Arias intensities calculated from strong motion acceleration records with the extent of earthquake-induced landslides were undertaken for areas affected by the October 1, 1987, Whittier, California earthquake and the November 23-24, 1987, Superstition Hills earthquakes in the Imperial Valley, California. Ground-based surveys of the extent of landslides outward from the epicentral areas of these earthquakes were conducted to compare with Arias intensity values to be calculated from records from the extensive strong motion networks existing in these two areas in southern California.

Efforts were continued in defining seismic slope susceptibility categories for data gathered from rock slopes along the Wasatch Front near Salt Lake City, Utah. The "rock-mass-quality" index (Q), a quantitative, empirical index that ranks the competence of rock based on various fracture characteristics for tunnel design, was modified for use on surficial slopes subject to rock falls and rock slides. Analysis of variance tests were performed on rock-slope data from the Wasatch Front to determine the separability of the various lithologic units present in the study area between Mill Creek and Little Cottonwood Creek.

## Results

Data is still being processed and analyzed for the Whittier and Superstition Hills earthquakes. The survey of landslides for the Whittier earthquake shows a strongly asymmetric pattern of landslide extent about the epicentral area. To the southeast of the epicenter landslides (mainly falls and slides of both rock and soil) extended only 22 km. To the west, they extended almost 46 km to Topanga Canyon north of Malibu.

Preliminary calculations of Arias intensities from 12 stations of the U.S.G.S. network in the Imperial Valley have provided a range of values for the threshold at which minor soil falls and small slumps in irrigation canal banks occurred from the $M = 6.6$ Superstition Hills earthquake. Figure 1 shows the approximate limit of earthquake induced slope failures and Arias intensity values next to the corresponding stations. From these preliminary data, we estimate that the landslide threshold for this earthquake ranged from about 0.2 to 0.9 m/s, a variation probably due to differences in strength properties of slope-forming materials. Further refinement in these threshold values is expected as the full complement of digitized acceleration records becomes available.

Preliminary statistical analyses of rock mass quality data mentioned above under investigations shows that lithologic units in the study area along the Wasatch Front near Salt Lake City, Utah can be separated into well-defined groups or categories of susceptibility to seismic-induced failure. Analysis of similar data from the 1980 Mammoth Lakes earthquakes in California show a good correlation between Q indices and the numbers of rock falls and rock slides. This correlation between seismically induced rock failures and Q values will serve as a qualitative yardstick to subdivide formations or lithologic subunits along the Wasatch Front into categories of relative seismic susceptibility to failure.

## Reports

Kobayashi, Yoshimasa, Harp, Edwin L., and Kagawa, Takao, (in review), simulation of rockfalls triggered by earthquakes, to be submitted to Engineering Rock Mechanics.

## References

Porcella, R., Etheredge, E., Maley, R., and Switzer, J., 1987, Strong-motion data from the Superstition Hills earthquakes of 0154 and 1315 (GMT), November 24, 1987: U.S. Geological Survey Open-File Report 87-672, 56 p.

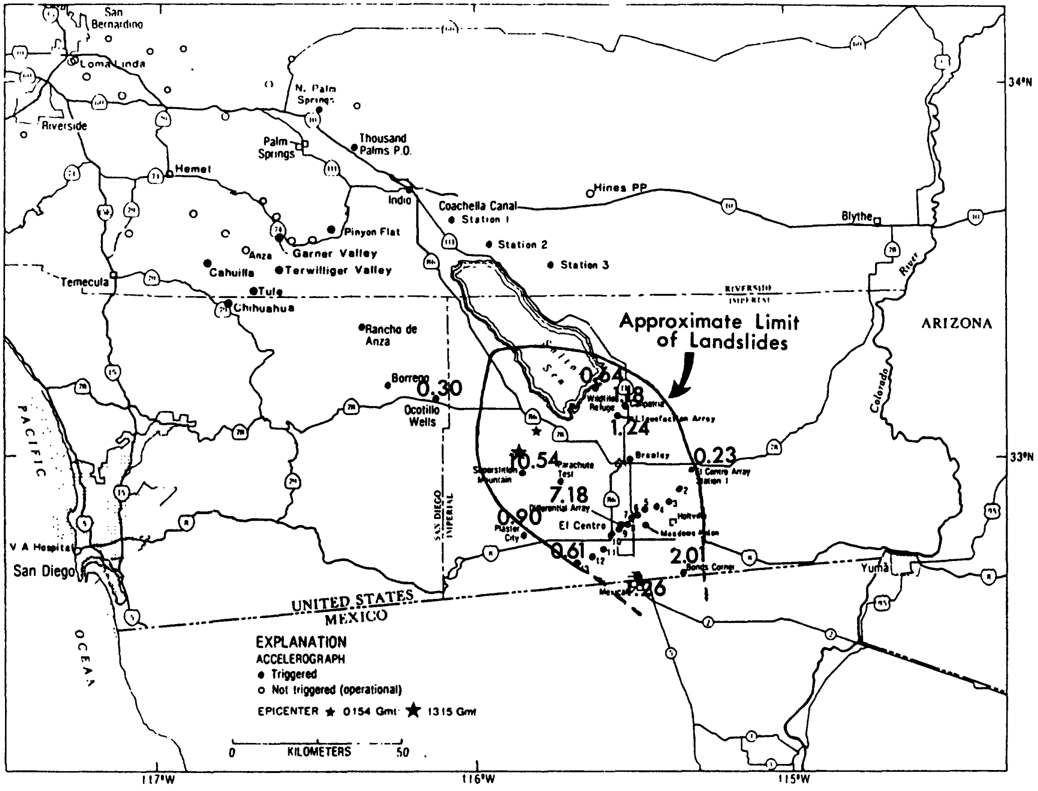

Figure 1. U.S.G.S. strong motion network, Arias intensities calculated for 12 of the stations from the M = 6.6 earthquake, and approximate limits of landslide occurrence (epicenters and locations of strong-motion stations from Porcella and others, 1988).

# Projecting the Risk from a Tsunami Generated in the Juan de Fuca Region

14-08-001-G1346

Gerald T. Hebenstreit
Marine Analysis Division
Science Applications International Corporation
McLean, Virginia 22102
703-827-4975

The purpose of this study is to examine, by means of existing numerical modeling techniques, the spread of distribution of wave energy along the western coast of Oregon, Washington, and British Columbia due to tsunamis generated by local subduction earthquakes. Even though such earthquakes have not occurred in recent historical time, the potential does exist, and the need to assess the tsunami potential also exists.

Articles in the two preceding volumes of this series have described the choice of source areas and source motions used to develop reasonable seafloor displacement patterns which could arise from subduction earthquakes in the Cascadia subduction zone. The overall source zone was examined in terms of three potential source areas: the Gorda plate zone, the southern end of the Cascadia subduction zone, and the northern end. A linearized long wave propagation model was used to simulate wave travel from the initial uplift region to coastal zones. No attempt to model wave runup or inundation was made during this study.

The key indicator of wave energy distribution in the simulations is the maximum predicted wave height at recording points along the coastline. Although the absolute values of wave height have little importance (being, as they are, directly related to the hypothetical earthquake-induced displacement) the relative pattern of heights can be used to infer which coastal zones are more or less likely to be susceptible to concentrations of tsunami energy.

Figure 1 shows the bathymetry of the Gorda plate model zone; superimposed as concentric ellipses are contours of seafloor uplift based on assumed earthquake parameters. Figure 2 shows the coastline and the locations of the points at which elevations were recorded. The the right of the coastline is a plot of the variation in wave elevation (as a function of location number) along the coast. The solid line gives the mean elevation level among all recording points. Notice that certain areas show noticeably higher levels of waves than others and that the highest waves were recorded in the region of the uplift. This pattern is repeated throughout the results of the simulations.

A project report detailing these findings is being completed and will be available in May 1988.

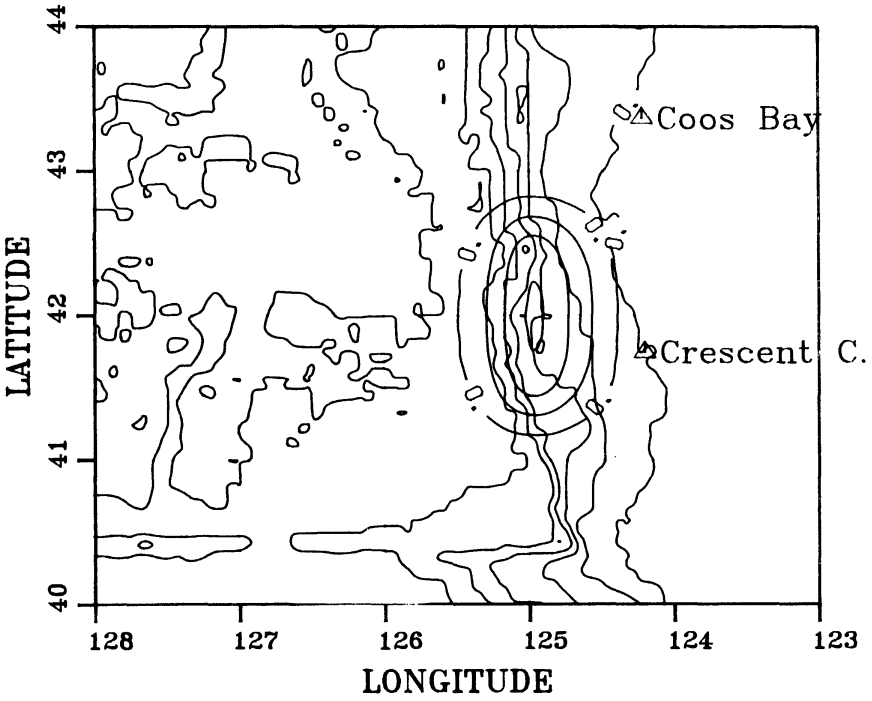

Figure 1. The bathymetry of the seafloor in the Gorda plate model zone. Superimposed as concentric ellipses are the contours of positive seafloor uplift for the hypothetical earthquake source. The maximum uplift in this case is approximately 1m.

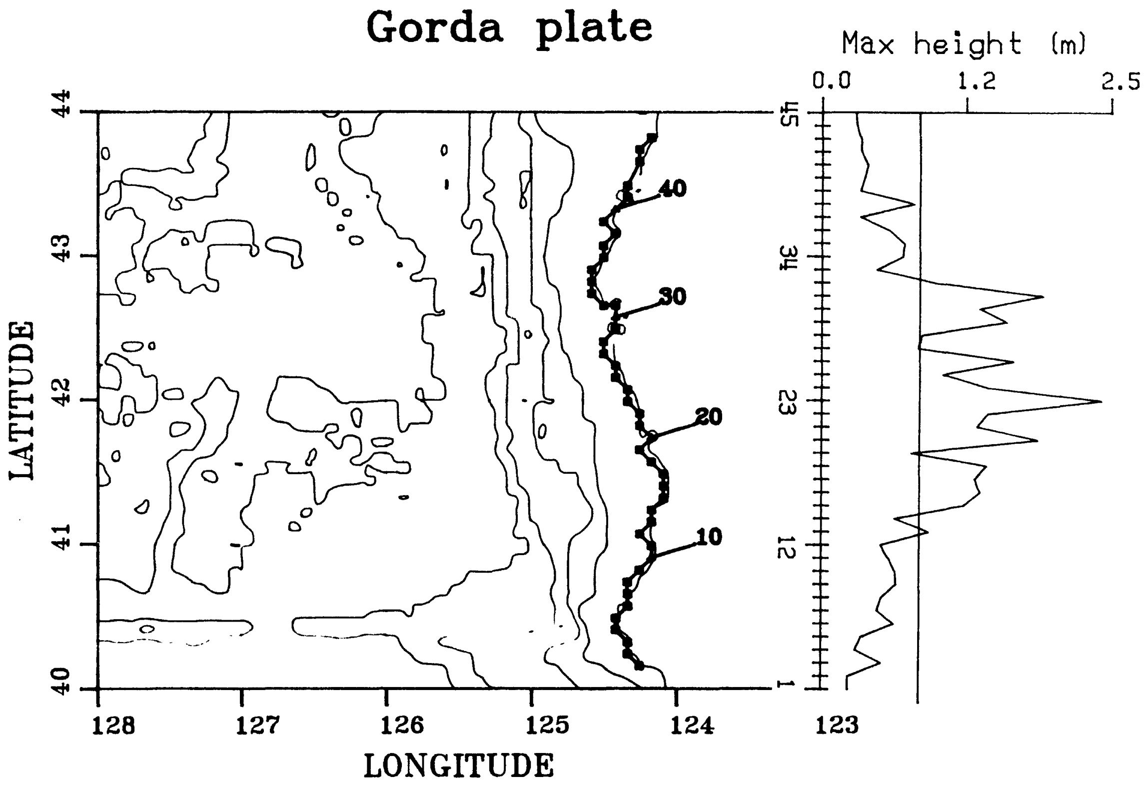

Figure 2. The locations of coastal recording points in the Gorda plate model are indicated in the left-hand figure. The right-hand figure shows the pattern of wave elevation for all recording points. The solid line is the average elevation for all points.

# U.S. ACTIVE FAULT RECONNAISSANCE

9950-04334

Darrell G. Herd
Branch of Geologic Risk Assessment
U.S. Geological Survey
922 National Center
Reston, Virginia 22092
703/648-5981; FTS 959-5981

An aerial-photographic search of unevaluated regions of the United States for active faults was initiated in FY 1988. A reconnaissance of several areas for geomorphic evidence of geologically recent faulting is underway to locate and map potentially active faults toward a more comprehensive appraisal of the earthquake tectonics of the Nation.

## EASTERN UNITED STATES

Investigations. Three areas of the Eastern United States are being surveyed for evidence of recent tectonism:

1. The southeast Tennessee-northwest Georgia seismic zone (highest level of current seismic activity in the Southeastern United States).

2. Areas surrounding the Meers fault in southwestern Oklahoma.

3. Meizoseismal area of the Charleston, South Carolina, earthquake of 1886.

Results.

1. A zone (50-100 km wide) of persistent microseismic activity (generally $M \leq 3$, with events as large as $M=5$) extends southwestward from near Knoxville, Tennessee, past Chattanooga into northwestern Georgia. The earthquake activity is broadly associated with the Valley and Ridge province, generally occurring east of the Cumberland Plateau but west of the Smoky Mountains. Southerly-trending elements of the adjacent Smoky Mountain fault (at the western foot of the Great Smoky Mountains) are scarp-like in character, with locally precipitous southwest-facing aspects and alluvial fans at their base. At least one ancient, high-standing erosional surface (in northwestern Georgia) ends abruptly at the escarpment.

2. Several northwest-trending faults in the Arbuckle Mountains near Ardmore, Oklahoma (100 km southeast of the Meers fault) appear potentially recent in age. A steep south-facing escarpment occurs along much of the length of the Mill Creek fault, offsetting a well-developed erosional surface cut across the dipping beds of the surrounding hills. (None of the Holocene alluvial fans, however, that cross the fault are evidently offset.) Smaller (but equally steep) north-facing scarps also occur along several nearby northwest-trending faults.

3. The swampy, planar floor of the Ashley River valley near Summerville, South Carolina (meizoseismal zone of the Charleston earthquake of 1886), is interrupted at Slands Bridge (1.5 km SW of Slandsville) by a broad, gentle rise (2-3 m in relief) that extends westward across the width of the valley. Approaching the rise, the course of the Ashley River is pressed northward against the valley wall by the east abutment of the rise into a narrow ravine. The rise effectively dams the upper Ashley River, impounding it more than 3 m above the lower channel. The rise must have developed within the last 200,000 years and may date from the Holocene: the rise now blocks an alluvium-flooded valley that was incised to a much-lowered sea level through estuarial deposits of both the penultimate and last glaciation. The rise is coincident with the epicentral location of the Charleston seismic zone. The possibility that the Slands Bridge rise is the consequence of near-surface fault movement is under current investigation.

## WESTERN UNITED STATES

Several regional maps (scale 1:250,000) and accompanying articles describing the active faults of the San Francisco Bay region and surrounding California Coast Ranges (from mapping by Herd in 1974-82) are in preparation.

# Earthquake Hazards Evaluation of the
# West Valley Fault Zone in the
# Salt Lake City Urban Area, Utah

Grant Number 14-08-0001-G1397

Jeffrey R. Keaton
EARTHSTORE, A Division of Dames & Moore
250 E. Broadway, Suite 200
Salt Lake City, Utah 84111-2480
(801) 364-1030

## INVESTIGATIONS

1. Trend surface analyses of existing subsurface geotechnical data in the vicinity of suspected traces of the northern part of the West Valley fault zone.

2. Field observations of morphostratigraphic relationships in preparation for drilling and/or trenching.

## RESULTS

Distinctive stratigraphic units encountered in borings permits use of marker horizons for evaluation of the presence or absence of deformations. First order trend surface representations provide insight into uniformity of the slope of pelagic lacustrine units; the distribution of residuals provides insight into localized deformation across discrete planes of offset. Significant problems exist with respect to 1) anthropogenic disturbance and obscuration of morphostratigraphy, 2) lack of existing geotechnical borings across suspected fault traces, 3) access difficulties for additional subsurface investigations, and 4) correlation of specific stratigraphic units between borings and within the context of the Bonneville Alloformation or post-Bonneville Holocene deposits.

# Urban Hazards Seismic Field Investigations and the Study of the Effects of Site Geology on Ground Shaking

9950-01919

K. W. King and A. C. Tarr
Branch of Geological Risk Assessment
U. S. Geological Survey
Denver Federal Center, MS 966
Denver, CO 80225
(303) 236-1591; (303) 236-1605

## INVESTIGATIONS

The objectives of this project are: (1) to improve the understanding of how shallow underlying geology affects ground motion, (2) to develop integrated techniques and methodologies for efficiently and effectively processing large quantities of digital seismic response data, seismic reflection and refraction data, seismic and geological borehole data, and building response data, and (3) to produce relative ground response maps for urban study areas. Specific goals for this reporting period were: (1) to conclude borehole velocity studies in the Wasatch Front urban area, (2) to conclude the first phase of seismic response and shallow seismic geophysics studies in the Puget Sound - Portland urban areas, (3) to complete shallow seismic studies of a site on the Hanford Reservation in Washington, (4) to conduct seismic studies at a site at White Sands National Monument, (5) to implement the design for a geotechnical data base which would link all data sets needed in the production of a relative ground response map, and (6) to begin the implementation of geographic information systems (GIS) technology for seismic hazards map production in the Pacific Northwest study area.

## RESULTS

### (1) Wasatch Front

The downhole geophysical surveys in the Salt Lake City urban area have been completed and the data have been analyzed. In addition, the final site response map has been completed and a final site response report is in progress. Correlation of response values with borehole, seismic reflection, and seismic refraction results is in progress.

### (2) Puget Sound - Portland

Digital recordings of nuclear tests at the Nevada Test Site (NTS), open-pit coal mine explosions near Centralia, Washington, microearthquakes near Seattle, and microtremors (small-amplitude seismic motions from natural sources) were acquired in late 1986 and in 1987 as the first-phase of studies related to assessment of seismic hazards in the Pacific Northwest. The recordings were made at sites in Seattle, Olympia, and Portland which were chosen to reflect a variety of geological and seismic ground response conditions. In addition, digital recordings were made to determine natural period and damping characteristics in low-rise and medium-rise structures in Seattle.

Geophysical data, in the form of seismic reflection and refraction profiles, were acquired at many of the ground response sites to determine shallow subsurface structural details. The profiles and geotechnical data from existing and planned boreholes are to be used in correlation of site geology with ground response.

Preliminary analysis of the data indicate that relative spectral ratios of ground response compare generally (although not totally) with observed MM intensities of the April 1965 Puget Sound earthquake; that is, higher spectral ratios are found near places of higher MM intensity. Spectral ratios derived from the several types of seismic sources are generally compatible, although reliable seismic response could not always be determined from coal mine explosions; thus far, microearthquakes seem to provide the best spectral ratio data to date.

Preliminary results of reflection and refraction line data from Seattle indicate the presence of a high-velocity bedrock unit (8500 ft/sec), presumably the same unit which is exposed at Seward Park, the location of the reference seismic response site. The velocity of the surficial soil layer was less than 1000 ft/sec and the velocity of the intermediate till layers ranged from 2400 ft/sec to 5100 ft/sec.

The low-rise building testing established the range of natural period and damping parameters in the West Seattle area. The predominant frequency of single-family dwellings ranged from 5.4 Hz to 14.8 Hz; the predominant frequency of the chimneys on the same dwellings ranged from 6.2 Hz to 13.7 Hz. The damping of the dwellings ranged from 2.5% to 6% of critical damping.

### (3) Hanford Reservation Experiment

The seismic experiment at Hanford, Washington was to determine if it is feasible to map the top of a buried basalt layer using the high-resolution, shallow-reflection method. The results indicate that the top surface and structure of a basalt layer, 20 feet or thicker and buried 200 feet to 400 feet, can be mapped using selective lay-out parameters of both sources and seismometers. The resolution of the method is about three to six feet for a 20-foot thick basalt layer buried under approximately 300 feet of sediments.

### (4) White Sands National Monument

The purpose of the seismic study at White Sands National Monument was to determination vibration engineering parameters for historic buildings and to study the vibration effects of local vehicular traffic and acoustic sources on the buildings. The field data have been collected and analysis is in progress.

### (5) Geotechnical Data Base

Production of a relative ground response map for a large urban area requires the acquisition and analysis of many hundreds of pieces of seismic, geological, and geotechnical data. The rational organization and manipulation of so much data requires a data base management system (DBMS) and a data base structure which permits linking many types of data. Portability of the DBMS and data sets to several kinds of computers and ability to access the data base in the field suggested implementation on a microcomputer system.

Following completion of the prototype design during the last reporting period, the design was implemented by extensive data entry from several study areas. During implementation, several modifications were made and several new data structures (including one for borehole logging) were added. A report by Tarr describing the implementation was revised and distributed for further review.

### (6) Geographic Information System (GIS)

Production of a seismic hazards map for an urban area requires integrating results of research (such as relative site response, landslide susceptibility, lifeline vulnerability) in a map format. GIS technology has shown promise in recent years as a powerful tool for spatial analysis and manipulation of data with geographical attributes. Because a seismic hazards map is multi-disciplinary, a interdivisional investigation was established to use GIS technology in production of preliminary seismic hazards maps; this project took the lead in the investigation.

An interdivisional proposal entitled "Applications of Geographical Information Systems Technology for Pacific Northwest Hazards Studies" was funded under the Director's GIS fund during the reporting period. The USGS participants are: A. Tarr (GD)and M. Crane (NMD). Under the proposal, a GIS project would be established to integrate expertise and data sets from the respective Divisions to produce seismic hazards maps expected from the Regional Earthquake Hazards Assessment of the Pacific Northwest urban hazards. The work would be performed on existing GIS systems at the NMD Rocky Mountain Mapping Center and at a new GIS processing facility in Golden. The proposal includes a pilot study, which would result in a seismic response and landslide susceptibility map of the Olympia urban area, to develop and test techniques and methodologies. Following completion of the pilot study, preparation of a seismic hazards map of Seattle will begin.

Acquisition of digital cartographic data sets has begun. Procurement of GIS hardware and software was initiated at the end of the reporting period. New hardware includes a GIS workstation, graphics terminal, and ERDAS workstation; new hardware includes Interactive Surface Mapping (IMS) and ERDAS image processing software.

## PUBLICATIONS

Brewer, W. A. and King, K. W., 1988, Nuclear waste site characterizations using shallow seismic profiling [abs.]: Waste Management 88, Tucson, Arizona.

# Quaternary Geology Along the Wasatch Fault Zone, Utah

9950-04182

Michael N. Machette
Branch of Geologic Risk Assessment
U.S. Geological Survey
Box 25046, MS 966, Denver Federal Center
Denver, Colorado 80225
(303) 236-1243

Project members: M.N. Machette, A.R. Nelson, S.F. Personius,
and K.A. Haller.

## Investigations

1. Continued synthesis of data pertaining to earthquake hazards along the Wasatch fault zone. Preliminary results on segmentation, recency of faulting, and temporal clustering of paleoearthquakes were presented at the March 1988 meeting of the Cordilleran section of GSA.

2. Continued compilation of data for a series of 1:50,000-scale maps showing the Quaternary geology along the Wasatch fault zone from Honeyville to Santaquin, Utah. These maps form a 6- to 15-km-wide strip along nine segments of the fault zone.

3. Machette, Nelson, Personius, and Wheeler presented papers at the December 1987 workshop on "Continuing Actions to Reduce Potential Losses from Earthquakes along the Wasatch Front, Utah", Salt Lake City, Utah.

4. Haller completed her field reconnaissance of the Lemhi and Beaverhead faults, Idaho, and the Red Rock fault, Montana. Photogrammetric mapping of the fault scarps is complete and the scarp morphology data has been interpreted. Results from this study (her M.S. thesis at Univ. of Colorado) will be presented at the May 1988 meeting of the Rocky Mountain section of GSA.

## Results

1. Completion of our 1986 cooperative-trenching efforts with the Utah Geological and Mineral Survey has given us a much expanded data base for analyzing recency and recurrence intervals of surface rupturing along the Wasatch fault zone (see fig. 1). We now have one to as many as three major trench sites on the seven most active segments and will be able to test our hypothesis that the Wasatch fault zone has more segments (10-12) than originally suggested by Schwartz and Coppersmith (1984). In addition, the results of radiocarbon analyses now permit us to place tighter constraints on the times of most recent movement along the critical, urbanized parts of the fault zone.

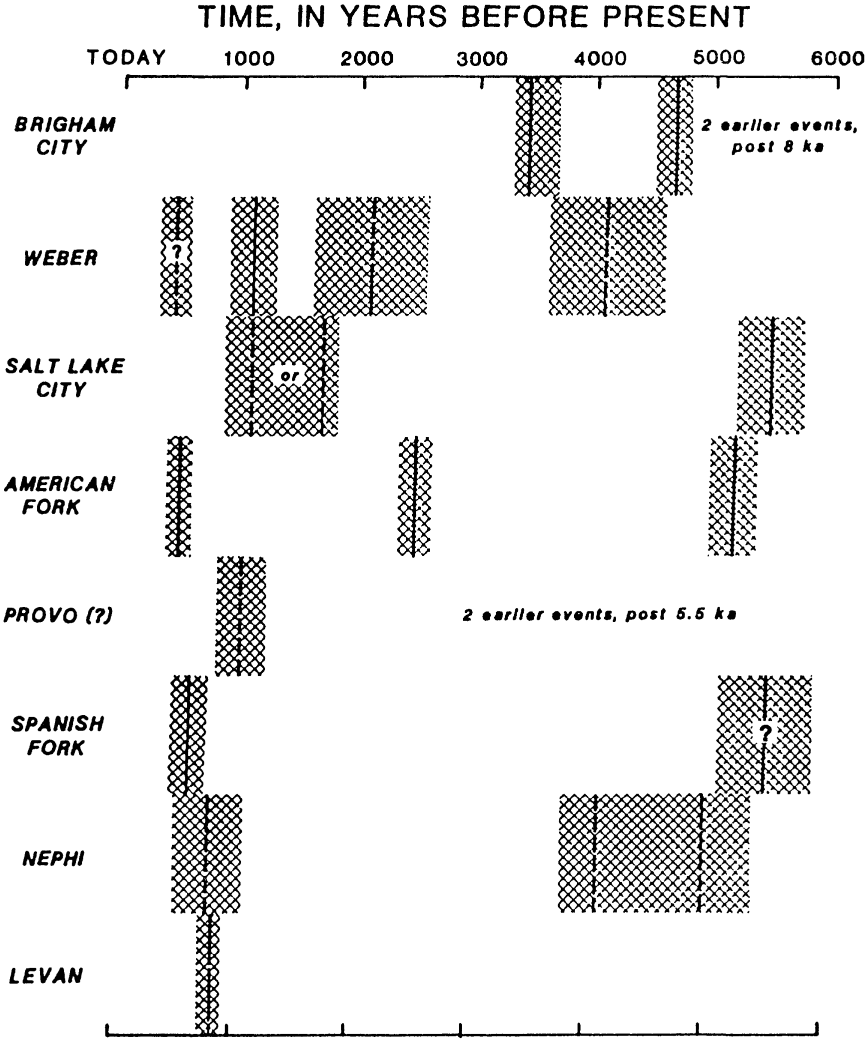

Figure 1.--Timing of faulting events on segments of the Wasatch fault zone that show Holocene movement. Vertical lines indicate probable times of faulting; cross-hachured patterns indicate probable limits on times of faulting. Data from this project, D.P. Schwartz and W.R. Lund (written commun., 1988), and Michael Jackson (written commun., 1988).

2. As of April, 1988, 36 radiocarbon age determinations of charcoal and concentrated soil organic matter have been received from a variety of laboratories. We have tried to correct these ages to calendric years, and are finalizing our interpretations of them. The resulting soil ages are calibrated apparent-mean-residence times (AMRT). The AMRT ages from buried and surface soils provide a ways to estimate the times of faulting along the Wasatch fault zone (see fig. 1). In addition, S.F. Forman and colleagues (INSTAAR, University of Colorado-Boulder) have finalized 12 thermoluminesence (TL) age estimates for materials exposed in our exploratory trenches. The general concordance of TL ages and corrected $^{14}C$ ages (fig. 2) from the trenches at East Odgen and American Fork Canyon are extremely encouraging. Although TL provides a second method of dating paleoseismic events along the Wasatch fault zone, a more important aspect is the widespread utility of the method. TL dates the time of last exposure of minerals to sunlight. TL light levels are measured from the 4-11$\mu$ fraction of sediments, such as soil A horizons, eolian sand and silt (loess), fine-grained overbank alluvium, glacial outwash, and lacustrine sediments. As such, the TL method could date a great variety of surficial materials from different environments.

3. The 1:50,000-scale map of the Brigham City segment received Directors Approval and is at the printers. This is the first of a series of maps that will show the surface trace of the Wasatch fault zone from Honeyville, Utah (on the north) to Santaquin, Utah (on the south). The surficial geologic units are subdivided by (1) genesis--lacustrine, eolian, alluvial, glacial, or colluvial; (2) age--late Holocene, mid- to early Holocene, latest Pleistocene (10-130 ka), and middle to early Pleistocene; and (3) by lithologic facies (that is, coarse versus medium versus fine grained). These maps will provide a comprehenive base for further evaluations of earthquake-hazards potential. We will publish the maps first in the MF series (black and white, limited distribution) for early release and later in the I series (color, wide distribution).

4. Kathy Haller's aerial-photo reconnaissance and field studies of the Lemhi and Beaverhead faults, Idaho, and the Red Rock fault, Montana, indicate that the faults are segmented and at least one segment of each fault has Holocene displacement. These segments are identified from distinct and persistent relations between scarp height and maximum slope-angle. Relative ages of the most recent movement of the individual segments have been determined by using scarp morphology and the presence of scarps on Quaternary deposits of different ages. The 150-km-long Lemhi fault consists of six segments that range from 12 to 43 km in length; three of the fault segments were active during the past 20,000 yr, and one of these has Holocene displacement. The Beaverhead fault is also 150 km long and consists of six segments that are 20 to 42 km long. There has been movement on one of the segments during the past 20,000 yr and on another two segments in during the Holocene. The Red Rock fault is less than 60 km long, but only the central 27 km of the fault is delineated by scarps on surficial deposits. This part of the fault consists of two segments; one is 16 km long and has Holocene displacment, and the second is 11 km long and has movement in the past 20,000 years. The average lengths of segments and the overall timing of surface displacement of these three faults are comparable to the 135-km-long Lost River fault to the west.

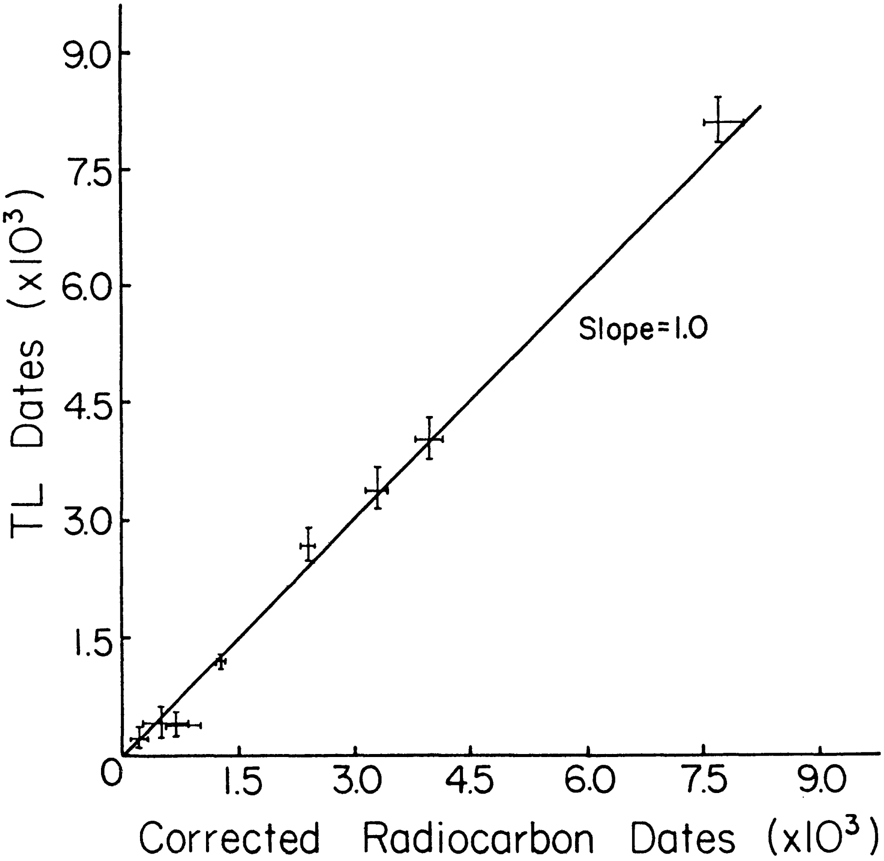

Figure 2.--Comparison of dendrochronologically calibrated $^{14}$C ages (years before present) and TL age (years ago) estimates from charcoal-bearing sediment and faulted A horizons along the Wasatch fault zone. Note the general concordance of the two dating methods (slope of isochron is 1.0).

## Reports

Forman, S.L., and Machette, M.N., Thermoluminescence dating, in Chapter 17, Dating methods applicable to the Quaternary, Rosholt, J.N., ed.: Geological Society of America Decade of North American Geology Volume K-2, Morrison, R.B., ed., Quaternary Non-Glacial Geology of the Conterminous United States; 11 ms pages, 3 figures (in press).

Haller, K.M., 1988, Proposed segmentation of the Lemhi and Beaverhead faults, Idaho, and Red Rock fault, Montana--Evidence from fault-scarp morphology: Geological Society of America Abstracts with Programs, v. 20, no. 5 (in press).

Jackson, M.E., Forman, S.L., and Machette, M.N., 1987, Dating of paleoseismic events using the thermoluminescence (TL) dating method--Preliminary results: Eos (Transactions, American Geophysical Union), v. 68, no. 44, p. 1287.

Machette, M.N., 1987, Changes in long-term versus short-term slip rates in an extensional environment, in Crone, A.J., and Omdahl, E.M. eds., Proceedings of Conference XXXIX--Directions in Paleoseismology: U.S. Geological Survey Open-File Report 87-673. p. 228-238.

Machette, M.N., Personius, S.F., and Nelson, A.R., 1987, Quaternary geology along the Wasatch fault zone--Segmentation, recent investigations, and preliminary conclusions,Chapter A in Hays, W.W., and Gori, Paula, eds., Assessment of Regional Earthquake Hazards and Risk along the Wasatch Front, Utah; U.S. Geological Survey Open-File Report 87-585, v. I, p. A1-A72.

Machette, M.N., Nelson, A.R., Personius, S.F., Schwartz, D.P., and Lund, W.E., 1988, The late Quaternary Wasatch fault zone, Utah--Evidence for segmentation, recent faulting, and clustering of earthquakes: Geological Society of America Abstracts with Programs, v. 20, no. 3, p. 177.

Nelson, A.R., 1987, A facies model of colluvial sedimentation adjacent to a single-event normal-fault scarp, in Crone, A.J., and Omdahl, E.M. eds., Proceedings of Conference XXXIX--Directions in Paleoseismology: U.S. Geological Survey Open-File Report 87-673. p. 136-145.

Personius, S.F., 1988, Preliminary surficial geologic map of the Brigham City segment and adjacent parts of the Weber and Collinston segments, Wasatch fault zone, Box Elder and Weber Counties, Utah: U.S. Geological Survey Miscellaneous Field Studies Map MF-2042, scale 1:50,000.

Wheeler, R.L., 1987, Boundaries between segments of normal faults--Criteria for recognition and interpretation, in Crone, A.J., and Omdahl, E.M. eds., Proceedings of Conference XXXIX--Directions in Paleoseismology: U.S. Geological Survey Open-File Report 87-673, p. 385-398.

Wheeler, R.L., and Krystinik, K.B., 1987, Persistent and nonpersistent segmentation of the Wasatch fault zone, Utah--Statistical analysis for evaluation of seismic hazard, in Hays, W.W., and Gori, Paula, eds., Assessment of regional earthquake hazards and risk along the Wasatch Front, Utah: U.S. Geological Survey Open-File Report 87-585, v. I, p. A1-B124.

# Earthquake-induced landslides and liquefaction in western Washington

9950-03789

Richard F. Madole
Robert L. Schuster
Alan F. Chleborad
Branch of Geologic Risk Assessment
U.S. Geological Survey
P. O. Box 25046, MS 966
Denver, Colorado 80225
(303) 236-1617

## Investigations

1. Prehistoric earthquake-induced liquefaction and landslides

2. Historic landslides and liquefaction

3. Landslide and liquefaction susceptibility mapping

## Results

### 1. Prehistoric earthquake-induced liquefaction and landslides.

Large areas on valley floors and deltas of several large rivers that drain into the Puget Sound are potentially susceptible to liquefaction. Unfortunately, natural exposures of the liquefaction-prone sediment are few; therefore, the search for liquefaction-disturbed strata has (1) concentrated on ground studies in areas of known (historic) liquefaction because liquefaction tends to recur in the same places, and (2) utilized remote sensing to explore for evidence of paleoliquefaction. Application of remote sensing to the search for evidence of paleoliquefaction assumes that features such as sand boils and fissures have a photomorphic expression, or have physical properties that differ from those of adjacent materials, and that features ranging in age from decades to possibly millenia can be recognized. This assumption is supported by the fact that thousands of sand boils are recognizable on aerial photographs of the New Madrid area, Missouri and Arkansas, even at scales as small as 1:60,000. Also, it seems reasonable to expect that sand boils should contrast with overbank sediment, which typically covers flood plains and deltas, in reflectance, bulk density, and other properties that permit detection by remote sensing.

Nothing comparable to the sand boils and fissures of the New Madrid area were observed on that part of the Skagit River deltaic plain for which aerial photography has been obtained, an area of about 175 $km^2$. However, little is known yet about the subsurface stratigraphy of the deltaic sediments, including whether or not sand beds thick enough to produce sand boils and fissures, if liquified, are present, or where such beds are likely to be found. It appears that the Holocene sediment beneath the deltas and estuaries of the region is as much as 30 m thick (Minard, 1985a, b, c). The uppermost strata over most of the deltaic plains and valley floors are estimated to be of late Holocene age on the basis of soil profile development. The soils in these areas consist of simple A/C profiles.

## 2. Historic landslides and liquefaction

Fourteen earthquakes, from 1872 to 1980, are known to have caused landslides or liquefaction in western Washington. Landslides occurred up to 180 km from the origin of the 1949 Olympia earthquake and 100 km from the 1965 Seattle-Tacoma earthquake. During the first half of FY 88, we began study of these historic incidences of ground failure. This work consisted of: (1) study of published information (newspaper and technical journal articles, and governmental agency accounts), (2) interviews with residents and local officials having information on historic earthquake-induced ground failure, and (3) field study of the ground-failure sites. We have only really started on efforts (2) and (3), but from evidence gathered thus far, much more ground failure occurred (due to these historic earthquakes) than has previously been reported.

## 3. Landslide and liquefaction susceptibility mapping

Work on a pilot map of the Olympia, Washington, area was begun with the objective of developing a methodology for producing earthquake-induced landslide susceptibility maps for selected urban areas of the Puget Sound lowland. Late in FY 87, a preliminary reconnaissance of historic earthquake-induced landslides was conducted in the Olympia, Washington, area; parts of Seattle and Tacoma, Washington; and Vashon Island. Data were collected and compared on the topography, geology, and landslide characteristics at selected sites. Additional information was compiled from a library search of published newspaper accounts, journal articles and other technical reports, and interviews with state and local officials. A 5-day training course on GIS (Geographic Information Systems) methods using ARC/INFO computer software was completed in March 1988.

## References cited

Minard, J.P., 1985a, Geologic map of the Arlington West quadrangle, Snohomish County, Washington: U.S. Geological Survey Miscellaneous Field Studies Map MF-1740; scale 1:24,000.

Minard, J.P., 1985b, Geologic map of the Stanwood quadrangle, Snohomish County, Washington: U.S. Geological Survey Miscellaneous Field Studies Map MF-1741; scale, 1:24,000.

Minard, J.P., 1985c, Geologic map of the Marysville quadrangle, Snohomish County, Washington: U.S. Geological Survey Miscellaneous Field Studies Map MF-1743; scale, 1:24,000.

## Reports

Advisory Committee on the International Decade for Natural Hazard Reduction, 1987, Confronting natural disasters--An international decade for natural hazard reduction: National Research Council, National Academy of Sciences, National Academy of Engineering, National Academy Press, Washington, D.C., 60 p. (Schuster was a Liaison Representative on the Advisory Committee and wrote the section on multiple hazards and much of the section on landslide hazards.)

Luza, K.V., Madole, R.F., and Crone, A.J., 1987, Investigation of the Meers fault, southwestern Oklahoma: Oklahoma Geological Survey Special Publication 87-1, 75 p.

Madole, R.F., 1988, Stratigraphic evidence of Holocene faulting in the Midcontinent--The Meers fault, southwestern Oklahoma: Geological Society of America Bulletin, v. 100, p. 392-401.

Madole, R.F., Ferring, C.R., Guccione, M.J., Hall, S.A., Johnson, W.C., and Sorenson, C.J., in press, Osage Plains and Interior Highlands, in Morrison, R.B., ed., Non-glacial Quaternary Geology--Conterminous United States: Boulder, Colorado, Geological Society of America, The Geology of North America.

Schuster, R.L., Chleborad, A.F., and Hays, W.H., 1987, Irrigation-induced landsliding in fluvial-lacustrine sediments, south-central Washington State: Conference Proceedings, 5th International Conference and Field Workshop on Landslides, Christchurch, p. 147-156.

# Investigation of the Seismic Hazard of Puerto Rico

14-08-0001-G1511

William R. McCann
Department of Geology
University of Puerto Rico, Mayaguez
Mayaguez, Puerto Rico 00709-5000

## Investigations:

1. Compilation of a new catalog of strong earthquakes for Puerto Rico for purposes of seismic hazard analysis.

2. Estimation of source region and focal mechanism of 1943 earthquake ($M_s$ 7.75), which occurred of the northwest coast of the island.

3. Calibration of Modified Mercalli scale for typical structures in Puerto Rico by design analysis in particular structures damaged by historic earthquakes.

## Results:

1. The work of the historians is to examine the 400 years of documents held at "Archivos de las Indias" in Seville, Spain. The historian (L. Feldman) and his assistant have arrived in Spain and work on those documents has begun. It will be another month or two before we receive sufficient information to make statements about the earthquake hazard of Puerto Rico in the 1500's and 1600's.

2. We have examined the seismograms of station SJP in Puerto Rico, in an attempt to better define the aftershock zone of the large earthquake of 1943. For some 30 well recorded aftershocks we measured for amplitude of P-wave on the N-S and E-W components as well as the S-P time. The data indicate that the aftershocks occurred some 195-295 kilometers from the station at an azimuth of 37 to 51 degrees west of north. This method of location places the aftershocks from 50 to 150 northwest of the epicenter of the mainshock as located by Kelleher et al. (1973). The aftershock zone as presently located lies on the north wall of the Puerto Rico Trench in a region about 100km long. Next, we will calibrate the $V_p/V_s$ and Vp used to determine the range of the events from SJP. Thus we will be able to calibrate the S-P derived distance and thus more confidently locate the aftershocks.

3. The calibration of the Modified Mercalli scale must await the arrival of specific damage reports from the historians in Spain.

## Reports:

None.

# Chronology of Paleoearthquakes on the Wasatch Fault Zone by Thermoluminescence (TL) Dating

Contract #:14-08-0001-G1396

James McCalpin
Dept. of Geology
Utah State University,
Logan, Utah 84322,
(801) 750-1220

Steven L. Forman
Center for Geochronological Research
Univ. of Colorado,
Boulder CO. 80309-450
(303) 492-6072

Objectives: This study focuses on developing and applying the relatively new thermoluminescence (TL) technique to date Holocene and Pleistocene surface-faulting events on the Wasatch fault zone. For the TL technique to be useful sediment must have been exposed to light for a sufficient time during sedimentation to reduce previously acquired TL. After deposition, the TL signal accumulates in the mineral grains by exposure to ionizing radiation from the decay of radioactive elements. The TL technique directly dates mineral grains, reflecting the time since deposition of the sediment.

Data Acquisition and Analysis: During the first year of this project over 100 TL samples were collected from 19 trenches or natural exposures on the Wasatch Fault zone. Additional modern calibration samples came from the 1983 Borah Peak scarp and the Doublesprings Pass trench.

1. Six sedimentary facies associated with deposition, and stabilization of the land surface before and after a faulting event were tested for the potential to be dated by TL. These facies include faulted alluvial fan sediments (mainly debris flows), scarp-derived colluvium (proximal and distal facies; see Nelson, 1987), sag pond muds, loess, and buried A horizons (Fig. 1). Progress in dating each facies is summarized below.

a. Proximal colluvium: stony proximal colluvium (debris facies of Nelson 1987, p.140) accumulates at the base of normal fault scarps while the free face continues to shed sediment. Because proximal colluvium immediately post-dates surface faulting, accurate dates on this facies could closely constrain age of faulting. Unfortunately, proximal colluvium is deposited by falling, toppling, slumping, and sliding of "blocks" of alluvium which may further disaggregate on the wedge surface, so sunlight exposure, a prerequisite for TL

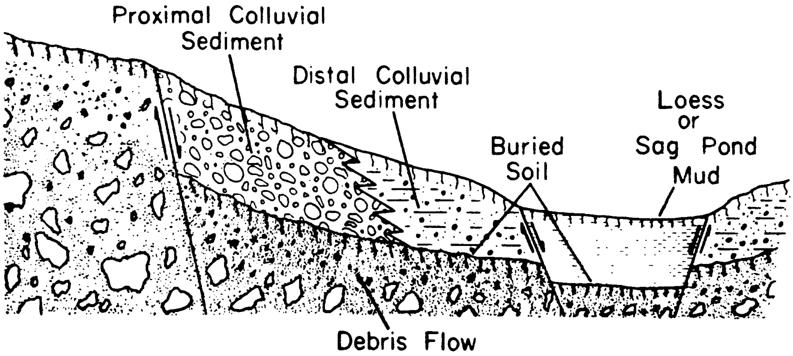

Figure 1: Sedimentary facies associated with deposition and stabilization of the land surface before and after a faulting event for many sites on the Wasatch Fault zone. These facies were tested for the potential to be dated by thermoluminescence.

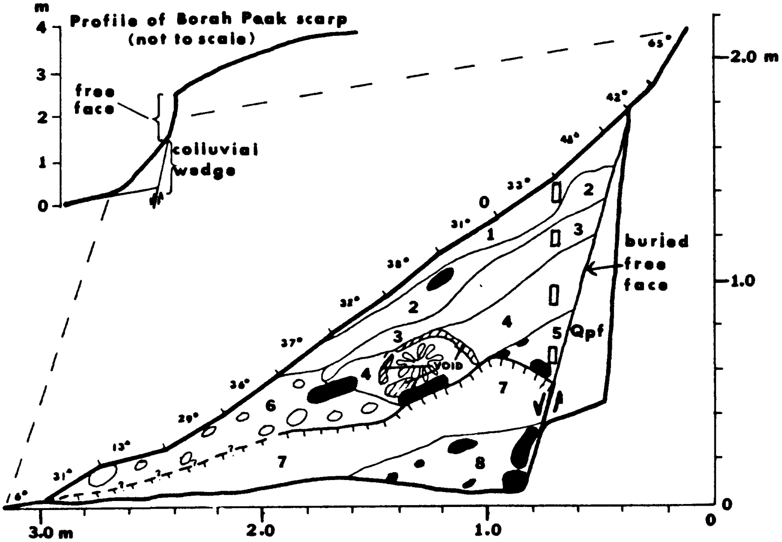

Figure 2: Diagram of a proximal colluvial wedge shed from the fault scarp formed by the 1983 Borah Peak Earthquake. Qpf: Pinedale fan alluvium; Units 7 and 8: Prehistoric proximal colluvium capped by a weak soil; Units 1-5: Proximal colluvium deposited post the October, 1983 earthquake. Vertical boxes at right show TL sample locations; unit 3 sample yielded an TL apparent age of 40 ± 4 ka (see text).

dating, is minimal. We sampled the colluvial wedge shed from the 1983 Borah Peak fault scarp in August, 1986 to test initial bleaching levels. The stratigraphy within the proximal wedge was surprisingly complex (Fig.2). Alternating beds of matrix-rich and matrix-poor colluvium may reflect seasonal variations between spring deposition (freeze-thaw generated slumping and toppling) versus summer/fall deposition (single clast falling and eolian winnowing). A matrix-rich sample (unit 3 in Fig. 2) yielded an apparent TL age of 40 ± 4 ka, despite the fact that it was deposited only 1-2 years ago. This age is even older than the accepted age of the parent material (Pinedale outwash, approx. 15-20 ka). Our interpretation is that the parent Pinedale outwash itself was poorly bleached during deposition 15-20 ka ago, and that essentially no further bleaching occurred during colluvial deposition. As expected, this facies shows little promise for TL dating; no further work is planned on debris facies in FY 88.

b. Distal Colluvium: Finer-grained distal colluvium (wash facies of Nelson, 1987;140) is inferred to result from sheetwash, rillwash, and rainsplash deposition after the scarp free face is buried. Detailed sampling of a 2.2 m-thick composite distal wedge at East Ogden, Utah (trench EO-1) showed the following trend:

| Depth below modern surface | TL age (ka) estimate | Sample No. | Radiocarbon Calibration |
|---|---|---|---|
| 50 cm | 1.2 ± 0.1 | ITL 47 | 1365 ± 40 yr. B.P. |
| 100 cm | 2.6 ± 0.2 | ITL 75 | overlies Holocene fan dated at 4.1-4.8 ka |
| 130 cm | 3.1 ± 0.2 | ITL 72 | |
| 180 cm | 2.5 ± 0.3 | ITL 24 | |

The sharp age discontinuity between 50 and 100 cm has no visible expression on the trench wall, but correlates well with the interval between two paleoevents expressed as separate proximal wedges closer to the fault. This result suggests that small-interval TL dating of homogenous-appearing thick distal colluvium can detect "invisible" unconformities related to faulting events. More work is planned in '88 to confirm this potential.

c. Debris flow alluvium, sag pond sediments, and loess: no new samples of these facies have been dated since the last Technical Report Summary.

d. Buried A horizons: A horizons which are moderately well developed (estimated 1 ka of pedogenesis) can be dated by TL, regardless of the initial bleaching of the parent material. Bleached silt within the A horizon, evidently illuviated from surface eolian dust, is exposed to sunlight and further mixed by bioturbation. Correspondence between TL age estimates and radiocarbon ages for sample pairs of A horizons in Wasatch trenches is excellent (see next section). Pursuing the limits of TL dating in this "facies" is a major goal in FY 88.

Calibration: Preliminary comparison of TL age estimates with corrected radiocarbon ages on nine sample pairs shows an impressive 1:1 correlation back to roughly 8 ka (Fig. 3). Twelve more TL/radiocarbon sample pairs are undergoing analysis, with preliminary confirmation of this 1:1 relationship. Facies which yield the best correspondence of TL to radiocarbon age estimates are A horizons, distal colluvium, and loess. It should be stressed that TL age estimates were produced without prior knowledge of the corresponding radiocarbon dates.

2. TL Age Constraints on Paleoseismic Events on the Wasatch Fault zone: TL age estimates have been incorporated by USGS trench loggers into chronologies of faulting at two sites to date. At American Fork, six TL age estimates and six radiocarbon ages on two trenches roughly bracket three faulting events: earliest, around 4.5 ± 0.1 ka; middle,2.5 ± 0.1 ka; and latest, 0.5 ± 0.1 ka. At the East Ogden site, three TL age estimates and seven radiocarbon ages also suggest three events: earliest, 4.1 ± 0.2 ka; middle, 3.1 ± 0.2 ka; and latest, 1.1 ± 0.2 ka. More TL dating is planned at the East Ogden site and elsewhere in the Weber segment for FY 88. In addition, M. Jackson (Univ. of Colorado) is analyzing TL and radiocarbon samples from four trenches on the Spanish Fork, Nephi, and Levan segments.

## Acknowledgments

Much of laboratory analyses were completed by M.E. Jackson and P. Maat. Jackson was also responsible for excavations on the Levan and Nephi Segments. We proffer sincere appreciation to M.N. Machette, A.R. Nelson, A.J. Crone and W. Lund for collaboration in the field and the laboratory.

## Publications

Forman, S. L., Jackson, M.J. and McCalpin, J., 1987: Thermoluminescence (TL) dating studies of colluvial and alluvial sediments from Utah and Colorado: preliminary results. Geological Society of America Abstracts with Programs, Rocky Mountain Section, v. 19(5): 275.

Jackson, M.J., Forman, S.L. and Machette, M.N. 1987: Dating paleoseismic events using the thermoluminescence (TL) dating method: Preliminary results. EOS Transactions, American Geophysical Union, 68(44): 1287.

Forman, S.L. 1987: The application of thermoluminescence (TL) to normal faulted terrain. IN: Crone, A.J. and Omdahl, E.M.(Eds), Directions in Paleoseismology, Proceedings of

Conference XXXIX, U.S. Geological Survey Open File Report 87-673: 42-49.

McCalpin, J. 1987: Geologic criteria for recognition of individual paleoseismic events in extensional environments. IN: Crone, A.J. and Omdahl, E.M.(Eds), Directions in Paleoseismology, Proceedings of Conference XXXIX, U.S. Geological Survey Open File Report 87-673: 102-114.

Forman, S.L., Maat, P. and Jackson, M.E. 1988: The Thermoluminescence dating of paleoearthquakes: recent results and future prospects. Geol. Soc. of Amer. Abstracts with Programs, Cordileran Section. 20(3) :161.

Forman, S.L. (in press): Application and limitation of thermoluminescence to date Quaternary sediments: IN: Rutter, N. and Brigham-Grette, J Eds. "INQUA Volume on Quaternary Dating Methods" Quaternary Science Reviews

Forman, S.L., Jackson, M.E., J. McCalpin and Maat, P., (in press): The potential of using thermoluminescence to date buried soils in colluvial and fluvial sediments from Utah and Colorado, U.S.A: preliminary results. Quaternary Science Reviews

## References Cited

Nelson, A.R. 1987: A facies model of colluvial sedimentation adjacent to a single event normal-fault scarp, basin and Range Province, western United States. IN: Crone, A.J. and Omdahl, E.M.(Eds), Directions in Paleoseismology, Proceedings of Conference XXXIX, U.S. Geological Survey Open File Report 87-673: 136-145.

Stuvier, M. and Reimer, P.J. 1986: A computer program for radiocarbon age calibration. Radiocarbon, 28:1022-1030.

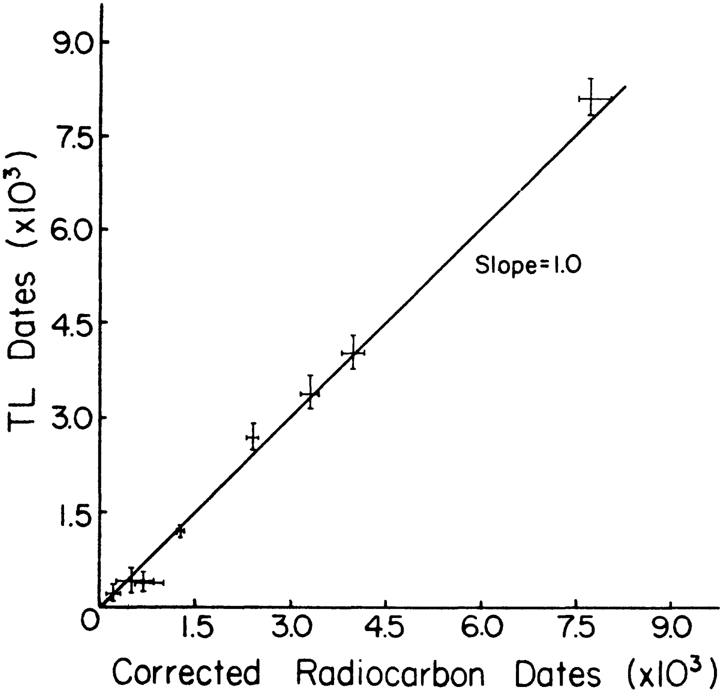

Figure 3: A plot comparing TL age estimates with corrected radiocarbon ages for nine sample pairs from the American Fork (AF) and the Weber (W) segment trench sites. Radiocarbon ages were corrected to calendar years using the IBM program of Stuiver and Reimer (1986). Seven of the nine radiocarbon dates are from the analysis of disseminated organics from buried A horizons; the remaining ages are for carbonized wood. To compensate for the mean residence time of organic carbon in soil A horizons 100 to 200 years was subtracted from the laboratory reported dates prior to the calendar year correction.

# Mississippi Valley Seismotectonics

New

Frank A. McKeown
Branch of Geologic Risk Assessment
U.S. Geological Survey
Box 25046, MS 966, Denver Federal Center
Denver, Colorado 80225
(303) 236-9355

## Investigations

This project is a renewal of a former project with the same name that was discontinued because of the unavailability of experienced personnel to continue studies of the New Madrid seismic zone (NMSZ) and its associated structural environment. The project has been revitalized primarily to utilize much neglected subsurface data that is critical to understanding the structural characteristics of the NMSZ.

1. Reprocess some and interpret all seismic-reflection data purchased several years ago.

2. Finish reprocessing and interpreting marine seismic-reflection data collected along the Mississippi River.

3. Macroscopic and Microscopic examination of samples from the Dow Wilson #1 deep exploratory drill hole in the upper Mississippi Embayment.

4. Compilation of all available stratigraphic data in the upper Mississippi Embayment region for entering into a digital data base.

## Results

1. Field tapes for five seismic-reflection profiles with a total length of about 150 km and that cross the NMSZ were processed to a depth of 12 s by Warren Agena (Branch of Petroleum Geology) and Bob Hamilton. The reprocessed data show below the previously known faulted antiform in Paleozoic rocks a zone of strong discontinuous reflectors below 4 s. The top of the zone is a synform from 4 to 6 s (10 to 16 km). Seismicity occurs between the antiform and synform. Generally flat-lying reflectors at about 9 s (about 25 km) occur under the synform. Comparison of the seismic-reflection data with seismic-refraction data indicates that the 4-6 s zone of reflectors correlates with the interface between a 6.2 km/s upper crust and a 6.6 km/s lower crust. The reflectors at about 9 s correlate with the interface between lower crust and a 7.3-km/s modified lower crust.

2. Correlation of the major reflectors within the Tertiary and Quaternary section of rocks below the Mississippi River continued (K.M. Shedlock and Gene Luzietti). Detailed processing and analysis of reflection data from the large meander of the Mississippi River south of New Madrid, Mo., show several faults that displace sediments up to near the bottom of the river. Loss of resolution in the data preclude determining if the bottom

may have been offset. Although resolution in the data is lost, the normal variable scouring and aggradation of river-bottom sediments would be expected to obliterate evidence of offset.

3. Macroscopic and preliminary microscopic examination of 18 "junk basket" samples of rocks from the Dow Wilson #1 deep exploratory drill hole (provided by E. Glick) appear to be providing information and insight of the early development of the Reelfoot rift (F. McKeown and Sharon Diehl). The samples were collected from depths ranging from 12,523 to 14,143 ft. Because of the way that the samples were collected, the depth reported for a sample means only that pieces of rock in the sample cam from no greater depth than that assigned to the sample. Nevertheless, the stratigraphic sequence indicated by the samples agrees reasonably well with other information from the drill hole. The fabric, mineralogy, alteration, and differences in grain size of the samples are suggestive of a more detailed history of the Reelfoot rift than can be obtained from geophysical data. Tentative interpretations of the section of rocks represented by the samples is that they are largely clastics of both marine and terrestial origin derived from provinces with low relief. Subsequent to slight metamorphism (largely quartz overgrowth) the rocks were subjected to a shear stress as suggested by lineation in planar structure normal to bedding.

4. Compilation of all available stratigraphic data from drill holes in the upper Mississippi Embayment region has been completed (Richard Dart). The data are being entered into a digital data base from which subcrop, structure contour, and isopach maps will be plotted.

## Reports

Dart, R. L., and Zoback, M. L., 1987, Application of the well-bore breakout stress method to areas within the Continental United States [abs.]: Second International Symposium on Borehole Geophysics for Minerals, Geotechnical and Ground-Water Applications, Minerals and Geotechnical Logging Society (Oct. 1987).

Dart, R. L., and Zoback, M. L., 1987, Application of the well-bore breakout stress method to areas within the Continental United States: Proceedings of the Second International Symposium on Borehole Geophysics for Minerals, Geotechnical, and Ground-Water Applications, Minerals and Geotechnical Logging Society, 20 p. (in press).

Dart, R. L., 1988, Stress implications and stratigraphic correlations of well-bore breakouts, Oklahoma and Texas Panhandle [abs]: Anadarko Basin Workshop, Oklahoma Geological Survey and the U.S. Geological Survey (April 5-6, 1988).

Hamilton, R.M., Agena, W.F., Lee, M.W., and McKeown, F.A., 1987, Deep structure of the New Madrid seismic zone interpreted from seismic-reflection profiles: EOS [Transactions of the American Geophysical Union]. v. 68, no. 44, p. 1355.

# Database Management

9910-03975

Charles S. Mueller
Branch of Engineering Seismology and Geology
U.S. Geological Survey
345 Middlefield Road, MS 977
Menlo Park, California 94025
(415) 329-5646

## Investigations

1. Development of techniques for data playback, processing, management, and export with emphasis on large datasets collected with portable digital event-recording seismographs (e.g., GEOS).

2. Design and implement relational databases for strong-motion (ESM) and aftershock/special-experiment data (ESGDB). The goal of the databases is to enhance researcher access to diverse Branch datasets.

## Results

1a. New datasets played back, processed and archived:
Whittier Narrows, California - aftershocks.
Superstition Hills, California - aftershocks.
Kilauea Volcano, Hawaii - volcanic tremor.

1b. Old datasets archived:
Enola, Arkansas - 1982 earthquake swarm.

1c. Datasets exported:
Enola, Arkansas, 1982 earthquake swarm -- USGS in Golden, Colorado.

## Reports

None.

04/88

# EARTHQUAKE RECURRENCE AND QUATERNARY DEFORMATION IN THE CASCADIA SUBDUCTION ZONE, COASTAL OREGON

**9950-04180**

Alan R. Nelson and Stephen F. Personius
U.S. Geological Survey
Branch of Geologic Risk Assessment
MS 966, Box 25046
Denver, CO 80225
(303) 236-1596; FTS 776-1596

## INVESTIGATIONS

There are two components to this project: (1) Nelson's study of middle and late Holocene sea level history as revealed by salt marsh stratigraphy, and (2) Personius' study of fluvial terrace remnants along major Coast Range rivers to determine style and rates of late Quaternary deformation.

## RESULTS

### Recurrence of Holocene earthquakes in central Oregon

Repeated, great plate-interface earthquakes have been postulated for the Cascadia subduction zone in western Washington and Oregon. The best evidence of the coseismic subsidence to be expected near the coast during great earthquakes is found in southwestern Washington where many exposures record repeated episodes of submergence of late Holocene marshes. Atwater and others have used consistent stratigraphic relationships, $^{14}$C ages, and plant macrofossils from sequences of interbedded marsh peats and intertidal muds to show that the 6 marsh peats buried in the last 4000 years throughout southwestern Washington were submerged suddenly. The late Holocene estuarine record in the central part of the subduction zone in Oregon is more difficult to interpret; there are very few good exposures, and coring at some sites has produced evidence of a gradual rise of late Holocene sea level while sea level rise appears to be jerky at other sites.

#### *Marsh foraminifera as sea level indicators*

One of our goals is to show if the peats we find interbedded with muds in cores from the central Oregon coast were submerged suddenly (coseismicaly), like those in Washington. Marsh foraminifera are more sensitive to changes in sea level than many marsh plants and are easier to identify in cores. Thus, we have begun to use foraminifera faunas in cores from Oregon marshes to test whether our buried peats represent jerky (repeated coseismic) marsh subsidence. Because no studies of modern marsh foraminifera from the region have been done, one of our first objectives is to show if modern marsh subenvironments at different elevations can be distinguished using foraminifera faunas.

Analyses of samples from surface transects of the first two of five Oregon marshes studied show the same strong correlation between foraminiferal assemblage zones and sea level found in other marshes worldwide. Three (informal) assemblage zones can be recognized in the transects studied so far: a high-marsh zone, an upper-low-marsh zone, and a low-marsh--mud-flat zone. Tide-gauge data are not available for either site, but the distribution of high and low marsh and the position of mean high water can be estimated from macrofloras. The highest samples in each transect, on the upland border, are barren of foraminifera. Samples from the upper part of the high-marsh zone are dominated by *Trochammina macrescens* and *Trochammina inflata* with lesser numbers of *Miliammina fusca* and *Haplophragmoides wilberti.* The percentage of *M. fusca* increases towards the base of the high marsh zone. Where *M. fusca* becomes the dominant species over *T. macrescens*, *T. inflata*, and other species we recognize an upper-low-marsh zone. In both transects this zone includes a 0.5- to 1-m-high, nearly vertical scarp resulting from modern erosion of the low marsh. In the low-marsh--mud-flat zone *M. fusca* and *Ammotium salsum* co-dominate, *Trochammina* is absent, and *Reophax nana* and calcareous species become increasing abundant with decreasing elevation. On the basis of these preliminary analyses, we should be able to identify former sudden changes in sea level of about 0.5-1.0 m in future analyses of cores from Oregon estuaries. Studies incorporating more accurate vertical control and more detailed sampling might be able to resolve significantly smaller changes in sea level.

### *Character of sea level rise indicated by marsh stratigraphy*

Preliminary coring and study of outcrops at 12 marsh sites in seven tidal inlets yields conflicting evidence for the history of relative sea-level along the south-central Oregon coast. Additional radiocarbon dates from most of these sequences are pending and all sites will be investigated in more detail later in FY88.

At sites in the eastern arms of Coos Bay, one probable buried marsh surface is found in the upper 1 m of most cores overlying 4-6 m of uniform mud. In some cores both upper and lower contacts of peaty units are gradational, but in most cores the thickest peat bed has a fairly abrupt upper contact suggesting sudden submergence of a marsh. A spruce root from this buried surface in Shinglehouse Slough was dated at 340 $^{14}$C yrBP. One interpretation of this type of marsh sequence is that sedimentation rates in most tidal inlets have been low during all but the last few hundred years of the late Holocene and that for this reason no evidence (buried marsh surfaces) of earlier sudden submergence events has been preserved. Another interpretation is that no sudden changes in sea level have occurred.

In contrast, at two sites in South Slough in western Coos Bay, cores show 6-8 abruptly buried marsh surfaces that are 0.4-1.2 m apart. Extensive coring in a small marsh along Winchester Creek revealed up to 8 buried marsh surfaces in sections 5-8 m thick. The 4 best-developed surfaces can be correlated across the inlet. The uppermost buried surface has a modern $^{14}$C age; it must have been buried by sedimentation following diking of the marsh. Lower surfaces date at 460 (2.2 m) and 2880 (2.8 m) $^{14}$C yrBP, indicating highly non-uniform sedimentation rates. A core from Day Creek, 4 km to the north, had a similar sequence of 6 buried surfaces. These sites are near the axis of the South Slough syncline, and tilted marine terraces on the west limb of the syncline document continued late Pleistocene folding of this structure. Thus, the South Slough buried surfaces may record local Holocene coseismic faulting or folding rather than regional deformation of the central Oregon coast during great plate-interface earthquakes. Alternatively, sudden deformation of the syncline might also occur primarily as a response to large subduction zone earthquakes.

Coring in South Inlet, an arm of the Siuslaw River estuary, shows that 4 m of fairly uniform peat overlies 4 m of mud. This type of marsh sequence suggests that late Holocene relative sea-level rise was gradual with no abrupt changes in the type or rate of sedimentation. Subtle, gradual lithologic changes within the peat section suggest only small, gradual changes in sea level. Abrupt lithologic changes found in some cores farther up the valley of South Inlet probably record stream flood events.

Most cores in the Umpqua River estuary showed peaty beds in the upper 1.5 m of the cores, but the upper and lower contacts of most beds were gradational. Abrupt contacts bounding some units could be due to sudden submergence or flooding. As in Coos Bay, below 1.5 m only muds were found to 7 m depth in the cores. A $^{14}$C age of 3.1 ka from a depth of 6 m in one core indicates that the relative rate of sea level rise here is twice the rate in Coos Bay, or that a great deal of differential compaction has taken place in these peat-mud sequences.

A single buried marsh surface was described in outcrop along the Coquille River at a depth of 1.2 m. A small spruce stump rooted in the surface was dated at 290 $^{14}$C yrBP. The estuarine muds that bury the surface are overlain by overbank silts from flooding of the river and by eolian sands derived from dune fields to the west.

Thus, the most recent buried marsh surface, which may date from about 300 yrBP, appears to be fairly widespread along this part of the Oregon coast. Good evidence for earlier submergence events is found only in South Slough. To show whether or not the earlier submergence events found in South Slough have regional extent emphasis in FY88 will be placed on coring less-protected sites in inlets with moderate-size streams. The moderately high sedimentation rates in marshes at these sites should have allowed marshes to develop and to be preserved following all major submergence events. Selected cores from Coos Bay and South Inlet will also be analyzed for foraminifera and diatoms to more accurately estimate the elevation and rate of change of former sea levels.

## Late Quaternary deformation rates indicated by fluvial terraces in central Oregon

The purpose of this part of the project is to evaluate some of the longer-term effects of subduction along the Cascadia subduction zone by examining the styles and rates of deformation of Quaternary deposits within the Oregon Coast Range (OCR). Extensive Quaternary deposits are relatively rare in the erosion-dominated OCR; however, fluvial terraces along several Coast Range rivers appear to be well enough preserved for stratigraphic, chronologic, and tectonic analysis. The three rivers examined in this study are the Umpqua River, the Smith River, a main tributary of the Umpqua, and the Siuslaw River. The Umpqua River has its headwaters in the Cascades; both the Smith and Siuslaw Rivers drain the western flank of the central OCR.

### *Geomorphology*

The poor preservation of fluvial terraces in most of the OCR reflects the processes that form these features. Most OCR terraces are strath terraces, which are fluvial benches cut into bedrock, covered by a thin veneer of fluvial sediment. This type of terrace is formed by fluvial downcutting in response to changes in base level. In the OCR, these changes are related to eustatic sea level changes and regional uplift. Strath terraces commonly do not form broad platforms along streams, so laterally extensive, paired terraces of this type are rarely preserved. OCR terraces are commonly preserved as scattered unpaired remnants, usually restricted to the insides of meander bends and along wider parts of river valleys, and less commonly in abandoned meander loops. All the rivers examined in this study are flowing in deeply incised valleys, which indicates that uplift of the OCR has been an ongoing, long-term process.

### *Stratigraphy*

Exposures of fluvial terrace sediments along the Umpqua, Smith, and Siuslaw Rivers show a remarkably consistent stratigraphic sequence. They typically consist of a 1-2-m-thick sandy pebble gravel that overlies a cut bedrock bench; this gravel is in turn overlain by a 2-5-m-thick silt or sandy silt. An exception to this sequence is seen in terraces very near the coast, where the sediments generally consist of much thicker deposits of sand and silt. These near-coastal deposits are probably overthickened by trapping of sediment in estuaries during periods of higher sea level. However, several high (>90 m), well exposed fluvial terraces near the coast show a thickened, but stratigraphically similar sequence of silt over gravel over bedrock, suggesting that processes of fluvial terrace formation are similar along the length of Coast Range rivers.

I have interpreted the gravel facies as bedload sediment deposited in channels, and the silt facies as overbank sediment deposited during periodic flooding. The modern river channels are flowing directly on bedrock except in estuarine settings near the coast. Terraces surfaces appear to be reoccupied only rarely by channel deposits, but are frequently reoccupied during seasonal flooding. This is evident because the silt units are remarkably uniform stratigraphically; they are generally massive or weakly stratified, with only minor thin, discontinuous sand and sandy gravel interbeds. Of over 40 exposures examined so far, only one outcrop showed a gravel deposit at the surface of a terrace deposit. Because the modern rivers are flowing directly on bedrock, contemporary uplift of the Coast Range is assumed. This uplift eventually results in raising the surface of the terrace beyond the reach of flood waters, and the terrace surface is abandoned. The massive nature of the silt facies and general lack of buried soils within these deposits suggests that overbank sedimentation occurs at regular intervals at fairly high rates until the terrace surface is abandoned.

### *Umpqua River*

Fluvial terraces are intermittently present along the length of the Umpqua River. Terraces are presently being examined from near the mouth of the river near Reedsport to Coles Valley, 160 river kilometers upstream. Terrace remnants vary in height, from the modern floodplain to over 100 m above modern river level. Correlation of these scattered remnants is difficult, but a dating program of radiocarbon and thermoluminescence (TL) analyses is being undertaken in an attempt to identify possible terrace deformation and to calculate rates of downcutting. Several radiocarbon dates have been obtained on charcoal in the lower terraces. Terraces about 13-15 m above river level, 120-130 km upstream are 7-10 ka. A terrace of similar height on Scholfield Slough, 15 km upstream from its confluence with the Umpqua near Reedsport, has a radiocarbon age of >26 ka. This relationship suggests that the coast may be subsiding relative to the inland Coast Range. Alternatively, this relationship may be explained by a decreasing stream gradient and subsequent convergence of terraces as the river approaches base level. Additional radiocarbon and TL dates and terrace profiles will be used to further analyze these problems.

### *Smith River*

The Smith River is a major tributary of the Umpqua River; the confluence of these two rivers is just upstream from the town of Reedsport, about 18 km from the mouth of the Umpqua River. The drainage basin of the Smith River is much smaller than that of the Umpqua River, and the Smith is shorter and has a much steeper gradient than the Umpqua. Several radiocarbon dates obtained on charcoal indicate that rates of downcutting are substantially faster on the Smith River. A 3 ka terrace surface 47 km upstream from the confluence is about 30 m above river level, whereas a correlative terrace surface 10 km upstream from the confluence is only about 10 m above river level. This relationship again suggests decreasing stream gradients and(or) subsidence near the coast. Additional dates and terrace elevations are pending.

### *Siuslaw River*

Earlier studies of the terraces along the Siuslaw River concluded that a high terrace surface on the north side of the river showed apparent westward tilt that may have been related to active folding. My studies along the Siuslaw River show that this "surface" is actually several terrace levels that may have been incorrectly mapped as a single surface. Terrace profiles are currently being constructed in order to assess possible deformation. Unfortunately, the only well preserved terrace surfaces along the Siuslaw river are those preserved at great height (80-110 m) above the modern river level. The degree of soil development on these surfaces (several-meter-thick Bt horizons with 2.5 YR colors, complete weathering of in situ gravel clasts) suggests that they may be several hundred thousand years old. This would suggest that these deposits are probably substantially older than the earlier estimate of 100 ka, and that they are beyond the range of TL dating.

## REPORTS

Nelson, A.R., 1987, Apparent gradual rise in relative sea level on the south-central Oregon coast during the late Holocene--Implications for the great earthquake hypothesis: EOS [Transactions of the American Geophysical Union], v. 68, no. 44, p. 1240.

Personius, S F., 1988, Analysis of fluvial terraces along the Umpqua, Smith, and Siuslaw Rivers, central Oregon Coast Range: Geological Society of America, Abstracts with Programs, v. 19, no. 6, .

Nelson, A.R., and Jennings, A.E., 1988, Use of salt-marsh foraminifera to identify coseismic changes in sea level in Oregon: American Quaternary Association, Program and Abstracts of the Tenth Biennial Meeting, University of Massachusetts, Amherst, (in press).

# Analysis of Liquefaction Susceptibility in San Jose, California

14-08-0001-G1359

M.S. Power, J.R. Wesling, F.H. Swan III, R.C. Perman, and R.R. Youngs
Geomatrix Consultants
One Market Plaza, Spear Street Tower, Suite 717
San Francisco, California 94105
(415) 957-9557

and

R.W. Mearns
City of San Jose
801 North First Street
San Jose, California 95110
(408) 277-4693

## Investigations

The city of San Jose is located in a region of high potential seismic activity. Large areas of the city are underlain by unconsolidated deposits that have a potential for liquefaction because of their relatively young geologic age, presence of sand layers, and relatively high groundwater levels. In this study, Quaternary geologic units within San Jose were mapped using aerial photographs, field checks, and previous geologic mapping by others (Helley and Brabb, 1971; Helley and others, 1979). The liquefaction susceptibility of these deposits has been characterized using information from a variety of sources. The major data source has been logs of borings contained in more than 1800 reports of geotechnical investigations conducted in San Jose during the period 1974 to 1987. Information on ground water levels, soil classifications, and penetration resistances (blow count values) of cohesionless soils were extracted from this data base and analyzed in detail. Other data that were collected and analyzed from previous investigations in the study area include cone penetrometer test data and shear wave velocity data. A limited program of borings with standard penetration test blow count measurements and cone penetrometer tests at selected locations was conducted during this study to supplement the existing data base. In addition to these data sources, evidence for historical liquefaction in the San Jose area (Lawson, 1908; Youd and Hoose, 1978) was reviewed.

## Results

Liquefaction susceptibility in the study area has been evaluated primarily on the basis of: correlations between susceptibility and penetration resistance and soil grain size characteristics presented by Seed and others (1985); correlations established between susceptibility and the geologic age and depositional environment of unconsolidated deposits (Youd and Perkins, 1978); and historical accounts of liquefaction.

Areas directly underlain by Pleistocene or older deposits are assessed to have a low susceptibility to liquefaction. In areas underlain by Holocene deposits, liquefaction susceptibility depends on the geologic origin of the deposit, depth to groundwater, and presence or absence of potentially liquefiable soil types (i.e. cohesionless sands, silts, and gravels). Depths to groundwater have been zoned throughout the study area and vary from less than 10 feet to greater than 30 feet. Proportions of potentially liquefiable cohesionless soils versus cohesive (clayey) soils having low liquefaction susceptibility have been evaluated. Within a depth range extending from the ground water table to 30 feet below the ground water table, cohesive soils generally predominate. This reduces liquefaction susceptibility overall. However, there are significant lateral variations in the proportions of cohesionless and cohesive soils that cannot be predicted on a regional scale. Thus, within given areas underlain by Holocene deposits, a range of susceptibility is assessed, reflecting variations in amounts of cohesionless soils as well as variations in ground water depths. Holocene alluvial fan deposits are assessed to have low to moderate liquefaction potential. Holocene fluvial and estuarine deposits in areas of shallow groundwater (generally less than 10 feet deep) have low to high susceptibility. These deposits are generally restricted to the northern part of the study area near San Francisco Bay and along channels of active streams throughout the study area. Susceptibility of Holocene fluvial deposits generally decreases toward the south and is assessed to be low to moderate for intermediate ground water depths (generally in the range of 10 to 30 feet deep) and low when groundwater is greater than 30 feet in depth.

Evaluation of both liquefaction susceptibility and liquefaction opportunity are necessary to fully assess liquefaction potential in San Jose. Liquefaction opportunity is a function of the seismicity of the area and the frequency of occurrence of earthquake ground motions capable of causing liquefaction in susceptible materials. In a second phase of study, currently being conducted, liquefaction opportunity is being assessed, and the probability of liquefaction, combining susceptibility and opportunity information, is being evaluated.

Results of these investigations will be displayed on USGS 1:24,000 scale topographic quadrangle maps. The maps will be filed with the Department of Public Works of the City of San Jose for use by city officials and general public.

## References

Helley, E.J. and Brabb, E.E., 1971, Geologic map of late Cenozoic deposits Santa Clara County, California: U.S. Geological Survey Miscellaneous Field Studies Map MF-335, Scale 1:62,500.

Helley, E.J., Lajoie, K.R., Spangle, W.E., and Blair, M.L., 1979, Flatland deposits of the San Francisco Bay region, California -- their geology and engineering properties and their importance to comprehensive planning: U.S. Geological Professional Paper 943.

Lawson, A.C., 1908, The California earthquakes of April 18, 1906, Report of the State Earthquake Investigation Commission, Carnegie Institute of Washington.

Seed, H.B., Tokimatsu, K., Harder, L.F., and Chung, R.M., 1985, Influence of SPT procedures in soil liquefaction resistance evaluations: Journal of Geotechnical Engineering, ASCE, v. 111, no. 12, p. 1425-1445.

Youd, T.L., and Hoose, S.N., 1978, Historic ground failures in northern California triggered by earthquakes: U.S. Geological Survey Professional Paper 993.

Youd, T.L., and Perkins, D.M., 1978, Mapping liquefaction-induced ground failure potential: Journal of the Geotechnical Engineering Division, ASCE, v. 104, no. GT4, p. 433-446.

# The Effect of Local Geology on Earthquake Intensity in the Seattle to Portland Region of Washington and Northern Oregon

14-08-0001-G1510

Anthony Qamar
Geophysics Program
University of Washington
Seattle, WA 98195
(202) 543-8020

## Objectives

This study examines the variation of strong ground-motion during earthquakes in the Puget Sound-to-Portland region of Washington and Oregon using intensity data from past earthquakes. Our goal is to find earthquake intensity patterns that show consistency from earthquake to earthquake. Ultimately, we hope to determine which geologic factors are responsible for the patterns observed and use this information to predict intensity patterns for large earthquakes in the future.

## Accomplishments

We have nearly finished digitizing earthquake intensity data for the 1981 Elk Lake Washington earthquake, a shallow, magnitude 5.5 earthquake that occurred 130 km south of Seattle on February 14, 1981. So far, we have digitized the locations of about 3,200 earthquake sites where we have felt reports obtained immediately after the earthquake. A portion of these data in the Seattle area are shown in Figure 1.

The intensities reported for the 1981 earthquake are not as large as those reported for the 60 km deep, magnitude 7.1 and 6.5 Puget Sound earthquakes of 1949 and 1965. However, the 1981 earthquake is valuable because of the large number of felt reports available, especially in the Seattle region. Although there is considerable variance in the apparent intensities reported for the 1981 earthquake, there are several patterns that emerge. One such pattern is the relatively large number of high intensities reported east of Lake Washington. In contrast, North Seattle showed a large number of low intensity values. A pattern of high intensity in West Seattle, noted during the 1965 earthquake, did not show up in the 1981 earthquake. Unfortunately, there are few data in 1981 along the river delta of the Duwamish river, an industrial area of Seattle that reported considerable damage in 1965. This is due to the fact that most of our data are taken from letters written by people in residential areas.

The next step on our analysis will be to smooth the data and calculate summary intensities on a uniform grid over regions where we have a sufficient number of felt reports. After this we will compare the estimated intensities with those of the 1949 and 1965 earthquakes.

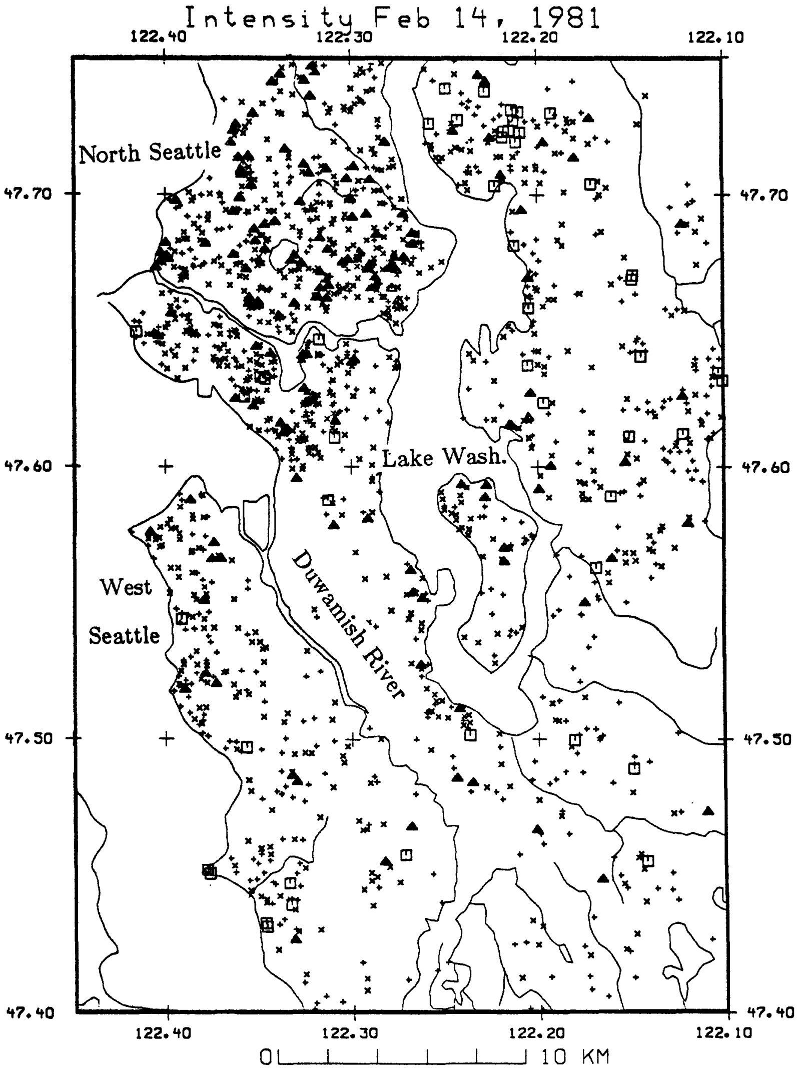

Figure 1. Observations of intensities for the 1981 Elk Lake earthquake in the Seattle, Washington region. Low intensities (I or II) are indicated by large triangles. Intensity III is indicated by a small cross and IV by a small plus-symbol. Large intensities (V or VI) are indicated by a large square.

# Simulation and Empirical Studies of Ground Motion Attenuation in the Seattle-Portland Region

14-08-0001-G1516

Paul Somerville
Woodward-Clyde Consultants
566 El Dorado Street
Pasadena, California 91101
(818) 449-7650

Objective: The objective of the project is to use strong ground motion simulation methods together with empirical strong motion data to estimate ground motion attenuation in the Seattle-Portland region due to potential large earthquakes on the shallow plate interface of the Cascadia subduction zone. The use of strong motion simulation procedures is motivated by the complete absence of subduction earthquakes on the Cascadia subduction zone during historical time (and the consequent absence of strong motion recordings of such events), and the sparsity of applicable strong motion recordings from other subduction zones. The simulation procedures are based on the summation of contributions from subregions of the fault rupture surface.

Validation of Simulation Procedures: Before proceeding to apply the ground motion simulation procedures in the Cascadia subduction zone, we are validating them by testing their performance against strong motion recordings of the magnitude 8 Michoacan, Mexico earthquake of 1985. This event is of special value for our purposes because of the abundance of recordings at close distances, the similarity of the subduction zone geometry between Michoacan and Cascadia, and the known source characteristics of the Michoacan earthquake. Preliminary results of this validation exercise are shown in Figures 1 and 2, which show the recorded and simulated acceleration time histories and response spectra at station La Villita. The two sets of time histories are quite similar in peak acceleration, duration, and the shape of the envelope of strongest ground motion. The acceleration response spectra also show good agreement over a wide frequency range.

Development of Source Models: The geometry of the shallow region of the Cascadia subduction interface, which constitutes the fault plane of potential interplate earthquakes, has been defined using the detailed analysis by Weaver and Baker (1988) of earthquake hypocentral locations within the underlying oceanic lithosphere. The rupture zone is assumed to be confined to depths less than 40 km.

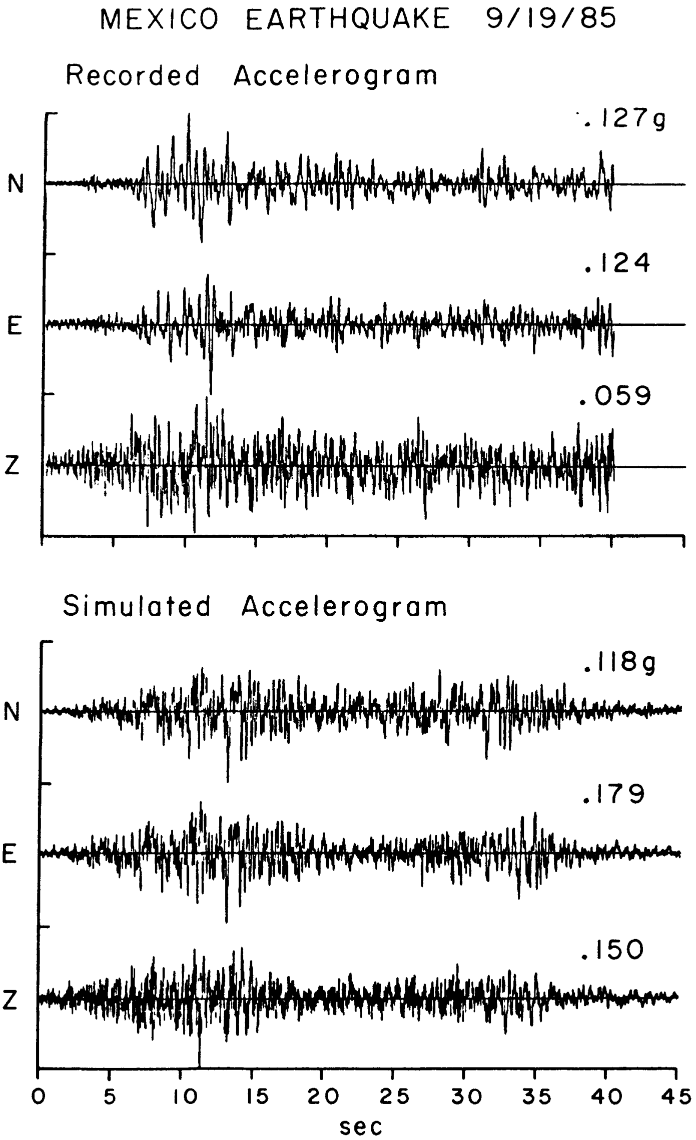

Figure 1. Recorded and simulated accelerograms of the magnitude 8 Michoacan, Mexico earthquake of September 19, 1985 at station La Villita.

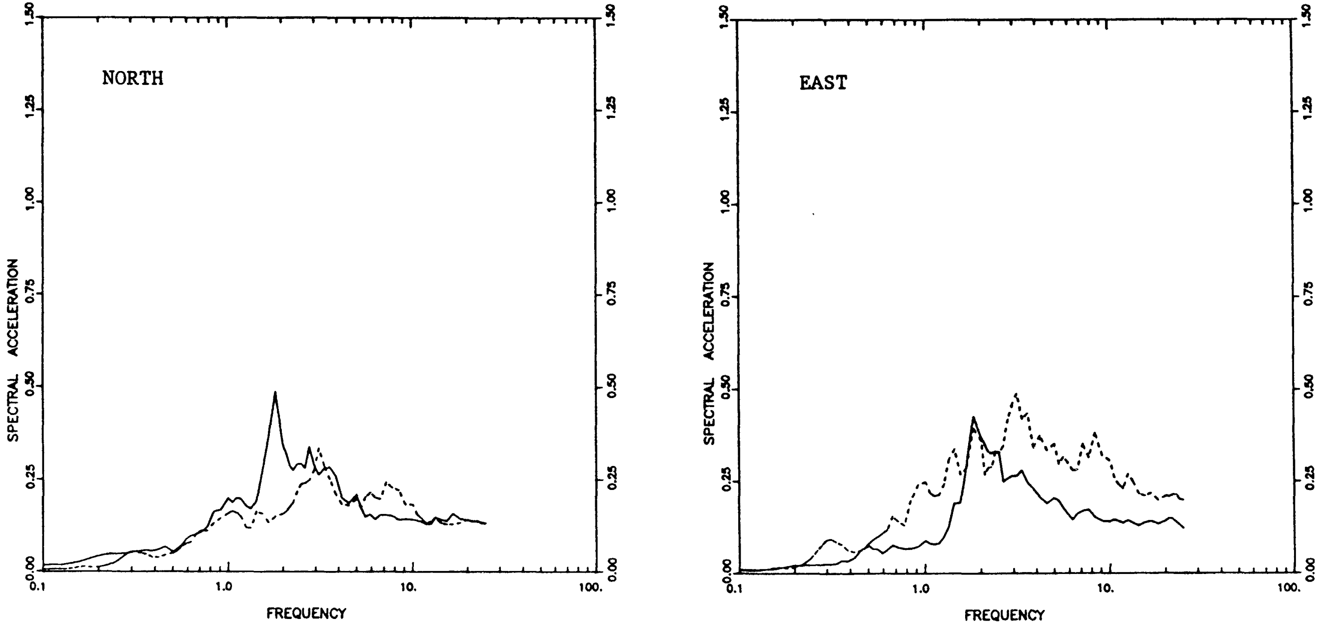

Figure 2. Comparison of recorded and simulated horizontal component response spectra at 5% damping of the magnitude 8 Michoacan, Mexico earthquake of September 19, 1985 at station La Villita. The recorded response spectrum is shown by the solid line and the simulated one by a dashed line.

# Quaternary Framework for Earthquake Studies
# Los Angeles, California

9540-01611

John C. Tinsley
Branch of Western Regional Geology
U.S. Geological Survey
345 Middlefield Road, MS 975
Menlo Park, California 94025
(415) 329-4928

## Investigations

1. Geology and relative ground motion, Wasatch Region:

Part of the assessment of seismic risk is the evaluation of seismic site response, relative to nearby hard rock, of soils and underlying geologic units to earthquake ground motions. Ground motion has been recorded at more than 70 sites throughout the Wasatch region and the site effects have been identified at soil sites relative to bedrock sites (Hays and King, 1982). The geology has been studied in detail at 43 of these sites using regional geologic studies, drilling and sampling by USGS field crews, laboratory analyses of soils and near-surface rock units to average depths of 200 ft subsurface, downhole P-wave and S-wave velocity profiles, high-resolution reflection profiles (Ken King, Golden, CO), and geologic and geotechnical data compiled from public and private sources. The analysis of these data are not yet complete, but results in the form of preliminary contour maps showing site response on alluvium relative to site response on rock in two period bands (0.2-0.7 sec and 0.7-1.0 sec) are shown in the accompanying figures. (J. Tinsley, K. King, R. Williams and D. Trumm).

2. Geology and relative ground-response - Puget Sound and Portland areas:

A contract has been submitted for bid for drilling and sampling at 14 sites in Seattle, WA and 6 sites in Olympia, WA during FY 88. The study will compare subsurface geology among several sites damaged during the 1949 and 1965 Puget Sound earthquakes and other sites located ostensibly on similar geologic materials that sustained little or no damage. These sites are arrayed in a transect across the Seattle and West Seattle area. This study is the initial phase of what will be at least a 3 to 4 year study to evaluate geologic aspects of site response in the glaciated and non-glaciated lowlands of the Pacific northwest. Emphasis in future years will shift southward and will include additional sites in southern Washington and in Oregon as time and circumstances permit. The inital emphasis on the Seattle area takes advantage of the patterns of damage sustained during historical earthquakes. (John Tinsley and D. Trumm).

3. Holocene stratigraphy and fold deformation rates near Coalinga, CA:

This study is concluding; a manuscript has been submitted to Editor M. Rymer for publication in the USGS Professional Paper dedicated to the Coalinga earthquake (B. Atwater, D. Trumm, J. Tinsley and R.S. Stein).

Results

1. Preliminary relative ground response maps in two period-bands for part of the Salt Lake Valley are shown in figures 1 and 2. Contours are drawn on the basis of on-going studies of the geology of the region and on the results of the ground motion studies program initiated by Walter Hays and Kenneth King during the middle and late 1970's. Positions of the contour lines are approximate, owing to sparse data in some areas, especially in the western and southwestern parts of the region, but we are including the maps here because they are an improvement over previous published data set for the area and because the contours are not likely to change radically during subsequent analyses. Specifically these maps include 95% of the new data recorded during the past 3 years and exclude records made previously at any recording stations that could be shown to be unreliable. Additional, new stations are located along and west of the Jordan River and show that relative site response decreases west of the Jordan River valley towards the bedrock of the Oquirrh Range, as sedimentary fill becomes more coarse and the Quaternary deposits thin progressively to the west. Published subsets of these data (Hays and King, 1982) showed the steeply increasing trend towards relative ground response in the 0.2 and 0.7-second period-bands from low values along the bedrock of Wasatch Front to high values along the Jordan River. However, they lacked the data to close the contours west of the Jordan River; this situation has been improved owing to the new stations, and revised but preliminary contour maps are shown in figures 1 and 2.

   **CAUTION:** These maps are preliminary and should not be used for hazard studies or earthquake loss estimates without considering other important factors including size of earthquake, distance to earthquake source, non-linear soil response to earthquake strains, type, design and condition of the structure, and duration of strong ground-motion. The authors reserve the right to amend the contour maps as they see fit during subsequent stages of the analysis and during preparation for publication in the forthcoming, second Wasatch Front Earthquake Hazards Professional Paper.

2. Drilling has not commenced in the Puget Sound region. Permission has been obtained from the cities of Olympia and Seattle, plus the departments of schools and parks and recreation for access. Detailed arrangements will be completed by mid-May, 1988.

3. Charcoal (5000 and 7000 $^{14}C$ YBP) recovered at two localities from high in the section within the Pleasant Valley Syncline effectively precludes large rates of vertical deformation of the Coalinga anticline and Pleasant Valley syncline during the middle and late Holocene. Radiocarbon analyses at four localities in this age range indicate that the buried 5000 year old floodplain of Los Gatos Creek is essentially parallel to the "present alluvial plain". The "present alluvial plain" was the active floodplain of Los Gatos Creek from about 500 radiocarbon-years BP until not less than about 100 $^{14}C$ YBP, when Los Gatos Creek began an episode of incision that continues in the present. After accounting for uncertainties in the topography of the buried alluvial floodplains the apparent repeat time for fold-belt earthquakes accompanied by coseismic uplifts on the order of 0.2 m may be as frequent as 200 years. However, if the floodplains are interpreted as being essentially parallel, the repeat time is on approximately 1500 years.

## Reports

Morton, D.M., Matti, J.C., and Tinsley, J.C., 1987, Cucamonga fault zone carps, Day Canyon alluvial fan, Eastern San Gabriel Mountains, Southern California, in Hill, M. (ed.) Geological Society of America Centennial Field Guide, Volume I, p. 199-200.

Morton, D.M., Matti, J.C., and Tinsley, J.C., 1987, Banning Fault, Cottonwood Canyon, San Gorgonio Pass, Southern California: in Hill, M. (ed.) Geological Society of America, Centennial Field Guide, Volume I, p. 191-192.

## References Cited

Hays, W.W. and King, K.W., 1982, Zoning of the earthquake ground shaking hazard, in International Earthquake Microzonation Conference, 3rd, Seattle, WA, 1982, Proceedings, p. 145-156.

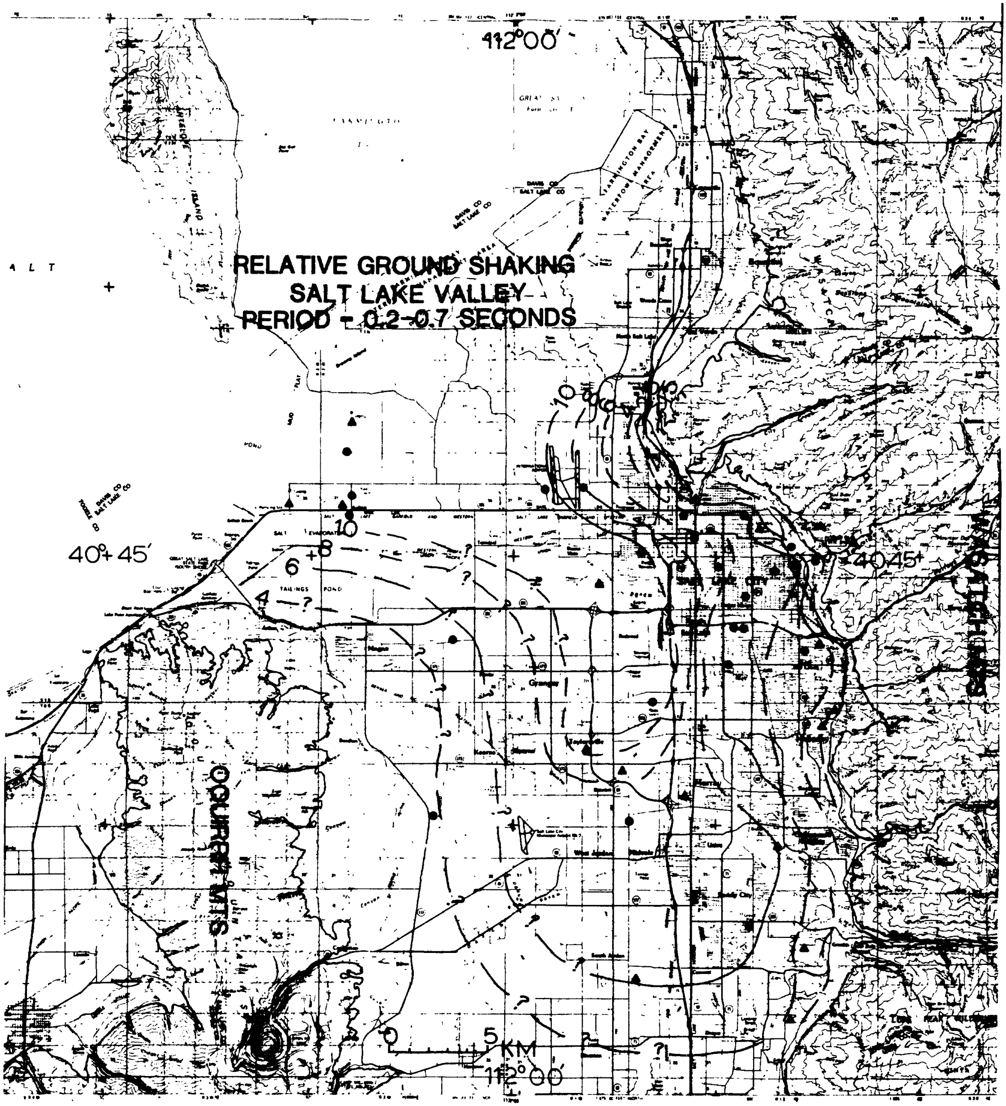

Figure 1. Map showing levels of ground shaking on alluvium relative to bedrock in the Salt Lake Valley in the period band 0.2-0.7 seconds, using the techniques of Hays and King (1982), but including additional geologic data. Map is preliminary and contours may be modified owing to further analysis of the data. Contours drawn by J. Tinsley on the basis of geology and using alluvium:rock spectral ratios recorded and computed by Kenneth W. King and Robert Williams.

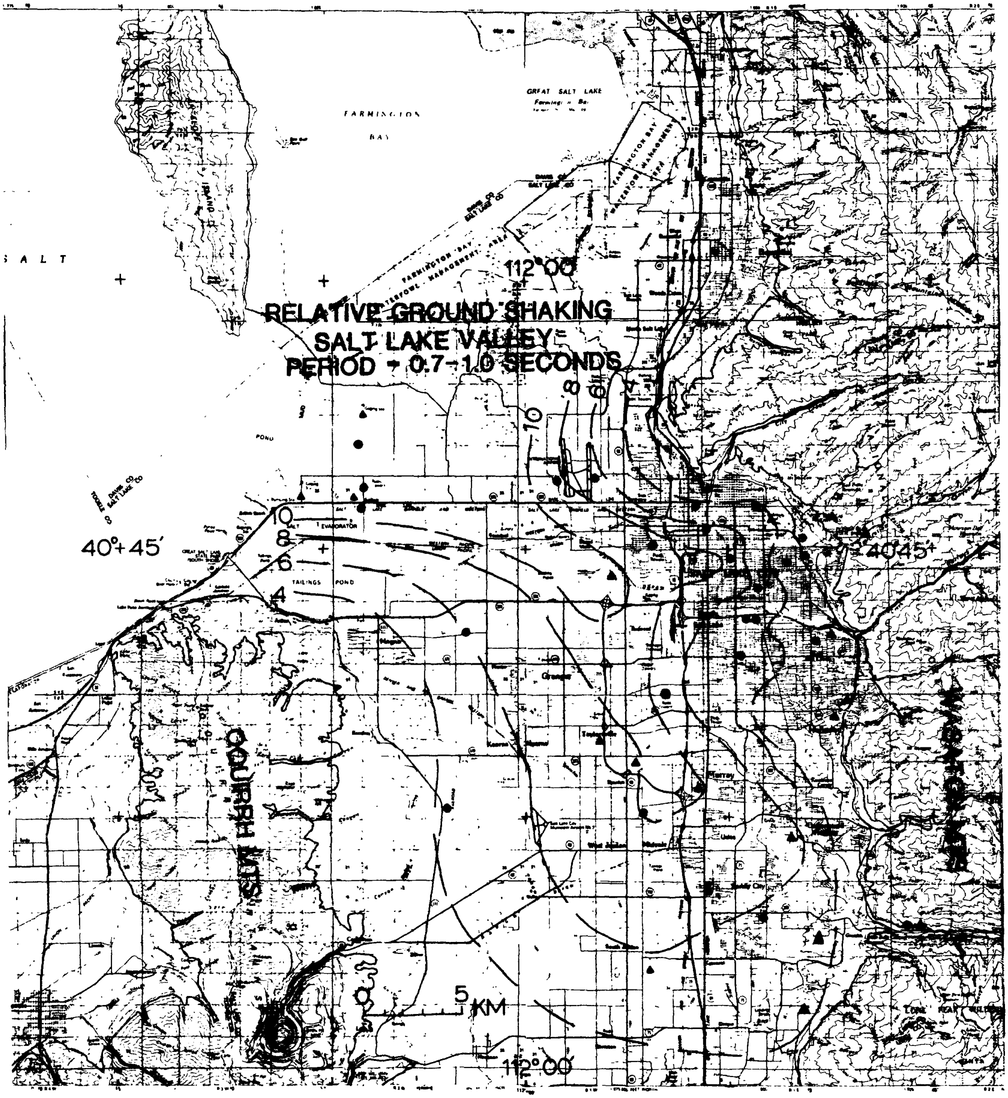

Figure 2. Map showing levels of ground shaking on alluvium relative to bedrock in the Salt Lake Valley in the period band 0.7-1.0 seconds, using the techniques of Hays and King (1982), but including additional geologic data. Map is preliminary and contours may be modified owing to further analysis of the data. Contours drawn by J. Tinsley on the basis of geology and using alluvium:rock spectral ratios recorded and computed by Kenneth W. King and Robert Williams.

# Seismic Reflection Investigations of Mesozoic Basins, Eastern U.S.

9950-03869

John D. Unger
Branch of Geologic Risk Assessment
U.S. Geological Survey
922 National Center
Reston, VA 22092
(703) 648-6790

## ONGOING INVESTIGATIONS

1. To consolidate and synthesize the available seismic reflection information that pertains to the internal and external structure of Mesozoic basins, with special emphasis on the hypocentral area of the present seismicity of Charleston, South Carolina and the Ramapo fault zone in New Jersey and Pennsylvania.

2. To use 2-D synthetic seismic reflection models of the basement structure along selected seismic reflection traverses in the Charleston and Ramapo regions as an aid to processing and interpretation of the seismic reflection data and to allow the use of ray-tracing algorithms to be used for earthquake relocation.

3. To use 2- and 3- dimensional GIS (Geographical Information System) techniques to display, analyze, and interpret geological and geophysical data collected in and around Mesozoic basins and other seismogenic structures in the Eastern U.S.

## RESULTS

Continuing studies using Dynamic Graphic's ISM software and ESRI's ARC/INFO software have resulted in promising possibilities for displaying the results of seismic reflection data analysis along with gravity, magnetic, and refraction information as three-dimensional models of the crust in and around Mesozoic basins. A key component of this process is the ability to use the high resolution color graphics available with the programs mentioned above in conjuction with software being written inhouse on high quality workstations such as the Sun 3 microcomputer now being used.

## REPORTS

Unger, J. D., 1987, Orientation of the decollement surface beneath the Chain Lakes massif: results of the 3-D seismic reflection study, Director's Approval 10/16/87.

Stewart, D. B., Unger, J. D., Phillips, J. D., Wright, B. E., and Luetgert, J. H., 1987, Prototype three-dimensional geographic information system (GIS) for deep crustal studies along a Global Geoscience Transect, GSA Annual Meeting Abstracts with Programs, v. 19, p. 885.

# A Search for Active Faults in the Willamette Valley, Oregon

14-08-0001-G1522

Robert S. Yeats
Department of Geology
Oregon State University
Corvallis, OR 97331-5506
503-754-2484

## Investigations

The Willamette Valley from Salem Hills to Portland is being studied by Ken Werner, and the Willamette Valley south of the Salem Hills is being studied by Erik Graven. We will work cooperatively with Ian Madin of DOGAMI in the Portland Hills and Portland Basin in providing information for a neotectonic map of the Portland metro area.

Seismic lines in the southern Willamette Valley, across the Salem Hills, and in the Tualatin Basin across the Gales Creek fault zone have been made available for our use.

A continuously-cored hole to 61 meters depth near Corvallis was drilled by the Oregon State Highway Division and logged by our group in cooperation with Alan Niem and Wendy Niem of OSU. This hole was designed to date a previously-unrecognized clay unit, the Calapooia Clay, that underlies the Wisconsinan Linn outwash gravels and overlies the Eocene Spencer Formation. Magnetostratigraphy will be done by Shaul Levi of OSU with support from this project.

Ken Werner, Erik Graven, Tom Berkman, and Mike Parker are using four-arm, dual-caliper dipmeter logs for deep wells in western Oregon to determine the orientation of principal compressive stress in western Oregon.

## Results

The Calapooia Clay was discovered during borehole investigations for a possible supercollider site in the southern Willamette Valley (CH2M Hill, 1987). It rests with angular unconformity on the Eocene Spencer Formation on a surface of moderate relief. Very preliminary age estimates based on pollen are Pleistocene, although a similar clay unit near Monroe was dzted as late Miocene-early Pliocene (Roberts and Whitehead, 1984). More detailed pollen investigations are forthcoming. The clay overlies a soil zone near the front of the Oregon Coast Range at Corvallis. We plan to date this clay unit and determine its structural relation with the nearby Corvallis fault, which has 450-600 meters vertical separation of Eocene marker horizons (Baker, 1988).

The seismic line across the Salem Hills near Amity demonstrates that the Salem Hills are not bounded by a fault but comprise the western limb of a syncline in Columbia River Basalt.

## References

Baker, L. J., 1988, The stratigraphy and depositional setting of the Spencer Formation, west-central Willamette Valley, Oregon: A surface-subsurface analysis: Corvallis, Oregon State University MS thesis

CH2M Hill, 1987, Superconducting Super Collider site proposal: University site, Oregon, v. 3, 1177 pp.

Roberts, M. C. and Whitehead, D. R., 1984, The palynology of a nonmarine Neogene deposit in the Willamette Valley, Oregon: Reviews of Palaeobotany and Palynology, v. 41, p. 1-12.

# Geophysical and Tectonic Investigations of the Intermountain Seismic Belt

9930-02669

Mary Lou Zoback
U. S. Geological Survey
Branch of Seismology
345 Middlefield Road, Mail Stop 977
Menlo Park, CA 94025
(415) 329-4760

## Investigations

1) Analysis of focal mechanism and fault slip data from the Wasatch front and Sierra Nevada-Great Basin transition region.

2) Continued compilation and analysis of global *in situ* stress data.

3) Analysis of the state of stress in the south-central United States, specifically in the vicinity of the Meers fault in south-central Oklahoma.

## Results

1) The direction of slip on a pre-existing fault plane depends on the orientation of the principal stresses with respect to that fault plane as well as their relative magnitudes. A forward modelling approach assuming principal stress orientations and using observed slip vectors for major earthquakes has been utilized to constrain relative stress magnitudes in actively deforming regions. This method was applied to the Owens Valley area, eastern California (site of a M~7.7 event in 1872) and to various other regions of active deformation in the province. One of the most significant results of this analysis is the indication of temporal variations in stress regime due to variations in relative stress magnitudes. Observations of nearly pure normal dip-slip and strike-slip events on sub-parallel faults are common within the Sierra Nevada-Basin and Range transition and the Basin and Range-Colorado transition. These observations are best explained by large fluctuation in the magnitude of the N-S horizontal principal stress (from $\approx S_V$ to $\approx S_{hmin}$).

2) *In-situ* stress data compiled by a variety of indicators show an excellent correspondence between orientations inferred from the different indicators despite the different depths sampled. The data indicate that the state of stress in the upper brittle crust is regionally uniform, permitting the definition of stress provinces. The intraplate stress regime is primarily compressive, extensional stresses occur almost exclusively in in anomalously high (thermally elevated) regions. A strong positive correlation between absolute plate velocity and $S_{Hmax}$ direction

in many midplate areas implies that the sources of stress are primarily plate tectonic origin and that the net balance of forces responsible for moving the plates is also responsible for stressing the plates. There is no indication that the state of stress in the crust is dominated by residual stresses from some past tectonic event.

Local geologic or crustal structure can strongly influence tectonic stress orientations. In a roughly 200 km wide band along the San Andreas fault zone principal stresses are aligned nearly parallel and perpendicular to to the fault. This pattern of stress can be explained by the slightly convergent relative plate motion and a very low shear strength for the San Andreas. Geologically young reverse faults and folds which generally parallel the San Andreas are well explained by fault normal compression.

Another example of the influence of local structure on stress orientations is observed in the western Atlantic outer continental shelf region. In this area extensional stresses acting along the passive continental margin result in rotation of the tectonic stresses to be approximately parallel and perpendicular to the trend on the margin.

3) Over 180 dipmeter logs were examined from a region extending from the Texas panhandle to the Mississippi River. Orientations were determined for over 1000 breakouts in these wells. Data from wells in the central to eastern part of the study area (from Oklahoma to the Mississippi River) form a high quality data set; a consistently orientated ENE $S_{Hmax}$ (maximum horizontal stress) direction was inferred from those data. This result is confirmed by hydrofracture studies in central Okalhoma and the Texas panhandle which indicate $S_{Hmax}$ orientations of N65°E and $N40 - 60°E$, respectively. The ENE $S_{Hmax}$ orientation is consistent with evidence of left-lateral reverse oblique slip on the WNW-striking Meers fault in south-central Okalahoma.

A possible deviation from the regional stress pattern was observed in the southwestern part of the study area. Here a nearly orthogonal pattern of breakouts suggest both NE and NW $S_{Hmax}$ orientations. One set of breakouts may be indicating the true $S_{Hmax}$ orientation (~NE). Additional well data (including leak-off tests) are now being examined to determine if one set of breakouts may in fact be drilling-induced hydrofractures which were later enlarged by erosion by motion of drilling fluids. Orthogonal sets of breakouts have been observed in numberous wells in coastal California and have been interpreted in a similar manner.

## Reports

Zoback, M. L., 1987, Global pattern of tectonic intraplate stresses: EOS (Trans. American Geophysical Union), v. 68, p. 1209-121. *presently being prepared as an invited review article for Nature.*

Dart, R. L., 1987, South-central United States well-bore breakout data catalog: U. S. Geological Survey Open-file Report 87-405, 95 p.

# Earthquake Loss Estimation Modeling of the Seattle Water System

14-08-0001-G1526

Donald Ballantyne
Kennedy/Jenks/Chilton
33301 Ninth Avenue South, Suite 100
Federal Way, Washington 98003
(206) 874-0555

Objective: The Puget Sound Region suffered magnitude 7.1 and 6.5 earthquakes in 1949 and 1965 respectively. USGS is currently evaluating potential for a magnitude 8+ earthquake in the region. While some California water utilities have done rigorous earthquake planning, water utilities in the Puget Sound region are not as advanced in their planning to mitigate earthquakes. The Seattle Water Department (SWD) is the largest water supplier in the state, serving City residents as well as wholesaling water to 31 purveyors. While SWD has recently undertaken a project focusing on vulnerability of system structural components, their system has not been evaluated for operability following an earthquake.

This project is developing and applying techniques for estimating earthquake losses to the water system. The SWD system is being inventoried, and then modeled to estimate the loss of function based on the severity of ground shaking.

Data Collection and Review: Geological and seismological data being developed by USGS will be identified and reviewed for its applicability for input into the model. Existing applicable data will be collected and organized.

The system is being inventoried by line and node number, facility category, and Geographic Base File data. System operation parameters, such as flow and pressure, are being determined. Earthquake vulnerability data such as pipe and joint material type and structural design criteria are being gathered.

System Characterization: Data for a system network model using KYPIPE (Kentucky program) are being developed, considering appropriate segmentation of the system. System features important to vulnerability assessment, such as isolation valve location, are being incorporated.

Hazard Definition: Hazards maps will be prepared to facilitate input of data currently under development by USGS.

Component Vulnerability: Algorithms will be developed for percent loss of function for categories of system components for varying design earthquakes. Algorithm input will be based on site-specific geotechnical data, as well as structural and mechanical design of the facilities.

System Vulnerability: A system vulnerability model will be developed to modify input data files to KYPIPE, based on component vulnerability algorithms. As part of this model, system connectivity will be assessed to allow operation of KYPIPE. Earthquake parameters will be varied to establish operational criticality of each component.

# Earthquake-Resistant Design and Structure Vulnerability

9950-04181

Edgar V. Leyendecker
Branch of Geologic Risk Assessment
U.S. Geological Survey
Denver Federal Center, M.S. 966
Denver, CO 80225
(303) 236-1601

## Investigations

1. Work is in progress to examine, evaluate, and improve the estimation of casualties and aggregate monetary losses associated with the occurrence of earthquakes in the United States.
2. Work is continuing on development of improved measures of vulnerability of structures to damage, including the refinement of our understanding of earthquake damage and the applicability of the existing data base on earthquake damage.
3. Investigations continue for development/identification of cost-effective techniques for determining inventory at risk.
4. The October 1, 1988 Whittier Narrows earthquake provided an occasion to evaluate and refine these procedures for loss-estimation and damage survey that are under development.

## Results

1. Plans are being made for development of an improved and consistent loss-estimation methodology that can be applied in a uniform way on a regional basis for the estimation of losses throughout the United States. Planning for a USGS Workshop on earthquake losses to be held in late FY 88 has started.

   Earthquake loss studies may be of the "deterministic" or "probabilistic" type. A scenario study might consider the consequences of one or more earthquakes; frequently this might be the largest likely earthquake. Such a study is very useful for purposes such as emergency planning. The probabilistic study considers both magnitude and frequency of occurrence and may be "more realistic" than the above "worst case" scenario. Both deterministic and probabilistic studies are being considered for the Puget Sound area, an area under current study in the Urban Hazards Program. Emphasis is being placed on developing the tools for use in loss studies rather than a complete assessment for the region. Accordingly a limited area of Seattle has been selecting for conducting a detailed study of losses. It includes West Seattle, an area with considerable damage in 1965, and portions of downtown Seattle.

2. Examination of current vulnerability relationships is underway with a review of existing earthquake damage data bases. Plans for the collection of earthquake damage data following selected earthquakes have been made, including development of data collection techniques. Improvement of vulnerability relationships, including parameter variability, depends heavily on the collection of earthquake damage data.

   The 1983 Insurance Services Office (ISO) classification system is being used for the inventory survey of buildings and vulnerability relationships. This classification uses a system of 5 major classes as shown below:

   Class 1: Wood frame structures
   Class 2: All-metal buildings
   Class 3: Steel frame buildings
   Class 4: Reinforced concrete buildings, combined reinforced concrete and structural steel buildings
   Class 5: Concrete, brick, or block buildings

   This system was selected for its relative simplicity and ease of use by a lay person with a limited amount of training.

   This system was used for work on the Whittier Narrows earthquake and is planned for use in the Seattle area.

3. Development of inventory at risk is costly and is a major impediment to accurate loss estimates. A study of the critical elements of inventory needed for loss assessment in urban areas, including field inventory techniques is in progress. Plans for preparation of inventory training procedures are underway. Both the survey and training procedures are being evaluated following trial use in Whittier.

   The data collection procedures are centered around (1) a simple system for classifying buildings, (2) the census tract as the basic area for data collection, and (3) machine read "mark-sense" sheets for compiling a computer data base. It should be noted that the procedures can be used for either inventory or damage surveys.

   The census tract is being used as a data collection unit in order to simplify the inventory of buildings. Since census data provide a relatively accurate count of residential construction, this is one component of an inventory that does not have to be compiled in detail. The type of residential construction (type of frame, siding, etc.) can be determinied relatively simple statistical sampling. Other types of structures require additional inventory work. Additional extensive sampling will be required in order to develop suitable inventories for structures other than dwellings.

   Data will be collected on "mark-sense" sheets which describe building class and various types of damage if it is a damage survey. The mark-sense sheets are preprinted forms with multiple choice responses that are filled out with a soft lead pencil. The "marks" by the soft lead pencil can be "sensed" by an optical scanning device and read into a computer data base.

A plan for an inventory in a limited portion of the Seattle urban area is being developed for using these techniques.

4. The methodologies under development were tested following the October 1, 1988 Whittier Narrows Earthquake. The survey procedures worked relatively well. However, it was concluded that the specific data recorded on the mark-sense sheets, while adequate, should be simplified as much as possible for use in future studies. There were also indications that minor modifications were desirable in the building classification system but major changes are not anticipated in the near term.

## Reports

Leyendecker, E.V., Highland, L.M., Hopper, M.G., Arnold, E.P., Thenhaus, P.C., and Powers, P.S., 1988, *Early Results of Isoseismal Studies and Damage Surveys for the Whittier Narrows Earthquake*, Spectra, Earthquake Engineering Research Institute.

# VULNERABILITY OF HIGH-RISE BUILDINGS IN CHICAGO AND ATLANTA TO A GREAT EARTHQUAKE IN THE NEW MADRID SEISMIC ZONE

Award Number: 14-08-0001-G1347

Principal Investigator: Dr. Lincoln E. Malik

URS/John A. Blume & Associates, Engineers
150 Fourth Street
San Francisco, California 94103
(415) 957-5300

The purpose of this study was to address concerns about the vulnerability of tall buildings (20 stories and greater in height) in Atlanta and Chicago to a great earthquake in the New Madrid seismic zone. These concerns are motivated in part by the historical precedent set by a sequence of very large earthquakes that occurred near New Madrid, Missouri, during the winter of 1811-1812. Research into this sequence has made earthquake engineers and disaster management officials more aware of the potential for seismic damage in areas heretofore considered virtually immune to such hazards. It has been observed that damaging levels of ground motion can propagate to much greater distances from these great events in the central United States than from similar events in the western United States. Furthermore, the duration of surface waves from the events will increase with distance. Thus, a great earthquake in the New Madrid seismic zone could cause long-duration, long-period motions in Chicago and Atlanta, which might be hazardous to tall buildings.

This concern was first addressed by a study that URS/John A. Blume & Associates, Engineers, conducted for the Federal Emergency Management Agency (FEMA) in 1985. The performance of tall buildings in Atlanta, Chicago, Dallas, and Kansas City (Missouri) were qualitatively evaluated for a major earthquake anywhere in the New Madrid seismic zone. Since the soil deposits at Chicago and Atlanta amplify ground motions at selected frequencies, the study recommended a more refined study for those two cities.

This study used a methodology that is an improvement over that used in the FEMA study, with improvements in the characterization of ground motion, the dynamic modeling of buildings, and the quantitative evaluation of damage. Ground motions in the two cities were synthesized using the numerical procedures of quantitative seismology. Bedrock ground motions were estimated to have peak ground accelerations (PGAs) of 0.020g and 0.013g in Atlanta and Chicago, respectively. Local soil conditions in Atlanta increase the PGA to 0.026g and amplify the motions by a factor of 2 for periods between 0.6 and 0.7 sec. In Chicago, local soils increase the PGA to 0.032g and amplify motions by a factor of 5 for periods between 0.6 and 0.7 sec.

Additional information obtained on the proportions, sizes, weights, and features of buildings in the two cities permitted development of dynamic models that were analyzed by a structural analysis computer program. Story shears, overturning moments, and interstory drifts were calculated for 20-, 40-, and

80-story generic buildings using modal superposition, response spectrum analysis.

A panel of experts was asked to estimate seismic damage by comparing the responses from the postulated earthquake and the design wind loads. The panel's estimate of damage levels indicates that tall buildings in Atlanta will sustain damage losses of about 1% to 2% of replacement cost, almost entirely nonstructural damage. This estimate applies to buildings that are free of irregular features such as high first stories, setbacks, and highly nonsymmetrical floor plans. Some slight, but not significant, structural damage may occur in a few regular buildings. Irregular buildings in Atlanta are expected to sustain greater losses, and some may experience significant structural damage.

In Chicago, the expected losses for regular buildings in the 20- to 50-story range are about 3% but are less than 1% for extremely tall buildings around 80 stories. Buildings with irregular floor plans, setbacks, and other irregular structural features are expected to sustain greater losses, and some may experience significant structural damage. Damage to irregular buildings could have a greater impact on the total damage in Chicago than in Atlanta because irregular features seem to be more common in Chicago.

It is recommended that more details on irregular building features be obtained and that their effects on damage be studied. Given the amount of amplification of motion around periods of 0.7 sec in Chicago, it is recommended that a similar study be conducted of buildings of 5 to 15 stories.

# Inventory Technique Development - Puget Sound/Oregon.

14-08-0001-G1515

Bruce C. Olsen
Consulting Engineer
1411 Fourth Avenue
Seattle, WA. 98101-2216
(206) 624-7045

## Initial Investigation

Work under this contract was initiated in January of 1988 and has proceeded through the following areas:

1. Literature Search and personal communications.
2. Establishment of scope of desired information to be obtained.
3. Development of data source contacts and list expansion. Correspondence with sources and initial interviews.
4. Concentrated localized urban area study. (City Center, Seattle.)
5. Development of suitable questionnaire for differing sources.

## Results

This work is being undertaken because there is relatively little guidance relative to inventory development readily generally applicable and without prohibitive effort and expense. The literature available from previous inventorying efforts is limited, and in some cases inappropriate. However, some procedures followed in prior work may be incorporated in guidelines resulting from this study.

Information which should be included in the inventorying effort includes many different elements. In order to investigate vulnerability as well as to perform loss estimation studies, there is a need for structural data, site condition information, nonstructural conditions and occupancy information.

To this point in the investigation it has been found that availability of data varies greatly with communities and their record-keeping systems. Computerising of information has potential for good inventory information, provided the data retained in the computerized records includes the material useful to subsequent investigation. This does not necessarily correspond to material which appears pertinent to the city or county. Additionally, the use of computerised records is quite recent, and much historical record is only available through manual search.

Appropriate information may be available through various public channels, including assessor records, building department records, and other related public body sources. Pursuing material through these sources is not necessarily fruitful, since the records retained are sometimes fragmentary and may be inadequate. Moreover, this material often requires extensive time and effort for interpretation and reduction. A careful look at the material which is considered essential must be taken, so that time is not wasted in pursuing material not readily available.

A detailed investigation has been carried out on a limited sample of an urban city center, involving a sidewalk survey approach compared with a study of community records. This provides some verification of records and also a picture of the usefulness of the material available from city records. It can also be useful in conjunction with a parallel loss estimation study.

In conjunction with the investigation questionnaires have been developed for city and county agencies, to obtain responses for the type of material desired. These have been used in conjunction with direct interviews, rather than as a mail-out questionnaire. In some cases it will be necessary to review and repeat the questionnaire, possibly modified. A modified questionnaire will be utilised in telephone follow-up with small communities which may have some information of interest.

Over the next quarter an effort will be made to expand the area of investigation to both the north and south, and also to digest some of the urban-area etailed study which has been performed in Seattle.

********************

# LATE QUATERNARY FAULTING, SOUTHERN SAN ANDREAS FAULT

9910–04098

Michael J. Rymer

Branch of Engineering Seismology and Geology
U.S. Geological Survey
345 Middlefield Road, MS/977
Menlo Park, CA 94025
(415) 329–5649

## Investigations

1. Postearthquake investigations of the November 23 and 24, 1987 Elmore Desert Ranch and Superstition Hills earthquakes, respectively.
2. Trenching investigation of the San Andreas fault in the Durmid Hill–Bombay Beach area.

## Results

1. Surface rupture along the Superstition Hills fault and related faults located to the northeast were mapped and measured by Rymer during the first 16 days following the Elmore Desert Ranch ($M_L$ = 6.2) and the Superstition Hills ($M_L$ = 6.6) earthquakes. Rymer concentrated on the central 10 km of surface rupture on the Superstition Hills fault and documented right-lateral surface displacements of as much as 80 cm, which includes approximately equal amounts of coseismic and postseismic slip; postseismic slip is continuing as of the time of this writing. Also, about 115 stations were occupied along the Superstition Hills fault, and about 45 stations along north-south-, northeast-southwest-, and northwest-southeast-trending faults. Many of the stations along the Superstition Hills fault were reoccupied for measurement of postseismic slip during February and March, 1988. (See report by R. V. Sharp, this volume, for more detail on the postseismic investigations following the earthquakes.)
2. A 28–m–long exploratory trench was exposed across the San Andreas fault in the "dog leg" section of the fault between Durmid Hill and Bombay Beach. The trench was as much as 3 m deep and exposed late Holocene(?) lacustrine and fluvial deposits. Investigations of the trench, with R. V. Sharp, revealed faults throughout its length; the fault zone was not entirely spanned by the trench. Five main breaks, with at least 1 m of right–lateral component of displacement (the width of the trench), were exposed. Also, dozens of secondary breaks with unknown but smaller displacements were exposed in the trench. Numerous marker beds are present in the exposures, along with channel-fill deposits that will aid in determining displacement across individual breaks and the entire fault zone. The uppermost unit, as much as 40 cm thick, is a lacustrine gastropod-rich sand that is not broken by any of the faults; all other sedimentary units are broken by one or more of the faults. The uppermost unit is presumably from Lake Cahuilla that dried up about 300 years ago; the site is at a higher elevation than the high stand of 1905–1907 Salton Sea flooding. The trench study of the fault zone at this location is preliminary. The complexity of the fault zone at the site indicates that an extensive effort is needed to fully understand the timing of earthquakes and the slip rate at the site. To date, we cannot rule out the possibility of only one earthquake producing the entire set of breaks exposed in the trench.

## Reports

None

# Historical Normal Fault Scarps -- Wasatch Front and Vicinity

9910-04102

David P. Schwartz
Branch of Engineering Seismology and Geology
U.S. Geological Survey
345 Middlefield Road, MS 977
Menlo Park, California 94025
(415) 329-5651, FTS 459-5651

## Investigations:

The project goal is to study historical and recent normal fault scarps in the Great Basin in order to calibrate geological techniques used to identify individual past earthquakes and the amount of displacement during each, quantify earthquake recurrence intervals, and evaluate earthquake recurrence models and fault segmentation models. Investigations have concentrated on 1) recurrence and segmentation along the 1983 Borah Peak, Idaho surface rupture and associated scarps of the Lost River fault zone, and 2) recurrence and paleo-displacements on the Wasatch fault zone at the Dry Creek site near the southern end of the Salt Lake segment and at the Mapleton site on the Provo segment.

## Results:

1. Lost River fault zone, Idaho (Schwartz and Crone)

   Results to date were summarized in U.S. Geological Survery Open-File Report 88-16. No new field work was conducted during the present report period (Fall 1987-Winter 1988). Additional charcoal samples have been submitted for dating. Mapping of existing trenches on the Warm Spring and Mackay segments, and scarp profiling to determine slip distribution during the pre-1983 earthquakes, will continue during Summer 1988.

2. Wasatch fault zone, Utah (Schwartz and Budding; W.R. Lund, Utah Geological and Mineral Survey)

   No new field work was conducted during the report period (Fall 1987-Winter 1988).

   A) Dry Creek Site. Bulk samples of an organic A-horizon soil that was buried by scarp colluvium at the time of the most recent surface-faulting earthquake were prepared and submitted for radiocarbon dating. It is hoped that the new dates will resolve ambiguities in the timing of this event, which appears to have occurred between 1,100 and 1,900 years ago.

   B) Mapleton site. New accelerator radiocarbon dates were obtained from faulted deposits at the Mapleton South trench site. Charcoal from a buried A-horizon soil that was displaced by two events yielded a date of 2810±95 $^{14}$C yr B.P.. A TL date from this same horizon had previously given an age of 5500±250 years. Charcoal from an overlying debris flow displaced by only the most recent event yielded an age of 1350±100 $^{14}C$ yr BP, consistent with a dendro-corrected age range of 1170 AD to 1480 AD for the same event in a trench 0.8 km to the north. Additional radiocarbon and TL dating of the displaced A-horizon is being undertaken to evaluate the reasons for the differences in age estimates using both techniques.

Reports:

Schwartz, D.P., and Crone, A.J., 1988, Paleoseismicity of the Lost River fault zone, Idaho: Earthquake recurrence and segmenttation [abs]: Geological Society of America Abstracts with Programs, Cordilleran Section, v. 20, no. 3, p. 228.

Schwartz, D.P., Lund, W.R., Mulvey, W.E., and Budding, K.E., 1988, New paleoseismicity data and implications for space-time clustering of large earthquakes on the Wasatch fault zone, Utah [abs.]: Seismological Society of America, Annual Meeting, Honolulu, Hawaii, Seismological Research Letters, in press.

# San Andreas Segmentation: Cajon Pass to Wallace Creek

9910-03983

David P. Schwartz, Robert V. Sharp, And Thomas Fumal
Branch of Engineering Seismology and Geology
U.S. Geological Survey
345 Middlefield Road, MS 977
Menlo Park, California 94025
(415) 329-5651, (415) 329-5652

## Investigations

The project goal is to refine existing and/or develop new segmentation and fault behavior models for the San Andreas fault between Wallace Creek and Cajon Pass.

1. Develop new slip rate and recurrence data from Wallace Creek to south of Cajon Creek.

2. Critically review published and unpublished data and, where possible, existing field relationships to define and quantify uncertainties in: a) timing, displacement, and lateral extent of individual past earthquakes; and b) location-specific slip rate estimates.

3. Map and characterize the style of secondary faulting along the San Andreas, particularly near the junction with the San Jacinto fault on the south and near Liebre Mountain on the north.

## Results

1. Wrightwood site. Field work during Fall, 1987 focused on three-dimensional trenching of the four secondary fault traces south of the main zone. Four trenches, each approximately 50 m long, were excavated and logged. Trench 6 was excavated parallel to and 2 m southeast of trench 1, which was the main trench excavated in 1986. Trenches 4 and 5 were excavated parallel to and approximately 25 m to the northwest-southeast respectively, of trench 1. Trench 3 connected the north ends of trenches 1, 4, 5 and 6, thus enabling us to trace the stratigraphy from one trench to the next.

   The southernmost secondary fault consistently dips to the north; a normal component of slip is dominant, in contrast to the other secondary fault traces. A peat, which yielded dates of 1436 to 1658 AD and occurs near the surface over much of the site, is buried by up to 2 meters of sediment at this fault. This sediment contains two distinct colluvial wedges apparently derived from the fault scarp, thereby suggesting two separate faulting events during the past 400 years.

   The other secondary faults generally exhibit variable geometry and break to different stratigraphic horizons along strike. Because of this variability, these fault traces are likely to be less useful for distinguishing individual faulting events. Large amplitude folds show much more consistency from trench to trench and may prove to be more useful for defining the number of events. Preliminary analysis suggests there may have been a 7 to 8 distinct episodes of folding during the past 1300 years.

Samples of ten of the peats occurring between the two dates previously reported from the top and bottom of the section exposed in these trenches have been submitted for dating. These samples should provide a detailed chronology of sedimentation events and deformational episodes at this site. (Fumal, Weldon, Schwartz)

2. D. Schwartz and R. Sibson (U.C. Santa Barbara) convened a USGS Workshop on Fault Segmentation and Controls of Rupture Initiation and Termination, Palm Springs, California, 6-9 March, 1988.

# Earthquake Hazards Studies, Metropolitan Los Angeles-Western Transverse Ranges Region

9540-02907

R.F. Yerkes
Branch of Western Regional Geology
345 Middlefield Road, MS 975
Menlo Park, California 94025
(415) 329-4946

## Investigations and results

1. Historic earthquakes (Yerkes and W.H.K. Lee). Evaluated structural setting and contributed to reports on the Whittier Narrows earthquake of 10/01/87. The $M_L$ 5.9 earthquake occurred at a depth of about 14 km and about 10 km below the basement-rock surface on a previously-unrecognized south-directed thrust that underlies an extensive east-west antiform in basement and superjacent rocks. The 1973 $M_L$ 5.9 Point Mugu and 1979 $M_L$ 5.0 Malibu reverse-fault earthquakes may be related to the same zone of deformation. The largest ($M_L \sim 5$) aftershock of the 1987 sequence occurred 3 km northwest of the mainshock epicenter, was a right-lateral strike-slip event trending N. 35° W., and was precisely aligned with a sharply-defined late Pleistocene fault-line scarp that marks the northeast margin of the Montebello Hills (immediately southwest of the 1987 earthquake zone). The sequence nowhere ruptured to the ground surface; peak accelerations from the main-shock reached 0.6g within 50 of the epicenter.

   Continued preparation of reports on 360 single-event fault-plane solutions derived from 2500 events for 1974-1985 within a 40 x 175-km segment of the south boundary zone of the Transverse Ranges between Santa Barbara Channel and the San Jacinto fault zone.

2. Quaternary stratigraphy, chronology, and tectonics, southern California region (Sarna-Wojcicki and Meyer, BWRG). This investigation is currently focusing on improvement of age control for Quaternary deposits, and on providing age control for studies of neotectonics in southern California and elsewhere in the Western Region.

   a. Continued investigations reported in vol. XXIV, p. 621-623, USGS OFR 87-374.

   b. Current results of studies in support of active faulting and tectonic studies are:

   (1) A suite of about 50 tephra layers was sampled from the area south of Fish Lake Valley, in order to provide age control for a study of late Cenozoic tectonics in the "seismic gap" area of west-central Nevada and east-central California, along the northern extension of the Furnace Creek fault zone (with Marith Reheis, BCRG, and Janet Slate, Univ. of Colorado, Boulder). Preliminary results based on electron-microprobe analyses of volcanic glass shards by Charles Meyer (BWRG) provide several correlations to tephra layers that have been

isotopically dated or are closely bracketed by age data at other sites. Among these tephra layers are the Putah and Nomlaki Tuffs (both dated at 3.4 Ma by K-Ar), found in the study area in the Esmeralda Fm.; Tuff C-83-6A, which we estimate to be 2.1 ±0.1 Ma, found near the top of the Esmeralda Fm.; several tephra layers in late Cenozoic deformed gravels overlying the Esmeralda Fm., which we correlate with the compound Tuff of Taylor Canyon, estimated to be between 2.0 and 1.7 Ma on the basis of K-Ar dates (John Nakata, BWRG), and the Bishop ash bed, found in faulted alluvium in Fish Lake Valley, and dated elsewhere at 0.74 Ma (table 1). Additional tephra layers collected from this area are also being currently analyzed.

(2) We have also identified the Nomlaki Tuff in northern Death Valley, in deformed late Cenozoic fan alluvium of the Nova Fm., west of the Furnace Creek/Death Valley fault zone, and a tephra layer in faulted fan alluvium that we correlate more generally with mid-Pleistocene tephra layers erupted from the Long Valley caldera, in the age range of about 0.74 to 1.2 Ma (coop. study with John Tinsley, BWRG).

(3) We have also identified the Nomlaki Tuff and Tuff C-83-6A (see above) in cores obtained from Bristol Dry Lake, Mojave Desert, CA (see table 1). (work for Mike Rosen, University of Texas, San Antonio).

(4) A suite of mid-Quaternary tephra layers found on Paoha Islnad in Mono Lake, and correlative tephra layers exposed at Benton Crossing, north of Lake Crawley in Long Valley caldera, east-central California, have been identified previously by this project and are associated with a brief magnetic reversal within the Brunhes Chron (coop. work with Ken Lajoie, BESG, Roy Bailey, BIGP, and Joe Liddicoat, Univ. of California, Santa Cruz). Our recent correlation of part of this sequence to tephra layers at Tulelake, Ca., and Summer Lake, Ore. (coop. with Dave Adam, BPAS, and others, and J. O. Davis, Desert Research Institute, Reno, Nev., respectively), indicate that the reversal is about 290 Ka in age, the same as that estimated for the Biwa 2 reversal found in cores of Lake Biwa, Japan (Duane Champion, BIG), and consequently is probably that event. This suite of tephra layers forms an important set of time and stratigraphic markers that can be used in assesment of seismic hazards, and volcanic hazards in the Long Valley caldera in post-Bishop Tuff time.

## Reports

R.F. Yerkes, Paia Levine, and W.H.K. Lee, 1987, Contemporary tectonics along the south boundary of the central and western Transverse Ranges, southern California (abs.): EOS, vol. 68, no. 44, p. 1510.

Haukkson, Egill, L.M. Jones, T.L. Davis, L.K. Hutton, A.G. Brady, P.A. reasenberg, A.J. Michael, R.F. Yerkes, and others, 1988, The 1987 Whittier Narrows earthquake in the Los Angeles metropolitan area, California: Science, vol. 239, p. 1409-1412.

Davis, T.L., and Yerkes, R.F., Application of retrodeformable cross sections to seismic risk evaluation of the Los Angeles basin and the Whittier Narrows earthquake (M 5.9) of October 1, 1987: submitted to Geology 3/88.

Table 1. Electron-microprobe analysis of volcanic glass shards from several tephra layers in the western U.S. that provide age control to neotectonic studies. C. E. Meyer (BWRG, Menlo Park), analyst. Values given are concentrations in weight percent, recalculated to 100 percent on a fluid-free basis.

| Sample | FLV-20-WW | 758-292 | FLV-21-WW | RSPL-1 | CAES-1 | FLW-52-WW | C-83-6A | CAES-2 | FLV-4-WP | BT-8 |
|---|---|---|---|---|---|---|---|---|---|---|
| $SiO_2$ | 74.98 | 74.90 | 77.21 | 77.27 | 77.55 | 72.48 | 72.50 | 73.23 | 77.93 | 77.40 |
| $Al_2O_3$ | 13.62 | 13.92 | 12.88 | 12.69 | 12.48 | 13.92 | 14.47 | 14.50 | 12.49 | 12.73 |
| $Fe_2O_3$ | 1.77 | 1.76 | 1.10 | 1.14 | 1.06 | 2.70 | 2.73 | 2.69 | 0.74 | 0.72 |
| MgO | 0.11 | 0.09 | 0.22 | 0.19 | 0.19 | 0.27 | 0.27 | 0.27 | 0.05 | 0.04 |
| MnO | 0.03 | 0.03 | 0.05 | 0.06 | 0.03 | 0.10 | 0.11 | 0.08 | 0.04 | 0.04 |
| CaO | 0.72 | 0.72 | 0.99 | 1.01 | 0.97 | 0.92 | 0.89 | 0.91 | 0.44 | 0.45 |
| $TiO_2$ | 0.14 | 0.14 | 0.21 | 0.24 | 0.19 | 0.32 | 0.29 | 0.31 | 0.06 | 0.06 |
| $Na_2O$ | 4.03 | 4.06 | 3.97 | 3.98 | 3.92 | 6.10 | 5.39 | 5.37 | 3.73 | 3.34 |
| $K_2O$ | 4.61 | 4.36 | 3.36 | 3.42 | 3.61 | 3.19 | 3.36 | 2.64 | 4.53 | 5.22 |
| Total[1] | 93.29 | 92.93 | 93.22 | 94.95 | 93.72 | 91.37 | 92.75 | 90.51 | 93.98 | 94.17 |

[1] Original total before recalculation to 100 percent.

FLV-20-WW - Tephra layer in Esmeralda Fm., Willow Wash section, south of Fish Lake Valley, Nev.

758-282 - Putah Tuff in Tehama Fm., southwestern Sacramento Valley, Ca., dated 3.4 Ma, by K-Ar (Sarna-Wojcicki, 1976).

FLV-21-WW - Tephra layer in Esmeralda Fm., Willow Wash section, stratigraphically above FLV-20-WW.

RSPL 1 - Nomlaki Tuff in Tuscan Fm. at Richardson Spring, eastern Sacramento Valley, Ca. (D. Harwood and A. M. Sarna-Wojcicki, unpublished data).

CAES-1 - Tephra layer at 829 feet in core 1, Bristol Dry Lake, Mojave Desert (M. Rosen, Univ. of Texas, San Antonion, written commun.).

FLV-52-WW - Tephra layer near top of Esmeralda Fm. or base of overlying late Cenozoic gravels, Willow Wash section, Fish Lake Valley, Nev. Stratigraphically overlies FLV-21-WW.

C-83-6A - Tephra layer in the lower part of the Tulare Fm., Kettleman Hills, west-central San Joaquin Valley, Ca. Age control at Kettleman Hills and at Willow Wash section constrain age of this layer to 2.1 Ma ±0.1 Ma (Obradovich and others, 1978, and A. M. Sarna-Wojcicki, M. Reheis, and C. E. Meyer, unpub. data).

CAES-2 - Tephra layer at 1499 feet in core 2, Bristol Dry Lake, as above.

FLV-4-WP - Tephra layer exposed in deformed alluvium at Wingate Pass, Inyo Mountains (M. Reheis and J. Slate, unpub. data).

BT-8 - Bishop ash bed underlying Bishop Tuff at Insulating Aggregates Quarry, north of Bishop, Ca. (Sarna-Wojcicki and others, 1984).

# A Demonstration Project on Seismic Risk Assessment and Hazard Mitigation through Land Use Planning

USGS Grant No. 14-08-0001-G1386

Philip C. Emmi
Department of Geography
University of Utah
Salt Lake City, Utah 84112
(801) 581-5562

## Research Objectives

A serious earthquake affecting lives and property along the Wasatch Front is a real possibility . Counties and municipalities are well advised to assess the risks and take appropriate action. The goal of this study is to compile and translate research on seismic and related geologic hazards in Salt Lake County, Utah, into a form which has meaning for public decision makers. Objectives include integration of hazards maps into a computer-based geographic information system, compilation of mapped data on cultural features, loss estimation, communication of seismic risk assessments, and evaluation of mitigation policy options.

## Accomplishments and Results

To date, we have collected over eighty-two data and digital map files. These include boundary files, digital maps on seismic and related geologic hazards, digital maps and data files on current and projected (2005) population, building inventories and land use, and digital map and data files on related elements of the built environment (lifelines, critical facilities, etc.). These are maintained on a geographic information system with digital cartographic overlay and analysis capabilities.

The most recent additions to our collection of digital map files are maps showing the distribution of residential structures by frame type, residential structures by value, and projections to year 2005 of residential structures by type and value. Development of a comparable set of files for commercial and industrial structures is now under way.

Our most significant results to date rely on earlier studies of probabalistic estimates of maximum bedrock velocities and bedrock-to-soil transfer functions to derive estimates of the intensity and spatial distribution of seismically induced ground shaking. The result are presented as a set of maps describing Modified Mercalli Intensities with a 10% chance of exceedence over 10, 50 and 250 year periods (Emmi, 1987). These maps are essential to an estimate of expected loss to property and lives due to seismic risk.

We have been engaged in an effort to improve upon the MMI maps in several different ways. Our earlier mapping efforts were based on Algermissen's (1982) estimates of peak bedrock velocities, bedrock-to-soil spectral transfer functions by Hayes and King (1982), and a velocity-to-MMI relationship presented by Everendon and Thompson (1985).

We are now exploring ways to use a 1987 report by Young and others on the earthquake ground shaking hazard along the Wasatch Front. This report provides a probabalistic assessment and mapping of peak ground acceleration along the Wasatch for different recurrence intervals. Our efforts are focused on defining the corresponding estimates for peak bedrock velocities. These would then substitute for Algermissen's estimates in our attempt to generate probabalistic estimates of MMI. Our efforts to define corresponding bedrock velocities has involved us in an exploration of the relationship between the velocity-to-acceleration conversion factor and the recurrence interval.

A second way to improve upon our earlier MMI mapping efforts is to base estimates of bedrock-to-soil spectral amplification on a current reworking of the 1982 Hayes and King report by King and Tinsley (Tinsley, 1987). While awaiting the release of revised spectral amplification maps, we have been addressing related issues in the interpretation of soil amplification data produced by nuclear blasts at the E.R.D.A. Nevada Test Site.

The first issues concerns the possibility raised by Hill (1988) of a bedrock shadowing effect. The proposition under consideration is the possible effect which the prism of unconsolidated geologic material in the Salt Lake Valley might have on seismic wave propagation originating from sites west of the Valley. Hill's simulation study indicates that the prism of unconsolidated material in the Valley will shadow the bedrock to the east of the Valley when seismic waves originate from the west. As a result, the ratio of simulated peak horizontal velocities on rock-to-soil are several times larger than the simulated rock-to-soil amplification ratio for an event originating more directly beneath the surface expression of the Wasatch Fault. Hill's simulation results provide an alternative explanation for the high amplification factors found by Hayes and King. Yet King (1988) argues that equivalent amplification factors were produced by explosions on the east side of the Wasatch fault. We feel a need to resolve this issue before proceeding with a revision of our earlier MMI mapping efforts and extending our work to an estimation of expected losses due to ground shaking.

A second issues concerns the rapid increase in uncertainty King (1988) reports with repect to rock-to-soil amplifications above the six-to-eight range. Confidence intervals around spectral amplification ratios below six are small enough to let one treat ratio differences as an interval scale measure. However, confidence intervals around spectral amplification ratios above eight are large enough to blur the differences between intervals on the scale. Thus one might be well advised to treat amplification ratios in this higher range as being simply "greater that eight". Surely, there is some interaction between this argument and the agrument regarding the typical nonlinear soil response to ground shaking at high strain levels. A nonlinear response to higher strain may significantly reduce spectral amplification ratios. Does one implicity accept the argument for nonlinear soil response by reducing to some lower factor all amplifications above eight? We feel a need to resolve this issue, too, before proceeding further.

By taking these steps, we hope to improve upon earlier estimates of ground shaking intensities. With the study by Young and other, we will have a more careful consideration of sources, magnitudes, recurrences and source-to-site geometries. With the revisions by King and Tinsley, we will have a greater density of observations on site amplification particularly on the west side of the Salt Lake Valley where previous observations were lacking. And with the above-mentioned issues considered directly, we will have a greater understanding of the current limits on the accuracy of seismic intensity microzonation.

A significant porportion of our efforts over the last six months were focused on remedial work with the County Assessor's Files on Commercial Properties. These files together with the Assessor's Files on Residential Properties are useful in estimating expected losses from exposure to seismic hazards. Unlike the residential property files, the Assessor's commercial property files are not now in digital form. Converting these files to digital form would have been an overwhelming task. Instead we took a stratified random sample of the paper records in the commercial file and converted the sample data to digital form. We succeeded in drawing a 10 to 25 percent sample of commercial records from each quarter-sections in our study area. However, in many quarter-sections, either the population of property records proved too small to be reliably sampled, or the sampling ratio was too low to reliably represent the characteristics of a small population of properties. While trying to sample at the quarter-section level, we have rudely encountered the limitations in the law of large numbers.

Our sampling design had failed to provide uniformly acceptable samples in each of the quarter-sections. To preserve the fine-grained spatial resolution in which our work was proceeding, we had to re-sample a large number of the quarter-sections to ensure that each had an adequately large sample size and sampling ratio. Procedures to do this efficiently were developed, and the corrective re-sampling has been completed.

To further ensure a high quality sample of the commercial properties file, we identified and heavily over-sampled all quarter-sections which contained regional shopping centers. The rationale for doing this is straightforward. The population of commercial structures in quarter-sections with regional shopping centers is highly heterogeneous. To get a reliable sample from a highly heterogeneous population, one need a larger than normal sampling ratio.

Work on the technical aspects of our database and analysis has limited our contact with local land use planners and public officials. However activity of this sort has not been completely absent. One team member presented a report on our work to date at the Association of Collegiate Schools of Planning (Los Angeles, November 5-8). He also presented a report on computer mapping of seismic hazard information at the USGS-sponsored Workshop on Continuting Actions to Reduce Potential Losses from Earthquakes along the Wasatch Front, Utah (Salt Lake City, December 1-2, 1987). The research team convened a technical working group containing University Faculty and Salt Lake County and UGMS officials to discuss issues relating to MMI mapping. They convened a second meeting to discuss implementation issues with officials from the Utah State Division of Comprehensive Emergency Management. Finally, a team member presented a report on MMI mapping and seismic hazard mitigation planning to the Governor's Conference on Comprehensive Hazards Reduction (Park City, May 5-6, 1988).

## References Cited

Algermissen, S. T. et al. 1982. Probabalistic estimates of maximum acceleration and velocity in rock in the contiguous United States. U.S. Geological Survey Open File Report 82-1033.

Emmi, Philip C. 1987. Seismic risk and mitigation policies: An assessment of problems and possibilities in Salt Lake County, Utah, Wasatch Front Forum, Vol. III, No. 3/4 (Spring/Summer).

Everendon, J. F. and Thomson, J. M. 1985. Predicting seismic intensities. In I. Ziony ed., Evaluating Earthquake Hazards in the Los Angeles Region - An Earth Science Perspective. U. S. Geological Survey Professional Paper 1360. U. S. Government Printing Office: Washington, D. C.

Hayes, W. W. and King, K. W. 1982. Zoning of earthquake shaking hazard along the Wasatch fault zone, Utah. Third International Earthquake Microzonation Conference, Seattle, v.3. p. 1307-1318.

Hill, J. 1988. A finite difference simulation of seismic wave propagation and resonance in Salt Lake Valley, Utah. M.S. thesis, Department of Geology and Geophysics, University of Utah.

King, K. W. 1988. Personal communication with Jeffrey Keaton.

Tinsley, J. C. 1987. A session III presentation regarding ongoing research on ground shaking within Salt Lake County, Utah. Workshop on Continuting Actions to Reduce Potential Losses from Earthquakes along the Wasatch Front, Utah. Salt Lake City, December 1-2, 1988.

Young, R.R., Swan, F.H., Power, M.S., Schwartz, D.P. and Green, R.K. 1987. Probabalistic analysis of earthquake ground shaking hazard along the Wasatch Front, Utah. In Gori, P.L. and Hayes, W.W. ed. Assessment of Regional Earthquake Hazards and Risks along the Wasatch Front, Utah, v.II, p. M1 - M110. U.S. Geological Survey Open File Report 87-585, Reston, VA.

# Experimental Investigation of Liquefaction Potential

9910-01629

Thomas L. Holzer
Branch of Engineering Seismology and Geology
U.S. Geological Survey
345 Middlefield Road, MS 977
Menlo Park, California 94025
(415) 329-5637

## Investigations

1. Establishment of an instrumented site in Parkfield, California, to monitor pore-pressure build-up in sand and strong ground motion during the predicted earthquake.
2. Post-earthquake field investigation of the October 1, 1987, Whittier Narrows, California, earthquake.
3. Post-earthquake field investigation of the November 23-24 Superstition Hills earthquakes and analysis of the record from the Wildlife liquefaction array.

## Results

1. Installation of a new array of pore-pressure transducers to replace the original failed array was completed. Fourteen transducers are now functioning at the array. The current array provides both redundancy in depth and variations in method of installation and transducer type. The recording system also was configured to permit quick installation of GEOS. During the installation of the transducers, undisturbed soil samples were taken for dynamic testing in the laboratory. Testing is presently underway.
2. Areas of high water with high liquefaction susceptibility as described in USGS Professional Paper 1360 were searched for evidence of liquefaction induced by the Whittier Narrows earthquake. Differential settlements were noted along embankments and at bridges, but no direct evidence for high fluid pressures was observed.
3. Following the Superstition Hills earthquake sequence of November 23-24, 1987, an extensive reconnaissance was conducted in the Imperial Valley for sites of liquefaction. Particular attention was paid to sites where liquefaction was previously caused by either the Imperial Valley earthquake of 1979 or Westmorland earthquake of 1981. The earthquake also triggered a special strong ground motion array that was installed in 1982 to measure pore pressure in sands concurrently with strong ground motion. The array is known as the Wildlife strong motion array. The array consists of six pore-pressure transducers and a downhole and surface accelerometer.

Liquefaction of natural deposits was observed in at least 10 areas. Liquefaction was also widespread in fills along the All-American canal. The most extensive liquefaction was mapped on the Elmore Ranch, the San Felipe Creek Delta, and in the Wildlife Refuge Area along the Alamo River. More than 100 acres in each of these areas was affected. The most damaging incident was destruction of the Worthington Road bridge across the New River where lateral spreading and vertical settlements forced long-term closure of the bridge. All of the liquefaction appears to have been caused by the M6.6 main shock.

Reliquefaction in areas that liquefied in 1979 and 1981 was only extensive in one area, the Wildlife Refuge Area. Identical areas were affected in both 1981 and 1987. Minor lateral spreading at a few other sites of previous liquefaction was noted, but damage was not nearly as serious as it had been in the earlier events.

Records from the Wildlife Liquefaction Array indicate that pore-pressures generated by the Superstition Hills earthquake reached overburden pressures throughout a 4.3-m-thick silty sand that underlies a 2.5-m-thick surficial layer of silt. The records are the first in which a deposit totally liquefied. Only 50 per cent of the pore-pressure build-up occurred during the earthquake. The cause of the delayed build-up is currently being investigated. Preliminary results suggest it was caused by soil disturbance during installation of the pore-pressure transducers.

## Reports

Holzer, T.L., Youd, T.L., Bennett, M.J., and Stepp, J.C., 1987, Parkfield liquefaction and strong motion experiment: EOS, Transactions, American Geophysical Union, v. 68, no. 44, p. 1350.

Holzer, T.L., Bennett, M.J., Youd, T.L., and Chen, A.T.F., 1988, Parkfield, California, liquefaction prediction: Bulletin of the Seismological Society of America, v. 78, no. 1, p. 385-389.

# The Implementation of an Earthquake Hazard Mitigation Program in Salt Lake County, Utah

Contract Number: 14-08-0001-G1531

Principal Investigators: Gary Madsen,
Jerold Barnes and Loren Anderson

Utah State University, Logan, Utah 84322

(801) 750-1233, (801) 468-2061, (801) 750-2775

## Investigations:

The investigations during the initial phase of the project have centered around the task of assessing earthquake hazard reduction priorities of Salt Lake County public technical staff. An interview schedule placing emphasis on standardized open-ended questions has been developed and reviewed by those having technical expertise in engineering, earth sciences, environmental planning and sociology. The interview schedule will be administered to Salt Lake County Planning staff, Salt Lake County Development Services staff, city building inspectors and city planning staffs. The data from such interviews will be analyzed to identify the most often proposed actions and priorities with respect to mitigating earthquake losses for new development as well as existing facilities.

## Results:

The interview schedule has been developed, the sample of public service staff has been drawn and there have been several organizational meetings of the project team. Copies of the schedule are being reviewed by representatives of Utah Geological and Mineral Survey, Utah Division of Comprehensive Emergency Management and USGS.

# WEST VALLEY CITY
# EARTHQUAKE HAZARDS REDUCTION PROGRAM
# PHASE II

14-08-00010-G1398

Joseph L. Moore, AICP
West Valley City Community Development Department
2470 So. Redwood Road
West Valley City, Utah 84119
801-974-5501

## SCOPE:

As stated in the grant application, the purpose of the Earthquake Hazards Reduction Program (EHRP) is to compile and analyze existing geologic/seismic data as part of a citywide effort to understand and eventually mitigate some of the consequences of a significant seismic event in our area. The Community Development Department of West Valley City has applied for this grant so that a greater knowledge of a potentially catastrophic earthquake occurrence could be considered in the planning and emergency management functions within City government.

## SPECIFIC OBJECTIVES:

1. **Define the Study Area** - the study area during Phase II became all of West Valley City. This is a City of 27 square miles and some 95,000 people. All of the locally demanded critical facilities are located within the area boundaries as well as a wide variety of land uses.

2. **Inventory and Digitally Map Study Area Attributes** - initially a base map at 1" = 1000' scale was produced showing streets and lot lines. Then overlays of the available geologic/seismologic data were drafted utilizing the versatile digital mapping system originally called GEO/GROUP, but now called GEO/GROUP Manitron.

These overlays included liquefaction (Anderson), faults (USGS), ground shaking (Hays & King), soil types (SCS), water table (SCS), landslides, tectonic subsidence (Anderson & Keaton). In addition, overlays of critical facilities were produece. During the study, some of the maps were further defined by the detailed research undertaken by Bruce Kaliser, our geologic consultant.

3. **The Digital Overlay Mapping of Study Area Attributes** - once the information for the maps identified in step 2 was complete they were layered upon each other with the intent of identifying high risk areas. This map and methodology is discussed in detail later in the report.

4. **Structural Analysis of Critical Facilities** - Reaveley Engineers, a local structural engineering firm, was under contract to study selected critical facilities within the City. The information derived proved to be extremely useful and is described in the critical facilities and implementation section of the report.

5. **Implementation** - with all this new found information, a on-going effort has

been initiated to disseminate information in the form of brochures for the public in terms of the business and residential sectors of the City, draft ordinances have been developed, more strict adherence to the Seismic 3 zone requirements of the UBC have been assured, modifications to the City's Emergency Operation Plan and some suggestions for modifications of several critical facilities.

## FINDINGS:

Our intent was not to generate new information but to compile and synthesize the existing geologic/seismic information. The question that has always concerned the researcher has been whether such information was readily available and usable by local officials. On the whole, adequate information exists, except in the area of ground shaking. Some gross information was compiled and then refined by the geologic consultant, but it still seems quite theoretical for our effort. It is hoped that during 1988-89 there will be a new more detailed study of ground shaking which can be incorporated at a later date into the report. That study is being completed by Dames and Moore, an geology/engineering firm.

In this study only ground shaking has been considered weak due to a lack of readily available information. In the pages that follow available information concerning liquefaction, faults, ground shaking, soil condition, watertable and landslides is reviewed, mapped and analyzed. Population density/critical facilities maps are also produced leading to an understanding of potential scenarios. The technical reports have been translated to a level of readability that a planner, public official or layman can easily interpret. In a sense, this readability was an important goal of this project.

The final section of the report covers implementation strategies. Much research has been completed utilizing examples from California and other states. Ordinances, building code modifications, Master Plan elements and other information has been compiled for our purposes. This section describes changes, processes and policies that are being implemented at this time.

April 9, 1987

## SEISMIC BIBLIOGRAPHY

### Book:

Arabasz, Walter J., Smith, R. B., and Richins, W.D. Earthquake Studies in Utah 1850 to 1978. Salt lake City, Utah University of Utah Seismograph Stations, Department of Geology and Geophysics, July 1979.

Brabb, E. E., ed. Progress on Seismic Zonation in the San Francisco Bay Region, Circular 807. Arlington, Virginia: U.S. Geological Survey, 1979.

Cluff, Lloyd S., Brogan, George E., and Glass, Carl E. Wasatch Fault, Northern Portion: Earthquake Fault Investigation & Evaluation: A Guide to Land Use Planning. Oakland, California: Woodward Clyde & Associated for Utah Geological and Mineral Survey, 1970.

Earthquake Safety in Utah and Recommendations for Risk Reduction, Utah State Seismic Safety Advisory Council. Salt Lake City, Utah: May 1981.

Gauchat, Urs P., Schodek, Daniel L., Luft, Rene. Patterns of Housing Type and Density: A Basis for Analyzing Earthquake Resistance. N.S.F. Grant No. PFR-780-258. Boston, Mass: Dept. of Architecture, Harvard University, 1984.

Governor's Conference on Geologic Hazards. Utah Geological and Mineral Survey Circular 74, Atwood, Genevieve, Director. Salt Lake City, Utah: Utah Geological and Mineral Survey, December, 1983.

Hays, Walter W., ed. Complied by Kitzmiller, Carla. A Workshop on "Probabalistic Earthquake-hazards Assessments," Open-File Report 86-185. San Francisco, California: U.S. Geological Survey, November 25-27, 1985.

Hays, Walter R., and Gori, Paula L., editors. A Workshop on "Evaluation of Regional and Urban Earthquake Hazards and Risk in Alaska," Open-File Report 86-70 September 5-7, 1985. Reston, Virginia: U.S. Geological Survey, 1986.

Hilpert, Lowell S., et al. Environmental Geology of the Wasatch Front. Salt Lake City, Utah: Utah Geological Association, Publication 1, 1971.

Model Recovery Program. Open-file report 85-371 from ICSSC TR-6 Committee members. Reston, Virginia: U.S. Geological Survey, July, 1984.

National Earthquake Hazards Reduction Program, Summaries of Technical Reports, Volume XXII, Open-File Report 86-383.

Menlo Park, California: U.S. Geological Survey, 1986.

Richins, William D., et al. Earthquake Data for the Utah Region July 1, 1978 to Dec. 31, 1980. Salt Lake City Utah: University of Utah Seismograph Stations, Department of Geology and Geophysics, University of Utah, October 1981.

Schnell, Mary L. and Herd, Darrell G. editors. National Earthquake Hazards Reduction Program: Fiscal Year 1983 Activities, Report to the United States Congress, Geological Survey Circular 918. Alexandria, Virginia: U.S. Geological Survey, 1984.

Seismic Safety Element Part V. San Diego, California: County of San Diego, Environment Development Agency, January 1975.

Wyner, Alan J., Mann, Dean E. Preparing for California's Earthquakes: Local Government and Seismic Safety. Berkeley, California: University of California, Berkeley, 1986.

## Periodicals:

Arabasz, Walter J., Smith R.B., and Richins, W.D. "Earthquake Studies Along the Wasatch Front, Utah: Network Monitoring, Seismicity, and Seismic Hazards." Bulletin of the Seismological Society of America, Vol. 70.No.5, pp. 1479-1499, October 1980.

Kockelman, William J. "Some Techniques for Reducing Landslide Hazards." Bulletin of the Association of Engineering Geologists, 1986.

Mabey, Don R., and Atwood, Genevieve. "Fluctuations of the Level of Great Salt Lake." Survey Notes Vol. 18, No.1. Salt Lake City, Utah: Utah Geological and Mineral Survey, Spring 1984, pp. 3-8.

Mabey, Don R. "Earthquake Hazards in Utah." Survey Notes Vol. 18, No. 4. Salt Lake City, Utah: Utah Geological and Mineral Survey, Winter 1985.

Marine, Wendell and Price, Don. "Geology and Ground-Water Resources of the Jordan Valley, Utah." Water Resources Bulletin #7, Salt Lake City, Utah: Utah Geological and Mineral Survey, (Dec. 1964(, pp. 7-10, 22-27.

Ringholz, Raye C. "The Inevitability of Earthquake." Utah Holiday, January 1981, pp. 54-58.

Smith, Robert B., and Richins, William D. "Seismicity and Earthquake Hazards of Utah and the Wasatch Front: Paradigm and paradox." U.S.G.S. Workshop, Evaluation of Regional and Urban Earthquake Hazards and Risk in Utah, Salt Lake City, Utah: U.S. Geological Survey (1984).

## Reports

Adhidjaja, J.I., Cook, K.L. & Serpa, 1.F., 1981, Satt Lake Valley gravity map and data, U.S.M.S. open file report 39.

Anderson, Loren R., et al. Liquefaction Potential map for Davis County, Utah. Eight plates, scale 1:48,000. Logan, Utah: Department of Civil and Environmental Engineering, University of Utah. U.S. Geological Survey, Professional paper, contract: 14-08-001-19127, February, 1982.

Anderson, Loren R., et al. Liquefaction Potential map, Salt lake County, Utah. Eight Plates, scale 1:48,000. Logan, Utah: Department of Civil and Environmental Engineering, Utah State University, and Dames and Moore Consulting Engineers, Salt lake City, Utah. U.S. Geological Survey, Professional paper, 1982.

Arabasz, Dr. Walter J. "Seismic Environment of the Intermountain Region." Workshop on Mitigating Risk In Older Buildings, Structural Facilities, Inc., and The National Science Foundation. Salt Lake City, Utah: The University of Utah, January, 16-18, 1985.

Arnold, Christopher, and Reitherman, Robert. Building Configurations Seismic Design, (excerpts). Salt Lake City, Utah: Reaveley Engineers and Associates. (Date not noted.)

Atwood, Genevieve, and Mabey, Don R. Earthquake Hazard Reduction In Utah. Salt Lake City, Utah: Utah Geologic and Mineral Survey, 1986.

Bapis, Jim. Geography Means a World of Difference. Salt Lake City, Utah: University of Utah, September, 1985.

Bruhn,R.L., et al. Structure of the Salt Lake Segment, Wasatch Normal Fault Zone; Implications for Rupture Propagation during Large Earthquakes. Salt Lake City, Utah: Department of Geology and Geophysics, University of Utah, 1985.

Currey, Donald R. Paleolake History in Reconstructing Neotechtonic History and Assessing Earthquake Hazards: The Special Case of Lake Bonneville and the Wasatch Front. Salt Lake City, Utah: Department of Geography, University of Utah, March, 1986.

Dowrick, D.J. Earthquake Resistant Design: A Manual for Engineers and Architects, (excerpts). (Publisher not noted)

Environmental Conditions: North Portion of Salt Lake County. R & M Consultants, Salt Lake City, Utah: Prepared for: Planning and Zoning Department, Salt Lake City Corporation, November 1983.

Gill, Harold. Utah Geological and Mineral Survey Excavation Inspection Program: A Tool for Earthquake Hazard Recognition in Utah. Salt Lake City, Utah: monograph, 1986.

Goode, Harry D. Field-Trip Guide Environmental Geology of the Middle Wasatch Front, Utah. Salt Lake City: Department of Geology and Geophysics, University of Utah, October 19, 1975.

Hays, Walter W. Evaluation of Local Site Amplification of Earthquake Ground Motion, An Important Consideration In Earthquake-Resistant Design In Utah. Reston, Virginia: U.S. Geological Survey, 1986.

Highland, Lynn M. Earthquake Hazards to Domestic Water Distribution Systems In Salt Lake City, Utah. Denver, Colorado: U.S. Geological Survey, 1986.

Intergovernmental Hazard Mitigation Report for the State of Utah. F.E.M.A. 680-DR-Utah. August 1, 1983.

Keaton, Jeffery R., Currey, Donald R., and Olig, Susan J. Paleoseismicity and Earthquake Hazards Evaluation Salt Lake City, Utah of the West Valley Fault Zone, Salt Lake Urban Area. Salt Lake City, Utah: Department of Geography and Department of Geology and Geophysics, University of Utah, 1985.

Keaton, Jeffery R., and Reaveley, Lawrence D. Field Guide to Selected Geologic Features and Building in Southern Davis and Northern Salt Lake Counties, Utah, Utah Earthquake Hazards Workshop. Salt Lake City, Utah: Utah Geological and Mineral Survey and U.S. Geological Survey, July 18, 1986.

King, Kenneth W. Efforts on Site Geology on the Level of Ground Shaking Along the Wasatch Front. Denver, Colorado: U.S. Geological Survey, 1986.

King, K.W., et al, 1983, Wasatch Front urban area seismic response data report: U.S.G.S. Open File Report 83-452.

Kockelman, William J. Five Critical Elements for Reducing Earthquake Hazards. Menlo Park, California: U.S. Geological Survey, 1986.

Kockelman, William J. "Using Earth-Science Information For Earthquake Hazard Reduction." Ziony, J.I. ed. Evaluating Earthquake Hazards in the Los Angeles Region An Earth-Science Perspective. U. S. Geological Survey Professional Paper 1360. Washington, D.C.: United States Government Printing Office, 1985.

Kockelman, William J. Reducing Losses From Earthquakes Through Personal Preparedness, Open-file Report 84-765. Menlo Park, California: U.S. Geological Survey, 1984.

Lund, William and Schwartz, David. Evaluation of Fault Behavior and Earthquake Recurrence at the Dry Creek Site Salt Lake Segment, Wasatch Fault Zone, Salt Lake County, Utah. Salt Lake City, Utah: Utah Geological and Mineral Survey and the U.S. Geological Survey, 1986.

Machette, Michael, Lund, William, and Arabasz, Walter J. Triad for Tectonic Framework and Earthquake Potential of the Wasatch Front Area and Other Parts of Utah, (Draft Report). Salt Lake City, Utah: U.S. Geological Survey, July 14, 1986

Machette, Michael N., et al. Quaternary Geology Along the Wasatch Front: Evidence for Ten Fault Segments and Large-Scale Changes in Slip Rate Along the Wasatch Fault Zone, (expanded abstract). Salt Lake City, Utah: monograph, 1986.

McCalpin, James, Robison, Robert M., and Garr, John D. Neotechtonics of the Hansel Valley-Pocatello Valley Corridor, Northern Utah and Southern Idaho. Logan, Utah: Department of Geology, Utah State University, 1986.

Miller, R.D., et al, 1981, Basic data report of selected samples collected from six test holes at five sites in the Great Salt Lake and Utah Lake Valleys, Utah; USGS Open File Report 81-179.

Oaks, Sherry D. The 1934 Hansel Valley, Utah Earthquakes Event and Institutional Response in Salt Lake City. Boulder, Colorado: Department of Geography, University of Colorado, 1986.

Perkins, David M. and Bender, Bernice K. Mathematical Modelling of Potential Large Earthquake Occurrences and Implications for Wasatch Hazard. Denver, Colorado: U.S. Geological Survey, 1986

Slosson, James E. Legal issues Related to Hazard Mitigation Policies, Paper No. 11. Van Nuys, California: Slosson and Associates, 1986.

Steinbrugge, Karl V. Earthquakes, Volcanoes, and Tsunamis: An Anatomy of Hazards. New York, N.Y: Skandia America Group, 1982.

Taylor, Craig E., Ward, D.B., and Haber, J.M. Earthquake Loss Estimates for Utility Systems and State-Owned buildings in Salt Lake and Davis Counties, U.S. Geological Survey Professional Paper. Salt Lake City, Utah: NTS Engineering and Structural Facilities, Inc., 1986.

Tingey, James L. and Findlay, Ralph F. Emergency Management in Utah for Earthquakes. Salt Lake City, Utah: Utah Division of Comprehensive Emergency Management, 1986.

Wallace, Gwynn J. Great Salt Lake Field Trip, In Conjunction With the Annual Meetings of Rocky Mountain Sections AAPG-SEPM. Salt Lake City, Utah: March 19, 1978.

Wheeler, Russell L. A Statistical Analysis of Segmentation of the Wasatch Fault, U.S. Geological Survey Professional Paper. Denver, Colorado: U.S. Geological Survey Branch of Engineering Geology and Tectonics, 1986.

Zoback, Mary Lou. Interpretation of a 30 km Seismic Reflection Profile Across the Wasatch Fault Zone Near Nephi, Utah. Menlo Park, California: U.S. Geological Survey, 1986.

# Global Digital Network Operations

9920-02398

Howell M. Butler
Branch of Global Seismology and Geomagnetism
U.S. Geological Survey
Albuquerque Seismological Laboratory
Building 10002, Kirtland AFB-East
Albuquerque, New Mexico 87115-5000
(505) 844-4637

## Investigations

The Global Digital Network Operations presently consists of 15 SRO/ASRO and 14 DWWSSN stations. The primary objective of the project is to provide technical and operational support to keep these stations operating at the highest percentage of recording time possible to provide high-quality digital seismic data to the seismic research community. This support includes operational supplies, replacement parts, repair service, modification of existing equipment, installation of systems and on-site maintenance, training and calibration. A service contract provides technicians to perform on-site maintenance and installations, as well as to perform repair-and-test of seismometers and all replaceable units that comprise the various network systems. Contract technicians are also provided for special projects such as on-site noise surveys, special telemetered system installations, system renovations, and evaluation and testing of seismological and related instrumentation. The following on-site station maintenance activity was accomplished:

CTAO - Charters Towers, Australia - ASRO - One maintenance visit
TAU - Tasmania, Australia - DWWSSN - One maintenance visit
TOL - Toledo, Spain - DWWSSN - One maintenance visit
BGIO - Bar Giygora, Israel - SRO - One maintenance visit
LEM - Lembang, Indonesia - DWWSSN - One maintenance visit
BOCO - Bogota, Colombia - SRO - One maintenance visit
ANMO - Albuquerque, New Mexico - SRO - Two maintenance visits

Special Activity. One programmer worked in the Data Processing Center primarily on the VAX System and the Chinese (CDSN) operating system. One Field Engineer was in China full time during this period assisting in maintenance and training of CDSN personnel. During this period one Field Engineer was assigned full time to the WWSSN heated-pen program for testing and check-out of the production units.

## Results

The Global Digital Network continues with a combined total of 29 SRO/ASRO/DWWSSN stations. The main effort of this project is to furnish the types of support at a level needed to keep the GSN at the highest percentage of operational time in order to provide the highest quality digital data for the worldwide digital data base.

# U.S. Seismic Network

9920-01899

Marvin A. Carlson
Branch of Global Seismology and Geomagnetism
U.S. Geological Survey
Denver Federal Center
Box 25046, Mail Stop 967
Denver, Colorado 80225
(303) 236-1506

## Investigations

U.S. Seismicity. Data from the U.S. Seismic Network (USSN) are used to obtain preliminary locations and magnitudes of significant earthquakes throughout the United States and the world.

## Results

As an operational program, the USSN operated normally throughout the report period. Data were recorded continuously in real time at the National Earthquake Information Center's (NEIC) main office in Golden, Colorado. At the present time, 120 channels of SPZ data are being recorded at Golden on develocorder film. This includes data telemetered to Golden via satellite from both the Alaska Tsunami Warning Center, Palmer, Alaska, and the Pacific Tsunami Warning Center, Ewa Beach, Hawaii. A representative number of SPZ channels are also recorded on Helicorders to give NEIC real-time monitoring capability of the more active seismic areas of the United States. In addition, 15 channels of LPZ data are recorded in real time on multiple pen Helicorders.

Data from the USSN are interpreted by record analysts and the seismic readings are entered into the NEIS data base. The data are also used by NEIS standby personnel to monitor seismic activity in the United States and world wide on a real time basis. Additionally, the data are used to support the Alaska Tsunami Warning Center and the Pacific Tsunami Warning Service. At the present time, all earthquakes large enough to be recorded on several stations are worked up using the "Quick Quake" program to obtain a provisional solution as rapidly as possible. Finally, the data are used in such NEIS publications as the "Preliminary Determination of Epicenters" and the "Earthquake Data Report."

Development is continuing on an Event Detect and Earthquake Location System to process data generated by the USSN. We expect the new system to be ready for routine operational use during 1988. At that time, the use of develocorders for data storage will be discontinued. Ray Buland and David Ketchum have been doing the developmental programming for the new system. A Micro Vax II will be used as the primary computer of the Event Detect and Earthquake Location System. PDP 11/23's and PDP 11/73's are being used as front ends to off load the real-time data collection from the Micro Vax II. A second Micro Vax II has been procured to serve as a backup to the primary system. The two Micro Vaxs share 1.3 gigabytes of disk storage.

During FY 1987, four stations of a pilot VSAT Network were installed. Three of the stations were former RSTN sites at McMinnville, Tennessee, St. Regis Falls, New York, and Black Hills, South Dakota, which are now operated by the Branch of Global Seismology and Geomagnetism. The fourth site is the first prototype National Seismic Network Station at Bergen Park, Colorado. The data is transmitted via satellite to a shared Master Earth Station and on to the NEIC at Golden, Colorado, via AT&T long line

# Earth Structure and its Effects upon Seismic Wave Propagation

9920-01736

George L. Choy
Branch of Global Seismology and Geomagnetism
U.S. Geological Survey
Denver Federal Center
Box 25046, Mail Stop 967
Denver, Colorado 80225
(303) 236-1506

## Investigations

1. Use of differential travel-time anomalies to infer lateral heterogeneity. We are investigating lateral heterogeneity in the Earth by analyzing differential travel times of phases that differ in ray path only in very narrow regions of the earth. Because such phases often are associated with complications near a cusp or caustic, their arrival times can not be accurately read without special consideration of the effects of propagation in the Earth as well as additional processing to enhance arrivals.

2. Use of body wave pulse shapes to infer attenuation in the Earth. We are developing techniques to determine the depth- and frequency-dependence of attenuation in the Earth. Resolution of this frequency dependence requires analysis of a continuous frequency band from several Hz to tens of seconds. It also requires consideration of the contributions of scattering and slab diffraction to apparent broadening of a pulse.

3. Enhancement of NEIC reporting services. We are incorporating techniques of analyzing broadband data into the data flow of the NEIC. However, the accuracy of source parameters extracted from digitally recorded data depends on the correct application of propagation corrections to waveforms. Broadband data can then be used on a routine basis to increase the accuracy of some reported parameters such as depth and to compute additional parameters such as radiated energy.

## Results

1. We have developed a source-deconvolution technique that resolves differential travel times of body waves near cusps and caustics. Application of this algorithm to PKP waves sampling the inner core suggests that regional velocity variations exist within the upper 200 km of the inner core. The regional variations are consistent with those obtained from global inversions of absolute PKP times. We are reading high quality arrival times of PcP and branches of PKP, corrected for propagation effects. This accumulation of data can be used to determine if propagation phenomena have biased the catalog data which have been used to derive models of lateral heterogeneity.

2. We are attempting to separate intrinsic attenuation from scattering in waveforms. We synthesize waveforms using a method that simultaneously models causal attenuation and source finiteness. Under the assumption that intrinsic attenuation can be described by minimum phase operators, we can attribute discrepancies in the waveforms to scattering.

3. A computer package has been implemented that routinely processes digital data received by the NEIC into broadband records using the method of Choy and Boatwright (1981) and Harvey and Choy (1982). The broadband data are now routinely used by the NEIC to determine with greater accuracy the depths of earthquakes. Techniques for determining depths of earthquakes using broadband data are described in Choy and Engdahl (1987). A semi-automated version of the algorithm of Boatwright and Choy (1986) has been implemented to compute the radiated energies of earthquakes with $m_b > 5.8$. The frequency-dependent Q model of Choy and Cormier (1987) has been incorporated into the energy algorithm.

## Reports

Choy, G. L., and Engdahl, E. R., 1987, Analysis of broadband seismograms from selected IASPEI events: Physics of the Earth and Planetary Interiors, v. 47, p. 80-92.

# Systems Engineering

9920-01262

Harold E. Clark, Jr.
Branch of Global Seismology and Geomagnetism
U.S. Geological Survey
Albuquerque Seismological Laboratory
Building 10002, Kirtland AFB-East
Albuquerque, New Mexico 87115-5000
(505) 844-4637

## Investigations

Continuation of the development and support of the China Digital Seismograph Network (CDSN).

## Results

CDSN System No. 12 construction and assembly is complete. CDSN System No. 12 will provide the same data recording techniques as the other eleven CDSN systems, and will also provide a satellite telemetry channel for data transmission. Work is continuing on a special satellite data receiving station to record and analyze the CDSN data. The initial satellite link will be tested using parts and equipment from the Sandia RSTN satellite network.

Most of the month of March was devoted to depot maintenance training for two People's Republic of China CDSN personnel. The Albuquerque Seismological Laboratory (ASL) operations group did not have sufficient resources or training on the CDSN equipment to conduct extended depot maintenance training, so the majority of the training was accomplished by the ASL Engineering Section. The China personnel received system training on the new CDSN System No. 12 system and the test equipment (ATE) that is in the Beijing CDSN Maintenance Facility. Special classes and demonstrations on the use of CD-ROM readers will allow interested seismologists in China to use the USGS NEIC earthquake data disks. The data from selected sites in the CDSN will eventually be part of the USGS NEIC earthquake digital data distributed by CD-ROM disks.

The specifications for the correct interface between CDSN Satellite Field Systems and the China satellite terminals are being finalized. As soon as the complete specifications are delivered to ASL, the special interface hardware and cables will be designed and assembled.

# Reanalysis of Instrumentally Recorded United States Earthquakes

9920-01901

J. W. Dewey
Branch of Global Seismology and Geomagnetism
U.S. Geological Survey
Denver Federal Center
Box 25046, Mail Stop 967
Denver, Colorado 80225
(303) 236-1506

## Investigations

1. Relocate instrumentally recorded U.S. earthquakes using the method of joint hypocenter determination (JHD) or the master event method, using subsidiary phases (Pg, S, Lg) in addition to first arriving P-waves, using regional travel-time tables, and expressing the uncertainty of the computed hypocenters in terms of confidence ellipsoids on the hypocentral coordinates.

2. Evaluate the implications of the revised hypocenters on regional tectonics and seismic risk.

## Results

1. J. W. Dewey is investigating the characteristics of midplate seismicity that is marginal to former rift-basins. For the purposes of this study, "rift basins" are the structural or topographic lows that mark sites of significant upper-crustal extension. A "former" rift basin is one that has not extended in the present geologic epoch, in contrast to a "present-day" rift basin, which has. "Marginal" seismicity is that reliably located external to the basin boundaries. Only rift-basins that are within or adjacent to continental lithosphere are considered in this study.

Many former rift-basins are bordered by belts of marginal seismicity that have widths of tens or hundreds of kilometers. Probably the most commonly accepted explanation for this marginal seismicity is that it is due to reactivation under the present-day stress field of minor preexisting faults that were formerly active in the period of extensional tectonism during which the rift basins were formed. The fact that marginal seismic belts are also associated with many present-day rift basins is consistent with the postulated presence of preexisting faults marginal to former rift-basins. Focal-mechanisms of shocks marginal to present-day rift basins imply that most of these shocks are due to movements of minor faults that have similar senses-of-slip to the major faults that bound the rift basins.

There are, however, several reasons for seeking beyond the reactivation of minor preexisting faults for mechanisms to explain seismicity marginal to former rift-basins. First, some former rift-basins have seismically active margins but historically inactive bounding faults and interiors. The hypothesis that minor preexisting rift-margin faults can be reactivated in the present-day stress field suggests that major, basin-bounding, faults might also be susceptible to reactivation. From the viewpoint of assessing seismic risk, it is therefore important to know if a mechanism exists that would localize seismicity on some rift-basin margins but that would not imply the reactivation of basin-bounding or basin-interior faults. Second, the evidence linking rift-margin earthquakes to minor preexisting faults is mostly indirect. As is true throughout midplate regions, very few earthquakes occurring on the margins of former rifts have hypocenters reliably located on mapped preexisting faults and have focal mechanisms consistent with slip on the faults. Third, in some regions in which seismic activity occurs both in the interiors of rift-basins and on the margins of the basins, the focal mechanisms of the shocks imply that the tectonic stress field is oriented differently in the two environments, suggesting that spatial variations in the stress-field, besides or in addition to the presence of preexisting faults, might play a role in the localization of seismicity on the margins of some rifts.

A hypothesis that would account for seismically active rift-basin margins and seismically inactive basin-interiors is that some processes associated with extension produce lithosphere that in later eras is less deformable, and hence less seismic, in the center of the basin than at the margins. This might be the case, for example, if the crust beneath the rift basin were depleted of volatiles by a high geothermal gradient. Another hypothesis that has been proposed to account for active margins and inactive interiors is that concentrations of small and moderate midplate earthquakes occur in uppermost crust that has high Young's modulus; the crystalline near-surface rock on the margins of rifts would have a much higher Young's modulus than the sedimentary near-surface rock of the basin interior. Some seismologists have invoked stresses generated by density inhomogeneities in the lithosphere or bending stresses induced in the lithosphere by external loads to explain regional variations in the orientations of the stress tensor.

2. J. W. Dewey and D W. Gordon have completed two reviews addressed to non-seismologists on respectively the seismotectonics and earthquake history of Pennsylvania. These will be published in a review volume on the geology of Pennsylvania.

3. J. W. Dewey has completed a review, co-authored with G. Suárez of the Universidad Nacional Autónoma de México, on the seismicity and tectonics of Middle America. The review will be published in the Decade of North American Geology volume on the Neotectonics of North America. Dewey also attended a workshop on Middle American Seismotectonics, San Jose, Costa Rica, and presented lectures to the workshop.

## Reports

Dewey, J. W., and Gordon, D. W., Chapter 27--Seismic framework, for inclusion *in* Shultz, C. H. (ed.), The Geology of Pennsylvania: To be published by the Pittsburgh Geological Society, 6 typescript pages and 3 figures (submitted).

Dewey, J. W., and Suárez, G., Seismicity of Middle America, for inclusion *in* Slemmons, D. B., Engdahl, E. R., Blackwell, D., Schwartz, D., and Zoback, M., (eds.), Neotectonics of North America: Geological Society of America Decade of North American Geology Associated Volume, GSMV-1, 30 typescript pages and 6 figures (submitted).

Gordon, D. W., 1987, Seismicity and tectonics in the Wyoming foreland [abs.]: Seismological Research Letters, v. 58, p. 97-98.

Gordon, D. W., and Dewey, J. W., Chapter 53--Earthquakes, for inclusion *in* Shultz C. H., (ed.), The Geology of Pennsylvania: To be published by the Pittsburgh Geological Society, 15 typescript pages, 1 table, and 5 figures (submitted).

# Global Seismology

9920-03684

E. R. Engdahl
and
J. W. Dewey

Branch of Global Seismology and Geomagnetism
U.S. Geological Survey
Denver Federal Center
Box 25046, Mail Stop 967
Denver, Colorado 80225
(303) 236-1506

## Investigations

1. Depth Phases. Develop procedures for the global analyses of earthquake depth phases and source characteristics using broadband seismograms of body waves.

2. Earthquake Location in Island Arcs. Develop practical methods to accurately locate earthquakes in island arcs.

3. Subduction Zone Structure. Develop techniques to invert seismic travel times simultaneously for earthquake locations and subduction zone structure.

4. Global Synthesis. Synthesize recent observational results on the seismicity of the earth and analyze this seismicity in light of current models of global tectonic processes.

## Results

1. Depth Phases. Source parameters have been systematically determined for all earthquakes $M_W \geq 5$ that occurred between 172° and 179° W. longitude in the Adak Island region of the central Aleutians during 1977-1986. Centroid-moment tensor (CMT) solutions yield stable results for 76 events. We relocate the events using a plate model developed for the region and use two alternative methods of depth determination. The first method uses broadband P-wave displacement seismograms and the long-period CMT data set in an inversion for the mechanism, depth, and time function of the source. The second method uses arrival times of direct and prominent reflected phases, primarily pwP, from short-period and broadband digital seismograms.

Systematic analysis of these events provides an unusually well-constrained data set for the study of stress release along an active subduction zone. Three earthquakes, which occurred seaward of the trench axis, are located just below the crust-mantle interface and show extension nearly perpendicular to the trench axis. Sixty-four events are located in the active thrust zone 50-130 km north of the trench axis, and, except for 5 unusual events, are characterized by thrust mechanisms with one nodal plane dipping north at a shallow angle. In map view, the horizontal projection of the slip vector of the moment tensors for these events is more northerly than the direction of relative plate motion for the region. In cross section, the thrust zone appears as a thin (thickness < 15 km) interplate region; the dip angle of the shallow dipping plane gently steepens with depth. Five earthquakes, which occurred as aftershocks of the May 7, 1986, earthquake ($M_W = 8$) in the crust of the overriding plate, are characterized by strike-slip mechanisms. Six events at depths greater that 50 km have null axes nearly parallel to the strike of the slab.

2. Earthquake Location in Island Arcs. Nothing new to report.

3. Subduction Zone Structure. Early work with body waveforms for slab modeling used ray trajectories and densities to estimate ray theoretical amplitudes and to identify multipathing, but could not calculate the frequency dependent effects of head waves and diffraction along slab boundaries and radiation having wavelengths on the order of or larger than slab width. Recently, however, the techniques of forward modeling of body waves in two- and three-dimensional structures have been systematically advanced to show these effects to be highly sensitive to slab width and its variations with depth. Application of these new techniques to the central Aleutian and Kurile subduction zones demonstrate that waveforms of P and S waves can provide important new constraints on slab structure that are independent of the information provided by their arrival times.

Some general features of wave propagation in subducted slabs are highlighted. The anomalous features are of three kinds: (1) faster material in the slab advances the arrivals that leave the source region in the plane of the slab; (2) faster material in the slab tends to defocus energy leaving the source region in the plane of the slab; (3) the waveforms of energy that leave the source region in the plane of the slab can be distorted, with emergent first arrivals and a long-period, late-diffracted arrival, which can make the full waveform appear as a broadened pulse. Slab diffraction is akin to a head wave traveling along the underside of the slab. It arrives late in the waveform because it is sensitive to the slower velocity structure that surrounds the higher velocity slab. In general, thinner slabs of a given length produce more waveform broadening and smaller amplitudes for signals that leave the source in the plane of the slab. It is also predicted that slab diffraction will be observed at all azimuths on the downdip side of a steeply dipping slab, strongest in a direction oblique to the normal to the strike of the slab, evolving into a prominent secondary phase along strike, and rapidly decaying on the side opposite to the dip. Slab diffraction effects have been demonstrated for both P and S waves, but are more pronounced in the case of S waves. However, attenuation affects S waves more than P waves, so that both types of body waves are needed to study waveform distortions due to slabs.

There seems to be strong evidence for slab diffraction effects in P waves from central Aleutian earthquakes. The observations reported by Vidale and Garcia-Gonzalez (1987) and Engdahl and Kind (1986), and the modeling reported by Vidale and Helmberger (1986) suggest that the central Aleutian slab is relatively thin, probably no more than 40-50 km thick. Further development of the inversion techniques of Engdahl and Gubbins (1987) and more investigation of broadband data and modeling is needed to confirm this result.

Thus far, the primary source of information on penetration of the Kurile slab beyond 670 km has been travel-time anomalies. However, slab length will still have some tradeoff with lateral variations in slab shape and velocity, and the magnitude of velocity perturbation within the slab. A priori constraints of thermal models and phase changes can reduce, but not eliminate these tradeoffs. The possibility of using amplitudes and waveforms as additional constraints on the modeling of slab structure has been demonstrated. Vidale and Helmberger (1986) presented evidence for slab diffraction effects along an azimuth perpendicular to the strike of the slab for a 135 km deep Kurile event, but not for an event at 540 km depth. Silver and Chan (1986) showed that a zone of multipathed arrivals can exist for S waves from deep focus Kurile earthquakes observed along azimuths parallel to the strike of the slab. The duration of the predicted multipathing, however, is too small to account for the duration of the tail in broadband waveforms of the S wave. Cormier (1987), based on modeling studies, suggests that the mechanism of slab diffraction is sufficient to explain the duration of observed S pulses in many azimuths without additional ray theoretical arrivals. Multipathing along strike, however, is consistent with the observations of high variability in S waveform widths and complexity for azimuths close to the strike of the slab (e.g., Silver and Chan, 1986; Beck and Lay, 1986). Thus, there is conflicting evidence in amplitude and waveform data on the geometry of the Kurile slab near and below the 670 km discontinuity and the data may require independent lower mantle lateral heterogeneity as well.

4. Global Synthesis. A highlight of the Decade of North American Geology (DNAG) program is the publication of seven new continent-scale maps (geological, gravity, magnetic, seismicity, stress, neotectonic, and thermal aspects), in color and on a common base at a scale of 1:5,000,000. Construction of the seismicity map required the rationalization of more than one-half million earthquake hypocenters from global, national, regional, and local catalogs. Duplicate entries were removed regionally based on a comparison of reported origin times, epicentral locations, and magnitudes. Only those data that exceeded the magnitude-completeness threshold for each region and time period were plotted. The reduced database spans an interval from the early 1500's through 1985. In all parts of the map, earthquakes of magnitudes less than 4 are represented by small dots, larger earthquakes by filled circles of various sizes in proportion to magnitude, and the great earthquakes ($M \geq 7$) by large rings. Different colors or shades are used to distinguish modern from historic data and to show deep ($h \geq 60$ km), intraplate earthquakes in subduction zones. This scheme of symbols and colors shows details of the seismotectonic fabric of North America that are revealed by the more accurate and complete modern data, yet preserves a perspective of historical earthquake occurrence.

A paper on the seismicity of the Aleutian arc has been prepared for the volume titled "Neotectonics of North America" which will accompany the neotectonic map series. The following summarizes the results of that review study: The Alaska-Aleutian arc extends 3600 km from the Gulf of Alaska to Kamchatka. The largest along-strike variation in the geometry of the subduction zone is in the shallow thrust plane where the great earthquakes occur. Almost all sections of the arc have been broken by great earthquakes in recent historic time with an average repeat time per segment of approximately 60 years. The dip of the thrust plane varies from 25-30° in the central Aleutians to 4-5° in the Gulf of Alaska. Associated with this decrease in dip is a widening of the main thrust zone. The zone of interplate seismicity extends arcward from near the trench ot a depth of 40-60 km where the dip steepens to 30-60° and the earthquakes become intraplate events. Minor seismic activity occurs above the base of the main thrust zone, between the accretionary prism and the volcanic arc, in the crust of the overriding plate. A double Wadati-Benioff zone has been observed at depths of 50-150 km, but except for the Shumagin Islands region, the two planes seem to show a lateral segmentation of the subducting slab and not a true double zone. A change from upper to lower plane seismicity in the eastern Aleutians may be related to the transition from oceanic to continental upper plate near long 164° W. Focal mechanisms generally exhibit down-dip compression in the upper plane and down-dip tension in the lower plane except locally in the Shumagins where the reverse appears to be true. A single plane of seismicity exists everywhere below 170 km and extends to nearly 300 km in depth. Teleseismic inversions have modeled the slab to continue at 100 km and possibly as much as 300 km beneath the deepest seismicity.

## Reports

Choy, G. L., and Dewey, J. W., 1988, Rupture process of an extended earthquake sequence--Teleseismic analysis of the Chilean earthquake of 3 March 1985: Journal of Geophysical Research, v. 93, p. 1103-1118.

Ekström, G., and Engdahl, E. R., 1987, Earthquake source parameters and stress distribution in the Adak Island region of the central Aleutian Islands, EOS (American Geophysical Union, Transactions), v. 68, p. 1352.

Engdahl, E. R., Vidale, J. E., and Cormier, V. F., Wave propagation in subducted lithospheric slabs, Proceedings of the 6th Course: Digital Seismology and Fine Modeling of the Lithosphere, Marjorana Center, Sicily (submitted).

Engdahl, E. R., and Rinehart, W. A., 1987, Seismicity map of North America: Proceedings of the Berkeley Centennial Symposium (submitted).

Taber, J. J., Billington, S. S., and Engdahl, E. R., Seismicity of the Aleutian Arc, in DNAG Associated Volume, Neotectonics of North America, GSMV-1 (submitted).

# Global Seismograph Network Evaluation and Development

9920-02384

Jon Peterson
Branch of Global Seismology and Geomagnetism
U.S. Geological Survey
Albuquerque Seismological Laboratory
Building 10002, Kirtland AFB-East
Albuquerque, New Mexico 87115-5000
(505) 844-4637

## Investigations

1. China Digital Seismograph Network (CDSN).

2. New Global Seismograph Network.

## Results

1. A formal acceptance and dedication ceremony was held for the China Digital Seismograph Network (CDSN) during October 1987. Scientists from the United States, Europe, and China inspected facilities in Beijing, Lanzhou, and Shanghai. The groups of experts submitting a favorable report to the State Seismological Bureau. This event marked the end of the deployment and testing phase of the CDSN. The network has functioned reliably and network data are being routinely distributed through the USGS. A joint report describing the CDSN network has been published.

2. Preliminary work in preparation for deployment of the new GSN data systems in cooperation with IRIS has been in progress. This has included meetings in New Zealand and Australia to discuss plans for modernization of their GDSN stations.

## Reports

________1987, The China Digital Seismograph Network--A joint report by the Institute of Geophysics, State Seismological Bureau and the Albuquerque Seismological Laboratory, U.S. Geological Survey, 91 p.

# Digital Data Analysis

9920-01788

Stuart A. Sipkin
Branch of Global Seismology and Geomagnetism
U.S. Geological Survey
Denver Federal Center
Box 25046, Mail Stop 967
Denver, Colorado 80225
(303) 236-1506

## Investigations

1. Moment Tensor Inversion. Apply methods for inverting body phase waveforms for the best point-source description to research problems.

2. Other Source Parameter Studies. Apply methods for inverting body phase waveforms for distributed kinematic and dynamic source properties.

3. Aftershock Source Properties. Examine mainshock and aftershock source properties to study the mechanics of aftershock occurrence.

4. Broadband Body-Wave Studies. Use broadband body phases to study lateral heterogeneity, attenuation, and scattering in the crust and mantle.

5. Earthquake Recurrence Statistics. Use earthquake recurrence statistics and related parameters to better understand the earthquake cycle and study how they can be used for prediction and forecasting purposes.

5. Real-Time Earthquake Location. Experiment with real-time signal detection, arrival-time estimation, and event location for regional earthquakes.

6. Data Collection Center. Develop a state-of-the-art data collection center to handle digital waveform data collection for the next decade.

7. NEIC Monthly Listing. Contribute both fault-plane solutions (using first-motion polarity) and moment tensors (using long-period body-phase waveforms) for all events of magnitude 5.8 or greater when sufficient data exists. Contribute waveform/focal-sphere figures of selected events.

## Results

1. Moment Tensor Inversion. An anomalous seismic event that occurred off the coast of Japan is being studied. The mechanism is consistent with the hypothesis that this event was caused by fluid injection. Other explanations for the anomalous radiation patterns are being investigated.

2. Other Source Parameter Studies. A journal article on the inversion of teleseismic P waveforms for the distribution of fault slip has been accepted for publication. The results suggest that rupture during moderate-to-large earthquakes involve a tress and/or strength heterogeneity along the fault

surface. The available strong-motion data for the 1985 Michoacan earthquake, one of the events studied teleseismically, is being inverted in a similar manner to refine the estimate of the slip pattern. Preliminary results indicate that the distribution of slip is similar to that obtained using teleseismic data.

3. Aftershock Source Properties. A paper comparing aftershock patterns following several moderate-to-large earthquakes with the corresponding distributions of coseismic slip has been accepted for publication. In this study, the mainshock slip patterns were obtained from previous analyses of the recorded strong ground-motion and teleseismic waveforms. Results of the comparison are consistent with aftershocks occurring as a result of a redistribution of stress following primary failure on the earthquake fault. Aftershocks occur mostly outside or near the edges of the mainshock source regions. This reflects either a continuation of slip beyond the limits of mainshock displacement or the activation of subsidiary faults within the surrounding volume.

4. Broadband Body-Wave Studies. High-quality digitally recorded broadband data sets from the Gräfenberg Array in West Germany and the Regional Seismic Test Network in North America have been collected. Multiple-ScS differential travel times have been computed by waveform cross-correlation. Estimates of the multiple-ScS attenuation operator have been obtained using a phase-equalization and stacking technique. For the tectonic Eurasia and North America path, we obtain $Q_{ScS}$ of 182±21 over the frequency band 0.017-0.117 Hz. In this band, there is no apparent frequency dependence.

5. Earthquake Recurrence Statistics. A paper describing a new earthquake forecasting algorithm has been published and the algorithm has been adopted by NEPEC. An extension of this algorithm, that does optimal estimation of forecast probability, has been completed. Work is underway on applying the algorithm to cases where only one recurrence interval is available, where the recurrence interval must be estimated from other information, and where only paleoseismic information is available.

6. Real-Time Earthquake Location. The station processor for the National Seismic Network (NSN) has been redesigned around a 24-bit digitizer. New developments have suddenly made this technology economically attractive. The network design has been finalized. Procurements for the NSN seismometers, telemetry, network processing system, mass storage, and field processing systems have been completed and submitted.

7. Data Collection Center. Software conversion is mostly done and the system is now operational. Hardware is now in its operational configuration except for the mass store. The new data distribution format (SEED) has been finalized and adopted. As of 1 January 1988, network-day tapes are being produced in the new format.

8. NEIC Monthly Listing. Since January 1981, first-motion fault-plane solutions for all events of magnitude 5.8 or greater have been contributed to the Monthly Listings. Since July 1982, moment-tensor solutions and waveform/focal-sphere plots have also been contributed. In the last six

months, solutions for approximately 71 events have been published. Maps showing the regional distribution of first-motion focal mechanisms, regional seismicity, global CD-ROM data sources and distribution, and proposed national seismograph station distribution and communication network, have been prepared and presented at various international and domestic meetings.

## Reports

Buland, R. P., and Massé, R. P, 1987, A national system of seismic networks [abs.]: EOS (American Geophysical Union, Transactions), v. 68, no. 44, p. 1358.

Mendoza, C., and Hartzell, S. H., 1987, Slip distribution during the 1985 Michoacan earthquake from teleseismic P waves [abs.]: GEOS, Special Issue (Abstracts, Mexican Geophysical Union Annual Meeting), p. 38.

Mendoza, C., and Hartzell, S. H., 1988, Inversion for slip distribution using GDSN P waves--North Palm Springs, Borah Peak, and Michoacan earthquakes: Bulletin of the Seismological Society of America, v. 78 (in press).

Mendoza, C., and Hartzell, S. H., 1988, Aftershock patterns and mainshock faulting [abs.]: Seismological Research Letters, v. 59 (in press).

Mendoza, C., and Hartzell, S. H., 1988, Aftershock patterns and mainshock faulting: Bulletin of the Seismological Society of America, v. 78 (in press).

Sipkin, S. A., 1987, Observation and analysis of broadband multiple-ScS phases [abs.]: EOS (American Geophysical Union, Transactions), v. 68 no. 44, p. 1376.

# Seismicity and Tectonics

9920-01206

William Spence
Branch of Global Seismology and Geomagnetism
U.S. Geological Survey
Denver Federal Center
Box 25046, Mail Stop 967
Denver, Colorado 80225
(303) 236-1506

## Investigations

Studies carried out under this project focus on detailed investigations of large earthquakes, aftershock series, tectonic problems, and Earth structure. Studies in progress have the following objectives:

1. Use earthquake focal mechanisms and integrative tectonics to infer the origins of present-day stresses acting at the proposed Cascadia subduction zone (W. Spence).

2. Explore the consequences of the slab pull force acting at the zone of plate bending that is downdip of the lower end of an interface thrust zone (W. Spence and W. Z. Savage).

3. Provide tectonic setting for and analysis of the 1974 Peru gap-filling earthquake (W. Spence and C. J. Langer).

4. Examine the seismicity and tectonics of the Isthmus of Panama using earthquake relocation methods and modern techniques of focal-mechanism determination (C. Mendoza).

5. Determine the maximum depth and degree of velocity anomaly beneath the Rio Grande Rift and Jemez Lineament by use of a 3-D, seismic ray-tracing methodology (W. Spence and R. S. Gross).

## Results

1. Earthquakes in the Juan de Fuca plate that is subducted beneath the State of Washington generally exhibit extensional stresses. These stresses are due to the slab pull force, the primary driving force for subduction and for shallow, subduction earthquakes. However, the 60 percent slowing of Cascadian subduction over the interval 6.5-0.5 m.y.B.P. (Riddihough, Journal of Geophysical Research, 1984) suggests that the local slab pull force is diminishing in its capability to lead to great subduction earthquakes. Magnetic anomaly lineations cannot resolve plate motions for the last 500,000 years; thus, present-day details of subduction of the Juan de Fuca plate must be inferred from recent geologic, tectonic, and seismic data.

The seismicity of the Cascadia subduction zone is anomalous when compared to other subduction zones. A synthesis of 19 focal mechanisms for the zone from Cape Mendocino to the Queen Charlotte fault shows that most of the offshore earthquakes are associated with maximum compressive stress axes that trend about N-S. The locations of these earthquakes indicate that much of the offshore plate system is being compressed by the northwestward motion of the Pacific plate. Similarly, there is considerable evidence for N-S compression in the shallow crust of the overriding North American plate, from Cape Mendocino northwards to Vancouver. The fact that the South Gorda block is not subducting but is being driven northward suggests that a N-S shear traction is being transmitted into the overriding plate, consistent with the observed landward focal mechanism data. The slowing of Cascadian subduction and the Pacific plate's motion leading to pervasive N-S compression in the Cascadian plate system suggest that the in-plate driving forces of the Juan de Fuca plate no longer dominate the Juan de Fuca plate's motion and that the cessation of subduction at Cascadia is in progress. This unusual subduction environment will complicate estimates of the timing and size of future subduction earthquakes at Cascadia.

2. Interface thrust zones typically have dips in the range 8-15°, whereas lithospheres that are subducted into the mantle typically have dips in the range 40-70°, giving an average dip increase in the mantle of about 45°. These dip increases often occur within 40-60 km of plate length. These zones of sharp dip increases (slab bends) have not been given much attention because generally they lack large earthquakes. This is in sharp contrast to the well-studied zones of bending beneath oceanic trenches where there are frequent normal-faulting earthquakes. It has been noted by Ruff and Kanamori (1983) that great, interface thrust earthquakes terminate their downdip ruptures at the updip part of mantle slab bends. Spence (1987) showed that the slab pull force is the primary force that causes shallow, subduction earthquakes. He also interpreted the mantle slab bends as a pivot for the summed slab pull force of the more deeply subducted plate. In this study, we model the stress distribution in the mantle slab bend, acting under a slab pull load. We find that the observed lack of earthquakes in the mantle slab bend is due to ductility there. However, the strength of the work-hardened ductile portion of the slab bend is more than sufficient to transmit the slab pull load into the shallow subduction zone.

3. The great 1974 Peru thrust earthquake ($M_S$ 7.8, $M_W$ 8.1) occurred in a documented seismic gap, between two earthquakes each with magnitude of about 8, occurring in 1940 and 1942. Additional major earthquakes occurred in this region in 1966 and in 1970; all but the 1970 shock represent thrust faulting. The stress release of the October 3, 1974, main shock and aftershocks occurred in a spatially and temporally irregular pattern. The multiple-rupture main shock produced a tsunami with wave heights of 0.6 ft at Hawaii and which was observed, for example, at Truk Island and at Crescent City. The aftershock series essentially was ended with the occurrence of a $M_S$ 7.1 aftershock on November 9, 1974. The several years of preseismicity data to this earthquake include an unusually clear example of the "Mogi donut" pattern.

4. Earthquakes occurring in the Costa Rica-Panama-Colombia region provide important information on the tectonic framework of the Panamanian Isthmus in Central America. Earthquake epicenters generally define the boundaries between the Cocos, Nazca, and Caribbean plates; focal mechanisms for these earthquakes reflect the relative motion of the plates. However, the boundary between the Caribbean and Nazca plates presently is not well defined by seismicity. A more detailed examination of the seismicity pattern is currently being conducted to obtain a more complete understanding of the seismotectonic characteristics of the Panama segment. Earthquake locations for events with $m_b \geq 5.0$ are being recomputed with the method of joint hypocenter determination (JHD). Also, focal mechanisms for many of these earthquakes are being recompiled from the published literature or are being determined using modern surface-wave techniques.

5. To a depth of about 160 km, the upper mantle P-wave velocity beneath the Rio Grande rift and Jemez lineament is 4-6 percent lower than beneath the High Plains Province. A 3-D, P-wave velocity inversion shows scant evidence for pronounced low P-wave velocity beneath the 240-km-long section of the Rio Grande rift covered by our array. However, the inversion shows a primary trend of 1-2 percent lower P-wave velocity underlying the northeast-trending Jemez lineament, down to a depth of about 160 km. The Jemez lineament is defined by extensive Pliocene-Pleistocene volcanics and late Quaternary faults. The upper mantle low-velocity segment beneath the Jemez lineament is at most 100 km wide and at least 150-200 km long, extending in our inversion from Mt. Taylor through the Jemez volcanic center and through the Rio Grande rift. A Backus-Gilbert resolution calculation indicates that these results are well-resolved.

Reports

Mendoza, Carlos and Hartzell, S. H., Inversion for slip distribution using GDSN P-waves--North Palm Springs, Borah Peak, and Michoacan earthquakes: Bulletin of the Seismological Society of America (submitted).

Spence, William, 1988, Anomalous subduction and the origins of stresses at Cascadia: Journal of Geophysical Research (submitted).

# United States Earthquakes

9920-01222

Carl W. Stover
Branch of Global Seismology and Geomagnetism
U.S. Geological Survey
Denver Federal Center
Box 25046, Mail Stop 967
Denver, Colorado 80225
(303) 236-1500

## Investigations

One hundred and thirty earthquakes in 21 states were canvassed by a mail questionnaire for felt and damage data. Fifty seven of these earthquakes occurred in California and 28 in Alaska. The most destructive one occurred near Whittier, California, on October 1, 1987, UTC, with magnitudes of 5.8 $m_b$, 5.8 $M_S$, 5.9 $M_L$ (PAS). Two aftershocks on October 4, 1987, and February 11, 1988, magnitudes 5.3 $M_L$ (PAS) and 5.0 $M_L$ (PAS), respectively, caused additional damage in the Whittier area. The Imperial Valley of southern California suffered damage from two earthquakes on November 24, 1987, UTC. These quakes had magnitudes of 6.2 $M_S$ and 6.6 $M_S$. The second earthquake injured 94 people and caused an estimated $2.6 million damage. The largest event occurred on November 30, 1987, UTC in the Gulf of Alaska, magnitude 7.6 $M_S$, and caused minor damage at Yakutat, Alaska.

Hypocenters for earthquakes in the United States for the period October 1, 1987, to March 31, 1988, have been computed and published in the Preliminary Determination of Epicenters (PDE) Weekly and Monthly Listings. A new publication, tentatively titled "History of United States Earthquakes" is being compiled. This publication will list all known earthquakes of intensity VI or larger and magnitude 4.5 or larger. It will also contain descriptions of the damage, isoseismal maps for large earthquakes, and some seismicity maps.

## Results

A preliminary maximum intensity of VII has been assigned to the October 1, 1987, Whittier Narrows earthquake. The most severe damage occurred in Whittier, primarily in the old Whittier commercial district where three buildings collapsed and 10 were damaged beyond repair. Most of these damaged buildings were constructed between 1900 and 1920. Newer buildings sustained little damage. Many chimneys fell or were broken at the roofline, masonry walls were severely cracked or partially collapsed, houses shifted off their foundations, and attached porches collapsed. It was felt over an area of approximately 100,000 km of California and Nevada, caused eight deaths, and caused an estimated $358 million in damage.

State seismicity maps for Colorado (MF-2036), New Mexico (MF-2035), and Texas (MF-2034), have been updated through 1983 and reprinted. United States Earthquakes, 1984, is completed and should be printed in June 1988. United States Earthquakes, 1985, is about 50 percent completed.

# Worldwide Standardized Seismograph Network (WWSSN)

9920-01201

Russ Wilson
WWSSN Project Chief
Branch of Global Seismology and Geomagnetism
U.S. Geological Survey
Albuquerque Seismological Laboratory
Building 10002, Kirtland AFB-East
Albuquerque, New Mexico 87115-5000
(505) 844-4637

Worldwide Standardized Seismograph Network (WWSSN)

## Investigations

1. Technical and operational support was provided to each station in the Worldwide Standardized Seismograph Network (WWSSN) as needed and required.

2. One hundred and three modules and components were repaired, and 180 separate items were shipped to 88 separate locations to support the WWSSN network during this period.

## Results

A continuous flow of high-quality seismic data from the cooperating WWSSN stations within the network was provided to users in the seismological community.

## WWSSN Maintenance and Calibration Visits.

1. Ponta Delgada, Azores (PDA) - Status not known. Replacement modules and parts sent December 30, 1987.
2. Seoul, Korea, (SEO) - Status not known. Replacement modules and parts sent January 7, 1988.
3. All other WWSSN stations are fully operational.

South Pole Antarctica (SPA) - Winter-Over. October 5-16, 1978, Mr. Eric Wong from Denver, Colorado, and Mr. Gregory Manual from Reston, Virginia, were trained to operate and maintain the SPA WWSSN station.

Heated-Stylus System for WWSSN Seismograph Networks. During the period of October 1987 through March 1988, 27 heated-stylus conversion kits were tested, calibrated and sent to the following WWSSN stations to be installed by station personnel:

1. University of Panama, Panama (MPA) - Three-LP, One-SP
2. Nurmijarvia, Finland (NUR) - Three-LP, One-SP
3. Kevo, Finland (KEV) - DWWSSN Digital Station
4. Bogota, Colombia (BOG) - Three-LP, Three-SP
5. Brasilia, Brazil (BDF) - DWWSSN Digital Station
6. Baguio City, Philippines (BAG) - One-LP, Three-SP

7. Davao, Philippines (DAV) - One-LP, Three-SP
8. Shillong, India (SHL) - Three-LP, One-SP
9. Quetta, Pakistan (QUE) - Three-LP, One-SP
10. Nairobi, Kenya (NAI) - Three-LP, One-SP
11. Poona, India (POO) - Three-LP, One-SP
12. L'Aquila, Italy - Three-LP, One-SP
13. Seoul, Korea (SEO) - One-LP, Three-SP
14. Songkhla, Thailand (SNG) - Three-LP, One-SP
15. Wellington (South Karori), New Zealand (WEL) - Three-LP, One-SP
16. Windhoek, South Africa (WIN) - Three-LP, One-SP
17. Lormes, France (LOR) - Three-LP, One-SP
18. Arequipa, Peru (ARE) - One-LP, Three-SP
19. Nana, Peru (NNA) - One-LP, Three-SP
20. Eskdalemuir, Scotland (ESK) - Three-LP, One-SP
21. Akureyri, Iceland (AKU) - One-LP, Three-SP
22. Riverview, Australia (RIV) - Three-LP, One-SP
23. Port Moresby, Paupa, New Guinea - Three-LP, One-SP
24. Athens, Greece (ATH) - Three-LP, One-SP
25. Silverton, South Africa (SLR) - DWWSSN Digital Station
26. Ponta Delgada, Azores (PDA) - Three-LP, One-SP
27. Porto, Portugal (PTO) - Three-LP, One-SP

As of April 1, 1988, 50 heated-stylus kits have been sent to WWSSN stations. To date, we have received confirmation that 35 WWSSN stations have been converted from photographic recording to heated-stylus (visual) recording by station personnel.

# Data Processing Section

9920-02217

John Hoffman
Branch of Global Seismology and Geomagnetism
U.S. Geological Survey
Albuquerque Seismological Laboratory
Building 10002, Kirtland AFB-East
Albuquerque, New Mexico 87115-5000
(505) 844-4637

## Investigations

1. IRIS/USGS Data Collection Center. The Incorporated Research Institutions for Seismology (IRIS) have designated the Albuquerque Seismological Laboratory (ASL) to be the data collection center (DCC) for a new global network of digitally recording seismograph stations. A new computer system has been purchased (primarily with IRIS funds) and installed, a new format has been developed, and a new code has been written to process the data.

2. Data Management System for the China Digital Seismograph Network. The Data Management System in Beijing is completely installed and fully operational. All software training at the ASL for China personnel has been completed, however, several hardware modifications are planned for this summer in Beijing.

3. Data Processing for the Global Digital Seismograph Network. All of the data received from the Global Digital Seismograph Network and other contributing stations is regularly reviewed and checked for quality.

4. Network-Day Tape Program. Data from the Global Network stations are assembled into network volumes which are distributed to regional data centers and other government agencies.

## Results

1. IRIS/USGS Data Collection Center. IRIS is planning to install a network of 50 or more digital recording seismograph stations around the world during the next five years. All of the data from this network will be forwarded to the DCC located at the ASL. As part of this program, IRIS is funding much of the new hardware required by the DCC to process this large amount of data. During the past several years, three Micro Vax II computer systems complete with approximately 2.5 gigabytes of disk memory were purchased with IRIS funds and installed at the ASL. A new format has been developed at the ASL which will be used both to record data in the field and also to distribute this data in the form of network volumes to interested users. This new format is known as the "Standard for the Exchange of Earthquake Data" (SEED). A detailed report explaining this format has been published and is available. A large amount of software has been written for the new Micro Vax II computer system to process the station data both in the old and new

format. During FY88, an optical/laser jukebox memory system will be purchased for use as online storage and also to archive the seismic data.

2. Data Management System for the China Digital Seismograph Network. The Data Management System located in Beijing, China, is now processing all of the data received from the China Digital Seismograph Network (CDSN). The Chinese are now producing network-day tapes which contain all of the data recorded by the CDSN for a specific calendar day on one digital tape. Due to hardware problems caused by the existing disk memory system, a new Winchester disk, DEC Model RA81, will be installed this summer to replace the existing disk drives. There is a severe air-pollution problem in Beijing particularly during the winter coal-burning season, and a Winchester drive with a sealed airflow should resolve most of the problem. During March 1988, two Chinese scientists spent four weeks at the ASL for training in all aspects of data processing operations. The data management system in Beijing regularly furnishes copies of digital tapes from five of the CDSN stations to the ASL for incorporation into the network-day tape program.

3. Data Processing for the Global Digital Seismograph Network. During the past six months, 581 digital tapes (218 SRO/ASRO, 271 DWWSSN, 86 CDSN, 6 IRIS1) from the Global Network and other contributing stations were edited, checked for quality, corrected when feasible, and temporarily archived at the ASL. The Global Network is presently comprised of 11 SRO stations, 4 ASRO stations, and 14 DWWSSN stations. In addition, there are eight contributing stations which include Glen Almond, Canada, the five stations from the CDSN, and two IRIS1 stations. The IRIS1 stations are located at Harvard, Massachusetts and Pasadena, California, record data in a continuous mode 20 samples per second in a compressed format, and will be included in the new network volumes effective January 1, 1988. Data from the Harvard station will be included effective January 1, and the effective data for the Pasadena station will be near the end of February 1988.

4. Network-Day Tape Program. The network-day tape program is a continuing program which assembles all of the data recorded by the Global Digital Seismograph Network plus the various contributing stations for a specific calendar day onto one magnetic tape. This tape includes all the necessary station parameters, calibration data, transfer functions, and time correction information for each station in the network. Copies of these tapes are distributed to several university and government research groups for detailed analysis. The network-day tape archive at the ASL contains tapes for each day beginning January 1, 1980, up to the present. Effective January 1, 1988, the format of the network-day tapes was changed to the new SEED format previously mentioned in Section 1. A new format was required to accommodate the large volumes of data that will become available to the seismic community over the next several years. By the end of 1990, a network volume for a particular day will approach 150 megabytes, and within two or three years from that date will probably exceed 300 megabytes each day.

## Reports

Hoffman, John, P., 1987, Data management system for the China digital seismograph network: Open-File Report 87-603, 24 p.

# Data Processing, Golden

9950-02088

Robert B. Park
Branch of Geologic Risk Assessment
U.S. Geological Survey
Box 25046, MS 966, Denver Federal Center
Denver, CO 80225
(303) 236-1638

## Investigations

The purpose of this project is to provide the day-to-day management and systems maintenance and development for the Golden Data Processing Center. The center supports Branch of Geologic Risk Assessment with a variety of computer services. The systems include a PDP 11/70, a VAX/750, a VAX/780, a MicroVAX, and two PDP 11/34's. Total memory is 14 mbytes and disk space is approximately 4 G bytes. Peripherals include four plotters, ten mag-tape units, an analog tape unit, two line printers, 5 CRT terminals with graphics, and a Summagraphic digitizing table. Dial-up is available on all the major systems and hardwire lines are available for user terminals on the upper floors of the building. Users may access any of the systems through a Gandalf terminal switch. Operating systems used are RSX11 (11/34's), Unix (11/70), RT11 (LSI's) and VMS (VAX's).

## Results

Computation performed is primarily related to the Hazards program; however, work is also done for the Induced Seismicity and Prediction programs as well as for DARPA, ACDA, and U.S. Bureau of Reclamation, among others.

The data center supports research in assessing seismic risk and the construction of national risk maps. It also provides capability for digitizing analog chart recordings and maps as well as analog tape. Also, most, if not all, of the research computing related to the hazards program are supported by the data center.

The data center also supports equipment for online digital monitoring of Nevada and Colorado Western Slope seismicity. Also, it provides capability for processing seismic data recorded on field analog and digital cassette tape in various formats.

# National Earthquake Information Service

9920-01194

Waverly J. Person
Branch of Global Seismology and Geomagnetism
U.S. Geological Survey
Denver Federal Center
Box 25046, Mail Stop 967
Denver, Colorado 80225
(303) 236-1500

## Investigations and Results

The Quick Epicenter Determinations (QED) continues to be available to individuals and groups having access to a 300-baud terminal with dial-up capabilities to a toll-free watts number or a commercial telephone number in Golden, Colorado. The time period of data available in the QED is approximately 3 weeks (from about 2 days behind real time to the current PDE in production). The QED program is available on a 24-hour basis, 7 days a week. From October 1, 1987, through March 31, 1988, we have had approximately 2,518 log-ins.

The weekly publication, Preliminary Determination of Epicenters (PDE) continues to be published, averaging about 100 earthquakes per issue. The QED, PDE Monthly Listing and Earthquake Data Report (EDR) are now being run on the NEIS VAX/8250, transferred from the VAX 8250.

Telegraphic data are now being received from the USSR on magnitude 6.5 or greater earthquakes. We are still having discussions with representatives from the Institute of the Physics of the Earth, trying to get data on a routine basis.

Data from the People's Republic of China via the American Embassy are being received in a very timely manner and in time for the PDE publication. We continue to receive four stations on a weekly basis from the State Seismological Bureau of the People's Republic of China. The Bulletins with additional data are now being received in time for the Monthly. Data are now being received from New Zealand by computer. Special efforts are being made to receive more data from the Latin American countries on a more timely basis. We have rapid data exchange (alarm quakes) with Centre Seismologique European-Mediterranean (CSEM), Strasbourg, France, and Instituto Nazionale de Geofisica, Rome, Italy, and Sicily, and data by telephone from Mundaring Geophysical Observatory, Mundaring, Western Australia and Japan Meteorological Agency (JMA).

The Monthly Listing of Earthquakes is up to date. As of March 31, 1988, the Monthly Listing and Earthquake Data Report (EDR) were completed through November 1987. A total of 5,760 events was published for the 6-month period. Total number of events published for 1986 were 12,709. Solutions continue to be determined when possible and published in the Monthly Listing and EDR for any earthquake having an $m_b$ magnitude $\geq$ 5.8. Centroid moment tensor solutions from Harvard University continue to be published in the Monthly Listing and EDR. Moment tensor solutions are being computed by the U.S. Geological Survey and are also published in the above publications. Waveform plots are being published for selected events having $m_b$ magnitudes $\geq$ 5.8. Beginning with the month of October 1985, depths for selected events were obtained from broadband displacement seismograms and waveform plots published in the Monthly.

The Earthquake Early Alerting Service (EEAS) continues to provide information on recent earthquakes on a 24-hour basis to the Office of Earthquakes, Volcanoes, and Engineering, scientists, news media, other government agencies, foreign countries, and the general public.

Fifty-nine releases were made from October 1, 1987, through March 31, 1988. The most significant earthquakes released in the United States were in Southern California: October 1, 1987, a magnitude 5.7 in the Whittier area; November 24, 1987, a magnitude 6.2 and a magnitude 6.6 in the Westmorland-El Centro area; November 17, 1987, a magnitude 7.0; November 30, 1987, a magnitude 7.6; and March 6, 1988, a magnitude 7.6 in the Gulf of Alaska. Foreign earthquakes: October 6, a magnitude 7.3 in the Tonga Islands; October 16, a magnitude 7.4 in the New Britain region; October 25, a magnitude 7.0 in West Irian; November 26, a magnitude 6.5 in Timor; and December 17, a magnitude 6.4 in Japan.

## Reports

Monthly Listing of Earthquakes and Earthquake Data Reports (EDR); six publications from June 1987 through November 1987. Compilers: W. Jacobs, L. Kerry, J. Minsch, R. Needham, W. Person, B. Presgrave, W. Schmieder.

Person, Waverly J., Seismological Notes: Bulletin of the Seismological Society of America, v. 77, no. 6, January-February 1987; v. 78, no. 1, March-April 1987.

Preliminary Determination of Epicenters (PDE); 26 weekly publications from October 8, 1987, through March 31, 1988, numbers 37-87 through 10-88. Compilers: W. Jacobs, L. Kerry, J. Minsch, R. Needham, W. Person, B. Presgrave, W. Schmieder.

Quick Epicenter Determination (QED) (daily): Distributed only by electronic media.

Monthly Listing of Earthquakes--July-September (Microfiche): Seismological Research Letters, v. 58, no. 3; July-September 1986, v. 58, no. 4; October-December 1987. Compilers: W. Jacobs, L. Kerry, J. Minsch, R. Needham, W. Person, B. Presgrave, W. Schmieder.

Person, Waverly J., Earthquake Information Bulletin "Earthquakes," v. 19, no. 2, November-December 1986.

# Seismic Review and Data Services

9920-01204

James N. Taggart
Branch of Global Seismology and Geomagnetism
U.S. Geological Survey
Denver Federal Center
Box 25046, Mail Stop 969
Denver, Colorado 80225
(303) 236-1506

## Investigations and Results

Technical review, quality control, and photography were carried out on 227 station-months of seismograms from the Worldwide Standardized Seismograph Network (WWSSN). During the first two months of the reporting period, diazo negatives for eight FY-87 standing orders were prepared and shipped by the contractor. Eleven standing orders for FY-88 and back orders for four fiscal years have been received during this reporting period. Two standing orders for Canadian Standard Network (CSN) films also have been received. Special requests for WWSSN, CSN, and pre-1963 historical seismogram films have been received at a slightly slower rate than during the previous six months.

Conversion to heated pen recording has been completed at WWSSN stations outside the continental United States by another project. Following our recommendations, four WWSSN stations in the continental United States will be given heated pen conversion kits, and several additional stations will continue to be supplied with photographic paper until they are replaced by the state-of-the-art digital seismograph stations of the U.S. National Seismograph Network.

No additional filmed historical seismograms were received during this reporting period. The holdings of the World Data Center A for Seismology archives now include silver negative and diazo films of 5,150,000 WWSSN seismograms (1962-1987), 800,000 CSN seismograms (1963-1987), and 600,000 historical seismograms (1899-1962).

# Computer and Data Analysis Services

9920-04151

Madeleine Zirbes
Branch of Global Seismology and Geomagnetism
U.S. Geological Survey
Denver Federal Center
Box 25046, Mail Stop 967
Denver, Colorado 80225
(303) 236-1506

## Investigations

1. NEIC Monthly Listing. Contribute waveform data for all events of magnitude 5.8 or greater when sufficient data exists.

2. Network Day Tape Support. Develop, distribute, and support FORTRAN programs to access network-day tapes and station tapes.

3. SEED Support. Develop, distribute, and support software for the Standard for the Exchange of Earthquake Data (SEED) format.

4. Event Tape Production and Distribution. Produce and distribute event tapes.

5. Event CD-ROM Production and Distribution. Produce and distribute event CD-ROM data.

## Results

1. NEIC Monthly Listing. Since July 1982, digital waveform plots have been contributed to the Monthly Listings. USGS fault-plane and moment tensor solutions, and broadband data have also been incorporated into the focal sphere plots.

2. Network Day Tape Support. FORTRAN software to read and extract digital data from station tapes (1976-1979) and network-day tapes (1980-1987) has been developed and distributed to the research community worldwide. Users are supported on a variety of computers.

3. SEED Support. A new Standard for the Exchange of Earthquake Data (SEED) has been created and tapes are now being produced and distributed by the Albuquerque Seismic Laboratory. FORTRAN software is being developed to read and extract the digital data from the SEED tapes, and this software will be made available to the research community.

4. Event Tape Production and Distribution. Event tapes have been produced from network-day tapes for data from 1980 through 1986 for all events with magnitude 5.5 or greater. These tapes are distributed to 25 institutions

worldwide along with a waveform catalog that provides a visual display of the data available for each event.

5. Event CD-ROM Production and Distribution. Data from the event tapes are reformatted and sent to a CD-ROM mastering facility for replication. The CD-ROMs are being distributed to over 150 universities across the U.S. and geophysical research institutes worldwide. Retrieval software has been developed for the IBM/PC/AT/386 compatibles and distributed. Menu-driven PC software is being developed for easier access to the digital data.

# National Strong-Motion Network: Data Processing

9910-02757

A.G. Brady
Branch of Engineering Seismology and Geology
U.S. Geological Survey
345 Middlefield Road, MS 977
Menlo Park, California 94025
(415) 329-5664

## Investigations

Four significant earthquakes in southern California in this reporting period have demanded complete attention of the staff in this project. The magnitude $M_L$=5.9 Whittier Narrows earthquake of October 1, 1987 triggered strong-motion instrumentation at 52 stations operated in the Los Angeles area as part of the National Strong-Motion Instrumentation Network (NSMIN). The aftershock of magnitude $M_L$=5.3 occurred on October 4, 1987 and triggered 30 of the main shock stations. In the following month, on November 24, a magnitude $M_L$=6.6 earthquake occurred at 1315 hr in the Superstition Hills area near the southern margin of the Salton Sea and triggered 42 stations. Among the 19 earthquakes of magnitude 4 or greater occurring that day, an $M_s$=6.2 earthquake, at 0154, triggered 25 stations. Selection of the significant records for digitizing and processing has proceeded with caution as simultaneous analysis indicates that there exists some long period signal content (out to 4 sec period) present in the records of the $M_L$ 5.9 Whittier Narrows event that would otherwide have been considered as noise and filtered out.

Digitizing details for 4 events.

| | Whittier Narrows, 1987 | | Superstition Hills | |
|---|---|---|---|---|
| | Oct. 1 | Oct. 4 | November 24, 1987 | |
| | | | 0154 hr | 1315 hr |
| Magnitude | $M_L$ 5.9 | $M_L$ 5.3 | $M_s$ 6.2 | $M_s$ 6.6 |
| Stations triggered | 52 | 30 | 25 | 42 |
| Stations with records chosen for digitization and processing | 27 | 7 | 5 | 28 |
| Total film records for digitizing | 54 | 11 | 5 | 28 |
| Total channels for digitizing | 197 | 33 | 24 | 93 |
| Digitizing duration, each event (sec) | 30 | 20 | 30 | 40 |
| At approx. 600 sps, total data points ($x10^6$) | 3.5 | 0.4 | 0.4 | 2.2 |

The number of channels per station varies from 3 (in a self-contained accelerograph with two horizontal and one vertical channel) to 33 (in a thoroughly instrumented building with several ground-level accelerographs). The October

1 event provided several significant sets of structural records (from Whittier, Alhambra, Norwalk, and Los Angeles). The $M_s$6.6 event at Superstition Hills has provided downhole accelerographs from a liquefaction array together with pore presure records from the liquefying layers.

Digitization and processing of the close-in October 1 records has included multiple records at structural stations. Displacements calculated by integrating are coherent over periods as long as 4 sec at each of two structural stations. We conclude from this that there are long period arrivals at many stations during the interval (approximately 2 sec) between triggering and the arrival of the shear wave. These long-period P-waves reach amplitudes of the order of 6 cm/sec/sec, or, perhaps, result in a tilting of the ground surface by 0.006 radian. The directions of these motions are approximately radial with respect to the epicenter.

Processing of the accelerograms and pore pressure records from the liquefaction array has forced a lowering of the high-frequency limits in the filtering procedures. Digitizing noise from the film traces, which are not as clear as usual, may require a high frequency cut of 20 Hz.

## Results

Routine processing, including digitizing (D), computer processing (P), and report preparation (R) of these accelerograms continues: 41 records (D), from Whittier Narrows earthquake of October 1, 1987, out to 31 km; 15 records (P, R) from Whittier Narrows, October 1, 1987; 2 records (D), from the liquefaction array during the Superstition Hills earthquakes, November 24, 1987.

## References

For copies of the records, refer to U.S. Geological Survey Open-File Reports 87-616, 87-672, and 88-38 for strong-motion data from the 1 October 1987 Whittier Narrows, 24 November 1987 Superstition Hills, and 4 October 1987 Whittier Narrows aftershock, respectively.

## Reports

Brady, A.G., Etheredge, E., and Porcella, R.L., 1988, A preliminary assessment of the strong-motion records from the October 1, 1987, M5.9, Whittier Narrows, California, earthquake: accepted by Spectra.

Brady, A.G., Mork, P.N., and Seekins, L.C., 1988, Processed strong-motion records; Whittier Narrows, California, earthquake; October 1, 1987, Volume 1: USGS-NSMIN stations within 15 km of the epicenter: submitted for U.S. Geological Survey Open-File Report.

Brady, A.G., Mork, P.N., and Seekins, L.C., 1988, Processed strong-motion records from the Imperial Wildlife liquefaction array during the Superstition Hills earthquakes, November 24, 1987: in preparation.

Hauksson, E., and others, 1988, The 1987 Whittier Narrows earthquake in the Los Angeles metropolitan area, California: Science, v. 239, no. 4846, p. 1409-1412.

# National Strong-Motion Network: Engineering Data Analysis

9910-02760

A.G. Brady and G.N. Bycroft
Branch of Engineering Seismology and Geology
U.S. Geological Survey
345 Middlefield Road, MS 977
Menlo Park, California 94025
(415) 329-5664 or (415) 329-5665

## Investigations

### Soil Structure Interaction

Studies on fundamental problems of soil structure interaction continue. These problems include the development of asymptotic solutions for the impedence functions of a layered elastic half space. Such solutions will give a better correlation between theory and the experimental results obstained in the Camp Parks experiments. These exeriments investigated the motion at the top surface of a low pedestal during the passage in the soil supporting the pedestal, of seismic waves from a multi-depth, sequential, explosive device simulating earthquake motion.

The relationships between the free-field motion and the motions on a trapezoidal section dam or ridge of the same section has been obtained and will be tested against experimental data. A multi-degree of freedom differential spectra model has been developed and will be applied to records obtained from the differential arrays at El Centro and Hollister.

### Analysis of Records from an Earth Dam

This study used records at Leroy Anderson Dam, Santa Clara County, California, which were obtained during the $M_L$=6.2 Morgan Hill earthquake of April 24, 1984 and the $M_L$=5.8 Mt. Lewis earthquake of March 31, 1986. Between the two earthquakes the instrumentation was extended from two 3-channel accelerographs (crest and downstream) to a 12-channel central recording system in addition to the crest instrument.

Modal responses of the dam obtained from both sets of records are compared with those predicted by current theories of earth dam behavior. Amplification spectra are used to derive modal frequencies reasonably accurately. 2-D homogeneous and non-homogeneous models closely predict the mode shapes and are used to estimate material properties. The design of the instrumentation array's locations was important in the recovery of these results.

# Preliminary Analysis of Structural Records from the Whittier Narrows, California, Earthquake, October 1, 1987

This earthquake provided a wide variety of significant records from buildings in the strongly shaken area in southern California:

| City | No. of Stories | Epicentral Distance (km) | Peak Horizontal Acceleration (g) Ground level | Instrumentation |
|---|---|---|---|---|
| Alhambra | 12 | 8 | 0.30 | 3 triaxial |
| Whittier | 10 | 10 | 0.63 | 3 triaxial |
| Norwalk | 8 | 15 | 0.21 | 4 triaxial |
| Norwalk | 7 | 15 | 0.21 | 3 triaxial<br>and 24 channels |
| Los Angeles | 8 | 16 | 0.16 | 3 triaxial |
| Los Angeles | 33 | 17 | 0.18 | 3 triaxial<br>and 12 channels |

A study of copies of the original records shows many of these buildings with first and second mode vibrations in both horizontal directions, some in-plane floor bending, and torsion. Periods of near-sinusoidal oscillations provide opportunities to calculate displacement amplitudes. The routine processed data for the first two buildings on the list confirm these preliminary findings. Further digitizing and processing continues.

## Reports

Fedock, J.J., and Brady, A.G., 1988, Analysis of strong-motion records from Leroy Anderson Dam: U.S. Geological Survey Open-File Report in preparation.

Brady, A.G., Etheredge, E., and Porcella, R.L., 1988, A preliminary assessment of the strong-motion records from the October 1, 1987, M5.9, Whittier Narrows, California, earthquake: accepted by Spectra.

Brady, A.G., Mork, P.N., and Seekins, L.C., 1988, Processed strong-motion records; Whittier Narrows, California, earthquake; October 1, 1987, Volume 1: USGS-NSMIN stations within 15 km of the epicenter: submitted for U.S. Geological Survey Open-File Report .

Brady, A.G., 1988, An engineering assessment of the structural records grom the USGS-maintained stations -- Whittier Narrows, October 1, 1987 [abs.]: Seismological Society of America, Honolulu.

04/88

# National Strong Motion Data Center

9910-02085

Howard Bundock
Branch of Engineering Seismology and Geology
U.S. Geological Survey
345 Middlefield Road, MS 977
Menlo Park, California 94025
(415) 329-5621, FTS. 459-5621

## Investigations:

The objectives of the National Strong Motion Data Center are to:

Maintain a strong capability for the processing, analysis, and dissemination of all strong motion data collected on the National Strong Motion Network and data collected on portable arrays;

Support research projects in the Branch of Engineering Seismology and Geology by providing programming and computer support including digitizing, graphics, processing and plotting capabilities as an aid to earthquake investigations;

Manage and maintain computer hardware and software so that it is ready to process data rapidly in the event of an earthquake.

The Center's facilities include a new VAX 8250 and a VAX 11/750 computer operating under VMS Version 4.6, a PDP 11/70 running RSX-11M+ and two PDP 11/73 computers. The Center's computers are part of a local area network with other branch, OEVE, Geologic Division, and ISD computers, and we have access to computers Survey-wide over Geonet. Project personnel join other office branches in the support of the OEVE VAX 11/785.

Investigations during the first six months of FY88 included study of new operating system software allowing network access to printers. We also prepared for the installation of hardware upgrades on the graphics systems used, and for installation of a number of new graphics terminals. The project has worked closely with persons involved with the Rolm data communications and also with those involved with moving back to permanent quarters after the asbestos removal project. The project has analyzed existing Branch computer resources so that our new VAX 8250 could be installed with a minimum of new peripheral hardware. Methods of tying our local area network into a wide area network or electronic mail facility were studied and the project continued preparation for maintenance of computer hardware under a Survey-wide, five-year contract. The project continues its support of the OEVE VAX 11/785 project. As an ongoing policy, the project has kept its hardware up to current revision levels, and operating system, network, and other software at the most recent versions.

Results:

As a result of these and previous investigations, the project has:

Installed a laser printer and set up software for Branch and Office computer systems, so that the printer can be accessed from any computer on the network;

Further developed and documented a complete procedure for digitizing and plotting map features such as fault lines, earthquakes, etc. and a procedure for making slides for presentation, and upgraded 3-D graphics workstations for plotting surfaces topography, faults and hypocenters, and other plots;

Installed a number of inexpensive graphics terminals for use of individual scientists and for use in the common terminal room;

The project has remained informed and has supported the new Rolm data communications and has installed equipment for its use;

The project has removed all computer equipment from temporary quarters during the asbestos removal project back to where it belongs, and has reinstalled it;

Installed a VAX 8250 BI computer for the Branch using a disk that can be shared with our VAX 11/750. This computer needed no other peripherals as it can be accessed over Ethernet and its system disk can be backed up using the VAX 11/750;

Gained access for Branch scientists needing access to BITNET, a widely used electronic mail network;

Did a complete inventory of all hardware on all Branch and Office computer systems in preparation for commencement of a Survey-wide, five-year hardware maintenance contract;

Managed and maintained the OEVE VAX 11/785 and joined with representatives from other Branches in managing the project;

Managed, maintained, updated Branch and office computer system hardware and software.

Reports:

None.

# Instrumentation of Structures

9910-04099

Mehmet Celebi
Branch of Engineering Seismology and Geology
U.S. Geological Survey
345 Middlefield Road, MS 977
Menlo Park, California 94025
(415) 329-5623

## Investigations:

1. The process of selection of structures to be recommended for strong-motion instrumentation has continued in Los Angeles, Orange County, northeastern United States (Boston), Alaska, Hawaii, and Puget Sound (Seattle) and Puerto Rico. This effort is being extended to Salt Lake City.

2. The process to design instrumentation schemes for selected structures has continued. Applicable permits for two structures, in San Bernardino, California, and one in Anchorage, Alaska, have been obtained. Current efforts are being made to obtain permits for structures in Hawaii and Boston.

3. The process of implementation of instrumentation for those structures for which instrumentation schemes have been designed has continued in Los Angeles (1100 Wilshire Finance Building), in Charleston, SC (the Charleston Place), and in San Bernardino, California. The strong-motion recording systems in these buildings are now operational. Non-destructive testing of 1100 Wilshire Finance Building will be made soon. Agreements have been made to instrument Salt Lake City and County Building in cooperation with the City of Salt Lake City. The building is the first building being retrofitted by base isolation. Non-destructive dynamic testing of the building is being carried out progressively to evaluate the dynamic characteristics of the building before and after being rehabilitated by base isolation. Design of instrumentation schemes for a building in Anchorage, Alaska and Boston, Massachusetts, are being carried out.

4. The minimal instrumentation in a building in Alhambra, Southern California, is being upgraded to contain extensive instrumentation to acquire sufficient data to study complete response modes of the building. New digital recording systems are being installed.

5. Agreements have been made with UCLA to convert the wind-monitoring system in the Theme Buildings in Los Angeles (previously financed by NSF) into a strong-motion monitoring system. Plans are being made to implement the conversion.

6. Studies of records obtained from instrumented structures are carried out. In particular, the records obtained during the October 1, 1987 Whittier Narrows earthquake from the 1100 Wilshire Finance Building (Los Angeles), the Bechtel Building (Norwalk), and the Santa Ana River Bridge (base-isolated) will be investigated as soon as they are available.

Results:

1. The report of the Alaska advisory committee for strong motion instrumentation of structures has been completed. This report will shortly be issued as an open-file report.

2. The report of the Los Angeles advisory committee for strong motion instrumentation of structures has been completed. This report will shortly be issued as an open-file report.

3. A draft of the report of the Boston area advisory committee for strong motion instrumentation of structures has been prepared. This report is now being finalized and will be issued shortly.

4. The Hawaii committee on strong motion instrumentation of structures has completed its deliberations and a draft report is being prepared.

5. Papers resulting from study of records obtained from structures are prepared.

Reports:

Celebi, M., Bongiovanni, G., Safak, E., and Brady, G., 1988, Seismic response of a large-span roof diaphragm (paper submitted to Earthquake SPECTRA).

Bongiovanni, G., and Celebi, M., and Safak, E., 1988, Seismic rocking response of a triangular building founded on sand: paper accepted for publication in Earthquake SPECTRA.

04/88

# STRONG-MOTION INSTRUMENTATION NETWORK
# DESIGN, DEVELOPMENT, AND OPERATIONS

9910-02764, 9910-02765

Ed Etheredge, Dick Maley, and Ron Porcella

Branch of Engineering Seismology and Geology
345 Middlefield Road, MS 977
Menlo Park, California 94025
(415) 329-5667

## Investigations

The Strong-Motion laboratory, in cooperation with federal, state, and local agencies and advisory engineering committees, designs, develops, and operates an instrumentation program in 41 states and Puerto Rico. Program goals include: (1) recording of potentially damaging ground motion in regional networks, and in closely spaced sensor arrays; and (2) monitoring the structural response of buildings, bridges and dams using sensors placed in critical locations. The present coordinated network consists of approximately 1,000 recording units installed at 600 ground sites, 27 buildings, 5 bridges, 56 dams, and 2 pumping plants.

## New Instrumentation

A 12-channel structural instrumentation system was installed in the San Bernardino County Government Center building located in the downtown area of San Bernardino, California. The building is a 6-story steel-frame structure, generally L-shaped, but with a varying configuration at different levels (figure 1). A free-field accelerograph was installed a few hundred feet east of the building.

Recent ground motion stations have been installed at the following locations:

| | |
|---|---|
| California | |
| Calaveras fault zone | 6 |
| Los Angeles - central rock site | 1 |
| San Bernardino array (see below) | 4 |
| Hawaii | |
| Hilo Hospital | 1 |
| Washington | |
| Olympia | 1 |

The San Bernardino array being developed along the San Andreas and San Jacinto faults and through the high potential liquefaction zone in central San Bernardino will more than double the number of accelerographs in the area. Thus far four new ground stations have been established: at Devore, two in north San Bernardino, and one in conjunction with instrumentation in the County government building. Accelerographs, all equipped with WWVB radio receivers, are being located in existing small buildings or Survey installed fiberglass housings.

The strong-motion group is conducting a program of upgrading the dam instrumentation network for the Sacramento District Corps of Engineers (COE). The COE is spending nearly $300,000 on their relatively small network to replace obsolescent instrumentation, add numerous real-time systems, and install fiberglass housings. This project will be completed during FY-88.

Planning is underway for the instrumentation of several buildings outside of California, chiefly those recommended by regional advisory committees. These include:

| | | |
|---|---|---|
| Tang Hall, MIT | 22 stories | Moderate instrumentation |
| Sohio Bldg. Anchorage | 13 stories | Extensive instrumentation |
| Salt Lake City County Bldg | 4 stories and tower | Extensive instrumentation |
| Seattle, WA | 62 stories | Extensive instrumentation |
| Honolulu, HI | Twin 41-story buildings on different soil conditions | 1) Extensive instrumentation<br>2) Moderate instrumentation |
| Hilo, HI | 5 stories | Extensive instrumentation |

## Recent Earthquake Records

During the past 12 months strong-motion records were recovered from California, Hawaii, and Alaska. The following summarizes some of the more important results.

| Earthquake Date (G.m.t.) | Published Magnitude | Location | Records | Peak Acceleration (g) |
|---|---|---|---|---|
| 1 October 1987 | 5.9 | Whittier Narrows, CA | 95 | 0.63 ground<br>0.61 structure |
| 4 October 1987 | 5.3 | Whittier Narrows, CA | 57 | 0.33 ground<br>0.53 structure |
| 24 November 1987 | 6.2 | Superstition Hills CA | 25 | 0.22 ground |
| 24 November 1987 | 6.6 | Superstition Hills CA | 42 | 0.91 ground |
| 11 February 1988 | 5.0 | Whittier Narrows, CA | 44 | 0.25 ground<br>0.18 structure |

The data recorded from these earthquakes are described in the publications listed below.

Recent Reports

Etheredge, E., and Porcella, R., 1987, Strong-Motion data from the October 1, 1987 Whittier Narrows earthquake: U.S. Geological Survey Open-File Report 87-616, 64 p.

Porcella, R., Etheredge, E., Maley, R., and Switzer, J., 1987, Strong-Motion data from the Superstition Hills earthquakes of 0154 and 1315 (GMT), November 24, 1987: U.S. Geological Survey Open-File Report 87-672, 56 p.

Etheredge, E., and Porcella, R., 1988, Strong-Motion data from the Whittier Narrows aftershock of October 4, 1987: U.S. Geological Survey Open-File Report 88-38, 32 p.

Egill Hauksson, et al., 1988, The 1987 Whittier Narrows earthquake in the Los Angeles metropolitan area, California: Science, V 239. No. 4846, 18 March 1988, p.1409-12.

Acosta, A. V., Nielson, and J., Switzer, J., 1988, Strong-Motion data from the Whittier Narrows aftershock of February 11, 1988: U.S. Geological Survey Open-File Report, 27 p., in press.

Brady, A. G., Etheredge, E. C., and Porcella, R. L., 1988, A preliminary assessment of the strong-motion records from the October 1, 1987 M=5.9 Whittier Narrows, California, earthquake: Spectra, V 4, No, 1, February 1988, in press.

# SAN BERNARDINO
# COUNTY GOVERNMENT CENTER

## STRONG-MOTION INSTRUMENTATION

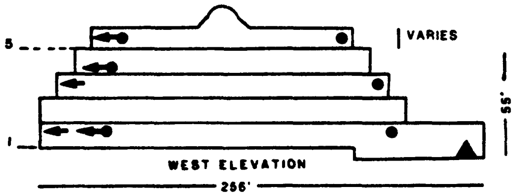

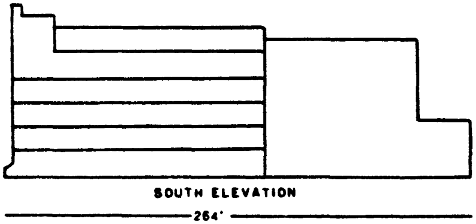

**STRUCTURE**
**Braced steel frame**

**ACCELEROMETER DIRECTION**

● INTO PLAN OF PLAN/ELEVATION

← AS SHOWN

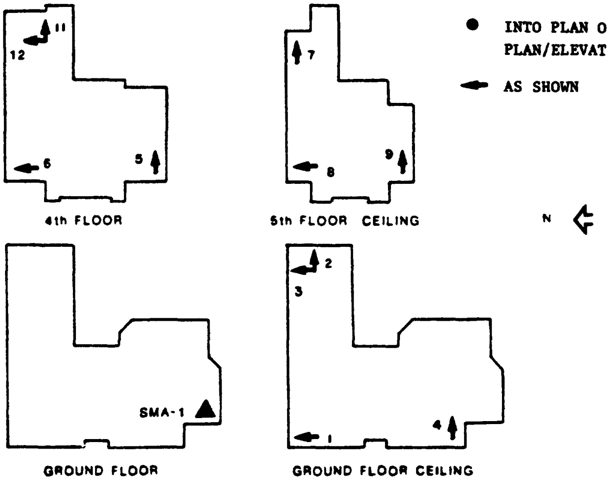

Figure 1.

# General Earthquake Observation System (GEOS)
# GEOS Analysis and Playback Systems (GAPS)

9910-03009

Gary L. Maxwell and Roger D. Borcherdt
U.S. Geological Survey
Branch of Engineering Seismology and Geology
345 Middlefield Road, Mailstop 977
Menlo Park, California 94025
(415) 329-5618 or (415) 329-5619

## Investigations

1. Development and construction of a portable, broad band, high-resolution digital data acquisition capability (GEOS) for seismology and engineering applications.
2. Development of mini- and micro-computer systems (hardware and software) (GAPS) for retrieval, processing, and archival of large columes of digital data.
3. Development of hardware and software components to improve functionality, versatility, and reliability of digital data acquisition and retrieval systems.

## Results

Design features and modifications to the General Earthquake Observation System (GEOS) incorporated or being investigated during this report period with assistance from M. Kennedy, J. Sena, C. Dietel, E.G. Jensen, and J. VanSchaack include:

1. Final engineering evaluation and testing for construction of fifty-five GEOS recorders (330 total data channels) under a construction contract awarded in FY87. Construction of first evaluation unit is expected during the next reporting period.
2. Final testing was underway for a low-power data buffer capable of storing over one million digital samples of seismic data, for use in extreme environments or in applications requiring a large pre-event memory window.
3. Integration of various software modules and features to provide more programmability by field operators to improve data quality, using higher density memory modules for containing GEOS software components.

## Reports Utilizing Data Recorded by GEOS and Processed by GAPS

Liu, H., Warrick, R.E., Westerlund, R.E., Fletcher, J.B., and Maxwell, G.L., An air-powered impulsive shear-wave source with repeatable signals: *Bulletin of the Seismological Society of America*, v. 78, p. 355.

Lindley, G.T., Archuleta, R.J., and Maxwell, G.L., Least squares fit of earthquake spectra in the Mammoth Lakes area of California (abstract): *American Geophysical Union*, 1987 Fall meeting.

# Structural Response in Support of National Strong Motion Program

9910-02759

Erdal Safak, Mehmet Celebi, A. Gerald Brady, and Richard Maley
Branch of Engineering Seismology and Geology
U.S. Geological Survey
345 Middlefield Road, MS 977
Menlo Park, California 94025
(415) 329-5648, FTS 459-5648

## Investigations

1. Implementation of structural instrumentation and design of instrumentation schemes for structures selected by instrumentation advisory committees.

2. Develop methodologies and computer software to analyze ground motion and structural vibration recordings.

3. Develop methodologies to estimate response spectra from seismological models of ground motion.

4. Continue on site response studies and structural damage correlation during the 3 March 1985 Chile earthquake.

5. Continue on structural characteristic evaluation during the 19 September 1985 Mexico earthquake.

6. Testing of the Salt Lake City and County building, which is the first building in the world to be retrofitted by base isolation.

## Results

1. As part of structural response study efforts through strong-motion instrumentation, and in accordance with recommendations of committees, two new structures are now instrumented. These are the 1100 Wilshire Building (33 stories) in Los Angeles and the Charleston Place Building (8 stories) in Charleston, South Carolina. A complete set of data has been obtained from the 1100 Wilshire Building during the October 1, 1987, Whittier Narrows earthquake.

2. A computer program is being developed to identify source and site amplification of earthquake motions from ground motion recordings, and frequency, damping, and mode shapes of buildings from the ambient and earthquake vibration recordings.

3. A method based on the random vibration theory has been developed to estimate response spectra from seismological models of ground motion. Also, a simpler model that uses only four parameters of the ground motion has been introduced for response spectra.

4. After the 3 March 1985 Chile earthquake ($M_s$=7.8), and as a result of observation of damages on ridges, as well as alluvial and sandy sites, site response studies were conducted. The results showed that there were topographical and geological amplification and these two factors contributed to the patterns of responses observed during post-earthquake surveys. In addition, data obtained from structures are being studied.

5. Approximately 15 structures in Mexico City were tested in January 1986. Some of these structures were tested in 1962 also. Studies are being finalized on the changes of dynamic characteristics of these structures.

5. Prior to installation of base isolaters, a set of vibration data from the building was obtained in September 1987 during a nuclear explosion test at the Nevada test site. Another set will be obtained after the base isolaters are installed.

## Reports

Safak, E., 1988, Analytical approach to calculation of response spectra from seismological models of ground motion: Earthquake Engineering and Structural Dynamics, v. 16, no. 1, p. 121-134.

Safak. E., Mueller, C., and Boatwright, J., 1988, A simple model for strong ground motions and response spectra: Earthquake Engineering and Structural Dynamics, v. 16, no. 2, p. 203-215.

Safak, E., and Boore, .D.M., 1988, On low-frequency errors of uniformly modulated, filtered, white-noise models for ground motion: Earthquake Engineering and Structural Dynamics, v. 16, no. 3, p. --- (March, 1988).

# Physical Constraints on Source of Ground Motion

9910-01915

D.J. Andrews
Branch of Engineering Seismology and Geology
U.S. Geological Survey
345 Middlefield Road, MS 977
Menlo Park, California 94025
(415) 329-5606

## Investigations

Implications of fault geometry for earthquake mechanics.

## Results

Work has started to model the interaction of many fault segments with arbitrary orientations. A boundary integral method in two-dimensional plane strain is being used to model interacting frictional surfaces in quasistatic equilibrium.

Modeling of two-dimensional in-plane deformation of an elastic solid containing faults leads to the following conclusions: A.) At a sharp bend in a fault there must be a fault branch, forming a triple junction. B.) Slip may occur at a triple junction in a limited number of earthquakes, with the junction gradually becoming a stronger barrier. Then a fresh fracture must be formed in a different location. For this reason there is little geologic expression of fault junctions. C.) A characteristic earthquake, defined by its barriers, changes a bit with each recurrence. D.) Slip on a fault branch may trigger slip on a main throughgoing fault.

## Reports

None.

04/88

# Ground Motion Prediction for Critical Structures

9910-01913

D. M. Boore
W. B. Joyner

Branch of Engineering Seismology and Geology
U. S. Geological Survey
345 Middlefield Road, MS 977
Menlo Park, California 94025

*Investigations:*

1. Study the $m_N$, M relation for eastern North American earthquakes.
2. Study the source scaling of earthquakes in the Northwest Territories of Canada.
3. Prepare a major review of the prediction of ground motion.

*Results:*

1. A stochastic model of ground motion has been used as a basis for comparison of data and theoretically-predicted relations between $m_N$ (commonly denoted by $m_{bLg}$) and moment magnitude for eastern North America (ENA) earthquakes. $m_N$ magnitudes are recomputed for several historical ENA earthquakes, to ensure consistency of definition and provide a meaningful data set. We show that by itself the magnitude relation cannot be used as a discriminant between two specific spectral scaling relations, one with constant stress and the other with stress increasing with seismic moment, that have been proposed for ENA earthquakes.
2. Spectral ratios of $P$-waves from a suite events occurring near the Nahanni River in the Northwest Territories of Canada and recorded 1400 km away on the WCTN network have been computed. Preliminary comparison with theoretical ratios shows that the $\omega^3$ model with a constant stress parameter does not fit the data. An $\omega^2$ model does fit the data, but the best stress parameter for this fit is over 300 bars.

*Reports:*

Atkinson, G. M. and Boore, D. M., 1987, On the $m_N$, M relation for eastern North American earthquakes, *Seismological Research Letters*, v. 58, p. 119–124.

Boore, D. M., 1988, The Richter scale–Its development and use for determining earthquake source parameters, ***Physics of the Earth and Planetary Interiors***, in press.

Joyner, W. B. and Boore, D. M., 1988, Measurement, characterization, and prediction of strong ground motion, *Proceedings Earthquake Engineering and Soil Dynamics II Conference*, Park City, Utah, June, 1988, American Society of Civil Engineers, in press.

4/15/88

# Anelastic Wave Propagation

9910-02689

Roger D. Borcherdt
Branch of Engineering Seismology and Geology
U.S. Geological Survey
345 Middlefield Road, MS 977
Menlo Park, California 94025
(415) 329-5619

## Investigations:

Volumetric strain measurements for inference of additional characteristics of anelastic seismic wave fields.

## Results:

Linear viscoelasticity accounts for anelasticity of the near-surface materials and provides a mathematical basis for interpretation of seismic radiation fields as detected simultaneously by co-located volumetric strain meters and and seismometers. The general theory provides an account of volumetric strain and displacement for general (homogeneous or inhomogeneous) P and S waves in an anelastic whole space. Solutions to the free-surface reflection problems for incident general P and S-I waves are used to evaluate the effect of the free surface on observations from co-located sensors. Corresponding expressions were derived for a Rayleigh-type surface wave on a linear viscoelastic half-space. The theory predicts a number of anelastic wave field characteristics that can be inferred from observation of volumetric strains and displacement fields as detected by co-located sensors that cannot be inferred from either sensor alone. Volumetric strain meters respond to P waves but not S waves, with simultaneous observations permitting the possible resolution of superimposed P and S wave fields into their respective components. The amplitude and phase for components of the displacement fields depend on angle of incidence, azimuth and inhomogeneity of the wave field. As volumetric strain shows no similar dependencies for direct waves, simultaneous measurement permits inference of these characteristics as well as in situ material parameters. Conversion of S energy to dilatational strain energy by the free surface is largest at angles of incidence for which inhomogeneity of the reflected P wave is near its physical limit (that is, amplitudes vary rapidly along surfaces of constant phase). For such angles of incidence in a low-loss anelastic half-space, the particle motions for the reflected P waves are elliptical, amplitudes near the surface increase with depth and phase propagation is not parallel to the free surface. Volumetric strain for a Rayleigh-type surface wave shows an exponentially damped sinusoidal dependence on depth not evident for a Rayleigh wave on an elastic half-space.

## Reports

Johnston, M.J.S., Linde, A.T., Gladwin, M., and Borcherdt, R.D., 1987, Fault failure for moderate earthquakes: Tectonophysics, v. 144, p. 189-206.

Borcherdt, R.D., Johnston, M.J.S., and Glassmoyer, G., 1987, On the use of volumetric strain meters to infer additional characteristics of seismic wave fields: Seismological Research Letter, v. 58, p. 24.

Borcherdt, R.D., Johnston, M.J.S., Linde, A., Lindh, A., Noce, T., Myren, D., Glassmoyer, G., and Maxwell, G., 1987, A high-fidelity strong-motion network surrounding the rupture zone of the 1966 Parkfield earthquake: EOS, Transactions, American Geophysical Union, v. 68, p. 1357.

Johnston, M.J.S., Borcherdt, R.D., Glassmoyer, G., and Linde, A.T., 1987, Static and dynamic strains during the July 21, 1986, Chalfant earthquake near the Long Valley Caldera, California: Seismological Research Letters, v. 58, p. 24.

Borcherdt, R.D., and Johnston, M.J.S., 1988, A broad-band, wide dynamic range, strong-motion network near Parkfield, California USA for measurement of acceleration and volumetric strain: Proceedings, Ninth World Conference on Earthquake Engineering, in press.

Myren, G.D., Johnston, M.J.S., Linde, A.T., Gladwin, M.T., and Borcherdt, R.D., 1987, Borehole strain array near Parkfield, California: EOS, Transactions, American Geophysical Union, v. 68, p. 1358.

Johnston, M.J.S., Borcherdt, R.D., Gladwin, M.T., Glassmoyer, G., and Linde, A.T., 1987, Static and dynamic strain during the $M_L$ 5.9 Banning, California, earthquake on July 8, 1986: EOS, Transactions, American Geophysical Union, v. 68, p. 1244.

Borcherdt, R.D., 1988, Volumetric strain and particle displacements for body and surface waves in a general viscoelastic half-space, accepted, Geophysical Journal of the Royal Astronomical Society.

# Velocity and Attenuation Measurements in Engineering Sesimology

9910-02413

Hsi-Ping Liu
Branch of Engineering Seismology and Geology
U. S. Geological Survey
345 Middlefield Road, MS 977
Menlo Park, California 94025
(415) 329-5643

## Investigations

1. Computation of near-field zero-offset vertical impulse response from a horizontal point force acting (i) in a homogeneous unbounded anelastic medium and (ii) on the free surface of an anelastic half space. These solutions are needed for data interpretation in the measurement of seismic attenuation using the pulse-broadening method in conjunction with the in-hole and down-hole method, respectively.
2. Construction of two borehole seismometers for the third site in the Anza Digital Seismic array. (The first two sites are at Keenwild, California, and at Pinon Flat Observatory, California.) Each borehole seismometer contains three orthogonal geophones having natural period of 0.5 s. The horizontal geophones are leveled to 0.1°, which is necessary to avoid nonlinear response and asymmetrical clipping.

## Results

1. Exact numerical Green's function solution of (i) a point force acting in an unbounded infinite anelastic medium, and (ii) a tangential point load acting on the surface of an anelastic half space, have been obtained for the anelastic behavior characterized by a band-limited constant Q. These results will be used in the interpretation of the seismic attenuation data obtained for the San Francisco bay mud.
2. The two borehole seismometers have been fabricated and pressure tested in a presure vessel in our laboratory. They are currently been assembled for field installation scheduled for late April, 1988.

## Reports

Liu, H. P., R. E. Warrick, R. E. Westerlund, J. B. Fletcher, and G. L. Maxwell, 1988, An air-powered impulsive shear-wave source with repeatble signals: *Bulletin of the Seismological Society of America* **78**, p. 355-369.

Liu, H. P., Effect of source spectrum on seismic attenuation measurements using the pulse-broadening method: director approval.

# Seismic Properties of the Carbonate Accumulation Layer in Quaternary Fans: Potential for Macroscopic Dating Technique

9910-04193

Hsi-Ping Liu
Branch of Engineering Seismology and Geology
U. S. Geological Survey
345 Middlefield Road, MS 977
Menlo Park, California 94025
(415) 329-5643

## Investigations

Calcareous soils found in alluvial fans cut by normal faults have been used to determine the ages and amounts of Quaternary faulting (*e.g.,* Machette, 1978). "Soils age, and hence fault ages, can be calculated by measuring the total pedogenic calcium carbonate content in a section of buried paleosols and by using an independently established maximum soil formation rate." Carbonate cementation also increases the shear rigidity of the soil; the product of shear rigidity and thickness of a paleosol is likely proportional to the length of period of tectonic stability during which the soil layer was exposed at the surface. The research objective of this project is to determine the shear rigidity of calcareous soils of known age by seismic methods using the shear-wave generator developed by Liu *et al.* (1988). The shear rigidity determined by the seismic methods will be correlated with the thickness and the known age of the paleosols.

## Results

Calcareous soils range from upper Pleistocene, middle to lower Pleistocene, and Pliocene in age are exposed on the surface of an alluvial fan near Mackay, Idaho. The shear-wave velocity of these calcareous soils have been determined *in situ* with the following results: $958 \pm 4$ m/s for the Pliocene soil, $808 \pm 3$ m/s for the middle Pleistocene soil, and $515 \pm 10$ m/s for the Upper Pleistocene soil. These results show that higher shear-wave velocity correlates with older calcareous soil, thereby substantiating the basic premise of this project.

## Reference Cited

Liu, H. P., R. E. Warrick, R. E. Westerlund, J. B. Fletcher, and G. L. Maxwell, 1988, An air-powered impulsive shear-wave source with repeatble signals: *Bulletin of the Seismological Society of America* **78**, p. 355-369.

Machette, M. N., 1978, Dating Quaternary faulting in the southwestern United States by using buried calcic paleosols, *Journal of Research, U.S. Geological Survey*, **6**, p.369-381.

# Strong Ground Motion Prediction in
# Realistic Earth Structures

9910-03010

P. Spudich
Branch of Engineering Seismology and Geology
U.S. Geological Survey
345 Middlefield Road, MS 977
Menlo Park, California 94025
(415) 329-5654

## Investigations

1. Studies of the S-wave coda of aftershocks of the 1984 Morgan Hill, California, earthquake.

2. Interpolation of empirical Green's functions (aftershocks) of the 1986 North Palm Springs, California, earthquake for use in analysis of the main shock recordings.

3. Recording and analysis of aftershocks of the 1987 Whittier Narrows, California, earthquake.

## Results

1. In our study of the coda of aftershocks of the 1984 Morgan Hill earthquake is a continuation and extension of the work of Spudich and Bostwick (1987), who studied the early coda of seismograms from a cluster of 19 aftershock. Because of the short extent of the seismograms available from the portable GEOS recorders, the previous work could only study the early coda. Our more recent work studies the same earthquake cluster, but recorded at local and regional Cal-net stations. These seismograms are much longer (60s duration) and enable us to study the composition of the late coda. Most of the reporting period was spent collecting the relevant seismograms and also validating the analysis method. Because the wave field comprising the late coda may be nearly random, we have had to ensure that any results inferred from the plane wave decomposition technique are reliable when the wave field is nearly isotropic. We have used the 2-dimensional finite difference code provided by A.F. Frankel to generate wave fields caused by known scatterer distributions. These wave fields are used to test the analysis procedure to ensure that our inferences about the coda are warranted.

2. Thirteen digital 6-channel GEOS recorders, each recording a triaxial L-22 geophone and a FBA-13 force-balance accelerometer, were deployed in the epicentral region of the Whittier Narrows earthquake within 36 hours of the main shock. In the first phase of the deployment, lasting until about October 13, GEOS recorders were primarily collocated with analog SMA-1 accelerographs that recorded the main shock. Aftershocks recorded by the GEOS will be used as empirical Green's functions for modeling the main shock ground motions. Occupied stations included USC stations 11,

19, 66, 69, 73 and 75, CDMG stations 24401, 24402, and 14368, and USGS stations at Garvey Reservoir (709) and Whittier Narrows Dam upstream (289). In addition, several free-field sites were occupied. The large aftershock (M5.5) of day 277 1059 UTC was recorded at ten of these sites, and anywhere from 1 to 50 aftershocks were recorded at each site. In the second phase of the deployment on October 23, five GEOS were emplaced in Whittier to determine whether there was a spatial variation of aftershock ground motion that correlates with damage. Sites occupied were Bright Avenue basement (USGS station 804), a free-field site near Bright, a site about 150 m northwest of Lincoln School, a site 150 m northwest of Sorensen School, and USC site 75. The former three sites are in areas of considerable damage. Preliminary data analysis has concentrated on determination of source spectral parameters. In addition, it appears that ground motions at USC station 75 in Whittier did not suffer any amplification of motions compared to other stations distributed in the epicentral area.

3. One of the primary causes of errors in source inversions is the use of inaccurate theoretical Green's functions. These Green's functions are inaccurate because of our ignorance of the earth's velocity substructure at short wavelengths and also because of our inability to calculate exact complete synthetic seismograms in 3-dimensionally varying earth structures. For this reason we have concentrated on using locally recorded aftershocks of the North Palm Springs earthquake as empirical Green's functions (EGFs). In principle, if a set of aftershocks were recorded that had hypocenters distributed densely over the source region, and if they all had the desired mechanism, they could be use directly in s source inversion. In practice we have only a limited number of aftershocks to work with, so some method must be used to interpolate between them to obtain an approximate EGF that corresponds to the seismogram that would have been recorded had an aftershock occurred in the desired position on the fault. In order to interpolate EGFs, we assume that the observer seismograms are a sum of P and S body waves, scattered from a set of point scatterers distributed throughout the 3-D volume containing the fault and stations. When an aftershock occurs, its radiation illuminates each scatterer, causing it to radiate with a time function related to the incident illumination. We use a process similar to migration to solve for the time function associated with the scatterer. This procedure allows us to do waveform modeling of the observer aftershock seismograms. Once we have solved for for the force and moment time series of these scatterers, we can use them to calculate synthetic seismograms for sources at locations other than the actual aftershocks. This is the actual interpolation because we are obtaining seismograms at locations where aftershocks did not occur.

We are looking at the aftershock data from the 8 July 1986 earthquake. The aftershock data being used were recorded on the U.S. Geological Survey portable GEOS instruments which were co-located with the permanent strong motion accelerographs in that area. There is a total of seven co-located GEOS stations. From each of these stations the seismograms which met the following two criteria were chosen for analysis:

1. The aftershock had to be of "A" quality in the hypocentral location procedure.

2. The travel time residual had to be less than a predetermined value (usually 0.1 seconds).

This gave us a windowed data set of 15 to 25 aftershocks per station. The seismograms have been time corrected to account for hypocentral location errors and to obtain better waveform consistency. Ultimately, these data will be used in the interpolation procedure to determine seismic waveforms at arbitrary locations.

This aftershock data are being used to test the migration program. When a source acts, it radiates energy which illuminates scatterers buried within the medium. Each scatterer acts as a secondary source of seismic energy an d can be represented by three components of force and six independent moment couples. The program solves for these forces and moments for a grid of scatterers distributed throughout the crust in the Palm Springs region.

One unknown is the total size of the scattering region. The data determines which scatterers will act as strong secondary sources. A preliminary analysis indicates that in the Palm Springs region a volume of scatterers approximately 65 km wide by 65 km long by 40 km deep is needed to account for the scattered energy within 10 seconds after the p waves of our data. Within this volume certain scatterers radiate a great deal of energy while others radiate very little. Scatterers outside this volume do not contribute to the first 10 seconds of the data. Determination of this scattering volume is important in scaling the problem along with saving computing time.

## References

Spudich, P., and Bostwick, T., 1987, Studies of the seismic coda using an earthquake cluster as a buried seismograph array: Journal of Geophysical Research, vol. 92, p. 10,526-10,546.

## Reports

Bonamassa, O., Dietel, C., Glassmoyer, G., Mueller, C., Noce, T., Sena, J., Sembera, E., and Spudich, P., 1988, Digital recording of aftershocks of the October 1, 1987, Whittier Narrows earthquake [abs.]: Transactions, American Geophysical Union, EOS, in press.

# INDEX 1

## INDEX ALPHABETIZED BY PRINCIPAL INVESTIGATOR

| | | Page |
|---|---|---|
| Ahrens, T. J. | California Institute of Technology | 394 |
| Algermissen, S. T. | U.S. Geological Survey | 449 |
| Allen, C. R. | California Institute of Technology | 1 |
| Allen, C. R. | California Institute of Technology | 278 |
| Allen, R. V. | U.S. Geological Survey | 185 |
| Anderson, R. E. | U.S. Geological Survey | 452 |
| Andrews, D. J. | U.S. Geological Survey | 619 |
| Arabasz, W. J. | University of Utah | 6 |
| Atwater, B. F. | U.S. Geological Survey | 125 |
| Bakun, W. H. | U.S. Geological Survey | 283 |
| Ballantyne, D. | Kennedy/Jenks/Chilton | 539 |
| Beavan, J. | Lamont-Doherty Geological Observatory | 186 |
| Beavan, J. | Lamont-Doherty Geological Observatory | 191 |
| Beavan, J. | Lamont-Doherty Geological Observatory | 298 |
| Berger, G. W. | Western Washington University | 126 |
| Berger, J. | University of California, San Diego | 10 |
| Berger, J. | University of California, San Diego | 305 |
| Birkeland, P. W. | University of Colorado | 132 |
| Boatwright, J. | U.S. Geological Survey | 55 |
| Bock, Y. | Massachusetts Institute of Technology | 196 |
| Bonilla, M. G. | U.S. Geological Survey | 134 |
| Boore, D. M. | U.S. Geological Survey | 620 |
| Borcherdt, R. D. | U.S. Geological Survey | 311 |
| Borcherdt, R. D. | U.S. Geological Survey | 622 |
| Bourgeois, J. | University of Washington | 135 |
| Brady, A. G. | U.S. Geological Survey | 603 |
| Brady, A. G. | U.S. Geological Survey | 605 |
| Brown, R. D. | U.S. Geological Survey | 139 |
| Buchanan-Banks, J. M. | U.S. Geological Survey | 453 |
| Bucknam, R. C. | U.S. Geological Survey | 140 |
| Bundock, H. | U.S. Geological Survey | 607 |
| Burford, R. | U.S. Geological Survey | 314 |
| Burford, S. S. | U.S. Geological Survey | 202 |
| Butler, H. M. | U.S. Geological Survey | 572 |
| Byerlee, J. D. | U.S. Geological Survey | 396 |
| Byerlee, J. D. | U.S. Geological Survey | 398 |
| Campbell, R. H. | U.S. Geological Survey | 454 |
| Carlson, M. A. | U.S. Geological Survey | 573 |
| Castle, R. O. | U.S. Geological Survey | 455 |
| Celebi, M. | U.S. Geological Survey | 609 |
| Chan, W. W. | Teledyne Geotech Alexandria Labs. | 456 |
| Choy, G. L. | U.S. Geological Survey | 57 |
| Choy, G. L. | U.S. Geological Survey | 207 |
| Choy, G. L. | U.S. Geological Survey | 575 |
| Clark, H. E. | U.S. Geological Survey | 577 |
| Clark, M. M. | U.S. Geological Survey | 142 |

| | | |
|---|---|---|
| Clough, G. W. | U.S. Geological Survey | 460 |
| Combellick, R. A. | State of Alaska | 463 |
| Crampin, S. | British Geological Survey | 209 |
| Cranswick, E. | U.S. Geological Survey | 465 |
| Crone, A. J. | U.S. Geological Survey | 471 |
| Crosson, R. S. | University of Washington | 9 |
| Crosson, R. S. | University of Washington | 60 |
| Davis, T. L. | Thomas L. Davis | 144 |
| Dewey, J. W. | U.S. Geological Survey | 578 |
| Dieterich, J. H. | U.S. Geological Survey | 400 |
| Diment, W. H. | U.S. Geological Survey | 474 |
| Emmi, P. C. | University of Utah | 556 |
| Engdahl, E. R. | U.S. Geological Survey | 581 |
| Espinosa, A. F. | U.S. Geological Survey | 477 |
| Etheredge, E. | U.S. Geological Survey | 611 |
| Evans, B. | Massachusetts Institute of Technology | 403 |
| Evernden, J. | U.S. Geological Survey | 405 |
| Fletcher, J. B. | U.S. Geological Survey | 213 |
| Galehouse, J. S. | San Francisco University | 320 |
| Gibbs, J. F. | U.S. Geological Survey | 480 |
| Gladwin, M. T. | University of Queensland | 327 |
| Gohn, G. S. | U.S. Geological Survey | 64 |
| Grant, W. P. | Shannon & Wilson, Inc. | 476 |
| Habermann, R. E. | Georgia Institute of Technology | 65 |
| Haimson, B. C. | University of Wisconsin | 406 |
| Hall, W. | U.S. Geological Survey | 12 |
| Hamburger, M. W. | Indiana University | 69 |
| Harden, J. W. | U.S. Geological Survey | 482 |
| Harding, S. T. | U.S. Geological Survey | 483 |
| Harp, E. L. | U.S. Geological Survey | 484 |
| Hauksson, E. | University of Southern California | 75 |
| Heaton, T. H. | U.S. Geological Survey | 215 |
| Hebenstreit, G. T. | Science Applications International Co. | 487 |
| Helmberger, D. V. | California Institute of Technology | 81 |
| Herd, D. G. | U.S. Geological Survey | 491 |
| Herring, T. A. | Harvard University | 218 |
| Herrmann, R. B. | Saint Louis University | 83 |
| Hoffman, J. P. | U.S. Geological Survey | 595 |
| Holzer, T. L. | U.S. Geological Survey | 560 |
| Irwin, W. P. | U.S. Geological Survey | 84 |
| Jacoby, G. C. | Lamont-Doherty Geological Observatory | 148 |
| Jachens, R. | U.S. Geological Survey | 333 |
| Jensen, E. G. | U.S. Geological Survey | 219 |
| Johnston, M. J. S. | U.S. Geological Survey | 335 |
| Jones, L. M. | U.S. Geological Survey | 221 |
| Julian, B. R. | U.S. Geological Survey | 407 |

| | | |
|---|---|---|
| Kanamori, H. | California Institute of Technology | 225 |
| Kanamori, H. | California Institute of Technology | 339 |
| Keaton, J. R. | Dames & Moore | 493 |
| Keller, E. A. | University of California, Santa Barbara | 152 |
| King, C. -Y. | U.S. Geological Survey | 230 |
| King, K. W. | U.S. Geological Survey | 494 |
| Kirby, S. H. | U.S. Geological Survey | 410 |
| Kisslinger, C. | University of Colorado | 14 |
| Kisslinger, C. | University of Colorado | 86 |
| Klein, F. W. | U.S. Geological Survey | 232 |
| Knuepfer, P. L. K. | State Univ. of New York, Binghamton | 153 |
| Koesterer, C. | U.S. Geological Survey | 234 |

| | | |
|---|---|---|
| Lahr, J. C. | U.S. Geological Survey | 21 |
| Lajoie, K. R. | U.S. Geological Survey | 156 |
| Lajoie, K. R. | U.S. Geological Survey | 159 |
| Langbein, J. | U.S. Geological Survey | 342 |
| Langer, C. J. | U.S. Geological Survey | 93 |
| Lee, W. H. K. | U.S. Geological Survey | 30 |
| Lee, W. H. K. | U.S. Geological Survey | 347 |
| Lester, F. W. | U.S. Geological Survey | 31 |
| Levine, J. | University of Colorado | 235 |
| Leyendecker, E. W. | U.S. Geological Survey | 541 |
| Lienkaemper, J. J. | U.S. Geological Survey | 95 |
| Lienkaemper, J. J. | U.S. Geological Survey | 96 |
| Lindh, A. G. | U.S. Geological Survey | 349 |
| Liu, H. -P. | U.S. Geological Survey | 624 |
| Liu, H. -P. | U.S. Geological Survey | 625 |
| Logan, J. M. | Texas A & M University | 412 |

| | | |
|---|---|---|
| Machette, M. N. | U.S. Geological Survey | 497 |
| Madole, R. F. | U.S. Geological Survey | 502 |
| Madsen, G. | Utah State University | 562 |
| Malik, L. E. | URS/John A. Blume Asso. | 544 |
| Maxwell, G. L. | U.S. Geological Survey | 615 |
| McCalpin, J. | Utah State University | 506 |
| McEvilly, T. V. | University of California, Berkeley | 355 |
| McEvilly, T. V. | University of California, Berkeley | 361 |
| McCann, W. R. | University of Puerto Rico, Mayaguez | 505 |
| McKeown, F. A. | U.S. Geological Survey | 512 |
| Moore, J. L. | West Valley City, Utah | 563 |
| Mortensen, C. E. | U.S. Geological Survey | 367 |
| Mueller, C. S. | U.S. Geological Survey | 514 |

| | | |
|---|---|---|
| Nelson, A. R. | U.S. Geological Survey | 515 |

| | | |
|---|---|---|
| Obermeier, S. F. | U.S. Geological Survey | 97 |
| Olsen, B. C. | Bruce C. Olsen | 546 |
| Oppenheimer, D. H. | U.S. Geological Survey | 236 |

| | | |
|---|---|---|
| Park, R. B. | U.S. Geological Survey | 597 |
| Park, S. K. | University of California, Riverside | 239 |
| Pavlides, L. | U.S. Geological Survey | 98 |
| Pavlis, G. L. | Indiana University | 99 |

| | | |
|---|---|---|
| Peppin, W. A. | University of Nevada | 103 |
| Perkins, J. A. | U.S. Geological Survey | 108 |
| Person, W. J. | U.S. Geological Survey | 598 |
| Peterson, C. D. | Oregon State University | 161 |
| Peterson, C. D. | Oregon State University | 165 |
| Peterson, J. | U.S. Geological Survey | 585 |
| Power, M. S. | Geometrix Consultants | 520 |
| Prescott, W. H. | U.S. Geological Survey | 243 |
| | | |
| Qamar, A. | University of Washington | 523 |
| | | |
| Reasenberg, P. A. | U.S. Geological Survey | 250 |
| Reimer, G. M. | U.S. Geological Survey | 369 |
| Robertson, E. C. | U.S. Geological Survey | 414 |
| Ross, D. C. | U.S. Geological Survey | 109 |
| Rudnicki, J. W. | Northwestern University | 416 |
| Rymer, M. J. | U.S. Geological Survey | 548 |
| | | |
| Safak, E. | U.S. Geological Survey | 617 |
| Sass, J. H. | U.S. Geological Survey | 418 |
| Sato, M. | U.S. Geological Survey | 255 |
| Savage, M. K. | University of Nevada | 34 |
| Scholz, C. H. | Lamont-Doherty Geological Observatory | 422 |
| Schwartz, D. P. | U.S. Geological Survey | 549 |
| Schwartz, D. P. | U.S. Geological Survey | 551 |
| Seeber, L. | Lamont-Doherty Geological Observatory | 166 |
| Segall, P. | U.S. Geological Survey | 371 |
| Sharp, R. V. | U.S. Geological Survey | 111 |
| Shaw, H. R. | U.S. Geological Survey | 423 |
| Sieh, K. | California Institute of Technology | 168 |
| Silverman, S. | U.S. Geological Survey | 378 |
| Simpson, R. W. | U.S. Geological Survey | 431 |
| Sims, J. D. | U.S. Geological Survey | 380 |
| Sipkin, S. A. | U.S. Geological Survey | 586 |
| Slaff, S. | University of Arizona | 175 |
| Smith, R. B. | University of Utah | 113 |
| Somerville, P. | Woodward Clyde Consultants | 525 |
| Spence, W. | U.S. Geological Survey | 447 |
| Spence, W. | U.S. Geological Survey | 589 |
| Spudich, P. | U.S. Geological Survey | 383 |
| Spudich, P. | U.S. Geological Survey | 626 |
| Stauder, W. V. | Saint Louis University | 38 |
| Stein, R. S. | U.S. Geological Survey | 385 |
| Stewart, S. W. | U.S. Geological Survey | 42 |
| Stone, D. B. | University of Alaska | 179 |
| Stover, C. W. | U.S. Geological Survey | 592 |
| Stuart, W. D. | U.S. Geological Survey | 436 |
| Sykes, L. R. | Lamont-Doherty Geological Observatory | 118 |
| Sylvester, A. G. | University of California, Santa Barbara | 388 |
| | | |
| Taber, J. | Lamont-Doherty Geological Observatory | 44 |
| Taber, J. | Lamont-Doherty Geological Observatory | 259 |
| Taggart, J. N. | U.S. Geological Survey | 600 |

| | | |
|---|---|---|
| Teng, T. | University of Southern California | 46 |
| Thurber, C. H. | University of New York, Stony Brook | 121 |
| Tinsley, J. C. | U.S. Geological Survey | 528 |
| Tullis, J. | Brown University | 438 |
| Tullis, T. E. | Brown University | 443 |
| Unger, J. D. | U.S. Geological Survey | 533 |
| Van Schaack, J. | U.S. Geological Survey | 50 |
| Weaver, C. S. | U.S. Geological Survey | 51 |
| Wentworth, C. M. | U.S. Geological Survey | 180 |
| Wesnousky, S. G. | Memphis State University | 181 |
| Wesson, R. L. | U.S. Geological Survey | 392 |
| White, R. A. | U.S. Geological Survey | 263 |
| Wilson, R. | U.S. Geological Survey | 593 |
| Wyatt, F. | University of California, San Diego | 265 |
| Wyatt, F. | University of California, San Diego | 269 |
| Wyatt, F. | University of California, San Diego | 271 |
| Wyatt, F. | University of California, San Diego | 276 |
| Wyss, M. | University of Colorado | 123 |
| Yeats, R. S. | Oregon State University | 182 |
| Yeats, R. S. | Oregon State University | 534 |
| Yerkes, R. F. | U.S. Geological Survey | 553 |
| Zirbes, M. | U.S. Geological Survey | 601 |
| Zoback, M. L. | U.S. Geological Survey | 536 |

# INDEX 2

## INDEX ALPHABETIZED BY INSTITUTION

| | | Page |
|---|---|---|
| Alaska, State of | Combellick, R. A. | 463 |
| Alaska, University of | Stone, D. B. | 179 |
| Arizona, University of | Slaff, S. | 175 |
| Brown University | Tullis, J. | 438 |
| Brown University | Tullis, T. E. | 443 |
| British Geological Survey | Crampin, S. | 209 |
| California Institute of Technology | Ahrens, T. J. | 394 |
| California Institute of Technology | Allen, C. R. | 1 |
| California Institute of Technology | Allen, C. R. | 278 |
| California Institute of Technology | Helmberger, D. V. | 81 |
| California Institute of Technology | Kanamori, H. | 225 |
| California Institute of Technology | Kanamori, H. | 339 |
| California Institute of Technology | Sieh, K. | 168 |
| California, University of, Berkeley | McEvilly, T. V. | 355 |
| California, University of, Berkeley | McEvilly, T. V. | 361 |
| California, University of, Riverside | Park, S. K. | 239 |
| California, University of, San Diego | Berger, J. | 10 |
| California, University of, San Diego | Berger, J. | 305 |
| California, University of, San Diego | Wyatt, F. | 265 |
| California, University of, San Diego | Wyatt, F. | 269 |
| California, University of, San Diego | Wyatt, F. | 271 |
| California, University of, San Diego | Wyatt, F. | 276 |
| California, University of, Santa Barbara | Keller, E. A. | 152 |
| Colorado, University of | Birkeland, P. W. | 132 |
| Colorado, University of | Kisslinger, C. | 14 |
| Colorado, University of | Kisslinger, C. | 86 |
| Colorado, University of | Levine, J. | 235 |
| Colorado, University of | Wyss, M. | 123 |
| Dames & Moore | Keaton, J. R. | 493 |
| Davis, Thomas L. | Davis, T. L. | 144 |
| Geomatrix Consultants | Power, M. S. | 520 |
| Georgia Institute of Technology | Habermann, R. E. | 65 |
| Harvard University | Herring, T. A. | 218 |

| | | |
|---|---|---|
| Indiana University | Hamburger, M. W. | 69 |
| Indiana University | Pavlis, G. L. | 99 |
| Kennedy/Jenks/Chilton | Ballantyne, D. | 539 |
| Lamont-Doherty Geological Observatory | Beavan, J. | 186 |
| Lamont-Doherty Geological Observatory | Beavan, J. | 191 |
| Lamont-Doherty Geological Observatory | Beavan, J. | 298 |
| Lamont-Doherty Geological Observatory | Jacoby, G. C. | 148 |
| Lamont-Doherty Geological Observatory | Scholz, C. H. | 422 |
| Lamont-Doherty Geological Observatory | Seeber, L. | 166 |
| Lamont-Doherty Geological Observatory | Sykes, L. R. | 118 |
| Lamont-Doherty Geological Observatory | Taber, J. | 44 |
| Lamont-Doherty Geological Observatory | Taber, J. | 259 |
| Massachusetts Institute of Technology | Bock, Y. | 196 |
| Massachusetts Institute of Technology | Evans, B. | 403 |
| Memphis State University | Wesnousky, S. G. | 181 |
| Nevada, University of, Reno | Peppin, W. A. | 103 |
| Nevada, University of, Reno | Savage, M. K. | 34 |
| New York State, University of, Binghamton | Knuepfer, P.L.K. | 153 |
| New York State, University of, Stony Brook | Thurber, C. H. | 121 |
| Northwestern University | Rudnicki, J. W. | 416 |
| Olsen, Bruce C. | Olsen, Bruce C. | 546 |
| Oregon State University | Peterson, C. D. | 161 |
| Oregon State University | Peterson, C. D. | 165 |
| Oregon State University | Yeats, R. S. | 182 |
| Oregon State University | Yeats, R. S. | 534 |
| Puerto Rico, University of, Mayaguez | McCann, W. R. | 505 |
| Queensland, University of | Gladwin, M. T. | 327 |
| Saint Louis, University of | Herrmann, R. B. | 83 |
| San Francisco State University | Galehouse, J. S. | 320 |
| Science Applications International Corp. | Hebenstreit, G. T. | 487 |
| Shannon & Wilson, Inc. | Grant, W. P. | 476 |
| Southern California, University of | Teng, T. | 46 |
| Teledyne Geotech Alexandria Laboratories | Chan, W. W. | 456 |
| Texas A & M University | Logan, J. M. | 412 |

| | | |
|---|---|---|
| U.S. Geological Survey | Algermissen, S. T. | 449 |
| U.S. Geological Survey | Allen, R. V. | 185 |
| U.S. Geological Survey | Anderson, R. E. | 452 |
| U.S. Geological Survey | Andrews, D. J. | 619 |
| U.S. Geological Survey | Atwater, B. F. | 125 |
| U.S. Geological Survey | Bakun, W. H. | 283 |
| U.S. Geological Survey | Boatwright, J. | 55 |
| U.S. Geological Survey | Bonilla, M. G. | 134 |
| U.S. Geological Survey | Boore, D. M. | 620 |
| U.S. Geological Survey | Borcherdt, R. D. | 311 |
| U.S. Geological Survey | Borcherdt, R. D. | 622 |
| U.S. Geological Survey | Brady, A. G. | 603 |
| U.S. Geological Survey | Brady, A. G. | 605 |
| U.S. Geological Survey | Brown, R. D. | 139 |
| U.S. Geological Survey | Buchanan-Banks, J.M | 453 |
| U.S. Geological Survey | Bucknam, R. C. | 140 |
| U.S. Geological Survey | Bundock, H. | 607 |
| U.S. Geological Survey | Burford, R. | 314 |
| U.S. Geological Survey | Burford, S. S. | 202 |
| U.S. Geological Survey | Butler, H. M. | 572 |
| U.S. Geological Survey | Byerlee, J. D. | 396 |
| U.S. Geological Survey | Byerlee, J. D. | 398 |
| U.S. Geological Survey | Campbell, R. H. | 454 |
| U.S. Geological Survey | Carlson, M. A. | 573 |
| U.S. Geological Survey | Castle, R. O. | 455 |
| U.S. Geological Survey | Celebi, M. | 609 |
| U.S. Geological Survey | Choy, G. L. | 57 |
| U.S. Geological Survey | Choy, G. L. | 207 |
| U.S. Geological Survey | Choy, G. L. | 575 |
| U.S. Geological Survey | Clark, H. E. | 577 |
| U.S. Geological Survey | Clark, M. M. | 142 |
| U.S. Geological Survey | Clough, G. W. | 460 |
| U.S. Geological Survey | Cranswick, E. | 465 |
| U.S. Geological Survey | Crone, A. J. | 471 |
| U.S. Geological Survey | Dewey, J. W. | 578 |
| U.S. Geological Survey | Dieterich, J. H. | 400 |
| U.S. Geological Survey | Diment, W. H. | 474 |
| U.S. Geological Survey | Engdahl, E. R. | 581 |
| U.S. Geological Survey | Espinosa, A. F. | 477 |
| U.S. Geological Survey | Etheridge, E. | 611 |
| U.S. Geological Survey | Evernden, J. | 405 |
| U.S. Geological Survey | Fletcher, J. B. | 213 |
| U.S. Geological Survey | Gibbs, J. F. | 480 |
| U.S. Geological Survey | Gohn, J. F. | 64 |
| U.S. Geological Survey | Hall, W. | 12 |
| U.S. Geological Survey | Harden, J. W. | 482 |
| U.S. Geological Survey | Harding, S. T. | 483 |
| U.S. Geological Survey | Harp, E. L. | 484 |
| U.S. Geological Survey | Heaton, T. H. | 215 |
| U.S. Geological Survey | Herd, D. G. | 491 |
| U.S. Geological Survey | Hoffman, J. P. | 595 |
| U.S. Geological Survey | Holzer, T. L. | 560 |
| U.S. Geological Survey | Irwin, W. P. | 84 |

| | | |
|---|---|---|
| U.S. Geological Survey | Jachens, R. | 333 |
| U.S. Geological Survey | Jensen, E. G. | 219 |
| U.S. Geological Survey | Johnston, M. J. S. | 335 |
| U.S. Geological Survey | Jones, L. M. | 221 |
| U.S. Geological Survey | Julian, B. R. | 407 |
| U.S. Geological Survey | King, C. -Y. | 230 |
| U.S. Geological Survey | King, K. W. | 494 |
| U.S. Geological Survey | Kirby, S. H. | 410 |
| U.S. Geological Survey | Klein, F. W. | 232 |
| U.S. Geological Survey | Koesterer, C. | 234 |
| U.S. Geological Survey | Lahr, J. C. | 21 |
| U.S. Geological Survey | Lajoie, K. R. | 156 |
| U.S. Geological Survey | Lajoie, K. R. | 159 |
| U.S. Geological Survey | Langbein, J. | 342 |
| U.S. Geological Survey | Langer, C. J. | 93 |
| U.S. Geological Survey | Lee, W. H. K. | 30 |
| U.S. Geological Survey | Lee, W. H. K. | 347 |
| U.S. Geological Survey | Lester, F. W. | 31 |
| U.S. Geological Survey | Leyendecker, E. W. | 541 |
| U.S. Geological Survey | Lienkaemper, J. J. | 95 |
| U.S. Geological Survey | Lienkaemper, J. J. | 96 |
| U.S. Geological Survey | Lindh, A. G. | 349 |
| U.S. Geological Survey | Liu, H. -P. | 624 |
| U.S. Geological Survey | Liu, H. -P. | 625 |
| U.S. Geological Survey | Machette, M. N. | 497 |
| U.S. Geological Survey | Madole, R. F. | 502 |
| U.S. Geological Survey | Maxwell, G. L. | 615 |
| U.S. Geological Survey | McKeown, F. A. | 512 |
| U.S. Geological Survey | Mortensen, C. E. | 367 |
| U.S. Geological Survey | Mueller, C. S. | 514 |
| U.S. Geological Survey | Nelson, A. R. | 515 |
| U.S. Geological Survey | Obermeier, S. F. | 97 |
| U.S. Geological Survey | Oppenheimer, D. H. | 236 |
| U.S. Geological Survey | Park, R. B. | 597 |
| U.S. Geological Survey | Pavlides, L. | 98 |
| U.S. Geological Survey | Perkins, J. A. | 108 |
| U.S. Geological Survey | Person, W. J. | 598 |
| U.S. Geological Survey | Peterson, J. | 585 |
| U.S. Geological Survey | Prescott, W. H. | 243 |
| U.S. Geological Survey | Reasenberg, P. A. | 250 |
| U.S. Geological Survey | Reimer, G. M. | 369 |
| U.S. Geological Survey | Robertson, E. C. | 414 |
| U.S. Geological Survey | Ross, D. C. | 109 |
| U.S. Geological Survey | Rymer, M. J. | 548 |
| U.S. Geological Survey | Safak, E. | 617 |
| U.S. Geological Survey | Sass, J. H. | 418 |
| U.S. Geological Survey | Sato, M. | 255 |
| U.S. Geological Survey | Schwartz, D. P. | 549 |
| U.S. Geological Survey | Schwartz, D. P. | 551 |
| U.S. Geological Survey | Segall, P. | 371 |
| U.S. Geological Survey | Sharp, R. V. | 111 |
| U.S. Geological Survey | Shaw, H. R. | 423 |
| U.S. Geological Survey | Silverman, S. | 378 |

| | | |
|---|---|---|
| U.S. Geological Survey | Simpson, R. W. | 431 |
| U.S. Geological Survey | Sims, J. D. | 380 |
| U.S. Geological Survey | Sipkin, S. A. | 586 |
| U.S. Geological Survey | Spence, W. | 447 |
| U.S. Geological Survey | Spence, W. | 589 |
| U.S. Geological Survey | Spudich, P. | 383 |
| U.S. Geological Survey | Spudich, P. | 626 |
| U.S. Geological Survey | Stein, R. S. | 385 |
| U.S. Geological Survey | Stewart, S. W. | 42 |
| U.S. Geological Survey | Stover, C. W. | 592 |
| U.S. Geological Survey | Stuart, W. D. | 436 |
| U.S. Geological Survey | Taggart, J. N. | 600 |
| U.S. Geological Survey | Tinsley, J. C. | 528 |
| U.S. Geological Survey | Unger, J. D. | 533 |
| U.S. Geological Survey | Van Schaack, J. | 50 |
| U.S. Geological Survey | Weaver, C. S. | 51 |
| U.S. Geological Survey | Wentworth, C. M. | 180 |
| U.S. Geological Survey | Wesson, R. L. | 392 |
| U.S. Geological Survey | White, R. A. | 263 |
| U.S. Geological Survey | Wilson, R. | 593 |
| U.S. Geological Survey | Yerkes, R. F. | 553 |
| U.S. Geological Survey | Zirbes, M. | 601 |
| U.S. Geological Survey | Zoback, M. L. | 536 |
| URS/John A. Blume Associates | Malik, L. E. | 544 |
| Utah State University | Madsen, G. | 562 |
| Utah State University | McCalpin, J. | 506 |
| Utah, University of | Arabasz, W. J. | 6 |
| Utah, University of | Emmi, P. C. | 556 |
| Utah, University of | Smith, R. B. | 113 |
| Washington, University of | Bourgeois, J. | 135 |
| Washington, University of | Crosson, R. S. | 9 |
| Washington, University of | Crosson, R. S. | 60 |
| Washington, University of | Qamar, A. | 523 |
| West Valley City, Utah | Moore, J. L. | 563 |
| Western Washington University | Berger, G. W. | 126 |
| Wisconsin, University of | Haimson, B. C. | 406 |
| Woodward-Clyde Consultants | Somerville, P. | 525 |

☆U.S. GOVERNMENT PRINTING OFFICE:1988-588-662/99244